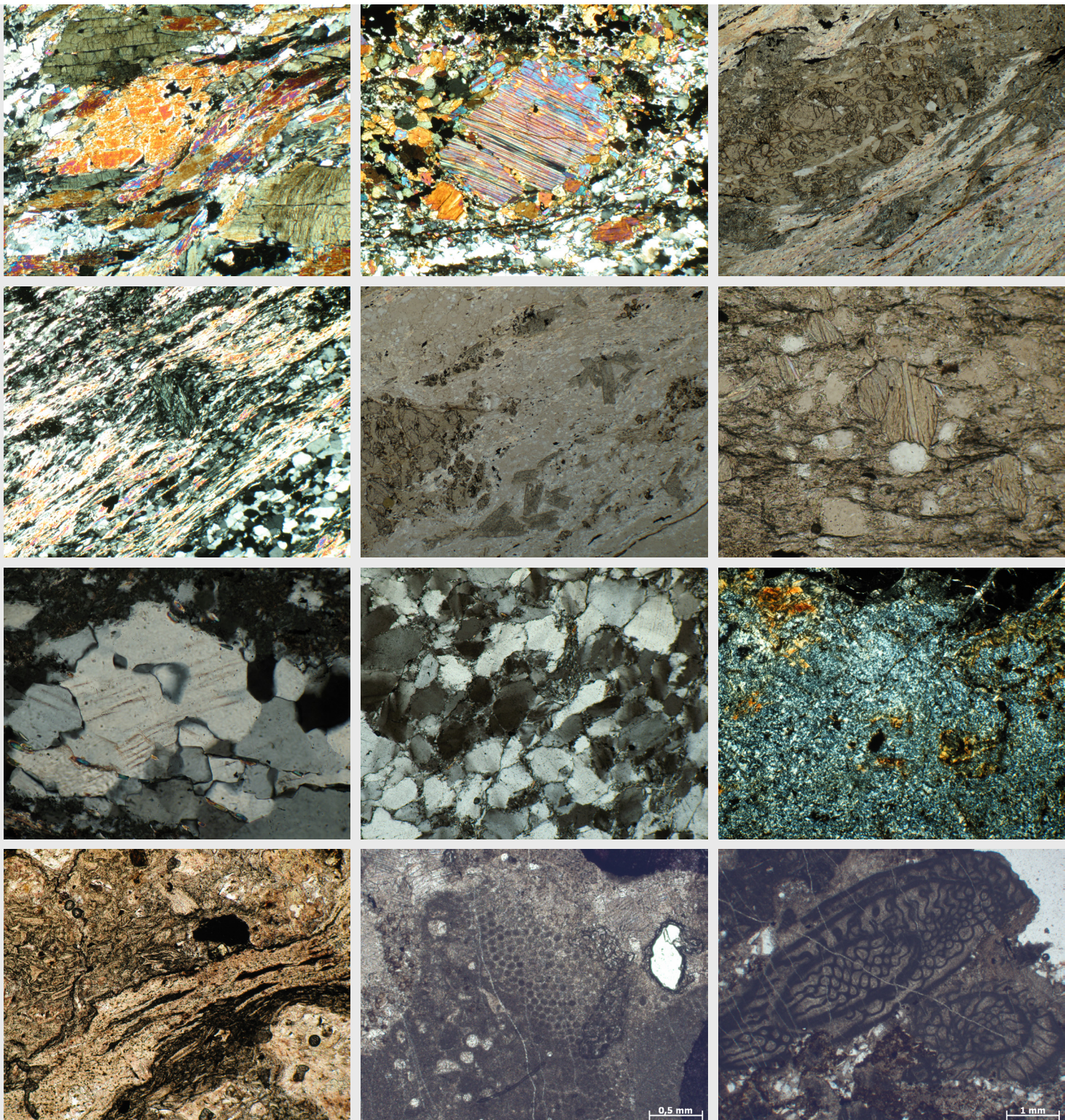


GELOGIJA

2024 | št.: **67/1**



ISSN

Tiskana izdaja / Print edition: 0016-7789

Spletna izdaja / Online edition: 1854-620X

GEOLOGIJA

67/1 – 2024



GEOLOGIJA	2024	67/1	1-185	Ljubljana
-----------	------	------	-------	-----------



Izdajatelj: Geološki zavod Slovenije, zanj direktor dr. Miloš Bavec

Publisher: Geological Survey of Slovenia, represented by Director dr. Miloš Bavec

Financirata Javna agencija za raziskovalno in inovacijsko dejavnost Republike Slovenije in Geološki zavod Slovenije

Financed by the Slovenian Research and Innovation Agency and the Geological Survey of Slovenia

UREDNIŠTVO / EDITORIAL TEAM

Glavna in odgovorna urednica / Editor-in-Chief:

dr. Mateja Gosar, Geological Survey of Slovenia, Ljubljana, Slovenia

Tehnična urednica / Technical Editor:

Bernarda Bole, Geological Survey of Slovenia, Ljubljana, Slovenia



ČLANI TEHNIČNEGA UREDNIŠTVA / TECHNICAL EDITORIAL TEAM

Vida Pavlica, Geological Survey of Slovenia, Ljubljana, Slovenia

Maks Šinigoj, Geological Survey of Slovenia, Ljubljana, Slovenia

Irena Trebušak, Geological Survey of Slovenia, Ljubljana, Slovenia

Marko Zakrajšek, Marko Zakrajšek, e-Tutor s.p., Kranj, Slovenia

UREDNIŠKI ODBOR / EDITORIAL BOARD

Dunja Aljinović, Faculty of Mining Geology and Petroleum Engineering, Zagreb, Croatia

Kristine Asch, Federal Institute for Geosciences and Natural Resources (BGR), Hannover, Germany

Maria João Batista, National Laboratory of Energy and Geology, Lisbon, Portugal

Giovanni Battista Carulli, University of Trieste, Department of Mathematics and Earth Sciences, Trieste, Italy

Miloš Bavec, Geological Survey of Slovenia, Ljubljana, Slovenia

Mihail Brenčič, University of Ljubljana, Faculty of Natural Sciences and Engineering and Geological Survey of Slovenia, Ljubljana, Slovenia

Stefano Covelli, University of Trieste, Department of Mathematics, Informatics and Geosciences, Trieste, Italy

Katica Drobne, Research Centre of the Slovenian Academy of Sciences and Arts, Ivan Rakovec Institute of Palaeontology, Ljubljana, Slovenia

Jadran Faganeli, University of Ljubljana, Biotechnical Faculty Ljubljana, Slovenia

László Földör, Eötvös Loránd University, Budapest, Hungary

Luka Gale, University of Ljubljana, Faculty of Natural Sciences and Engineering and Geological Survey of Slovenia, Ljubljana, Slovenia

Špela Goričan, Research Centre of the Slovenian Academy of Sciences and Arts, Ivan Rakovec Institute of Palaeontology, Ljubljana, Slovenia

Andrej Gosar, Slovenian Environment Agency and University of Ljubljana, Faculty of Natural Sciences and Engineering, Ljubljana, Slovenia

János Haas, Etvos Lorand University, Budapest, Hungary

Mitja Janža, Geological Survey of Slovenia, Ljubljana, Slovenia

Mateja Jemec Aušlič, Geological Survey of Slovenia, Ljubljana, Slovenia

Bogdan Jurkovšek, Geological Survey of Slovenia, Ljubljana, Slovenia

Roman Koch, GeoZentrum Nordbayern, Institute of Palaeontology, Erlangen, Germany

Marko Komac, Marko Komac s.p., Ljubljana, Slovenia

Harald Lobitzer, GeoSphere Austria, Vienna, Austria

Tamara Marković, Croatian Geological Survey, Zagreb, Croatia

Miloš Miler, Geological Survey of Slovenia, Ljubljana, Slovenia

Rinaldo Nicolich, University of Trieste, Trieste, Italy

Simon Pirc, University of Ljubljana, Faculty of Natural Sciences and Engineering, Ljubljana, Slovenia

Frank Preusser, University of Freiburg, Institute of Earth and Environmental Science, Freiburg, Germany

Roberto Rettori, University of Perugia, Department of Physics and Geology, Perugia, Italy

Mihail Ribičič, University of Ljubljana, Faculty of Natural Sciences and Engineering, Ljubljana, Slovenia

Nina Rman, Geological Survey of Slovenia, Ljubljana, Slovenia

Boštjan Rožič, University of Ljubljana, Faculty of Natural Sciences and Engineering, Ljubljana, Slovenia

Milan Sudar, University of Belgrade, Faculty of Mining and Geology, Beograd, Serbia

Kristina Šarić, University of Belgrade, Faculty of Mining and Geology, Beograd, Serbia

Sašo Šturm, Institut »Jožef Stefan«, Ljubljana, Slovenia

Gevorg Tepanosyan, Center for Ecological-Noosphere Studies NAS RA, Yerevan, Armenia

Timotej Verbovšek, University of Ljubljana, Faculty of Natural Sciences and Engineering, Ljubljana, Slovenia

Miran Veselič, Faculty of Civil and Geodetic Engineering, University of Ljubljana, Ljubljana, Slovenia

Michael Wagreich, University of Vienna, Department of Geology, Vienna, Austria

Nina Zupančič, University of Ljubljana, Faculty of Natural Sciences and Engineering, Ljubljana, Slovenia

Naslov uredništva / Editorial Office: GEOLOGIJA Geološki zavod Slovenije / Geological Survey of Slovenia
Dimičeva ulica 14, SI-1000 Ljubljana, Slovenija
Tel.: +386 (01) 2809-700, Fax: +386 (01) 2809-753, e-mail: urednik@geologija-revija.si
URL: <https://www.geologija-revija.si/>

GEOLOGIJA izhaja dvakrat letno. / GEOLOGIJA is published two times a year.
GEOLOGIJA je na voljo tudi preko medknjižnične izmenjave publikacij. /
GEOLOGIJA is available also on exchange basis.

Izjava o etičnosti

Izdajatelji revije Geologija se zavedamo dejstva, da so se z naglim naraščanjem števila objav v svetovni znanstveni literaturi razmahnili tudi poskusi plagiatorstva, zlorab in prevar. Menimo, da je naša naloga, da se po svojih močeh borimo proti tem pojavom, zato v celoti sledimo etičnim smernicam in standardom, ki jih je razvil odbor COPE (Committee for Publication Ethics).

Publication Ethics Statement

As the publisher of Geologija, we are aware of the fact that with growing number of published titles also the problem of plagiarism, fraud and misconduct is becoming more severe in scientific publishing. We have, therefore, committed to support ethical publication and have fully endorsed the guidelines and standards developed by COPE (Committee on Publication Ethics).

Baze, v katerih je Geologija indeksirana / Indexation bases of Geologija: Scopus, Directory of Open Access Journals, GeoRef, Zoological Record, Geoscience e-Journals, EBSCOhost

Cena / Price

Posamezni izvod / Single Issue

Posameznik / Individual: 15 €

Institucija / Institutional: 25 €

Letna naročnina / Annual Subscription

Posameznik / Individual: 25 €

Institucija / Institutional: 40 €

Tisk / Printed by: TISKARNA JANUŠ d.o.o.

Slika na naslovni strani: Mikrofaciesi klastov pliocensko-pleistocenskih sedimentov Dravsko-Ptujskega bazena
(foto: Eva Mencin Gale).

Cover page: Microfacies of the clasts in the Pliocene-Pleistocene sediments in the Drava-Ptuj Basin (photo: Eva Mencin Gale).

VSEBINA – CONTENTS

Članki - Articles

Žvab Rožič, P.	
Hydrogeochemical and Isotopic Characterisation of the Učja Aquifer, NW Slovenia	7
Hidrogeokemična in izotopska karakterizacija vodonosnika Uče, SZ Slovenija	
Gale, L. & Rožič, B.	
Signs of crustal extension in Lower Jurassic carbonates from central Slovenia	25
Znaki ekstenzije skorje v spodnjejurskih karbonatih osrednje Slovenije	
Gosar, M., Bavec, Š., Miler, M. & Gaberšek, M.	
Vsebnosti potencialno strupenih elementov v sedimentih in vodah reke Meže in njenih pritokov, ki odvodnjavajo odlagališča rudarskih odpadkov.....	41
Contents of potentially toxic elements in sediments and waters of the Meža river and its tributaries draining mine waste deposits	
Dernov, V.	
Palaeoecological significance of the trace fossil <i>Circulichnis</i> Vyalov, 1971 from the Carboniferous of the Donets Basin, Ukraine.....	63
Paleoekološki pomen fosilne sledi <i>Circulichnis</i> Vyalov, 1971 iz karbona Doneškega bazena v Ukrajini	
Skaberne, D., Čar, J., Pristavec, M., Rožič, B. & Gale, L.	
Middle Triassic deeper-marine volcano-sedimentary successions in western Slovenia	71
Srednjetriaspna globljemorska vulkansko-sedimentna zaporedja v zahodni Sloveniji	
Kanduč, T. & Markič, M.	
Isotopic composition of carbon ($\delta^{13}\text{C}$) and nitrogen ($\delta^{15}\text{N}$) of petrologically different Tertiary lignites and coals.....	105
Izotopska sestava ogljika ($\delta^{13}\text{C}$) in dušika ($\delta^{15}\text{N}$) petrološko različnih terciarnih lignitov in premogov	
Placer, L., Popit, T. & Rižnar, I.	
Tectonics and gravitational phenomena, part two: The Trnovski gozd-Banjšice-Šentviška Gora degraded plain	129
Tektonika in gravitacijski pojavi, drugi del: Trnovsko-banjško-šentviška degradirana uravnava	

Podatkovni članki - Data Articles

Mencin Gale, E., Kralj, P., Trajanova, M., Gale, L. & Skaberne, D.	
Petrology dataset of Pliocene-Pleistocene sediments in northeastern Slovenia.....	157
Podatki o petrologiji pliocensko-pleistocenskih sedimentov severovzhodne Slovenije	

Poročila in ostalo - Reports and More

Rajver, D.: 7. Svetovni geotermalni kongres WGC 2023, Peking (Kitajska) 15.–17. september 2023.....	161
Novak, M.: Poročilo slovenskega nacionalnega odbora za geoznanosti in geoparke (IGGP) za leto 2023.....	169
Švara, A.: Poročilo o aktivnostih Slovenskega geološkega društva v letu 2023	171

Nove publikacije - New Publications

Veselič, M.: Decrouez, D., Finger, W., Haldimann, P., Hofstetter, J.-C., Kündig, R., Meyer, C., Mumenthaler, T., Sieber, N., Spescha, R., Testaz, G. et al. (eds.) 2018: Stein und Wein: Entdeckungreisen durch schweizerischen Rebbaugebiete, AS Verlag & Grafik, Zürich: 612 p. 178



Hydrogeochemical and Isotopic Characterisation of the Učja Aquifer, NW Slovenia

Hidrogeokemična in izotopska karakterizacija vodonosnika Učje, SZ Slovenija

Petra ŽVAB ROŽIČ

University of Ljubljana, Faculty of Natural Sciences and Engineering, Department of Geology, Aškerčeva 12,
SI-1000 Ljubljana, Slovenia; e-mail: petra.zvabrozic@ntf.uni-lj.si

Prejeto / Received 23. 10. 2023; Sprejeto / Accepted 2. 2. 2024; Objavljeno na spletu / Published online 7. 2. 2024

Key words: groundwater, hydrogeochemistry, isotopes, cross-border aquifer, Učja Valley

Ključne besede: podzemna voda, hidrogeokemija, izotopi, čezmejni vodonosnik, dolina Učje

Abstract

The groundwater characteristics of the Učja aquifer were investigated using geochemical and isotopic data. The water discharge and physico-chemical properties of the groundwater and the Učja River reflect the climate that is characteristic of the area. The mixed snow/rainfall regime is characteristic for the Učja Valley, with the highest discharges appearing during the spring snowmelt and autumn precipitation, and the lowest discharges in the winter and especially summer months. The temperature of the groundwater and the Učja River is lower in winter and higher in summer. The specific electrical conductivity values indicate a very permeable carbonate aquifer. Higher conductivity values were observed in spring and autumn at all sampling sites, which is related to snowy and rainy periods. The groundwater from the Učja aquifer indicates a uniform type of water ($\text{Ca}-\text{Mg}-\text{HCO}_3$), with Ca^{2+} , Mg^{2+} and HCO_3^- the most abundant ions. Differences in Ca^{2+} and Mg^{2+} concentrations and in the $\text{Mg}^{2+}/\text{Ca}^{2+}$ molar ratio between sampling sites were observed. Those springs with lower Mg^{2+} and lower $\text{Mg}^{2+}/\text{Ca}^{2+}$ molar ratios indicate limestone recharge areas, and those springs with higher Mg^{2+} and molar ratios indicate interaction with the dolomite hinterland. The pH values confirm alkaline waters characteristic of carbonate aquifers. The hydrogen ($\delta^2\text{H}$) and oxygen ($\delta^{18}\text{O}$) isotope values suggest the main source of water is from precipitation from a complex mixing of maritime and continental air masses. An altitude isotopic effect is observed with minor $\delta^{18}\text{O}$ and $\delta^2\text{H}$ depletion at higher altitude sampling sites compared to those springs at lower altitudes. The altitude isotopic effect is most prominent in spring. The $\delta^{13}\text{C}_{\text{DIC}}$ values indicate the dissolution of carbonates and the degradation of organic matter.

Izvleček

Značilnosti podzemne vode vodonosnika doline Učje so bile raziskane z uporabo geokemijskih in izotopskih podatkov. Pretoki in fizikalno-kemijski parametri reke Učje in podzemne vode na izviroh odražajo podnebne značilnosti območja. Za dolino Učje je značilen mešani snežno-dežni režim z največjimi pretoki v času spomladanskega taljenja snega in jesenskih padavin ter najnižjimi pretoki pozimi in predvsem poleti. Temperatura podzemne vode in reke Učje je pozimi nižja in poleti višja. Rezultati specifične elektroprevodnosti kažejo na zelo prepusten karbonatni vodonosnik. Na vseh vzorčnih mestih so bile izmerjene višje vrednosti spomladini in jeseni, kar povezujem s snežnimi in deževnimi obdobji. Podzemna voda vodonosnika doline Učje je enotnega tipa ($\text{Ca}-\text{Mg}-\text{HCO}_3$) z najvišjimi koncentracijami Ca^{2+} , Mg^{2+} in HCO_3^- ionov. Med vzorčnimi mesti so bile ugotovljene razlike v koncentracijah Ca^{2+} in Mg^{2+} ter molskim razmerjem $\text{Mg}^{2+}/\text{Ca}^{2+}$. Izviri z nižjimi vrednostmi Mg^{2+} in nižjim molskim razmerjem izkazujejo apnenčevno napajalno območje, izviri z višjimi vrednostmi Mg^{2+} in višjim molskim razmerjem pa interakcijo z dolomitom. Vrednosti pH potrjujejo alkalnost voda, značilnih za karbonatne vodonosnike. Vrednosti izotopov vodika ($\delta^2\text{H}$) in kisika ($\delta^{18}\text{O}$) kažejo, da so glavni vir vode v vodonosniku padavine, ki nastanejo ob kompleksnem mešanju morskih in celinskih zračnih mas. Višinski izotopski efekt je opazen v nižjih vrednostih $\delta^{18}\text{O}$ in $\delta^2\text{H}$ na vzorčnih mestih višjih nadmorskih višin v primerjavi z izviri na nižjih nadmorskih višinah. Višinski izotopski učinek je najizrazitejši spomladini. Vrednosti $\delta^{13}\text{C}_{\text{DIC}}$ odražajo raztopljanje karbonatov in razgradnjo organske snovi.

Introduction

Geochemical studies of surface and groundwater play an important part in understanding the mechanisms determining water chemistry (Gibbs, 1970). Karst and fractured aquifers pose a specific challenge due to their heterogeneity and the special geochemical processes at work in aquifers (Ford & Williams, 2007; Moral et al., 2008; Newman, 2005; White, 1988). Understanding the water flow in aquifers and the connections between the atmosphere and deeper aquifers is essential (Allshorn et al., 2007; Keim et al., 2012; Maurice et al., 2021). The characteristics of spring water are the result of the mixing of groundwaters, interaction with the host rocks in the aquifer, and fresh surface water from precipitation with specific climate-related characteristics (Khadka & Rijal, 2020; White, 2010). Karst springs often respond very quickly and intensively to rainy events, while their response to snowmelt varies in space and time (Weber et al., 2016) and also depends on other climatic factors. Both sources of water contribute considerably to aquifer recharge and are useful in understanding the impact of the composition of precipitation on groundwater (spring water).

Hydrogeochemical and isotopic data provide us with information about groundwater sources and residence times, aquifer properties, water-rock interaction along the flow path, and the mixing of different types of water (Cartwright et al., 2012). The temporal and spatial variability of major ions in karstic waters is important in an understanding of chemical and physical processes influenced by geological conditions, climate, and anthropogenic activities (Gibbs, 1970; Meybeck, 1987). The isotopic compositions of hydrogen and oxygen of water and carbon in the dissolved inorganic carbon, in combination with meteorological, hydrological, hydrogeological, and physicochemical data all help us to characterise and trace waters through the hydrological cycle (Dansgaard, 1964; Kendall & Doctor, 2003; Kanduč et al., 2012; Torkar et al., 2016; Calligaris et al., 2018; Shamsi et al., 2019; Serianz et al., 2021 and others). Stable isotopes of hydrogen ($\delta^2\text{H}$) and oxygen ($\delta^{18}\text{O}$) are used to determine the source of the water and residence time, the flow of water through the water body, or to quantify exchanges of water, solutes, and particulates between hydrological compartments to indicate the potential water inputs to the system and characterize the influence of different processes during infiltration, and to determine the mixing of waters of different origins within the system (Aggarwal et al., 2005; Clark & Fritz, 1997; Glynn &

Plummer, 2005; Rodgers et al., 2005). Carbon isotopes help us to assess the origin of dissolved inorganic carbon (DIC), the main component in waters draining carbonate systems. The isotope composition of dissolved inorganic carbon ($\delta^{13}\text{C}_{\text{DIC}}$) is used to understand the biogeochemical reactions controlling alkalinity and to trace the origin of the bicarbonate ion, which is the dominant anion in the shallow groundwater (Bullen & Kendall, 1998).

Almost half of the Slovenian territory is characterized by karst (Gams, 1974, 2004; Gostinčar & Stepišnik, 2023). These systems are often vast reservoirs of high quality water and thus important sources of drinking water (Ravbar & Kovačič, 2006). Studies of karst aquifers are complex but pose important research challenges within the frame of determining and protecting potential sources of drinking water.

In the past, various hydrogeological research has been carried out in the area of the Kanin (Komac, 2001; Turk et al., 2014; Zini et al., 2014; Russo, 2015) and Kobariški stol aquifers (Brenčič et al., 2001), while the Učja Valley has not yet been studied in detail. The Učja aquifer represents a cross-border karstic aquifer, which may contain large amounts of quality groundwater (Brenčič et al., 2001; Rejc, 2014), and could in the future represent an important source of drinking water or a commercial source as well, as it could be used as a significant water resource for cross-boundary supply. As a result, a comprehensive survey of the potential of the Učja aquifer was carried out.

Various geological studies have been made of the wider investigated area in the past, which provide basic data for detailed lithological and structural maps of the territory. The first geological studies were made already in the 1970s and 1980s to produce basic geological maps (Kuščer, 1974; Buser, 1986, 1987). Later, due to the very complex tectonic structure of the area, numerous regional and local studies of the Učja Valley and its surroundings were elaborated (Čar & Pišljar, 1991, 1993; Vrabec, 2012). The lithology of the Mt. Kobariški Stol area, which represents the southern slopes of the Učja Valley, was described by Šmuc (2012) and is currently investigated in greater detail (Rožič et al., 2022; Vantur, 2023). From the hydrogeological point of view, the springs of the wider area were listed and described (Brenčič et al., 2001; Janež, 2002), whereas within the framework of national monitoring only hydrological measurements of surface water on the Učja River are carried out. A basic hydrogeological analysis of the Učja was also described (Rejc, 2014).

The aim of this paper is to characterise the groundwater of the Učja aquifer. Physico-chemical parameters (T, EC, pH), hydrogeochemical composition (cations and anions) and isotopic tracers ($\delta^2\text{H}$, $\delta^{18}\text{O}$, $\delta^{13}\text{C}_{\text{DIC}}$, ${}^3\text{H}$) were used to characterize the (1) water–rock interaction in the aquifer, (2) the origin of the groundwater using isotopic tracers, and (3) the origin of carbon in the dissolved inorganic carbon to evaluate the biogeochemical processes at work in the groundwater. The presented results, in combination with other segments of the aquifer (geological conditions, climate land use characteristics, geochemical modeling etc.), will provide a useful basis for the further planning of the use and protection of the Učja water resource. The importance of the results extends beyond Slovenia's borders, in terms of cross-border sharing of knowledge, coordination, and the potential cross-border planning and management of common water resources.

Study area

Sampling location

The Učja Valley is located in NW Slovenia between the towns of Bovec and Kobarid. The valley extends in the W-E direction, and is bounded

on the south and north by mountain ridges: the Kobariški stol ridge (with the highest peak Stol or Veliki Muzec, 1673 m) in the south and the ridge with the Skutnik peak (1721 m), which is part of the Kanin ridge in the north. The western border is defined by the state border with the Republic of Italy, and to the east by the Soča River valley near the village of Žaga (Fig. 1). The W-E orientation of the Učja Valley is unique from a tectonic point of view, as it almost perpendicularly cuts the entire fault zone of the Idrija fault (Fig. 2), one of the most prominent fault zones in western Slovenia (Čar & Pišljar, 1991; Vrabec, 2012).

The area has a typical mountain morphology with steep slopes in the north and south, with the gorge of Učja River between them (Fig. 1). The northern and southern slopes descend towards the valley at an average gradient of 25–45°, with vertical slopes of some mountains, ridges, and gorges. The northern slopes in some parts above the river rise vertically up to 300 m, but then decrease slightly (on average 40°). Due to the prominent ruggedness and especially steep slopes of the terrain, some parts are completely impassable and work in such areas is very difficult. Towards the west of the researched area, where the Učja River flows into the Soča River, the slope of the

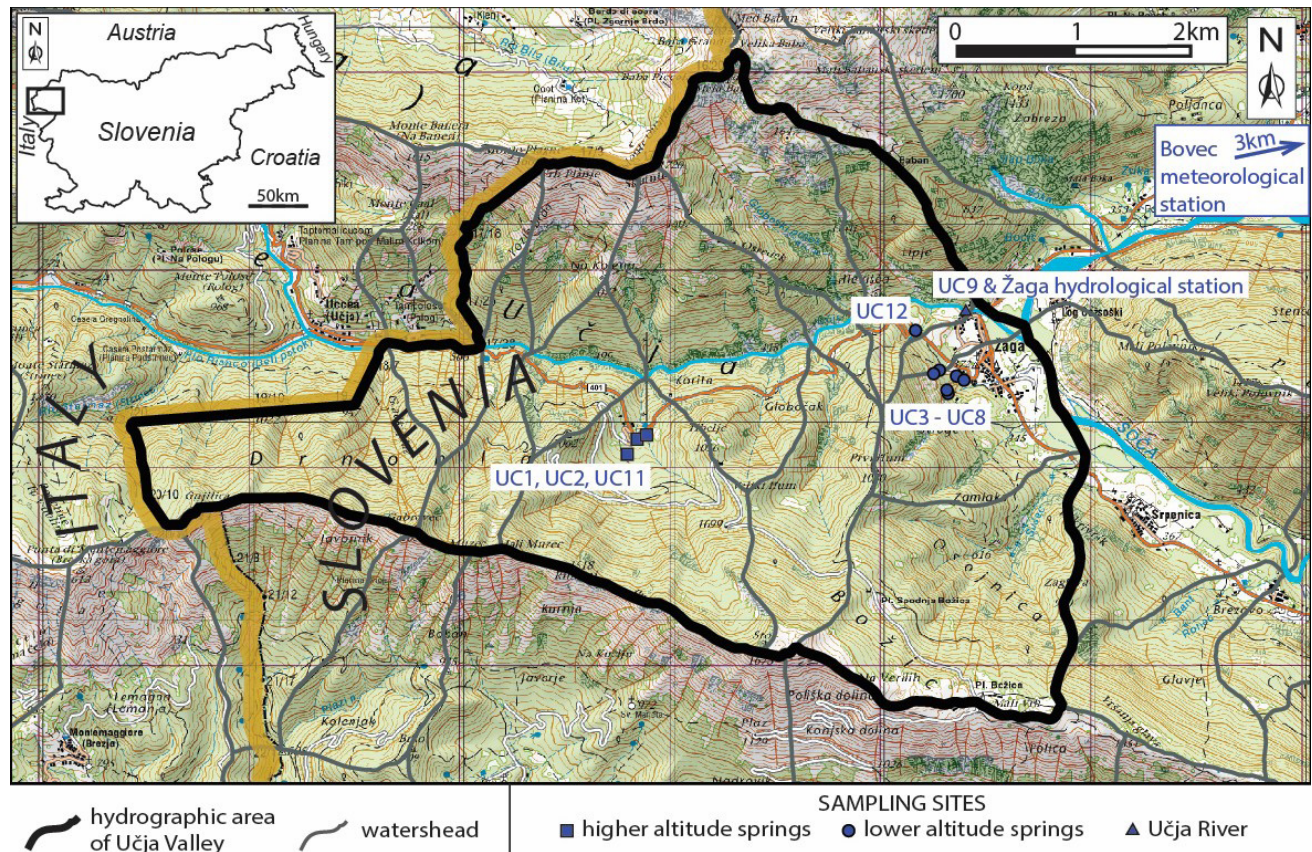


Fig. 1. Geographic location of the Učja Valley with marked sampled springs in the study area (source map Geopedia; 13.36402° W, 13.52413° E, 46.33777° N, 46.26382° S). The hydrographic area of the Slovenian part of the Učja Valley is presented (ARSO, 2019b).

terrain decreases considerably ($15\text{--}20^\circ$) and finally levels out on the alluvial plain of the Soča River. The Učja river originates under the western slopes of the Kanin ridge in Italy and flows into Slovenia through a narrow gorge. After 18 km, the Učja River flows into the Soča River as the right and second largest tributary near the village of Žaga. The Učja gorge is registered in the Nature Conservation Atlas (ZRSVN, 2023) as Natural Value (ID 775).

The Hydrogeological characteristics of the Učja Valley are directly dependent on the geological characteristics of the wider area (Fig. 2). Most of the main springs are located at the foot of the mountain slopes near the transition to the alluvial plain of the Soča Valley and appear along the Idrija fault (Fig. 1 and 2). A few springs were defined along the Učja riverbed (Čar & Pišljar, 1991), and individual springs higher up on the slopes, most likely linked to lithological changes or strong tectonic structures. Part of the groundwater (springs) is captured for drinking water in the public water supply network, while some springs are used for private drinking water supply. These springs also have water permits. Water protection zones are not defined for any of the springs (ARSO, 2019a).

Water for geochemical and isotopic analyses was sampled at 13 locations in the Učja Valley (Fig. 1 and 2). The spring water (groundwater) was sampled at twelve sampling sites (UC1-UC8, UC10-UC13) as well as one additional water sample from the Učja River (surface water, UC9). In this work, the results of 11 sampling sites are presented (Table 1), while two sites (UC10, UC13) are not considered in the evaluation due to a lack of data. Seven sampling sites were positioned at the foot of the mountain slopes (UC3-UC8, UC12; on figures marked with circles), near the transition to the alluvial plain of the Soča Valley. These springs are located west of the Idrija fault zone and one of them (UC12) in the fault zone. These sampling sites are located at altitudes of 389–480 m asl. Three sampling sites (UC1, UC2, UC11; on figures marked with squares) are located on the slopes of the Kobariški stol ridge near the former border crossing station with the Republic of Italy. These sampling sites are located at altitudes of 758–700 m asl. Sampling site UC9 (Učja stream water; on figures marked with a triangle) was located approximately 50 m upstream of the road bridge at the Žaga hydrological station.

Table 1. Details of sampling locations in the Učja Valley (*not considered in this research), sampling periods of in-situ field measurements (physico-chemical parameters) and periods of laboratory analyses (geochemical and isotopic analyses – $\delta^{18}\text{O}$, $\delta^2\text{H}$, total alkalinity, $\delta^{13}\text{C}_{\text{DIC}}$, ${}^3\text{H}$).

Label	LAT [$^\circ$]	LONG [$^\circ$]	Altitude [m]	Water type	Sampling period (in-situ field measurements)	Sampling period (laboratory measurements)		
						Geochemical analyses	$\delta^{18}\text{O}$, $\delta^2\text{H}$, total alkalinity, $\delta^{13}\text{C}_{\text{DIC}}$	Tritium (${}^3\text{H}$)
UC1	46,29615	13,43663	758	Spring	December 2017, January 2018, March 2018, April 2018, 2x June 2018, July 2018, August 2018, October 2018, November 2018, December 2018, March 2019	December 2017, April 2018	December 2017, April 2018, July 2018, October 2018	December 2017
UC2	46,29750	13,43778	707	Spring	December 2017, January 2018, March 2018, April 2018, 2x June 2018, November 2018, December 2018, March 2019	Same as UC1	December 2017, April 2018	Same as UC1
UC3	46,30250	13,47594	437	Spring	Same as UC1	Same as UC1	Same as UC1	Same as UC1
UC4	46,30222	13,47611	449	Spring	Same as UC1	Same as UC1	Same as UC1	Same as UC1
UC5	46,30398	13,47432	480	Spring	Same as UC1	Same as UC1	Same as UC1	Same as UC1
UC6	46,30431	13,47498	451	Spring	Same as UC1	Same as UC1	Same as UC1	Same as UC1
UC7	46,30347	13,47806	389	Spring	Same as UC1	Same as UC1	Same as UC1	Same as UC1
UC8	46,30377	13,47710	411	Spring	Same as UC1	Same as UC1	Same as UC1	Same as UC1
UC9	46,30972	13,47805	342	River	Same as UC1	Same as UC1	Same as UC1	Same as UC1
UC10*	46,30996	13,47887	367	Spring	December 2017, January 2018, March 2018, April 2018, June 2018	–	–	–
UC11	46,29795	13,43901	700	Spring	January 2018, March 2018, April 2018, 2x June 2018, November 2018, December 2018, March 2019	April 2018	December 2017, April 2018	–
UC12	46,30787	13,47196	447	Spring	December 2017, January 2018, March 2018, April 2018, 2x June 2018, October 2018, November 2018, December 2018, March 2019	April 2018	April 2018, October 2018	–
UC13*	46,29218	13,44839	985	Spring	June 2018	–	–	–

Geological setting

The area of the Učja Valley structurally belongs to the Southern Alps and is characterized by Miocene south-directed thrusting (Fig. 2). The major part of the Učja Valley consists of a succession of the Tolmin Nappe, i.e. the lowest of the South-alpine nappes, whereas the highest peaks of the Kanin ridge (northern slopes of Učja Valley) are composed of the structurally higher Krn (Julian) Nappe. Thrust units are further displaced by neotectonic strike-slip faults (Placer, 1999, 2008). The most prominent is the NW-SE oriented Idrija fault zone that generally runs east of the Učja Valley, i.e. along the Soča Valley between the town of Tolmin and the village of Žaga, through the Kanin ridge and enters the Rezija (Resia) Valley near Mt. Skutnik. A few minor faults parallel to the Idrija fault zone run across the Učja Valley. On the southern slopes of the Učja Valley important E-W trending vertical faults divide two slightly diverse stratigraphic successions (Buser, 1987).

The entire area is dominated by a thick succession of Upper Triassic carbonates (Fig. 2). In the Kobariški stol ridge the succession starts with the Norian Hauptdolomit (Main Dolomite) formation passing upward into the Norian-Rhaetian Dachstein Limestone formation, which is covered further by Lower Jurassic platform limestone (Buser, 1986,

1987). Above the stratigraphic gap, the Middle Jurassic limestone breccia and thin-bedded hemipelagic limestone follows and is in turn replaced by Upper Jurassic ammonitico rosso-type limestone of the Prehodavci formation, and finally the end Jurassic-earliest Cretaceous pelagic Biancone Limestone formation. These three units are condensed, only reaching several tens-of-meters in thickness (Šmuc, 2012; Rožič et al., 2022; Vantur, 2023). Above, an end-Cretaceous Upper flyschoid formation is deposited, composed of alternating shale/marl and graded sandstone. At the base of the formation, laterally discontinuous limestone breccia beds are deposited. Similar beds occur also as interbeds within flysch-type deposits (Vantur, 2023).

North of the E-W trending fault, i.e. in the central part of the Učja Valley, only the Norian-Rhaetian is developed as the Hauptdolomit formation. With the erosional contact, it is overlain with Upper Cretaceous deep-marine Volče Limestone formation (resedimented and pelagic limestone) and upwards by an Upper flyschoid formation highly similar to the one described above. The Krn Nappe, which is thrust over the soft bed of the Upper flyschoid formation, is composed almost exclusively of the Norian-Rhaetian Dachstein Limestone formation with only local occurrences of dolomite (Buser, 1986, 1987).

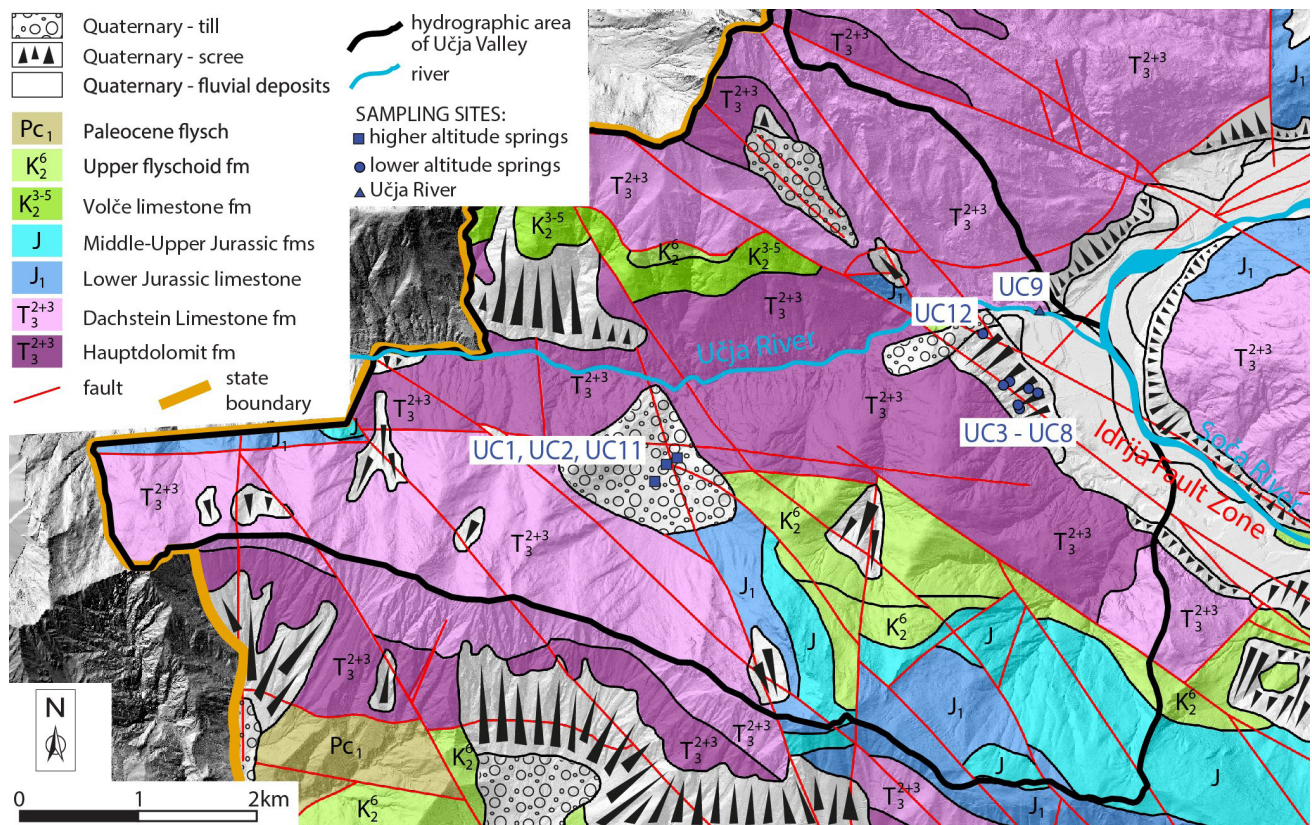


Fig. 2. Geological map of the Učja Valley with sampled springs marked (modified after Buser, 1987; source map in background from ARSO, 2019a; 13.36482° W, 13.50750° E, 46.33294° N, 46.27038° S). The hydrographic area of the Slovenian part of the Učja Valley is presented (ARSO, 2019b).

Materials and methods

In-situ measurements and water sampling were carried out from December 2017 to March 2019. Information about sampling and laboratory analyses for individual sampling sites is presented in Table 1. The missing measurements in the table are the result of the absence of spring water (springs were dry) at the time of sampling.

The measurements of *physico-chemical parameters* (temperature, pH, specific electrical conductivity) were measured on a monthly basis or at least every two months (Table 1) using a WTW Multi 3430 Multiparameter probe (WTW GmbH, Weilheim, Germany). Additionally, the *discharge* of springs was observed and, where possible, measured in the field using a bucket (Fig. 5). The Učja River discharge and the precipitation of the area is measured in the frame of the Slovenian national monitoring system. Data from the gauging hydrological station Žaga – Učja (46.30978° N, 13.47774° E, 342 m a.s.l.) was used to analyse the discharge of the Učja River (ARSO, 2019c). Discharge measurements at the gauging station are monitored every 10 minutes. Data from the Bovec meteorological gauging station (46.33171° N, 13.55382° E, 441 m a.s.l.) was used to analyse the precipitation fluctuations in the area (ARSO, 2023). The amount of precipitation at the gauging station is measured every half hour.

Two rounds of hydrogeochemical analysis and four rounds of isotopic analysis were performed on a seasonal basis (Table 1). Water samples for *hydrogeochemical analysis* were collected in 50 mL in high-density polyethylene HDPE bottles. For cations, the water was further filtered through a 0.45 µm nylon filter and pre-treated with HNO_3^- on site. Analyses were performed in the ActLabs accredited laboratory (Activation Laboratories Ltd., Ancaster, ON, Canada). Cations (major, minor, and trace) were analysed using Inductively Coupled Plasma-Mass Spectrometry (ICP-MS), with some of the major cations (e.g. Ca^{2+} , Mg^{2+}) also analysed using Overrange Inductively Coupled Plasma-Optical Emission Spectrometry (ICP-OES) due to some excessively high concentrations for ICP-MS, and major anions (Br^- , Cl^- , F^- , NO_2^{2-} , NO_3^- , PO_4^{3-} , SO_4^{2-}) were determined using Ion Chromatography (IC). Internal laboratory reference materials and independent quality control with duplicates (one for each measurement campaign) were measured. Detection limits for each element or compound for individual methods are reported on the ActLabs homepage (ActLabs, 2023).

Water samples for oxygen ($\delta^{18}\text{O}$) and hydrogen isotope ($\delta^2\text{H}$) analysis (Table 1) were collected in

50 mL HDPE bottles. The isotopic composition of oxygen and hydrogen was determined at the Jožef Stefan Institute using the $\text{H}_2 - \text{H}_2\text{O}$ (Coplen et al., 1991) and $\text{CO}_2 - \text{H}_2\text{O}$ (Avak & Brand, 1995; Epstein & Mayeda, 1953) equilibration technique on a dual inlet isotope ratio mass spectrometer (Finnigan MAT DELTA plus) with a $\text{CO}_2 - \text{H}_2\text{O}$ and $\text{H}_2 - \text{H}_2\text{O}$ HDOeq 48 automatic equilibrator and a water bath at 18°C (Kanduč et al., 2018a, 2018b, 2018c, 2018d). CO_2 (Messer 4.7) and H_2 (IAEA) gasses were used as working standards for water equilibration. Two laboratory reference materials (LRM), such as W-3896 and W-3871, calibrated to the international VSMOW-SLAP scale, were used to normalize the data. LRM W-45 and commercial reference materials USGS 45, USGS 46, and USGS 47 were used for the independent quality control of measurements as also described in Žvab Rožič et al. (2021). The average repeatability of the samples was 0.02 ‰ for $\delta^{18}\text{O}$ and 0.3 ‰ for $\delta^2\text{H}$, with results expressed as a δ -value per mil (‰).

For the analysis of *total alkalinity (TA)* and *isotope composition of dissolved inorganic carbon ($\delta^{13}\text{C}_{\text{DIC}}$)* (Table 1), water was filtered through a 0.45 µm pore-sized membrane filter. Samples were stored in 30 mL HDPE bottles for TA and 12 in mL Labco glass vials with septum, without headspace, for $\delta^{13}\text{C}_{\text{DIC}}$ analyses. Before TA analyses in the laboratory, pH was measured using a pH meter (Mettler Toledo AG 8603, Schwerzenbach, Switzerland). Total alkalinity (TA) was measured within 24 hr after sampling using the Gran titration method (Gieskes, 1974; Kanduč, 2006) to determine the results with an accuracy of $\pm 1\%$. Approximately 8 g of the water sample was weighed into a plastic container and placed on a magnetic stirrer. A calibrated pH electrode (7.00 and 4.00 ± 0.02) was placed in the sample and the initial pH was recorded. Titration was performed using a CAT titrator (Ingenierbüro CAT, M. Zipperer GmbH Ballrechten-Dottingen, Germany). Reagencon HCl 0.05 N (0.05 M) was used for the titration (Kanduč et al., 2018a, 2018b, 2018c, 2018d). The method is described in detail by Zuliani et al. (2020).

The isotope composition of dissolved inorganic carbon ($\delta^{13}\text{C}_{\text{DIC}}$) was determined according to the Spötl procedure (Spötl, 2005; Kanduč, 2006). Ampoules of saturated phosphoric acid (100–20 µL) were flushed with pure helium, 6 ml of the water sample was added, and headspace CO_2 was measured. The $\delta^{13}\text{C}_{\text{DIC}}$ values were determined using a continuous flow Europa Scientific 20-20 isotope mass spectrometer with the ANCA - TG preparation module (Sercon Limited, Crewe, UK). A standard solution of Na_2CO_3 (Carlo Erba reagents,

Val de Ruil, France) and a Scientific Fischer sample with known $\delta^{13}\text{C}_{\text{DIC}}$ values of $-10.8 \text{ ‰} \pm 0.2 \text{ ‰}$ and $-4.8 \text{ ‰} \pm 0.1 \text{ ‰}$ were used to calibrate the measurements. Messer reference gas with known $\delta^{13}\text{C}_{\text{CO}_2}$ $-35.5 \text{ ‰} \pm 0.2 \text{ ‰}$ was also used. The reference material (Carlo Erba solution) was used to convert the analytical results to the Vienna Pee Dee Belemnite (VPDB) scale. The average sample repeatability was 0.2 ‰ . Two replicates of each sample were measured. Results are expressed as a δ -value per mil (‰) (Kanduč et al., 2018a, 2018b, 2018c, 2018d).

For tritium (${}^3\text{H}$) the water was sampled once in 1 L HDPE bottles. The tritium (${}^3\text{H}$) was measured

in Hydrosys Labor Ltd. in Budapest using a liquid scintillation counting (LSC) TriCarb 3170 TR/SL (PerkinElmer, Waltham, MA, USA). Before analysis, the sample was treated and prepared using electrolytic enrichment. Analysis error was $\pm 0.3 \text{ TU}$, with a detection limit of 3 TU.

Results and discussion

Climate conditions and discharge regime

The wider Učja Valley is located in a transition area between Alpine and Sub-mediterranean climate zones. Winters are long and snowy, with December and January the coldest months (Fig. 3).

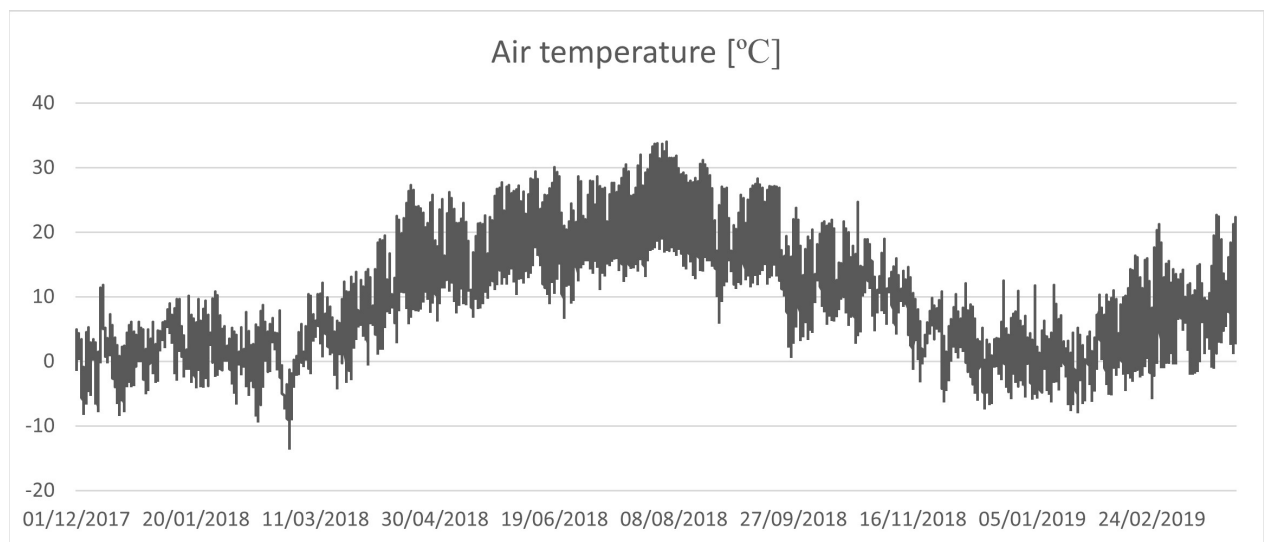


Fig. 3. Air temperature measured at the Bovec meteorological gauging station (ARSO, 2023).

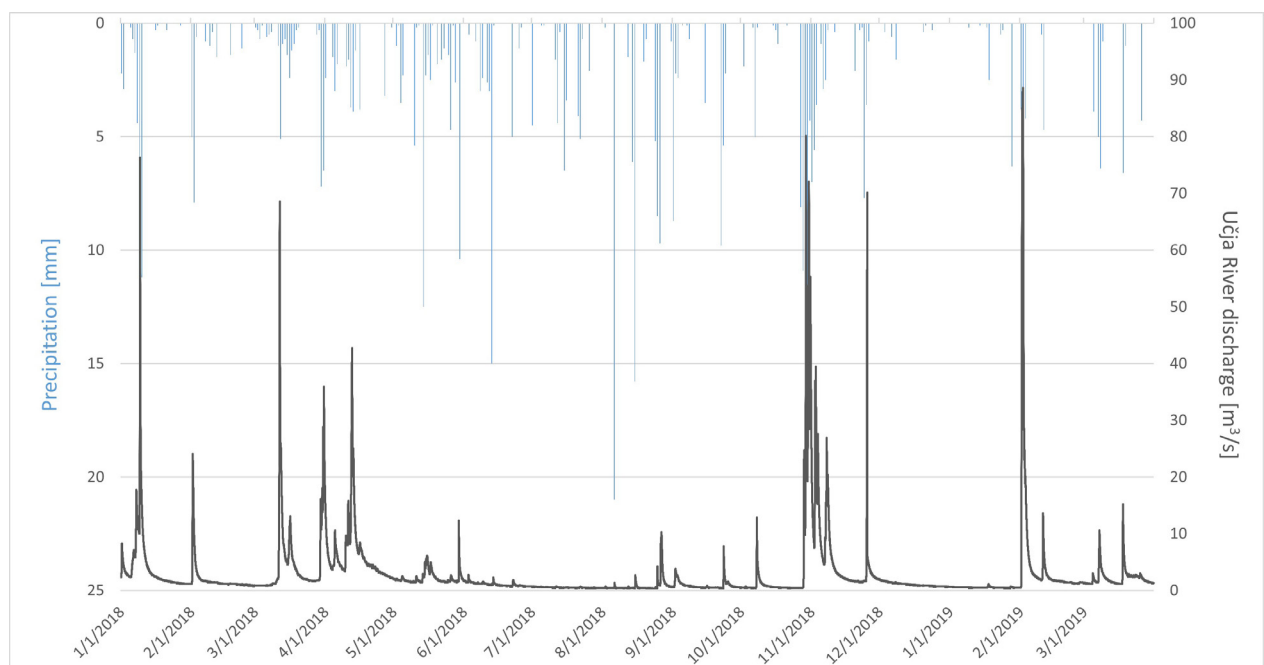


Fig. 4. Precipitation (blue) measured at the Bovec meteorological gauging station (ARSO, 2023) and discharge (dark grey) of the Učja River at the Žaga – Učja hydrological gauging station (ARSO, 2019c) for 2018.

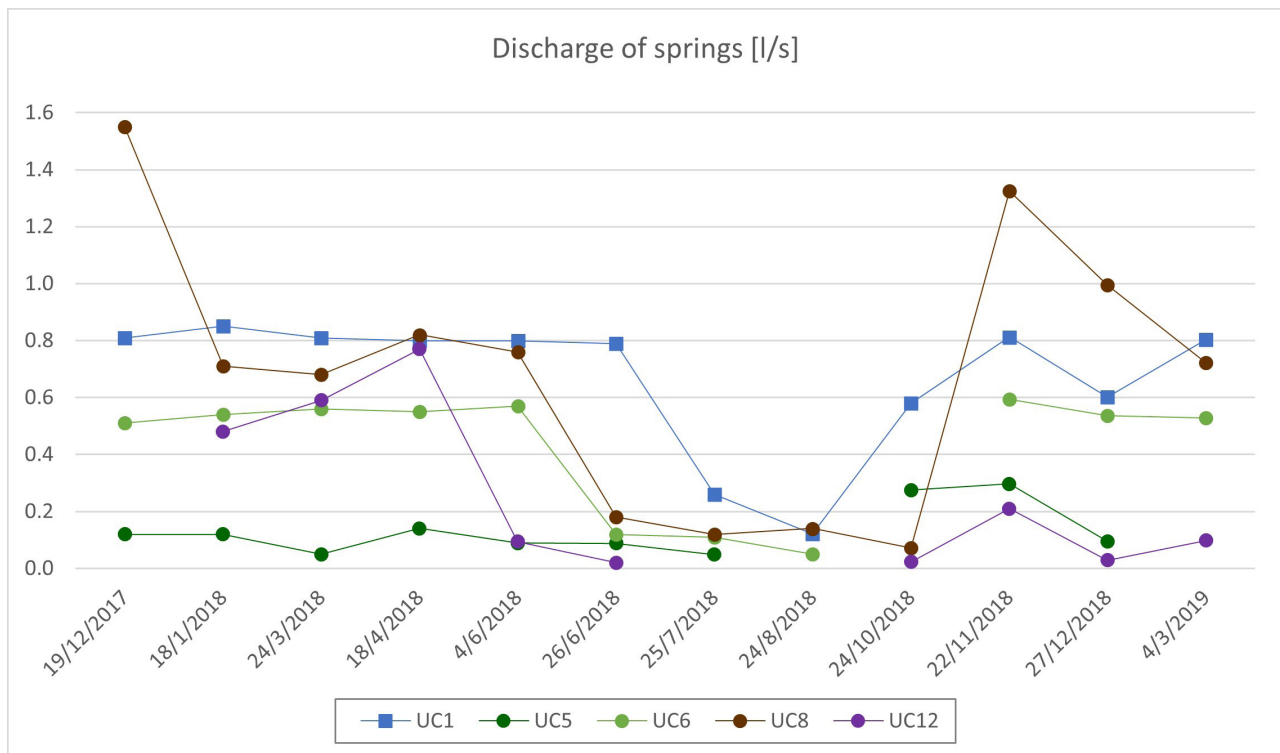


Fig. 5. Discharge of springs where taking of measurements was possible. Missing measurements are the result of the absence of spring water (springs were dry) at the time of sampling.

Summers are moderately warm (around 20 °C) with rare air temperatures above 30 °C (Fig. 3). Higher amounts of precipitation fall in autumn and spring, and lower amounts in winter and summer (local showers) (Fig. 4). Precipitation in the region (measured at Bovec meteorological gauging station; ARSO, 2023) and at the Učja River discharge (measured at the Žaga – Učja hydrological gauging station; ARSO, 2019c) is plotted in Fig. 4. The most pronounced increase of Učja River discharge in spring (March-April) and autumn (November) is in accordance with the mixed snow/rainfall regime. Lower discharges are recorded in winter and especially during summer, and the highest discharges during the spring snowmelt and with autumn precipitation. A quick and intense response in the discharge of the river is also observed twice in winter. During the summer, the response of river discharge to precipitation is not so intense, which may be the result of short and local summer showers (the Bovec gauging station is located some 10s of km northwest in the Soča Valley) and more intense evapotranspiration. Similar trends are also seen in the measured springs, with two periods of higher water discharge in the spring and autumn, and low or even no discharge in the summer (Fig. 5).

Physico-Chemical Parameters of Učja aquifer

Measured physico-chemical parameters are presented in Figures 6 and 7. The entire range of results are presented in common database in Pangaea repository (Žvab Rožič et al., 2024). The groundwater temperature of the springs and water from Učja River (Fig. 6) generally follow the fluctuations in air temperature (Fig. 3), and therefore reflect the significant seasonal temperature conditions of the area. The highest water temperatures were measured in summer (max 18.7 °C at UC6 in July 2018) and the lowest in winter (min 3.6 °C at UC9 in December 2017 and 2018). More noticeable changes are recorded at the springs where the watershed area of the springs is smaller and significantly lower discharges were observed in the summer months. The quick response of groundwater temperature to fluctuations in air temperature is also the result of water heating in the shallow or surface pipelines and reservoirs from which the water was sampled. The springs at higher altitudes (UC1, UC2, UC11; Fig. 1, Table 1) show less markable temperature fluctuations. This may be the result of higher elevations and the shadier locations of spring areas in the valley and probably deeper local recharge areas. The temperature trend of these springs is also less than entirely clear, because the temperature was not measured at some sampling sites (UC2, UC11) due to a lack of water in the summer months.

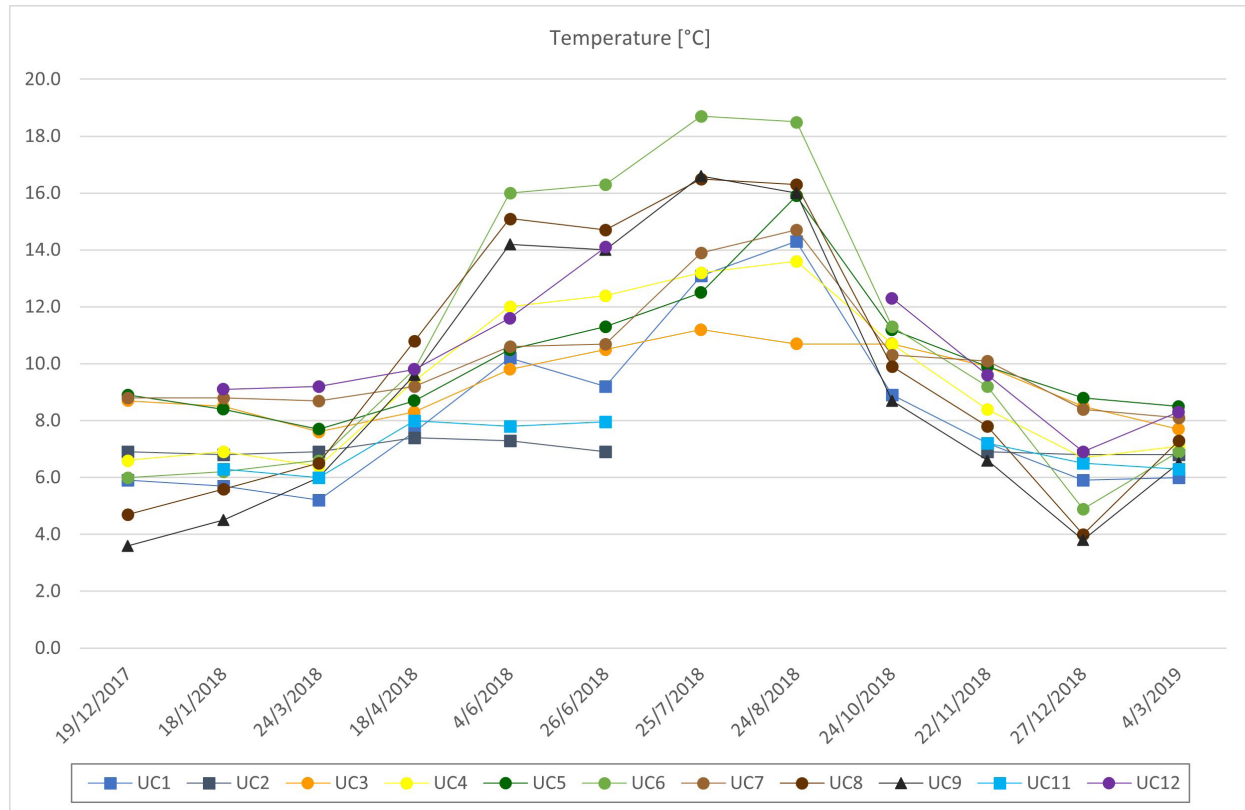


Fig. 6. Measured water temperatures (°C) at sampling sites in the Učja Valley.

The specific electrical conductivity (EC) of sampling water ranges from 186 to 438 $\mu\text{S}/\text{cm}$ (average 266 $\mu\text{S}/\text{cm}$) (Fig. 7). The EC values indicate a highly permeable carbonate aquifer with a low resistance time as also described in Torkar & Brenčič (2015). The highest EC was observed at

sampling site UC12 (max 438 $\mu\text{S}/\text{cm}$) and the lowest at sampling site UC2 (min 186 $\mu\text{S}/\text{cm}$). Lower EC values were generally measured in spring waters at higher altitudes (UC1, UC2, UC11 – marked with squares; Fig.1, Table 1) and in the water from the Učja River (UC9 – marked with

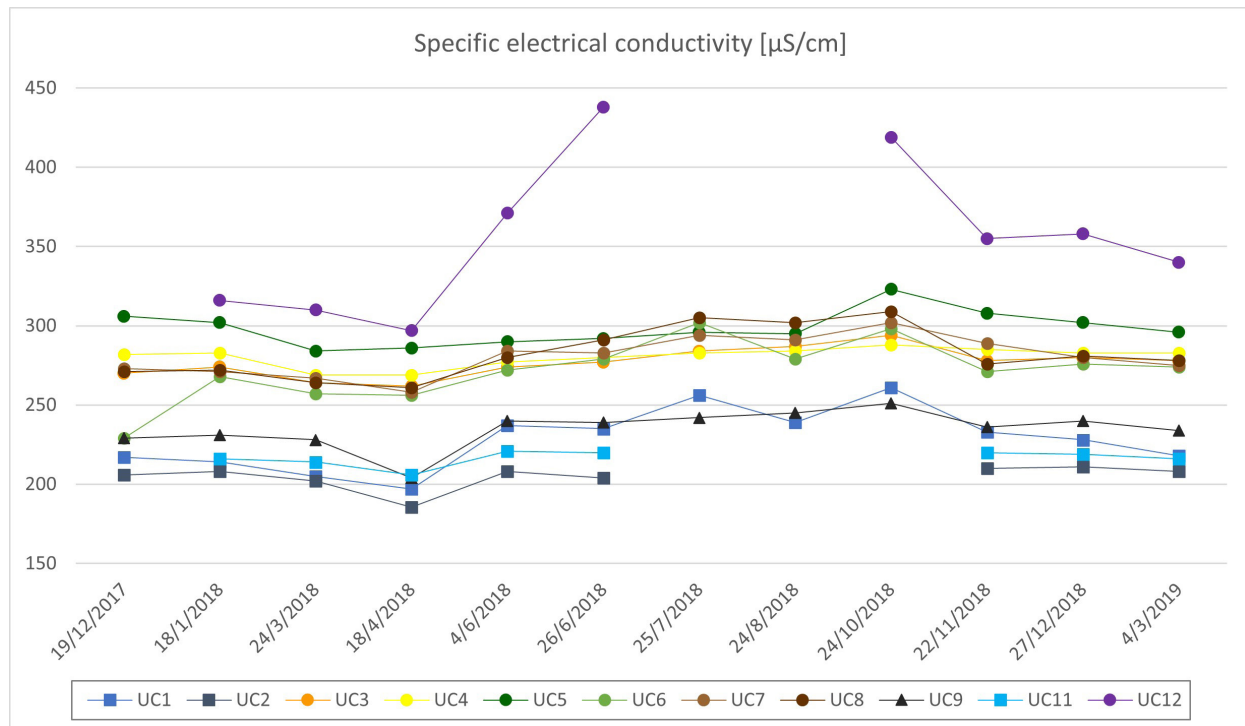


Fig. 7. Field measurements of specific electrical conductivity ($\mu\text{S}/\text{cm}$) at sampling sites in the Učja Valley.

a triangle). The EC inversely related to elevation was also described for fractured dolomite aquifers in central Slovenia (Verbovšek & Kanduč, 2016). Slight fluctuations in EC values at all sampling sites is observed throughout the year. Rather lower EC values were recorded in April-March and November-December, and related to snowmelt in spring and rainy periods in autumn (Fig. 4), and most likely also to lower evapotranspiration. A more prominent EC fluctuation is noticeable at the UC12 sampling site, with the lowest values in the spring and a marked decrease in November, which is associated with rainy periods (Fig. 4), and the highest in the summer before the spring dries up. The spring is also located within the tectonic zone of the Idrja fault (Čar & Pišljar, 1991, 1993; Vrabc, 2012), where inflow and mixing with deeper waters with higher EC could occur. However, more precise explanations and processes in the aquifer remain to be developed and investigated.

The pH of sampled water varied from 7.60 to 8.96, with an average value of 8.12, and reflects the common characteristics of a carbonate aquifer, with no differences between sampling sites. The pH values are comparable with groundwater samples from fractured dolomite aquifers in central Slovenia (Verbovšek & Kanduč, 2016).

Hydrogeochemistry of the Učja aquifer

The geochemical results for the Učja Valley aquifer are part of a common database in Pangaea repository (Žvab Rožič et al., 2024). The major composition of groundwater from the Učja aquifer does not change between the two sampling campaigns (December 2017 and April 2018) and is dominated by HCO_3^- , Ca^{2+} , and Mg^{2+} ions (Fig. 8), which is characteristic for carbonate types of waters. All samples belong to the Ca-Mg-HCO₃ facies with low K^+ , Na^+ , Cl^- , NO_3^- and SO_4^{2-} content (Jäckli, 1970). Comparable results are also described for karstic

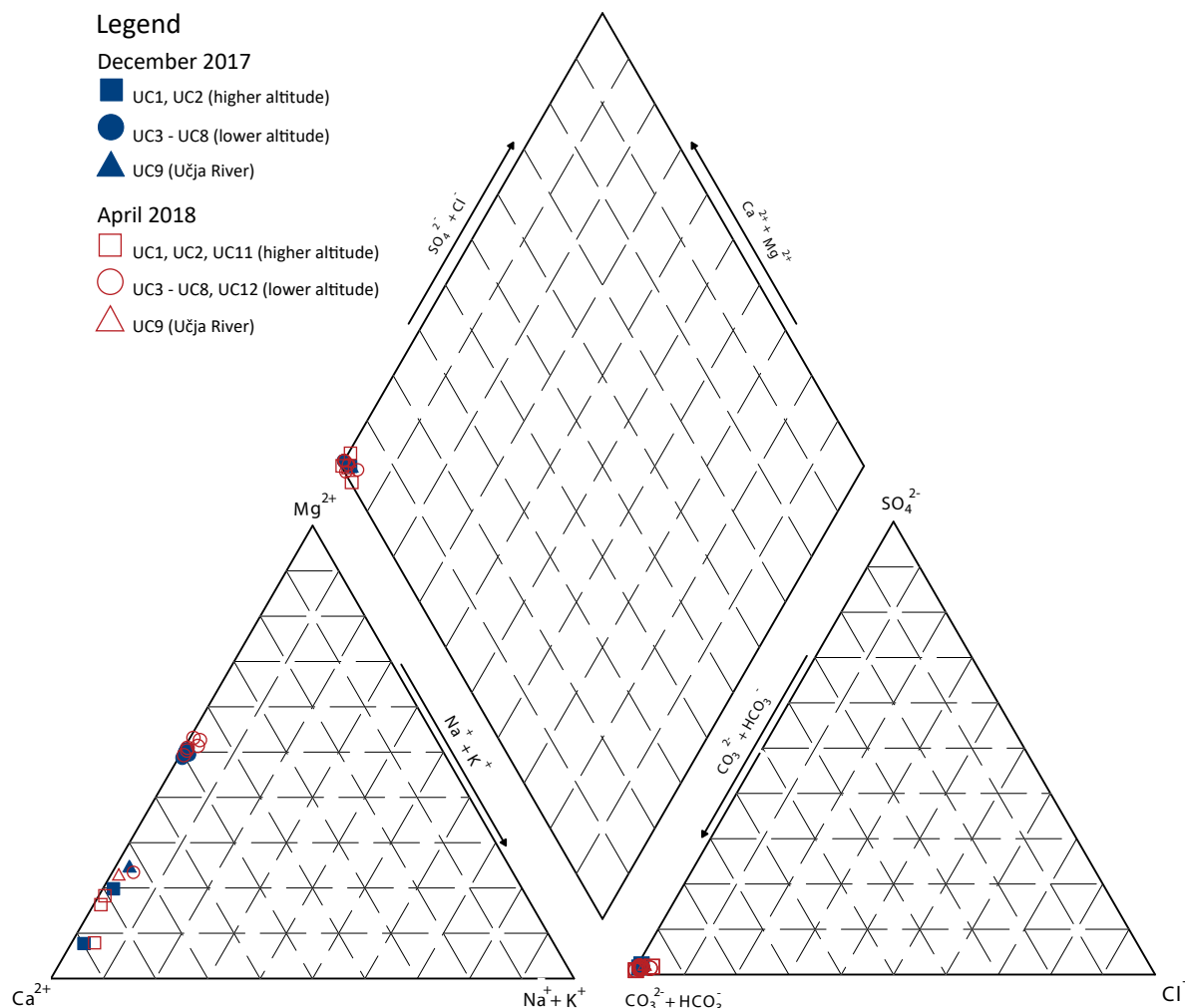


Fig. 8. Piper plot diagram of the Učja Valley water samples.

and fractured aquifers in Central Slovenia (Verbovšek & Kanduč, 2016) and for the Triglavská Bistrica River in Northern Slovenia (Serianz et al., 2021). Total alkalinity ranged from 1.95 mM (UC1) to 3.40 mM (UC5), and concentrations of Ca^{2+} and Mg^{2+} from 27.0 mg/L (UC6) to 47.9 mg/L (UC12) and from 1.96 mg/L (UC1) to 20.9 mg/L (UC5), respectively. The $\text{Mg}^{2+}/\text{Ca}^{2+}$ molar ratio, which indicates the relative contribution of dolomite and calcite to the intensity of carbonate weathering in the groundwater, differs significantly between sampling sites: group I (UC1, UC2 and UC11) exhibits ratios ranging from 0.08 to 0.25 and group II (UC3-UC8) ratios ranging from 1.00 to 1.15. Sampling sites UC9 (Učja River) and UC12 show a $\text{Mg}^{2+}/\text{Ca}^{2+}$ molar ratio of 0.32. The same grouping is also visible on the Piper plot diagram (Fig. 8). The $\text{Mg}^{2+}/\text{Ca}^{2+}$ molar ratios are slightly higher than those found in descriptions of fractured dolomite aquifers in central Slovenia (Verbovšek & Kanduč, 2016). The results can be explained by the geological conditions of the area (Fig. 2). The springs from group II indicate that dolomite (the main rock in the catchment area) weathering is the source of the major solutes within the aquifer, while for group I the Ca^{2+} contribution from limestone layers (limestone breccia or thick platform limestone succession, as both are located south of the E-W trending fault) prevail (Fig. 2).

Isotopic characteristics of the Učja aquifer

The isotopic results for the Učja Valley aquifer are presented entirely in database in Pangaea repository (Žvab Rožič et al., 2024). The $\delta^{18}\text{O}$ and $\delta^2\text{H}$ values for the groundwater from the Učja Valley vary from $-8.7\text{\textperthousand}$ to $-7.4\text{\textperthousand}$ (average $-8.0\text{\textperthousand}$) and from $-54.9\text{\textperthousand}$ to $-45.1\text{\textperthousand}$ (average $-49.5\text{\textperthousand}$), respectively. The surface water of the Učja River has $\delta^{18}\text{O}$ values from $-8.7\text{\textperthousand}$ to $-8.1\text{\textperthousand}$ (average $-8.4\text{\textperthousand}$) and $\delta^2\text{H}$ values from $-55.3\text{\textperthousand}$ to $-50.4\text{\textperthousand}$ (average $-52.6\text{\textperthousand}$). $\delta^{18}\text{O}$ and $\delta^2\text{H}$ values vary seasonally at all sampling sites (Fig. 9). In general, the lowest values were measured during the spring sampling campaign (average $-8.2\text{\textperthousand}$ for $\delta^{18}\text{O}$ and $-51.8\text{\textperthousand}$ for $\delta^2\text{H}$) and the highest during the winter sampling campaign (average $-7.8\text{\textperthousand}$ for $\delta^{18}\text{O}$ and $-48.0\text{\textperthousand}$ for $\delta^2\text{H}$). Differences in the $\delta^{18}\text{O}$ values are noticeable between sampling sites (Fig. 9). Higher $\delta^{18}\text{O}$ values were recorded in springs UC1 and UC2 (from 0.6 to 0.7‰) and the Učja River (0.6‰), while in the remaining springs (UC3-UC8, UC12) the amplitudes are lower (from 0.3 to 0.5‰). This may indicate rather longer residence times for the springs at lower altitudes (UC3-UC8, UC12) due to the dolomite rocks in the watershed (Torkar et al., 2016).

The results of $\delta^{18}\text{O}$ and $\delta^2\text{H}$ measurements of Učja groundwater and the Učja River are presented in Figure 10. For comparison, the results of selected previous studies from Northern and Central Slovenia (Kanduč et al., 2012; Zega et al., 2015; Verbovšek & Kanduč, 2016; Torkar et al., 2016; Serianz et al., 2021) are presented together with selected water lines: global meteoric water line (GMWL; $\delta^2\text{H} = 8 \times \delta^{18}\text{O} + 1\text{\textperthousand}$; Craig, 1961), local meteoric water line for Kredarica (LMWL_K ; $\delta^2\text{H} = 8.42 (\pm 0.19) \times \delta^{18}\text{O} + 18.98 (\pm 2.09)$; SLONIP, 2023), local meteoric water line for Zgornja Radovna (LMWL_{ZR} ; $\delta^2\text{H} = 7.98 (\pm 0.13) \times \delta^{18}\text{O} + 11.13 (\pm 1.21)$; SLONIP, 2023), and local meteoric water line for Portorož (LMWL_P ; $\delta^2\text{H} = 8.09 (\pm 0.2) \times \delta^{18}\text{O} + 9.99 (\pm 1.34)$; SLONIP, 2023). For Local meteoric lines the precipitated weighted reduced major axis regression (PWRMA LMWL) was used (Vreča et al., 2022; SLONIP, 2023). The isotopic composition of the groundwater from the Učja aquifer and the Učja River is similar to the isotopic composition of the Žveplenica sulfur karst spring (Zega et al., 2015), which is influenced by similar climate conditions. If we compare the results with the springs from Northern Slovenia (Kanduč et al., 2012), from karst and fractured aquifers in Central Slovenia (Verbovšek & Kanduč, 2016), Radovna Valley (Torkar et al., 2016), and Triglavská Bistrica (Serianz et al., 2021) (Fig. 10) the groundwater from the Učja Valley is enriched with heavier isotopes (i.e. ^2H and ^{18}O). This is attributed to the proximity of the Mediterranean climate, and the continental isotopic effect is reflected in precipitation (Kern et al., 2020; Vreča & Malenšek, 2016). The results from the Učja Valley show that all water samples are above the GMWL, LMWL_{ZR} and LMWL_P , plotted between local meteoric water lines for Zgornja Radovna LMWL_{ZR} and especially for Kredarica LMWL_K . As already described in some previous studies (Vreča et al., 2006; Torkat et al., 2016), the results from the Učja Valley suggest a complex mixing of maritime and continental air masses.

The $\delta^{18}\text{O}$ and $\delta^2\text{H}$ values in the groundwater of the Učja Valley reveal isotopic depletion (altitude isotopic effect) in the sampling locations (UC1, UC2, UC11) at higher altitudes (app. 720 m asl) compared to the locations (UC3-UC8, UC12) at lower altitudes (app. 440 m asl). In view of the difference between the UC1 (758 m asl) and UC7 (389 m asl) sampling sites, the average altitude effect for the Učja Valley is 0.11‰ per 100 m for $\delta^{18}\text{O}$ (the same as for the Radovna Valley; Torkar et al., 2016) and 0.45‰ per 100 m for $\delta^2\text{H}$. The altitude isotopic effect varies between seasons.

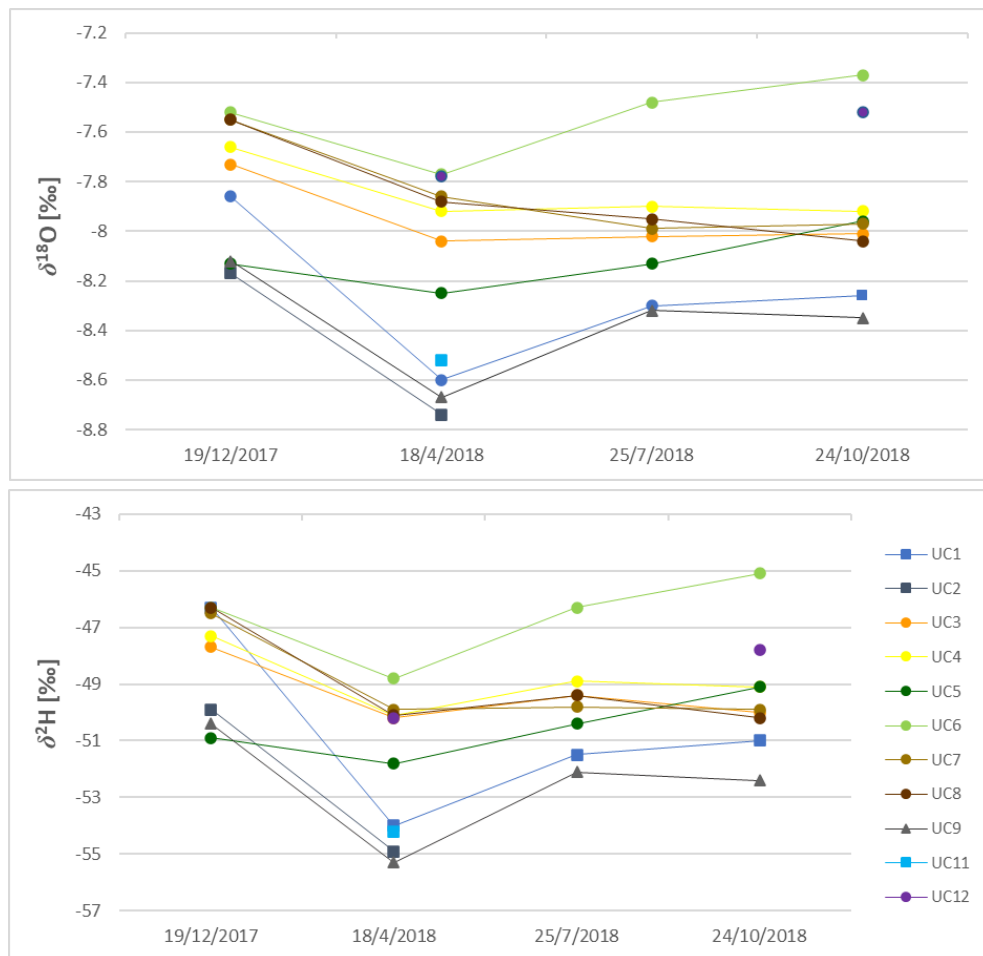


Fig. 9. Time series of isotopic compositions of $\delta^{18}\text{O}$ and $\delta^2\text{H}$ in groundwater of the Učja aquifer and the Učja River.

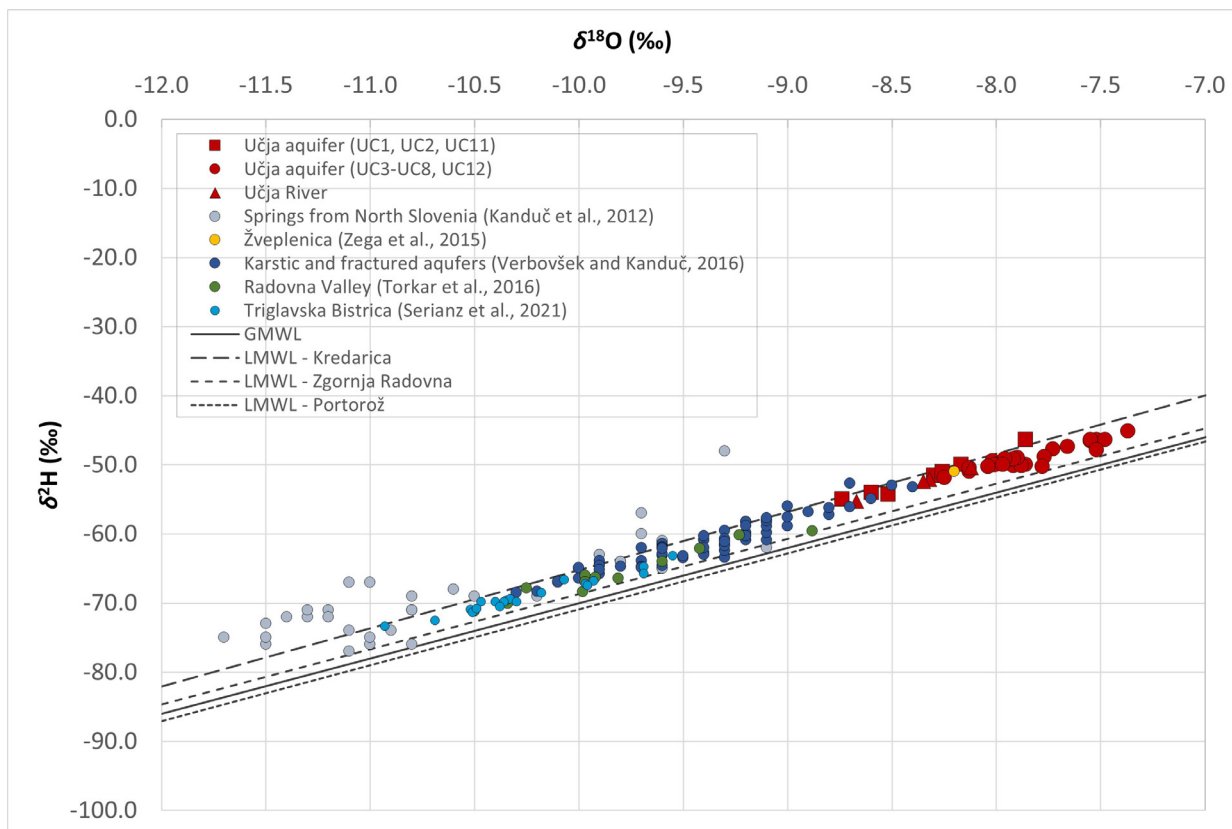


Fig. 10. Plot of $\delta^{18}\text{O}$ versus $\delta^2\text{H}$ values for groundwater of the Učja aquifer (groundwater) and the Učja River, the results from selected previous studies from Northern and Central Slovenia (Kanduč et al., 2012; Zega et al., 2015; Verbovšek & Kanduč, 2016; Torkar et al., 2016; Serianz et al., 2021), together with the global meteoric water line (GMWL) and the local meteoric water lines from Kredarica (LMWL_K), Zgornja Radovna (LMWL_{ZR}) and Portorož (LMWL_p) (Vreča et al., 2022; SLONIP, 2023).

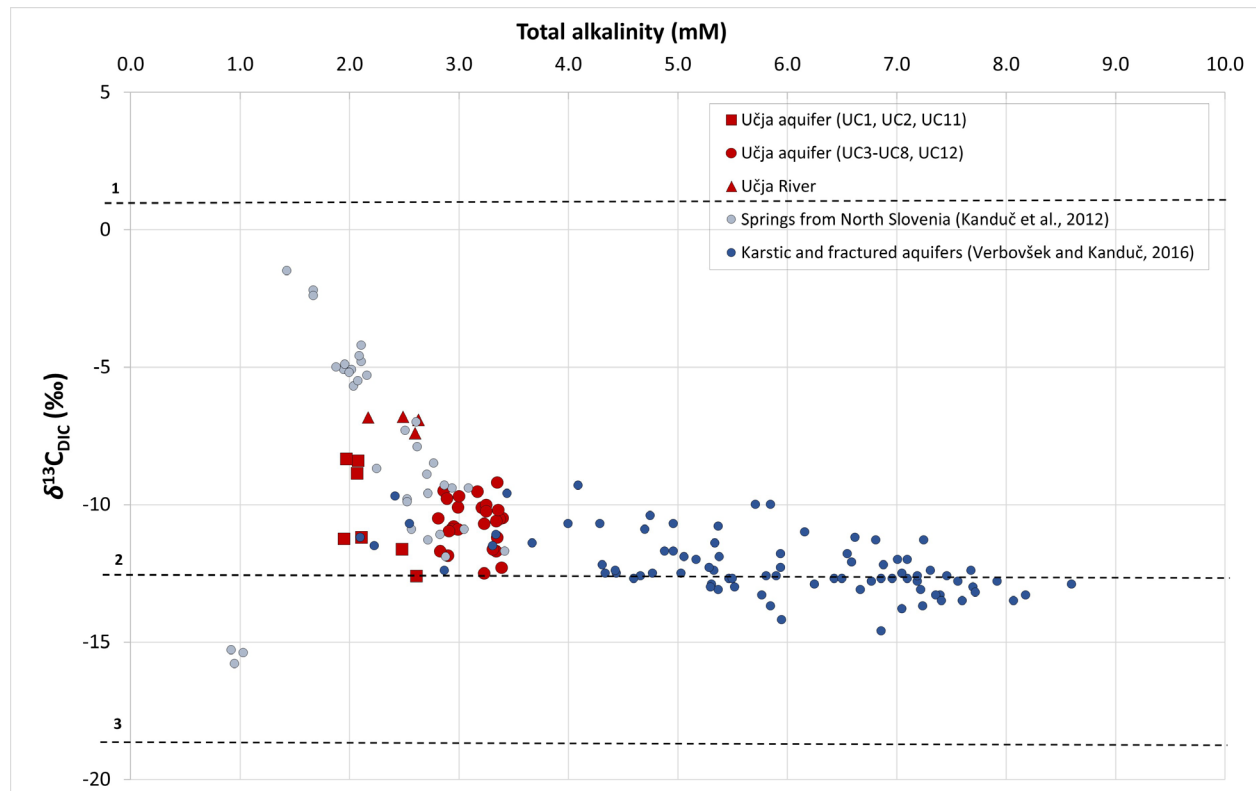


Fig. 11. Total alkalinity versus isotopic composition of dissolved inorganic carbon ($\delta^{13}\text{C}_{\text{DIC}}$) of groundwater from the Učja aquifer and the Učja River, together with groundwater from northern Slovenia (Kanduč et al., 2012) and karstic and fractured aquifers from Central Slovenia (Verbovšek & Kanduč, 2016). See the explanation of dotted lines 1, 2, and 3 in Verbovšek & Kanduč (2016).

The least prominent altitude effect was found in winter (0.08 ‰ per 100 m for $\delta^{18}\text{O}$ and 0.05 ‰ per 100 m for $\delta^2\text{H}$), and the highest in spring (0.2 ‰ per 100 m for $\delta^{18}\text{O}$ and 1.11 ‰ per 100 m for $\delta^2\text{H}$). Seasonal differences in altitude effect were also described in precipitation across the Adriatic–Pannonian region (Kern et al., 2020).

The $\delta^{13}\text{C}_{\text{DIC}}$ values for the groundwater of the Učja Valley vary from –12.6 ‰ to –8.3 ‰ (average –10.7 ‰) and alkalinity from 2.0 mM and 3.4 mM (average 2.9 mM). The surface water of the Učja River has higher $\delta^{13}\text{C}_{\text{DIC}}$ values, from –7.4 ‰ to –6.8 ‰ (average –7.0 ‰), while the alkalinity is slightly lower than in groundwater, from 2.2 mM and 2.6 mM (average 2.5 mM). Seasonal variations of $\delta^{13}\text{C}_{\text{DIC}}$ are generally observed with slightly higher values in the summer and noticeably lower values in the winter. Similar trends were described for the Radovna Valley (Torkar et al., 2016). The geochemical processes influencing the $\delta^{13}\text{C}_{\text{DIC}}$ values in groundwater are presented in Figure 11 and described in Kanduč et al. (2012, 2016). Geochemical processes were calculated as follows: line1 (with a value of +1.2 ‰) – dissolution of carbonates according to the average $\delta^{13}\text{C}_{\text{CaCO}_3}$ value – predicted value (Kanduč et al., 2012) resulting in 1 ‰ enrichment in ^{12}C in

DIC (Romanek et al., 1992), line 2 (with a value of –12.5 ‰) – nonequilibrium carbonate dissolution by carbonic acid produced from soil zone CO_2 (Kanduč et al., 2012; Verbovšek & Kanduč, 2016), and line 3 (with a value of –18.2 ‰) open system equilibration of DIC with soil CO_2 originating from the degradation of organic matter with $\delta^{13}\text{C}_{\text{soil}} = -27.2$ ‰ (Kanduč et al., 2012; Verbovšek & Kanduč, 2016) (Fig. 8). There are a number of possible sources of carbon. All $\delta^{13}\text{C}_{\text{DIC}}$ values (Fig. 11) indicate that the groundwater from the Učja Valley is a resulting mixture of the dissolution of carbonates and the degradation of organic matter. The results are comparable with groundwater samples from springs of Northern Slovenia (Kanduč et al., 2012), individual karstic and fractured dolomite aquifers in Central Slovenia (Verbovšek & Kanduč, 2016), the Triassic aquifers of the Velenje Basin (Kanduč et al., 2016) and $\delta^{13}\text{C}_{\text{DIC}}$ measurements from the Radovna Valley (Torkar et al., 2016).

Tritium (^3H) concentrations in the groundwater from the Učja aquifer ranged from 3.0 to 4.5 TU (average 3.5 TU), which is close to the detection limit of the method. More measurements would be needed to understand the age of the water in more detail, and should be further investigated in the future.

Conclusions

The groundwater from the Učja aquifer, a cross-border karst aquifer in NW Slovenia, was characterised using geochemical and isotopic data. Analysis was carried out on water samples from 10 springs (groundwater) and on (surface) water from the Učja River. The measurements were performed over the period December 2017 to March 2019.

The water discharge and physico-chemical parameters of the Učja groundwater and the Učja River reflect the climate that is characteristic of the area. The mixed snow/rainfall regime is characteristic for the Učja Valley. Lower discharges of the Učja River are recorded in winter and especially during summer, with the highest discharges seen during the spring snowmelt (March-April) and in autumnal precipitation (November). Similar trends are also seen in groundwater from the area (spring water measurements), with two periods of higher water discharge in the spring and autumn, and low or no discharge (dry springs) in the summer. The temperatures of both the groundwater and the Učja River are lower in winter (min 3.6 °C) and higher in summer (max 18.7 °C). The EC values indicate a highly permeable carbonate aquifer with a low residence time. The fluctuation of specific electrical conductivity at all sampling sites throughout the year reflects depletions during the dry season and higher values in spring (March-April) and autumn (November-December) and are related to periods of snow and rain. Slight differences in physico-chemical parameters were observed between sampling sites of higher and lower elevations.

All water samples indicate the same Ca-Mg-HCO₃ facies, with the most abundant ions Ca²⁺, Mg²⁺, and HCO₃⁻, and low concentrations of K⁺, Na⁺, Cl⁻, NO₃⁻, and SO₄²⁺. Differences in concentrations of Ca²⁺ and Mg²⁺ and of the Mg²⁺/Ca²⁺ molar ratio between the two groups of springs are observed. The limestone defines the recharge area for the first group of springs (UC1, UC2, UC11), while the dolomite prevails in the second group of springs (UC3-UC8, UC12). The Mg²⁺/Ca²⁺ molar ratios for UC9 (Učja River) and UC12 (within the Idrija Fault zone) are rather higher than for first group of springs. The pH values (average 8.12) also indicate the rather alkaline waters characteristic of carbonate aquifers.

The hydrogen ($\delta^2\text{H}$) and oxygen ($\delta^{18}\text{O}$) isotope values suggest the complex mixing of maritime and continental air masses. The isotopic composition of Učja groundwater reflects its proximity to the Mediterranean climate and to some degree the influence of continental precipitation as well.

Minor depletions in the altitude isotopic effect are noted (0.11 ‰ per 100 m for $\delta^{18}\text{O}$ and 0.45 ‰ per 100 m for $\delta^2\text{H}$) at sampling locations from springs at higher altitudes (UC1, UC2, UC11) compared to those springs at lower altitudes (UC3-UC8, UC12). The altitude isotopic effect varies between seasons and is most prominent in spring. The $\delta^{13}\text{C}_{\text{DIC}}$ values indicate the dissolution of carbonates and the degradation of organic matter.

The results contribute to a considerably better understanding of the aquifer recharge area, the origin of the water, and groundwater dynamics, and provide us with an important basis for a comprehensive interpretation of a potential natural water resource in the future.

Acknowledgments

The research was financially supported by the Slovenian Research Agency (ARRS) within the postdoctoral project Z1-8154 (Evaluation of Učja Valley karstic aquifer as a potential source of drinking water (NW Slovenia) and research programme P1-0195 (Geoenvironment and geomaterials). The results of this study have been discussed within the COST Action: "WATSON" CA19120 (www.cost.eu). Special thanks to all my colleagues for their assistance in the fieldwork performed (A. Grkman, B. Miklavič, D. Rehakova, B. Rožič, T. Verbovšek), to M. Švob, and B. Rožič for their preparation of the cartographic images, and to Jeff Bickert for his copy edit of the text.

References

- ActLabs, 2023: Tools for buried deposit targets, Hydrogeochemistry. Available online: <https://actlabs.com/geochemistry/tools-for-buried-deposit-targets/hydrogeochemistry/> (20. 10. 2023).
- Aggarwal, P.K., Froehlich, K.F. & Gat, J.R. 2005: Isotopes in the Water Cycle. Springer: Dordrecht, The Netherlands: 382 p.
- Allshorn, S.J.L., Bottrell, S.H., West, L.J. & Odling, N.E. 2007: Rapid karstic bypass flow in the unsaturated zone of the Yorkshire chalk aquifer and implications for contaminant transport. In: Parise, M. & Gunn, J. (eds.): Natural and Anthropogenic Hazards in Karst Areas: Recognition, Analysis and Mitigation. Special Publications. Geological Society, London, UK: 111 p.
- ARSO 2019a: Agency of Republic of Slovenia for Environment. Atlas okolja. Available online: <https://gis.arso.gov.si/atlasokolja/> (20. 10. 2023)

- ARSO 2019b: Agency of Republic of Slovenia for Environment. Archive of hydrological data. Available online: <http://www.arso.gov.si/vode/podatki/> (20. 10. 2023)
- ARSO 2019c: Agency of Republic of Slovenia for Environment. Archive of meteorological data. Available online: <https://gis.arso.gov.si/geoportal/> (20. 10. 2023)
- ARSO 2023: Agency of Republic of Slovenia for Environment. Archive of meteorological data. Precipitation. Available online: <https://meteo.arso.gov.si/met/sl/archive/> (20. 10. 2023)
- Avak, H. & Brand, W.A. 1995: The Finning MAT HDO-Equilibration - A fully automated H_2O /gas phase equilibration system for hydrogen and oxygen isotope analyses. Thermo Electronic Corporation, Application News, 11: 1–13.
- Brenčič, M., Premru, U., Toman, M., Trček, B., Bole, Z., Kralj, A., Tršič, N., Andjelov, M. & Marinko, M. 2001: Raziskave ležišč pitne vode v območju Posočja. Zaključno poročilo o rezultatih opravljenega raziskovalnega dela na projektu v okviru ciljnih raziskovalnih programov (CRP). Geološki zavod Slovenije: 72 p.
- Bullen, T.D. & Kendall, C. 1998: Chapter 18-tracing of weathering reactions and water flowpaths: multi-isotope approach. In: McDonnell, C.K.J. (ed.): Isotope tracers in catchment hydrology. Elsevier, Amsterdam: 611–646. <https://doi.org/10.1016/B978-0-444-81546-0.50025-2>
- Buser, S. 1986: Osnovna geološka karta SFRJ 1:100.000. Tolmač lista Tolmin in Videm (Udine). Zvezni geološki zavod Jugoslavije, Beograd: 103 p.
- Buser, S. 1987: Osnovna geološka karta SFRJ 1:100.000. List Tolmin in Videm (Udine). Zvezni geološki zavod Jugoslavije, Beograd.
- Calligaris, C., Mezga, K., Slepko, F.F., Urbanc, J. & Zini, L. 2018: Groundwater characterization by means of conservative ($\delta^{18}O$ and δ^2H) and non-conservative ($^{87}Sr/^{86}Sr$) isotopic values: the Classical Karst region aquifer case (Italy–Slovenia). Geosciences, 8: 321. <https://doi.org/10.3390/geosciences8090321>
- Cartwright, I., Weaver, T.R., Cendón, D.I., Keith Fifield, L., Tweed, S.O., Petrides, B. & Swane, I. 2012: Constraining groundwater flow, residence times, inter-aquifer mixing, and aquifer properties using environmental isotopes in the southeast Murray Basin, Australia. Applied Geochemistry, 27: 1698–1709. <https://doi.org/10.1016/j.apgeochem.2012.02.006>
- Clarke, I.D. & Fritz, P. 1997: Environmental Isotopes in Hydrogeology. Lewis, New York: 328 p.
- Coplen, T.B., Wildman, J.D. & Chen, J. 1991: Improvements in the gaseous hydrogen-water equilibration technique for hydrogen isotope-ratio analysis. Analytical Chemistry, 63/9: 910–912. <https://doi.org/10.1021/ac00009a014>
- Craig, H. 1961: Isotopic variations in meteoric waters science. Science, 133/3465: 1702–1703. <https://doi.org/10.1126/science.133.3465.1702>
- Čar, J. & Pišljar, M. 1991: Geološke in hidrogeološke posebnosti doline reke Učje. Idrija: 37 p.
- Čar, J. & Pišljar, M. 1993: Presek Idrijskega preloma in potek doline Učje glede na prelomne strukture. Rudarsko metalurški zbornik (RMZ), 40/1-2: 79–101.
- Dansgaard, W. 1964: Stable isotopes in precipitation. Tellus, 16: 436–468.
- Epstein, S. & Mayeda, T. 1953: Variation of O^{18} content of waters from natural sources. Geochimica et Cosmochimica Acta, 4/5: 213–224. [https://doi.org/10.1016/0016-7037\(53\)90051-9](https://doi.org/10.1016/0016-7037(53)90051-9)
- Ford, D. & Williams, P.W. 2007: Karst hydrogeology and geomorphology, Rev. ed. John Wiley & Sons Ltd, Chichester: 562 p.
- Gams, I. 1974: Kras: zgodovinski, naravoslovni in geografski oris. Slovenska matica, Ljubljana: 358 p.
- Gams, I. 2004: Kras v Sloveniji v prostoru in času. Založba ZRC, Ljubljana, Slovenia.
- Gibbs, R.J. 1970: Mechanisms controlling world water chemistry. Science, 170: 1088–1090.
- Gieskes, J.M. 1974: The alkalinity - total carbon dioxide system in seawater. In: Goldberg, E.D. (ed.): The Sea: Ideas and Observations on Progress in the Study of the Sea. Volume 5: Marine Chemistry. Wiley, New York, N.Y., pp. 123–152.
- Glynn, P. & Plummer, L.N. 2005: Geochemistry and the understanding of ground-water systems. Hydrogeology Journal, 13: 263–287. <https://doi.org/10.1007/s10040-004-0429-y>
- Gostinčar, P. & Stepišnik, U. 2023: Extent and spatial distribution of karst in Slovenia. Acta geographica Slovenia, 63/1: 111–129. <https://doi.org/10.3986/AGS.11679>
- Janež, J. 2002. Veliki kraški izviri v zgornjem Posočju. Geologija, 45/2: 393–400. <https://doi.org/10.5474/geologija.2002.038>
- Jäckli, H. 1970: Kriterien zur Klassifikation von Grundwasservorkommen. Eclogae Geologicae Helvetiae, 63/2, 389–434.
- Kanduč, T. 2006. Hidrogeokemične značilnosti in kroženje ogljika v porečju reke Save v Sloveniji.

- Doktorska disertacija. Univerza v Ljubljani, Naravoslovnotehniška fakulteta, Ljubljana.
- Kanduč, T., Mori, N., Kocman, D., Stibilj, V. & Grassa, F. 2012: Hydrogeochemistry of Alpine springs from North Slovenia: Insights from stable isotopes. *Chemical Geology*, 300-301: 40–54. <https://doi.org/10.1016/j.chemgeo.2012.01.012>
- Kanduč, T., Mori, N., Koceli, A. & Verbovšek, T. 2016: Hydrogeochemistry and isotopic geochemistry of the Velenje basin groundwater. *Geologija*, 51/1: 7–22. <https://doi.org/10.5474/geologija.2016.001>
- Kanduč, T., Vreča, P. & Žigon, S. 2018a: Izotopska sestava raztopljenega anorganskega ogljika ($\delta^{13}\text{C}_{\text{DIC}}$), celokupna alkalinost, izotopska sestava kisika ($\delta^{18}\text{O}$) in izotopska sestava vodika ($\delta^2\text{H}$). Analizno poročilo št. GEO 001/2018, 5 p.
- Kanduč, T., Vreča, P. & Žigon, S. 2018b: Izotopska sestava raztopljenega anorganskega ogljika ($\delta^{13}\text{C}_{\text{DIC}}$), celokupna alkalinost, izotopska sestava kisika ($\delta^{18}\text{O}$) in izotopska sestava vodika ($\delta^2\text{H}$). Analizno poročilo št. GEO 007/2018: 5 p.
- Kanduč, T., Vreča, P. & Žigon, S. 2018c: Izotopska sestava raztopljenega anorganskega ogljika ($\delta^{13}\text{C}_{\text{DIC}}$), celokupna alkalinost, izotopska sestava kisika ($\delta^{18}\text{O}$) in izotopska sestava vodika ($\delta^2\text{H}$). Analizno poročilo št. GEO 011/2018: 4 p.
- Kanduč, T., Vreča, P. & Žigon, S. 2018d: Izotopska sestava raztopljenega anorganskega ogljika ($\delta^{13}\text{C}_{\text{DIC}}$), celokupna alkalinost, izotopska sestava kisika ($\delta^{18}\text{O}$) in izotopska sestava vodika ($\delta^2\text{H}$). Analizno poročilo št. GEO 019/2018: 4 p.
- Keim, D.M., West, L.J. & Odling, N.E. 2012: Convergent flow in unsaturated fractured chalk. *Vadose Zone Journal*, 11/4. <https://doi.org/10.2136/vzj2011.0146>
- Kendall, C. & Doctor, D.H. 2003: 5.11—stable isotope applications in hydrologic studies. In: Heinrich, D.H. & Karl, K.T. (eds.): *Treatise on geochemistry*. Pergamon, Oxford: 319–364. <https://doi.org/10.1016/B0-08-043751-6/05081-7>
- Kern, Z., Hatvani, I.G., Czuppon, G., Fórízs, I., Erdélyi, D., Kanduč, T., Palcsu, L. & Vreča, P. 2020: Isotopic ‘altitude’ and ‘continental’ effects in modern precipitation across the Adriatic-Pannonian region. *Water*, 12/6: 1797. <https://doi.org/10.3390/w12061797>
- Khadka, K. & Rijal, M.L. 2020: Hydrogeochemical assessment of spring water resources around Melamchi, Central Nepal. *Water Practice & Technology*, 15/3: 748–758. <https://doi.org/10.2166/wpt.2020.066>
- Komac, B. 2001: The karst springs of the Kanin massif. *Acta Geographica*, 41: 43 p.
- Kuščer, D. 1974: Geološke raziskave med Bovcem in Kobaridom. *Geologija*, 17: 425–476.
- Maurice, L., Farrant, A.R., Mathewson, E. & Atkinson, T. 2021: Karst hydrogeology of the Chalk and implications for groundwater protection. In: Farrell, R.P., Massei, N., Foley, A.E., Howlett, P.R. & West, L.J. (eds.): *The Chalk Aquifers of Northern Europe*. Special Publication. Geological Society, London, UK.
- Meybeck, M. 1987: Global chemical weathering of surficial rocks estimated from river dissolved loads. *American Journal of Science*, 287/5: 401–428. https://ui.adsabs.harvard.edu/link_gateway/1987AmJS..287..401M/doi:10.2475/ajs.287.5.401
- Moral, F., Cruz-Sanjulián, J.J. & Olías, M. 2008: Geochemical evolution of groundwater in the carbonate aquifers of Sierra de Segura (Betic Cordillera, southern Spain). *Journal of Hydrology*, 360/1-4: 281–296. <https://doi.org/10.1016/j.jhydrol.2008.07.012>
- Neuman, S.P. 2005: Trends, prospects and challenges in quantifying flow and transport through fractured rocks. *Hydrogeology Journal*, 13: 124–147. <https://doi.org/10.1007/s10040-004-0397-2>
- Placer, L. 1999: Contribution to the macro-tectonic subdivision of the border region between Southern Alps and External Dinarides. *Geologija*, 41/1: 223–255. <https://doi.org/10.5474/geologija.1998.013>
- Placer, L. 2008: Principles of the tectonic subdivision of Slovenia. *Geologija*, 51/2: 205–217. <https://doi.org/10.5474/geologija.2008.021>
- Ravbar, N. & Kovačič, K. 2006: Karst water management in Slovenia in the frame of vulnerability mapping. *Acta carsologica*, 35/2: 73–82. <https://doi.org/10.3986/ac.v35i2-3.230>
- Rejc, U. 2014: Hidrogeološka analiza porečja Uče = hydrogeological analysis of Učja river basin. Diplomsko delo (in Slovenian with English abstract). Univerza v Ljubljani, Naravoslovnotehniška fakulteta, Ljubljana: 44 p.
- Rodgers, P., Soulsby, C., Waldron, S. & Tetzlaff, D. 2005: Using stable isotope tracers to assess hydrological flow paths, residence times and landscape influences in a nested mesoscale. *Hydrology and Earth System Sciences*, 9/3: 139–155. <https://doi.org/10.5194/hess-9-139-2005>
- Romanek, C.S., Grossman, E.L. & Morse, J.W. 1992: Carbon isotopic fractionation in synthetic aragonite and calcite; effects temperature

- and precipitation rate. *Geochimica et Cosmochimica Acta*, 46: 419–430. [https://doi.org/10.1016/0016-7037\(92\)90142-6](https://doi.org/10.1016/0016-7037(92)90142-6)
- Rožič, B., Udovč, J., Žvab Rožič, P., Gale, L. & Gerčar, D. 2022: How far to the west was the Slovenian basin extending? In: Program, Abstracts and Field Trip Guide. Budapest: 97.
- Russo, S. 2015: Hydrogeochemistry of karst springs in the transboundary area Italy – Slovenia (Kanin Mountain). *Plinius*, 41: 5 p.
- Serianz, L., Cerar, S. & Vreča, P. 2021: Using stable isotopes and major ions to identify recharge characteristics of the Alpine groundwater-flow dominated Triglavská Bistrica River. *Geologija*, 64/2: 205–220. <https://doi.org/10.5474/geologija.2021.012>
- Shamsi, A., Karami, G. H., Hunkeler, D. & Taheri, A. 2019: Isotopic and hydrogeochemical evaluation of springs discharging from high-elevation karst aquifers in Lar National Park, northern Iran. *Hydrogeology Journal*, 27/2: 655–667. <https://doi.org/10.1007/s10040-018-1873-4>
- SLONIP 2023: SLOvenian Network of Isotopes in Precipitation. Ljubljana: Institut "Jožef Stefan". Available online: <https://slonip.ijz.si/data/3> (1. 12. 2023)
- Spötl, C. 2005: A robust and fast method of sampling and analysis of $\delta^{13}\text{C}$ of dissolved inorganic carbon in ground waters. *Isotopes in Environmental Health Studies*, 41/3: 217–221. <https://doi.org/10.1080/10256010500230023>
- Šmuc, A. 2012: Middle to Upper Jurassic succession at Mt Kobariški Stol (NW Slovenia) = srednje- do zgornjejursko zaporedje na Kobariškem Stolu (SZ Slovenija). Materials and geoenvironment (RMZ), 59/2-3: 267–284.
- Torkar, A. & Brenčič, M. 2015: Spatio-Temporal distribution of discharges in the Radovna River Valley at low water conditions. *Geologija*, 58/1: 47–56. <https://doi.org/10.5474/geologija.2015.003>
- Torkar, A., Brenčič, M. & Vreča, P. 2016: Chemical and isotopic characteristics of groundwater-dominated Radovna River (NW Slovenia). *Environmental earth sciences*, 75/18: 1–18. <https://doi.org/10.1007/s12665-016-6104-5>
- Turk, J., Malard, A., Jeannin, P.-Y., Petrič, M., Gabrovšek, F., Ravbar, N., Vouillamoz, J., Slabe, T. & Sordet, V. 2014: Hydrogeological characterization of groundwater storage and drainage in an alpine karst aquifer (the Kanin massif, Julian Alps). *Hydrological Processes*, 29: 1986–1998. <https://doi.org/10.1002/hyp.10313>
- Vantur, N. 2023: Sedimentarna analiza jurskih in krednih plasti profila na Drnohli v dolini Uče = Sedimentary analysis of the Jurassic and Cretaceous beds of the Drnohla section in the Učja Valley. Diplomsko delo (in Slovenian with English abstract). Univerza v Ljubljani, Naravoslovnotehniška fakulteta, Ljubljana: 43 p.
- Verbovšek, T. & Kanduč, T. 2016: Isotope Geochemistry of Groundwater from Fractured Dolomite Aquifers in Central Slovenia. *Aquatic Geochemistry*, 22: 131–151. <https://doi.org/10.1007/s10498-015-9281-z>
- Vrabec, M. 2012: Znaki kvartarne tektonske aktivnosti v coni Idrijskega preloma pri Učji. Materiali in geookolje (RMZ), 59/1–2: 285–298.
- Vreča, P. & Malenšek, N. 2016: Slovenian Network of Isotopes in Precipitation (SLONIP) – A review of activities in the period 1981–2015. *Geologija*, 59/1: 67–84. <https://doi.org/10.5474/geologija.2016.004>
- Vreča, P., Bronić, I.K., Horvatinčić, N. & Barešić, J. 2006: Isotopic characteristics of precipitation in Slovenia and Croatia: comparison of continental and maritime stations. *Journal of Hydrology*, 348: 457–469. <https://doi.org/10.1016/j.jhydrol.2006.04.005>
- Vreča, P., Pavšek, A. & Kocman, D. 2022: SLONIP—A Slovenian Web-Based Interactive Research Platform on Water Isotopes in Precipitation. *Water*, 14/13: 2127. <https://doi.org/10.3390/w14132127>
- Weber, M., Bernhardt, M., Pomeroy, J.W., Fang, X., Härrer, S. & Schulz, K. 2016: Description of current and future snow processes in a small basin in the Bavarian Alps. *Environmental Earth Sciences*, 75, 1223. <https://doi.org/10.1007/s12665-016-6027-1>
- White, W.B. 1988: Geomorphology and hydrology of karst terrains. Oxford University Press, New York.
- White, W.B. 2010: Springwater geochemistry. In: Krešić, N. & Stevanović, Z. (eds.): *Groundwater Hydrology of Springs: Engineering, Theory, Management, and Sustainability*. Butterworth-Heinemann: Burlington, NJ, USA, 2010: 231–268.
- Zega, M., Rožič, B., Gaberšek, M., Kanduč, T., Žvab Rožič, P. & Verbovšek, T. 2015: Minerlogical, hydrogeochemical and isotopic characteristics of the Žveplenica sulphide karstic spring (Trebuša Valley, NW Slovenia). *Environmental Earth Sciences*, 74: 3287–3300. <https://doi.org/10.1007/s12665-015-4357-z>
- Zini, L., Casagrande, G., Calligaris, C., Cucchi, F., Manca, P., Treu, F., Zavagno, E. & Biolchi, S.

- 2015: The karst hydrostructure of the Mount Canin (Julian Alps, Italy and Slovenia). In: Bartolomé, A., Carrasco, F., Durán, J.J., Jiménez, P. & LaMoreaux, J.W. (eds.): Hydrogeological and Environmental Investigations in Karst Systems. Environmental Earth Sciences 1. Springer-Verlag Berlin Heidelberg, 2015: 219–226. https://doi.org/10.1007/978-3-642-17435-3_24
- ZRSVN, 2023: Nature Conservation Atlas – NV. Available online: <https://www.naravovarstveni-atlas.si/web/profile.aspx?id=NV@ZRSVNJ> (20. 10. 2022)
- Zuliani, T., Kanduč, T., Novak, R. & Vreča, P. 2020: Characterization of Bottled Waters by Multielemental Analysis, Stable and Radioactive Isotopes. Water, 12: 2454. <https://doi.org/10.3390/w12092454>
- Žvab Rožič, P., Polenšek, T., Verbovšek, T., Kanduč, T., Mulec, J., Vreča, P., Strahovnik, L. & Rožič, B. 2022: An Integrated Approach to Characterising Sulphur Karst Springs: A Case Study of the Žvepovnik Spring in NE Slovenia. Water, 14: 1249. <https://doi.org/10.3390/w14081249>
- Žvab Rožič, P., Grkman, A., Verbovšek, T., Vreča, P., Kanduč, T. & Rožič, B. 2024: Hydrogeochemical and Isotopic data of Učja aquifer, NW Slovenia. PANGAEA. <https://doi.org/10.1594/PANGAEA.964981>



Signs of crustal extension in Lower Jurassic carbonates from central Slovenia

Znaki ekstenzije skorje v spodnjejurskih karbonatih osrednje Slovenije

Luka GALE^{1,2} & Boštjan ROŽIČ²

¹Department of Geology, University of Ljubljana, Aškerčeva 12, SI–1000 Ljubljana, Slovenia;
e-mail: luka.gale@ntf.uni-lj.si; bostjan.rozic@ntf.uni-lj.si

²Geological Survey of Slovenia, Dimičeva ulica 14, SI– 1000 Ljubljana, Slovenia; e-mail: luka.gale@geo-zs.si

Prejeto / Received 7. 8. 2023; Sprejeto / Accepted 27. 2. 2024; Objavljeno na spletu / Published online 29. 3. 2024

Key words: carbonate platform, External Dinarides, Early Jurassic, Podbukovje Formation, neptunian dyke, breccia
Ključne besede: karbonatna platforma, Zunanji Dinaridi, zgodnja jura, Podbukovška formacija, neptunski dajk, breča

Abstract

The Lower Jurassic Podbukovje Formation represents a succession of shallow marine carbonate rocks deposited on the former Southern Tethyan Megaplatform and one of its successors, the Adriatic Carbonate Platform. Several outcrops of the Podbukovje Formation from central Slovenia (southern margin of the Ljubljana Moor) are presented, bearing possible evidence of Early Jurassic extensional tectonics. Peritidal facies of the lowermost, Hettangian – Sinemurian, part of the Podbukovje Formation locally interfingers with bodies of matrix supported pervasively dolomitized polymictic breccia, several metres to tens of metres thick and is locally cut by neptunian dykes some few decimetres to metres wide. The same or slightly younger part of the formation locally contains grabens/half-grabens metres to tens of metres deep and filled with poorly sorted pervasively dolomitized matrix supported polymictic breccia. Small miliolid foraminifera are present within the clasts and in the matrix. Finally, partly dolomitized blocky breccia tens of metres thick locally overlies the Pliensbachian – lowermost Toarcian limestone with lithiotid bivalves. Besides completely and partly dolomitized clasts, the breccia contains a variety of limestone clasts and preserves common radial ooids and some bioclasts within the partially dolomitized matrix.

The Hettangian-Sinemurian breccias and dykes are presumably related to the early, diffused rifting stage of the Penninic (Alpine Tethys) Ocean, whereas Toarcian breccias relate to the main, focused rifting stage. Together with evolving biota and changing paleo-oceanographic conditions, the extensional tectonics may have been an important factor behind the facies changes observed within the Podbukovje Formation.

Izvleček

Spodnjejurska Podbukovška formacija predstavlja zaporedje plitvomorskih karbonatnih kamnin, odloženih na nekdanji Južnotetidini karbonatni megaplatformi in Jadranski karbonatni platformi. V članku predstavljamo nekaj izdankov Podbukovške formacije iz osrednje Slovenije (južni rob Ljubljanskega barja), v katerih so vidni možni dokazi za zgodnjejursko ekstenzijsko tektoniko. Periplimski facies najnižjega, hettangijsko-sinemurijskega dela Podbukovške formacije se lokalno prepleta z nekaj metri do nekaj deset metri debelimi plastmi muljasto podprte povsem dolomitizirane polimiktne breče. Drugod plasti periplimskih karbonatov sekajo neptunski dajki, ki so široki do nekaj metrov in zapolnjeni z dolomikritom. Iсти ali nekoliko višji deli formacije ponekod vsebujejo tektonske grabne/polgrabne, zapolnjene z nekaj metri ali desetinami metrov povsem dolomitizirane slabo sortirane, muljasto podprte polimiktne breče. V klastih in vezivu so prisotne drobne miliolidne foraminifere. Delno dolomitizirana blokovna breča je prisotna tudi v zgornjih delih Podbukovške formacije nad pliensbachijsko – spodnjetoarcijskim litiotidnim apnencem. Poleg povsem in delno dolomitiziranih klastov breča vsebuje tudi raznolike klaste apnanca. V vezivu so prisotni radialno žarkoviti ooidi in nekaj bioklastov.

Hettangijsko-sinemurijske breče in dajke povezujemo z zgodnjo, razpršeno fazo razpiranja Peninskega oceana (Alpske Tetide), toarcjske breče pa z glavno, fokusirano fazo razpiranja. Ekstenzijska tektonika je skupaj z razvojem biote in spremembami v paleo-oceanografskih razmerah pomembno vplivala na faciesne spremembe med nižjimi in višjimi deli Podbukovške formacije.

Introduction

The Late Triassic to Early Jurassic paleogeography of central Pangea and the western Tethys Ocean was greatly affected by the opening of the Central Atlantic and related systems of basins belonging to the Penninic Ocean (Ratschbacher et al., 2004; Meschede & Warr, 2019). The main rifting phase started during or at the end of the Pliensbachian and into the Toarcian, and is reflected in the Southern Alps in the subsidence and eventual drowning of smaller platform areas, together with the establishment of marine plateaus (Buser, 1989; Bosellini, 2004; Šmuc, 2005; Berra et al., 2009; Rožič & Šmuc, 2009; Šmuc, 2010; Rožič et al., 2014). The main rifting event was preceded by a phase of diffuse early rifting, which occurred from the late Hettangian to the Sinemurian. In the western and central Southern Alps,

this phase is manifested through the subsidence of the Lombardian and Belluno basins (Winterer & Bosellini, 1981; Bertotti et al., 1993; Sarti et al., 1993; Clari & Masetti, 2002; Berra et al., 2009), whereas accelerated subsidence, increase in slope inclination, segmentation, and block tilting have been documented in the basin areas in the eastern Southern Alps (Rožič et al., 2017).

In the External Dinarides, major shifts in carbonate platform facies were described from the uppermost Pliensbachian – Toarcian successions (Dragičević & Velić, 2002; Črne & Goričan, 2008; Sabatino et al., 2013; Martinuš & Bucković, 2015; Ettinger et al., 2021), but the earlier tectonic events are not as well documented and their influence on the evolution of the platform has not yet been fully evaluated (Dozet & Strohmenger, 1996; Knez et al., 2003).

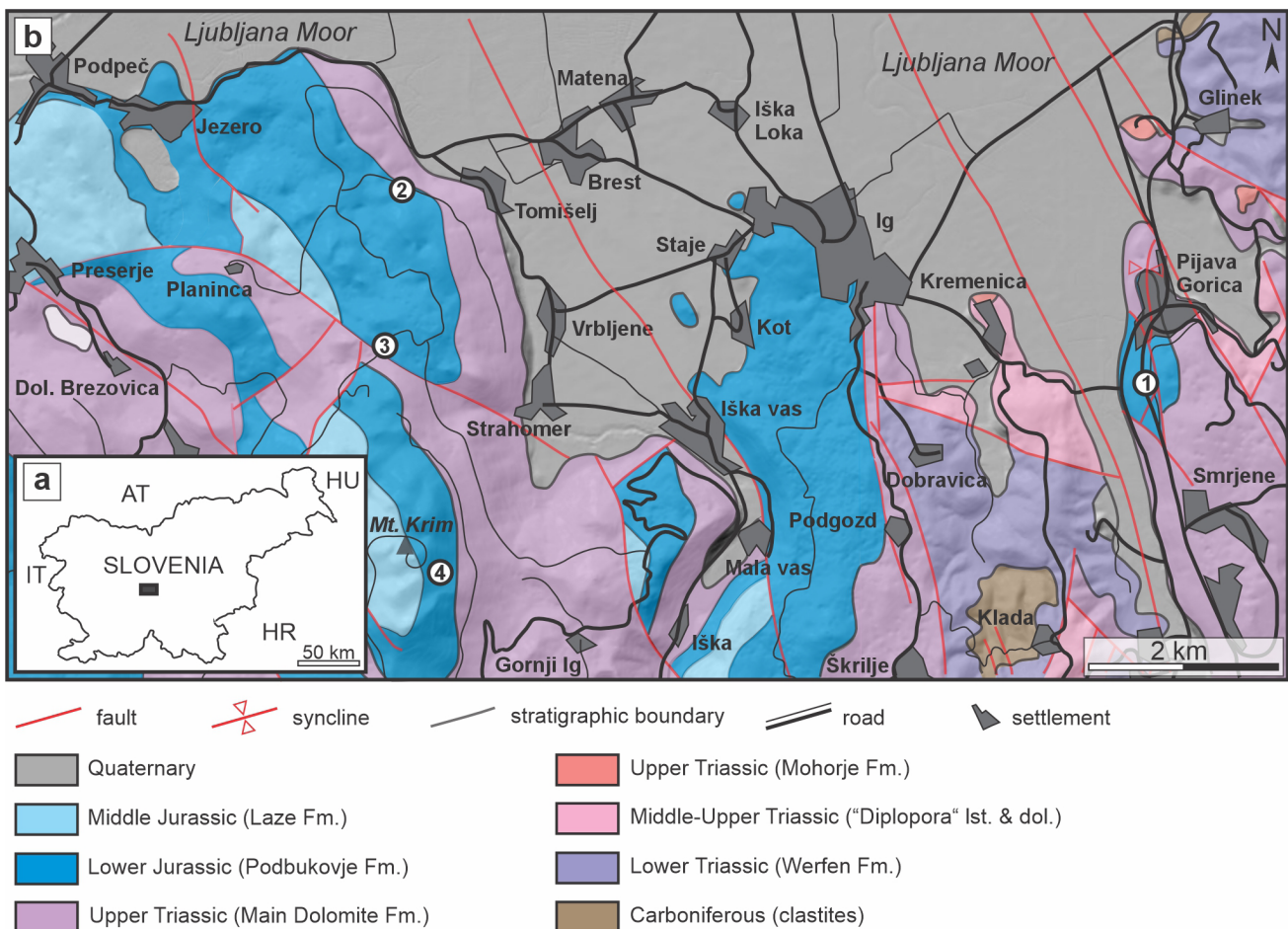


Fig. 1. Location and geological map of the study area. **a:** Outline of Slovenia. Position of the area, shown in Fig. 1b is indicated by a black rectangle. **b:** Detailed map and geological map of the studied area. Position of the described outcrops 1–4 (see text and Table 1) is indicated by the circled numbers 1–4. Geological map (Buser et al., 1967; Buser, 1968) is drawn over the LIDAR digital model of the relief, 2015. Data source: Slovenian Environment Agency. Accessed via portal Geopedia (Sinergise d.o.o.) in May 2023.

The aim of this paper is to present possible evidence for the Early Jurassic extensional tectonics in the area of the present-day External Dinarides (central Slovenia) related to both tectonic phases mentioned above. We suggest that Early Jurassic extensional tectonics was an important force behind the transition from the Hettangian facies association of intertidal flats to the Sinemurian and Pliensbachian shallow lagoon and shoal facies.

Geological Setting

The presented successions of Lower Jurassic rocks deposited in the shallow marine environments of the Southern Tethyan Megaplatform (sensu Vlahović et al., 2005). During the late Early Jurassic, this large entity broke up into several smaller (but still relatively large) carbonate platforms, one of which was the Adriatic Carbonate Platform, which extended from present-day NE Italy to Montenegro and Albania (Dragičević & Velić, 2002; Vlahović et al., 2002, 2005). To the north (present orientation), the platform faced the Slovenian Basin (Buser, 1989, 1996). The Adriatic Carbonate Platform was separated from other platform areas to the west through the formation of the Adriatic Basin that connected the Belluno and the Ionian Basins (Vlahović et al., 2005). The

presented outcrops are located in central Slovenia, on the southern rim of the Ljubljana Moor Basin (Fig. 1). Structurally, the area belongs to the Hrušica Nappe of the External Dinarides (Placer, 1999), and is dissected by major SSE-NNW directed dextral strike-slip and associated faults (Buser et al., 1967; Pleničar, 1970; Buser, 1968, 1974).

The Lower Jurassic succession has been assigned to the Podbukovje Formation and subdivided into four to five members (Fig. 2) (Dozet & Strohmenger, 2000; Dozet, 2009; Brajković et al., 2022). The lowermost Krka Limestone Member represents bedded intertidal limestone and dolostone (Dözet, 1993). According to Gale (2015), and Gale and Kelemen (2017), Lofer-type cycles of the Hettangian part of this member upwards pass into predominantly subtidal micritic and oolitic limestone. The following Orbitopsella Limestone Member is dominated by thick-bedded limestone in which foraminifera Orbitopsella first occurs. Breccia, oncoid, gastropod, and megalodontid limestone beds are sporadically present (Dözet, 2009). The following Lithiotis Limestone Member contains variety of facies types, deposited under restricted subtidal and intertidal conditions. Lithiotid bivalves occur at several levels and are a distinctive feature of this member (Dözet, 2009). The next, Oolitic Limestone

		Suha Krajina (Dözet & Strohmenger, 2000)	Radensko Polje (Dözet, 2009)	Mt. Krim area (Gale, 2015; this work)
MIDDLE JURASSIC		Laze Formation	Laze Formation	oolitic limestone
EARLY JURASSIC	PODBUKOVJE FORMATION	Spotted Limestone	Spotty limestone	nodular & oolitic limestone
		Oolitic Limestone	Oolitic limestone	breccia ④
		Lithiotis Limestone	Lithiotis limestone	micritic, oolitic, bioclastic limestone, lithiotid limestone
		Orbitopsella beds	Orbitopsella limestone	breccia
		Krka Limestone	banded micritic limestone	micritic limestone, fine-grained oolite
LATE TRIASSIC	Norian- Rhaetian	Main Dolomite	Main Dolomite	laminated & crystalline dolomite

Fig. 2. Lithostratigraphic units of the Lower Jurassic carbonates of central Slovenia and approximate stratigraphic position of the presented outcrops. Schemes for Suha Krajina and for Radensko Polje are drawn after Dözet and Strohmenger (2000) and Dözet (2009), respectively. The lithological units from the Mt. Krim area are modified after Gale (2015).

Member is characterised by oolitic limestone facies (Dozet & Strohmenger, 2000; Dozet, 2009). The Podbukovje Formation ends with the Spotted (or Spotty) Limestone Member, representing succession of thin to medium thick beds of dark grey limestone of nodular-like appearance. Limestone is mostly micritic (Dözet, 2009).

Previous records of Lower Jurassic breccias in southern Slovenia

Although it remains valid to this day that the Lower Jurassic platform carbonates of the southern Slovenia show little or no evidence of Early Jurassic extension, there are a few mentions of breccias that could be related to palaeotectonics. Breccias positioned atop the Upper Triassic Main Dolomite Formation were mentioned from the vicinity of Logatec (Buser, 1965). Ogorelec and Rothe (1993) described breccias at the boundary between the Upper Triassic platform carbonates and Jurassic deposits in the Čepovan-Lokovec section. Blocky breccias exceed 10 m or 20 m in thickness and laterally pinch-out. Fragments of corals within the breccia indicate earliest Jurassic age. Knez et al. (2003) described poorly sorted (clasts ranging in size from very fine pebble to boulder), chaotic, matrix- and clast-supported dolomitic breccia discordantly lying on peritidal carbonates. No fossils were found, but based on the superposition the breccia was formed close to the Triassic-Jurassic boundary. Authors interpreted breccia as "synsedimentary, fault, fissure, or small graben-related, tectonically influenced phenomenon" (Knez et al., 2003, p. 34–35). From younger beds, Buser (1965, 1974) mentioned limestone breccia beds alternating with light grey lower and middle Lower Jurassic limestone in the area between Ivančna Gorica and Trebnje. Lithiotid bivalves have been found in some of the limestone beds, indicating that the sedimentation of breccias lasted up to the Pliensbachian (Buser, 1974). Upper Lower Jurassic to Middle Jurassic dolomitic breccias were also documented between Velika Gora and Loški Potok (Buser, 1965). Breccias were also illustrated in a schematic column of middle Lower Jurassic (?) beds at Korinj, but not explained in detail (Strohmenger &

Dözet, 1991). Finally, from the area of Mt. Krim studied herein, Miler and Pavšič (2008) described breccias within the Hettangian and Sinemurian, as well as the Pliensbachian and the Toarcian parts of the succession. The thickness of the breccia beds is not indicated, but the authors mention up to 15 cm large clasts in Toarcian breccias, which have wackestone matrix containing ooids and bioclasts, including miliolid foraminifera.

Methods and materials

The sections of Lower Jurassic shallow marine carbonates presented herein were investigated between the years 2014 and 2022. The sections are situated along roads or hiking trails. The stratigraphic thickness of the studied successions varies from a few metres to several tens of metres and is indicated in the Results sections. For the purpose of petrographic description, 63 samples of rock were cut for thin sections of 28 × 47 mm in size. Thin sections were investigated with a polarizing microscope. Carbonates were classified according to Dunham (1962), and Embry and Klovan (1971). In forming the textural name, we follow recommendations by Wright (1992) putting the predominant component first. Fifteen thin sections of breccias and the surrounding rock were stained with Alizarin Red S dye in order to determine the presence of dolomite. The texture of the dolomite was described in accordance with Sibley and Gregg (1987). Although the term "dolostone" has not gained wide usage among sedimentary petrologists, we use this term here to distinguish dolomitic rock from the mineral dolomite (see also Warren, 2000, p. 7).

Results

The examined outcrops are presented according to superposition. The coordinates of the sections are given in Table 1. Due to the presence of stromatolites, herein presented outcrops 1–3 and the lower part of the section 4 lithostratigraphically belong to the lowermost, Krka Member. Breccias overlying the Lithiotid Limestone Member in the upper part of the section 4 are likely positioned lateral to the lower part of the Spotted/Spotty Member sensu Dozet and Strohmenger (2000) and Dözet (2009).

Table 1. "Coordinates of the presented outcrops and sections."

Locality	Stratigraphic position	Latitude	Longitude
Pijava Gorica (Outcrop 1)	Krka Limestone Member (Hettangian)	45°56'40.29" N	14°34'17.68" E
Tomišelj (Outcrop 2)	Krka Limestone Member (Sinemurian)	45°57'46.69" N	14°28'19.15" E
Strahomer (Outcrop 3)	Krka Limestone Member (Sinemurian)	45°56'57.24" N	14°28'0.86" E
Mt. Krim (Outcrop 4, lower)	Krka Limestone Member (Hettangian)	45°55'16.31" N	14°28'38.02" E
Mt. Krim (Outcrop 4, upper)	Unnamed member (Toarcian)	45°55'38.72" N	14°28'28.90" E

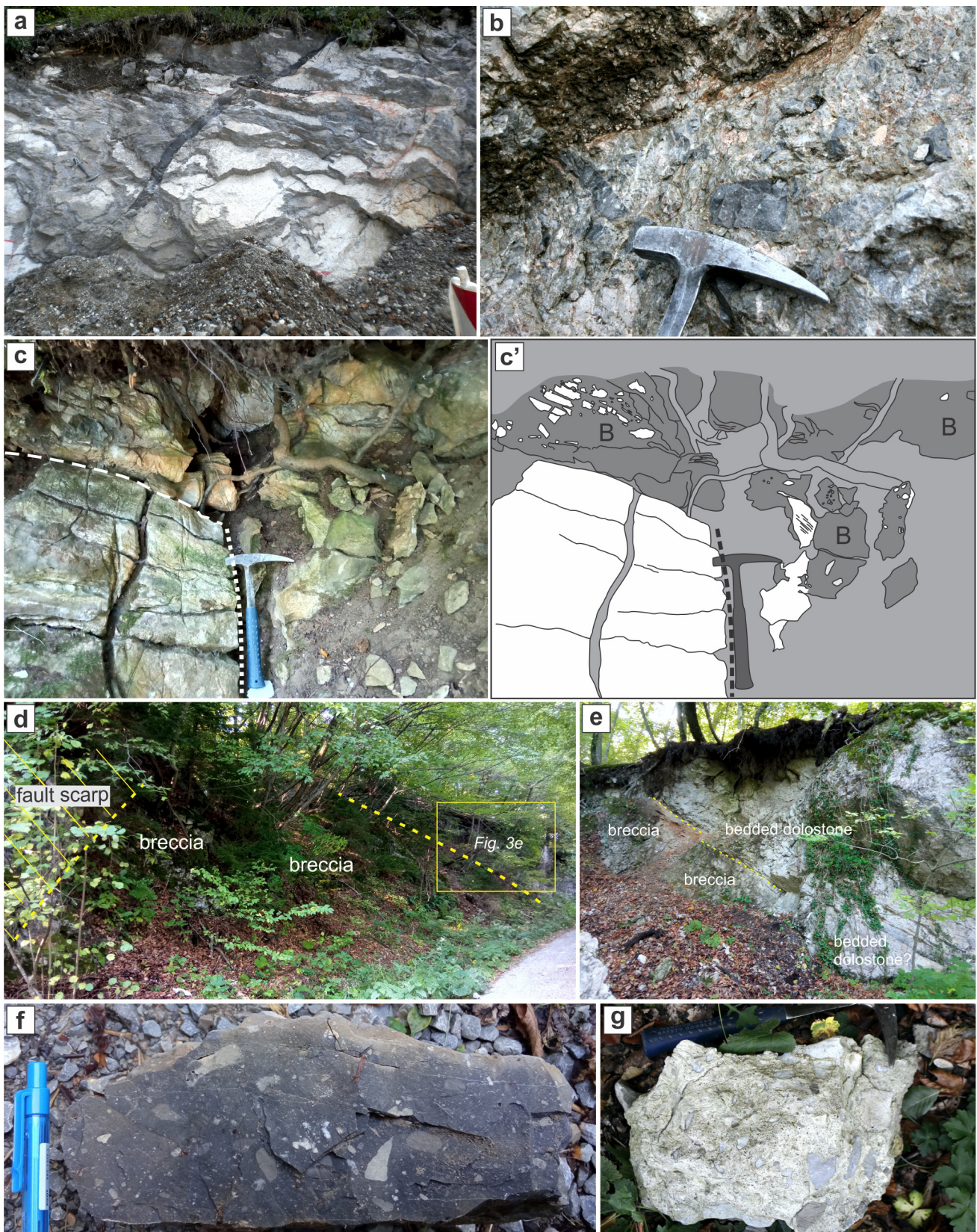


Fig. 3. Field view of the outcrops 1–3. **a:** Neptunian dykes cutting through Lower Jurassic dolostone at Pijava Gorica (outcrop 1). **b:** Clasts of dolostone floating in dolomircite filling the Neptunian dykes at Pijava Gorica (outcrop 1). **c–c'**: Base of the matrix-supported dolomitic breccia in outcrop 2 above Tomišelj (lower 4 m of sedimentary log in Fig. 4). **d**: Eastern side of the outcrop of dolomitic breccia at the roadcut between the Slemec, Strmec, and Trešenk summits west of Strahomer (outcrop 3). Yellow lines indicate the position of a paleo-fault plane (left side) and the bedding plane separating the breccia from the overlying stromatolitic dolomite. **e**: Western side of the outcrop depicted in Figure 3d. Yellow line indicates the position of the upper bedding plane of breccia. **f**: Hand sample of matrix-supported dolomitic breccia from outcrop 2. Note the different colours of clasts and that some clasts (left side of the sample) themselves are matrix-supported breccia. **g**: Hand sample of Toarcian breccia, outcrop 4 (upper).

Outcrop 1: Neptunian dykes within the Krka Limestone Member at Pijava Gorica (Hettangian – ?Sinemurian)

The roadcut between Pijava Gorica and Smrjene exposes medium thick-bedded dark grey dolostone (dolomicrite). The section is crossed by numerous smaller faults, and the bedding orientation changes, so the actual thickness of the succession cannot be determined. Planar laminations (stromatolites) are locally visible. The dolostone is crosscut by dykes filled with darker dolostone (dolomicrite), which locally contains angular clasts of dolostone lithologically identical to the surrounding rock (Fig. 3a–b). The size of clasts ranges from 5 mm to 50 cm. Some of the clasts closely fit together, indicating very short transport, while others float within the matrix.

Outcrop 2: Syndepositional breccia within the Krka Limestone Member above Tomišelj (Hettangian – Sinemurian)

Dolomitized matrix-supported carbonate conglomeratic breccia with characteristic brownish-grey matrix is found at several localities around Mt. Krim. However, due to the intense weathering of the dolostone and the dense vegetation, outcrops with visible relationships with the surrounding lithologies are difficult to find. Dolomitic breccia a few metres thick was discovered roughly west of Tomišelj along a forest road running along the eastern slopes of the small summits Gadna (elevation 521 m) and Srobotnik (elevation 603 m) (Fig. 1).

The described section is approximately 10 m thick (Fig. 4). It starts with thin to thick beds of light grey dolostone (dolosparite and dolomicrite). Stromatolites and desiccation cracks are present in dolomicrite. Upwards (immediately below the breccia level) lies a bed of light grey dolostone 140 cm thick with stromatolite intraclasts in its lower part. The described beds dip at 240/55 and laterally end at a steep scarp, interpreted as a normal paleofault (Fig. 3c). The succession continues with pervasively dolomitized conglomeratic breccia, which covers the paleofault and fills the graben. The breccia is matrix-supported and at least 4.5 m thick within the graben. The clasts vary in colour and are angular to subrounded. Some are shattered into mosaic-like configurations. Clast dimensions decrease upwards: close to the paleofault they measure up to 15 cm, while they are up to 2 cm large near the top of the breccia. In the graben-filling succession (basinward sensu Matenco & Haq, 2020), the breccia is followed by several thinner and possibly internally lay-

ered beds of pervasively dolomitized fine-grained polymict breccia. The clasts in this fine-grained breccia consist of crystalline dolostone, as well as completely dolomitised calcimudstone, peloidal-bioclastic packstone, and bioclastic packstone, transitioning to calcimudstone. Dolomitized bioclastic packstone is relatively abundant in miliolid foraminifera (Fig. 5a–b, e). The same foraminifera can also be found within the finely crystalline dolomitized breccia matrix, indicating the same/similar age of the matrix and (at least part of) the clasts. Sinemurian foraminifera were determined from beds lying approximately 60 stratigraphic metres higher in the succession (section “Tomišelj 1” in Gale & Kelemen, 2017).

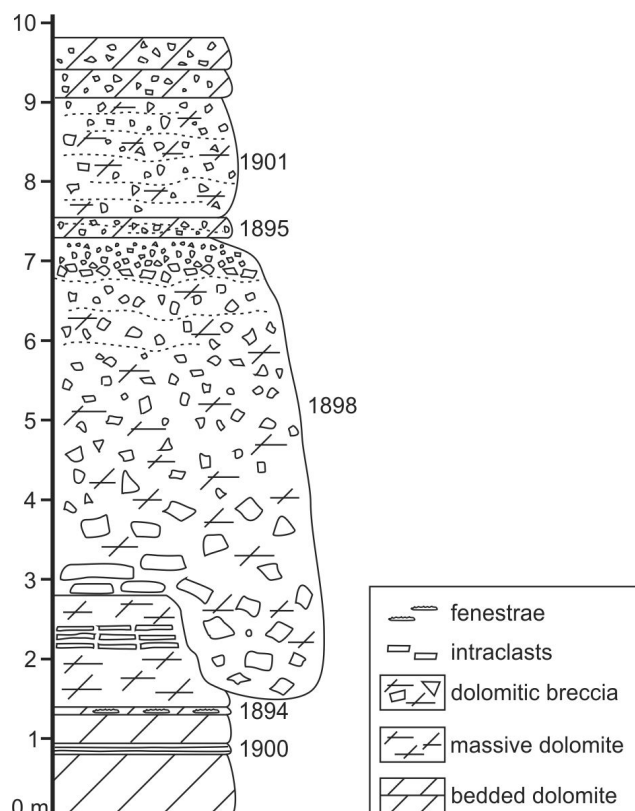


Fig. 4. Sedimentary log of the breccia body within the Lower Jurassic (Hettangian?) Krka Limestone Member above Tomišelj (outcrop 2). Numbers to the right indicate thin section numbers.

Outcrop 3: Matrix-supported dolomitic breccia within the Krka Limestone Member west of Strahomer (Hettangian – Sinemurian)

Roadcuts between the Sleme, Strmec, and Trešenk summits west of Strahomer feature long exposures of pervasively dolomitized matrix-supported breccia, macroscopically identical to the breccia in outcrop 2, described above. At the eastern (lowermost) side of the outcrop bedded light grey dolostone (dolosparite and dolomicrite with rare fenestrae) is exposed (Fig. 3d). The bedded

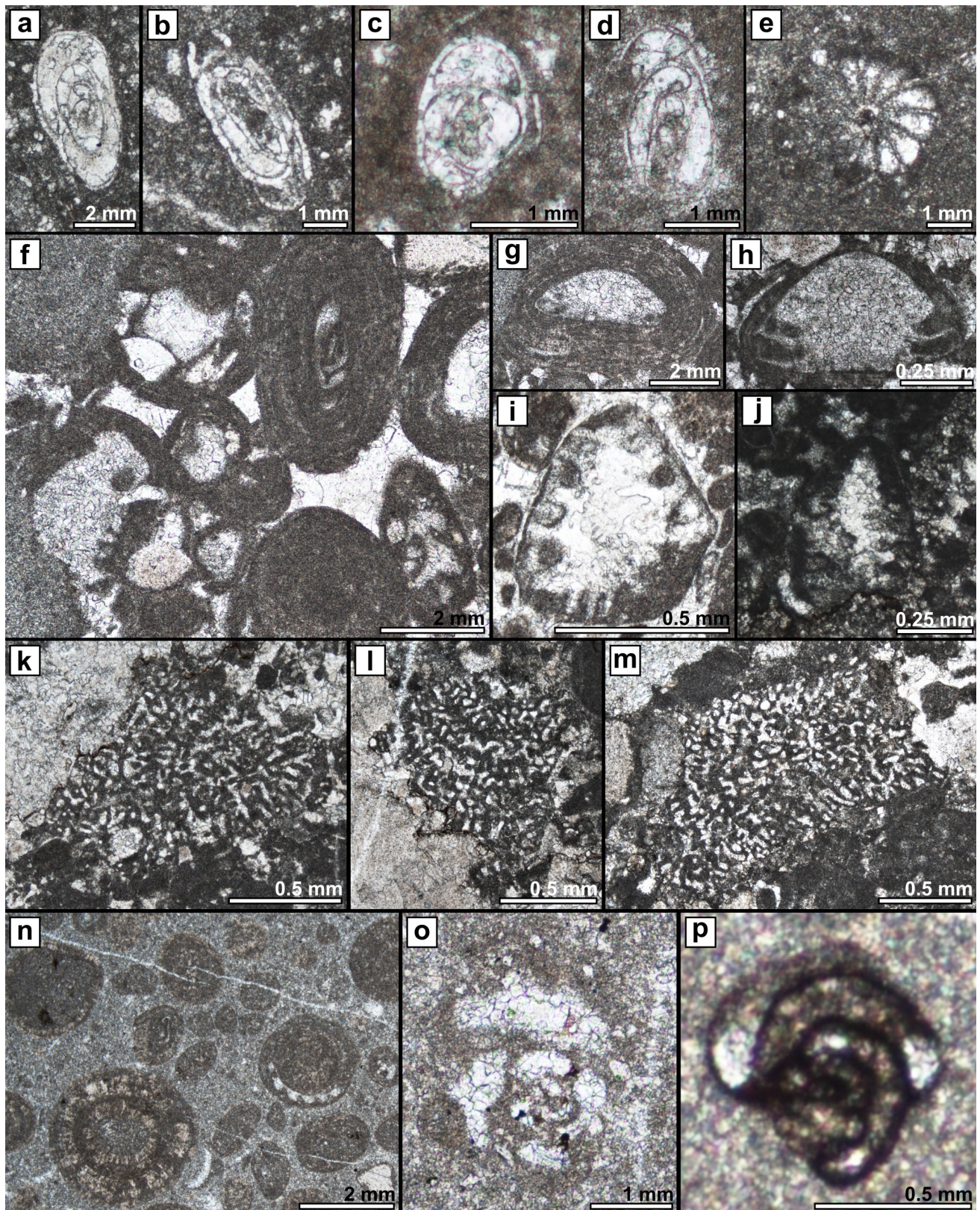


Fig. 5. Selected foraminifera from the described outcrops. **a–b:** Miliolid foraminifera (?*Istriloculina* sp.). Outcrop 2. Thin section 1895. **c–d:** Miliolid foraminifera (?*Istriloculina* sp.). Outcrop 3. Thin section 1903. **e:** Undetermined foraminifera. Outcrop 2. Thin section 1895. **f:** Various foraminifera in ooids (Trocholinidae and Miliolida) and as free particles (?*Ammobaculites* or ?*Everticyclammina* sp.). Outcrop 4 (upper). Thin section 1927. **g:** Trocholinidae (cf. *Trocholina conica* (Schlumberger)). Outcrop 4 (upper). Thin section 1927. **h:** Trocholinidae (cf. *Trocholina conica* (Schlumberger)). Outcrop 4 (upper). Thin section 1920. **i:** Trocholinidae (cf. *Coscinococonus alpinus* Leupold in Leupold and Bigler). Outcrop 4 (upper). Thin section 1933. **j:** *Coscinococonus* sp. Outcrop 4 (upper). Thin section 1916. **k–m:** *Socotraina serpentina* Banner, Whittaker, BouDagher-Fadel and Samuel. Outcrop 4 (upper). Thin section 1930. **n:** Sessile foraminifera on radial ooids. Outcrop 4 (upper). Thin section 1932. **o:** ?*Ammobaculites* sp. Outcrop 4 (upper). Thin section 1914. **p:** *Meandrovoluta asiagoensis* Fugagnoli and Rettori. Outcrop 4 (upper). Thin section 1911.

dolostone dips at 300/25. The beds are truncated along a subvertical (120/80) plane, a possible palaeofault that separates the bedded dolostone from the breccia. The matrix-supported to locally clast-supported breccia is poorly exposed and attains a thickness of at least 25–30 m. Clasts within the breccia are very poorly sorted (Fig. 3f–g). On average, they form approximately 20 % of the rock, but are more abundant near the mentioned paleofault. The clasts are generally a centimetre in size, but the size of the clasts varies considerably between the samples. The largest recorded clasts measure approximately 15 cm, while the smallest are less than 0.2 mm in size. Macroscopically, they are white, greyish-brown, and brown laminated dolomiticrite. At the microscopic level, the following lithoclasts can be distinguished: dolomitic tectonic breccia, crystalline dolostone, pervasively dolomitized lithoclasts with recognisable primary composition of mudstone, fenestral mudstone, laminated mudstone (stromatolite), peloidal wackestone, bioclastic-peloidal wackestone and packstone, and intraclastic grainstone. Clasts are angular to subrounded, and highly variable in shape. No connection between lithological composition and roundness was noted. The matrix is brownish dolomiticrite. Small benthic foraminifera are rare, both within the clasts and in the matrix (Fig. 5c–d). The breccia is crosscut by younger veins, up to 2 cm thick and filled with dolomitic cement.

At the opposite, western side of the roadcut the breccia at the top laterally and vertically passes into bedded light grey dolostone (dolosparite) and laminated dolostone (dolomiticrite) (Fig. 3e). Small-scale cracks, filled with black dolomiticrite (seemingly identical to the neptunian dykes in outcrop 1), are present within beds of light grey dolosparite overlying the breccia.

Outcrop 4 (lower part): Dolomitic breccia within the Krka Limestone Member on the NE slope of Mt. Krim (Hettangian-Sinemurian)

A thick succession of pervasively dolomitized breccia is exposed within a 280 m long succession underlying Sinemurian and Pliensbachian limestone on the hiking path from Gornji Ig to Mt. Krim. The area was covered also by a detailed geological map of Miler and Pavšič (2008), where the same breccias are briefly described. The succession was logged schematically because of the poor visibility of bed boundaries (Fig. 6). The lower 100 m of the succession is represented by bedded dolostone, in which stromatolites, birdseyes fenestrae, stromatolitic intraclasts, and black pebbles

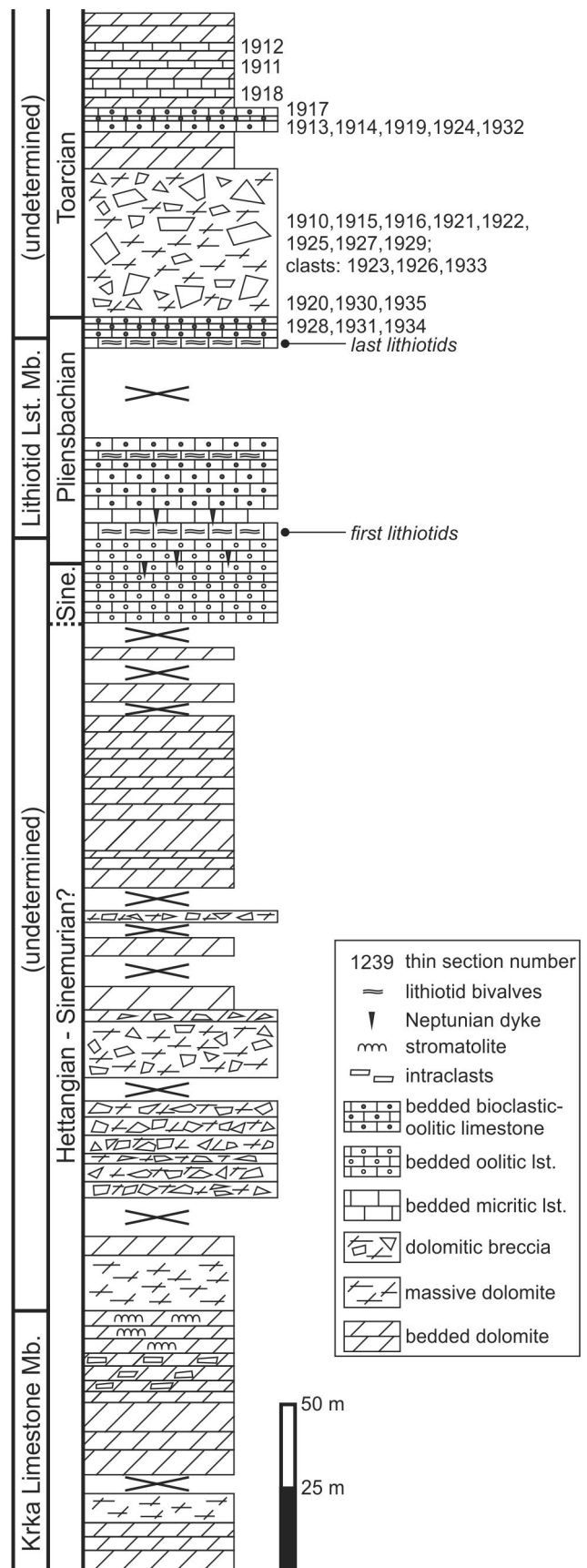


Fig. 6. Stratigraphic succession of Lower Jurassic (Hettangian – Toarcian) beds on the NE slope of Mt. Krim (all of outcrop 4). Numbers to the right indicate thin section numbers.

are locally present. Fractures filled with dark dolostone (dolomiticrete) resembling neptunian dykes from outcrop 1, were noticed in the upper part of this interval. The next 50 m of the succession is dominated by chaotic and poorly sorted dolomitic breccias, deposited in beds 3–17 m thick. Breccia is clast or matrix-supported, with clasts ranging from 1 mm to at least 30 cm in size. The average clast size is approximately 5 cm. Clasts are angular to rounded, dolomicritic or dolosparitic, and of different colours. The section continues upwards with thick to massive beds of dolostone, with a single bed of dolomitic breccia at 190 m of the succession. At approximately 290 m of the succession, the dolostone is succeeded by bedded limestone. The lower part of the limestone succession roughly corresponds to the *Orbitopsella* Limestone Member (although *Orbitopsella* first occurs approximately 30 m above the first limestone bed). The lowest occurrence of the lithiotid bivalves, 41 m above the base of the limestone part of the section, defines the base of the approximately 85-m-thick Lithiotid Limestone Member (Fig. 6). Within the limestone interval, oolitic and bioclastic limestones predominate, with bioclasts becoming more common in the Lithiotid Limestone Member. Micritic limestone is subordinate. Beds are between 5 cm and 160 cm thick. Small-scale neptunian dykes are locally present within this member.

Outcrop 4 (upper part): Dolomitized blocky breccia overlying the Lithiotid Limestone Member on the NE slope of Mt. Krim (Toarcian)

After the highest occurrence of the lithiotid bivalves, a few beds of nearly black limestone (intraclastic-bioclastic grainstone with oncoids) follow. Foraminifera *Haurania deserta* Henson is numerous in some beds, while *?Bosniella oenensis* Gušić and *Involutina liassica* (Jones) are less common. According to Velić (2007), the stratigraphic range of *H. deserta* is from the late Sinemurian to the end of the Pliensbachian, and *B. oenensis* is limited to the Pliensbachian. Other bioclasts are fragments of bivalve shells, gastropods, calcimicrobes, microproblematica *Thaumatoporella*, echinoderms, and dasycladacean algae.

Limestone is followed by poorly exposed dolostone (dolosparite) with small lithoclasts overlain by one or several beds (this part of the section is mostly covered) of very poorly sorted, coarse-grained partly dolomitized polymictic breccia (Figs. 3g, 6). Clasts are rounded to angular, and on average 3–5 cm large. The largest clasts are up to 30 cm in size. Some clasts completely escaped dolomitization or are only partially dolomitized (mud-

stone, bioclastic wackestone, oolitic grainstone, pelletal grainstone, bioclastic-intraclastic-oolitic grainstone, peloidal-oolitic-crinoidal grainstone, peloidal-bioclastic grainstone, peloidal grainstone, and lithoclastic-bioclastic rudstone), while the others are completely replaced by dolomite and rarely show their original texture and composition (one exception being oolitic grainstone, mimetically replaced by coarse, planar-s dolomite). The lithoclastic-bioclastic rudstone clasts contain *Socotrina serpentina* Banner, Whittaker, BouDagher-Fadel, and Samuel (Fig. 5k–m), *Siphovalvulina* sp., *Meandrovoluta asiagoensis* Fugagnoli & Rettori, and *Haurania deserta* Henson. Trocholinidae (Fig. 5f–j), Miliolida, and *Pseudopfenderina* were determined from other clasts. Besides the lithoclasts, non-dolomitized radial ooids, fragments of corals, sponges, gastropods, and echinoderms are present in the dolomitized matrix of the breccia. Some ooids formed around tests of foraminifera Miliolida and *?Siphovalvulina*.

Poorly sorted breccias are followed by poorly exposed dolostone (dolosparite), followed by thin- to medium thick-bedded, almost black limestone (oolitic wackestone, packstone and grainstone, mudstone, rare spiculitic packstone, and bioclastic-pelletal packstone). Ooids are of the radial type. Skeletal material is relatively rare: echinoderms, gastropods, bivalves, ostracods, pelagic crinoids, foraminifera, sponge spicules, and calcareous spheres (radiolarians?) are present. Foraminiferal assemblage comprises common agglutinated sessile forms (Fig. 5n), *?Ammobaculites* sp. (Fig. 5o), *Meandrovoluta asiagoensis* Fugagnoli & Rettori (Fig. 5p), *Ophthalmidium* sp., *Lenticulina* sp., nodosariids, Textulariida, and Epistominidae. The section ends with bedded dolostone.

For the breccia described above, Toarcian age is assumed. This is supported by the findings of *S. serpentina*, which was described from the upper Lower Jurassic (Toarcian) beds (Banner et al., 1997; Martinuš & Bucković, 2015; BouDagher-Fadel, 2018). Based on the presence of *M. asiagoensis* with the stratigraphic range from Sinemurian to Toarcian (Velić, 2007), Toarcian age is also presumed for the oolites overlying the breccia.

Dolomitization

Although all of the breccias described above show some degree of dolomitization, there are some notable differences between the Hettangian-Sinemurian and the Toarcian breccias. The Hettangian-Sinemurian breccias from outcrops 2, 3, and 4 (lower part) are completely (pervasively) dolomitized (Fig. 7a–b). Non-mimical dolomitization

of the clasts includes the growth and replacement of original textures by medium (0.025 mm) to coarse (0.330 mm) subhedral dolomite crystals of equal or different sizes (unimodal or polymodal). Other clasts show mimical replacement by very small subhedral dolomite. Staining with Alizarin Red S revealed that micritic clasts are also composed of dolomite, which is thus very finely

crystalline and mimically replaces fine-grained calcimudstone. Pervasive mimical dolomitization by very small crystals of dolomite was also recognized in peloidal grainstone and laminated (stromatolitic) dolomiticrite. The matrix of the Hettangian-Sinemurian breccias is non-mimically replaced by equigranular, rarely polymodal, anhedral (?) to subhedral dolomite.

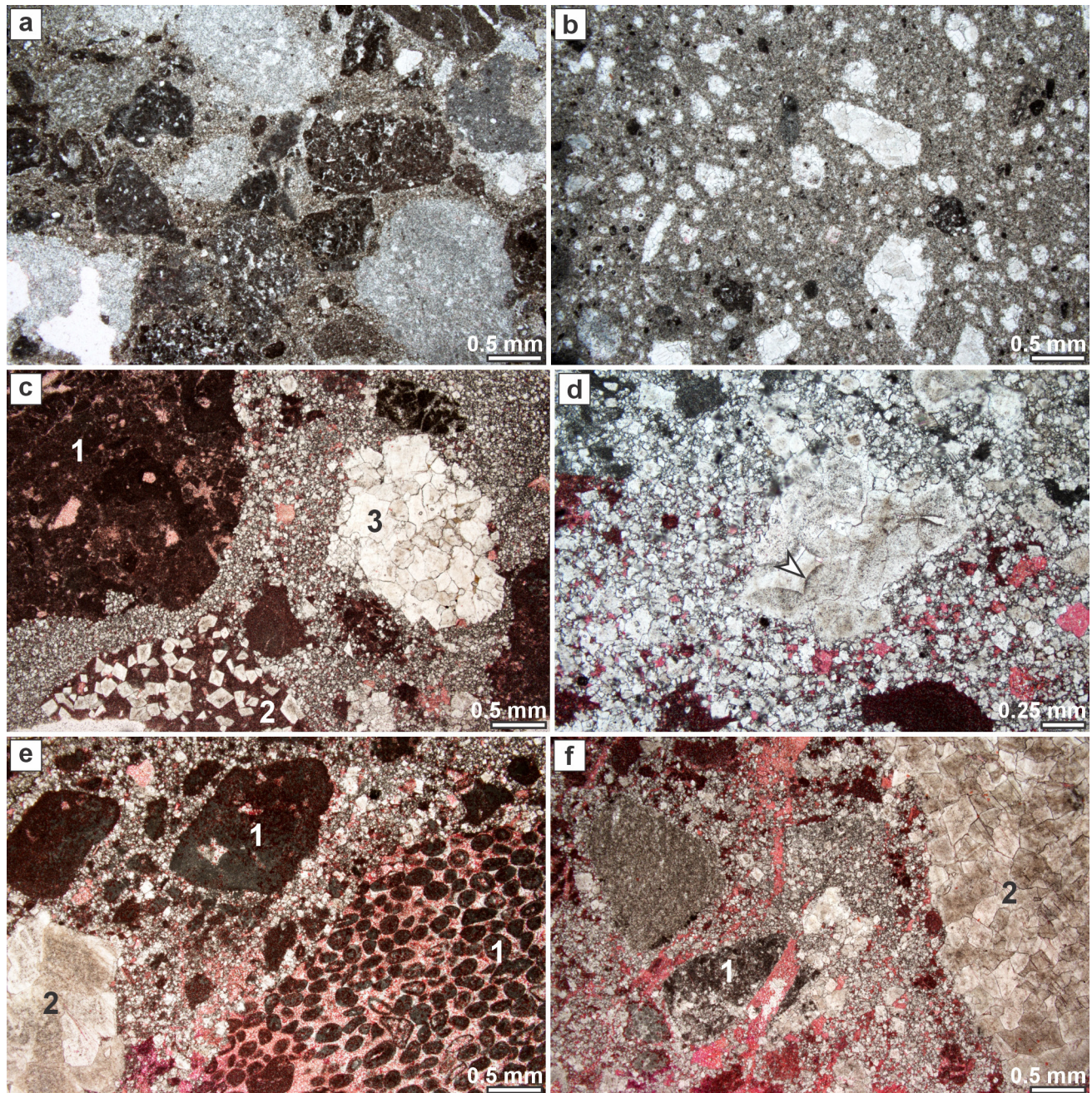


Fig. 7. Dolomitization of Lower Jurassic breccias. All pictures are from the stained parts of the thin sections. **a:** Pervasive dolomitization of clasts and matrix. Thin section 1903; outcrop 3; Sinemurian. **b:** Pervasive dolomitization of clasts and matrix. Most dolomite in the clasts is non-mimetic, subhedral. Thin section 1906; outcrop 3; Sinemurian. **c:** Different degrees of dolomitization of breccia. Some clasts are undolomitized (1), others partly dolomitized with euhedral rhomboidal dolomite (2), and some non-mimically replaced by subhedral dolomite (3). The breccia matrix is mostly dolomitized. Thin section 1921; outcrop 4 (upper); Toarcian. **d:** Mimical dolomitization of oolitic grainstone. Outlines of ooids is indicated by the arrowhead. Thin section 1915; outcrop 4 (upper); Toarcian. **e:** Partial dolomitization of breccia, with undolomitized (1) and completely dolomitized clasts (2). Thin section 1916; outcrop 4 (upper); Toarcian. **f:** Partial dolomitization of breccia. Mimical (1) and non-mimical (2) dolomitization of clasts. Thin section 1916; outcrop 4 (upper); Toarcian.

In contrast, Toarcian breccia shows only partial dolomitization (Fig. 7c–f). Some of the clasts are completely devoid of dolomitization or are only partly dolomitized. These are calcimudstone (partially dolomitized clasts show non-mimical growth of euhedral, rhombic dolomite crystals), peloidal packstone, and bioclastic wackestone. Oolitic grainstone is present in a non-dolomitized as well as completely dolomitized variety. The latter comprises mimical replacement by coarse subplanar dolomite. Completely dolomitized clasts include non-mimical, unimodal, subhedral dolomite, and polymodal, non-mimical subhedral dolomite. The matrix of the breccia is partially or completely dolomitized, non-mimically replaced by euhedral crystals of dolomite of different sizes (polymodal), or by both, subplanar and euhedral crystals of dolomite.

Discussion

Interpretation of described outcrops

The outcrops described above contain two types of sedimentary bodies that are here interpreted as evidence for extensional tectonics: (1) neptunian dykes, and (2) breccias associated with palaeofaults.

Neptunian dykes are “sedimentary dykes and sills formed by sediment filling of submarine fissures or cavities” (Lehner, 1991, p. 593). They can be “caused by extensional movement of lithified and indurated sediment due to gravitational mass movement or differential tectonic movement” (Lehner, 1991, p. 593). Alternatively, open spaces could be created by dissolution by meteoric waters during the emergence of the platform (Winterer et al., 1991). Early Jurassic tectonics was advocated as a possible cause for the formation of the neptunian dykes cutting through the shallow platform deposits of the former Trento Platform in the Sasso Rosso region in Trentino, northern Italy (Lehner, 1991), and for the dykes transecting the Upper Triassic and Lower Jurassic peritidal facies of the Julian Carbonate Platform in the Julian Alps, Slovenia (Babić, 1981; Šmuc, 2005; Črne et al., 2007). These last are dated as probably Pliensbachian in age (Črne et al., 2007). Small-scale neptunian dykes have also been recognized in Sinemurian limestone from the vicinity of Ig, but they are filled with intraclastic-bioclastic packstone containing Upper Jurassic microfossils (Rožič et al., 2018). Evidence of neptunian dykes and sills is unambiguous in outcrop 1. No fossils were found in the infill of neptunian dykes at Pijava Gorica. Based on lo-

cally derived clasts that are barely detached from the sides of the dykes and sills, we assume that their age is similar to that of the host rock, i.e. Hettangian – ?Sinemurian in age.

In the case of outcrops 2 and 3, it seems that breccia deposited along fault-scars. Combining the existence of paleo-scars and the large thickness of the breccia in outcrops 2 and 3, interpretation of this as intraformational breccia related to subaerial exposures and the Lofer cycle-type of sedimentation can be excluded. Instead, breccias deposited at the base of the scarp, which itself was created by a normal fault in the form of submarine talus (see Mišík et al., 1994; Ruiz-Ortiz et al., 2004; Aubrecht & Szulc, 2006; Ortner et al., 2008). The matrix-supported nature of the breccia suggests deposition from submarine debris flows (Fig. 2 in Ribes et al., 2019), rather than via collapse of the footwall (Ortner et al., 2008). As described above, the breccia from outcrop 2 is of Sinemurian age or slightly older. Seemingly the same miliolid foraminifera were found in the clasts and matrix of breccias from outcrops 2 and 3, so Hettangian – Sinemurian age is also assumed for the latter too. In the section below the summit of Mt. Krim (outcrop 4), carbonate breccias occur below as well as above the Lithiotid Limestone Member. The first breccia is lithologically identical to the breccia recorded in outcrops 2 and 3, but the geometry of the breccia could not be determined, nor were any palaeofaults identified.

The breccia overlying the Lithiotid Limestone Member clearly differs from the above mentioned breccias in age, in the composition of the clasts and matrix, in the manner of dolomitization, and in their being under- and overlain by subtidal carbonates. Here also, the geometry of the breccia body is not determined due to the vegetative cover of the area. However, the variety of clasts, which are mixed with ooids, sponge and coral fragments, derived from an active carbonate platform suggests that this too could be scarp breccia.

The late Pliensbachian – Toarcian extension is clearly manifested in the partial disintegration of the north-eastern margin of the Southern Tethyan Megaplatform margin (Dragičević & Velić, 2002), the deepening of some other areas of the same platform (Masetti et al., 2012; Sabatino et al., 2013; Ettinger et al., 2021), and the break-up and partial subsidence of the Julian Carbonate Platform (Šmuc, 2005; Šmuc & Goričan, 2005; Rožič et al., 2014; Gale et al., 2021). The effects of the earlier, Hettangian–Sinemurian extensional tectonics on the Southern Tethyan Megaplatform, are less clear, since the tectonics coincide with eustatic

sea-level changes (Haq et al., 1988; Hallam, 2001), as well as the recovery of skeletal-carbonate producing biota after the biotic crisis at the Triassic/Jurassic boundary (Hallam, 1996; Barattolo & Romano, 2005; Damborenea et al., 2017). Nevertheless, we hypothesise that the extensional tectonics, through the establishment of rugged palaeotopography, played an important role in the recorded facies changes (see Ruiz-Ortiz et al., 2004; Lachkar et al., 2009). This tectonic phase may potentially coincide with the subsidence of the margin, the increased sedimentation of the slope sediments, and the tilting of tectonic blocks in the Slovenian Basin (Rožič et al., 2017).

Timing and style of dolomitization

Despite the differences in the completeness of dolomitization (pervasive dolomitization of the Hettangian–Sinemurian breccia, and the partial dolomitization of the Toarcian breccia), subhedral and euhedral dolomite textures predominate in both cases. Planar dolomite forms early during diagenesis at temperatures below 50 °C (Gregg & Sibley, 1984; Warren, 2000), so an early diagenetic dolomitization is assumed for both types of breccia.

Early, even penecontemporaneous dolomitization has been postulated for the lowermost Jurassic peritidal dolomites of the Mt. Krim area (Ogorelec, 2009), as well as for analogous Upper Triassic dolomites from Slovenia and Hungary (Ogorelec & Rothe, 1993; Haas & Demény, 2002; Haas et al., 2015). For the peritidal facies of the Krka Member, microbially induced precipitation of the Ca–Mg carbonate precursor to dolomite is assumed, coupled with penecontemporaneous mimetic dolomitization via evaporative pumping or seepage influx. In contrast, dolomitization via reflux of slightly evaporated seawater after deposition of the sediment was suggested for the subtidal facies (Haas et al., 2015).

In the case of the Hettangian–Sinemurian breccia, we thus assume that some of the clasts were dolomitized already prior to brecciation, and that pervasive dolomitization of the rest of the clasts, as well as the matrix of the breccia, took place via the reflux of seawater after the deposition of the breccia and its subsequent burial by younger peritidal deposits. The variations in dolomite textures between different clasts and matrix could be explained by precursor grain size and mineralogical composition, and/or differences in concentrations of Mg ions in dolomitizing fluids (see Sibley &

Gregg, 1987). The coarse-grained dolomite fabrics observed in some clasts, probably formed during later stages of diagenesis from finer-grained precursors (Warren, 2000; Haas & Demény, 2002; Ogorelec, 2009).

A similar early diagenetic dolomitization is assumed for the Toarcian breccia. However, due to deposition in a completely subtidal environment, it is possible that some other mechanism of dolomitization should be applied, such as one of the normal marine dolomite models (see Warren, 2000, fig. 10).

Conclusions

Early Jurassic extensional tectonics is manifested in the northern sector of the Southern Tethyan Megaplatform of the central Slovenia in the presence of neptunian dykes and sills cutting through the peritidal dolostone, and in possible scarp breccias. The latter occur at two stratigraphic levels. The Hettangian – Sinemurian breccias are pervasively dolomitized. Clasts are poorly sorted and matrix supported. Their occurrence could be related to the “diffused rifting stage” recognized across the western and central Southern Alps at the beginning of the Jurassic. The younger breccias some metres thick are Toarcian in age. They are matrix-supported with poorly sorted clasts. Limestone clasts predominate over dolomitic ones and are more variable in texture. Radial ooids, coral and sponge fragments occur within the matrix.

Extensional tectonics had a significant effect on the architecture of the Southern Tethyan Megaplatform in the Early Jurassic. While the late Pliensbachian – Toarcian extension had a regional impact, leading to the breaking-up of the Southern Tethyan Megaplatform, the earlier extension may have governed the Hettangian – Pliensbachian transition from peritidal facies towards the predominantly subtidal lagoon and shoal facies observed within the Podbukovje Formation.

Acknowledgements

The research was supported by the Slovenian Research Agency (research core fundings No. P1-0011 and P1-0195). Thin sections were prepared at the Geological Survey of Slovenia. We thank the reviewers for their thorough reading of and constructive remarks on the manuscript.

References

- Aubrecht, R. & Szulc, J. 2006: Deciphering of the complex depositional and diagenetic history of a scarp limestone breccia (Middle Jurassic Krasin Breccia, Pieniny Klippen Belt, Western Carpathians). *Sed. Geol.*, 186/3-4: 265–281. <https://doi.org/10.1016/j.sedgeo.2005.11.020>
- Babić, L. 1981: The origin of "Krn Breccia" and the role of the Krn area in the Upper Triassic and Jurassic history of the Julian Alps. *Vjesnik Zavoda za geološka i geofizička istraživanja*, ser. A, *Geologija*, 38/39: 59–87.
- Banner, F.T., Whittaker, J.E., BouDagher-Fadel, M.K. & Samuel, A. 1997: *Socotraina*, a new hauraniid genus from the upper Lias of the Middle East (Foraminifera, Textulariina). *Rev. Micropaleontol.*, 40/2: 115–123. [https://doi.org/10.1016/S0035-1598\(97\)90514-6](https://doi.org/10.1016/S0035-1598(97)90514-6)
- Barattolo F. & Romano R. 2005: Shallow carbonate platform bioevents during the Upper Triassic-Lower Jurassic: an evolutive interpretation. *Boll. Soc. Geol. It.*, 124: 123–142.
- Berra, F., Galli, M.T., Reghellin, F., Torricelli, S. & Fantoni, R. 2009: Stratigraphic evolution of the Triassic–Jurassic succession in the Western Southern Alps (Italy): the record of the two-stage rifting on the distal passive margin of Adria. *Basin Res.*, 21: 335–353. <https://doi.org/10.1111/j.1365-2117.2008.00384.x>
- Bertotti G., Picotti V., Bernoulli D. & Castellarin A. 1993: From rifting to drifting: tectonic evolution of the Southalpine upper crust from the Triassic to the early Cretaceous. *Sediment. Geol.* 86: 53–76. [https://doi.org/10.1016/0037-0738\(93\)90133-P](https://doi.org/10.1016/0037-0738(93)90133-P)
- Bosellini, A. 2004: The western passive margin of Adria and its carbonate platforms. In: Crescimenti, V., D'Offizi, S., Merlino, S. & Sacchi, L. (eds.): *Geology of Italy*, Special volume of the Italian Geological Society for the IGC 32 Florence-2004. Societa Geologica Italiana, Roma: 79–91.
- BouDagher-Fadel, M. 2018: Evolution and geological significance of larger benthic foraminifera (2nd edition). UCL Press, London: 693 p.
- Brajkovič, R., Djurić, B., Gerčar, D., Cvetko Tešović, B., Rožič, B. & Gale, L. 2022: Mid-Cretaceous calcarenite in stone products from the Roman colony of Emona, Regio X (modern Ljubljana, Slovenia). *Archeometry*, 2022: 1–19. <https://doi.org/10.1111/arcm.12814>
- Buser, S. 1965: *Stratigrafski razvoj jurskih skladov na južnem Primorskem, Notranjskem in zahodni Dolenjski* (dissertation). University of Ljubljana, Faculty of Natural Sciences and Technology, Department for Mineralogy and Geology, Ljubljana: 101 p.
- Buser, S. 1968: Osnovna geološka karta SFRJ 1: 100.000. List Ribnica. Zvezni geološki zavod, Beograd.
- Buser, S. 1974: Osnovna geološka karta SFRJ 1: 100.000. Tolmač lista Ribnica. Zvezni geološki zavod, Beograd: 60 p.
- Buser, S. 1989: Development of the Dinaric and the Julian carbonate platforms and of the intermediate Slovenian Basin (NW Yugoslavia). *Boll. Soc. Geol. Ital.*, 40: 313–320.
- Buser, S. 1996: Geology of Western Slovenia and its paleogeographic evolution. In: Drobne, K., Goričan, Š. & Kotnik, B. (eds.): *International workshop Postojna '96: The role of impact processes and biological evolution of planet Earth*. Scientific Research Centre SAZU, Ljubljana: 111–123.
- Buser, S., Grad, K. & Pleničar, M. 1967: Osnovna geološka karta SFRJ 1: 100.000. List Postojna. Zvezni geološki zavod, Beograd.
- Clari, P. & Masetti, D. 2002: The Trento Ridge and the Belluno Basin. In: Santantonio M. (ed.): *General Field Trip Guidebook, VI International Symposium on the Jurassic System*, 12-22 September 2002. Palermo: 271–315.
- Črne, A.E. & Goričan, Š. 2008: The Dinaric Carbonate Platform margin in the Early Jurassic: a comparison between successions in Slovenia and Montenegro. *Boll. Soc. Geol. It. (Ital. J. Geosci.)*, 127: 389–405.
- Črne, A.E., Šmuc, A. & Skaberne, D. 2007: Jurassic neptunian dykes at Mt Mangart (Julian Alps, NW Slovenia). *Facies*, 53: 249–265. <https://doi.org/10.1007/s10347-007-0102-8>
- Damborenea, S.E., Echevarría, J. & Ros-Franch, S. 2017: Biotic recovery after the end-Triassic extinction event: Evidence from marine bivalves of the Neuquén Basin, Argentina. *Palaeogeogr., Palaeoclimatol., Palaeoecol.*, 487: 93–104. <https://doi.org/10.1016/j.palaeo.2017.08.025>
- Dozet, S. 2009: Lower Jurassic carbonate succession between Predole and Mlačovo, Central Slovenia. *RMZ - Min. Mettal. Quarterly*, 56: 164–193.
- Dozet, S. & Strohmenger, C. 1996: Late Malm carbonate breccias at Korinj and their significance for eustasy and tectonics (central Slovenia). *Geologija*, 37/38: 215–223. <https://doi.org/10.5474/geologija.1995.008>
- Dozet, S. & Strohmenger, C. 2000: Podbukovje Formation, central Slovenia. *Geologija*, 43: 197–212. <https://doi.org/10.5474/geologija.2000.014>

- Dragičević, I. & Velić, I. 2002: The northeastern margin of the Adriatic Carbonate Platform. *Geol. Croatica*, 55: 185–232. <https://doi.org/10.4154/GC.2002.16>
- Dunham, R.J. 1962: Classification of carbonate rocks according to depositional texture. In: Han, W.E. (ed.): *Classification of carbonate rocks, A symposium*. American Ass. Petrol. Geol.: 108–121.
- Embry, A.F. & Klovan, J.E. 1971: A late Devonian reef tract on northeastern Banks Island, N.W.T. *Bull. Can. Petrol. Geol.*, 19: 730–781.
- Ettinger, N.P., Larson, T.E., Kerans, C., Thibodeau, A.M., Hattori, K.E., Kacur, S.M. & Martindale, R.C. 2021: Oceanic acidification and photic-zone anoxia at the Toarcian Oceanic Anoxic Event: insights from the Adriatic Carbonate Platform. *Sedimentology*, 68: 63–107. <https://doi.org/10.1111/sed.12786>
- Gale, L. 2015: Microfacies characteristics of the Lower Jurassic lithiotid limestone from northern Adriatic Carbonate Platform (central Slovenia). *Geologija*, 58/2: 121–138. <https://doi.org/10.5474/geologija.2015.010>
- Gale, L. & Kelemen, M. 2017: Early Jurassic foraminiferal assemblages in platform carbonates of Mt. Krim, central Slovenia. *Geologija*, 60/1: 99–115. <https://doi.org/10.5474/geologija.2017.008>
- Gale, L., Kukoč, D., Rožič, B. & Vidervol, A. 2021: Sedimentological and paleontological analysis of the Lower Jurassic part of the Zatrnik Formation on the Pokljuka plateau, Slovenia. *Geologija*, 64/2: 173–188. <https://doi.org/10.5474/geologija.2021.010>
- Gregg, J.M. & Sibley, D.F. 1984: Epigenetic dolomitization and the origin of xenotopic dolomite texture. *J. Sed. Petrol.*, 54, 908–931. <https://doi.org/10.1306/212F8535-2B24-11D7-8648000102C1865D>
- Haas, J. & Demény, A. 2002: Early dolomitisation of Late Triassic platform carbonates in the Transdanubian Range (Hungary). *Sed. Geol.*, 151/3-4: 225–242. [https://doi.org/10.1016/S0037-0738\(01\)00259-7](https://doi.org/10.1016/S0037-0738(01)00259-7)
- Haas, J., Lukoczki, G., Budai, T. & Demény, A. 2015: Genesis of Upper Triassic peritidal dolomites in the Transdanubian Range, Hungary. *Facies*, 61/8. <https://doi.org/10.1007/s10347-015-0435-7>
- Hallam, A. 1996: Recovery of the marine fauna in Europe after the end-Triassic and early Toarcian mass extinctions. In: Hart, M.B. (ed.): *Biotic recovery from mass extinction events*. *Geol. Soc. Spec. Publ.*, 102: 231–236. <https://doi.org/10.1144/GSL.SP.1996.001.01.16>
- Hallam, A. 2001: A review of the broad pattern of Jurassic sea-level changes and their possible causes in the light of current knowledge. *Palaeogeogr., Palaeoclimatol., Palaeoecol.*, 167/1-2: 23–37. [https://doi.org/10.1016/S0031-0182\(00\)00229-7](https://doi.org/10.1016/S0031-0182(00)00229-7)
- Haq, B.U., Hardenbol, J. & Vail, P.R. 1988: Mesozoic and Cenozoic chronostratigraphy and cycles of sea-level change. In: *Sea-level changes – an integrated approach*. *SEPM Spec. Publ.*, 42: 71–108. <https://doi.org/10.2110/pec.88.01.0071>
- Knez, M., Otoničar, B. & Slabe, T. 2003: Subcutaneous stone forest (Trebnje, central Slovenia). *Acta Carsologica*, 32/1: 29–38. <https://doi.org/10.3986/ac.v32i1.362>
- Lachkar, N., Guiraud, M., El Harfi, A., Dommergues, J.-L., Dera, G. & Durlet, C. 2009: Early Jurassic normal faulting in a carbonate extensional basin: characterization of tectonically driven platform drowning (High Atlas rift, Morocco). *J. Geol. Soc.*, 166: 413–430. <https://doi.org/10.1144/0016-76492008-084>
- Lehner, B.L. 1991: Neptunian dykes along a drowned carbonate platform margin: an indication for recurrent extensional tectonic activity? *Terra Nova*, 3: 593–602. <https://doi.org/10.1111/j.1365-3121.1991.tb00201.x>
- Martinuš, M. & Bucković, D. 2015: Lithofacies, biostratigraphy and discontinuity surfaces recorded in deposits across the Pliensbachian–Toarcian transition (Lower Jurassic) in southern Lika and Velebit Mt. (Croatia). In: Wacha, L. & Horvat, M. (eds.): *Abstracts book, 5th Croatian Geological Congress with international participation, Osijek 23.–25.09.2015*. Hrvatski geološki institut, Zagreb: 162–163.
- Masetti, D., Fantoni, R., Romano, D.S. & Trevisani, E. 2012: Tectonostratigraphic evolution of the Jurassic extensional basins of the eastern southern Alps and Adriatic foreland based on an integrated study of surface and subsurface data. *AAPG Bull.*, 96/11: 2065–2089. <https://doi.org/10.1306/03091211087>
- Matenco, L.C. & Haq, B.U. 2020: Multi-scale depositional successions in tectonic settings. *Earth-Sci. Rev.*, 200: 102991. <https://doi.org/10.1016/j.earscirev.2019.102991>
- Meschede, M. & Warr, L.N. 2019: *The Geology of Germany – a process-oriented approach*. Springer Nature Switzerland, Cham: 304 p.
- Miler, M. & Pavšič, J. 2008: Triassic and Jurassic beds in Krim Mountain area (Slovenija).

- Geologija, 51/1: 87–99: <https://doi.org/10.5474/geologija.2008.010>
- Mišík, M., Sýkora, M. & Aubrecht, R. 1994: Middle Jurassic scarp breccias with clefts filled by Oxfordian and Valanginian-Hauterivian sediments, Krasin near Dolná Súča (Pieniny Klippen Belt, Slovakia). *Geol. Carpathica*, 45: 343–356.
- Ogorelec, B. 2009: Lower Jurassic beds at Preserje near Borovnica (Central Slovenia). *Geologija*, 52/2: 193–204. <https://doi.org/10.5474/geologija.2009.019>
- Ogorelec, B. & Rothe, P. 1993: Mikrofazies, Diagenese und Geochemie des Dachsteinkalkes und Hauptdolomits in Süd-West-Slowenien. *Geologija*, 35: 81–181. <https://doi.org/10.5474/geologija.1992.005>
- Ortner, H., Ustaszewski, M. & Rittner, M. 2008: Late Jurassic tectonics and sedimentation: breccias in the Unken syncline, central Northern Calcareous Alps. *Swiss J. Geosci.*, 101, suppl. 1: 55–71. <https://doi.org/10.1007/s00015-008-1282-0>
- Placer, L. 1999: Contribution to the macrotectonic subdivision of the border region between Southern Alps and External Dinarides. *Geologija*, 41: 223–255. <https://doi.org/10.5474/geologija.1998.013>
- Pleničar, M. 1970: Osnovna geološka karta SFRJ 1: 100.000. Tolmač lista Postojna. Zvezni geološki zavod, Beograd: 62 p.
- Ratschbacher, L., Dingeldey, C., Miller, C., Hacker, B.R. & McWilliams, M.O. 2004: Formation, subduction, and exhumation of Penninic oceanic crust in the Eastern Alps: time constraints from $^{40}\text{Ar}/^{39}\text{Ar}$ geochronology. *Tectonophysics*, 394/3-4: 155–170. <https://doi.org/10.1016/j.tecto.2004.08.003>
- Ribes, C., Ghienne, J.-F., Manatschal, G., Decarlis, A., Karner, G.D., Figueiredo, P.H. & Johnson, C.A. 2019: Long-lived mega fault-scarps and related breccias at distal rifted margins: insights from present-day and fossil analogues. *J. Geol. Soc.*, 176: 801–816. <https://doi.org/10.1144/jgs2018-181>
- Rožič, B. & Šmuc, A. 2009: Jurska evolucija prehodne cone med Julijsko karbonatno platformo in Slovenskim bazenom. *Geološki zbornik*, 20: 146–151.
- Rožič, B., Venturi, F. & Šmuc, A. 2014: Ammonites from Mt Kobla (Julian Alps, NW Slovenia) and their significance for precise dating of Pliensbachian tectono-sedimentary event. *RMZ – Min. Mettal. Quarterly*, 61: 191–201.
- Rožič, B., Kolar-Jurkovšek, T., Žvab Rožič, P. & Gale, L. 2017: Sedimentary record of subsidence pulse at the Triassic/Jurassic boundary interval in the Slovenian Basin (eastern Southern Alps). *Geol. Carpathica*, 68/6: 543–561. <https://doi.org/10.1515/geoca-2017-0036>
- Rožič, B., Gale, L., Brajkovič, R., Popit, T. & Žvab Rožič, P. 2018: Lower Jurassic succession at the site of potential Roman quarry Staje near Ig (central Slovenia). *Geologija*, 61/1: 49–71. <https://doi.org/10.5474/geologija.2018.004>
- Ruiz-Ortiz, P.A., Bosence, D.W.J., Rey, J., Nieto, L.M., Castro, J.M. & Molina, J.M. 2004: Tectonic control of facies architecture, sequence stratigraphy and drowning of a Liassic carbonate platform (Betic Cordillera, Southern Spain). *Basin Res.*, 16: 235–257. <https://doi.org/10.1111/j.1365-2117.2004.00231.x>
- Sabatino, N., Vlahović, I., Jenkyns, H.C., Scopeliti, G., Neri, R., Prtoljan, B. & Velić, I. 2013: Carbon-isotope record and palaeoenvironmental changes during the early Toarcian oceanic anoxic event in shallow-marine carbonates of the Adriatic Carbonate Platform in Croatia. *Geol. Mag.*, 150: 1085–1102. <https://doi.org/10.1017/S0016756813000083>
- Sarti, M., Bosellini, A. & Winterer, E. L. 1993: Basin geometry and architecture of the Tethyan passive margin (Southern Alps, Italy): implications for rifting mechanisms. In: Watkins, J. S. et al. (eds): *Geology and Geophysics of continental margins*. AAPG Mem. 53: 241–258. <https://doi.org/10.1306/M53552C13>
- Sibley, D.F. & Gregg, J.M. 1987: Classification of dolomite rock textures. *J. Sed. Petrol.*, 57: 967–975. <https://doi.org/10.1306/212F8CBA-2B24-11D7-8648000102C1865D>
- Strohmenger, C. & Dozet, S. 1991: Stratigraphy and geochemistry of Jurassic carbonate rocks from Suha krajina and Mala gora mountain (Southern Slovenia). *Geologija*, 33: 315–351. <https://doi.org/10.5474/geologija.1990.008>
- Šmuc, A. 2005: *Jurassic and Cretaceous stratigraphy and sedimentary evolution of the Julian Alps, NW Slovenia*. ZRC Publishing, ZRC SAZU, Ljubljana: 98 p.
- Šmuc, A. 2010: *Jurassic and Cretaceous neptunian dikes in drowning successions of the Julian High (Julian Alps, NW Slovenia)*. RMZ – Min. Mettal. Quarterly, 57: 195–214.
- Šmuc, A. & Goričan, Š. 2005: *Jurassic sedimentary evolution of a carbonate platform into a deep-water basin, Mt. Mangart (Slovenian-Italian border)*. *Riv. Ital. Paleont. Strat.*, 111: 45–70. <https://doi.org/10.13130/2039-4942/6269>

- Velić, I. 2007: Stratigraphy and palaeobiogeography of Mesozoic benthic Foraminifera of the Karst Dinarides (SE Europe). *Geol. Croatica*, 60: 1–113.
- Vlahović, I., Tišljar, J., Velić, I. & Matičec, D. 2002: The karst Dinarides are composed of relics of a single Mesozoic platform: facts and consequences. *Geol. Croatica*, 55: 171–183.
- Vlahović, I., Tišljar, J., Velić, I. & Matičec, D. 2005: Evolution of the Adriatic Carbonate Platform: Palaeogeography, main events and depositional dynamics. *Palaeogeogr., Palaeoclimatol., Palaeoecol.*, 220: 333–360. <https://doi.org/10.1016/j.palaeo.2005.01.011>
- Warren, J. 2000: Dolomite: occurrence, evolution and economically important associa-
- tions. *Earth-Sci. Rev.*, 52: 1–81. [https://doi.org/10.1016/S0012-8252\(00\)00022-2](https://doi.org/10.1016/S0012-8252(00)00022-2)
- Winterer, E.L. & Bosellini, A. 1981: Subsidence and sedimentation on a Jurassic passive continental margin, Southern Alps (Italy). *Am. Assoc. Petroleum Geol. Bull.*, 65: 394–421. <https://doi.org/10.1306/2F9197E2-16CE-11D7-8645000102C1865D>
- Winterer, E.L., Metzler, C.V. & Sarti, M. 1991: Neptunian dykes and associated breccias (Southern Alps, Italy and Switzerland): role of gravity sliding in open and closed systems. *Sedimentology*, 38/3: 381–404. <https://doi.org/10.1111/j.1365-3091.1991.tb00358.x>
- Wright, P. 1992: A revised classification of limestones. *Sed. Geology*, 76: 177–185.



Vsebnosti potencialno strupenih elementov v sedimentih in vodah reke Meže in njenih pritokov, ki odvodnjavajo odlagališča rudarskih odpadkov

Contents of potentially toxic elements in sediments and waters of the Meža river and its tributaries draining mine waste deposits

Mateja GOSAR, Špela BAVEC, Miloš MILER & Martin GABERŠEK

Geološki zavod Slovenije, Dimičeva ulica 14, SI-1000 Ljubljana, Slovenija; e-mail: mateja.gosar@geo-zs.si

Prejeto / Received 5. 12. 2023; Sprejeto / Accepted 20. 3. 2024; Objavljeno na spletu / Published online 29. 3. 2024

Ključne besede: rudarjenje, odlagališča rudarskih odpadkov, kovine in metaloidi, sedimenti, površinska voda, monitoring, rudnik Mežica

Key words: mining, mine waste deposits, metals and metalloides, sediments, stream water, monitoring, Mežica mine

Izvleček

Predstavljeni so rezultati spremeljanja vsebnosti potencialno strupenih elementov (PSE) v sedimentih (v letih 2013, 2017, 2020) in vodah (v letih 2017, 2020) reke Meže ter njenih pritokov, ki odvodnjavajo odlagališča rudarskih odpadkov. Skupno 13 vzorčnih mest je vzpostavljenih v vzorčni shemi, ki omogoča dolgoročno opazovanje vpliva odlagališč rudarskih odpadkov. V sedimentih so zaradi vplivov več kot 300-letnega delovanja rudarsko-predelovalne industrije močno povečane vsebnosti PSE, predvsem Pb, Zn, Cd, Mo in As, ki s časom precej nihajo. Razlike v vsebnostih na istih lokacijah v različnih letih so najbolj izrazite v pritokih reke Meže, ki drenirajo odlagališča rudarskih odpadkov. Na vsebnosti imajo pomemben vpliv hidrološki pogoji, saj so ob višjem vodostaju in višjem pretoku vsebnosti PSE večje. Vodna erozija odlagališč ima pomemben vpliv na dotok onesnaženega materiala v vodotoke. V nasprotju s pritoki, v zgornjem toku reke Meže nismo opazili večjega vpliva višjega vodostaja in pretoka na vsebnosti PSE v sedimentih. Dolvodno od Žerjava so nihanja vsebnosti med posameznimi leti oz. različnimi hidrološkimi pogoji tudi v Meži večja. Predstavljeni rezultati kažejo, da so v sedimentih reke Meže in njenih pritokov vsebnosti Pb, Zn, Cd, Mo in As zelo velike ter krepko presegajo zakonsko določeno kritično vrednost za tla. V površinski vodi so vsebnosti PSE lokalno povečane in se s časom bistveno ne spreminja. Glede na primerjavo z zakonodajnimi smernicami, so v obravnavanih vodah lokalno presežene koncentracije Pb, Cd in Zn. Ocenujemo, da je dinamika obremenjenosti sedimentov reke Meže s PSE vzdolž krajev Črna na Koroškem, Žerjav in Mežica zelo kompleksna. Poleg odlagališč rudarskih odpadkov na vsebnosti PSE v sedimentih in vodah vplivajo tudi razpršeni viri v okolju, kot so onesnažena tla in poplavne ravnice ter njihova različna stopnja onesnaženosti, saj je okolje obremenjeno zaradi dolgoletnih rudarskih in talilniških dejavnosti. Dodaten okoljski vpliv ima morda tudi sedanja industrijska dejavnost v dolini reke Meže.

Abstract

The results of the monitoring of the contents of potentially toxic elements (PTE) in sediments (2013, 2017, 2020) and waters (2017, 2020) of the Meža River and its tributaries, which drain mining waste deposits, are presented. A total of 13 sample sites were established in a sample scheme that enables long-term observation of the impact of mining waste deposits. In the sediments, the content of PTE, especially Pb, Zn, Cd, Mo and As, is greatly elevated and fluctuates with time. The study area is affected by more than 300 years of mining and ore processing industry. The differences in the contents in various years are most pronounced in the Meža River tributaries, which drain the mining waste dumps. Hydrological conditions have a significant influence on the contents in sediments, as PTE content increases with higher water level and higher water flow. Water erosion of mining waste dumps has a significant impact on the discharge of contaminated material into watercourses. In contrast, in the upper part of the Meža River, we did not observe strong influence of higher water level on the content of PTE in the sediments. Fluctuations in the content between individual years and fluctuations between various hydrological conditions are higher again in the middle part of the Meža river, downstream from Žerjav. The presented results demonstrate that the contents of Pb, Zn, Cd, Mo and As in the sediments of the Meža River and its tributaries are very high and that they by far exceed the legislative critical value for the soil. PTE contents in the surface water are elevated in some locations and do not change significantly over time. The local concentrations of Pb, Cd and Zn exceed the legislative guidelines. We estimate that the dynamics of the sediment load in the Meža River along the towns of Črna na Koroškem, Žerjav and Mežica is very complex. In addition to mining waste deposits, the content of PTE in sediments and waters is also affected by scattered sources in the environment, such as contaminated soil and floodplains and their varying degrees of pollution, as the environment has been burdened by long-term mining, ore processing and smelting activities. Current industrial activity may also have an additional environmental impact.

Uvod

Dolgoletno rudarjenje, različna industrija, promet in druge človekove dejavnosti lahko povzročijo povečanje vsebnosti nekaterih elementov v okolju (npr. v tleh, sedimentih) ter spremembe naravnega kroženja elementov. Človekove dejavnosti so geološko recentne in lahko izrazito vplivajo na naše okolje in so globalno prevladujoči vzrok za večino sodobnih okoljskih sprememb (Lewis & Maslin, 2015). Geokemično kartiranje tal v kontinentalnem merilu (projekt GEMAS) je pokazalo, da so prisotnost rudišč s spremljajočo rudarsko-predelovalno industrijo, litološka sestava in podnebje pomembni dejavniki, ki vplivajo na porazdelitve elementov v tleh. Na primer, pozitivne anomalije svinca zaznamujejo večino mineraliziranih območij po Evropi (Reimann et al., 2012), delovanje največjega rudnika živega srebra (Almadén) pa je povzročilo veliko pozitivno anomalijo živega srebra v osrednji Španiji (Ottesen in sodelavci, 2013; Ballabio et al., 2021). Tudi v Sloveniji so bili ugotovljeni lokalni in regionalni vplivi dolgoletnega pridobivanja kovinskih mineralnih surovin (Šajn & Gosar, 2004; Gosar et al., 2006; Fux & Gosar, 2007; Gosar & Miler, 2011; Miler & Gosar, 2012; Žibret et al., 2018; Gosar et al., 2019; Miler et al., 2022). Kovine in drugi potencialno strupeni elementi (PSE), prvotno sproščeni v okolje zaradi rudarjenja in predelave rud, so po nekaj letih razpršeno prisotne v različnih predelih površja kot difuzna onesnaževala v tleh in sedimentih ter nakopičene v različnih odlagališčih, od katerih so najpomembnejša odlagališča rudarskih odpadkov (Salomons & Förstner, 1988; Kesler, 1994; Boni et al., 1999).

Po hujših okoljskih nesrečah povezanih tudi z odloženimi rudarskimi odpadki v svetu v zadnjih 30-tih letih (na primer Aznacolar leta 1998 (Galán et al., 2002) in Baia Mare leta 2000 (Cunningham, 2005), se je pokazala potreba po ustreznejši zakonodaji. Evropska komisija je leta 2006 sprejela Uredbo o ravnanju z odpadki iz rudarskih in drugih ekstraktivnih dejavnosti (v nadaljevanju Direktiva 2006/21/ES), s katero je določila ukrepe, postopke in smernice za preprečevanje ali zmanjševanje škodljivih vplivov na okolje, zlasti na vodo, zrak, tla, favno in floro, pokrajine, ter tveganj za zdravje ljudi, ki so nastali kot posledica ravnanja z odpadki iz ekstraktivnih dejavnosti. Ti ukrepi zajemajo ravnanje z odpadki, ki nastanejo pri raziskovanju, pridobivanju, bogatenju in skladiščenju mineralnih surovin. Direktiva 2006/21/ES je bila leta 2008 prenesena tudi v pravni red Slovenije (Uradni list RS, št. 43/08, 30/11, 64/21 in 44/22 – ZVO-2). V omenjeni direktivi je med drugim navedeno, da

mora vsaka država članica zbrati podatke o zaprtih in opuščenih odlagališčih rudarskih odpadkov ter opredeliti ali obstaja potencialna nevarnost, da bi ta odlagališča lahko povzročila resne škodljive vplive na okolje in srednjeročno ali kratkoročno postala resna grožnja za zdravje ljudi ali okolje. Geološki zavod Slovenije (GeoZS) je zbiral potrebne podatke o zaprtih in opuščenih odlagališčih rudarskih odpadkov ter po posebni metodologiji, ki smo jo podrobno opisali Gosar in sodelavci (2014; 2017; 2020; 2021), določil tista zaprta odlagališča rudarskih odpadkov, ki bi lahko povzročila resne škodljive vplive na okolje in bi zato lahko obstajala resna grožnja za zdravje ljudi ali okolje ter jih je zato potrebno, skladno z omenjeno direktivo, redno (na vsaka 3 leta) opazovati oz. spremljati.

Zaradi več kot 300 let trajajoče rudarsko-predelovalne dejavnosti je območje zgornje Mežiške doline močno obremenjeno. Analize tal (Kugonič & Zupan, 1999; Vreča et al., 2001; Šajn, 2006; Zupan et al., 2008; Finžgar et al., 2014) so pokazale močno onesnaženost s Pb, Zn in Cd. Z geokemičnim kartiranjem tal sta Šajn in Gosar (2004) ugotovila, da so tla najbolj onesnažena v okolici Žerjava in Črne. Območje kritično onesnaženih tal se nadaljuje s prekinjvami vzdolž reke Meže vse do Raven na Koroškem. Prva sistematična analiza sedimentov vodotokov (reka Meža in njeni pritoki) je pokazala, da so med PSE vsebnosti Pb, Zn in Cd večinoma velike ali povečane (Bole et al., 2002). Kasnejše sistematične analize (Fux & Gosar, 2007; Gosar & Miler, 2011) so pokazale močno onesnaženost sedimentov zgornjega toka reke Meže s Pb, Zn, Mo, Cd in deloma z As, v nižjih delih pa so bile vsebnosti teh elementov manj velike, še vedno pa so močno presegale vrednosti naravnega ozadja. Poleg tega so bile vsebnosti Co, Cr, Cu in Ni povečane na območju Raven zaradi železarske industrije. Skupna ugotovitev študij sedimentov (Svete et al., 2001; Bole et al., 2002; Fux & Gosar, 2007; Gosar & Miler, 2011; Miler & Gosar, 2012) je bila, da so izjemno velike vsebnosti PSE (še posebno Pb, Zn in Cd) v sedimentih Helenskega potoka posledica odvodnjavanja odlagališč rudarskih odpadkov (Helena in Štoparjev odval). Bole in sodelavci (2002) so ugotovili, da so v Helenskem potoku vsebnosti Pb, Cd in Zn povečane tudi v površinski vodi. Miler in Gosar (2012) sta primerjala in ugotovila dobro ujemanje med mineralnimi oblikami ter količinami rudnih mineralov, ki vsebujejo PSE v sedimentu iz Helenskega potoka ter materialu iz gorvodnega odlagališča rudarskih odpadkov (Štoparjev odval). Podobno so Gošar in sodelavci (2015) opazili, da so, zaradi prisotnosti rudarskih odpadkov v zaledju, koncentracije Cr, Cu, Pb in Zn

v vodi v Helenskem potoku nekoliko povečane. V reki Meži dolvodno od Mežice pa so opazili izrazito večje koncentracije Pb in Zn ter v manjši meri tudi Cd, kar so pripisali vplivu rudarskih odpadkov v zaledju in najverjetneje tudi prisotnosti tovarne baterij in druge metalurške industrije na tem območju (Gošar et al., 2015). Novejše raziskave porazdelitve vsebnosti v sedimentih in površinski vodi v reki Meži in pritokih (Goltnik et al., 2022; Miler et al., 2022) so potrdile, da so vsebnosti Pb, Zn in Cd ter v manjši meri Mo in As v sedimentih še vedno zelo velike, medtem ko so v površinski vodi povečane v pritokih Meže, predvsem tistih, ki drenirajo odlagališča rudarskih odpadkov, v Meži pa predvsem na lokacijah dolvodno od Žerjava, kjer se nahaja trenutno dejavna industrija. Miler in sodelavci (2022) so z razmerji Pb izotopov ugotovili, da obstajajo različni viri Pb v sedimentih. Pomemben vir so primarni Pb rudni minerali, ki se nahajajo v orudenih kamninah. Drugi viri so produkti preverjanja, vplivi sedanje industrije v Žerjavu (reciklaža Pb odpadkov) in različna litologija. Poleg tega so izmerili ekstremno velike vsebnosti Pb, Zn in Cd na odlagališčih rudarskih odpadkov, močno sta povečana tudi As in Mo. Z uporabo geoakumulacijskega indeksa so ugotovili, da so sedimenti dolvodno od odlagališč rudarskih odpadkov večinoma močno do zelo močno obremenjeni s PSE. Goltnik in sodelavci (2022) so ocenili, da zaradi velikih vsebnosti PSE, obstaja visoko tveganje za vpliv PSE na vodne organizme, da so vsebnosti Pb, Zn in Cd večje v frakciji < 0,063 mm v primerjavi s frakcijo < 0,150 mm, ter da se razmerja Pb izotopov prostorsko razlikujejo, kar pomeni, da so na območju prisotni različni viri Pb.

Med viri onesnaženja na preiskovanem območju so v preteklosti prevladovali rudarjenje in predelava rude (talilnica svinca). V novejšem času pa poleg močno obremenjenega okolja, še reciklaža svinčevih odpadkov in ostali zelo raznoliki viri (promet, druga industrija, urbanizacija, kmetijstvo). Tako so danes med najpomembnejšimi viri odlagališča rudarskih odpadkov (Budkovič et al., 2003; Miler & Gosar, 2012; Miler et al., 2022), nekdanji rudarski revirji z metalurško dejavnostjo, onesnažene poplavne ravnice (Bidovec, 1997) in onesnažena tla (Šajn & Gosar, 2004). Dodatno k onesnaženju prispeva tudi današnja sekundarna predelava Pb odpadkov (Svete et al., 2001; Miler & Gosar, 2013, 2019; Žibret et al., 2018; Miler et al., 2022). Pomemben pretekli vir obremenitve vodotokov je bilo sproščanje mulja iz separacijske jalovine v reko Mežo do leta 1980 (Žibret et al., 2018). Po letu 1980 so začeli mulj odlagati v opuščene dele rudnika, v stare odkope in tako razbremenili reko

Mežo (Fajmut Štrucl & Pungartnik v Eržen et al., 2002). Poleg imisij v tleh, prahu, zraku in drugih okoljskih medijih so sedaj pomembni viri Pb in nekaterih drugih PSE odlagališča rudarskih odpadkov in dejavnosti, povezane z industrijo. V kamnolomu Žerjav rudarski odpadni material, ki vsebuje veliko svinca in drugih PSE (Miler & Gosar, 2012), reciklirajo v prodajne izdelke za uporabo v gradbeništvu. Gradbeni material se pogosto uporablja v lokalnem okolju. V Žerjavu se izvajajo dejavnost recikliranja odpadkov za pridobivanje Pb, končni odpadki iz procesa recikliranja pa se odlagajo na bližnje odlagališče nevarnih odpadkov (NOMO). Upravljanje odlagališča je pod nadzorom Ministrstva za okolje, podnebje in energijo. V Črni na Koroškem obratuje proizvodnja startnih baterij. Oba industrijska objekta sta uvrščena med industrijske dejavnosti, ki lahko povzročijo onesnaževanje okolja v večjem obsegu, zato sta zavezana k stalnemu monitoringu. Na sliki 1 so prikazana večja odlagališča rudarskih odpadkov, industrijski objekti in odlagališči za nevarne in nenevarne odpadke.

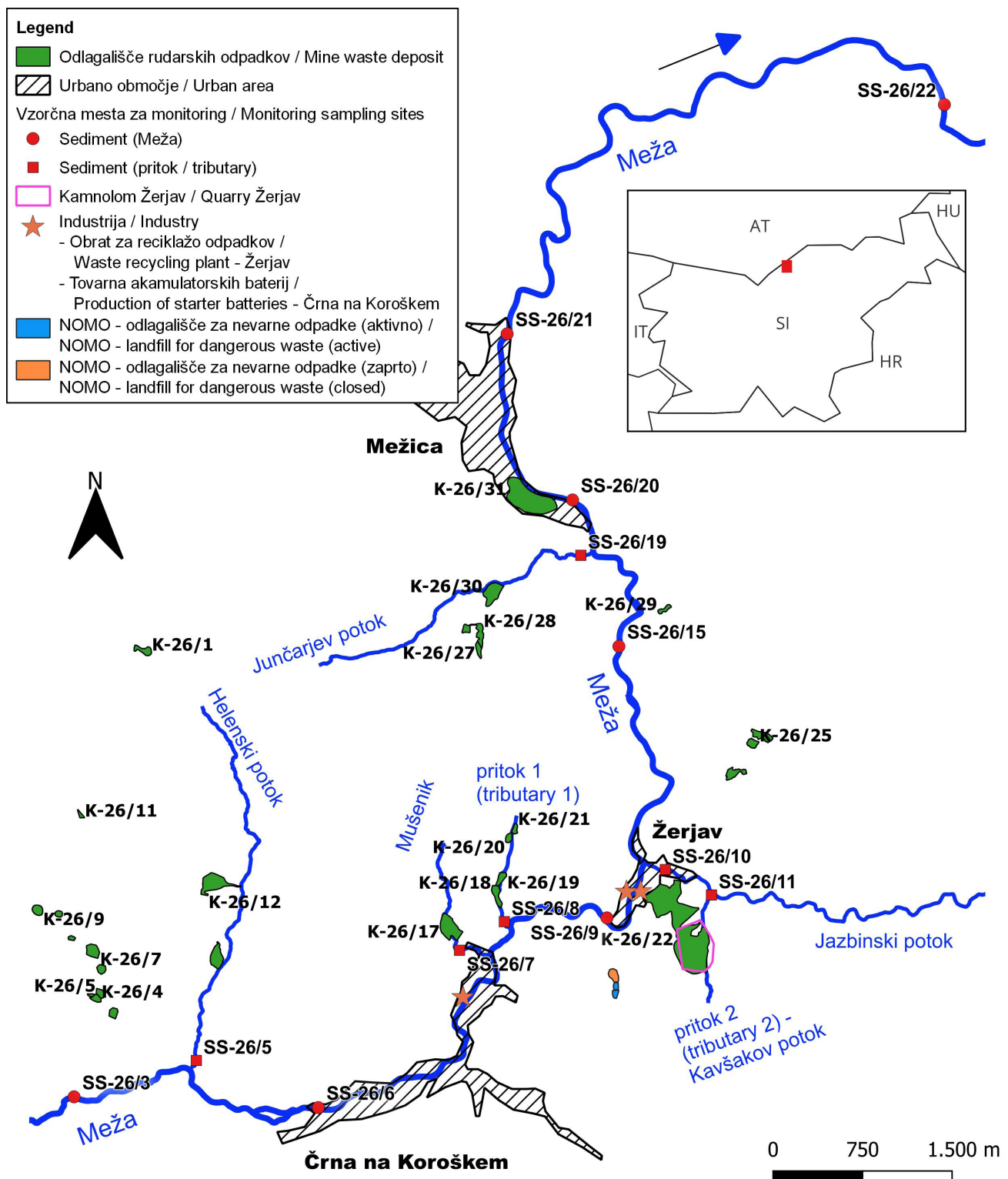
Namen pričujočega članka je strokovni in splošni javnosti predstaviti izsledke raziskav vpliva zaprtih odlagališč rudarskih odpadkov na sedimente in površinske vode na območju nekdanjega rudnika v Mežici od leta 2013 do leta 2020. Posebno pozornost smo posvetili vsebnostim PSE v sedimentih in površinskih vodah dolvodno od omenjenih odlagališč ter njihovi časovni variabilnosti in vplivu hidroloških pogojev na vsebnosti PSE v sedimentih.

Metode

Preiskovano območje, vzorčenje, priprava in analiza vzorcev

Preiskovano območje zajema del vodotoka reke Meže s pritoki (celotno porečje Meže meri 551,68 km²; Kolbezen & Pristov, 1998), kjer se v hidrološkem zaledju nahajajo odlagališča rudarskih odpadkov. To je od območja po pritoku potoka Topla do Prevalj (sl. 1).

Na preiskovanem območju se nahaja zaprti rudnik Mežica, kjer so 300 let pridobivali rudo, iz katere so pridobivali svinec, cink in v zadnjih desetletjih delovanja tudi molibden. Rudišče je epigenetsko tipa Mississippi Valley (MVT), kjer poteka mineralizacija v srednje- do zgornjetriasnih dolomitih in apnencih (Drovenik et al., 1980; Štrucl, 1984; Zeeh et al., 1998; Spangenberg et al., 2001). Glavna rudna minerala sta bila galenit in sfalerit (Drovenik et al., 1980; Štrucl, 1984). Spektralne analize rudnih mineralov iz Mežice kažejo, de je slednih prvin v sfaleritu malo. Edina prvina,



Sl. 1. Shematski prikaz obravnavanega območja z označenimi opazovanimi rudarskimi odlagališči in vzorčnimi mesti za sedimente in vode.
Fig. 1. Schematic study area map with marked observed mining waste deposits and sampling sites for sediments and water.

ki jo vsebujejo vsi vzorci v večji količini je Cd. V skorjastem sfaleritu je sorazmerno veliko As in Tl. Galenit vsebuje le malo slednih prvin, izjema je As, ki ga je v nekaterih vzorcih veliko, v drugih pa manj. Za mežiški galenit sta značilni izredno majhna vsebnost Ag in rahla obogatitev s Sb. Molibden v mežiškem rudišču je vezan v wulfenit, ki

je najbolj razširjen v zgornjem delu rudišča, njegova količina pa z globino upada (Drovenik et al., 1980). Pridobivanje Pb-Zn rude in primarno taljenje Pb na območju Mežice sta prenehala leta 1995, talilnica pa se je preoblikovala v obrat za reciklažo Pb-odpadkov in izrabljenih Pb-kislinskih baterij (sekundarna predelava Pb).

Tabela 1. Podatki o vzorčnih lokacijah.

Table 1. Sampling locations data.

Oznaka lokacije / Mark of sampling site	Zemljepisna dolžina / Longitude	Zemljepisna širi- na / Latitude	Vodotok / Watercourse	Odlagališče rudarskih odpadkov / Mine waste spoil heaps
SS-26/3	14,8083	46,4682	Meža	-
SS-26/5	14,8216	46,4709	Helenski potok	K-26/1 (Drče), K-26/11 (Pavel Mulb), K-26/12 (Štoparjev odval), K-26/13 (Helena)
SS-26/6	14,8349	46,4674	Meža	-
SS-26/7	14,8503	46,4793	Mušenik	K-26/17 (Igrče)
SS-26/8	14,8552	46,4814	Pritok 1/Tributary 1 ¹	K-26/18 (Unionski odval), K-26/19 (Matjaževe odlagališče), K-26/20 (Svitni), K-26/21 (Frančišek)
SS-26/9	14,8664	46,4817	Meža	-
SS-26/10	14,8728	46,4854	Jazbinski potok	K-26/22 (Kavšakovo odl.), K-26/23 (Žerjavski odval)
SS-26/11	14,8778	46,4835	Pritok 2/Tributary 2 ¹	K-26/22 (Kavšakovo odl.)
SS-26/15	14,8677	46,5022	Meža	-
SS-26/19	14,8635	46,5091	Junčarjev potok	K-26/27 (Srce), K-26/28 (Lekšeče), K-26/30 (Fridrih)
SS-26/20	14,8626	46,5132	Meža	-
SS-26/21	14,8554	46,5257	Meža	K-26/31 Glančnik
SS-26/22	14,9031	46,5431	Meža	-

¹manjši vodotoki, ki nimajo uradnega geografskega poimenovanja / smaller watercourses that do not have an official geographical name

Na območju Mežice je 32 deponij rudarskih odpadkov s skupno prostornino približno 7.400.000 m³ (Gosar et al., 2020), kjer so odpadni materiali odlagali na odlagališča v bližnjih ozkih dolinah in na strmih pobočjih manjših potokov. Večinoma so odlagališča sestavljena iz karbonatnih kamnin v katerih se nahaja rudišče (Gosar & Miler, 2011; Miler & Gosar, 2012; Miler et al., 2022 in tam navedeni viri), a tudi iz revne rude in separacijske jalovine ali žlindre.

Pritoki Meže, ki smo jih obravnavali, so Helenski potok, Mušenik, Jazbinski potok, Junčarjev potok z dvema pritokoma, ki nimata jasnega geografskega imena, zato smo jih poimenovali kot pritok 1 (*ang. tributary 1*) in pritok 2 (*ang. tributary 2*; po nekaterih virih imenovan tudi Kavšakov potok). Odlagališča odpadkov, ki jih potoki drenirajo, so podana v tabeli 1 in prikazana na sliki 1. Helenski potok in Jazbinski potok spadata med večje pritoke, medtem ko so ostali pritoki manjši. Reka Meža ima pretežno hudourniški značaj, medtem ko imajo njeni pritoki izrazit hudourniški značaj in s tem tudi veliko erozijsko moč (Kuzmič & Suhadolnik, 2005), ki je bila v primeru izjemno obilnih padavin tekom vremenske ujme v začetku avgusta 2023 tudi rušilna. Struge Meže in pritokov so v naseljih delno regulirane, izven naselij pa so zaradi velikih

vzdolžnih padcev dna ter hudourniškega značaja pogosto izpostavljene eroziji (Kuzmič & Suhadolnik, 2005).

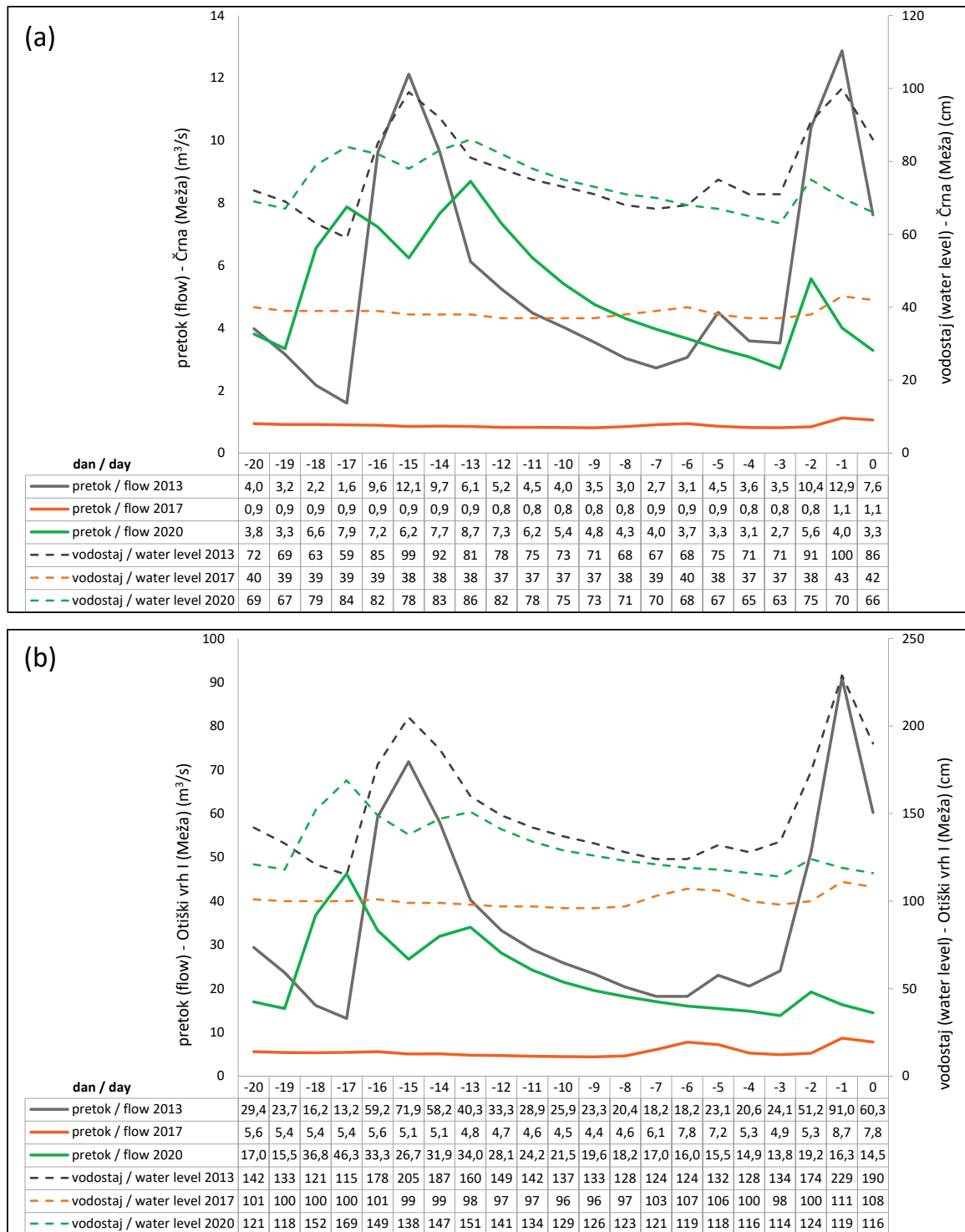
Vzorčenje potočnih in rečnih sedimentov je bilo izvedeno leta 2013 (25. 11. in 28. 11.), leta 2017 (8. 6.) in leta 2020 (29. 10. in 30. 10.), vsakič na skupno 13 vzorčnih mestih v Meži in njenih pritokih, ki so podana v tabeli 1 in prikazana na sliki 1. V letih 2017 in 2020 je bil sočasno z vzorčenjem sedimentov na istih mestih odvzet tudi vzorec vode.

Vodostaj in pretok reke Meže v času vzorčenj povzemamo po podatkih arhiva površinskih voda Agencije Republike Slovenije za okolje, in sicer za postaji Črna (Č) in Otiški vrh I (OV). Pri vodomerni postaji Otiški vrh I je potrebno upoštevati, da se pred njo v Mežo izliva večji pritok Mislinja. Na prvi dan vzorčenja sta bila pretok in vodostaj največja leta 2013 (Č: 86 cm in 7,6 m³/s ter OV: 190 cm in 60,3 m³/s) in najmanjša leta 2017 (Č: 42 cm in 1,1 m³/s ter OV: 108 cm in 7,8 m³/s) (sl. 2a, b). Leta 2020 sta bila vodostaj in pretok nekoliko večja kot leta 2017 (Č: 66 cm in 3,3 m³/s ter OV: 116 cm in 14,5 m³/s). Poleg tega sta bila vodostaj in pretok leta 2020 dlje časa (skupno 3 tedne) pred vzorčenjem konstantna, medtem ko sta v letu 2013 in 2017 nihala (eden ali več intenzivnejših padavinskih dogodkov). Padavinski dogodki leta 2013

so bili bolj intenzivni kot leta 2017. Nihanja vodo-staja in pretoka sta v opazovanih obdobjih 2023 in 2017 podobna na obeh vodomernih postajah (sl. 2a,b).

Drobnozrnat sediment je bil na vsakem vzorčnem mestu odvzet na najmanj petih lokacijah v medsebojni razdalji 5 do 10 metrov. Tako

pridobljen združeni vzorec je tehtal od 1 do 2 kilograma. Zračno posušene vzorce sedimentov smo presejali s sitom iz nerjavečega jekla na frakcijo $< 0,125$ mm, v kateri smo analizirali vsebnosti PSE. Kemična analiza vzorcev sedimentov je bila opravljena v laboratoriju Bureau Veritas Mineral Laboratories (mednarodna akreditacija ISO/IEC



Sl. 2. Vodostaj (cm) in pretok (m^3/s) na vodomernih postajah Črna (a) in (b) Otiški vrh I (po pritoku Mislinje) na reki Meži v 20. dneh pred začetkom in prvi dan vzorčenja v letu 2013, 2017 in 2020 (Vir podatkov: Arhiv površinskih voda, Agencija Republike Slovenije za Okolje).

Fig. 2. Water level (cm) and flow (m^3/s) at the water measuring stations of Meža river (a) Črna and (b) Otiški vrh I (after Mislinja confluent) 20 days before the start and on the 1st day of sampling in 2013, 2017 and 2020 (Source of data: Archive of surface waters, Slovenian Environment Agency).

17025:2017), v Vancouvru v Kanadi. Za določitev vsebnosti 11 elementov (As, Ba, Cd, Co, Cr, Cu, Hg, Mo, Ni, Pb, Zn) je bilo 15 g vzorca (izjemoma 0,5 g, v primeru da vzorca ni bilo dovolj) prelitega z modificirano zlatotopko (mešanica kislin HCl in HNO_3 ter vode v razmerju 1:1:1), eno uro segrevalo na 95 °C in potem primerno razredčeno z destilirano vodo. Vsebnosti elementov v raztopini (kislinskem izvlečku) so bile določene z induktivno sklopljeno plazemsko (ICP) masno spektrometrijo (MS) ali optično emisijsko spektrometrijo (OES). Na podlagi ponovitev štirih vzorcev in analize standardov OREAS 45d ter 45e je bila kakovost analitike ocenjena kot ustrezna.

Vzorci vode so bili na terenu prefiltrirani preko filtra < 0,45 µm in shranjeni v 60 ml HDPE plastenke, ki so bile predhodno dvakrat sprane z vzorčeno vodo. Ob vzorčenju vode smo izmerili pH, temperaturo vode (T), oksidacijsko-redukcijski potencial (Eh), električno prevodnost (EC) in količino raztopljenega kisika (DO). Odvzeti vzorci vode so bili shranjeni na hladno (8–10 °C). Kemične analize vode so bile opravljene v laboratoriju Activation Laboratories Ltd. (Actlabs; mednarodna akreditacija ISO/IEC 17025:2017) v Kanadi. V laboratoriju so bili vzorci najprej za nekaj dni zakisani z ultra čisto dušikovo kislino na pH < 2, da so se morebitno oborjene snovi ponovno raztopile. Nato so bili analizirani z induktivno sklopljeno plazemsko (ICP) masno spektrometrijo (MS) in optično emisijsko spektrometrijo (OES). Kakovost analitike je bila zagotovljena s ponovitvami šestih vzorcev in uporabo standarda IV-STOCK-1643 (ICP/MS).

Rezultati in razprava

Vsebnosti potencialno strupenih elementov v sedimentih

Vsebnosti 11 PSE (As, Ba, Cd, Co, Cr, Cu, Hg, Mo, Ni, Pb, Zn) v obravnavanih vzorcih sedimentov so podane v tabeli 2. Ker slovenska okoljska zakonodaja trenutno ne predpisuje standardov kakovosti za potočne oz. rečne sedimente, smo vsebnosti PSE primerjali z normativnimi (mejni in kritičnimi) vrednostmi za tla (tabela 2), ki so predpisane v Uredbi o mejnih, opozorilnih in kritičnih imisijskih vrednostih nevarnih snovi v tleh (Uradni list RS, št. 68/96, 41/04 – ZVO-1 in 44/22 – ZVO-2). Mejne in kritične vrednosti za tla po slovenski uredbi so zelo blizu vrednostim po t.i. nizozemski listi »The New Dutch list« (VROM, 2000), ki je veljala tako za tla kot sedimente. Za Ba smo vzeli mejno vrednost po nizozemski listi (VROM, 2000), ker v slovenski zakonodaji ni de-

finirana. Posebej smo izpostavili vsebnosti, ki presegajo 2 × kritično vrednost, da bi izpostavili s PSE zelo obremenjena območja (tabela 2).

V pritokih Meže so vsebnosti Pb (tabela 1, sl. 3) v sedimentih v vseh opazovanih letih presegale kritično vrednost v Helenskem potoku (SS-26/5), v pritoku 1 (SS-26/8), v pritoku 2 (SS-26/11) in v Junčarjevem potoku (SS-26/19). Nekoliko manjše vsebnosti, a še vedno večinoma nad kritično vrednostjo, smo izmerili v Jazbinskem potoku (SS-26/10) ter v Mušeniku (SS-26/7). Ugotavljamo, da so bile vsebnosti Pb v sedimentih iz pritokov Meže, ki neposredno drenirajo odlagališča (z izjemo Jazbinskega potoka in pritoka 2), največje v letu 2013, ko sta bila pretok in vodostaj najvišja. Slednje verjetno odraža močan vpliv vodne erozije odlagališč na povečanje vsebnosti v sedimentih pritokov Meže. Slednje ne velja za Jazbinski potok in pritok 2. Zelo verjetno je vzrok temu dobra zaježitev materiala pod Kavšakovo haldo, katere odtočne vode napajajo pritok 2, ki se izliva v Jazbinski potok in slednji v Mežo. Kavšakovo haldo vrsto let uporablja kot vir nekovinskih mineralnih surovin, predvsem za gradbene namene. Jazbinski potok pred pritokom 2 v zaledju drenira le nekaj majhnih odlagališč rudarskih odpadkov (Gosar et al., 2021). Sklepamo, da sta majhen vpliv odlagališč rudarskih odpadkov v zaledju Jazbinskega potoka pred izlivom pritoka 2 ter dobra zaježitev iztoka materiala iz Kavšakovega odlagališča glavna vzroka za podobne vsebnosti Pb v času različnih vodostajev in pretokov.

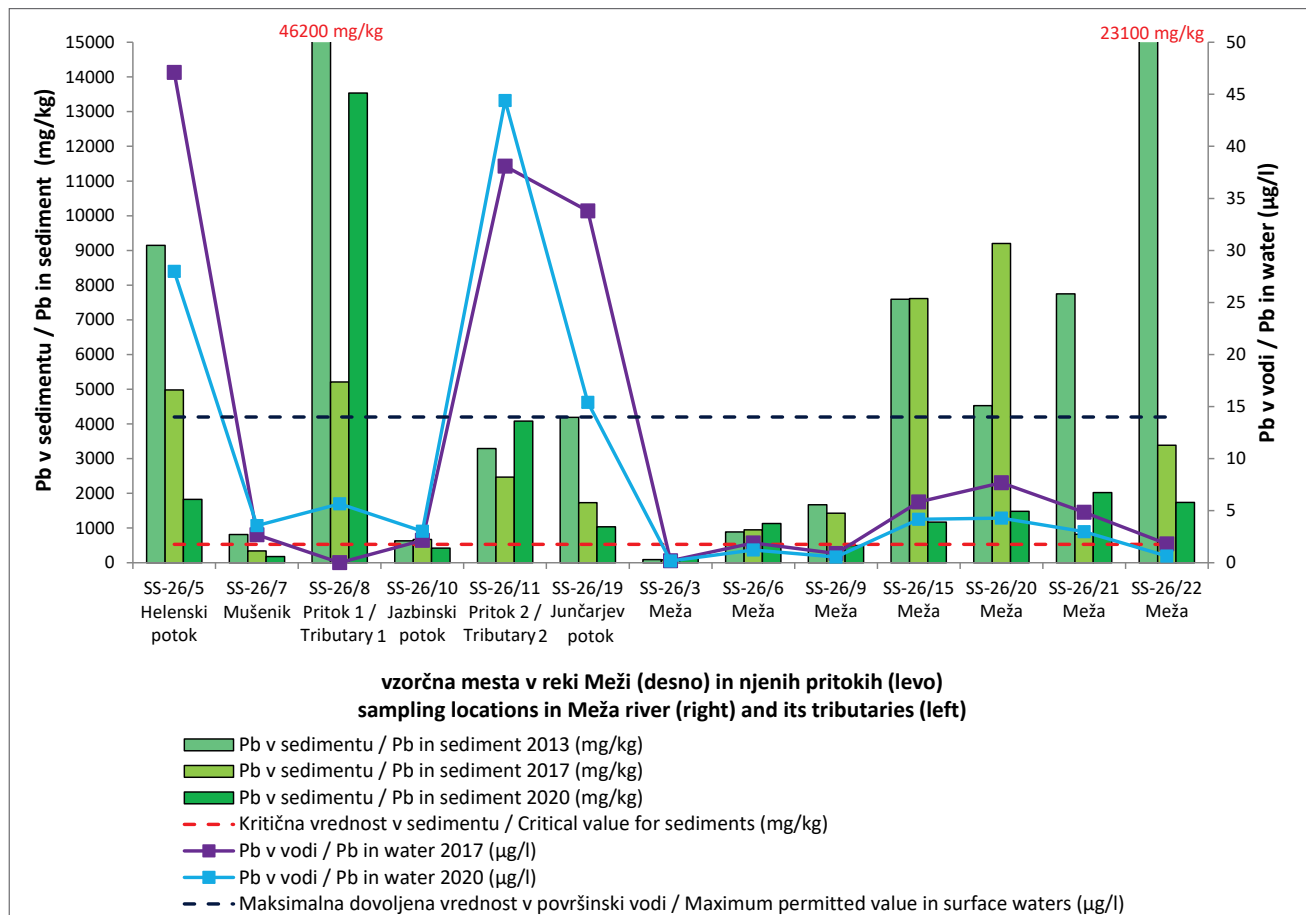
Na večini vzorčnih mest v Meži so bile vsebnosti Pb velike. Kritična vrednost za Pb je bila presežena v vseh opazovanih letih na vseh lokacijah, z izjemo lokacije SS-26/9 v letu 2020, kjer je bila vsebnost Pb med mejno in kritično vrednostjo ter lokacije SS-26/3, ki je v zgornjem toku Meže. Na slednji so bile vsebnosti glede na ostale lokacije zelo majhne, kar je pričakovano, saj se nahaja gorvodno od večine v uvodu predstavljenih virov Pb. V nasprotju z večino pritokov, vsebnosti Pb v sedimentih Meže niso bile znatno večje v obdobju povišanega vodostaja in pretoka, razen na lokacijah SS-26/21 in SS-26/22 (večkratno povišanje v 2013 v primerjavi z letoma 2017 in 2020), ki sta izmed 13 vzorčnih mest najbolj oddaljeni (dolvodno) od virov Pb v Zgornji Mežiški dolini. Možen razlog za izrazito večje vsebnosti v letu 2013 bi lahko bila povečana erozija s Pb močno obremenjenih poplavnih ravnic. Poleg tega je potrebno upoštevati, da se lokacija SS-26/22 nahaja tik za rovom, ki drenira rudnik, in da so bile na tej lokaciji vedno ugotovljene velike vsebnosti Pb ter prisotnost velike količine Pb-oksidnih/karbonatnih mineralov

Tabela 2. Vsebnosti As, Ba, Cd, Co, Cr, Cu, Hg, Mo, Ni, Pb in Zn (v mg/kg).

Table 2. Contents of As, Ba, Cd, Co, Cr, Cu, Hg, Mo, Ni, Pb and Zn (in mg/kg).

Vzorčeno mesto / Sampling site	Leto / Year	Vodotok / Watercourse	As	Ba	Cd	Co	Cr	Cu	Hg	Mo	Ni	Pb	Zn	
SS-26/3	2013 ¹	Meža	6,4	28	1,4	7,0	18,3	11,4	0,04	1,7	16,7	93	288	
	2017 ¹		8,8	30	2,2	8,2	16,2	14,8	0,09	1,8	19,2	83	358	
	2020		6,5	28	1,9	6,1	17,5	9,6	0,11	2,1	14,5	135	336	
SS-26/5	2013 ¹	Helenski potok	33,7	53	102,9	4,3	17,6	28,4	0,15	149	15,1	9149	18200	
	2017 ¹		23,8	60	64,9	7,5	15,9	37,4	0,13	97,7	22,4	4982	8169	
	2020		14,3	47	24,7	7,4	13,8	21,3	0,08	21,1	19,7	1828	3507	
SS-26/6	2013 ¹	Meža	7,7	33	5,6	6,6	21,5	12,4	0,16	14,1	14,9	887	805	
	2017 ¹		11,2	40	11,4	8,9	17,6	16,2	0,10	18,3	19,8	929	1561	
	2020		8,1	34	8,2	5,9	18,1	12,1	0,09	26,2	14,0	1130	1216	
SS-26/7	2013 ¹	Mušenik	6,7	28	5,4	2,1	7,4	8,5	0,02	15,8	6,6	815	656	
	2017 ¹		4,5	12	2,6	1,4	3,2	4,2	0,04	8,9	3,0	337	364	
	2020		3,4	9	1,5	1,3	3,9	2,8	0,02	4,9	2,3	178	180	
SS-26/8	2013 ¹	pritok 1 /tributary 1	71,8	205	81,1	2,3	14,4	13,3	0,34	3310	9,1	46200	14500	
	2017 ¹		25,3	108	40,2	3,3	10,4	12,0	0,26	286	8,8	5213	5107	
	2020		40,2	165	57,2	4,2	16,2	13,8	0,37	749	11,4	13533	7684	
SS-26/9	2013 ¹	Meža	13,1	150	7,2	11,5	30,6	24,7	0,85	33,3	21,9	1672	1235	
	2017 ¹		13,5	128	9,5	12,0	23,9	27,7	0,31	18,3	21,8	1430	1341	
	2020		8,4	85	5,1	14,2	32,9	24,6	0,20	10,2	31,8	498	814	
SS-26/10	2013 ¹	Jazbinski potok	6,0	95	1,7	4,0	10,3	13,2	0,29	5,2	10,7	634	282	
	2017 ¹		10,2	44	6,0	3,0	8,3	18,7	0,13	6,6	9,3	671	529	
	2020		6,8	61	2,0	4,9	10,1	12,2	1,15	4,9	11,8	419	306	
SS-26/11	2013 ¹	pritok 2 / tributary 2	23,7	307	103,9	1,1	7,2	10,5	0,10	17,7	6,7	3289	16600	
	2017 ¹		29,1	308	116,3	1,9	7,1	14,0	0,13	21,5	7,0	2470	17600	
	2020		37,0	196	94,8	5,4	19,1	73,6	0,38	38,2	33,1	4079	13800	
SS-26/15	2013 ¹	Meža	27,6	124	14,7	9,1	28,3	42,9	0,19	104	21,8	7593	2665	
	2017 ¹		27,4	89	18,6	7,4	27,7	85,0	0,75	92,1	32,1	7611	2208	
	2020		10,8	77	5,8	10,7	26,0	23,8	0,12	11,3	26,3	1171	844	
SS-26/19	2013 ¹	Junčarjev potok	20,6	285	25,5	1,2	6,2	8,8	0,04	122	5,2	4187	5834	
	2017 ¹		23,1	271	20,3	3,0	9,1	16,1	0,11	50,6	7,9	1733	3854	
	2020		13,0	212	12,8	1,1	4,9	4,9	0,04	32,1	3,7	1035	2530	
SS-26/20	2013 ¹	Meža	17,1	119	8,0	9,3	25,2	30,8	0,79	70,2	21,9	4527	1337	
	2017 ¹		34,3	110	22,7	9,6	33,8	57,3	0,56	160	29,0	9198	3027	
	2020		11,5	84	7,2	10,5	26,6	24,5	0,19	17,1	25,8	1481	1144	
SS-26/21	2013 ¹	Meža	24,6	132	23,0	8,7	26,9	35,0	0,13	113	19,5	7751	3728	
	2017 ¹		8,9	87	10,0	8,8	24,0	47,1	0,24	6,5	23,2	825	1090	
	2020		11,9	77	9,6	10,1	26,7	24,4	0,15	29,2	26,0	2019	1460	
SS-26/22	2013 ¹	Meža	37,9	128	30,1	10,3	44,0	54,3	0,79	361	25,3	23100	5083	
	2017 ¹		22,1	136	17,0	13,2	33,5	45,9	0,22	70,7	32,4	3383	2302	
	2020		13,9	74	7,7	12,1	29,8	24,3	0,10	38,3	29,4	1737	1269	
mejna vrednost / border (mg/kg) ²			20	160 ³	1	20	100	60	0,8	10	50	85	200	
kritična vrednost (mg/kg) ²			55	625 ³	12	240	380	300	10	200	210	530	720	

¹Podatki povzeti po Miler et al. (2022) / Data after Miler et al. (2022)²Mejne in kritične vrednosti povzete iz Uredbe o mejnih, opozorilnih in kritičnih imisijskih vrednostih nevarnih snovi v tleh (Ur. l. RS, št. 68/96, 41/04 – ZVO-1 in 44/22 – ZVO-2) / (Limit and critical values summarized from the Decree on limit values, alert thresholds and critical levels of dangerous substances into the soil (Ur. l. RS, št. 68/96, 41/04 – ZVO-1 in 44/22 – ZVO-2)³Vrednosti povzete iz »The New Dutch list« (VROM, 2000) / Values summarized from »The New Dutch list« (VROM, 2000)S črno barvo so zapisane vsebnosti pod mejno, z modro med mejno in kritično vrednostjo, z rdečo ne-odebeljeno vsebnosti nad kritično in pod 2 × kritično vrednostjo ter **odebeljeno rdeče** vsebnosti nad 2 × kritično vrednostjo / Contents below limit values are colored black, between limit and critical value in blue, above the critical value and below the 2 × critical value in red and above the 2 × critical value in bold red



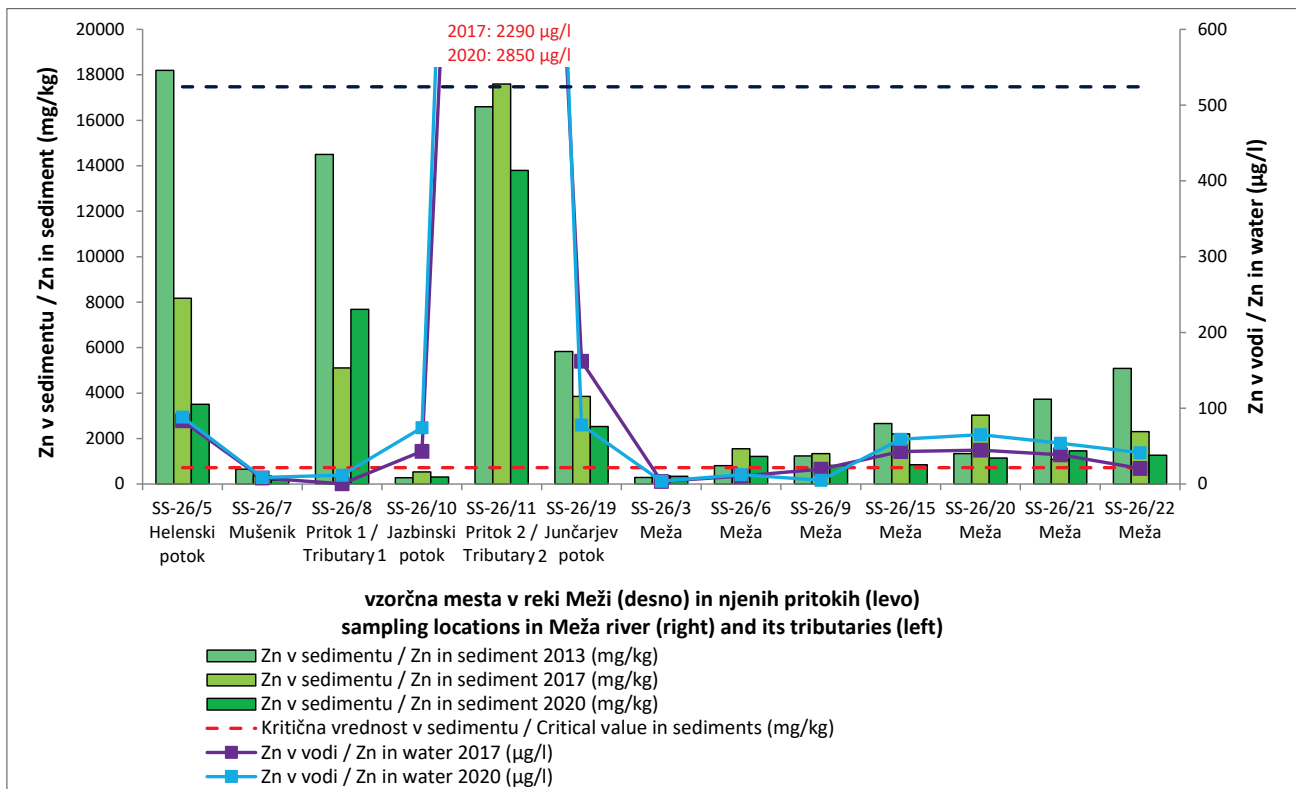
Sl. 3. Pb v sedimentih (v mg/kg) v letih 2013, 2017 in 2020 ter Pb v površinski vodi (v µg/l) v letih 2017 in 2020 (podatki iz leta 2013 in 2017 povzeti po Miler et al., 2022) skupaj z zakonodajnimi vrednostmi. Na levi so prikazane vzorčne lokacije v pritokih, ki spirajo material iz odlagališč, na desni pa v reki Meži. Vzorčne lokacije si na diagramu sledijo kot v naravi po toku navzdol.

Fig. 3. Pb in sediments (in mg/kg) in the years 2013, 2017 and 2020 and Pb in surface water (in µg/l) in the years 2017 and 2020 (data from 2013 and 2017 are summarized after Miler et al., 2022). Sampling locations of the tributaries, which wash the material from the waste sites, are presented on the left and of Meža River on the right. Sampling locations on the chart follow each other like in nature downstream.

v sedimentih (Miler et al., 2022). Na preostalih lokacijah v Meži, ki se nahajajo bližje virom Pb, so bile največje vsebnosti izmerjene v letu 2017 ali 2020, ko sta bila vodostaj in pretok nižja kot leta 2013, ali pa so si bile vsebnosti kljub veliki razlike v vodostaju in pretoku podobne v vseh opazovanih letih. V zgornjem toku Meže nismo opazili, da bi višji vodostaj in močnejši pretok neposredno vplival na večje vsebnosti PSE v sedimentih. Dolvodno od Mežice so nihanja vsebnosti tudi v Meži precejšnja, kar je lahko odraz gradbenih del v strugi dolvodno od Žerjava. Ocenujemo, da je dinamika onesnaženosti vodotoka Meže vzdolž krajev Črna na Koroškem, Žerjav in Mežica zelo kompleksna. Menimo, da imajo poleg odlagališč rudarskih odpadkov pomemben vpliv tudi ostali razpršeni viri PSE v okolju (onesnažena tla, poplavne ravnice in njihova različna ter kompleksno porazdeljena stopnja onesnaženosti) saj je okolje zaradi več kot 300-letnega izkoriščanja rude močno obremenjeno, kot smo podrobno opisali v uvodnem delu. Poleg tega verjetno vpliva na okolje tudi sedanja

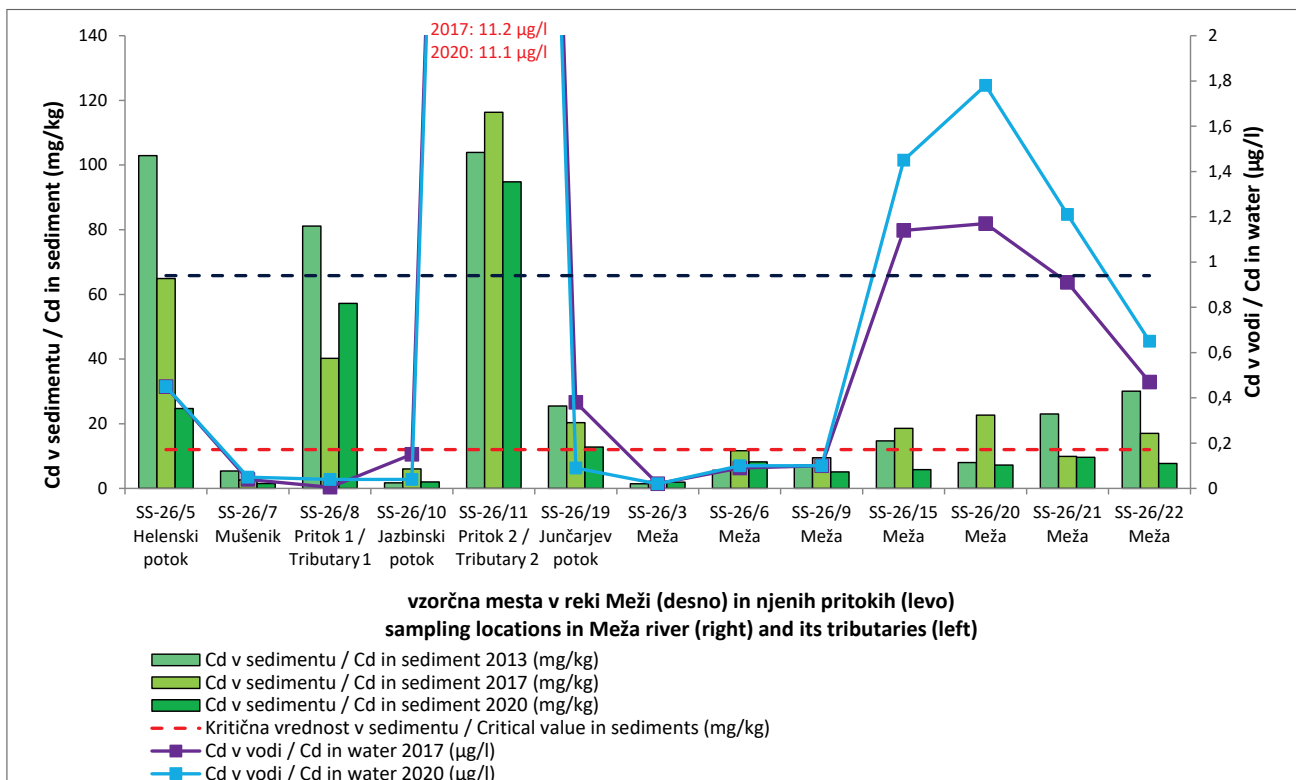
industrijska dejavnost. Močnejša vodna erozija struge lahko vpliva na vsebnosti na posamezni lokaciji, saj se že odloženi sedimenti v rečnem koritu ob višjem vodostaju ponovno mobilizirajo in prenesajo po toku navzdol ter ponovno odložijo, ko energija toka nekoliko upade.

Porazdelitev vsebnosti Zn (sl. 4) je zelo podobna porazdelitvi Pb. V vseh opazovanih letih so vsebnosti Zn v sedimentih presegale kritično vrednost v vseh pritokih Meže, razen v Mušeniku (SS-26/7), kjer so bile vsebnosti med mejno in kritično vrednostjo v letih 2013 in 2017, v letu 2020 pa pod mejno vrednostjo. Ravno tako so bile vsebnosti Zn v sedimentih Meže nad kritično vrednostjo v vseh opazovanih obdobjih na vseh lokacijah, razen na lokaciji SS-26/3, ki leži gorvodno od večine odlagališč odpadkov in rudarskih revirjev. Na tej lokaciji so bile vsebnosti Zn v vseh opazovanih obdobjih med mejno in kritično vrednostjo. Podobno kot v primeru Pb, so bile vsebnosti Zn v pritokih Meže večinoma največje leta 2013 (z izjemo Jazbinskega potoka



Sl. 4. Zn v sedimentih (v mg/kg) v letih 2013, 2017 in 2020 ter Zn v površinski vodi (v µg/l) v letih 2017 in 2020 (podatki iz leta 2013 in 2017 povzeti po Miler et al., 2022) skupaj z zakonodajnimi vrednostmi. Na levi so prikazane vzorčne lokacije v pritokih, ki spirajo material iz odlagališč, na desni pa v reki Meži. Vzorčne lokacije si na diagramu sledijo kot v naravi po toku navzdol.

Fig. 4. Zn in sediments (in mg/kg) in the years 2013, 2017 and 2020 and Zn in surface water (in µg/l) in the years 2017 and 2020 (data from 2013 and 2017 are summarized after Miler et al., 2022). Sampling locations of the tributaries, which wash the material from the waste sites, are presented on the left and of Meža River on the right. Sampling locations on the chart follow each other like in nature downstream.



Sl. 5. Cd v sedimentih (v mg/kg) v letih 2013, 2017 in 2020 ter Cd v površinski vodi (v µg/l) v letih 2017 in 2020 (podatki iz leta 2013 in 2017 povzeti po Miler et al., 2022) skupaj z zakonodajnimi vrednostmi. Na levi so prikazane vzorčne lokacije v pritokih, ki spirajo material iz odlagališč, na desni pa v reki Meži. Vzorčne lokacije si na diagramu sledijo kot v naravi po toku navzdol.

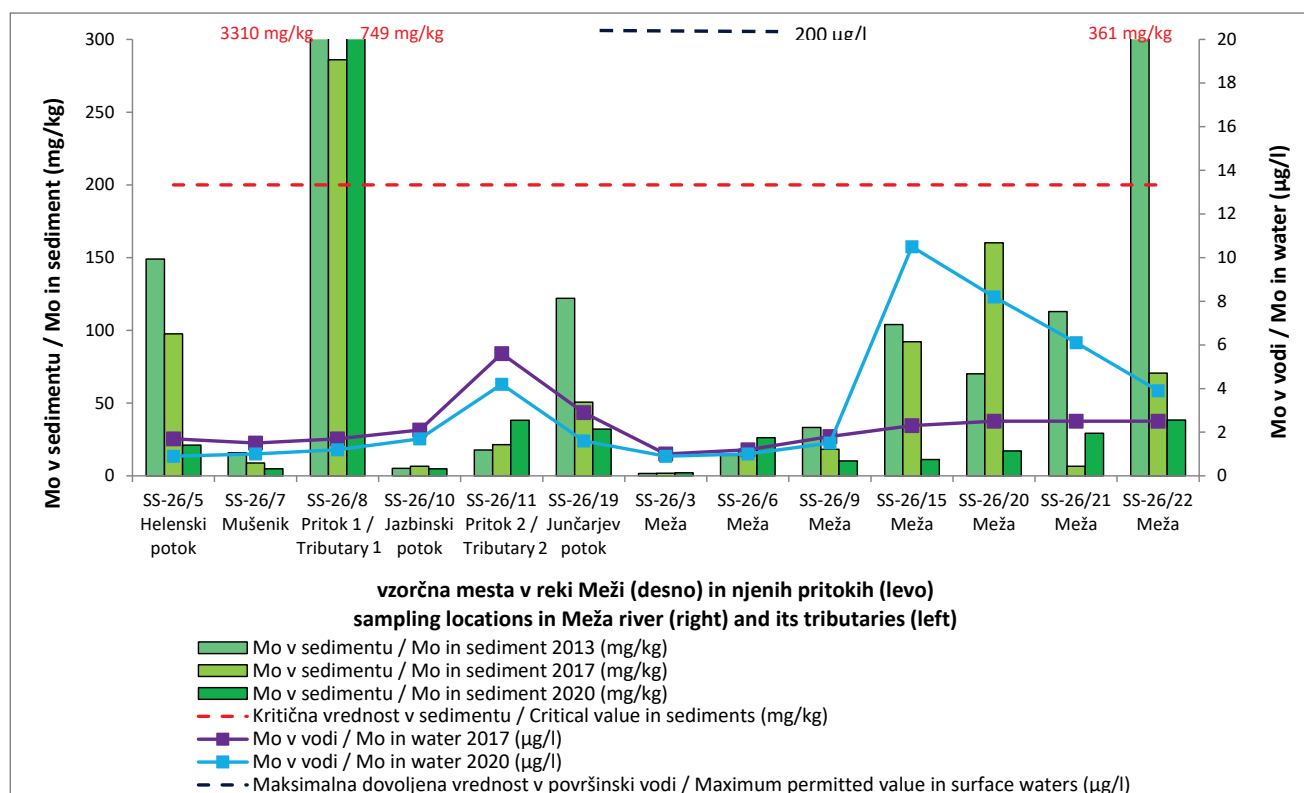
Fig. 5. Cd in sediments (in mg/kg) in the years 2013, 2017 and 2020 and Cd in surface water (in µg/l) in the years 2017 and 2020 (data from 2013 and 2017 are summarized after Miler et al., 2022). Sampling locations of the tributaries, which wash the material from the waste sites, are presented on the left and of Meža River on the right. Sampling locations on the chart follow each other like in nature downstream.

in pritoka 2), torej v času največjega pretoka in najvišjega vodostaja. Vsebnosti Zn v sedimentih Meže so bile v letu 2013 največje na lokaciji SS-26/15 ter lokacijah SS-26/21 in SS-26/22, ki sta od virov Pb najbolj oddaljeni (dolvodno). Na preostalih lokacijah so bile največje vsebnosti Zn v Meži izmerjene bodisi v letu 2017 ali 2020, ko sta bila pretoka nizka in precej podobna ali pa so si bile vsebnosti podobne v vseh opazovanih letih. Odvisnost vsebnosti Zn od vodostaja in pretoka tako v pritokih kot v Meži kaže podobne lastnosti kot vsebnosti Pb.

Vsebnosti Cd (sl. 5) so presegale kritično vrednost v vseh pritokih Meže, razen v Mušeniku (SS-26/7) in Jazbinskem potoku (SS-26/10), kjer so bile vsebnosti med mejno in kritično vrednostjo. Na lokacijah v Meži velja obratno, saj so bile vsebnosti Cd večinoma med mejno in kritično vrednostjo, z izjemo SS-26/15 v letih 2013 in 2017, SS-26/20 v letu 2017 ter SS-26/22 v letih 2013 in 2017, kjer so vsebnosti presegale kritično vrednost. Glede na vodostaj in pretok, vsebnosti Cd kažejo enak trend kot vsebnosti Pb in Zn; vsebnosti so največje v letu 2013 v pritokih reke Meže (z izjemo Jazbinskega potoka in pritoka 2) ter v Meži na lokacijah SS-26/21 in SS-26/22.

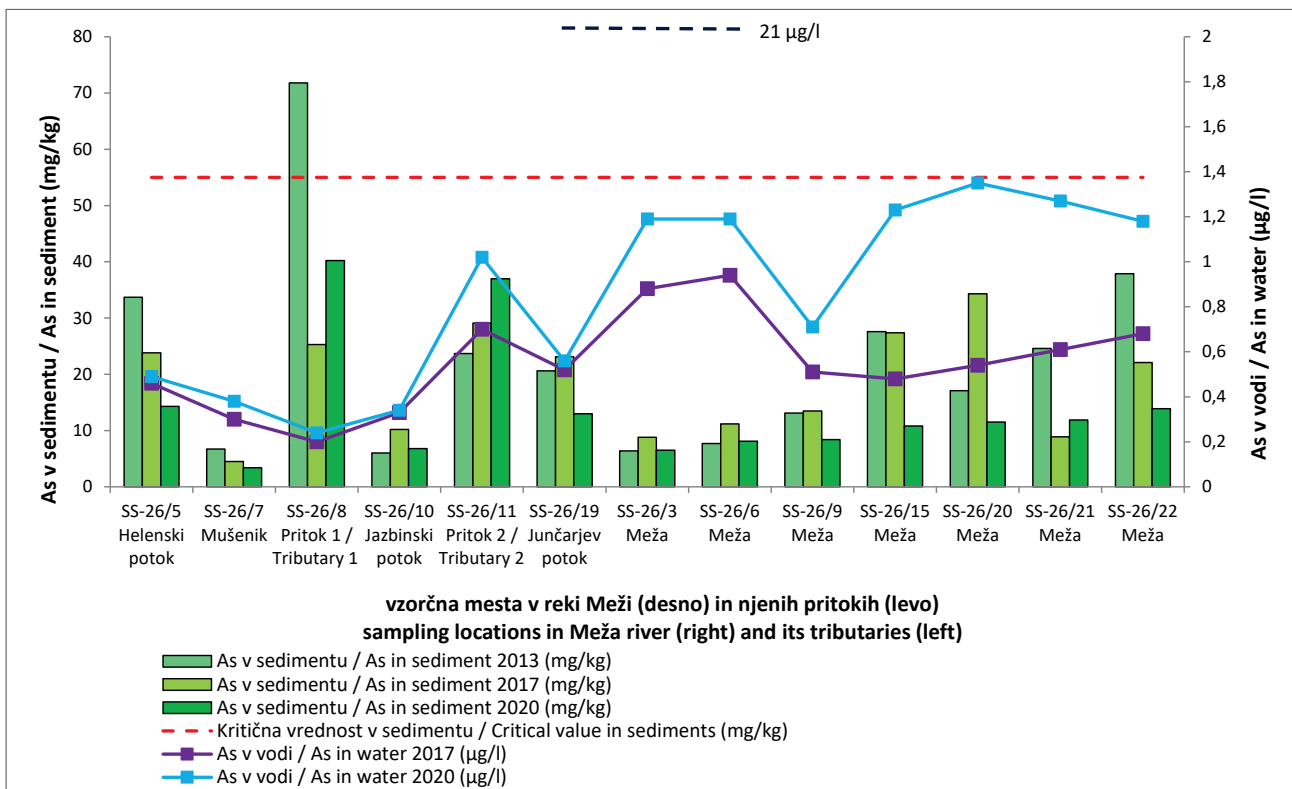
Vsebnosti Mo (sl. 6) so v pritokih Meže presegale kritično vrednost samo v pritoku 1 (SS-26/8), medtem ko so bile v preostalih pritokih med mejno in kritično vrednostjo oz. pod mejno vrednostjo v Jazbinskem potoku v vseh opazovanih obdobjih, ter v Mušeniku v letu 2017 in 2020. Na lokacijah v Meži so bile vsebnosti Mo večinoma med mejno in kritično vrednostjo, z izjemo lokacije SS-26/22, kjer je bila v letu 2013 vsebnost nad kritično vrednostjo, ter lokacije SS-26/21, kjer je bila vrednost v letu 2017 pod mejno vrednostjo. Pod mejno vrednostjo so bile tudi vsebnosti Mo na lokaciji SS-26/3 v vseh opazovanih obdobjih. Glede na vodostaj in pretok, vsebnosti Mo kažejo podoben trend kot vsebnosti Pb, Zn in Cd; vsebnosti so bile največje v letu 2013 v pritokih (z izjemo Jazbinskega potoka in pritoka 2), v Meži pa na lokacijah SS-26/15, SS-26/21 in SS-26/22.

Vsebnost As (sl. 7) je v pritokih Meže presegala kritično vrednost samo v pritoku 1 (SS-26/8) leta 2013, medtem ko je bila v letih 2017 in 2020 med mejno in kritično vrednostjo. Poleg tega so bile vsebnosti med mejno in kritično vrednostjo še v Helenskem potoku (SS-26/5) in Junčarjevem potoku (SS-26/19) leta 2013 ter 2017 ter v pritoku 2 (SS-26/11) v vseh opazovanih obdobjih. Na lokacijah



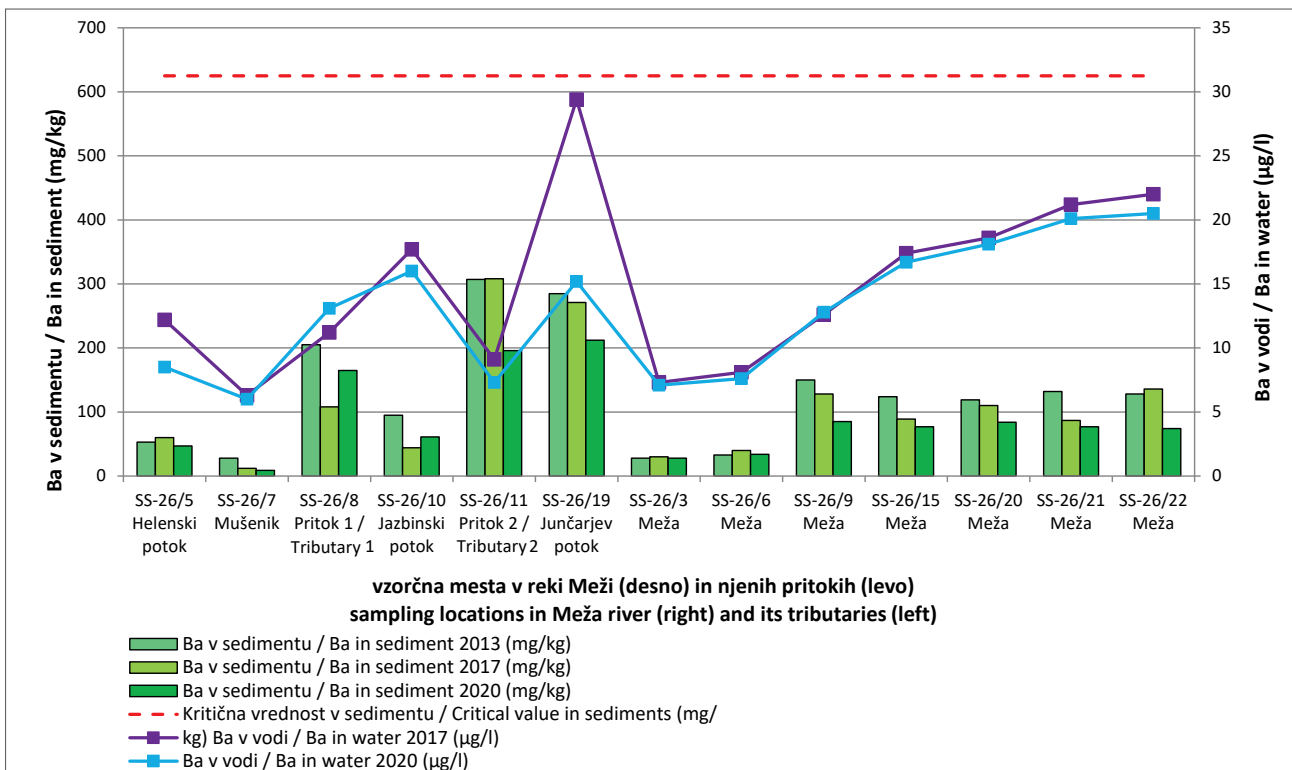
Sl. 6. Mo v sedimentih (v mg/kg) v letih 2013, 2017 in 2020 ter Mo v površinski vodi (v µg/l) v letih 2017 in 2020 (podatki iz leta 2013 in 2017 povzeti po Miler et al., 2022) skupaj z zakonodajnimi vrednostmi. Na levi so prikazane vzorčne lokacije v pritokih, ki spirajo material iz odlagališč, na desni pa v reki Meži. Vzorčne lokacije si na diagramu sledijo kot v naravi po toku navzdol.

Fig. 6. Mo in sediments (in mg/kg) in the years 2013, 2017 and 2020 and Mo in surface water (in µg/l) in the years 2017 and 2020 (data from 2013 and 2017 are summarized after Miler et al., 2022). Sampling locations of the tributaries, which wash the material from the waste sites, are presented on the left and of Meža River on the right. Sampling locations on the chart follow each other like in nature downstream.



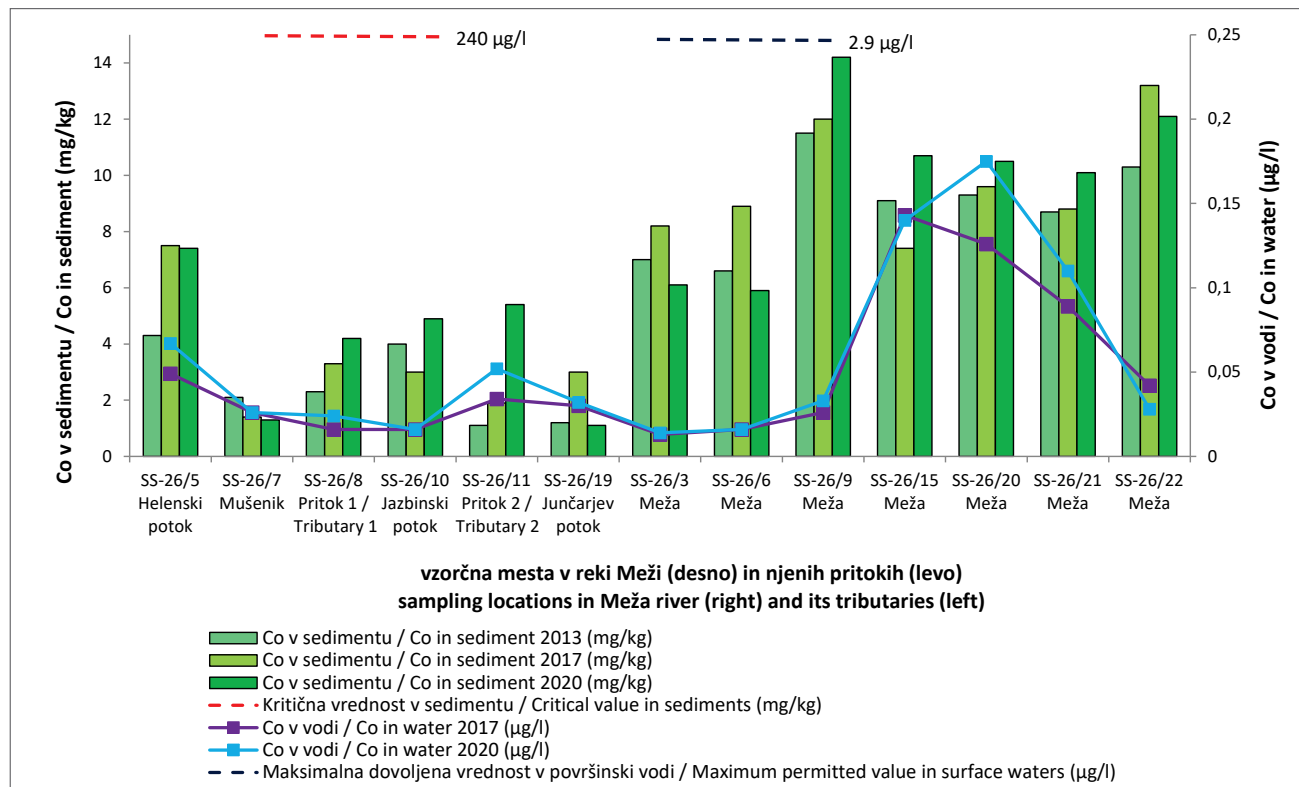
Sl. 7. As v sedimentih (v mg/kg) v letih 2013, 2017 in 2020 ter As v površinski vodi (v µg/l) v letih 2017 in 2020 (podatki iz leta 2013 in 2017 povzeti po Miler et al., 2022) skupaj z zakonodajnimi vrednostmi. Na levi so prikazane vzorčne lokacije v pritokih, ki spirajo material iz odlagališč, na desni pa v reki Meži. Vzorčne lokacije si na diagramu sledijo kot v naravi po toku navzdol.

Fig. 7. As in sediments (in mg/kg) in the years 2013, 2017 and 2020 and As in surface water (in µg/l) in the years 2017 and 2020 (data from 2013 and 2017 are summarized after Miler et al., 2022). Sampling locations of the tributaries, which wash the material from the waste sites, are presented on the left and of Meža River on the right. Sampling locations on the chart follow each other like in nature downstream.



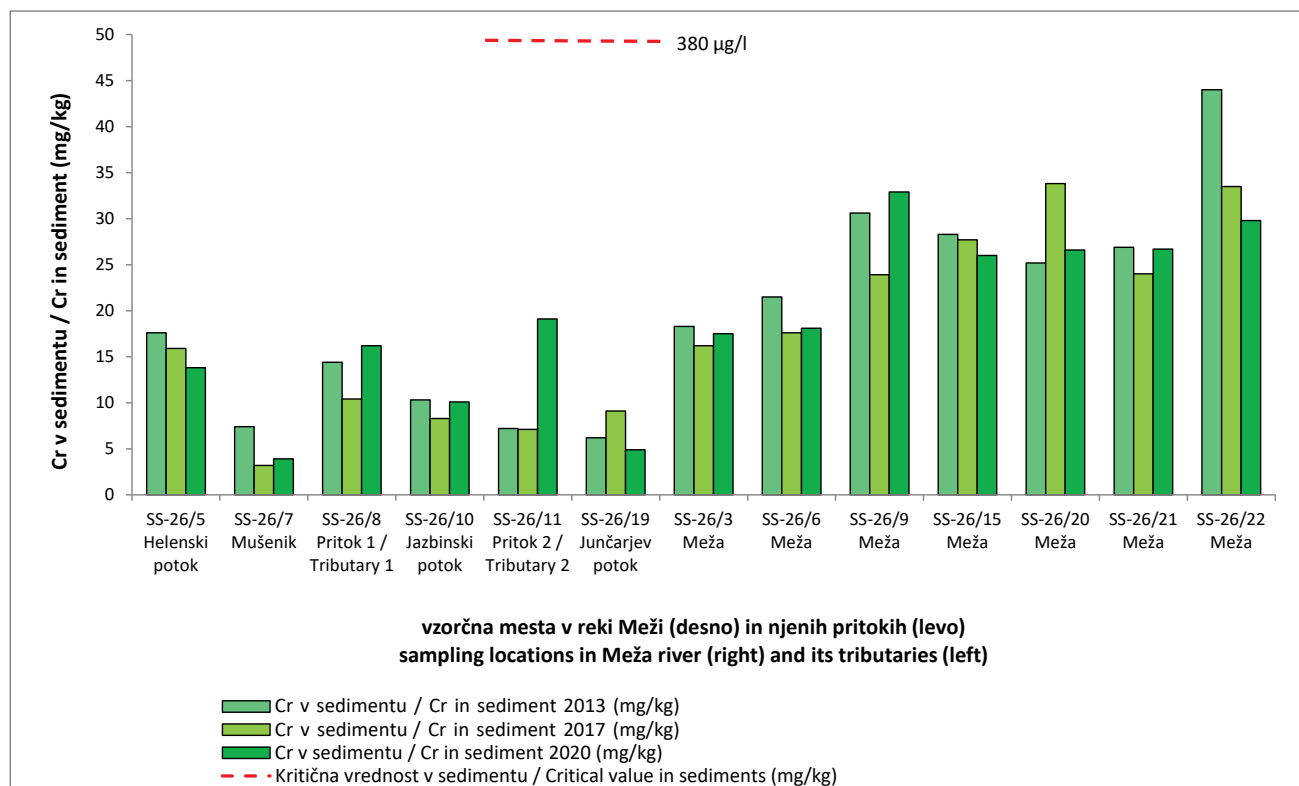
Sl. 8. Ba v sedimentih (v mg/kg) v letih 2013, 2017 in 2020 ter Ba v površinski vodi (v µg/l) v letih 2017 in 2020 (podatki iz leta 2013 in 2017 povzeti po Miler et al., 2022) skupaj z zakonodajnimi vrednostmi. Na levi so prikazane vzorčne lokacije v pritokih, ki spirajo material iz odlagališč, na desni pa v reki Meži. Vzorčne lokacije si na diagramu sledijo kot v naravi po toku navzdol.

Fig. 8. Ba in sediments (in mg/kg) in the years 2013, 2017 and 2020 and Ba in surface water (in µg/l) in the years 2017 and 2020 (data from 2013 and 2017 are summarized after Miler et al., 2022). Sampling locations of the tributaries, which wash the material from the waste sites, are presented on the left and of Meža River on the right. Sampling locations on the chart follow each other like in nature downstream.



Sl. 9. Co v sedimentih (v mg/kg) v letih 2013, 2017 in 2020 ter Co v površinski vodi (v µg/l) v letih 2017 in 2020 (podatki iz leta 2013 in 2017 povzeti po Miler et al., 2022) skupaj z zakonodajnimi vrednostmi. Na levi so prikazane vzorčne lokacije v pritokih, ki spirajo material iz odlagališč, na desni pa v reki Meži. Vzorčne lokacije si na diagramu sledijo kot v naravi po toku navzdol.

Fig. 9. Co in sediments (in mg/kg) in the years 2013, 2017 and 2020 and Co in surface water (in µg/l) in the years 2017 and 2020 (data from 2013 and 2017 are summarized after Miler et al., 2022). Sampling locations of the tributaries, which wash the material from the waste sites, are presented on the left and of Meža River on the right. Sampling locations on the chart follow each other like in nature downstream.



Sl. 10. Cr v sedimentih (v mg/kg) v letih 2013, 2017 in 2020 (podatki iz leta 2013 in 2017 povzeti po Miler et al., 2022) skupaj z zakonodajnimi vrednostmi. Na levi so prikazane vzorčne lokacije v pritokih, ki spirajo material iz odlagališč, na desni pa v reki Meži. Vzorčne lokacije si na diagramu sledijo kot v naravi po toku navzdol.

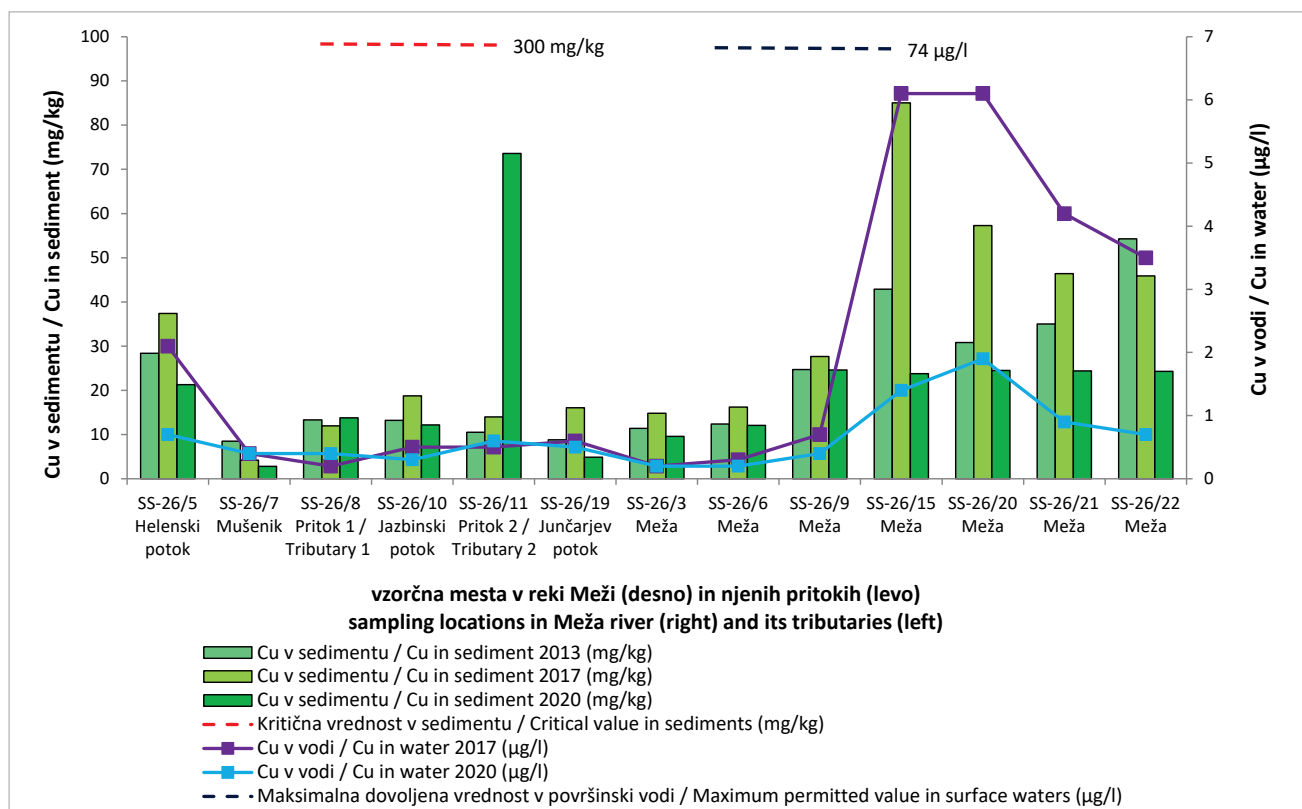
Fig. 10. Cr in sediments (in mg/kg) in the years 2013, 2017 and 2020 (data from 2013 and 2017 are summarized after Miler et al., 2022). Sampling locations of the tributaries, which wash the material from the waste sites, are presented on the left and of Meža River on the right. Sampling locations on the chart follow each other like in nature downstream.

v Meži so vsebnosti As nihale med mejno in kritično vrednostjo na lokacijah SS-26/15 in SS-26/22 leta 2013 ter 2017, na lokaciji SS-26/20 leta 2017 in na lokaciji SS-26/21 leta 2013. Glede na vodostaj in pretok, vsebnosti As v pritokih kažejo delno podoben trend kot vsebnosti Pb, Zn in Cd, z izjemo, da se vsebnosti As z višjim vodostajem in pretokom poleg Jazbinskega potoka in pritoka 2 ne povečajo tudi v Junčarjevem potoku. Na lokacijah v Meži je trend enak, vsebnosti As so bile nekoliko večje leta 2013 na lokacijah SS-26/21 in SS-26/22, ki sta od virov Pb in ostalih PSE v okolju najbolj oddaljeni.

Vsebnosti preostalih PSE (Ba, Co, Cr, Cu, Ni, Hg; sl. 8–13) so večinoma na nivoju naravnega ozadja in le izjemoma presegajo mejne vrednosti. Vsebnosti Ba (sl. 8) so bile nad mejno vrednostjo v pritoku 1 (SS-26/8) v letu 2013 ter v pritoku 2 (SS-26/11) in Junčarjevem potoku v vseh opazovanih obdobjih. Vsebnost Hg je bila nad mejno vrednostjo samo leta 2013 v Meži na lokaciji SS-26/9 (sl. 13), Cu pa leta 2017 v Meži na lokaciji SS-26/9 in pritoku 1 (SS-26/11) leta 2020 (sl. 11). Za omenjene PSE je večinoma značilno, da njihove vsebnosti v opazovanem obdobju oz. ob spremenljivem vodostaju ter pretoku ne nihajo močno,

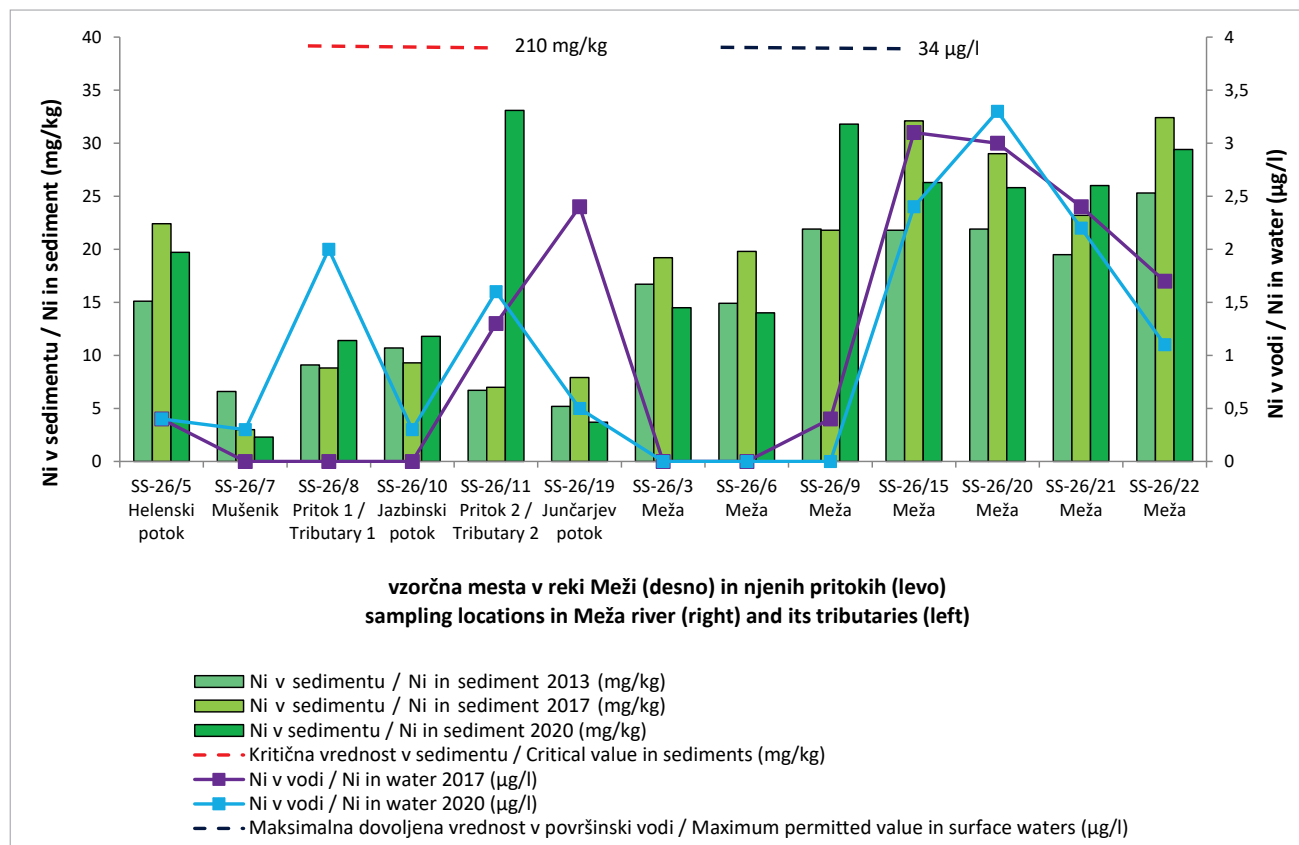
ampak so na istem vzorčnem mestu relativno podobne. Kaže, da se z višjim vodostajem in večjim pretokom še najbolj povečajo vsebnosti Cr na lokaciji SS-26/22 (sl. 10) in vsebnosti Hg na vzorčnih mestih SS-26/9, SS-26/20, SS-26/22 (sl. 13), vse v Meži. Nihanja v vsebnostih Ba, Co, Cr, Cu, Ni in Hg na posameznih vzorčnih mestih skozi leta so v primerjavi z nihanji vsebnosti Pb, Zn, Cd, Mo in As precej manj izrazita.

Rezultati nazorno prikazujejo (sl. 3–8, tabela 2), da so vsebnosti Pb, Zn, Mo, Cd ter deloma tudi As v sedimentih pritokov močno nad geokemičnim ozadnjem. Vsebnosti Cd, Pb in Zn v sedimentih vodotokov, ki odvodnjavajo odlagališča, z izjemo Mušenika in Jazbinskega potoka ter Cd v Junčarjevem potoku (2017, 2020), za več kot 2 × presegajo kritične vrednosti v vseh opazovanih letih. Poglavitni vzrok temu je neustrezeno stanje odlagališč. Odlagališča so bila sanirana pred več kot 25 leti, potem pa niso bila več vzdrževana. Na nekaterih lokacijah so brežine odlagališč strme in neporasle, odvodnjavanje ni pravilno urejeno (Gosar in sodelavci, 2021). Zaradi tega ima erozija odlagališč močan vpliv na dotok materiala v pritoke Meže in nadalje po toku navzdol.



Sl. 11. Cu v sedimentih (v mg/kg) v letih 2013, 2017 in 2020 ter Cu v površinski vodi (v µg/l) v letih 2017 in 2020 (podatki iz leta 2013 in 2017 povzeti po Miler et al., 2022) skupaj z zakonodajnimi vrednostmi. Na levih so prikazane vzorčne lokacije v pritokih, ki spirajo material iz odlagališč, na desni pa v reki Meži. Vzorčne lokacije si na diagramu sledijo kot v naravi po toku navzdol.

Fig. 11. Cu in sediments (in mg/kg) in the years 2013, 2017 and 2020 and Cu in surface water (in µg/l) in the years 2017 and 2020 (data from 2013 and 2017 are summarized after Miler et al., 2022). Sampling locations of the tributaries, which wash the material from the waste sites, are presented on the left and of Meža River on the right. Sampling locations on the chart follow each other like in nature downstream.



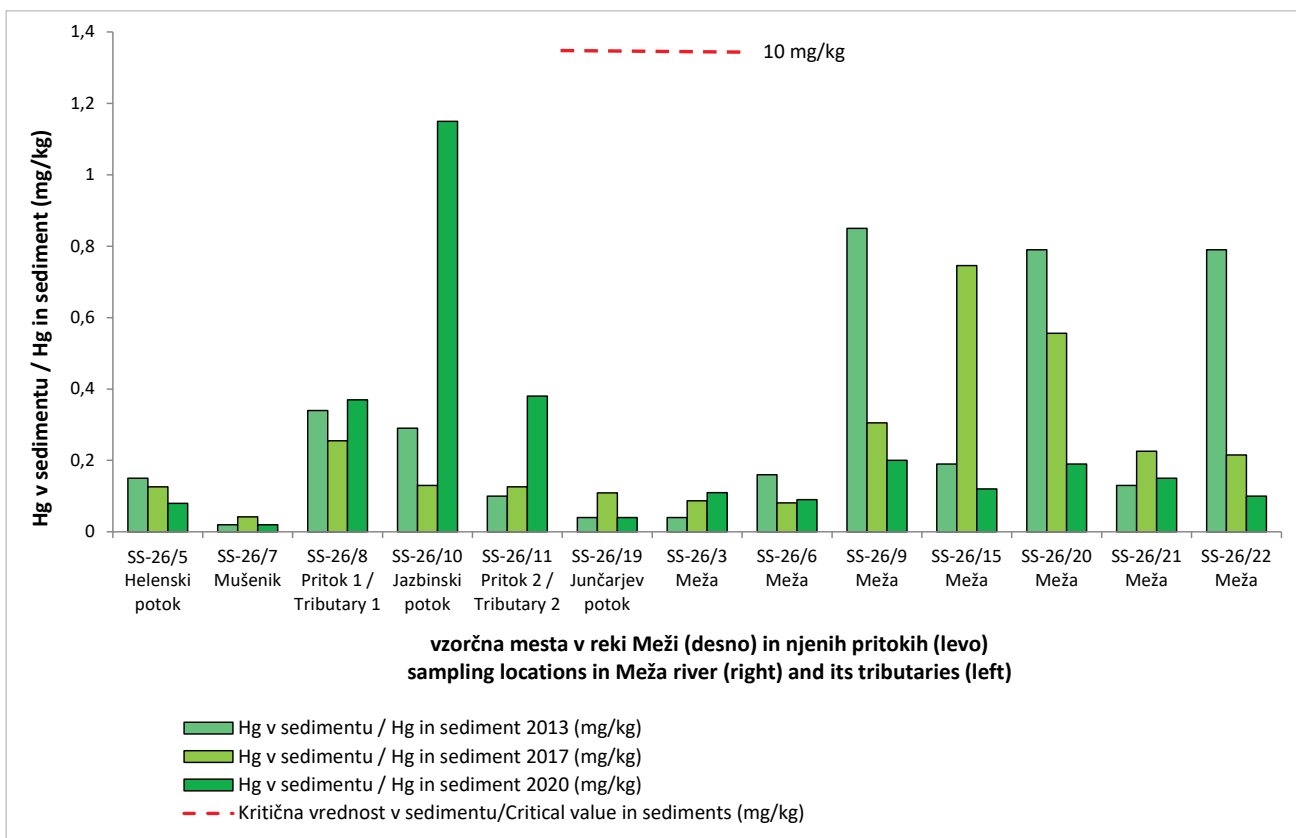
Sl. 12. Ni v sedimentih (v mg/kg) v letih 2013, 2017 in 2020 ter Ni v površinski vodi (v µg/l) v letih 2017 in 2020 (podatki iz leta 2013 in 2017 povzeti po Miler et al., 2022) skupaj z zakonodajnimi vrednostmi. Na levi so prikazane vzorčne lokacije v pritokih, ki spirajo material iz odlagališč, na desni pa v reki Meži. Vzorčne lokacije si na diagramu sledijo kot v naravi po toku navzdol.

Fig. 12. Ni in sediments (in mg/kg) in the years 2013, 2017 and 2020 and Ni in surface water (in µg/l) in the years 2017 and 2020 (data from 2013 and 2017 are summarized after Miler et al., 2022). Sampling locations of the tributaries, which wash the material from the waste sites, are presented on the left and of Meža River on the right. Sampling locations on the chart follow each other like in nature downstream.

Vsebnosti PSE so tudi v sedimentih Meže zelo velike in na splošno močno nihajo med posameznimi vzorčnimi mesti in med posameznimi leti, v katerih so bile izvedene meritve. V zgornjem toku je vpliv odlagališč rudarskih odpadkov na vsebnosti PSE v sedimentih Meže bolj izrazit, medtem ko je dolvodno od Mežice zakrit zaradi preostalih virov, verjetno zaradi prispevka sedanje industrijske dejavnosti (Miler et al., 2022) in erozije onesnaženih tal ter poplavnih ravnic. Velik vpliv ima tudi hidrološki pogoji. Pritoki imajo večinoma hidourniški značaj, za reko Mežo pa je značilno, da ima ob visokem vodostaju velik pretok, zaradi česar delno erodira lastno korito in v njem odložene sedimente. Glede na hidrološke pogoje v času vzorčenja in med različnimi leti so bile v Meži v 30 % dosežene ugodne razmere za erozijo in transport sedimenta obremenjenega s PSE (Miler et al., 2022). Zaradi tega se del onesnaženih sedimentov v obliki suspenzije ali po dnu struge transportira dolvodno v reko Dravo in dalje. To nakazuje tudi zelo drobna zrnavost trdnih nosilcev PSE v sedimentu in materialu odlagališč (Miler in sodelavci, 2022) in potrjujejo visoke vrednosti nekaterih

PSE v sedimentih Drave (Fux & Gosar, 2007; Gaberšek & Gosar, 2023) dolvodno od pritoka Meže. Akumulacijo onesnaženih sedimentov predstavlja jo poplavne ravnice v srednjem in spodnjem toku Meže, ki jih močna erozija ob izjemnih dogodkih lahko erodira.

Hudourniški značaj in izredno erozijsko moč Meže ter njenih pritokov smo opazovali tudi v začetku avgusta 2023, ko je v skupno 72 urah, od 3. avgusta zvečer do 6. avgusta zjutraj, v večjem delu Slovenije padlo med 100 in 300 mm dežja (ARSO, 2023), kar je povzročilo katastrofalne poplave in številne plazove, med drugim tudi v porečju Meže. Ob izrednem padavinskem in posledično poplavnem ter erozijskem dogodku so bile v mežiški dolini premeščene ogromne količine materiala, predvsem iz predhodno odloženih poplavnih ravnic, melišč, tal in tudi odlagališč rudarskih odpadkov. Mnogo premeščenega in nižje odloženega materiala, predvsem drobnozrnatega, je zagotovo vsebovalo velike vsebnosti PSE. To dokazujejo tudi podatki, ki jih je objavila Agencija republike Slovenije za okolje (ARSO) za vsebnosti nekaterih PSE v sedimentih, ki so se ob poplavah odložili



Sl. 13. Hg v sedimentih (v mg/kg) v letih 2013, 2017 in 2020 (podatki iz leta 2013 in 2017 povzeti po Miler et al., 2022) skupaj z zakonodajnimi vrednostmi. Na levi so prikazane vzorčne lokacije v pritokih, ki spirajo material iz odlagališč, na desni pa v reki Meži. Vzorčne lokacije si na diagramu sledijo kot v naravi po toku navzdol.

Fig. 13. Hg in sediments (in mg/kg) in the years 2013, 2017 and 2020 (data from 2013 and 2017 are summarized after Miler et al., 2022). Sampling locations of the tributaries, which wash the material from the waste sites, are presented on the left and of Meža River on the right. Sampling locations on the chart follow each other like in nature downstream.

(internet 1). Največjo vsebnost PSE v naplavljenem sedimentu so določili v Poljani (3800 mg/kg Zn, 590 mg/kg Pb, 25 mg/kg Cd, (podatki povzeti iz internet 1)). Vsebnosti PSE v sedimentih so velike in pričakovane, glede na podatke, ki jih obravnavamo v tem prispevku. Dogodek tovrstnega obsega je zagotovo močno spremenil geokemične lastnosti preučevanega območja, zato bo v bodoče zanimivo izvesti dodatne raziskave in opraviti primerjavo s podatki predstavljenimi v tem prispevku.

Vrednosti fizikalno-kemičnih parametrov in vsebnosti PSE v površinski vodi

Terenske meritve osnovnih fizikalno-kemičnih parametrov vode (pH, T, Eh, EC in DO) na posameznih vzorčnih mestih so podane v tabeli 3. Izmerjeni fizikalno-kemični parametri so osnovni indikatorji stanja vode. Pomembno vplivajo na obnašanje trdnih snovi v vodi, tudi tistih, ki vsebujejo PSE ter posledično na vsebnosti PSE v vodah. Mejne vrednosti osnovnih fizikalno-kemičnih parametrov v površinskih vodah v uredbah niso posebej predpisane.

Vrednosti pH so bile leta 2020 med 7,4 in 8,6, kar je nekoliko manj kot leta 2017 (8,1–8,8). Vzrok temu je lahko izvedba meritve v različnih letnih časih. Leta 2017 smo meritve izvedli poleti, ko je sproščanje organskih snovi iz rastlin v vodo intenzivnejše, kot jeseni, v času katere smo meritve izvajali leta 2020. V pritokih, ki odvodnjavajo odlagališča, je bila v obeh letih najmanjša vrednost izmerjena v pritoku 2 (SS-26/11), največja pa leta 2017 v Mušeniku (SS-26/7), leta 2020 pa v Helenskem potoku (SS-26/5). V reki Meži so se vrednosti pH gibale med 7,4 in 8,4. Vrednosti Eh so bile med 478 in 592 mV. Najmanjša vrednost v pritokih je bila izmerjena v Mušeniku (SS-26/7), največja pa v pritoku 2 (SS-26/11). Vrednosti v Meži so bile med 487 in 592 mV. Električna prevodnost (EC), ki odraža delež raztopljenih trdnih snovi v vodi oziroma je neposredno odvisna od ionskih oblik elementov, se v meritvah giblje med 183 in 685 µS/cm, kar je zelo podobno vrednostim iz leta 2017 (181–609 µS/cm). V obeh letih smo najmanjše vrednosti v pritokih izmerili v Jazbinskem potoku (SS-26/10), največji pa v

Tabela 3. Terenske meritve osnovnih fizikalno-kemičnih parametrov vode (pH, Eh, EC, DO, T).

Table 3. Field measurements of basic physico-chemical parameters of water (pH, Eh, EC, DO, T).

Vzorčno mesto / Sampling site	Leto / Year	Vodotok / Watercourse	pH	Eh (mV)	EC ($\mu\text{S}/\text{cm}$)	DO (%)	DO (mg/l)	T (°C)
SS-26/3	2017 ¹	Meža	8,54	/	180,9	101,6	11,06	8,5
	2020		7,37	592	182,6	101,7	11,43	7,4
SS-26/5	2017 ¹	Helenski potok	8,74	/	376,5	100,9	10,67	9,7
	2020		8,55	533	465,7	101,6	11,27	7,7
SS-26/6	2017 ¹	Meža	8,62	/	191,8	102,6	10,99	9,3
	2020		7,97	534	200,0	101,1	11,26	7,6
SS-26/7	2017 ¹	Mušenik	8,79	/	362,8	100,1	10,34	11,0
	2020		8,50	478	436,7	100,5	10,95	8,6
SS-26/8	2017 ¹	pritok 1/ tributary 1	8,77	/	348,1	100,7	10,39	10,7
	2020		8,46	502	410,1	100,2	10,90	8,8
SS-26/9	2017 ¹	Meža	8,12	/	260,9	96,6	9,46	13,4
	2020		8,36	506	270,0	99,5	10,90	8,5
SS-26/10	2017 ¹	Jazbinski potok	8,68	/	319,6	101,3	11,16	12,4
	2020		8,40	493	355,7	100,7	11,02	8,6
SS-26/11	2017 ¹	pritok 2/ tributary 2	8,24	/	609,0	100,7	11,18	7,9
	2020		7,90	567	684,9	96,8	10,70	8,2
SS-26/15	2017 ¹	Meža	8,58	/	324,4	100,1	9,42	15,5
	2020		8,42	487	383,7	97,9	10,55	9,6
SS-26/19	2017 ¹	Junčarjev potok	8,68	/	348,7	99,2	9,95	12,6
	2020		8,53	537	401,5	97,9	10,63	9,2
SS-26/20	2017 ¹	Meža	8,64	/	324,7	100,8	9,28	16,6
	2020		8,39	511	373,2	98,5	10,65	9,5
SS-26/21	2017 ¹	Meža	8,61	/	331,4	99,6	9,32	16,0
	2020		8,34	490	376,4	98,3	10,57	9,9
SS-26/22	2017 ¹	Meža	8,71	/	298,0	99,4	9,48	15,0
	2020		8,26	503	325,7	97,1	10,46	10,0

pritoku 2 (SS-26/11). V reki Meži so bile vrednosti v splošnem nekoliko manjše. Koncentracije v vodi raztopljenega kisika (DO) so bile leta 2020 (10,5–11,4 mg/l) malenkost večje, kot so bile leta 2017 (9,3–11,2 mg/l). V pritokih je bila vrednost DO v obeh letih najmanjša v Junčarjevem potoku (SS-26/19). Največjo vrednost DO v pritokih smo leta 2017 ugotovili v pritoku 2 (SS-26/11), leta 2020 pa v Helenskem potoku (SS-26/5). Vrednosti v Meži so bile v območju med 10,5 in 11,4 mg/l.

Glede na izmerjene vrednosti parametrov pH, Eh in DO je okolje v večini vodotokov na območju obravnavanih odlagališč rudarskih odpadkov nevtralno do rahlo bazično in relativno dobro prezračeno. V takih pogojih so trdni nosilci PSE Pb-karbonati in sulfidi ter Fe-oksihidroksidi večinoma stabilni, medtem ko so Zn-karbonati in sulfidi ter Fe-oksihidroksi sulfati s Pb in Zn nestabilni, zaradi česar se lahko del PSE iz njih izloči v vodo.

Vsebnosti 11 potencialno strupenih elementov (As, Ba, Cd, Co, Cr, Cu, Hg, Mo, Ni, Pb in Zn) v obravnavanih vzorcih površinskih vod so podane v tabeli 4. Za vrednotenje koncentracij PSE v obravnavanih vodah na vzorčnih mestih smo uporabili mejne vrednosti, določene z Uredbo o stanju površinskih voda (Uradni list RS, št. 14/09, 98/10, 96/13, 24/16 in 44/22 – ZVO-2). Tako so v tabeli 4 navedene vrednosti naravnega ozadja (NO) in najvišje dovoljene koncentracije za površinske vode. Z rdečo barvo so označene koncentracije, ki presegajo normativ za površinske vode. Vsebnost kadmija (Cd) je v normativu za površinske vode odvisna od trdote vode, ki je razdeljena v pet razredov. Ravno tako je od trdote vode odvisna vrednost cinka (Zn) in je razdeljena v tri razrede. Glede na meritve terenskih parametrov in litološko sestavo smo priveli, da je trdota vode v obravnavanih vzorcih za Cd od 100 do < 200 mg CaCO₃/l, s čimer je nor-

Tabela 4. Vsebnosti As, Ba, Cd, Co, Cr, Cu, Hg, Mo, Ni, Pb in Zn (v µg/l) v površinskih vodah.

Table 4. Contents of As, Ba, Cd, Co, Cr, Cu, Hg, Mo, Ni, Pb and Zn (in µg/l) in surface waters.

Vzorčno mesto / Sampling site	Leto / Year	Vodotok / Watercourse	As	Ba	Cd	Co	Cr	Cu	Hg	Mo	Ni	Pb	Zn	
SS-26/3	2017 ¹	Meža	0,88	7,3	0,02	0,013	< 0,5	0,2	< 0,2	1,0	< 0,3	0,18	3,3	
	2020		1,19	7,1	0,02	0,014	< 0,5	0,2	< 0,2	0,9	< 0,3	0,17	3,7	
SS-26/5	2017 ¹	Helenski potok	0,46	12,2	0,45	0,049	< 0,5	2,1	< 0,2	1,7	0,4	47,1	83,6	
	2020		0,49	8,5	0,45	0,067	< 0,5	0,7	< 0,2	0,9	0,4	28,0	88,4	
SS-26/6	2017 ¹	Meža	0,94	8,1	0,09	0,016	< 0,5	0,3	< 0,2	1,2	< 0,3	1,90	10,6	
	2020		1,19	7,6	0,10	0,016	< 0,5	0,2	< 0,2	1,0	< 0,3	1,23	12,4	
SS-26/7	2017 ¹	Mušenik	0,30	6,3	0,04	0,026	< 0,5	0,4	< 0,2	1,5	< 0,3	2,69	8,1	
	2020		0,38	6,0	0,05	0,026	< 0,5	0,4	< 0,2	1,0	0,3	3,57	8,6	
SS-26/8	2017 ¹	pritok 1 / tributary 1	0,20	11,2	< 0,01	0,016	< 0,5	0,2	< 0,2	1,7	< 0,3	< 0,01	< 0,5	
	2020		0,24	13,1	0,04	0,024	< 0,5	0,4	< 0,2	1,2	2,0	5,65	11,6	
SS-26/9	2017 ¹	Meža	0,51	12,6	0,10	0,026	< 0,5	0,7	< 0,2	1,8	0,4	0,89	19,7	
	2020		0,71	12,8	0,10	0,033	< 0,5	0,4	< 0,2	1,5	< 0,3	0,56	4,9	
SS-26/10	2017 ¹	Jazbinski p.	0,33	17,7	0,15	0,016	< 0,5	0,5	< 0,2	2,1	< 0,3	2,15	43,3	
	2020		0,34	16,0	0,04	0,016	< 0,5	0,3	< 0,2	1,7	0,3	3,02	74,4	
SS-26/11	2017 ¹	pritok 2 / tributary 2	0,70	9,1	11,20	0,034	< 0,5	0,5	< 0,2	5,6	1,3	38,1	2290	
	2020		1,02	7,3	11,10	0,052	< 0,5	0,6	< 0,2	4,2	1,6	44,4	2850	
SS-26/15	2017 ¹	Meža	0,48	17,4	1,14	0,143	< 0,5	6,1	< 0,2	2,3	3,1	5,84	42,9	
	2020		1,23	16,7	1,45	0,140	< 0,5	1,4	< 0,2	10,5	2,4	4,17	59,0	
SS-26/19	2017 ¹	Junčarjev potok	0,52	29,4	0,38	0,030	< 0,5	0,6	< 0,2	2,9	2,4	33,8	162	
	2020		0,56	15,2	0,09	0,032	< 0,5	0,5	< 0,2	1,6	0,5	15,4	78	
SS-26/20	2017 ¹	Meža	0,54	18,6	1,17	0,126	< 0,5	6,1	< 0,2	2,5	3,0	7,68	44,8	
	2020		1,35	18,1	1,78	0,175	< 0,5	1,9	< 0,2	8,2	3,3	4,28	65,1	
SS-26/21	2017 ¹	Meža	0,61	21,2	0,91	0,089	< 0,5	4,2	< 0,2	2,5	2,4	4,86	38,6	
	2020		1,27	20,1	1,21	0,110	< 0,5	0,9	< 0,2	6,1	2,2	2,98	53,9	
SS-26/22	2017 ¹	Meža	0,68	22,0	0,47	0,042	< 0,5	3,5	< 0,2	2,5	1,7	1,80	20,5	
	2020		1,18	20,5	0,65	0,028	< 0,5	0,7	< 0,2	3,9	1,1	0,64	41,4	
Naravno ozadje / Natural background (NO; µg/l) ²			/	/	0,04	0,100	/	1,0	0,0025	/	/	/	4,2	
Površinske vode-največja dovoljena koncentracija / Surface waters-highest permissible level (µg/l) ³			21	/	r.4 ^a : 0,9+NO	2,8 +NO	160	73 +NO	0,07 +NO	200	34	14	520 ^b +NO	
Odpadne vode (neposredno v vodo) Waste water (directly in water) (µg/l) ⁴			100	5000	25	30	500	500	5	1000	500	500	2000	

¹Podatki povzeti po Miler et al. (2022) / Data after Miler et al. (2022)^{2,3}Uradni list RS, št. 14/09, 98/10, 96/13, 24/16 in 44/22 – ZVO-2. Uredba o stanju površinskih voda / Decree on surface water status⁴Uradni list RS, št. 64/12, 64/14, 98/15, 44/22 – ZVO-2, 75/22 in 157/22. Decree on the emission of substances and heat when discharging waste water into waters and the public sewage system.

mativ za Cd 0,9 + NO µg/l ter za Zn \geq 100 mg Ca-CO₃/l, s čimer je normativ za Zn 520 + NO µg/l.

Izmerjene vsebnosti Pb v vzorcih vode (tabla 4, sl. 3) so leta 2017 presegale normativ za površinske vode za svinec (14 µg/l) na vzorčnih mestih v Helenskem potoku (SS-26/5; 47,1 µg/l), v pritoku 2 (SS-26/11; 38,1 µg/l) in v Junčarjevem potoku (SS-26/19; 33,8 µg/l). Preseganje normativne vrednosti in dobro ujemanje z vrednostmi iz leta

2017 na omenjenih treh lokacijah smo ugotovili tudi leta 2020. Vsebnosti Pb na vzorčnih mestih SS-26/5 (28 µg/l) in SS-26/19 (15,4 µg/l) sta bila le nekoliko manjši kot leta 2017, na vzorčnem mestu SS-26/11 pa rahlo večja (44,4 µg/l). Na vseh omenjenih lokacijah smo tudi v sedimentih v obeh letih ugotovili močno povečane vsebnosti Pb, ki presegajo kritične vrednosti za Pb.

Vsebnosti Zn (tabela 4, sl. 4) so leta 2017 presegale normativ za površinske vode za Zn (524,2 µg/l) samo v pritoku 2 (SS-26/11; 2290 µg/l). Podobno stanje smo ugotovili tudi leta 2020, ko je bila vsebnost Zn na vzorčnem mestu SS-26/11 nekoliko večja (2850 µg/l). Tudi vsebnosti Zn v sedimentu na istem vzorčnem mestu sta v obeh letih močno presegali kritično vrednost za Zn.

Vsebnosti Cd (tabela 4, sl. 5) so leta 2017 presegale normativ za površinske vode za Cd (0,94 µg/l) na treh vzorčnih mestih: v pritoku 2 (SS-26/11; 11,2 µg/l) ter na dveh lokacijah v Meži (SS-26/15; 1,14 µg/l in SS-26/20; 1,17 µg/l). Na vseh omenjenih lokacijah so tudi vsebnosti Cd v sedimentih presegale pripadajočo kritično vrednost. Tudi v letu 2020 smo ugotovili preseganje normativa za površinske vode za Cd v pritoku 2 (SS-26/11; 11,1 µg/l) ter v Meži na lokacijah SS-26/15 (1,45 µg/l) in SS-26/20 (1,78 µg/l). Dodatno smo leta 2020 ugotovili preseganje še na eni lokaciji v Meži (SS-26/21; 1,21 µg/l). Vsebnosti Cd v sedimentu v letu 2020 so bile na vzorčnem mestu SS-26/11 nad kritično vrednostjo za Cd, na preostalih treh vzorčnih mestih pa med mejno in kritično vrednostjo.

Vsebnosti Mo (sl. 6), As (sl. 7), Ba (sl. 8), Co (sl. 9), Cr (sl. 10), Cu (sl. 11) in Ni (sl. 12) v površinski vodi niso presegale zakonodajnih smernic, izmerjeni vrednosti na posameznem vzorčnem mestu sta si v obeh opazovanih letih večinoma zelo podobni. Prostorska porazdelitev vsebnosti posameznih elementov je podana v nadaljevanju. Vsebnosti Mo v površinski vodi so bile v obeh letih v pritokih Meže (z izjemo pritoka 2) in v zgornjem toku Meže do naselja Žerjav (na lokacijah SS-26/3, SS-26/6 in SS-26/9), nekoliko manjše kot v pritoku 2 ter lokacijah v Meži dolvodno od Žerjava (SS-26/15, SS-26/20, SS-26/21 in SS-26/22). Ob tem so bile vsebnosti na vzorčnih mestih dolvodno od Žerjava leta 2020 izrazito večje, kot leta 2017. Vsebnosti As v površinski vodi so bile nekoliko večje v pritoku 2 in na vseh lokacijah v Meži (z izjemo lokacije SS-26/9), predvsem leta 2020. Vsebnosti Ba so nekoliko večje v Jazbinskem (SS-26/10) in Junčarjevem potoku (SS-26/19) ter v Meži na lokacijah SS-26/15, SS-26/20, SS-26/21 in SS-26/22. Nakazuje se, da vsebnosti Ba naraščajo navzdol po toku Meže. Vsebnosti Co so nekoliko večje v Helenskem potoku in pritoku 2 ter v Meži na lokacijah SS-26/15, SS-26/20 in SS-26/21. Vsebnosti Cu v površinski vodi so bile leta 2017 na vzorčnih mestih SS-26/5 in v Meži dolvodno od Žerjava izrazito večje, kot leta 2020. Tudi leta 2020 so bile vsebnosti v Meži nižje od Žerjava nekoliko večje od preostalih. Vsebnosti Ni

so bile v obeh letih največje na vzorčnih mestih v Meži dolvodno od Žerjava, v posameznih pritokih pa se obe vsebnosti precej razlikujeta. Leta 2017 je bila izmed pritokov največja na vzorčnem mestu SS-26/8 in SS-26/11, leta 2020 pa na SS-26/11 in SS-26/19.

Izkazalo se je, da so površinske vode reke Meže s pritoki manj obremenjene s PSE v raztopljeni in bolj s PSE v trdni obliki. Ugotovili smo le lokalno velike vsebnosti v vodi, predvsem v vodotokih, ki odvodnjavajo odlagališča. To so koncentracije Pb v Helenskem potoku, pritoku 2, ki odvodnjava Kavšakovo odlagališče in Junčarjevem potoku, koncentracije Zn v pritoku 2 in koncentracije Cd v pritoku 2. V Meži pa je površinska voda obremenjena s Cd na lokacijah SS-26/15, SS-26/20, SS-26/21, to je nižje od Žerjava, v Mežici in dolvodno od Mežice. Miler in sodelavci (2022) so s pomočjo izluževalnih testov (z vodo) ugotovili, da material iz odlagališč Štoparjev odval (Helenski potok), Igrče (Mušenik), Kavšakovo odlagališče (pritok 2, Jazbinski potok) in Fridrih (Junčarjev potok) vsebuje Pb, ki se lahko izlužuje in vpliva na vsebnosti Pb v vodni raztopini. Poleg tega se iz materiala odlagališč Fridrih in Kavšakovo odlagališče izlužujeta tudi Cd oziroma Zn. To pomeni, da ima zadrževanje vode v odlagališčih pomembno vlogo pri dotoku raztopljenih oblik Pb, Zn in Cd v pritoke Meže. Z uporabo SEM/EDS mikroskopije v kombinaciji s PHREEQC simulacijami (Miler in sodelavci, 2022) je bilo ugotovljeno tudi, da je veliko rudnih mineralov (Zn-karbonati in sulfidi), ki se pojavljajo v materialu odlagališč in sedimentih, korodiranih, kar kaže na raztopljanje mineralov in sproščanje PSE v okolje pod pogoji, ki trenutno vladajo v površinskih vodah. V sedimentih in odlagališčih se pojavljajo tudi sekundarni produkti preperevanja rudnih mineralov s PSE, med katrimi so pri danih pogojih v vodah Fe-oksihidroksi sulfati nestabilni, Fe-oksihidroksidi pa večinoma stabilni. Pri spremembah teh pogojev pa lahko hitro postanejo nestabilni, pri čemer se PSE sprostijo nazaj v vodno raztopino.

Zaključek

Z zaprtjem rudnika in predelovalno-metalurških obratov na območju Mežice, se je neposreden vnos PSE v okolje močno zmanjšal. Še vedno pa na okolje vplivajo stara bremena in sedanje antropogene dejavnosti. Kot posreden vir potencialno strupenih elementov (PSE) so ostala odlagališča rudarskih odpadkov (siromašne rude in odpadkov nastalih pri predelavi rude), iz katerih se PSE spirajo v bližnje potoke ter z njimi potujejo v Mežo ter dalje v Dravo. Na vsebnosti PSE v sedimentih

vplivajo poleg odlagališč rudarskih odpadkov tudi vsespolno obremenjeno naravno in urbano okolje. Iz vseh segmentov s kovinami obremenjenega okolja se izpira material v vodotoke.

V obravnavanih sedimentih so vsebnosti PSE, predvsem Pb, Zn, Cd, Mo in As močno nad nivojem ozadja in večkratno presegajo kritično vrednost za tla. Njihove vsebnosti močno nihajo med posameznimi vzorčnimi mesti in tudi med posameznimi leti (2013, 2017, 2020) na istih vzorčnih mestih. Nihanja med opazovanimi leti so najbolj izrazita v pritokih reke Meže, kjer se vsebnosti zradi povečane erozije in transporta materiala kot posledica višjega vodostaja in pretoka, znatno popovečajo. Vsebnosti v površinski vodi se bistveno ne spreminjajo. Pojavljajo se le zmerna povečanja Pb, Zn in Cd v vodi, ki so lokalnega značaja.

Na podlagi rezultatov ugotavljamo, da so sedimenti v dolini Meže še vedno močno obremenjeni s PSE. Zaradi erozijskih procesov na odlagališčih rudarskih odpadkov so ta pomemben vir materiala bogatega s PSE, ki se spirala v vodotoke, ki jih odvodnjavajo. Zato je potrebna njihova sanacija in še nadaljnje spremljanje stanja odlagališč in nivojev PSE v sedimentih in vodah.

Zahvala

Raziskave smo izvedli s finančno podporo Ministrstva za okolje in prostor v okviru projekta »Spremljanje zaprtih objektov za ravnanje z odpadki iz rudarskih in drugih dejavnosti izkoriščanja mineralnih surovin (2020 – 2021) (št. pogodbe 2550 – 20 – 340122)«, ki je bil izведен na Geološkem zavodu Slovenije. Raziskava je bila delno financirana s strani Javne agencije za znanstvenoraziskovalno in inovacijsko dejavnost Republike Slovenije (ARIS) preko raziskovalnih programov »Podzemna voda in geokemija (P1-0020)« in »Mineralne surovine (P1-0025)«, ter raziskovalnega projekta »Dinamika in snovni tok potencialno šrapenih elementov (PSE) v urbanem okolju (J1-1713)«. Finančno pomoč je nudila tudi Slovenska nacionalna komisija za UNESCO, Nacionalni odbor Mednarodnega programa za geoznanost in geoparke.

Literatura

ARSO 2023: Nalivi in obilne padavine od 3. do 6. avgusta 2023. Preliminarno poročilo. Republika Slovenija, Ministrstvo za okolje, podnebje in energijo, Agencija Republike Slovenije za okolje, Urad za meteorologijo, hidrologijo in oceanografijo: 25 p. <https://meteo.arso.gov.si/uploads/probase/www/climate/text/sl/we->

[ather_events/padavine_3-6avg2023-preliminaro.pdf](#) (17. 11. 2023)

Ballabio, C., Jiskra, M., Osterwalder, S., Borrelli, P., Montanarella, L. & Panagos, P. 2021: A spatial assessment of mercury content in the European Union topsoil. *Sci Total Environ*, 769: 144755.

Bidovec, M. 1997: Uporaba poplavnega sedimenta za ugotavljanje geokemičnega ozadja in stopnje onesnaženja. Magistrsko delo. Univerza v Ljubljani, Naravoslovnotehniška fakulteta, Oddelek za geologijo, Ljubljana: 132 p.

Bole, M., Druks, P., Rošer Drev, A. & Vetrih, M. 2002: Segment: vode. In: Ribarič-Lasnik, C. (ed.): Primerjalna študija o onesnaženosti okolja v Zg. Mežiški dolini med stanji v letih 1989 in 2001, končno poročilo, zvezek 3: 185 p.

Boni, M., Costabile, S., De Vivo, B. & Gasparriini M. 1999: Potential environmental hazard in the mining district of southern Iglesiente (SW Sardinia, Italy). *J Geochem Explor*, 67: 417–430. [https://doi.org/10.1016/S0375-6742\(99\)00078-3](https://doi.org/10.1016/S0375-6742(99)00078-3)

Budkovič, T., Šajn, R. & Gosar, M. 2003: Vpliv delajočih in opuščenih rudnikov kovin in topilniških obratov na okolje v Sloveniji. *Geologija*, 46/1: 135–140. <https://doi.org/10.5474/geologija.2003.015>

Direktiva 2006/21/ES Evropskega parlamenta in Sveta z dne 15. marca 2006 o ravnanju z odpadki iz rudarskih in drugih ekstraktivnih dejavnosti ter o spremembji Direktive 2004/35/ES. Izjava Evropskega parlamenta, Sveta in Komisije. <https://eur-lex.europa.eu/legal-content/SL/ALL/?uri=CELEX:32006L0021>

Eržen, I., Kugonič, N., Pokorný, B., Končnik, D., Svetina, M., Justin, B., Druks, P., Bole, M., Rošer Drev, A., Vetrih, M., Flis, J., Kotnik, K., Mausar, R., Pačnik, L. & Savinek, K. 2002: Uvod. 1. Zvezek. In: Ribarič-Lasnik, C. (ed.): Primerjalna študija o onesnaženosti okolja v Zg. Mežiški dolini med stanji v letih 1989 in 2001, končno poročilo, zvezek 1: 32 p.

Finžgar, N., Jež, E., Voglar, D. & Leštan, D. 2014: Spatial distribution of metal contamination before and after remediation in the Meza Valley, Slovenia. *Geoderma*, 217–218: 135–143. <https://doi.org/10.1016/j.geodema.2013.11.011>

Fux, J. & Gosar, M. 2007: Vsebnosti svinca in drugih težkih kovin v sedimentih na območju Mežiške doline (Lead and other heavy metals in stream sediments in the area of Meža valley). *Geologija*, 50/2: 347–360. <https://doi.org/10.5474/geologija.2007.025>

- Gaberšek, M. & Gosar, M. 2023: Odraz preteklega rudarjenja v dravskih sedimentih. *Proteus*, 85/6–9: 288–292.
- Goltnik, T., Burger, J., Kranjc, I., Turšič, J. & Zuliani, T. 2022: Potentially toxic elements and Pb isotopes in mine-draining Meža River catchment (NE Slovenia). *Water*, 14/7, 998-1–998-13. <https://doi.org/10.3390/w14070998>
- Gosar, M. & Miler, M. 2011: Anthropogenic metal loads and their sources in stream sediments of the Meža River catchment area (NE Slovenia). In: Fortner, S. K. & Munk, L.(eds.): Sources, transport and fate of trace and toxic elements in the environment. Amsterdam: Elsevier. *Appl. Geochem.*, 26/11: 1855–1866. <https://doi.org/10.1016/j.apgeochem.2011.06.009>
- Gosar, M., Šajn, R. & Biester, H. 2006: Binding of mercury in soils and attic dust in the Idrija mercury mine area (Slovenia). *Sci Total Environ*, 369: 150–162. <https://doi.org/10.1016/j.scitotenv.2006.05.006>
- Gosar, M., Šajn, R. & Miler, M. 2014: Izdelava popisa zaprtih objektov za ravnanje z odpadki iz rudarskih in drugih dejavnosti izkoriščanja mineralnih surovin: poročilo 3. faze projekta. Geološki zavod Slovenije, Ljubljana: 49 p.
- Gosar, M., Miler, M. & Bavec, Š. 2017: Spremljanje zaprtih objektov za ravnanje z odpadki iz rudarskih in drugih dejavnosti izkoriščanja mineralnih surovin. Poročilo o izvedenih delih za Ministrstvo za okolje in prostor (RS). Geološki zavod Slovenije, Ljubljana: 67 p.
- Gosar, M., Šajn, R., Bavec, Š., Gaberšek, M., Pezdir, V. & Miler, M. 2019: Geochemical background and threshold for 47 chemical elements in Slovenian topsoil. *Geologija*, 62/1: 7–59.
- Gosar, M., Šajn, R., Miler, M., Burger, A., & Bavec, Špela. 2020: Overview of existing information on important closed (or in closing phase) and abandoned mining waste sites and related mines in Slovenia. *Geologija*, 63/2, 221–250. <https://doi.org/10.5474/geologija.2020.018>
- Gosar, M., Bavec, Š., Miler, M., Demšar, M. & Gaberšek, M. 2021: Spremljanje zaprtih objektov za ravnanje z odpadki iz rudarskih in drugih dejavnosti izkoriščanja mineralnih surovin (2020–2021). Poročilo o izvedenih delih za Ministrstvo za okolje in prostor (RS). Geološki zavod Slovenije, Ljubljana: 60 p.
- Gošar, D., Costa, M. R., Ferreira, A. & Štrucl Fajmut, S. 2015: Assessment of past and present water quality in closed Mežica Pb-Zn Mine (Slovenia). *Comunicações Geológicas*, 102/1: 71–75.
- Kesler, S.E. 1994; Mineral resources, economics, and the environment. Maxwell Macmillan International, New York: 434 p.
- Kolbezen, M. & Pristov, J. 1998: Površinski vodotoki in vodna bilanca Slovenije. Ministrstvo za okolje in prostor, Hidrometeorološki zavod republike Slovenije. 50 let organizirane hidrometeorološke službe na Slovenskem 1947–1997. Ljubljana: 79 p. http://www.arno.si/vode/publikacije%20in%20poro%c4%8dila/bilanca6190_2_BESEDILO.pdf (5. 7. 2023)
- Kugonič, N. & Zupan, M. 1999: Vsebnosti Pb, Cd in Zn v tleh in nekaterih rastlinah v Zgornji mežiški dolini (Contents of Pb, Cd and Zn in soil and plants in upper Meža Valley). In: Ribarič-Lasnik, C., Pokorny, B. & Pačnik, L. (eds.): Problem težkih kovin v Zgornji Mežiški dolini: zbornik referatov. Environmental Research & Industrial Co-operation Institute ERICO, Velenje: 66–78.
- Kuzmič, R. & Suhadolnik, A. 2005: Urejanje voda kot varstvo pred poplavami. In: 16. Mišičev vodarski dan 2005, Maribor: 65–71. <http://mvd20.com/LETO2005/R9.pdf> (5. 7. 2023)
- Lewis, S.L. & Maslin, M.A. 2015: Defining the Anthropocene. *Nature*, 519: 171–180. <https://doi.org/10.1038/nature14258>.
- Miler, M. & Gosar, M. 2012: Characteristics and potential environmental influences of mine waste in the area of the closed Mežica Pb-Zn mine (Slovenia). *J. Geochem. Explor.*, 112, 152–160. <https://doi.org/10.1016/j.gexplo.2011.08.012>
- Miler, M. & Gosar, M. 2013: Assessment of metal pollution sources by SEM/EDS analysis of solid particles in snow: a case study of Žerjav, Slovenia. *Microsc. Microanal.*, 19/6: 1606–1619. <https://doi.org/10.1017/S1431927613013202>
- Miler, M. & Gosar, M. 2019: Assessment of contribution of metal pollution sources to attic and household dust in Pb-polluted area. *Indoor Air*, 29/3: 487–498. <https://doi.org/10.1111/ina.12548>
- Miler, M., Bavec, Š. & Gosar, M. 2022: The environmental impact of historical Pb-Zn mining waste deposits in Slovenia. *J. Environ. Manag.*, 308: 114580. <https://doi.org/10.1016/j.jenvman.2022.114580>
- Reimann, C., Flem, B., Fabian, K., Birke, M., Ladenberger, A., Négre, P., Demetriades, A. & Hoogewerff, J. 2012: The GEMAS Project Team. Lead and lead isotopes in agricultural soils of Europe – The continental perspective. *Appl Geochem*, 27: 532–542.
- Ottesen, R.T., Birke, M., Finne, T.E., Gosar, M., Locutura, J., Reimann, C. Tarvainen, T. & the

- GEMAS Project Team 2013: Mercury in European agricultural and grazing land soils. *Appl Geochem*, 33: 1–12. <https://doi.org/10.1016/j.apgeochem.2012.12.013>
- Salomons, W. & Förstner, U. 1988: Environmental management of solid waste: Dredged materials and mine tailings. Springer-Verlag, Berlin: 396 p.
- Svetec, P., Milačič, R. & Pihlar, B. 2001: Partitioning of Zn, Pb and Cd in river sediments from a lead and zinc mining area using the BCR three-step sequential extraction procedure. *J. of Environ. Monit.*, 3/6: 586–590. <http://doi.org/10.1039/b106311c>
- Šajn, R. 2006: Factor Analysis of Soil and Attic-dust to Separate Mining and Metallurgy Influence, Mežica Valley, Slovenia. *Mathem. Geol.* 38/6: 735–747. <https://doi.org/10.1007/s11004-006-9039-7>
- Šajn, R. & Gosar, M. 2004: Pregled nekaterih onesnaženih lokacij zaradi nekdanjega rudarjenja in metalurških dejavnosti v Sloveniji. *Geologija*, 47/2: 249–258. <https://doi.org/10.5474/geologija.2004.020>
- Uradni list RS, št. 43/08, 30/11, 64/21 in 44/22 – ZVO-2: Uredba o ravnanju z odpadki iz rudarskih in drugih dejavnosti izkoriščanja mineralnih surovin. <http://www.pisrs.si/Pis.web/pregleđPredpisa?id=URED4693>
- Uradni list RS, št. 68/96, 41/04 – ZVO-1 in 44/22 – ZVO-2: Uredba o mejnih, opozorilnih in kritičnih imisijskih vrednostih nevarnih snovi v tleh. <http://www.pisrs.si/Pis.web/pregleđPredpisa?id=URED114>
- Uradni list RS, št. 14/09, 98/10, 96/13, 24/16 in 44/22 – ZVO-2: Uredba o stanju površinskih voda. <http://pisrs.si/Pis.web/pregleđPredpisa?id=URED5010>
- Uradni list RS, št. 64/12, 64/14, 98/15, 44/22 – ZVO-2, 75/22 in 157/22: Uredba o emisiji snovi in toplotne pri odvajjanju odpadnih voda v vode in javno kanalizacijo. <http://pisrs.si/Pis.web/pregleđPredpisa?id=URED6070>
- Vreča, P., Pirc, S. & Šajn, R. 2001: Natural and anthropogenic influences on geochemistry of soils in the terrains of barren and mineralized carbonate rocks in the Pb-Zn mining district of Mežica, Slovenia. *J. of Geochem. Explor.* 74/1–3: 99–108. [https://doi.org/10.1016/S0375-6742\(01\)00177-7](https://doi.org/10.1016/S0375-6742(01)00177-7)
- VROM, 2000: Ministerie van Volkshuisvesting, Ruimtelijke Ordening en Milie (The Ministry of Housing, Spatial Planning and the Environment). Dutch Target and Intervention Values, (the New Dutch List). https://www.esdat.net/Environmental%20Standards/Dutch/annexS_I2000Dutch%20Environmental%20Standards.pdf (19. 9. 2023)
- Zupan, M., Grčman, H. & Lobnik, F. 2008: Raziskave onesnaženosti tal v Sloveniji (Research of soil pollution in Slovenia). Agencija RS za okolje, Ljubljana: 68 p. http://agromet.mkgp.gov.si/Publikacije/raziskave_onesnazenosti_tal.pdf (17. 11. 2023)
- Žibret, G., Gosar, M., Miler, M. & Alijagić, J. 2018: Impacts of mining and smelting activities on environment and landscape degradation - Slovenian case-studies. *Land Degrad. Dev.* 29/12: 4457–4470. <https://doi.org/10.1002/ldr.3198>
- Internet 1: <https://www.he-ss.si/objava/rezultati-vzorcenja-sedimenta-in-prvotnih-tal-na-poplavljenih-podrocjih.html> (24. 11. 2023)



Palaeoecological significance of the trace fossil *Circulichnis* Vyalov, 1971 from the Carboniferous of the Donets Basin, Ukraine

Paleoekološki pomen fosilne sledi *Circulichnis* Vyalov, 1971 iz karbona Doneškega bazena v Ukrajini

Vitaly DERNOV

Institute of Geological Sciences, National Academy of Sciences of Ukraine, 55 b, Oles Honchar Str., Kyiv, 01054, Ukraine,
e-mail: vitalydernov@gmail.com

Prejeto / Received 24. 2. 2023; Sprejeto / Accepted 15. 4. 2024; Objavljeno na spletu / Published online 11. 6. 2024

Key words: trace fossils, *Circulichnis*, Pennsylvanian, Ukraine

Ključne besede: fosilne sledi, *Circulichnis*, pennsylvanij, Ukrajina

Abstract

The ichnogenus *Circulichnis* Vyalov is a horizontal a ring- or ellipse-shaped burrow and/or locomotion trace of an unknown producer, most likely an annelid or a “worm”, preserved on the bedding plane. This ichnogenus is known over a wide age interval (Ediacaran–Oligocene). *Circulichnis* demonstrates a wide ecological range and has been found in continental (Mermia ichnofacies), shelf, and relatively deep-water (turbidites) deposits. It is commonly interpreted as a sediment feeding trace, but the peculiarities of its formation remain somewhat mysterious, as it is unclear how the tracemaker reached the sediment surface, as lateral branches of the ring-shaped traces are extremely rare and have only been observed by a few researchers. A rather large specimen of *Circulichnis montanus* Vyalov, 1971 with a preserved lateral branch was found in the Mospyne Formation (upper Bashkirian, Lower Pennsylvanian) of the Donets Basin. This discovery confirmed the assumption made by Alfred Uchman and Bruno Ratazzi regarding the peculiarities of formation of *Circulichnis*. According to these authors, a single ring-shaped *Circulichnis* indicates an attempt to forage at a specific level in the sediment, while the lateral branches of *Circulichnis* are part of a vertical shaft leading to another level within the sediment. The study of *Circulichnis montanus* from the Donets Basin has confirmed that at least variant C of the *Circulichnis* formation scheme proposed by Uchman and Ratazzi is correct, i.e. the lateral branch is a horizontal or subhorizontal part of a generally vertical shaft. However, it is important to note that the correctness of variants A and B of the Uchman and Ratazzi scheme cannot be excluded. To answer this question unequivocally, new finds of well-preserved *Circulichnis* are necessary.

Izvleček

Ihnofosilni rod *Circulichnis* Vyalov, 1971 je vodoravna, obročasto ali elipsasto oblikovana sled vrtanja in/ali premikanja neznanih organizmov, najverjetneje anelidov ali „črvov“, ki so se ohranili na površini plasti. Ta ihmofosilni rod je poznan v širokem starostnem intervalu (ediakarij–oligocen). *Circulichnis* izkazuje širok ekološki razpon in je bil najden v kontinentalnih (Mermia ihmofacies), šelfnih in razmeroma globokomorskih (turbiditnih) sedimentih. Običajno ga tolmačijo kot sled prehranjevanja s sedimentom, vendar posebnosti njegovega nastanka ostajajo nekoliko skrivnostne, saj ni jasno, kako je organizem, ki je pustil sled, dosegel površino sedimenta, saj so stranske veje obročastih sledi izjemno redke in jih je opazilo le nekaj raziskovalcev. V formaciji Mospyne (zgornji baškirij, spodnji pennsilvanij) v Doneškem bazenu je bil najden precej velik primerek vrste *Circulichnis montanus* Vyalov, 1971. Na tem primerku je ohranjena stranska veja, kar je, kot je navedeno zgoraj, precej redko. To odkritje je potrdilo domnevo Alfreda Uchmana in Bruna Ratazzija o posebnostih nastanka rodu *Circulichnis*. Po tej domnevi je posamezen obroč *Circulichnis* poskus prehranjevanja na določeni ravni v sedimentu, medtem ko so stranske veje *Circulichnis* del vertikalnega rova, ki vodi na drugo raven v sedimentu. Raziskava *Circulichnis montanus* iz Doneškega bazena je pokazala, da je pravilna vsaj varianta C sheme nastanka rodu *Circulichnis*, ki sta jo predlagala Uchman in Ratazzi, tj. stranska veja je horizontalni ali subhorizontalni del sicer vertikalnega rova. Vendar to ne izključuje pravilnosti variant A in B Uchmanove in Ratazzijeve sheme. Nedvoumen odgovor na to vprašanje bodo lahko dale le nove najdbe dobro ohranjenih primerkov rodu *Circulichnis*.

Introduction

Circulichnisis Vyalov, 1971 is a burrow or trail of enigmatic producers, most likely annelids or “worms”, in the form of a ring or ellipse preserved on bedding surfaces (Pickerill & Keppie, 1981; Pickerill et al., 1988; Blissett & Pickerill, 2004; Uchman & Rattazzi, 2018). This ichnogenus ranged from the Ediacaran to the Oligocene (Uchman & Rattazzi, 2018; Morgan et al., 2023). *Circulichnisis* shows a wide environmental range, from continental (Mermia ichnofacies) via shelf to deep-sea (turbiditic) deposits (e.g., Pickerill & Keppie, 1981; Fillion & Pickerill, 1984; McCann & Pickerill, 1988; Buatois & Mángano, 1993; Buatois et al., 1998a). *Circulichnisis* is generally considered to be

a fodinichnion (Pickerill & Keppie, 1981; Mángano et al., 1997; Buatois et al., 1998a, b; Buatois et al., 2006).

Carboniferous trace fossils from the Donets Basin have not yet been studied sufficiently. However, they are of great palaeoecological importance, since the Carboniferous carbonate platform (Tournaisian–Viséan (part)), paralic coal-bearing (Serpukhovian–Kasimovian (part)), and continental red-bed (Kasimovian (part)–Gzhelian) strata in the Donets Basin were formed under different depositional conditions, from relatively deep-water shelf areas to lowland land, located in humid and arid climates (Logvinenko, 1953; Feofilova & Levenshtein, 1963; Novik, 1974; Kozitskaya &

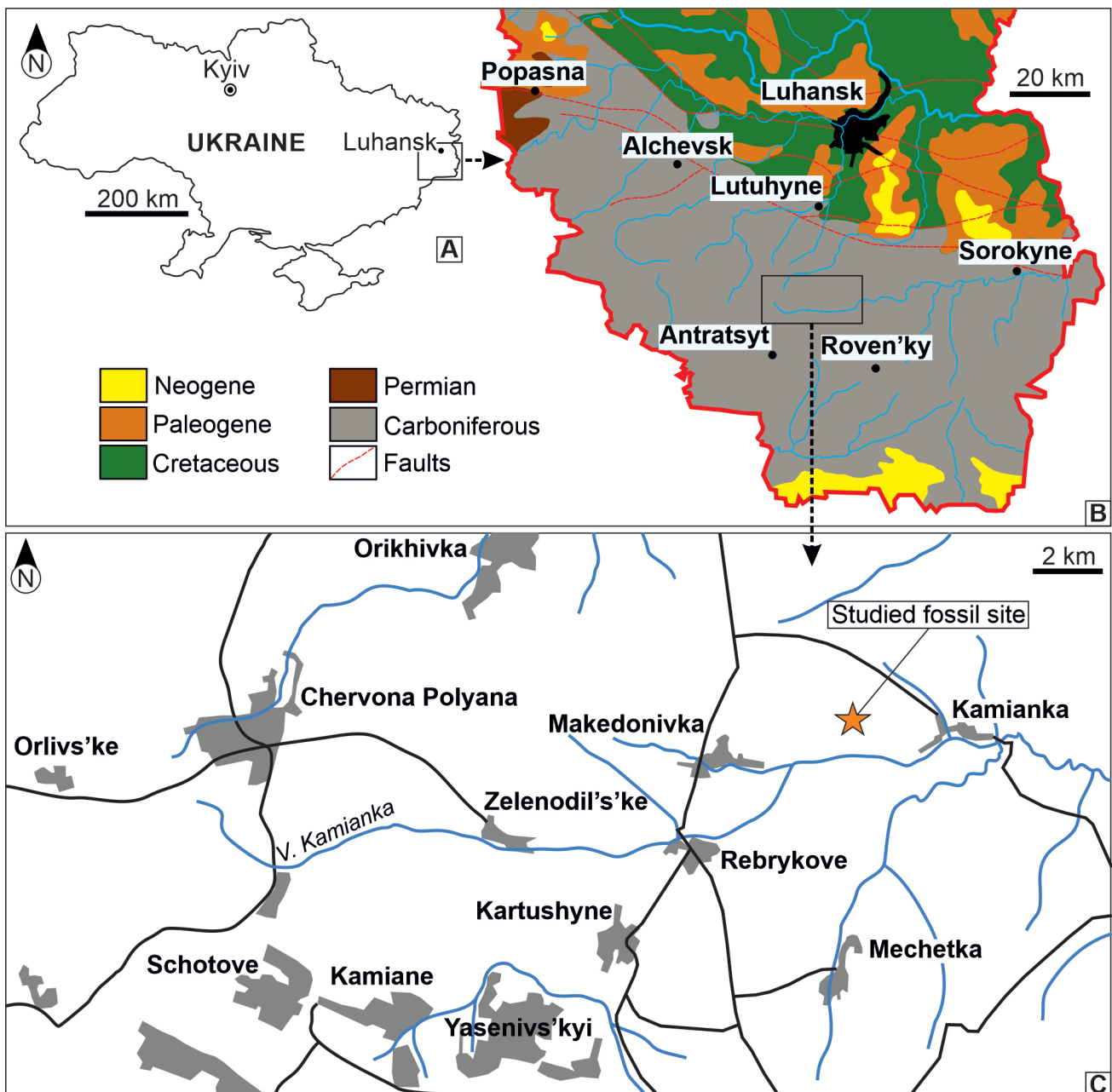


Fig. 1. Geographical location of the fossil site with *Circulichnisis montanus* Vyalov, 1971. Abbreviation: V. Kamianka – Velyka Kamianka River. Geological map in Fig. 1B modified after Fissunenko (2004).

Schegolev, 1993). As a result, they characterised different habitat conditions for animals and plants.

This paper describes the ichnospecies *Circulichnis montanus* Vyalov, 1971 from the upper Bashkirian (Pennsylvanian) Mospyne Formation of the Donets Basin (Ukraine), which is important for clarifying the ethology of its tracemakers. In Ukraine, the trace fossils *Circulichnis* have been recorded in the Ediacaran deposits of Podillia (Gureev, 1983), in the Triassic and Jurassic deposits of Crimea (Dmitrieva et al., 1963; Shalimov, 1978) and in the sandstone bed below the G₁² limestone layer of the Mospyne Formation in the study area (author's unpublished data), i.e. about 300 m below the sandstone bed from which the trace fossil described here originates. Therefore, this study is also a documentation of the new record of *Circulichnis* in Ukraine.

Geological setting and material

Bashkirian-aged coal-bearing deposits in the Donets Basin were accumulated mainly in a large alluvial-deltaic plain, which was flooded periodically by the epicontinental seas. Only the central part of the Donets Basin was characterized by a continuous regime of marine sedimentation in the Bashkirian.

The sandstone bed with *Circulichnis montanus* Vyalov, 1971 lies in the upper part of the Mospyne Formation (Fig. 2A, B), which is a 315 to 730 m-thick sequence of mudstone, siltstone, sandstone, limestone, and coal (Feofilova & Levenstein, 1963; Dunaeva, 1969; Aisenverg et al., 1975; Poletaev et al., 2011; Nemyrovska & Yefimenko, 2013). These rocks were deposited in shallow marine, lagoonal, lacustrine, prodeltaic, deltaic, peat and clastic swamp environments (Logvinenko, 1953; Feofilova & Levenshtein, 1963). The Mospyne Formation corresponds to the lower part of the Zuyivkian Horizon (lower half of the Kayalian Regional Stage) of the Regional Stratigraphic Scheme of the Dnipro-Donets Downwarp (Poletaev et al., 2011; Nemyrovska & Yefimenko, 2013). This formation contains remains of typical Langsettian terrestrial plants (Novik, 1974; Dernov & Udovychenko, 2019a) and

cally by the epicontinental seas. Only the central part of the Donets Basin was characterized by a continuous regime of marine sedimentation in the Bashkirian.

The sandstone bed with *Circulichnis montanus* Vyalov, 1971 lies in the upper part of the Mospyne Formation (Fig. 2A, B), which is a 315 to 730 m-thick sequence of mudstone, siltstone, sandstone, limestone, and coal (Feofilova & Levenstein, 1963; Dunaeva, 1969; Aisenverg et al., 1975; Poletaev et al., 2011; Nemyrovska & Yefimenko, 2013). These rocks were deposited in shallow marine, lagoonal, lacustrine, prodeltaic, deltaic, peat and clastic swamp environments (Logvinenko, 1953; Feofilova & Levenshtein, 1963). The Mospyne Formation corresponds to the lower part of the Zuyivkian Horizon (lower half of the Kayalian Regional Stage) of the Regional Stratigraphic Scheme of the Dnipro-Donets Downwarp (Poletaev et al., 2011; Nemyrovska & Yefimenko, 2013). This formation contains remains of typical Langsettian terrestrial plants (Novik, 1974; Dernov & Udovychenko, 2019a) and

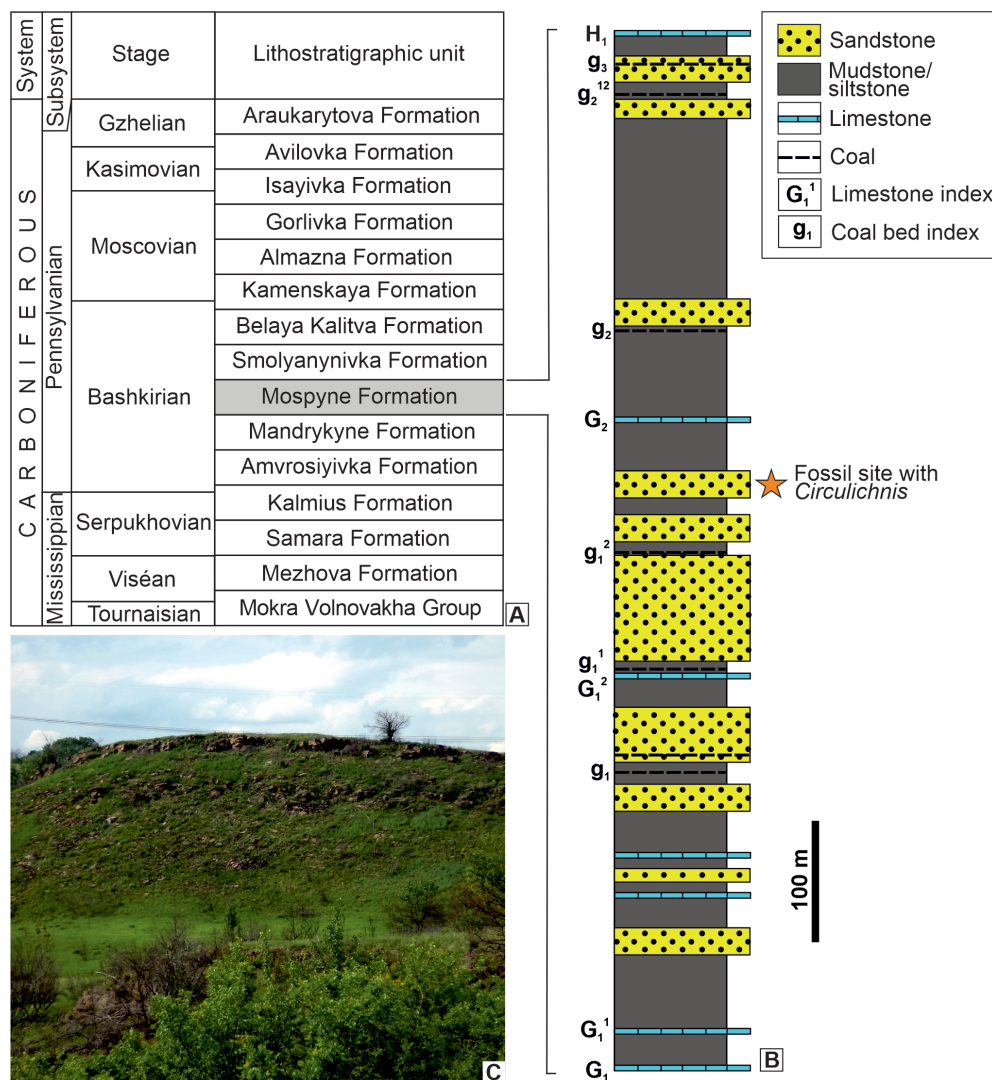


Fig. 2. Stratigraphic position (A, B) and the general view of the *Circulichnis*-bearing fossil site (C).

ammonoids (Popov, 1979; Dernov, 2022b), the non-marine bivalves of the upper part of the *lenisulcata* Zone and the lower part of the *communis* Zone (Dernov, 2022a), the late Bashkirian conodonts (Nemyrovska, 1999), and other marine and terrestrial biota, such as miospores, foraminifers, corals, bryozoans, brachiopods, scaphopods, gastropods, horseshoe crabs, millipedes, insects and fishes.

Some trace fossils from the Mospyne Formation, such as the ichnospecies of the ichnogenera *Arborichnus*, *Arenicolites*, *Avetoichnus*, *Archaeonassa*, *Aulichnites*, *Bergaueria*, *Chondrites*, *Cochlichnus*, *Conichnus*, *Cyclopuncta*, *Diplichnites*, *Diplocraterion*, *Diplopodichnus*, *Gordia*, *?Halopoa*, *Helminthopsis*, *Kouphichnium*, *Lockeia*, *?Lophoctenium*, *Mammillichnus*, *Monocraterion*, *Monomorphichnus*, *Paleophycus*, *Phycodes*, *Phycosiphon*, *Planolites*, *Ptychoplasma*, *Protovirgularia*, *Rhizocorallium*, *Rogerella*, *Rusophycos*, *Saerichnites*, *Scolithos*, *Selenichnites*, *Treptichnus* and evidences of arthropod-plant interaction have been previously described or figured by the author (Dernov, 2019a, b; Dernov & Udovychenko, 2019b; Dernov, 2021, 2022c, 2023).

The studied specimen GMLNU-15/01 is a single trace fossil *Circulichnus montanus* Vyalov, 1971 on a slab of fine-grained, polymictic, horizontally-bedded, grey sandstone. It was collected by the author from the sandstone bed in the upper part of the Mospyne Formation. This sandstone bed is exposed in the Dubova Ravine, located 2 km west of the village of Kamianka (Ukraine, Luhansk Region: 48°14'54.8"N 39°20'48.0"E; Fig. 1). The section is poorly exposed here (Fig. 2C), but in the neighbouring Sukha Ravine and near the village of Makedonivka, it has been exposed in small quarries. No *Circulichnus* has been found at these other sites, but numerous other trace fossils, such as *Archaeonassa*, *Aulichnites*, *Bergaueria*, *Planolites*, and *Treptichnus* are present. The specimen GMLNU-15/01 is housed in the Geological Museum of the Luhansk Taras Shevchenko National University (Poltava, Ukraine).

Systematic ichnology

Ichnogenus *Circulichnus* Vyalov, 1971

Type ichnospecies: *Circulichnus montanus* Vyalov, 1971; by original designation.

Diagnosis: Horizontal, approximately circular to oval, cylindrical ring (after Uchman & Rattazzi, 2018).

Remarks: Keighley & Pickerill (1998) proposed to change the spelling of the ichnogenus from *Circulichnus* to *Circulichnus*, arguing that in the original description of this ichnotaxon by Vyalov (1971),

there was a mistake in the spelling of its ending. I see no reason for such a decision, because nowhere is it officially stated that the names of ichnogenera should end in *-ichnus*. Moreover, in the text of the work of Vyalov (1971), the spelling *Circulichnis* is used everywhere, so the ending *-ichnis* cannot be a typographical error. This opinion is shared by many other researchers (for example, Uchman & Rattazzi, 2018; Morgan et al., 2023).

Occurrence: Ediacaran–Oligocene (Palaeogene); worldwide distribution.

Circulichnus montanus Vyalov, 1971

Fig. 3

(See Uchman & Rattazzi (2018, pp. 4, 5) for synonymy)

Material: One well-preserved specimen (GMLNU-15/01).

Description: Horizontal, smooth, unlined, ring-shaped and subcylindrical burrow, 10 to 15 mm wide and 12.5 cm and 10.0 cm in external diameters, preserved as a concave epirelief on the upper bedding plane. The width of the burrow varies considerably, which may be a taphonomic artefact caused by the fact that it is exposed to different depths. A much narrower, slightly curved burrow, about 50 mm long and 8–9 mm wide, extends from the ring at an acute angle. The burrow fill is identical to the host rock.

Remarks: In addition to the type species, several ichnospecies have been described under the name *Circulichnus/Circulichnis*, such as *Circulichnus ngariensis* Yang & Song, 1985, *Circulichnus spiralis* Li, 1993, and *Circulichnus sinensis* Yang, 1990, but they are not related to *Circulichnus* or are synonymous with *Circulichnus montanus* (Uchman & Rattazzi 2018). However, Fan et al. (2021) have reviewed *C. sinensis* as a valid ichnospecies, despite the fact that this ichnospecies, as well as *Circulichnus leomonti* Morgan, Juntunen, Scott & Landreth, 2023, differs from *Circulichnus montanus* in its segmental structure. *Circulichnus montanus* described above differs from *Circulichnus ligisticus* Uchman & Rattazzi, 2018 by the regular elliptical course of the burrow.

The specimen GMLNU-15/01 differs somewhat from the holotype of *Circulichnus montanus* figured by Vyalov (1971, pl. 1, fig. 1) and Uchman & Rattazzi (2018, fig. 2), namely: (1) the holotype is much smaller (the large diameter is about three times smaller than that of the specimen GMLNU-15/01; (2) the holotype is represented by a convex hyporelief, whereas the specimen GMLNU-15/01 is preserved as a concave epirelief; (3)

the holotype is composed by a cylindrical annular ridge, whereas the specimen GMLNU-15/01 is either a partially destroyed cylindrical or subcylindrical burrow. However, the morphology of the specimen GMLNU-15/01 does not contradict the diagnosis of *Circulichnis montanus* given in the revision by Uchman & Rattazzi (2018, p. 5), namely: "horizontal, cylindrical burrow, which shows a course along a regular circle or ellipse". The specimen GMLNU-15/01 is much larger than the holotype of *Circulichnis montanus*, but the size is not of ichnotaxonomic significance (Pickerill, 1994). From the Cretaceous deposits of Alaska, McCann & Pickerill (1988) described specimens of *Circulichnis montanus* similar in size to *Circulichnis montanus* described above.

Locality: Ukraine, Luhansk Region, left slope of the Dubova Ravine, 2 km west of the village of Kamianka; upper part of the Mospyne Formation (late Bashkirian, Early Pennsylvanian).



Fig. 3. *Circulichnis montanus* Vyalov, 1971 from the Mospyne Formation of the Donets Basin (specimen GMLNU-15/01). Scale bar = 10 mm.

Discussion and concluding remarks

Vyalov (1971) and Keighley & Pickerill (1998) suggested that *Circulichnis* could not be unbranched, as its tracemaker could not have appeared from nowhere and had to somehow get to the area of the seabed where it subsequently formed the trace. Probably, in most cases, the incoming (and outgoing) branch could not be preserved, since, for example, it could be located in a different plane relative to the main part of the trace (Vyalov, 1971; Pickerill & Keppie, 1981).

Pickerill & Keppie (1981), suggested that *Circulichnis* and *Helminthopsis* from the Cambrian–Ordovician deposits of Nova Scotia (Canada) were produced by the same producers, most likely annelid worms. This conclusion was supported by

the fact that these traces occur on the same bedding surfaces and sometimes overlap (Häntzschel, 1975, fig. 2a on p. W71; Pickerill & Keppie, 1981, fig. 3c).

Uchman & Rattazzi (2018) proposed a model for the function of *Circulichnis*, according to which, *Helminthoidichnites*, *Gordia*, and *Helminthopsis* are burrows or trails used for feeding, locomotion, or both. The trace makers probably used these structures to explore the environment at different sediment depths, primarily for feeding, and often along bedding interfaces. According to this model, the rejoining of the shaft can occur at the point where the vertical to subvertical shaft connects with the ring, or with the shaft bent to a horizontal position near the ring, or with the shaft diverging in the lower part and transitioning to an imperfect ring that is not closed on the same level.

However, a vertical or subvertical shaft hypothetically connecting *Circulichnis* to another level within the sediment has never been observed, but only documented cases of a horizontal short branch of the *Circulichnis* ring (Uchman & Rattazzi, 2018), as in the specimen GMLNU-15/01. The lateral branch of the specimen GMLNU-15/01, if found in isolation from the ring, could be assigned to the ichnogenus *Planolites* or *Palaeophycus*, so there is good reason to believe that the producers of these ichnogenus, as well as *Helminthoidichnites*, *Gordia*, and *Helminthopsis*, could also produced *Circulichnis*.

The studied material suggests that at least the variant of the *Circulichnis* ethological model proposed by Uchman & Rattazzi (2018, fig. 6A, B – variant C; see fig. 4) is correct. However, it is not yet clear whether it is the only possible one.

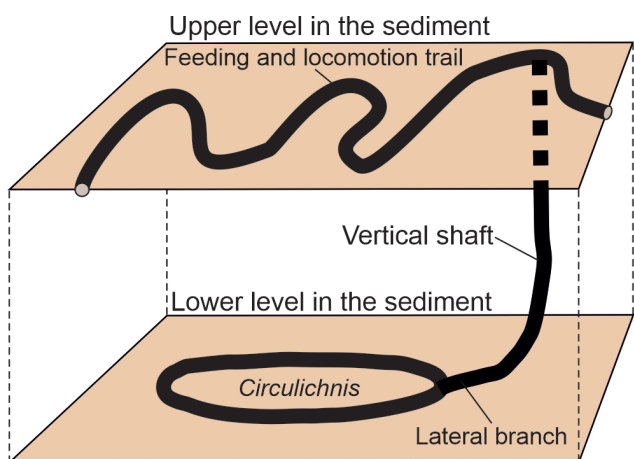


Fig. 4. Model of *Circulichnis*. Modified from Uchman & Rattazzi (2018, fig. 6).

Acknowledgements

I would like to thank the anonymous reviewers whose comments and suggestions improved the quality of the final version of the manuscript. The research was carried out within the framework of the scientific theme "Late Precambrian and Phanerozoic biota of Ukraine: biodiversity, revision of systematic composition and phylogeny of leading groups" (No. 0122U001609).

References

- Aisenverg, D.E., Belenko, N.G., Dedov, V.S., Levenshtein, M.L. & Makarov I.A. 1975: Stratigraphic excursion. In: Aizenverg, D.E., Lagutina, V.V., Levenshtein, M.L., Popov, V.S. (eds.): Field excursion guidebook for the Donets Basin. Nauka, Moscow: 201–245. (In Russian)
- Blissett, D.J. & Pickerill, R.K. 2004: Soft-sediment ichnotaxa from the Cenozoic White Limestone Group, Jamaica, West Indies. Scripta Geologica, 127: 341–378.
- Buatois, L.A. & Mángano, M.G. 1993: Trace fossils from the Carboniferous turbiditic lake: Implications for the recognition of additional nonmarine ichnofacies. Ichnos, 2/3: 237–258. <https://doi.org/10.1080/10420949309380098>
- Buatois, L.A., Mángano, M.G., Maples, C.G. & Lanier, W.P. 1998a: Allostratigraphic and sedimentologic applications of trace fossils to the study of incised estuarine valleys: an example from the Virgilian Tonganoxie Sandstone Member of eastern Kansas. Current Research in Earth Sciences, 241: 1–27.
- Buatois, L.A., Mángano, G.M., Maples, C.G. & Lanier, W.P. 1998b: Ichnology of an Upper Carboniferous fluvio-estuarine paleovalley: the Tonganoxie Sandstone, Buildex quarry, eastern Kansas, USA. Journal of Paleontology, 72/1: 152–180. <https://doi.org/10.1017/S0022336000024094>
- Buatois, L.A., Netto, R.G., Mángano, M.G. & Ballistieri, P.R.M.N. 2006: Extreme freshwater release during the late Paleozoic Gondwana deglaciation and its impact on coastal ecosystems. Geology, 34/12: 1021–1024. <https://doi.org/10.1130/G22994A.1>
- Dernov, V. 2019a: On the study of the non-marine fauna of the Mospino Formation (Middle Carboniferous, Donets Basin). Tectonics and Stratigraphy, 46: 105–115. (In Russian) <https://doi.org/10.30836/igs.0375-7773.2019.208882>
- Dernov, V. 2019b: Taphonomy and paleoecology of fauna and flora from deltaic sandstones of the Mospinka Formation (Middle Carboniferous) of Donets Basin. GEO&BIO, 18: 37–63. <https://doi.org/10.15407/gb1805>
- Dernov, V. 2021: The earliest insect endophytic oviposition (Early Pennsylvanian, eastern Ukraine). Visnyk of Taras Shevchenko National University of Kyiv. Geology, 95/4: 16–24. <https://doi.org/10.17721/1728-2713.95.02>
- Dernov, V. 2022a: Nonmarine bivalves from the Mospyne Formation (upper Bashkirian) of the Donets Basin: taxonomy, paleoecology, and stratigraphic significance. Geologichnij zhurnal, 380/3: 34–56. (In Ukrainian) <https://doi.org/10.30836/igs.1025-6814.2022.3.255491>
- Dernov, V. 2022b: Late Bashkirian ammonoids from the Mospyne Formation of the Donets Basin, Ukraine. Fossil Imprint, 78/2: 489–512. <https://doi.org/10.37520/fi.2022.021>
- Dernov V. 2022c: *Mamillichnis monstrum* isp. nov., a new sea anemone trace fossil from the Carboniferous of the Donets Basin, Ukraine. GEO&BIO, 23: 65–76. <https://doi.org/10.15407/gb2306>
- Dernov, V. 2023: Horseshoe crab trace fossils *Arborichnus* Romano et Meléndez, 1985 from the Bashkirian (Carboniferous) of the Donets Basin, Ukraine. Fossil Imprint, 79/1: 9–25. <https://doi.org/10.37520/fi.2023.002>
- Dernov, V.S. & Udovychenko, N.I. 2019a: On the palaeobotanical characteristics of the Mospino Formation. Visnyk of V.N. Karazin Kharkiv National University, Geology, Geography, Ecology, 51: 67–82. (In Russian) <https://doi.org/10.26565/2410-7360-2019-51-05>
- Dernov, V.S. & Udovychenko, N.I. 2019b: New fossil sites in deposits of the Bashkirian Stage (Lower Pennsylvanian) of the Donets Basin. Collection of scientific works of the Institute of Geological Sciences of NAS of Ukraine, 12: 40–47 (In Russian). <https://doi.org/10.30836/igs.2522-9753.2019.185717>
- Dmitrieva, E.V., Yershova, G.I. & Oreshnikova, E.I. 1963: Atlas of sedimentary rock structures. Part 1. Terrigenous rocks. Gostoptekhizdat, Moscow: 578 p. (In Russian)
- Dunaeva, N.M. 1969: Open Donets Basin. In: Bondarchuk, V.G. (ed.): Stratigraphy of the Ukrainian SSR. Vol. V. Carboniferous. Naukova Dumka, Kyiv: 21–48. (In Ukrainian)
- Fan, R., Zong, R. & Gong, Y. 2021: Deep-time geometricians and hints on motor control evolution of marine invertebrates. Palaeogeography, Palaeoclimatology, Palaeoecology, 567: article 110255. <https://doi.org/10.1016/j.palaeo.2021.110255>

- Feofilova, A.P. & Levenshtein, M.L. 1963: Features of the sedimentation and coal accumulation in the Early and Middle Carboniferous of the Donets Basin. Publishing House of the Academy of Sciences of the USSR, Moscow: 175 p. (In Russian)
- Fillion, D. & Pickerill, R.K. 1984: Systematic ichnology of the Middle Ordovician Trenton Group, St. Lawrence Lowland, eastern Canada. *Atlantic Geology*, 20/1: 1–41. <https://doi.org/10.4138/1572>
- Fissunenko, O.P. 2004: Geological map. In: *Atlas of Luhansk Region*. Kyiv, Kartographia: p. 6. (In Ukrainian)
- Gureev, Yu.A. 1983: Ring-like trace fossils from the Kanyliv Group of the Dniester River area. *Geologichnij zhurnal*, 43/1: 130–132. (In Russian)
- Häntzschel, W. 1975: Trace fossils and Problematica. In: Teichert, C. (ed.): *Treatise on Invertebrate Paleontology*. Part W. *Miscellanea*. Suppl. 1. Geological Society of America and University of Kansas Press, Lawrence: W3–W269.
- Keighley, D.G. & Pickerill, R.K. 1998: Systematic ichnology of the Mabou and Cumberland groups (Carboniferous) of western Cape Breton Island, eastern Canada, 1: burrows, pits, trails, and coprolites. *Atlantic Geology*, 34/2: 83–112. <https://doi.org/10.4138/2041>
- Kozitskaya, R.I. & Schegolev, A.K. 1993: Moscovian Age. In: Tsegelnyuk, P.D. (ed.): *Geological history of Ukraine*. Naukova Dumka, Kyiv: 144–147). (In Russian)
- Li, R.-H. 1993: Trace fossils and ichnofacies of Middle Ordovician Gongwusu Formation, Zhuozishan, Inner Mongolia. *Acta Palaeontologica Sinica*, 32/1: 88–104.
- Logvinenko, N.V. 1953: Lithology and paleogeography of the Carboniferous coal-bearing sediments of the Donets Basin. Kharkiv University, Kharkiv: 436 p. (In Russian)
- Mángano, M.G., Buatois, L.A., Maples, C.G. & Lamer, W.P. 1997: *Tonganoxichnus*, a new insect trace from the Upper Carboniferous of eastern Kansas. *Lethaia*, 30/2: 113–125. <https://doi.org/10.1111/j.1502-3931.1997.tb00451.x>
- McCann, T. & Pickerill, R.K. 1988: Flysch trace fossils from the Cretaceous Kodiak Formation of Alaska. *Journal of Paleontology*, 62/3: 330–348. <https://doi.org/10.1017/S0022336000059138>
- Morgan, R.F., Juntunen, K.L., Scott, A. & Landreth, M. 2023: *Circulichnus leomonti*, a new ring-like ichnospecies (trace fossil) from the Late Cambrian Lion Mountain Member, Riley Formation, Burnet County, Texas. *Texas Journal of Science*, 75/1 (Article 1): 12 p. https://doi.org/10.32011/tjsci_75_1_Article1
- Nemyrovska, T.I. 1999: Bashkirian conodonts of the Donets Basin, Ukraine. *Scripta Geologica*, 119: 1–116.
- Nemyrovska, T.I. & Yefimenko, V.I. 2013: Middle Carboniferous (Lower Pennsylvanian). In: Gozhik, P.F. (ed.): *Stratigraphy of the Upper Proterozoic and Phanerozoic of Ukraine*. Vol. 1. *Stratigraphy of the Upper Proterozoic, Paleozoic and Mesozoic*. LAT&K, Kyiv: 283–303. (In Ukrainian)
- Novik, E.O. 1974: Regularities of development of the Carboniferous flora of the south part of the European part of the USSR. *Naukova Dumka*, Kyiv: 140 p. (In Russian)
- Pickerill, R.K. 1994: Nomenclature and taxonomy of invertebrate trace fossils. In: Donovan, S.K. (ed.): *The palaeobiology of trace fossils*. John Wiley and Sons, Chichester, 3–42.
- Pickerill, R.K. & Keppie, J.D. 1981: Observations on the Ichnology of the Meguma Group (? Cambro-Ordovician) of Nova Scotia. *Atlantic geology*, 17/3: 130–138. <https://doi.org/10.4138/1381>
- Pickerill, R.K., Fyffe, L.R. & Forbes, W.H. 1988: Late Ordovician–Early Silurian trace fossils from the Matapedia Group, Tobique River, western New Brunswick, Canada. II. Additional discoveries with descriptions and comments. *Atlantic geology*, 24/2: 139–148. <https://doi.org/10.4138/1646>
- Poletaev, V.I., Vdovenko, M.V., Shchogolev, O.K., Boyarina, N.I. & Makarov, I.A. 2011: Stratotypes of the Carboniferous and Lower Permian regional stratigraphic units of the Dniro-Donets Downwarp. Logos, Kyiv: 236 p. (In Ukrainian)
- Popov, A.V. 1979: Carboniferous ammonoids of the Donets Basin and their stratigraphic significance. Nedra, Leningrad: 119 p. (In Russian)
- Shalimov, A.I. 1978: Trace fossils in the terrigenous flysch of the Tavria Group (Crimean Mountains) and their palaeogeographic significance. In: Kulikov, M.V., Khozatsky, L.I. & Djalilov, M.R. (eds.): *The issues of taphonomy and palaeobiology*. Donish, Dushanbe: 142–149. (In Russian)
- Uchman, A. & Rattazzi, B. 2018: The trace fossil *Circulichnus* as a record of feeding exploration: New data from deep-sea Oligocene-Miocene deposits of northern Italy. *Comptes Rendus Palevol*, 18/1: 1–12. <https://doi.org/10.1016/j.crpv.2018.05.002>

- Vyalov, O.S. 1971: A rare Mesozoic problematica from Pamir and Caucasus. *Paleontologicheskiy Sbornik*, 7: 85–93. (In Russian)
- Yang, S. 1990: Palaeoichnology. Geological Publishing House, Beijing: 194 p.
- Yang, S. & Song, Z. 1985: Middle–Upper Triassic trace fossils from Zhada, Ngari, southwest Xizang (Tibet), and its geologic significance. *Tibet Geology*, 1: 1–14.



Middle Triassic deeper-marine volcano-sedimentary successions in western Slovenia

Srednjetriasna globljemorska vulkansko-sedimentna zaporedja v zahodni Sloveniji

Dragomir SKABERNE^{1,2}, Jože ČAR^{3,4}, Maja PRISTAVEC^{3,5}, Boštjan ROŽIČ³ & Luka GALE^{2,3,*}

¹Medvedova c. 10, SI-1000 Ljubljana, Slovenia; e-mail: dskaberne@gmail.com

²Geological Survey of Slovenia, Dimičeva ulica 14, SI-1000 Ljubljana, Slovenia;

*corresponding author: luka.gale@geo-zs.si

³Department of Geology, Faculty of Natural Sciences and Engineering, University of Ljubljana, Aškerčeva cesta 12, SI-1000 Ljubljana, Slovenia; e-mail: bostjan.rozic@ntf.uni-lj.si; luka.gale@ntf.uni-lj.si

⁴Finžgarjeva ulica 18, SI-5280 Idrija, Slovenia; e-mail: joze.car@siol.net

⁵Brnica 58, SI-1430 Hrastnik, Slovenia; e-mail: maja.pristavec@gmail.com

Prejeto / Received 12. 2. 2024; Sprejeto / Accepted 7. 5. 2024; Objavljeno na spletu / Published online 11. 6. 2024

Key words: stratigraphy, carbonate-siliciclastic deposits, Slovenian Basin, Middle Triassic, Ladinian, Carnian, Pseudozilja formation, Amphicline formation

Ključne besede: stratigrafija, karbonatno-siliciklastični sediment, Slovenski bazen, srednji trias, ladinij, karnij, psevdoziljska formacija, amfiklinska formacija

Abstract

A Ladinian – Carnian volcano-sedimentary succession from western Slovenia, paleogeographically belonging to the western Slovenian Basin, is presented in 17 sections. Except for the lowermost part, which is dominated by volcanics and volcaniclastics, most of the succession is dominated by shale, sandstone, and micritic limestone. Various authors use the name Pseudozilja and/or Amphicline formation for this part, which is dominated by clastics, but they disagree on the differences between the formations. The lower Pseudozilja formation, represented by the Malenski Vrh section, comprises diabase, tuf and shale. No substantial differences in lithological composition have been observed between the upper Pseudozilja formation and the Amphicline formation, which are predominantly composed of shale, sandstone, and limestone. The shale and sandstone are largely composed of quartz, feldspar, and lithic grains (especially volcanics), which vary in proportions. Limestone varieties comprise hemipelagic limestones and resedimented carbonates deposited by gravity-flows. Deposition of the Ladinian – Carnian volcano-sedimentary succession took place on or near the continental slope that was generally inclined to the S, with the direction of transport mainly from N to S.

Izvleček

V članku v 17 profilih predstavljamo ladinjsko – karnijsko vulkansko-sedimentno zaporedje zahodne Slovenije, paleogeografsko umeščeno v zahodni del Slovenskega bazena. Spodnji del psevdoziljske formacije, posnet na Melenskem vrhu, sestavlja diabaz, tuf in laminiran muljevec. Zgornji del psevdoziljske formacije in amfiklinska formacija sta litološko identična. V večjem delu ju sestavlja laminiran muljevec, peščenjak in apnenec. Glavne sestavnine muljevca in peščenjaka so kremen, glinenci in litična zrna (predvsem predornin) v različnih razmerjih. Apnenec obsega hemipelagični apnenec in resedimentirane karbonate. Sedimentacija ladinjsko – karnijskega vulkansko-sedimentnega zaporedja je potekala na ali v bližini kontinentalnega pobočja z nagibom proti jugu. Transport sedimenta je v glavnem potekal od severa proti jugu.

Introduction

The time range and paleogeographic extent of the Slovenian Basin, a deeper marine sedimentary basin situated on the western Tethyan margin, is based on a succession of open-marine Mesozoic rocks, which today are exposed between Tolmin in western Slovenia and Neogene sediments of the Central Paratethys in eastern Slovenia (Buser, 1989, 1996; Buser et al., 2008). The lowermost/oldest rocks of the Slovenian Basin are volcanics

(rhyolite, diabase, and basalt), tuffs, volcaniclastic sandstone, feldspar-quartz-lithic sandstone and shale with intercalations of conglomerate, muddy conglomerate and breccia, bedded hemipelagic limestone, and carbonate olistoliths (bioherms?) (Stur, 1858; Teller, 1885, 1889; Kossamat, 1901, 1910, 1913; Winkler, 1936; Rakovec, 1950; Ramovš, 1970; Grad & Ferjančič, 1976; Placer & Čar, 1977; Čar et al., 1981; Turnšek et al., 1982; Buser, 1986; Šmuc & Čar, 2002; Dozet & Buser, 2009;

Demšar, 2016; Gale et al., 2016; Čar et al., 2021). While some authors (e.g. Turnšek et al., 1982; Buser, 1986) distinguished between the Ladinian (informal) Pseudozilja (also Pseudozilian, Pseudogailtal) formation and the Carnian Amphiclina formation based on the presence or, respectively, absence of volcaniclastics, others argue that the entire succession should be treated as one, that is, as the Pseudozilja formation (e.g., Čar et al., 1981, 2021). We note here that although neither name follows modern stratigraphic standards, the International Stratigraphic Guide states that “traditional or well-established names [...] should not be abandoned, providing they are or may become well defined or characterized” (Murphy & Salvador, 19.06.2023). The lower part of the volcano-sedimentary succession is relatively poorly dated. The succession rests unconformably on Lower Triassic shallow-water deposits or, more commonly, its base is tectonically cut-off. Rare fossil finds (bivalves) from tuff beds suggest that deeper-water sedimentation in the Slovenian Basin started in the Ladinian (Teller, 1889; Jurkovšek, 1984; Buser, 1986). However, the deepening could already have begun in the late Anisian during the regional extension of the crust and the formation of horst-and-graben relief (e.g. Buser, 1989; Gianolla et al., 1998a; Celarc et al., 2013; Smirčić et al., 2020).

The uppermost part of the investigated succession is represented by interchanging beds of dark limestone and shale dated with conodonts as late Carnian (Tuvalian) in age (Buser & Krivic, 1979; Kolar-Jurkovšek, 1982, 1990; Demšar, 2016). After a few meters, this transitional interval gives way to bedded dolostone with chert nodules known as the (also informal) Bača dolomite (i.e. dolostone) formation (Kossmat, 1901; Buser, 1986; Gale, 2010). In the more proximal settings, earlier (i.e. late Ladinian or early Carnian) transition to platform carbonates has been recorded (Čar et al., 2021).

With a combined thickness of 600 m (estimation based on profiles on geological maps; Buser, 1986; Demšar, 2016), the Pseudozilian/Amphiclina formations represent a notable zone of rheological weakness, along which important thrusting took place during the formation of the Alps (Placer & Čar, 1998; Placer, 1999; Placer et al., 2000). From the stratigraphic point of view, this succession is a sedimentary record of the early evolution of the Slovenian Basin, bearing information about the paleogeography, paleoclimate, and oceanographic conditions in this part of the Tethys during the Ladinian and Carnian. Due to the absence of data on the biostratigraphic and radiometric age, the

lack of known and described sedimentary sections as well as abrupt lateral and vertical changes in lithologies, however, we have yet to find the key to access such information.

The purpose of the present paper is to show the lithological composition of the volcano-sedimentary succession lying below the Bača dolomite formation. Some of the sections end with the transition to the Bača dolomite formation and thus have a well-known stratigraphic position. For others, we have no biostratigraphic or other data to determine the age; these were stratigraphically positioned based on the geological map (Buser, 1987; Demšar, 2016).

Methods

The Middle – lower Upper Triassic volcano-sedimentary succession of the Slovenian Basin was logged in 17 sections from 13 localities. Sections were logged between the years 1982 and 1990 by authors D.S. and J.Č. at scales of 1:50, 1:100 and 1:500. Approximately 270 thin sections were made for more detailed investigation under a polarizing petrographic microscope. Carbonates were classified according to Dunham (1962), modified by Wright (1992), and Lokier and Junaibi (2016). The terminology of the volcanically derived deposits follows Di Capua et al. (2022). In addition to thin section analysis, 38 samples of fine-grained clastic rocks were investigated using a Philips X-Ray Diffractometer with vertical goniometer and monochromator with a Cu cathode, CuK-0,1542 nm, powered up to 40 kW and 20 mA.

Structural setting and stratigraphic position of the sections

The logged sections lie between Železniki in the east, Koritnica in the west, and Cerkno in the south (Figs. 1–2; Table 1). In addition, Figure 1 also shows the positions of previously documented sections at Vrh Bače (Gale, unpubl. 2012), Crngrob (Gale et al., 2017), and Martinj Vrh (Pristavec et al., 2021). Except for the Malenski vrh section, which structurally lies in the Trnovo Nappe that belongs to the External Dinarides, all the other presented sections belong to the Tolmin Nappe of the eastern Southern Alps, more precisely to the Podmelec subnappe (Table 1). The Vrh Bače, Crngrob, and Malenski Vrh sections are structurally positioned in higher Kobla and Rut subnappes of the Tolmin Nappe, respectively.

Both the External Dinarides and the Tolmin Nappe of the Southern Alps are marked by the NE to SW thrusting that took part approximately from the Oligocene to the early Miocene (Vrabec

& Fodor, 2006). Later in the Miocene, the area of the Southern Alps experienced N-S to SE-NW-directed compression, which additionally resulted in the formation of S- to SE-verging folds and thrusts (Vrabec & Fodor, 2006). On a more detailed level all of the mentioned nappes further contain inner thrust blocks and smaller inner thrust-sheets, particularly at the transition between the Southern Alps and the Dinarides (Placer & Čar, 1998; Čar et al., 2021). Younger tectonic deformations of the area include local extension along NW-SE-trending normal faults that were reactivated as dextral strike-slip faults that today displace both sets of older folds and thrusts (Fig. 3) (Placer & Čar, 1998; Vrabec & Fodor, 2006).

The stratigraphic position of the presented sections is taken after Demšar (2016) and/or the lithological composition of the sections. According to Demšar (2016), the lower part of the Ladinian –

lowermost Carnian Pseudozilja formation consists of volcanics laterally and vertically passing into shale and tuff. Bedded limestone is subordinate and intercalated among volcanics. The higher part of the Pseudozilja formation is represented by volcanoclastic sandstone, shale, conglomerate, tuff, and subordinate bedded and massive limestone. The Carnian Amphiclina formation is defined by the same lithologies, except for the absence of tuff. In the upper part, the Amphiclina formation is mostly shale, sandstone, and quartz-carbonate lithic sandstone, with the addition of limestone, conglomerate, and breccia. The latter two locally contain abundant matrix. Nearing the transition into the Bača dolomite formation, the uppermost Amphiclina formation mostly comprises interchanging beds of limestone and shale (Demšar, 2016).

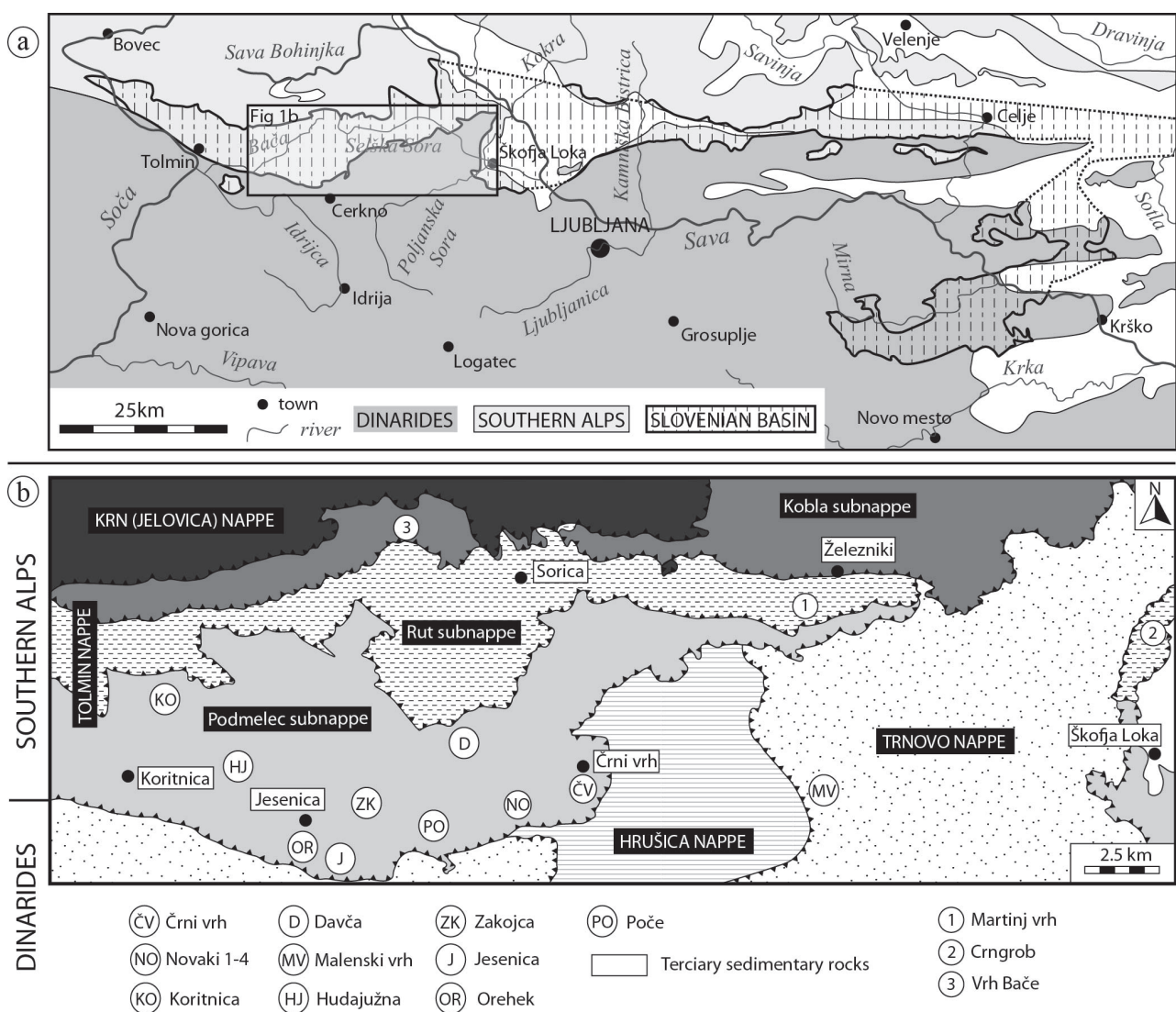


Fig. 1. Geographic position and structure of the studied area. a: Geotectonic units of central Slovenia, with present-day distribution of rocks deposited in the Slovenian Basin. Modified after Buser et al. (2007). b: Geographical position of the logged sections and the general structure of the studied area. Modified after Grad and Ferjančič (1974), Buser (1987), and Demšar (2016). Sections Martinj Vrh (1), Crngrob (2), and Vrh Bače (3) were previously investigated by Pristavec et al. (2021), Gale et al. (2017), and Gale (2012, unpubl.), respectively.

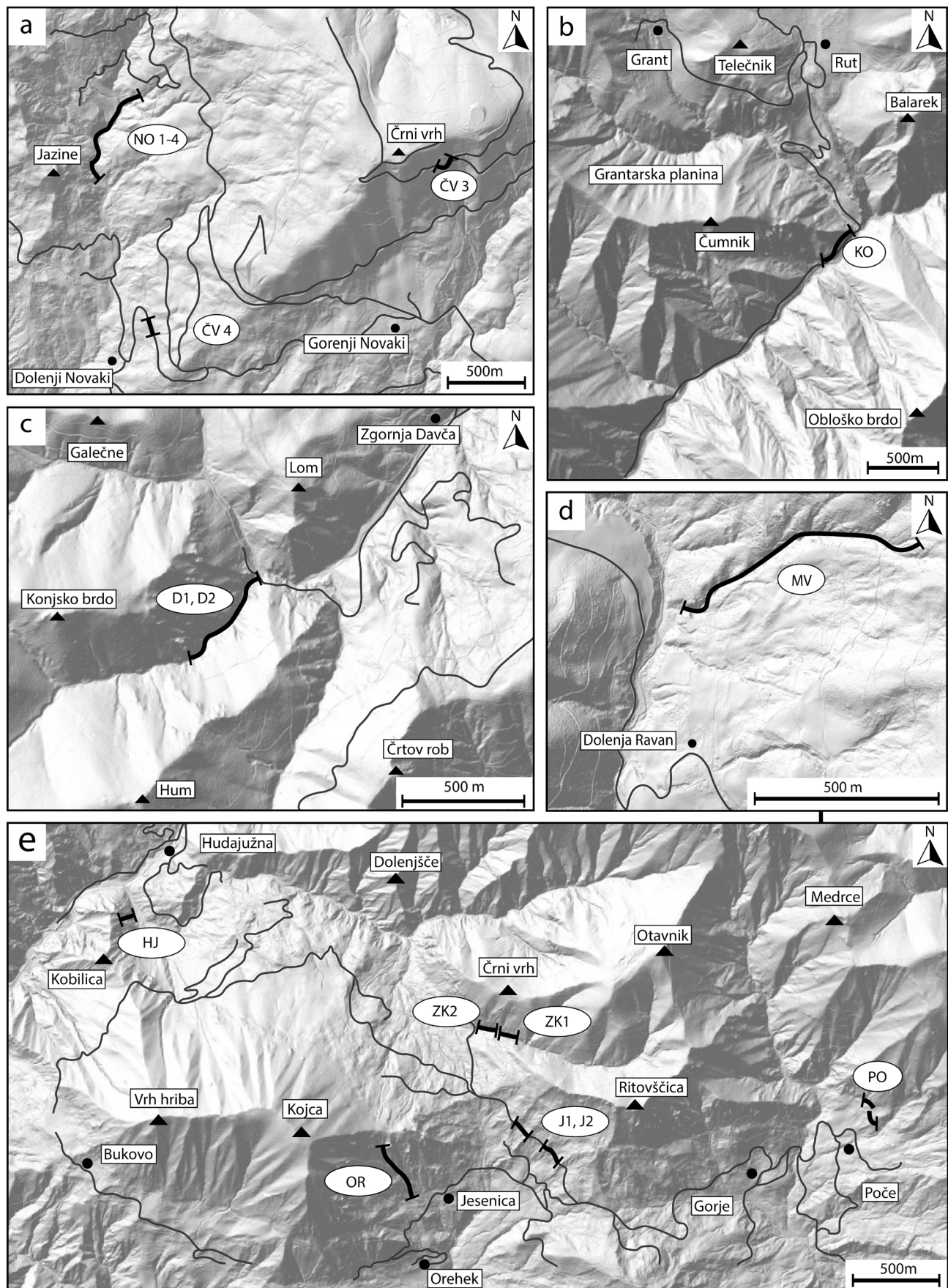


Fig. 2. Detailed position of the studied sections. **a:** Sections Novaki (NO 1–4), and Črni Vrh (ČV 3, ČV 4). **b:** Section Koritnica (KO). **c:** Sections Davča (D1, D2). **d:** Section Malenski Vrh (MV). **e:** Sections Hudajužna (HJ), Zakoča (ZK 1, ZK 2, ZK 3), Jesenica (J1, J2), Orehek (OR), and Poče (PO). LIDAR digital model of the relief, 2015. Source: Slovenian Environment Agency. Accessed via portal Geopedia (Sinergise d.o.o.) in May 2023. For geographic coordinates see Table 1.

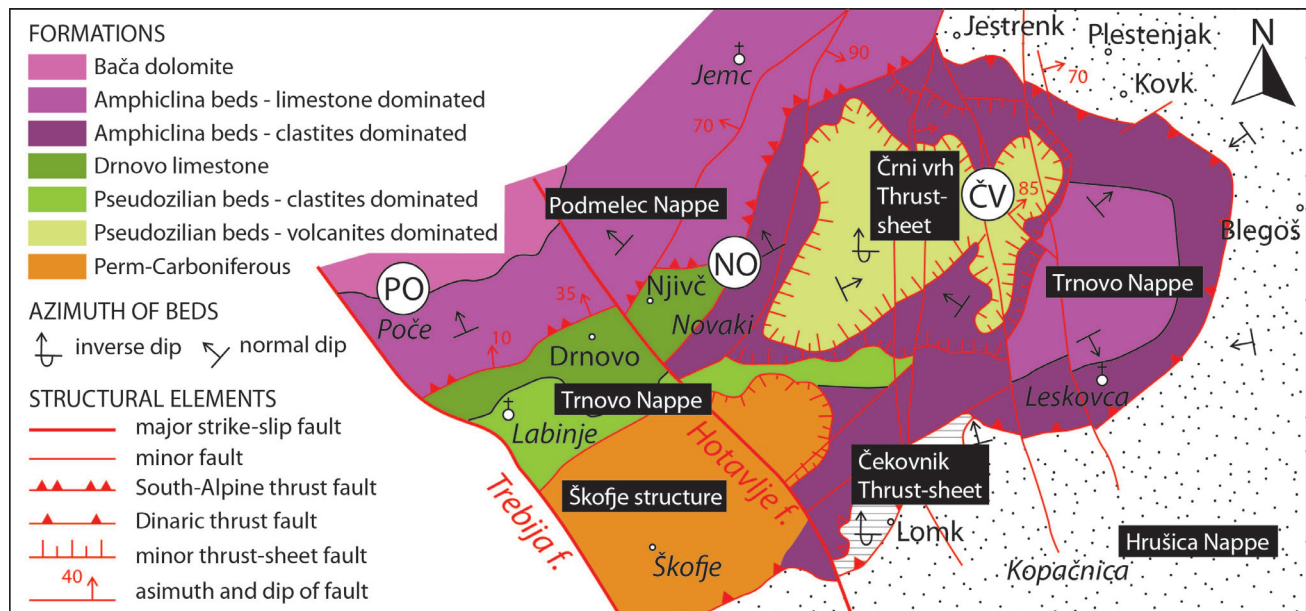


Fig. 3. Example of the minor thrust-sheet near Črni Vrh (coloured green) that is positioned just above the main South-Alpine Thrust Fault and characterized by partly overturned beds (for abbreviations of logged sections see Fig. 1). Note that in older publications (e.g., Placer & Čar, 1998; Placer, 1999, 2008) the structural unit marked here as the Trnovo Nappe was considered a thrust-sheet within the Hrušica Nappe.

Description of sections

Descriptions of logged successions are ordered according to their stratigraphic position (Table 1), starting with the lower part of the Pseudozilja formation and ending with the uppermost part of the Amphiclinia formation sensu Demšar (2016). The stratigraphic position of the sections Jesenica 1 and 2 is ambiguous; they could represent either

the upper part of the Pseudozilja formation or the lower part of the Amphiclinia formation. Most of the sedimentary rocks of the Pseudozilja/Amphiclinia formation are medium to dark grey, nearly black, so their colour will not be recorded in the subsequent description of the logged sections. The general aspect of the Pseudozilja/Amphiclinia formations is shown in Figure 4.

Section	Stratigraphic position	Start of section	End of section	Structural position
Malenski Vrh	Lower & upper Pseudozilja fm.	46°9'18.41"N, 14°8'30.84"E	46°9'23.54"N, 14°8'58.73"E	External Dinarides (Malenski vrh klippe)
Črni Vrh 3 (in inverse position)	Upper Pseudozilja fm.	46°9'43.86"N, 14°3'47.80"E	46°9'46.22"N, 14°3'51.12"E	
Črni Vrh 4 (in inverse position)	Upper Pseudozilja fm.	46°9'43.86"N, 14°3'47.80"E	46°9'46.22"N, 14°3'51.12"E	
Jesenica 1	Upper Pseudozilja/lower Amphiclinia fm.	46°9'14.49"N, 13°56'58.45"E	46°9'10.96"N, 13°57'2.76"E	
Jesenica 2	Upper Pseudozilja/lower Amphiclinia fm.	46°9'8.57"N, 13°57'10.45"E	46°9'3.30"N, 13°56'41.89"E	
Novaki 1–4	Lower Amphiclinia fm.	46°9'40.65"N, 14°2'16.86"E	46°9'56.28"N, 14°2'26.47"E	
Davča 1–2	Upper Amphiclinia fm.	46°10'29.26"N, 13°59'59.93"E	46°10'19.30"N, 13°59'47.62"E	
Poče	Upper Amphiclinia fm.	46°9'15.12"N, 13°59'13.77"E	46°9'21.29"N, 13°59'7.99"E	Southern Alps, Tolmin Nappe, Podmelec subnappe
Zakojca 1	Upper Amphiclinia Fm.	46°9'37.56"N, 13°56'59.27"E	46°9'39.06"N, 13°56'53.37"E	
Zakojca 2	Upper Amphiclinia Fm.	46°9'39.24"N, 13°56'44.74"E	46°9'43.66"N, 13°56'46.52"E	
Orehek	Upper Amphiclinia fm.	46°8'52.23"N, 13°56'19.35"E	46°9'7.67"N, 13°56'7.68"E	
Hudajužna	Upper Amphiclinia fm.	46°10'5.57"N, 13°54'29.60"E	46°10'6.79"N, 13°54'35.73"E	
Koritnica (in inverse position)	Upper Amphiclinia fm.	46°11'43.41"N, 13°53'41.82"E	46°11'36.44"N, 13°53'31.32"E	

Table 1. Geographic coordinates, structural and stratigraphic position of the studied sections (see text).

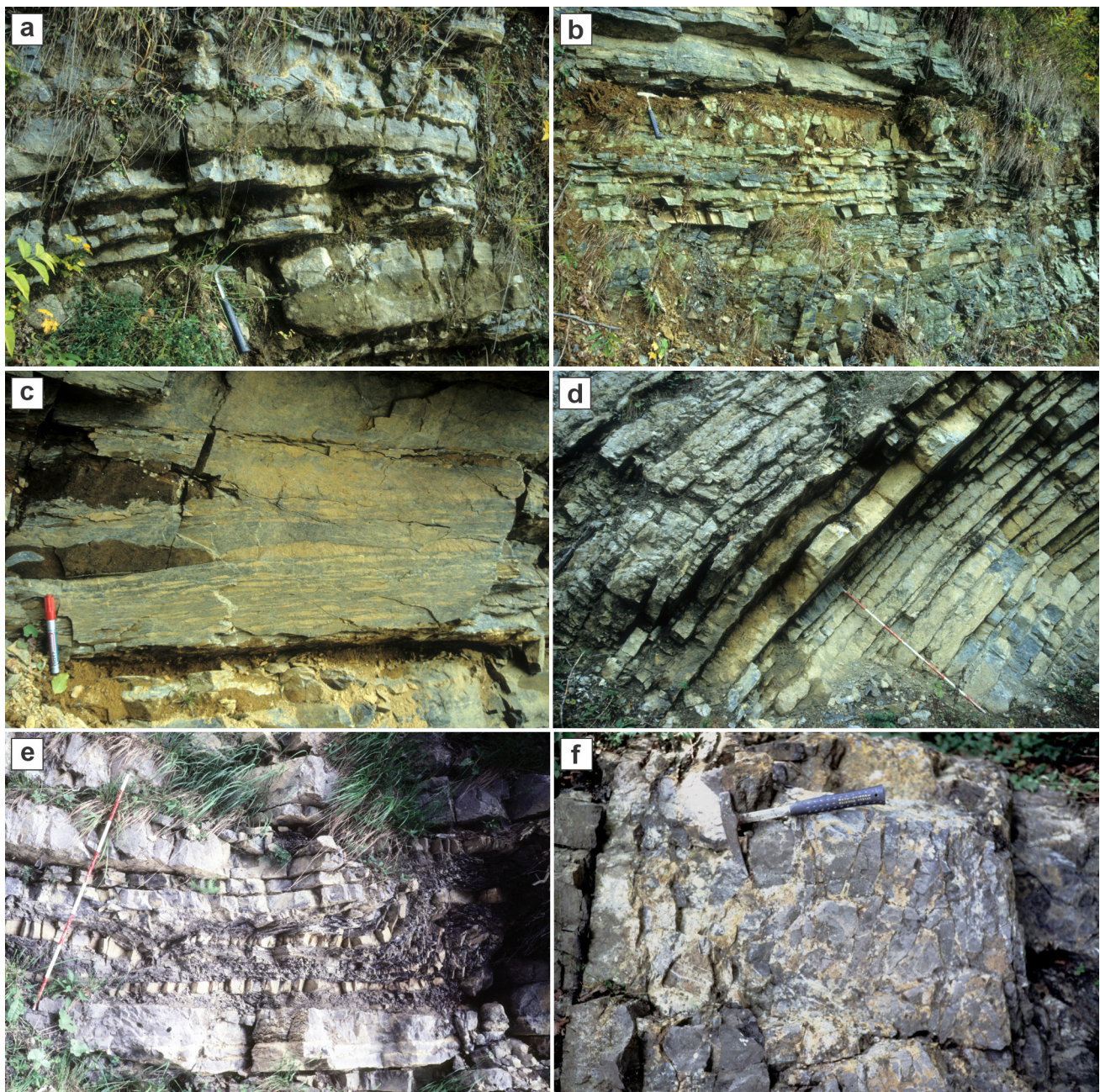


Fig. 4. Lithofacies of the Ladinian – Carnian volcano-sedimentary succession of the Slovenian Basin (Pseudozilja and Amphiclina formations sensu Demšar, 2016). **a:** Limestone interbedded with shale. Davča 1, 0.2–1.2 m. **b:** Interchange of shale-dominated heterolithic intervals with conglomerate and sandstone beds. Davča 1, 18.5 m. **c:** Lenticular bedding and ripple marks; sandstone interbedded in shale. Davča 1, 24.0 m. **d:** Transition from uppermost Amphiclina formation (right side of the picture) to the Bača dolomite formation (left side of the picture). Davča 2, 14.5–17.0 m. **e:** Sindepositional fold (slump). Interchange of calcarenite and shale. Koritnica 1, 45–46.3 m. **f:** Blocky limestone conglomerate. Koritnica 1, 33.0 m.

Pseudozilja formation (Malenski Vrh)

The Malenski Vrh section includes the lowermost part of the Pseudozilja formation and its clastics-dominated upper part. The entire volcano-sedimentary succession on the western slope of Malenski Vrh unconformably overlies Lower Triassic oolitic limestone (Fig. 5; also see Skaberne & Čar, 1986). The lowermost part of the Pseudozilja formation consists of 25 m of diabase with vacuoles filled by calcite and chlorite, followed by lithoclastic-crystallloclastic tuff with intercalations of

diabase that is pyritized in places. The diabase and tuff unit is approximately 190 m thick and is 35 % covered. It is followed by a succession of siliciclastic and carbonate rocks 260 m thick. The lower part of this interval, approximately 170 m thick, is partly covered and shale dominated, with rare thin interlayers and lenses of sandstone and limestone (mostly wackestone, subordinate pack- and grainstone). Approximately 90 m from the start of the siliciclastic and carbonate unit, which is dominated by shale, a lens-shaped body of pebbly sand-

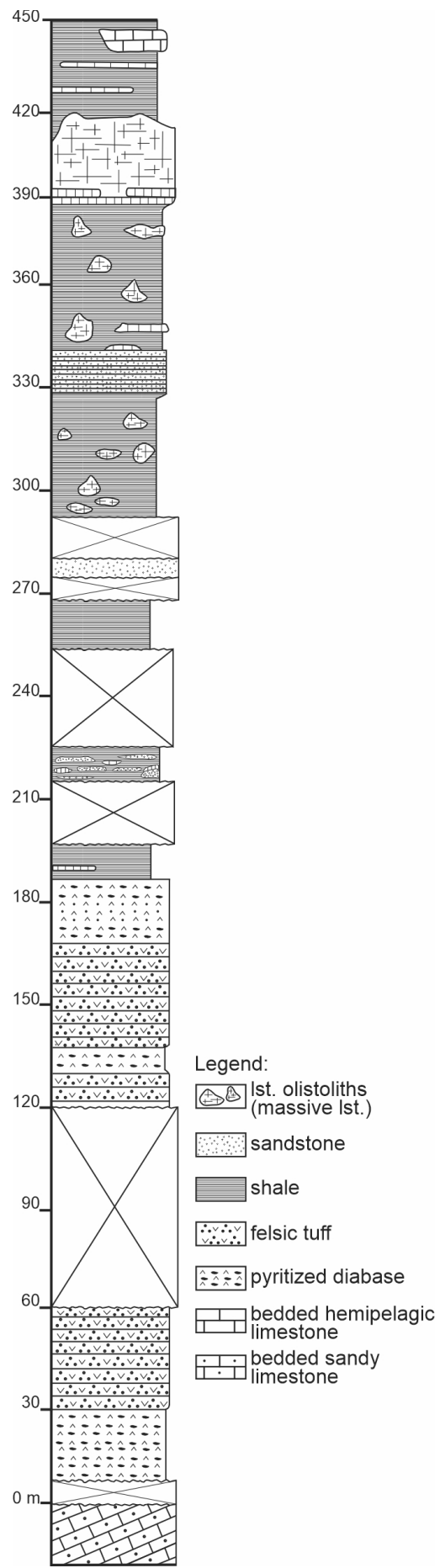


Fig. 5. Sedimentary log of the Malenski Vrh section. The section was logged schematically.

stone is recorded. It is characterised by a sharp, erosive lower boundary, and reaches up to 7 m in thickness. The sandstone consists mostly of feldspar, very altered volcanic lithic fragments, and quartz grains, with some chlorite and muscovite floating in quartz-sericite matrix and corrosion calcite cement. Approximately 160 m thick succession of shale follows. Locally, up to 25 m thick blocks of massive, in the lower part bedded limestone are present within the shale. No deformations around the massive limestone bodies were observed. Shale consists of 28–41 % of quartz, 6–15 % of feldspar, 19–34 % of muscovite /illite, 17–37 % of chlorite, and 0–26 % of calcite.

Upper Pseudozilja formation (Črni Vrh 3–4)

The sections Črni Vrh 3–4 are in overturned position. They are structurally situated in the Črni Vrh internal thrust sheet, in the tectonic zone between the Southern Alps and the External Dinarides. Approximately 12 m of the Pseudozilja formation recorded in the Črni vrh 3 section represent a fining-upward succession (Fig. 6). The lower part of the section displays normally graded sequences of conglomerate, upwards transitioning into coarse-grained sandstone with shale rip-up clasts. Conglomerates have erosive lower bedding planes. Pebbles in conglomerate are flattened, partly imbricated, and largely represented by rhyolites, felsic tuffs, and subordinate quartz grains. The last conglomerate bed overlies a 0.8 m bed of micritic limestone, laterally passing into shale. The top of the section is represented by sandstone, passing into shale. All coarser-grained beds are normally graded.

The Črni Vrh 4 section was logged in an abandoned quarry and stratigraphically lies above the Črni Vrh 3 section. The Črni Vrh 4 section comprises 43.6 m of the upper Pseudozilja formation, principally sandstone and conglomerate, intercalated with shale. Conglomerate mostly contains pebbles of rhyolites, felsic tuffs, subordinate quartz, and locally rip-up shale clasts. Several fining- and thinning-upward conglomerate-sandstone sequences can be recognized, each measuring 0.4–5 m in thickness. Sequences from the lower part of the section are thicker and are amalgamated or with thin intervals of shale in places. The sequences from the upper part of the section are finer-grained and thinner. The fine-grained part of sequences mostly consists of heterolithic intervals with 60–70 % of the interval consisting of fine-grained sandstone and 30–40 % shale.

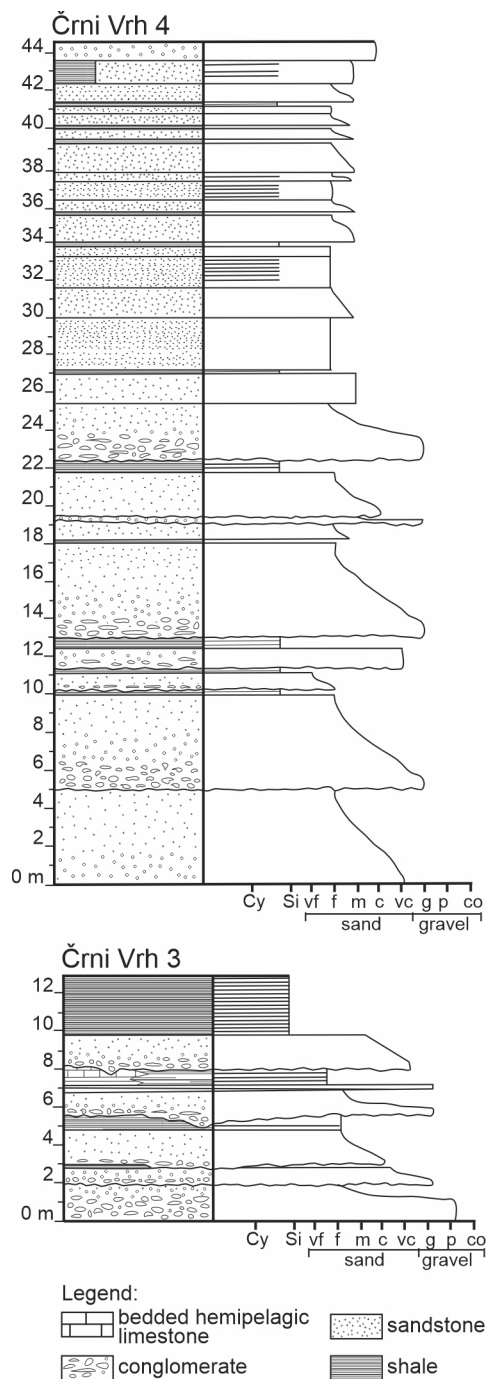


Fig. 6. Sedimentary log of the Črni Vrh sections. Right-side markings delineate grain sizes: Cy- clay, Si- silt, vf- very fine sand, f- fine sand, m- medium sand, c- coarse sand, vc- very coarse sand, g- granule, p- pebble, co- cobble.

Upper Pseudozilja formation and/or lower Amphiolina formation (Jesenica 1–2)

The Jesenica 1 section comprises 160 m of siliciclastic rocks, which are 50 % covered (Fig. 7). Even so, a coarsening-upward trend can be detected from the bottom to the top of the section. The lowermost 38 m of the section is shale-dominated. Approximately 15 % of this interval is represented by fine and very-fine sandstone that forms interchanging beds and lenses 2–20 cm thick. Sand-

stone is locally planar- and cross-laminated. After a 21 m thick gap, a 14.5 m thick heterolithic interval is exposed. Sandstone represents 30 % of the interval and is present in beds up to 10 cm thick. Small-scale slumps are present in the lower part of this interval. After another 13 m of covered interval, the next part of the section comprises a 13 m thick heterolithic interval, in which sandstone forms 50 % of the lithology, forming beds 5–40 cm thick. Lower bed boundaries are often erosional, and channelized, with scours running in a N–S direction. Load casts on lower bedding planes and ripple marks on upper bedding planes are common. Sandstone beds often contain rip-up clasts of shale in their lowermost parts, and display normal grading and planar and cross lamination in their upper parts. After another 19 m thick gap, a sandstone-dominated (60 %), interval 20 m thick follows. Sandstone beds are up to 50 cm thick and display the same characteristics as the underlying beds, with more pronounced cross lamination and ripple marks. Above a bed of normally graded pebbly to fine-grained sandstone, another heterolithic interval 3.4 m thick that is dominated by shale follows. Up to 20 cm thick, often normally graded and/or planar-laminated or normally graded beds of sandstone represent 20 % of this interval. Up to 3 m thick, matrix-supported conglomerate follows, bearing up to 30 cm large clasts of sandstone. The conglomerate is overlain by a heterolithic interval 1.5 m thick, which is dominated by shale. The next 12 m thick part of the section is covered. Matrix-supported muddy conglomerate approx. 5 m thick with large sandstone clasts up to 50 cm, follows. This is covered by a 5 m thick heterolithic, shale-dominated interval containing approx. 40 % of fine and very fine-grained sandstone.

The Jesenica 2 section, which measures 56 m in thickness (Fig. 8) lies in a slightly higher stratigraphic position than the succession described in the Jesenica 1 section. The first 39.6 m of the succession exhibits a coarsening-upward trend. This part is composed of heterolithic intervals comprising 60–90 % shale that is often bioturbated and in places contains calcite concretions and 10–40 % of sandstone in beds and lenses up to 10 cm thick. Shale-dominated heterolithic intervals from the upper half of the succession are interrupted by more sandy intervals, or by beds of conglomerate up to 60 cm thick, grading into sandstone showing planar and cross lamination. The conglomerate has erosive lower boundaries, with the proportion of coarser intervals increasing upwards. After a prominent bed of a matrix-supported conglomerate 5 m thick with sandstone and limestone clasts

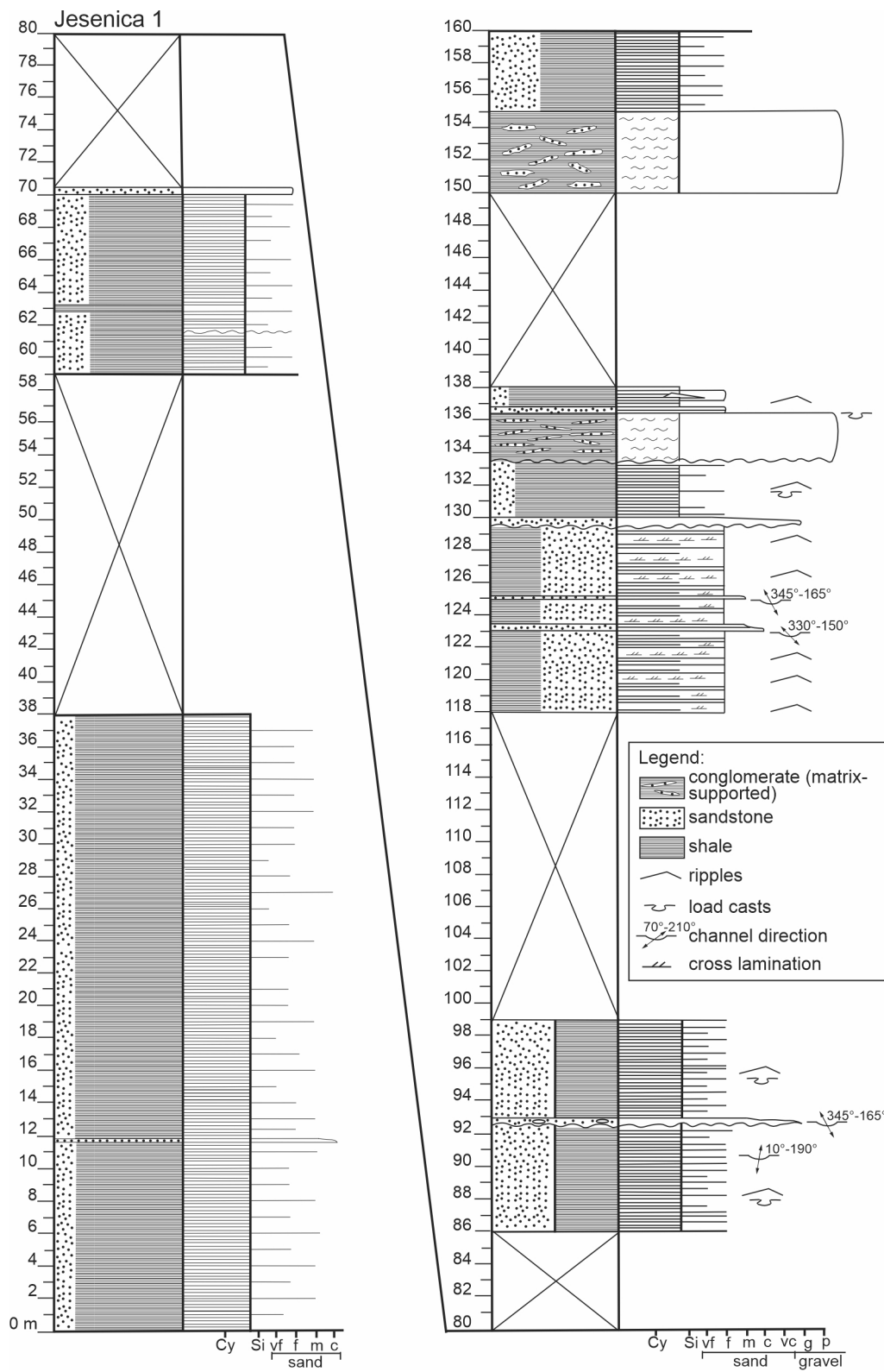


Fig. 7. Sedimentary log of the Jesenica 1 section. Right-side markings delineate grain sizes: Cy- clay, Si- silt, vf- very fine sand, f- fine sand, m- medium sand, c- coarse sand, vc- very coarse sand, g- granule, p- pebble.

up to 20 cm large, a finning-upward succession of shale 16.4 m thick follows. Shale is bioturbated, interbedded by normally graded conglomerate and thin sandstone beds with load casts. A single bed of micritic limestone is present near the top of the section.

Lower Amphiclina formation (Novaki 1-4)

The Novaki 1 section comprises a succession 39.6 m thick dominated by coarse- to fine-grained siliciclastic rocks (Fig. 9). The 1.5 m thick heterolithic, shale-dominated interval contains thin beds

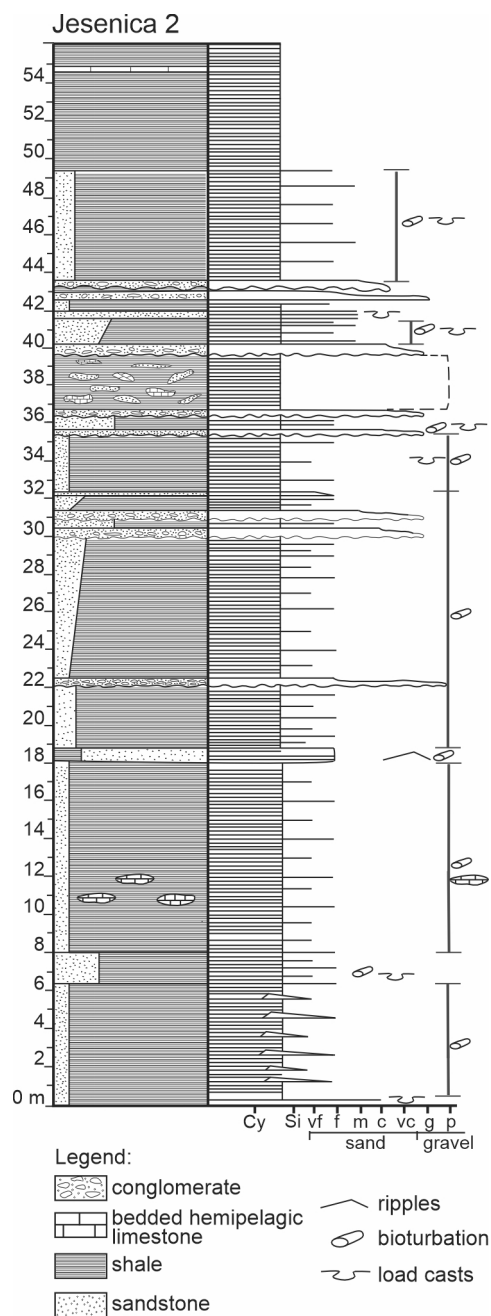


Fig. 8. Sedimentary log of the Jesenica 2 section. Right-side markings delineate grain sizes: Cy- clay, Si- silt, vf- very fine sand, f- fine sand, m- medium sand, c- coarse sand, vc- very coarse sand, g- granule, p- pebble.

and lenses of limestone (mudstone). It is overlain by an 11 m thick coarse-grained interval comprising normally graded, amalgamated beds of conglomerate and sandstone. The conglomerate beds contain mostly limestone pebbles and gradually pass to coarse-, medium- and fine-grained sandstone. The interval is overlain by 5 m thick shale, followed by 22 m of shale-dominated succession. Shale interchanges with calcareous conglomerate and siliciclastic sandstone. Sandstone is normally graded, planar-, and cross-laminated.

The Novaki 2 section reaches a thickness of 34 m (Fig. 9). It begins with a 10 m thick hetero-

lithic interval consisting of shale and subordinate (25 %) beds of limestone (wackestone). A 4 m thick package of medium-grained massive sandstone follows, overlain by a 20 m thick succession comprising several sedimentary sequences. The lowermost sequences begin with conglomerate, containing mostly non-calcareous pebbles. Conglomerate gradually passes into sandstone. Other sequences begin with coarse- to medium-grained sandstone and are partly normally graded. Finer parts of the sequences mostly consist of heterolithic intervals in which shale prevails over thin sandstone beds.

The Novaki 3 section comprises 20.5 m of mostly sandstone and subordinate darker shale (Fig. 9). They are subdivided into several sedimentary sequences of different thicknesses. Sequences begin mostly with an erosional surface, followed by medium- to very coarse-grained sandstone, which is pebbly in the upper part of the section. The sandstone beds are 0.5–2.5 m thick, normally graded, and in some beds planar-laminated in the upper parts. The upper, fine-grained parts of the sequences are 1–1.8 m thick heterolithic intervals comprised of 60 % shale and 40 % sandstone in thin beds and lenses.

The Novaki 4 section measures 22.5 m in thickness (Fig. 9). The lower 6 m are represented by interchanging thin beds of shale and 20–30 cm thick beds of normally graded fine-grained sandstone. The remaining 16.5 m of the section are subdivided into 0.7–5.2 m thick sedimentary sequences. Sequences are dominated by sandstone and pebbly sandstone. Normally graded sandy conglomerate with erosional base is subordinate. Shale forms upper fine-grained parts 0.2–1 m thick of the sequences.

Upper Amphiclina formation (Davča 1–2, Poče, Zakojca 1–2, Orehek, Hudajužna, Koritnica)

The described sections are ordered according to their geographic position from E to W.

The Davča 1 section represents the upper 80 m of the Amphiclina formation (Fig. 10). The section starts with an 8.4 m thick fining-upward succession, comprising sequences of coarse-grained sandstone, pebbly sandstone, and conglomerate. These beds are mostly normally graded and gradually pass into limestone (wackestone), or heterolithic intervals composed of limestone (wackestone) interbedded with thin beds and laminae of shale (Fig. 4a). A bed of slumped pebbly mudstone approx. 2 m thick follows after a sharp erosive surface. Muddy matrix forms 80 % of this bed. Dispersed within the matrix of the pebbly mudstone are clasts of shale, sandstone, and limestone up

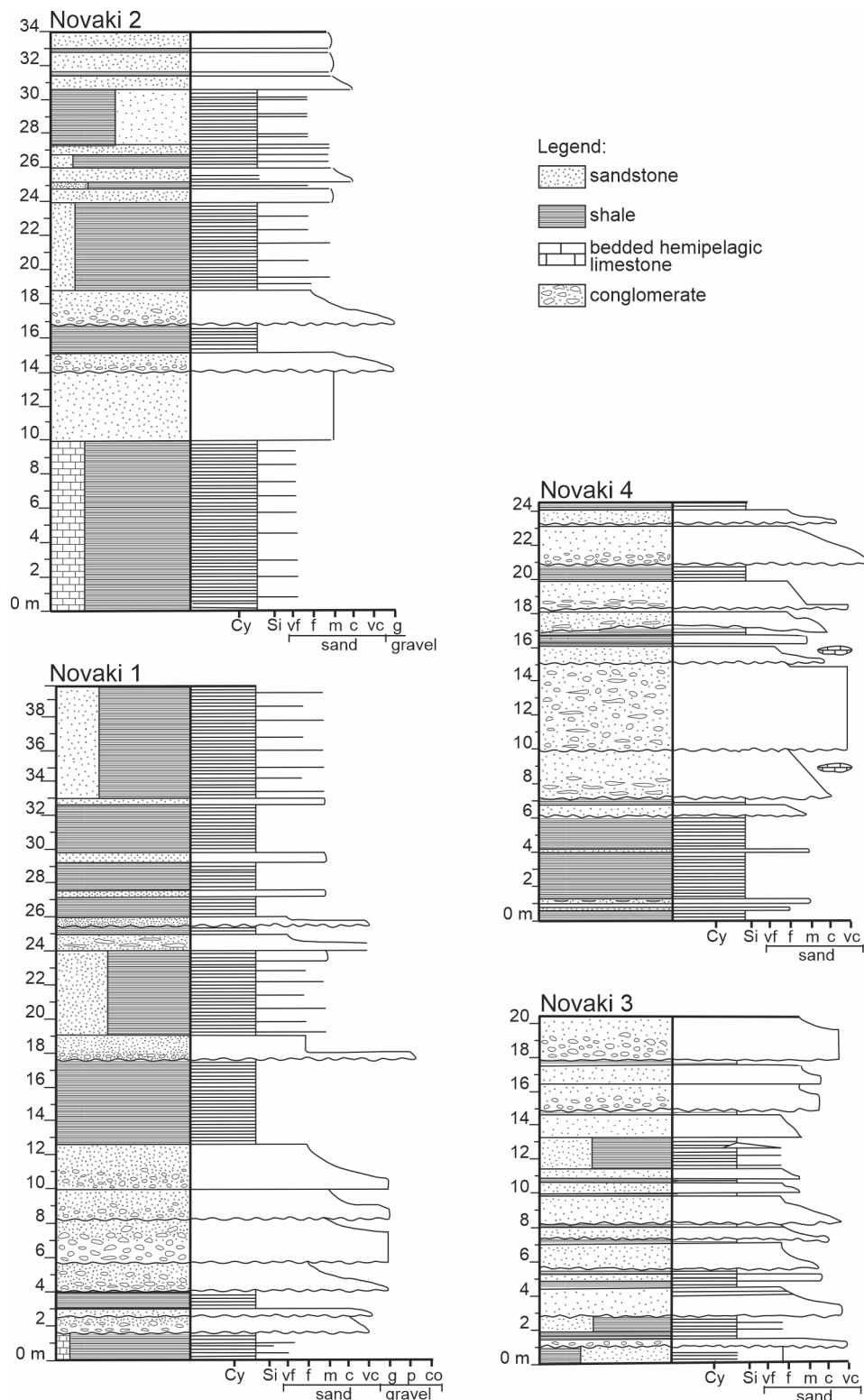


Fig. 9. Sedimentary log of the Novaki sections. Right-side markings delineate grain sizes: Cy- clay, Si- silt, vf- very fine sand, f- fine sand, m- medium sand, c- coarse sand, vc- very coarse sand, g- granule, p- pebble, co- cobble.

to 20 cm in size. The following 1.5 m of the section is covered. The covered interval is followed by a fining-upward succession 31 m thick. The lowermost 7.6 m of the interval is mostly sandstone, with subordinate locally bioturbated shale (Fig. 4b). Sandstone beds are up to 70 cm thick, with erosional, locally channelized bases and with

cross, planar lamination, flaser bedding, and ripple marks on some of the upper bedding planes. Three sedimentary sequences were singled out in the next 25.4 m of the section (from approx. 18 m to 45 m in Fig. 10) and are 7.4 m, 9.6 m and 8.4 m thick. Each sequence begins with beds of normally graded conglomerate up to 40 cm thick, transi-

tioning to planar- and cross-laminated sandstone. This is followed by 40 cm to 3 m thick shale-dominated heterolithic intervals with 10–40 % thin beds, laminae, and lenses of fine-grained sandstone and thin beds of limestone (wackestone). Load casts are present on the lower bedding planes of sandstone, and ripple marks were observed on some of the upper bedding planes (Fig. 4c). Some upper parts of the sandstone beds are weathered and pass into brown mudstone some few cm thick. After a 13.4 m thick covered part of the section, a 16.2 m thick succession of heterolithic shale-dominated interval follows. Intercalations of thin beds, laminae, and lenses of cross-laminated fine-grained sandstone represent 15 % of the interval. Load casts are present on the lower bedding planes of sandstone beds. Ripple marks are present on the upper bedding planes. Shale is often bioturbated. The heterolithic clastic interval is followed by a predominantly calcareous, heterolithic interval 2 m thick containing 70–85 % of limestone (wackestone) in beds 10–15 cm thick, and 15–30 % of shale in thinner beds. The interval is overlain by 1 m of bedded fine crystalline dolostone. The section ends with a clastic heterolithic interval 1.4 m thick with the same characteristics as the underlying one.

The Davča 2 section spans 21.5 m of a carbonate-dominated succession (Fig. 10). The lower 10.2 m thick succession is characterized by increasing terrigenous component. The lowermost, 6 m thick part consists of limestone-dominated heterolithic intervals. Limestone (wackestone) in beds up to 20 cm thick forms 10–95 % of intervals and interchanges with thin beds of shale. Most of the contacts between the two lithologies are wavy. Heterolithic parts are interbedded by packages of bedded limestone (wackestone) 1 m thick. The lower part of the section ends with 4.2 m of shale, above which follow 5.8 m of calcareous-prevailing succession with heterolithic intervals containing 60–90 % of limestone (wackestone) interbedded by shale. Pyrite can be found in the lower part. Shale is locally bioturbated and ripple marks were observed on some bedding planes of limestone beds. Small chert nodules are present within the limestone in the upper part of the succession. The section ends with an interval of fine crystalline dolostone 5.6 m thick in beds 5–50 cm thick belonging to the lowermost part of the Bača dolomite formation (Fig. 4d). Dolostone often contains chert nodules and chert horizons up to 10 cm thick.

The Poče section represents the upper 128 m of the Amphiclina formation (Fig. 11). The section is interrupted by two covered parts that are 9 m and

25 m long respectively and is dissected by three minor faults. The section begins with a 14.6 m thick coarsening-upward siliciclastic-dominated succession. The lower, 11 m thick part consists of shale that is interbedded with fine-grained sandstone. The upper part comprises 0.7–1.3 m thick sequences composed of normally graded and partly planar-laminated sandstone, intercalated by beds of shale up to 30 cm thick. The next 5 m of the section consists of a heterolithic interval in its lower part. The heterolithic interval is composed of 75 % of shale and 25 % sandstone lenses. Upwards, the interval transitions into an interval of shale 4 m thick with a thin lenticular bed of limestone (mudstone). The next, 9 m thick part of the section is covered, and is followed by a predominantly shaly succession 22 m thick. In the lower part (4 m) is a heterolithic interval with 80 % shale, interbedded with fine-grained sandstone and thin beds and lenses of limestone (wackestone). The upper part of the interval consists of an interval of shale 18 m thick with two thicker beds of fine-grained sandstone. The succession is interrupted by a minor fault. Three heterolithic intervals follow, the first of which is 4 m thick, and consists of 85 % shale and 15 % limestone in lenses 2 cm thick. The second and third heterolithic intervals consist of 80–95 % locally bioturbated shale, interchanging with thin beds, laminae, and lenses of fine-grained sandstone. The section is interrupted by a covered interval 25 m thick. After the covered interval, a succession of bedded limestone (wackestone) 2.8 m thick follows. It is interbedded by a calcareous conglomerate with limestone and chert pebbles. This interval is overlain by a calcareous conglomerate 2 m thick with rip-up clasts of shale. The limestone pebbles are up to 7 cm in diameter, and on the outer side crusted in finely crystalline quartz. Clasts are partly imbricated. The conglomerate bed is followed by a package of beds of intra-bioclastic grainstone limestone that is cut by a minor fault. Above the fault, a 5 m thick interval of bedded limestone (wackestone) and heterolithic intervals follows. Heterolithic parts consist of 50–80 % of limestone (wackestone), interchanging with beds of shale up to 1 m thick. This limestone dominated interval is overlain by a 14 m thick clastic heterolithic interval consisting of shale (75 %) and sandstone (25 %) in thin, partly cross-laminated beds, laminae, and lenses. Load casts are often present on lower bedding planes. The heterolithic interval is followed by three thick sequences, each 2 m thick. Sequences start with heterolithic interval up to 1.4 m thick composed of 80 % bedded limestone (wackestone) and 20 %

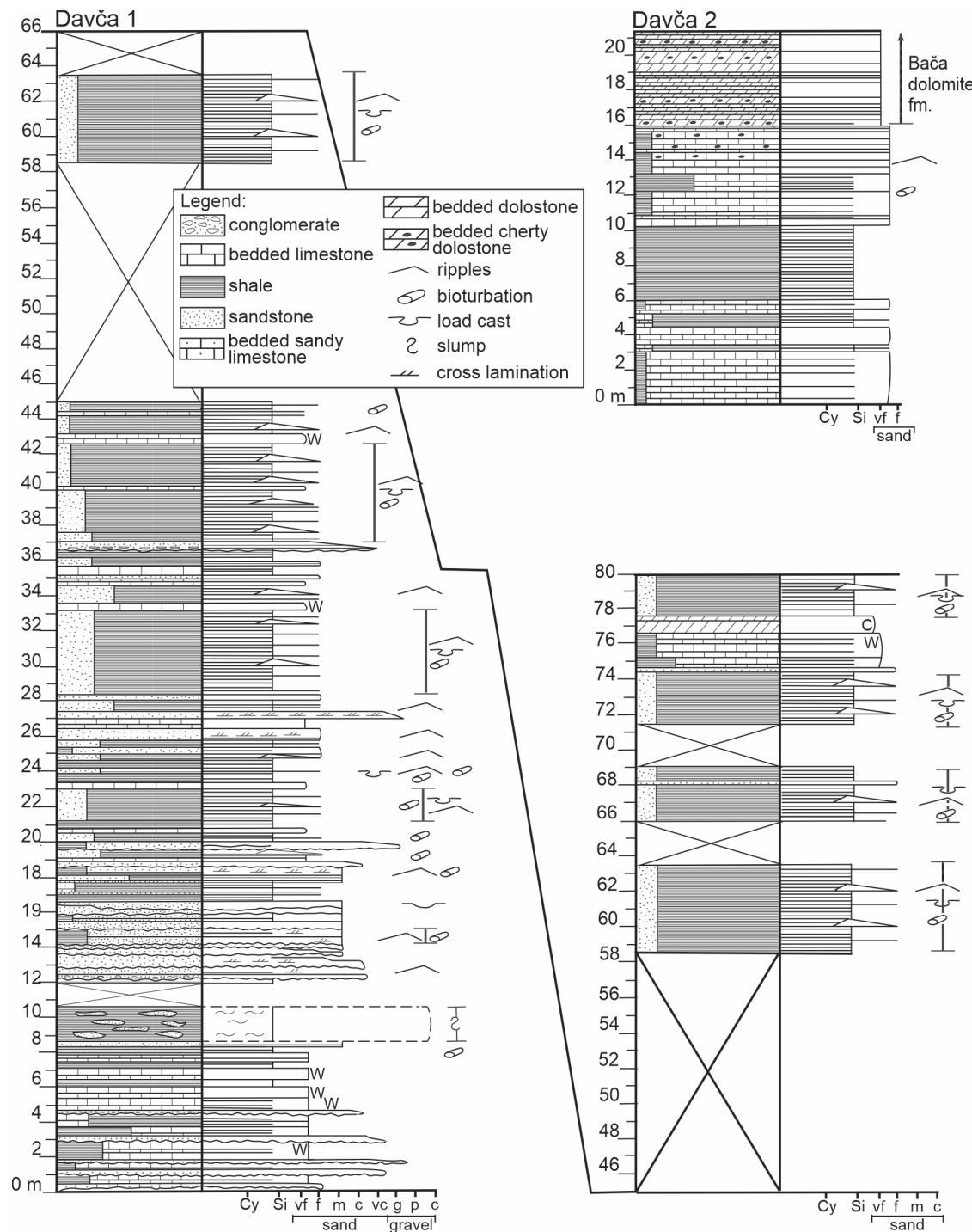


Fig. 10. Sedimentary log of the Davča sections. Right-side markings delineate grain sizes: Cy- clay, Si- silt, vf- very fine sand, f- fine sand, m- medium sand, c- coarse sand, vc- very coarse sand, g- granule, p- pebble, co- cobble. Letterings: W- wackestone, C- crystalline.

shale. The heterolithic parts are followed by clastic heterolithic intervals 0.8–1.4 m thick with 80–90 % of shale, interbedded with fine-grained sandstone in thin beds, laminae, and lenses. Load casts are present on some of the lower bedding planes. Ripple marks are present on the upper bed surfaces. Two more sequences follow, which are 1.6 m and 3 m thick, respectively. The lower one starts with bedded limestone (wackestone), followed by a

heterolithic interval consisting of 80 % limestone (wackestone) and 20 % shale. A lens of calcareous conglomerate is present near the base. The upper interval is shale-dominated, with 15–50 % of the interval limestone (wackestone). The transition from the Amphiclina formation to the Bača dolomite formation lies within a heterolithic interval 2 m thick, containing 80 % of fine crystalline dolostone interbedded by 15 % of shale.

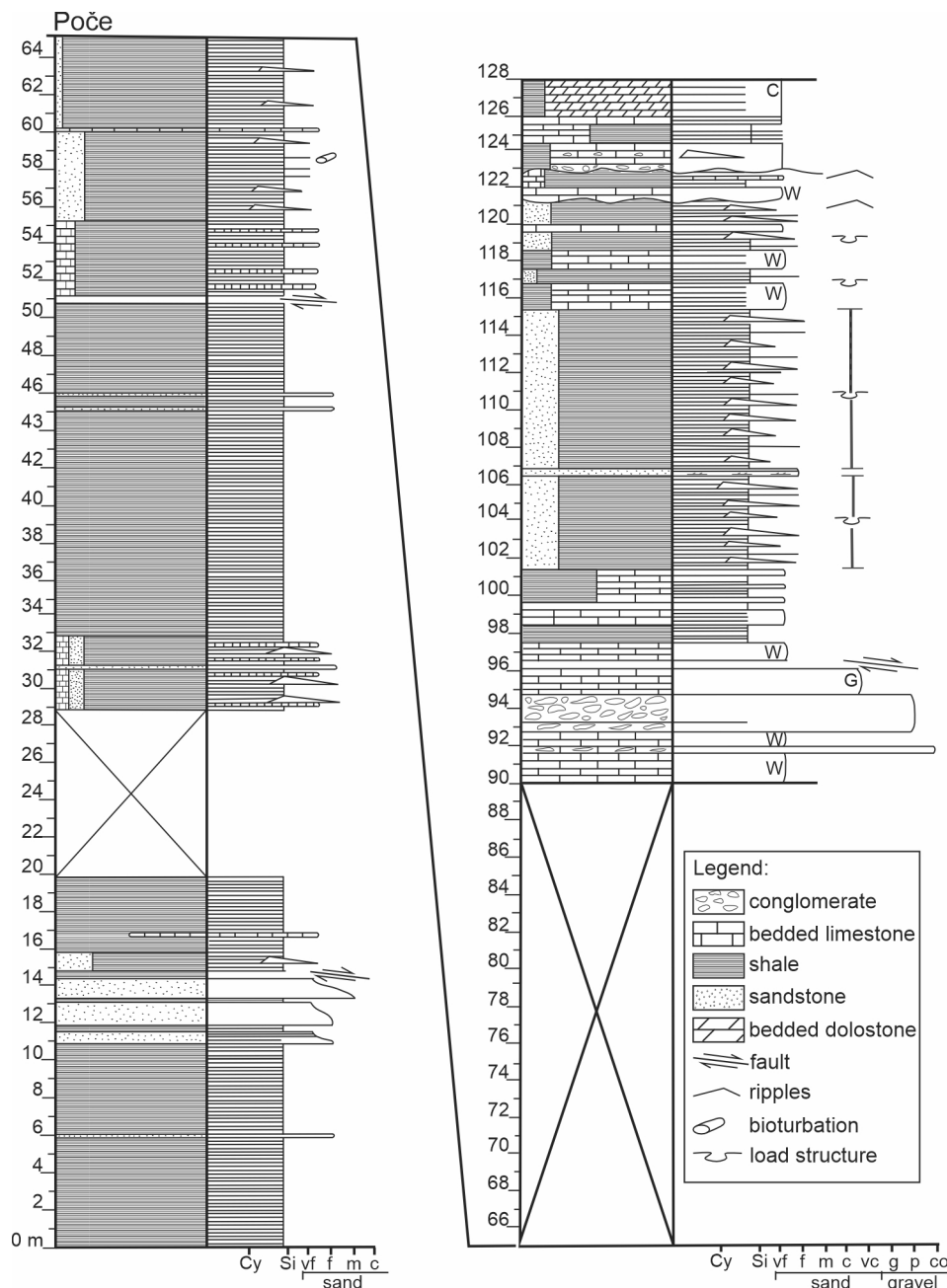


Fig. 11. Sedimentary log of the Poče section. Right-side markings delineate grain sizes: Cy- clay, Si- silt, vf- very fine sand, f- fine sand, m- medium sand, c- coarse sand, vc- very coarse sand, g- granule, p- pebble, co- cobble. Letterings: W- wackestone, G- grainstone.

The transition from the uppermost Amphiclina formation into the Bača dolomite formation in the surroundings of the village of Zakojca is exposed in two sections (Fig. 12).

The section Zakojca 1 represents a succession of sedimentary rocks 15 m thick. The lowest 12 m of the section consists of two sedimentary sequences with an upwardly increasing clastic component. The sequences are 7 m and 5 m thick, respectively. The lower parts contain heterolithic intervals 1–4.4 m thick with 60–70 % dark grey limestone (wackestone) in beds 5–25 cm thick interchanging with shale (30–40 %) in thin beds and laminae.

The section continues with clastic, shale-dominated intervals 2.6–4 m thick with 70 % shale interchanging with 30 % fine-grained sandstone in thin beds and lenses. The uppermost part of this 3-m thick section is dominated by carbonate rocks. It begins with limestone (wackestone) followed by partly dolomitized limestone. The section ends with a heterolithic interval 1.6 m thick consisting of fine crystalline dolostone (85 %) in beds 10–20 cm thick with chert nodules up to 20 cm in size interbedded by thin beds of shale (15 %). This interval belongs to the lowermost part of the Bača dolomite formation.

Section Zakojca 2 is located 300 m to the west of the former section, separated from it by a strike-slip fault. It was logged in a thickness of 35 m. It begins with a heterolithic interval 60 cm thick dominated by limestone (wackestone), interbedded with thin beds of shale. It is overlain by a bed of calcareous breccia 2.4 m thick with limestone clasts up to 50 cm in diameter. Clasts are silicified at the margin and partly imbricated. This breccia is very similar in composition and structure to the limestone conglomerate bed in the Poče section. The breccia is succeeded by a heterolithic interval 7 m thick containing 75 % limestone (wackestone) in beds up to 50 cm thick interbedded with thin beds of shale and a bed of calcareous breccia. This interval was partly eroded by a 2 m thick matrix-supported very coarse breccia with limestone clasts up to 1.5 m in size. The breccia passes into a 1.8 m thick bed of inversely graded muddy conglomerate with limestone pebbles 4–5 cm in diameter. The amount of muddy matrix is lower than in the former breccia layer. Breccias are followed by a 2 m thick bed of inversely graded fine- to medium-grained calcarenite and a 1.6 m thick bed

of calcareous breccia. The latter is overlain by a bed of matrix-supported limestone breccia 1.8 m thick with an erosional base. It is succeeded by a 1.4 m thick interval of medium-grained sandstone, limestone (wackestone) and shale. An erosional channel up to 30 cm deep is cut into the shale, and is filled with calcareous conglomerate with an admixture of smaller pebbles of quartz, rhyolites, chert, and sandstone. The conglomerate is followed by limestone (wackestone). Both are partly cut by matrix-supported breccia 4–5 m thick with clasts of sandstone and shale. The channel is oriented in a N–S direction. The muddy breccia is followed by 7 m of shale. The section ends with a heterolithic interval 2 m thick consisting of 85 % bedded, finely crystalline dolostone and 15 % shale belonging to the Bača dolomite formation.

The Orehek section is a heterogeneous succession approx. 430 m thick (Fig. 13). It starts with 5 m of shale with rare calcareous nodules. Above the erosional surface follows an approximately 15 m thick, matrix-supported blocky olistostrome breccia with deformational textures (from 5 m to 20 m in Fig. 13). Limestone clasts (olistoliths) are

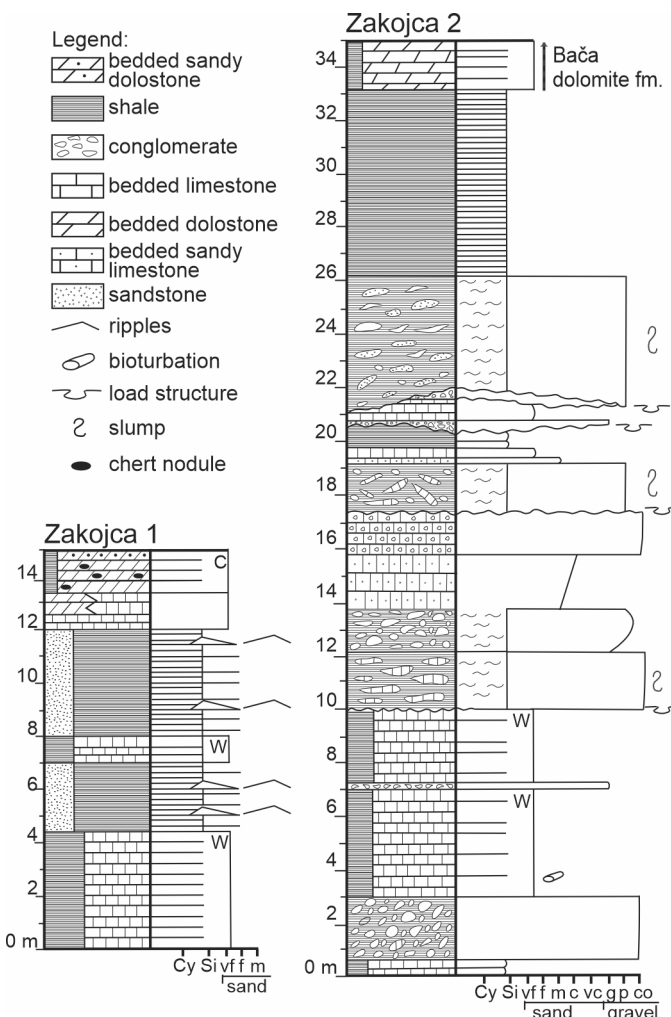


Fig. 12. Sedimentary log of the Zakojca sections. Right-side markings delineate grain sizes: Cy- clay, Si- silt, vf- very fine sand, f- fine sand, m- medium sand, c- coarse sand, vc- very coarse sand, g- granule, p- pebble, co- cobble. Letterings: W- wackestone, C- crystalline.

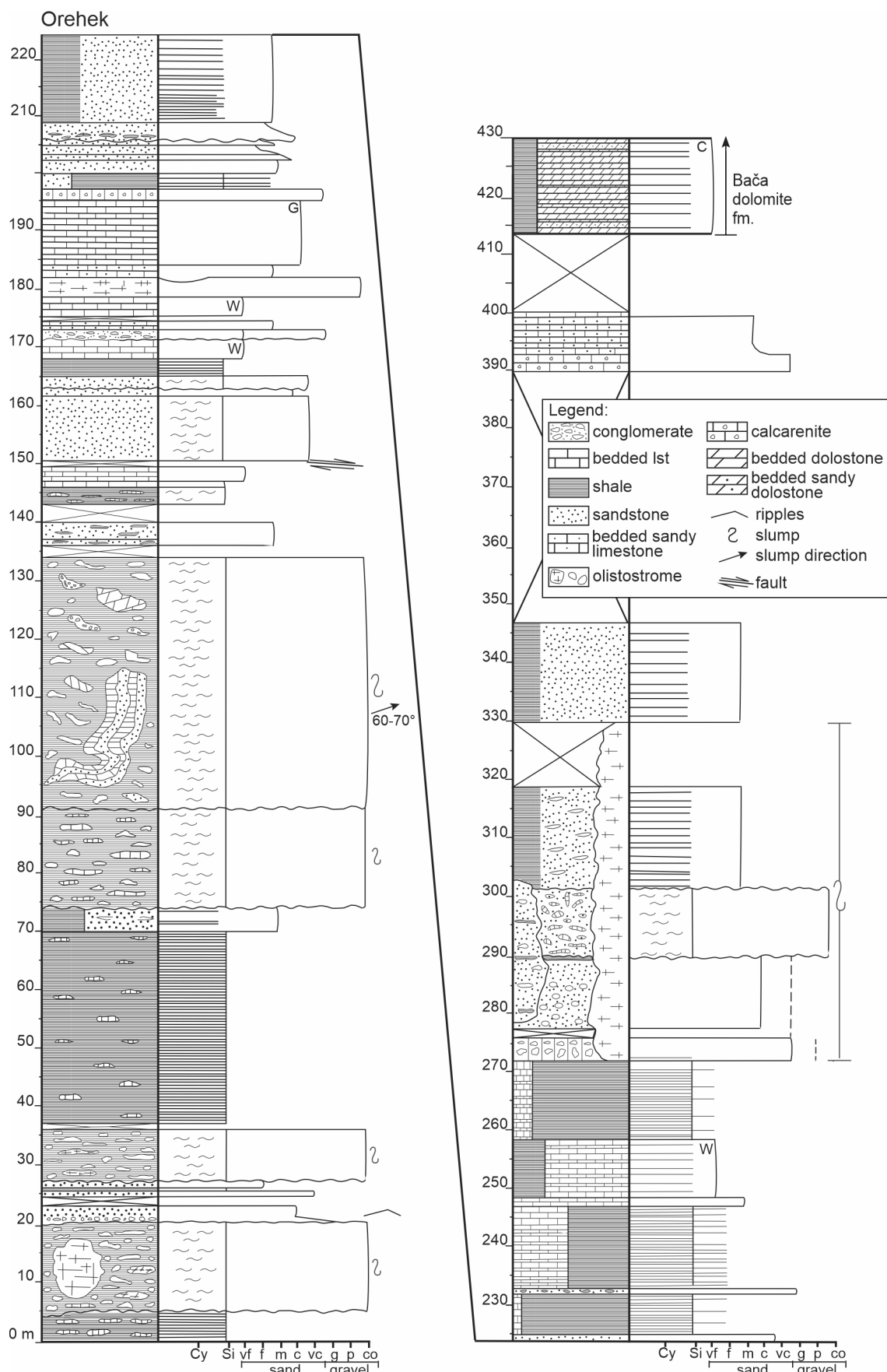


Fig. 13. Sedimentary log of the Orehek section. Right-side markings delineate grain sizes: Cy- clay, Si- silt, vf- very fine sand, f- fine sand, m- medium sand, c- coarse sand, vc- very coarse sand, g- granule, p- pebble, co- cobble. Letterings: W- wackestone, G- grainstone.

up to 10 m in size. Theolistostrome passes upwards into calcareous breccia, which in turn passes into sandstone. Another 9 m thick olistostrome with an erosional base follows (from 27 m to 36 m in Fig. 13). It is overlain by 37 m of shale with rare calcareous nodules and a heterolithic interval consisting of 65 % sandstone and 35 % shale. The following two olistostromes, 17 m and 43 m thick, respectively, contain olistoliths up to 20 m in size. An internal deformational fold axis indicates slumping towards the E-NE. The second olistostrome is overlain by calcareous sandstone, sandy shale with calcareous nodules, and limestone (wackestone) in a partly covered, 16 m thick interval (from 134 m to 150 m in Fig. 13). Passing a smaller fault, the succession continues with an olistostrome 18 m thick with smaller clasts. Olistostrome intercalates with coarse-grained sandstone gradually passing into shale. This is overlain by a succession of limestone, interbedded with sandy limestone breccia and calcarenite 29 m thick (from 168 m to 197 m). This interval includes a limestone block (mud mound or olistolith?) 3.5 m thick covered by calcarenite and dark grey, locally laminated limestone (grainstone) in beds 3–40 cm thick passing into limestone breccia. The limestone-dominated interval is succeeded by a clastic succession 28 m thick containing a shale-dominant heterolithic interval at the base, followed by sandstone in mostly normally graded beds up to 3 m thick with planar lamination at the top. A sandy interval is followed by a heterolithic interval 15 m thick consisting of 65 % medium-grained sandstone interbedded with shale and topped by coarse-grained sandstone. The heterolithic interval is followed by 33.5 m of shale-dominated heterolithic intervals 7–18 m thick containing 30–90 % shale and 10–70 % dark grey limestone (wackestone), interbedded by beds of calcareous conglomerate and limestone (wackestone) 1 m thick. An olistostrome approx. 58 m thick follows (starts slightly below 272 m in Fig. 13) and is divided into four sections according to predominant lithology. The first section consists mostly of calcareous breccia with clasts of limestone (wackestone) up to 70 cm large containing echinoderms. The following interval consists of a sandy conglomerate with pebbles of quartz, rhyolite, chert, limestone (mudstone), shale, and coarse-grained sandstone. This interval is overlain by matrix-supported sandy breccia with an erosive base. Clasts within the breccia are predominantly dark grey limestone (mudstone), up to 1 m in diameter. Breccia is overlain by a heterolithic interval, consisting of 70 % sandstone and 30 % shale. The upper part is covered, except for

58 m of olistostrome breccia. The lower part of the breccia includes an olistolith 24 m thick composed of normally graded, planar-, and cross-laminated sandstone with shale intercalations. The olistostrome is covered by a heterolithic interval 17 m thick (from 330 m to 347 m) with 70 % sandstone and 30 % shale. Approximately 40 m of the section are poorly exposed. Shale and sandstone outcrop locally. An interval of limestone breccia approx. 9 m thick, passing into coarse-grained calcarenite follows. After 14 m of covered part the Bača dolomite formation follows.

The Hudajužna section reaches a thickness of 66 m. It is composed of carbonate-clastic deposits that represent the upper part of the Amphicrina formation. The top of the section lies approx. 15 m below the contact with the Bača dolomite formation (Fig. 14). Conodonts studied by Flügel and Ramovš (1970) from a section in the vicinity provided late Carnian, Tuvalian age. According to a prevailing lithology, the section can be divided into two parts: the lower part is 20 m thick and largely consists of heterolithic intervals up to 2 m thick. Each interval consists of 70–95 % limestone (wackestone), and 5–30 % shale, and is interbedded by beds of limestone (wackestone) 40–60 cm thick and two beds of calcareous conglomerate, 1.4 m and 0.4 m thick, respectively. The second part, some 46 m thick and consisting mostly of shale occupies the rest of the section. The succession is characterized by the increasing-upwards content of the calcareous component. The heterolithic intervals alternate between predominantly limestone and shale and form sequences ranging from 0.4 m to 11 m in thickness. Sequences most often start with heterolithic intervals that are 0.8–3.4 m thick, consisting of 40–95 % limestone (wackestone) and 5–60 % shale, or with beds of limestone (wackestone) 20–40 cm thick. The upper, clastic-dominated heterolithic intervals include 70–95 % of shale, interbedded with thin beds, laminae, and lenses of very fine- to fine-grained sandstone. Shale is partly bioturbated. Some sandstone beds are planar- and/or cross-laminated and have ripple marks on some of the upper bedding planes.

The Koritnica section is the westernmost logged section. Beds are in an overturned position, slightly folded in the lower third of the section, and intersected by a minor normal fault with a displacement of about 2 m. Both irregularities were restored, so the complete section is present. The section comprises a succession 89 m thick of a highly variegated exchange of lithology: shale, bedded limestone (texturally mostly wackestone, subordinate pack-

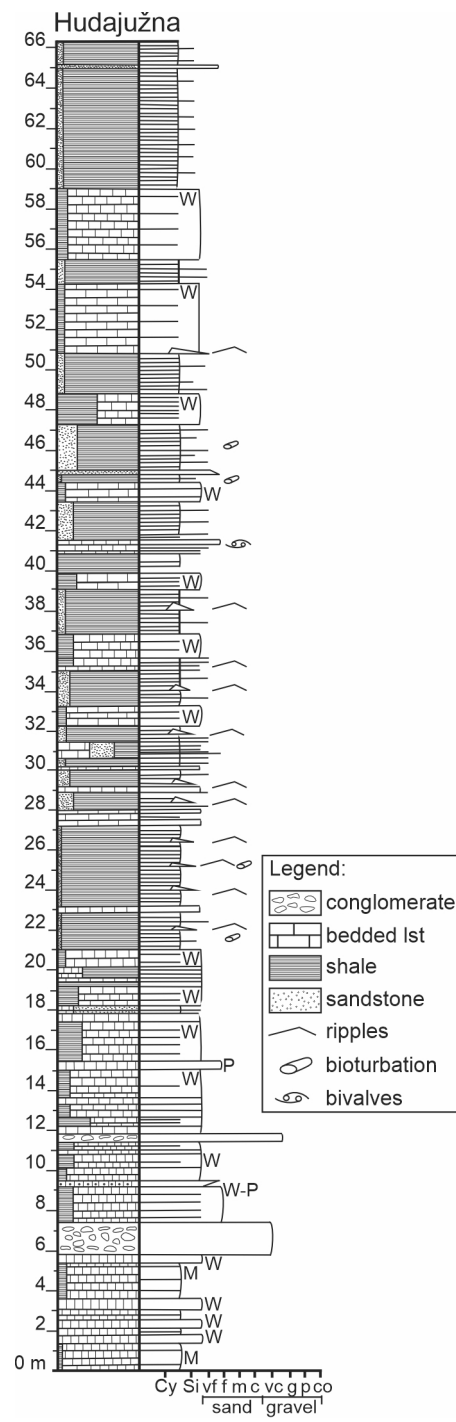


Fig. 14. Sedimentary log of the Hudajužna section. Right-side markings delineate grain sizes: Cy- clay, Si- silt, vf- very fine sand, f- fine sand, m- medium sand, c- coarse sand, vc- very coarse sand, g- granule, p- pebble, co- cobble. Letterings: W- wackestone, P- pack-stone.

stone, and grainstone), calcarenite, muddy breccia and conglomerate, and sandstone and dolostone with chert in the uppermost part of the section (Fig. 15). The complete succession was divided into ten intervals of different thickness and with specific characteristics. The first interval is 1.4 m thick and includes shale and limestone (mud- to wackestone). The second interval is 5.6 m thick and begins with muddy flat pebble calcareous conglomerate with erosional lower and upper bed-

ding plane, followed by interchanging calcareous conglomerate, calcarenite, some normally graded, and heterolithic intervals with 20–70 % of shale interbedded with limestone (mud- and packstone). The third interval is 10.8 m in thickness (approx. 7 m to 17.8 m in Fig. 15). Limestone (wackestone) is dominant, composed mostly of heterolithic intervals 0.8–3 m thick with 70–80 % limestone, 20–30 % shale, and 20–100 cm thick packages of bedded limestone interbedded with calcareous conglomerate and calcarenite. The fourth interval (from 17.8 m to 31.6 m) is 13.8 m thick and clastic-dominated, containing beds of conglomerate 20–80 cm thick. Some beds are calcareous, muddy breccia, sandstone, and calcarenite, interbedded by a heterolithic interval 0.6–1.4 m thick with 50–70 % limestone (wackestone) and 30–50 % shale. In this interval, two sandstone beds with ripples indicate the N–S direction of the current (at 23.5 m and 25.5 m). The fifth interval (from 31.6 to 43.2 m) measures 11.6 m in thickness. It is also dominated by clastic components. Four fining-upward successions start (at 31.5 m in Fig. 15) with beds of breccia 40–80 cm thick with an erosional base (Fig. 4f), passing upwards into coarse- to medium-grained sandstone, usually normally graded, interbedded with thin limestone (wackestone) beds or heterolithic intervals up to 60 cm thick with 85 % limestone (wackestone) and 15 % shale. In one of them, a thin bed of finely crystalline dolostone was detected. The upper part of the succession comprises two heterolithic intervals consisting of 60–85 % bedded limestone (wackestone), and 15–40 % shale interbedded with calcarenite. The sixth interval (from 43.2 to 59.4 m) occupies 16.2 m of the section and shows the coarsening-upwards trend. The lower part of the succession consists of interchanging thin beds of calcareous breccia, subordinate siliciclastic conglomerates, limestone (wackestone), and heterolithic intervals, some of which are calcareous and some siliciclastic-dominant, and a thin bed of finely crystalline dolostone. Sedimentary slumps were observed in two intervals. It is important to mention a heterolithic interval 1.4 m thick with 60 % shale and 40 % sandstone in which beds are broken and folded around a block of bedded limestone (at app. 46 m in Fig. 15; Fig. 4e). The limestone block apparently slid from N to S, indicating slope inclination in the same direction. The upper part of the succession is composed of siliciclastic conglomerate and muddy breccia up to 1.4 m thick, both with erosional bases interbedded with limestone in thin lenses and filling small depressions on uneven upper bedding surfaces

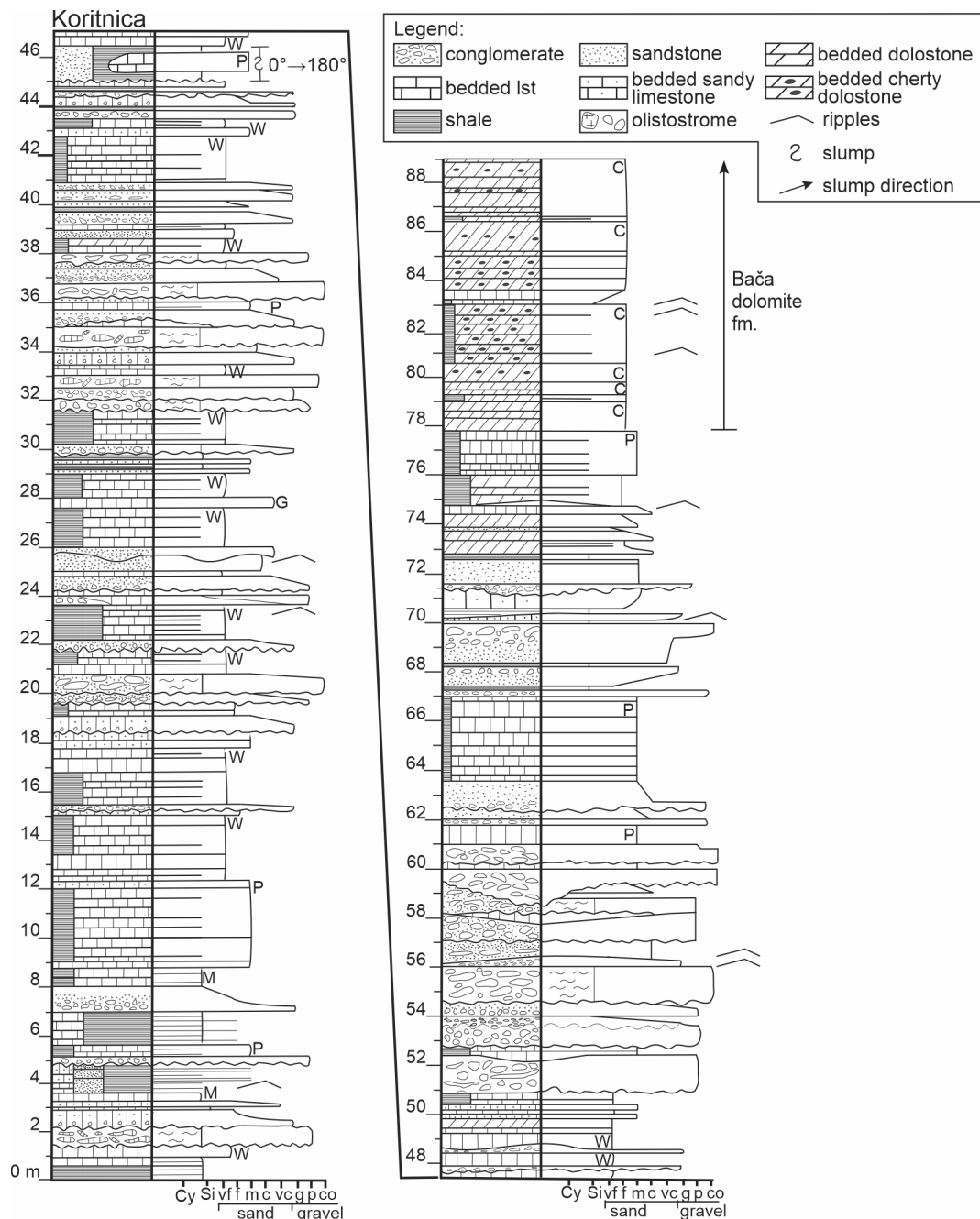


Fig. 15. Sedimentary log of the Koritnica section. Right-side markings delineate grain sizes: Cy- clay, Si- silt, vf- very fine sand, f- fine sand, m- medium sand, c- coarse sand, vc- very coarse sand, g- granule, p- pebble, co- cobble. Letterings: M- mudstone, W- wackestone, P- packstone, G- grainstone, C- crystalline.

of conglomerate, which are somewhere overlain by normally-graded sandstone or dunes with ripple marks. The seventh interval is 7.6 m thick with a fining-upward beds track. It begins with a channelized erosional surface cutting some 80 cm into underlying sediments (at app. 59 m in Fig. 15) and is overlain by two sequences with calcareous conglomerate with elongated, partly imbricated limestone clasts up to 50 cm in size, followed by sandstone or limestone (wackestone). The upper sequence also has a channelized erosional base. Channels run in the N-S direction. The succession ends with a heterolithic interval 3.4 m thick consisting of 90 % bedded limestone (packstone) and

10 % shale (from 63.5 m to 67 m in Fig. 15). The eight interval, which is 8 m thick, can be divided into two parts: the lower, 4.2 m thick, mostly contains inversely graded fine- to coarse-grained sandstone; the thickest bed at 2 m is inversely graded into siliciclastic conglomerate, which in the uppermost part is muddy and contains only limestone pebbles. The upper part is 3.8 m thick. It starts with channelized erosional surface (71 m in Fig. 15), overlain by a thin layer of conglomerate, followed by normally-graded coarse- to fine-grained sandstone, which is in the upper parts planar- or cross-laminated. Ripple marks are locally present. The sandstone is dolomitized. The

ninth interval is 7.1 m thick, consisting of heterolithic intervals dominated by bedded dolostone or limestone. The heterolithic intervals are 1.2–2.6 m thick. They consist of 60–90 % bedded dolostone and 19–40 % shale. The limestone-dominated heterolithic interval, 1.8 m thick, consists of 80 % limestone (packstone) and 20% shale. The succession is capped by a lens of limestone (wackestone) with some ripple marks (75 m in Fig. 15). The tenth interval covers 11 m of the section and consists of bedded crystalline dolostone and a heterolithic interval 2.4 m thick dominated by dolostone with 10 % of shale. The dolostone contains nodules and thin, uneven beds of chert. This interval belongs to the Bača dolomite formation.

Microfacies

Table 2 lists microfacies varieties of clastic sedimentary rocks and limestone from the upper Pseudozilja and Amphicilina beds. Late diagenetic changes are omitted from the description. Volca-

nics and volcanoclastics of the Malenski Vrh section were already described by Skaberne and Čar (1986).

Selected microfacies types of limestones and coarser (sand- to gravel-size) clastic rocks are presented in Figures 16–18. Limestone comprises a variety of microfacies types. The most common is wackestone, dominated by thin-shelled bivalves, echinoderms, and radiolarians. Also common are carbonate mudstone and radiolarian wackestone, whereas other limestone types are less common. Sandstone is mostly dominated by quartz, feldspar, and lithic grains (mostly fragments of acidic volcanic rocks) in various proportions. Rare bioclasts, such as thin-shelled bivalves, and echinoderms, are found in sandstone. A single silicified foraminifera *Lamelliconus* ex gr. *ventroplanus* (Oberhauser) was found in one sample (Fig. 18c). The stratigraphic range of *L. ex gr. ventroplanus* extends from the Ladinian to the Carnian (Rettori, 1995; Pérez-López et al., 2005).

Table 2. Description of microfacies types from the Ladinian – Carnian volcano-sedimentary succession of the western Slovenian Basin.

Microfacies	Composition	Interpretation	Samples
Carbonate mudstone (Fig. 16a)	Less than 10 % of clasts (mostly bioclasts, small admixture of terrigenous grains); micritic matrix predominates. Different degrees of bioturbation. Elongated grains oriented parallel to the bedding (could be due to compaction). Rare samples show faint parallel lamination. Bioclasts: echinoderms, fragments of thin-shelled bivalves, sponge spicules. Terrigenous grains: include quartz, feldspar, mica.	Hemipelagic background sedimentation.	Hudajužna: 10.5, 17.4, 24.6, 38.5, 45.8, 62.0; Davča 1: 20.4; Davča 2: 18.9, 23.3; Jesenica 2: 1, 4, 5, 9; Poče: 1, 2, 9, 11, 15, 28, 37; Koritnica: 48.6, 59.4, 96.4.
Filament-echinoderm wackestone and packstone (Fig. 16b–c)	10–50% of grains (bioclasts, some samples with 0–2% of terrigenous grains), 50–90% of micritic matrix. Poorly to moderately sorted; elongated grains concordant to bedding. Possible bioturbations locally present. Locally interchanges with bioclastic packstone in laminae. Some samples with geopetal structures (umbrella-type porosity beneath valves, geopetal infillings of gastropods). Bioclasts: dominant thin-shelled bivalves (fragmented), echinoderms (often bored); subordinate radiolarians, sponge spicules, gastropods, ostracods, foraminifera. Terrigenous grains: poorly preserved, strongly carbonatized; feldspar, fragments of volcanics, quartz. Some samples contain very rare intraclasts.	Hemipelagic background sediment, mixed with allochthonous components; reworked by bioturbation and/or weak currents.	Hudajužna: 1.7, 3.2, 9.1, 9.6, 10.8, 12.5, 14.2, 15.7, 18.4, 19.5, 28.8, 41.1, 52.0, 56.7; Davča 1: 2.7, 5.5, 33.5, 94.7; Davča 2: 2.7, 3.5, 5.7, 10.3, 13.9, 15.3; Poče: 3, 9, 11, 12, 15; Zakoča 1: 2, 2a, 14, 20.6, 47; Koritnica: 11.6, 15.7, 39.5, 83.7.
Filament packstone (Fig. 16d)	80% of grains, 20% of microsparite and carbonate cement. Faint parallel lamination, caused by different amount of peloids. Thin-shelled bivalves are parallel to bedding, in long contacts. Grains: thin-shelled bivalves predominate (70% of rock); peloids and echinoderms together represent 10% of rock.	Reworked hemipelagic sediment.	Zakoča 2: 53; Koritnica: 57.4, 91.6, 95.8.
Radiolarian wackestone (Fig. 16e)	15–30% of grains (mostly bioclasts), 70–85% of micritic matrix. Grains are poorly sorted. Bivalves are oriented parallel to bedding. Umbrella-type porosity under the valves is present in some samples. Bioclasts: dominant radiolarians, followed by thin-shelled bivalves, gastropods, echinoderms, thick-shelled bivalves, ostracods, foraminifera. Terrigenous grains are rare, including grains of quartz and lithic grains. Lithoclasts of carbonate mudstone are also sporadically present.	Hemipelagic background sedimentation.	Hudajužna: 36.2; Davča 1: 2.3, 43.0, 75.0, 97.8; Davča 2: 0.7; Poče: 11, 24, 26; Zakoča 2: 17, 20.6; Koritnica: 12.0, 45.8, 80.8.
Bioclastic wackestone (Fig. 16f)	20% of grains, 80% of micritic matrix. Grains are well sorted, less than 0.5 mm in size. They comprise angular sparitic fragments of bioclasts.	Diluted gravity flow deposit (waning turbidite)?	Poče: 7.

Crinoid wackestone and packstone (Fig. 16g)	40% of grains, 40% of micritic matrix, 20% of syntaxial calcite cement. Grains are overall poorly sorted, but individual components show good sorting. Grains are matrix supported or are in point, rarely planar contacts. Grains: predominant are echinoderms predominate (30–35% of rock); subordinate are thin-shelled bivalves, fragments of brachiopods, lithoclasts (intraclasts?) of carbonate mudstone.	Diluted gravity flow deposit (waning turbidite)?	Poče: 8; Zakojca 2: 30; Koritnica: 83.7.
Peloid packstone (Fig. 16h)	50% of grains (peloids), 50% of recrystallized micritic matrix. Microfacies is very limited in extent, associated with carbonate mudstone. Peloids are very well sorted, rounded, in point contacts and elliptical in shape due to compaction. Fragments of thin-shelled bivalves and ostracods are rarely present.	Very diluted gravity flow deposit (waning turbidite)?	Poče: 2; Koritnica: 57.4.
Pelletal-bioclastic packstone	60% of grains (35% pellets, 15% bioclasts), 40% of micritic matrix, 10% of terrigenous grains. Poorly to moderately sorted. Locally weakly expressed parallel lamination indicated by a greater proportion of non-calcareous grains. Some samples are bioturbated. Bioclasts: dominantly thin-shelled bivalves; subordinate ostracods, radiolarians. Terrigenous grains: unequally distributed, angular; mostly feldspar, subordinate quartz, sericite. Cement: syntaxial rim.	Hemipelagic background sedimentat, mixed with allochthonous components; reworked by bioturbation and/or weak currents.	Hudajužna: 41.1; Poče: 9, 11; Koritnica: 39.5.
Bioclastic-intraclastic packstone (Fig. 17a)	60% of grains (50% bioclasts, 10% intraclasts), 5–35% micritic matrix, 5–35% calcite cement. Moderately sorted. Bioturbated, partly laminated. Bioclasts: dominant thin-shelled bivalves (concentrated in laminae, most fragmented), echinoderms; subordinate radiolarians, gastropods, foraminifera (<i>Nodosaria ordinata</i> Trifonova, <i>Endoteba</i> sp.). Intraclasts: carbonate mudstone, 0.06–1.5 mm in size; subrounded, moderately sorted. Cement: granular and syntaxial rim.	Hemipelagic background sedimentat, mixed with allochthonous components; reworked by bioturbation and/or weak currents.	Hudajužna: 7.3; Zakojca 2: 3, 8, 5.1; Koritnica: 86.6, 90.5.
Intraclastic-bioclastic packstone	75% of grains (50% intraclasts, 20% bioclasts, 5% terrigenous grains), 20% of micritic matrix, 5% of cement. Normal grading. Grain size 0.1–2 mm (dominant 0.2 mm), well sorted. Grains are in point, planar, rarely concavo-convex contacts. Elongated grains are oriented parallel to the bedding. Bioclasts: fragmented bivalves, echinoderms, foraminifera. Intraclasts are micritic, rounded. Terrigenous grains: subangular to subrounded; include quartz, feldspar, lithic grains (volcanics, chert). Cement: granular and syntaxial rim calcite cement.	Gravity flow deposit (turbidite?).	Koritnica: 16.5, 28.4, 51.4, 70.1.
Intraclastic-bioclastic grainstone (Fig. 17b, c)	50% of grains, 50% of carbonate cement. Grains are moderately sorted, of average size 0.4 mm. Intraclasts (carbonate mudstone, rarely peloidal grainstone) represent 30% of the rock. Bioclasts (echinoderms, foraminifera, bivalves) form 20% of the rock.	Gravity flow deposit (turbidite?).	Davča 1: 97.7; Zakojca 1: 7.9.
Bioclastic floatstone with bioclastic-intraclastic grainstone matrix (Fig. 17d)	50% of grains (40% of bioclasts, 10% of intraclasts), 50% of carbonate cement. Grains are poorly sorted, between 0.05 mm and 2 cm in size (the largest grain is a fragment of a solenoporacean algae, overgrown by a thin crust of microbialite). Average grain size is 0.75 mm. Larger grains are oriented parallel to bedding and elongated due to compaction. Bioclasts are dominated by sparitic particles (solenoporacean algae, but most are unrecognisable); echinoderms are rare.	Gravity flow deposit (turbidite?).	Poče: 6, 7.
Sandy mudstone (Fig. 17e)	Silt-sized grains predominate. Sand grains (up to 0.15 mm in size) represent app. 10% of the rock. They comprise quartz, feldspar, and opaque grains. Grains are somewhat rotated due to compaction; pseudo fluvial texture is visible. Some samples show parallel lamination.	Diluted gravity flow deposit.	Jesenica 2: 4; Poče: 2, 10, 14, 16, 21, 25, 27, 40, 43.
Fine-grained sandstone (Fig. 17f–h)	60–70% of grains, 25% of calcite cement, 5% of other cement, up to 20% of epimatrix. Locally interchanging in laminae with pebbly, sandy mudstone. Grains are 0.03–0.25 mm (mostly 0.07 mm) in size, angular to subrounded, isometric to elongated. They are in point, planar and concavo-convex contacts. Elongated grains are oriented parallel to the bedding. Grains: quartz, feldspar, lithic grains, biotite, heavy minerals (opaque minerals, zircon, rutile).	Gravity flow deposit.	Črni Vrh: 1, 1.3, 3, 4.5, 6, 8, 10; Davča 1: 85.5; Davča 2: 5.0; Jesenica 1: 2, 5, 6, 8; Novaki: 28.1, 40.0, 62.9; Poče: 2, 10, 14, 18, 21, 33, 37, 42; Zakojca 1: 5.4; Zakojca 2: 3.0; Koritnica: 26.6, 33.5, 41.1, 61.9, 69.0.

Medium-grained sandstone (Fig. 18a–c)	<p>40–70% grains (10–20% quartz, 10–30% feldspar, 20–45% lithic grains), 25–60% cement, 1–5% epimatrix.</p> <p>Homogeneous structure or parallel lamination, caused by the difference in grain sizes or concentration in accessory heavy minerals. Some samples are graded. Elongated grains are oriented parallel to the bedding. Grains are poorly to moderately sorted; grain size 0.04–2 mm (dominant size 0.3–0.5 mm). Grain shape isometric to elongated, angular to rounded. Grains are in point, planar, concavo-convex or stylolitic contacts, rarely matrix-supported. The least abraded grains belong to quartz, often present as subhedral crystals.</p> <p>Grains: dominant (in different order) are feldspar (plagioclase and alkali feldspars), lithic grains (rhyolite and granitoids; very rare micritic limestone), quartz (mostly monocrystals, some with embayment structures); accessory are heavy minerals (zircon, rutile, titanite, opaque minerals) and mica (biotite, muscovite).</p> <p>Some samples with notable presence of carbonate mudstone lithoclasts (intraclasts).</p> <p>Very rare are bioclasts (fragments of bivalves, echinoderms, very rare fragments of thick-shelled bivalves).</p> <p>Cement: calcite, dolomite and feldspar.</p>	Gravity flow deposit.	<p>Črni Vrh 4: 0.7, 0.8, 1.6, 2, 2.5, 5, 12; Hudajužna: 22.0, 23.8, 31.8, 44.6, 64.8; Davča 1: 1.0, 8.9, 12.5, 13.8, 19.6, 27.5, 35.1, 38.9, 95.8; Novaki 1: 1, 3, 18, 84.7; Poče: 17, 18, 19, 22, 34, 36, 41; Koritnica: 43.9, 48.6, 63.7.</p>
Coarse-grained sandstone (Fig. 18d)	<p>60–80% of grains, 5–20% of epimatrix, 5–40% of carbonate cement. The amount of epimatrix increases with grain compaction.</p> <p>Grains are 0.15–2.5 mm in size, although most are in the range between 0.45 mm and 0.79 mm. They are poorly sorted, subangular to angular, isometric to slightly elongated. Planar contacts prevail, while point, concavo-convex and stylolitic contacts are locally present.</p> <p>Grains: quartz (monocrystals, rarely polycrystalline), feldspar, lithic grains (volcanics, mudstone); subordinate are opaque minerals and bioclasts (echinoderms, thin-shelled bivalves).</p>	Gravity flow deposit.	<p>Jesenica 1: 1, 7, 9; Jesenica 2: 3/1, 3/2, 6; Novaki: 10.3, 11.5, 18, 18.2, 27.5; Poče: 38; Zakoča 2: 18; Koritnica: 18.7, 33.5, 59.4.</p>
Coarse-grained pebbly sandstone (Fig. 18e–f)	<p>50–80% of grains (5–20% quartz, 10–30% feldspar, 30–50% lithic grains), 20–50% of matrix.</p> <p>Locally interchanging in laminae with fine-grained sandstone. 5–30% of grains larger than 2 mm, 40% of sand-sized grains, 50% of grains smaller than 0.03 mm.</p> <p>Grains are 0.03–7 mm in size, very poorly sorted. Larger grains are angular to well rounded. Smaller grains are mostly subangular to subrounded. Grains are isometric, rarely elongated. Most grains are supported by matrix; some are in point, planar, concavo-convex or stylolitic contacts.</p> <p>Grains: quartz (monocrystals, most with undulating extinction, some with embayment structures), feldspar (plagioclase and alkali feldspars), lithic grains (acidic volcanic rocks, basic volcanic rocks, tuff, chert), accessory are zircon, opaque minerals, mica (biotite).</p> <p>Matrix mostly ortho- and pseudomatrix, along cracks and grains illite-sericite epimatrix showing pseudofluidal texture around grains. Epimatrix prevails in tectonically-stressed samples.</p>	Gravity flow deposit.	<p>Črni Vrh: 4, 4.5; Davča 1: 9.5, 85.5; Davča 2: 5.0; Novaki: 1.0, 6.3, 14.0, 21.5, 33.3, 51.6, 57.4, 60.7; Koritnica: 23.2, 24.6, 33.2, 61.5, 73.5, 76.1.</p>
Pebble breccia (lithoclastic rudstone) (Fig. 18g)	<p>50% of clasts, 50% of carbonate cement.</p> <p>Clasts are poorly sorted. Their average size is 4 mm. The smallest grains measure 0.2 mm, while the largest grains measure 12 mm in size. Clasts are subangular to rounded. They comprise (not in order) carbonate mudstone, peloid packstone, filament mudstone, intraclastic-bioclastic wackestone-packstone, bioclastic grainstone, peloid grainstone, microbial boundstone, oncoids, bivalve shells, echinoderms, coral fragment, rhyolite lithoclasts, idiomorphic crystals of feldspar, quartz grains, and chert lithoclast.</p>	Gravity flow deposit.	<p>Poče: 4; Jesenica 2: 2, 7, 12; Koritnica: 15.7b, 55.3.</p>
Cobble breccia/conglomerate (Fig. 18h)	<p>85% of grains larger than 2 mm, 8% of grains smaller than 2 mm, 7% of cement.</p> <p>Grains in concave-convex and stylolitic contacts. Grain size 0.5–15 cm, poorly sorted, angular to rounded, most subrounded, isometric to elongated in shape.</p> <p>Grains: dominantly limestone clasts (mostly bioclastic wackestone, followed by carbonate mudstone, pelletal-bioclastic packstone, and bioclastic-intraclastic packstone with rare ooids). Sand-sized grains are of the same composition. Bioclasts are presented by echinoderms.</p> <p>Selective silicification.</p>	Gravity flow deposit.	<p>Hudajužna: 6.8; Koritnica: 31.0.</p>

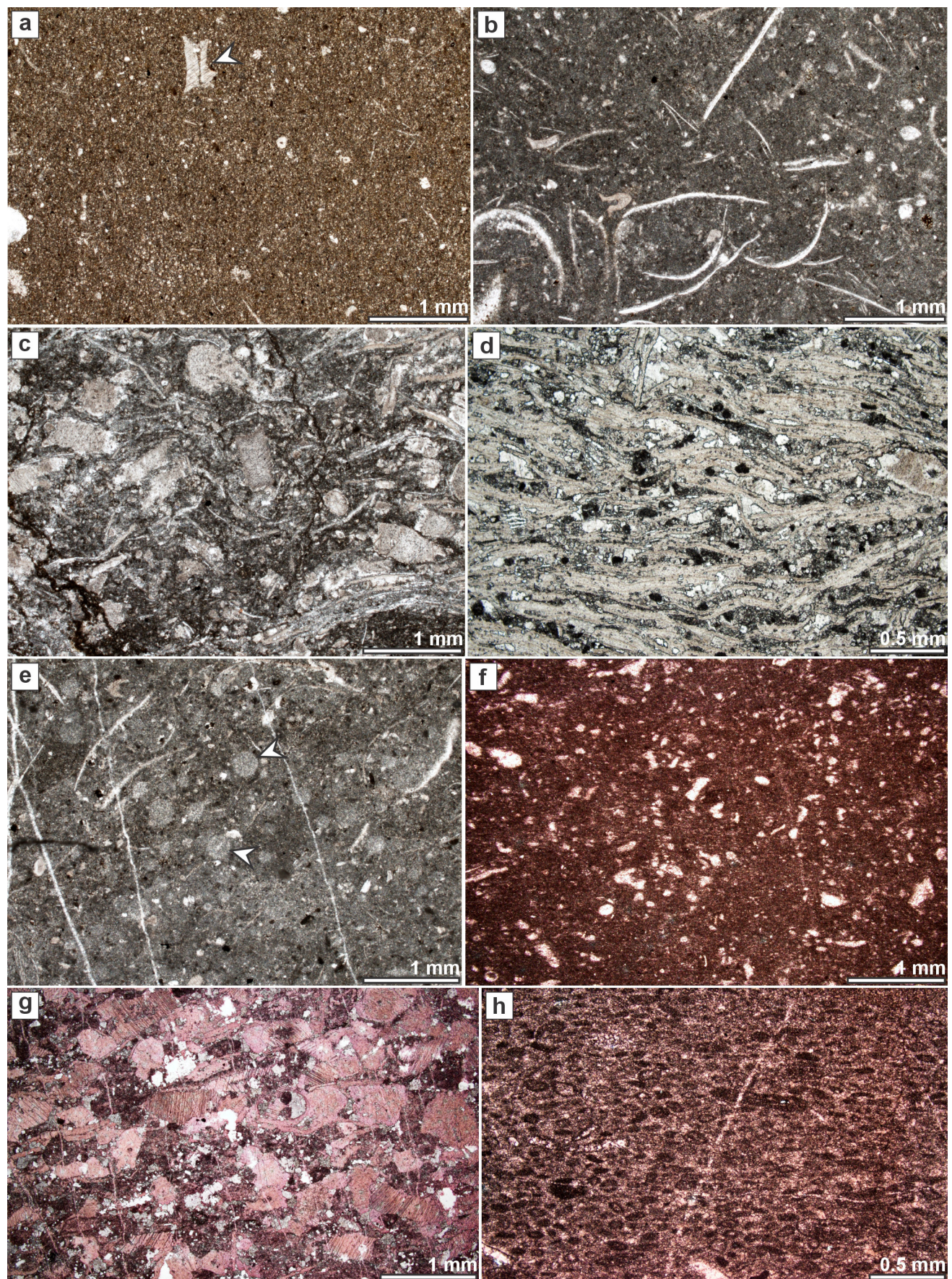


Fig. 16. Carbonate microfacies of the Ladinian – Carnian sedimentary succession of the Slovenian Basin (Pseudozilja and Amphiclina formations). **a:** Carbonate mudstone. Arrowhead points at the echinoderm. Sample Davča D1:23.3. **b:** Filament-echinoderm wackestone. Sample Hudajužna H19.5. **c:** Filament-echinoderm packstone. Sample Hudajužna H9.1. **d:** Filament packstone. Sample Zakojca ZK2:53. **e:** Radiolarian wackestone. Arrowheads point at calcified radiolarians. Note also the presence of filaments. Sample Hudajužna H36.2. **f:** Bioclastic wackestone. Sample Poče PO1:7. **g:** Crinoid packstone. Sample Zakojca ZK2:30. **h:** Peloid packstone. Sample Poče Po1:2.

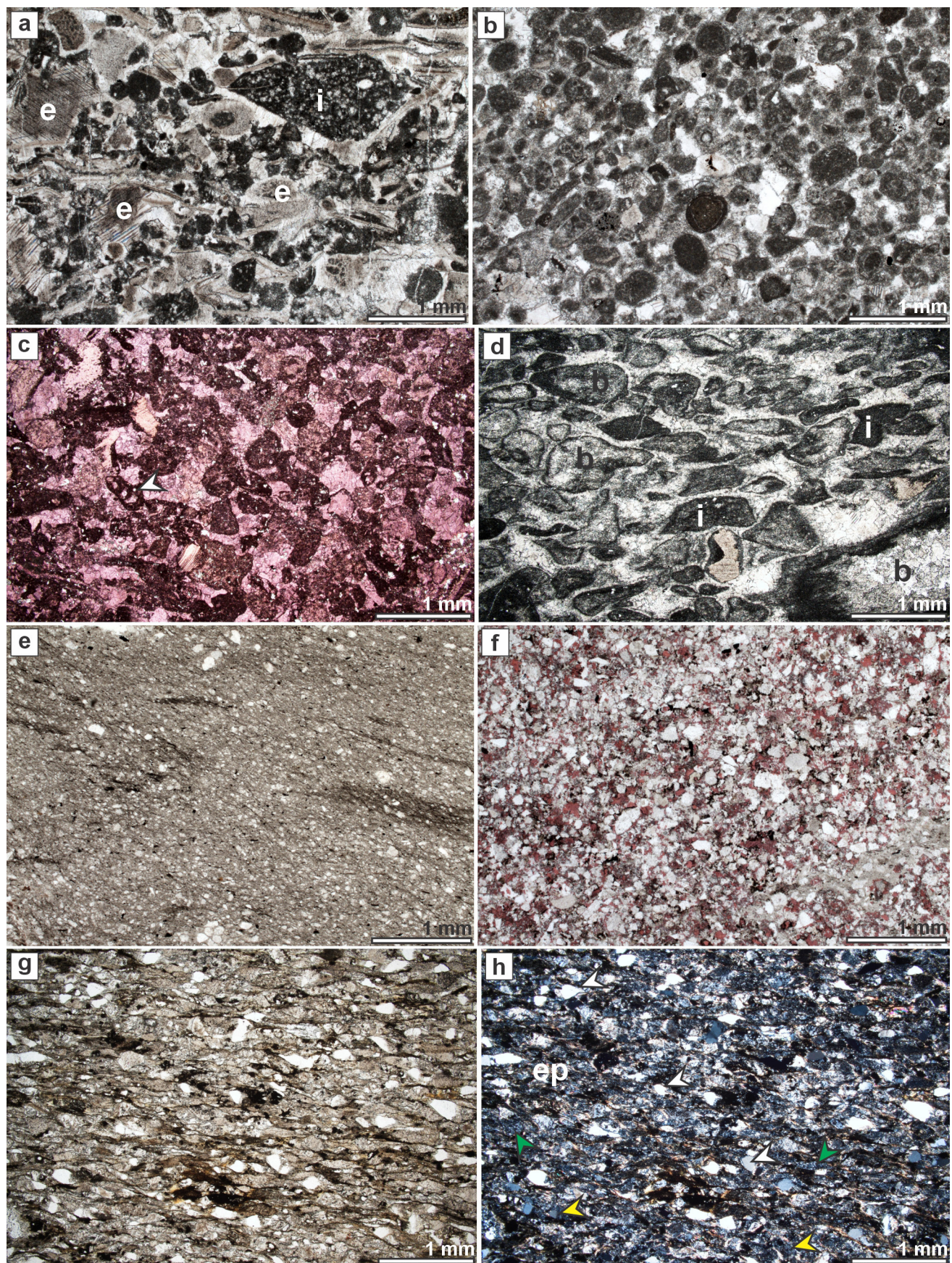


Fig. 17. Microfacies of the Ladinian – Carnian sedimentary succession of the Slovenian Basin (Pseudozilja and Amphiclina formations). **a:** Bioclastic-intraclastic packstone. Markings: e- echinoderm, i- intraclast. Sample Hudajužna H7.3. **b:** Intraclastic-bioclastic grainstone. Sample Davča D1:97.7. **c:** Intraclastic-bioclastic grainstone. Arrowhead points at the foraminifera. Sample Zakoječa ZK1:7.9. **d:** Bioclastic floatstone with bioclastic-intraclastic grainstone matrix. Markings: b- bioclast, i- intraclast. Sample Poče Po:1.6. **e:** Sandy mudstone. White grains belong to quartz and felsic volcanic rocks. Sample Davča D1:85.5. **f:** Fine-grained sandstone. Sample Davča D1:85.5. **g:** Fine-grained sandstone. Sample Črni Vrh CV1:6. **h:** Same sample, crossed Nichols. White arrowheads point at quartz, green arrowheads point at grains of felsic volcanic rocks, yellow arrowheads point at feldspar. Quartz-sericite matrix is marked with "ep".

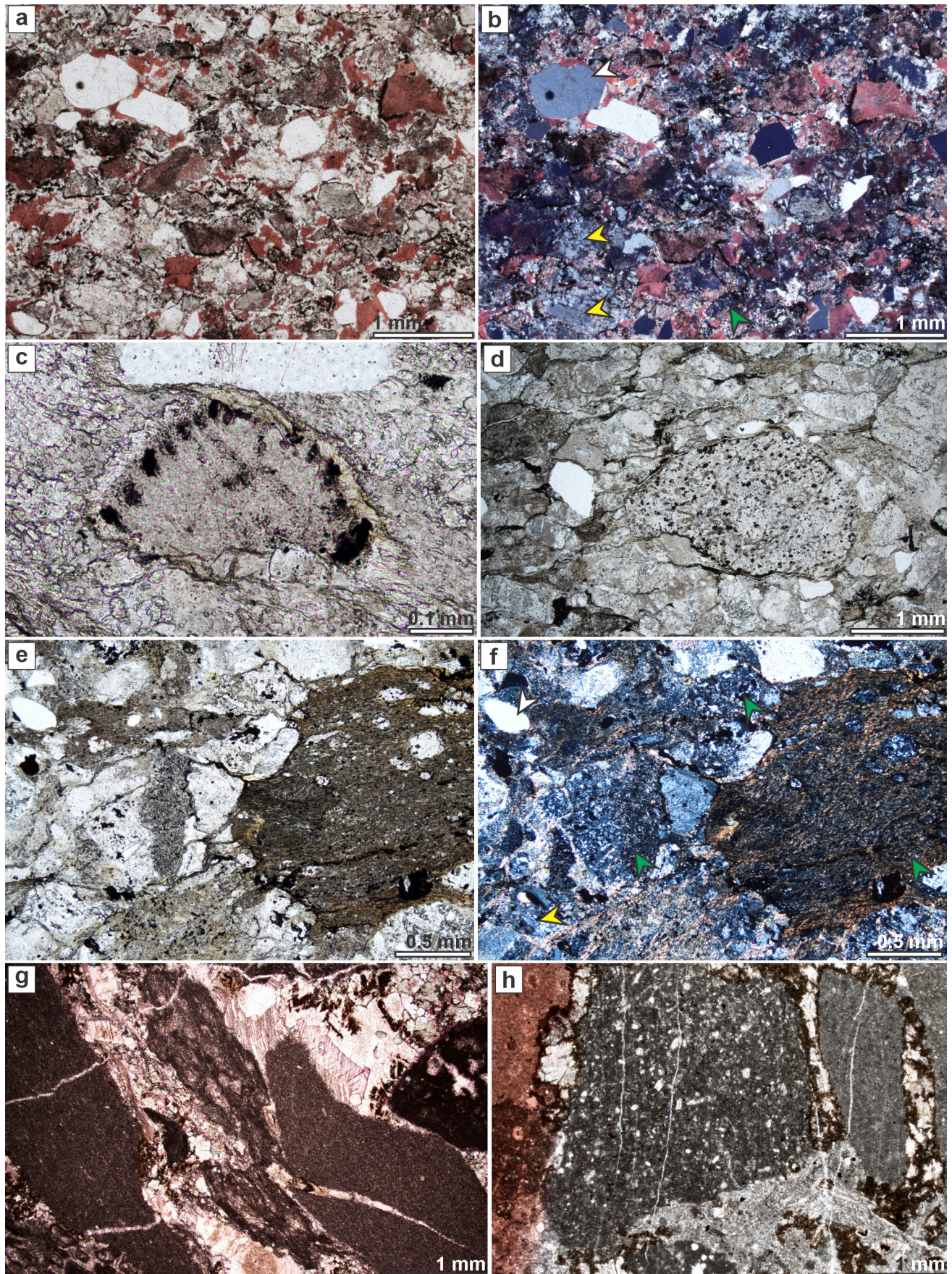


Fig. 18. Microfacies of the Ladinian – Carnian sedimentary succession of the Slovenian Basin (Pseudozilja and Amphiclinia formations). **a:** Medium-grained sandstone. Calcitization is revealed by staining. Sample Hudajužna H:64.8. **b:** Same sample, crossed Nichols. White arrowheads point at quartz, green arrowheads point at grains of felsic volcanic rocks, yellow arrowheads point at feldspar. **c:** *Lamelliconus ex gr. ventroplanus* (Oberhauser). Sample Novaki N1:18.0. **d:** Coarse-grained sandstone. The large grain in the middle belongs to volcanic rock. Sample Novaki N5:18.2. **e:** Coarse-grained pebbly sandstone. Sample Novaki N4:1.0. **f:** Same sample, crossed Nichols. White arrowheads point at quartz, green arrowheads point at grains of felsic volcanic rocks, yellow arrowheads point at feldspar. **g:** Pebby breccia (lithoclastic rudstone). Sample Poče Po1:4. **h:** Cobble breccia. Sample Hudajužna H6.8.

Discussion

One or two formations

For over 150 years, the volcano-sedimentary succession underlying the Bača dolomite formation has presented a considerable stratigraphic challenge. Based on the presence or absence of volcanics and tuff, respectively, some distinguished between the Ladinian Pseudozilja formation and the Carnian Amphiclina formation (Rakovec, 1950; Turnšek et al., 1982; Buser, 1986; Buser & Ogorelec, 1987), even though the early descriptions of both formations, based on observations from different geographic areas, do not mention volcanics or tuffs (Stur, 1858; Teller, 1885, 1889; Kossmat, 1901, 1907, 1910, 1913). Other authors suggest that the two represent the same formation (Kossmat, 1910, 1913; Čar et al., 1981; Ogorelec, 2011). The main volcanism in the eastern Southern Alps and the northern External Dinarides took place from the late Anisian to the early Ladinian (Gianolla et al., 1998; Kralj & Celarc, 2002; Dozet & Buser, 2009; Celarc et al., 2013; Smirčić et al., 2018; Gianolla et al., 2019; Kukoč et al., 2023; Oselj et al., 2023; Kukoč et al., 2024). However, reliably dated successions from the region show renewed volcanism in the late Ladinian and at the transition to the early Carnian (e.g. Jurkovšek, 1984; Kolar-Jurkovšek, 1991; Jelaska et al., 2003; Celarc, 2004, 2007; Kolar-Jurkovšek & Jurkovšek, 2019). Thus, the products of volcanism may indeed be limited to the upper Anisian – uppermost Ladinian/lowermost Carnian successions.

From the described sections, we summarize that the lithological compositions of the upper Pseudozilja and the Amphiclina formations (*sensu* Demšar, 2016) are virtually the same, comprising shale, siltstone, sandstone, bedded hemipelagic limestone, conglomerate, and breccia (including olistostromes) in varying proportions. Unfortunately, precise correlation between the sections is not possible due to the lack of biostratigraphic data. Although it would be expected from their position on the geological map that tuffs and/or volcanics would be present in the Črni Vrh (and maybe also in the Jesenica) sections this is not the case, even though the Črni Vrh section reaches 44 m in thickness. Volcanics and tuffs were recorded instead only in the Malenski Vrh section that belongs to the lower Pseudozilja formation. It must be emphasized, however, that the Malenski Vrh section is located in a different tectonic unit, in the Trnovo Nappe, which belongs to the External Dinarides. Thus, a question appears whether the tuffs and/or volcanics are common enough after the lower

Ladinian to be useful as a distinct feature for the entire Pseudozilja formation. Instead, it could be said that volcanics and tuffs may indicate that the observed succession is of the late Anisian – latest Ladinian age, but their absence is not enough to recognize the observed unit as the Amphiclina formation. More sections from the upper Pseudozilja formation should be logged in order to further substantiate this proposition.

Sedimentary environment

The depositional environment of the described volcano-sedimentary succession has mostly only been hinted at (e.g. Rakovec, 1950; Turnšek et al., 1982; Flügel & Ramovš, 1970; Ramovš, 2004). Flügel and Ramovš (1970) interpreted the sedimentation of muddy sediments in the aphotic zone of the sedimentary basin within low energetic water conditions, with interruptions of carbonate sedimentation. The sections from Zgornja Davča were already investigated by Babić and Zupanič (1978), who interpreted the limestone beds as autochthonous marine sediments, and the sandstone as sediment of turbidity currents in a relatively shallow basin. Ramovš (2004) suggested deposition of fine-grained conglomerate, sandstone, and shale from turbidite flows. Rakovec (1950), Čar et al. (1981), and Skaberne and Čar (1986) all envisioned deposition in the transitional zone between the shoreline and the shelf (Čar et al. 1981). An interpretation of the sedimentary environment will be given based largely on the logged sections, and later on, drawing from more regional aspects.

The only section enclosing the lowermost succession of the Pseudozilja formation (*sensu* Demšar, 2016) is the Malenski Vrh section, which is, as mentioned before, located in an entirely different tectonic position, in the Trnovo Nappe, which belongs to the External Dinarides. The succession of volcanic rocks followed by lithoclastic-crystalloclastic tuff with intercalations of diabase unconformably overlies the Lower Triassic oolitic limestone. The overlying, shale dominated succession with some larger sandstone lenses, interpreted as sand bars, indicates a relatively quiet shelf environment.

The other sections, representing the upper Pseudozilja formation (Črni Vrh 3–4), the upper Pseudozilja/the lower Amphiclina formation (Jesenica 1–2), and the lower Amphiclina formation (Novaki 1–4) have similar lithological compositions. Clastic sedimentary rocks prevail in all of these sections. The composition of conglomerate and sandstone is dominated by siliciclastic components, by fragments of volcanic rocks

and their tuffs, followed by quartz and feldspar grains. In the muddy conglomerates that are present only in sections Jesenica 1 and 2, pebbles of sandstone predominate, although some limestone pebbles were also found in the Jesenica 2 section. Sediments were partly transported by turbidity currents and debris flows, as indicated by sedimentary textures (normal grading for turbidites, matrix support for debris flow deposits), and partly as hemipelagic deposits. Small scour channels indicate a N–S direction of transport. The coarsening-upward sequence of the Jesenice 1 section corresponds to the progradation of submarine fan deposits, with lower fan, dominated by turbidite deposits passing upwards into middle and perhaps upper fan, dominated by debris-flow deposits (Walker & Mutti, 1973).

The somewhat larger number of sections (Davča 1–2, Poče, Zakojca 1–2, Orehek, Hudajužna, Koritnica) logging the upper Amphiclina formation (*sensu* Demšar, 2016) allows us to observe vertical and lateral differences in sediment composition and in sedimentation within roughly the same stratigraphic interval. The Davča sections are the most eastward lying of these sections. The lowermost sedimentary succession of the Divača 1 section indicates predominantly calcareous and subordinate muddy hemipelagic sedimentation, interrupted by turbidity currents transporting sandy siliciclastic material. The rest of the section is characterised by predominately siliciclastic, fining-upward, retrograding succession. It begins with slump/debris flow deposits followed by sandy deposits of proximal turbidites, passing into muddy hemipelagic deposits and distal turbidites. Limestone hemipelagic sediments prevail in the upper part of the section. The Davča 2 section is dominated by hemipelagic limestone. In the upper part of the section, the non-terrigenous siliceous component within the sediment increased and was later concentrated in chert nodules.

The Hudajužna section and the lower part of the Poče section are characterized by the longest lasting relatively quiet sedimentary conditions. The lower part of the Hudajužna section comprises mostly hemipelagic limestone, interrupted by higher energy currents, and depositing conglomerate with limestone clasts. The upper part of the Hudajužna section and lower part of the Poče section indicate prevailing muddy sedimentation, interchanging with hemipelagic limestone sedimentation with intercalations of siliciclastic sandy sediments deposited by (mostly distal) turbidity currents.

The Zakojca sections show quick lateral changes of sedimentary conditions. The Zakojca 1 section indicates relatively quiet, muddy and hemipelagic limestone sedimentation that was locally interrupted by distal turbidity currents. In contrast, the sedimentary successions in the Zakojca 2 section indicate energetic, highly variable, predominately high energy sedimentary conditions with debris flows and high- and low-density turbidity currents, interchanging with hemipelagic sedimentation. In the lower two-thirds of the section, hemipelagic limestone prevails, with some admixture of siliciclastic components in the upper part. The uppermost muddy breccia deposited from debris flow, has only noncarbonate clasts, mostly of sandstone and shale. Debris flow was followed by hemipelagic muddy sedimentation. The orientation of the erosional channels indicates transport in a N–S direction; the sediments were deposited on or near the continental slope.

The Orehek section includes the thickest part of the upper Amphiclina formation and is characterized by the most intensive slumping – debris flows. Syndepositional folds indicate transport from the NE. Massive blocks of limestone from this section are currently interpreted as *in-situ* mud mounds.

The Koritnica section is the westernmost section of the upper Amphiclina formation. Its heterogeneous composition indicates particularly versatile sedimentary conditions. The lower part of the succession is dominated by hemipelagic carbonate sedimentation, interrupted by slumps/debris flows, turbidity, and higher energy currents transporting calcareous and siliciclastic sediments. The middle part of the section shows the most dynamic sedimentary conditions and is dominated by slide, slump, debris flow, and turbidity current deposits. The slumps indicate N to S transport of the sediment. Subordinate to the mass-flow deposits are hemipelagic sediments. Sedimentation largely took place on a slope generally inclined towards the south.

To summarize, the upper Pseudozilja formation and the Amphiclina formation consist of hemipelagic deposits intercalated with sediment that was transported via slides, slumps, debris flows, and turbidity currents. Sedimentation mostly took place on or near the continental slope, generally inclined towards the south, and the transport was largely from north to south. Only olistostromes in the Orehek section indicate a more easterly direction of sedimentary transport.

It appears that sedimentary conditions became more uniform towards the end of the Carnian, when carbonate sedimentation completely prevails

over siliciclastics in all the sections. This could be due to the relative rise of the sea level, the shift of the coastline and/or change in the fluvial network, and the subsequent spreading of carbonate platforms (see Gianolla et al., 1998; Haas & Budai, 1999; Gawlick & Böhm, 2000; Gianolla et al., 2003; Berra et al., 2010).

Regional comparisons

The described volcano-sedimentary succession from the Slovenian Basin differs from contemporaneous volcano-sedimentary formations in the region in its pronounced thickness and in its higher shale content. Depending on the palaeogeographic position, the Pseudozilja/Amphiclina formations are succeeded either by the Bača dolomite formation in the late Carnian in the central part of the Slovenian Basin, or earlier (late Ladinian/early Carnian) by platform carbonates in the marginal parts of the basin (Šmuc & Čar, 2002).

According to Placer and Kolar-Jurkovšek (1990), the southernmost exposure of the Pseudozilja formation is the Zagorje area in the Posavje Hills. Considerable differences can be observed among individual sections further south, which structurally belong to the External Dinarides (see Dozet & Buser, 2009; Kolar-Jurkovšek & Jurkovšek, 2019; Oselj et al., 2023). Tuffs and volcanogenic sandstone usually occur in association with bedded limestone, dolostone, and marlstone (Buser, 1974; Jurkovšek, 1984; Dozet, 2006). A thick succession some hundreds of metres thick of Ladinian volcano-sedimentary succession from the Rute plateau in central-southern Slovenia was recently described by Kocjančič et al. (2022) and Rožič et al. (2024). This laterally highly variable succession consists of packages of tuff, volcanogenic sandstone, shale, marlstone, laminated limestone (calcimudstone), hemipelagic limestone, and resedimented limestones (calcarenite and limestone breccia).

In the Julian Alps and the Kamnik-Savinja Alps (Julian Nappes of the eastern Southern Alps), the volcano-sedimentary series occurs between Anisian platform limestone/dolostone (Contrin Formation) and Ladinian massive carbonates of the Schlern Formation (Jurkovšek, 1987; Celarc et al., 2013; Goričan et al., 2022; Gale et al., 2023). The most widespread unit, which can be considered the equivalent of the Buchenstein Formation from the western Julian Alps and the Dolomites (Celarc et al., 2013; Gale et al., 2023), consists of tuff, sandy claystone, marlstone, sandstone (some beds with plant fragments), and bedded limestone, with intercalations of volcanics and rarely volcan-

iclastic breccia (Ramovš, 1990). Limestone locally contains numerous involutinid foraminifers, small coral colonies, and bivalves (Ramovš, 1990; Gale et al., 2023). In the smaller half-grabens developed on top of the Contrin platform the Buchenstein Formation locally overlies pinkish nodular pelagic limestone of the Loibl (Ljubelj) Formation, and tuff and rhyolites and/or pinkish nodular limestone of the Vernar member, and the Uggowitz Breccia (Celarc et al., 2013; Gale et al., 2023). The cumulative thickness of the upper Anisian – lower Ladinian succession between the two platform units reaches up to a few tens of meters. Volcaniclastics also occur near the top of the Schlern Formation in the form of “pietra verde” tuffs associated with thin-bedded limestone with chert nodules and calcarenites, described as the Korošica Formation (Jurkovšek, 1984; Celarc, 2004, 2007).

Buchenstein-type facies is further present in many successions in Croatia and Bosnia and Herzegovina (Smirčić et al., 2018). Much thinner siliciclastic-dominant facies than in the Tolmin Nappe was documented in the Donje Pazarište section on the Velebit Mts. The series consists of 18 m of volcaniclastic (lithic) sandstone and shale, and 28 m of carbonate shale. Akin to sandstone from the herein described sections, sandstone from Donje Pazarište shows planar and cross lamination, and grading. The siliciclastic facies deposited via turbidity currents in a deepened basin, probably on a distal part of a submarine fan (Smirčić et al., 2020). The following lithologies consist of pyroclastic density-current facies, platy limestone with pyroclastics, limestone breccia, and slumped limestone with pyroclastics and chert (Smirčić et al., 2020).

Basinal deposits continue into the Carnian in the Southern Alps and the Internal Dinarides, whereas shallow water and terrestrial conditions prevail in the External Dinarides (Buser, 1989; Dozet, 2009; Gerčar et al., 2017). In the western Julian Alps, the Eastern and the Northern Dolomites, the Buchenstein Formation is followed by the Ladinian Zoppè Sandstone (arkosic turbiditic sandstone; slope fan), Aquatona Formation (pelagic limestone, tuff), Fernazza Formation (volcanics and volcaniclastics, chaotic breccia), the uppermost Ladinian Wengen Formation (volcanic-detritic sediments, gravity flow deposits), and the uppermost Ladinian - Carnian San Cassiano Formation (Gianolla et al., 1998; Neri et al., 2007; Mietto et al., 2020). The latter consists of alternating shale, marlstones, marly to pure micritic limestone, oolitic calcarenite, bioclastic and oncolytic calcarenite, and calcirudite. Volcaniclastic

sandstone is present in various proportions, depending on the paleotopography. Mixing of carbonate and siliciclastic grains is frequent. Sandstone layers show erosional bases, normal grading, and planar and cross lamination, indicating turbiditic transport with episodes of debris flow and slumping (Neri et al., 2007). In the proximity of the Cassian platform, the lower boundary of the San Cassiano Formation can be defined based on the lowest occurrence of oolitic calcarenites, whereas elsewhere the boundary with the Wenigen Formation may be difficult to decide (Neri et al., 2007). The lateral variability within the San Cassiano Formation, depending on the paleotopography, is consistent with the lateral variability observed among the sections studied herein. The San Cassiano Formation differs from the Carnian successions from the Slovenian Basin in greater proportion of calcarenites. In the Internal Dinarides, the upper Anisian shallow marine carbonates are locally overlain by breccia, tuffite and basalt, and/or the hemipelagic cherty limestone and distal turbiditic cherty limestone of the Kopaonik Formation (Schefer et al., 2010). Drowning of the platform took place in the late Anisian and onward up until the end of the early Ladinian. Sedimentation of the Kopaonik Formation lasted at least into the Norian (Schefer et al., 2010).

Finally, a notable terrigenous input characterises the upper Julian (Carnian) Tor Formation in the Julian Alps. The Tor Formation overlies peritidal carbonates and consists of siltstone, marly limestone and dolostone, micritic limestone, bivalve lumachellas, marlstone, and claystone (De Zanche et al., 2000; Gianolla et al., 2003; Gale et al., 2015). The siliciclastic input is thus notably younger and less pronounced than in the Tolmin Basin.

Conclusions

The Ladinian – Carnian volcano-sedimentary succession from the Slovenian Basin consists largely of shale, sandstone, and limestone (hemipelagic and gravity-flow deposits), with subordinate breccia/conglomerate. According to the present data, only the lower part of the Pseudozilja formation comprises lithologically distinct facies assemblage, with a substantial proportion of diabase and tuff. Despite previous suggestions by some authors, the lithological similarities between the upper part of the Pseudozilja formation and the Amphiclinia formation documented herein seem to preclude a distinction between the two formations. Based on the continuous presence of thin-shelled bivalves and radiolarians, the entire succession deposited in an open marine setting.

The common occurrence of carbonate gravity-flow deposits, debris breccias, slump and channel structures, suggests the succession deposited on or near continental slope. Channel directions and slump fold-axes suggest slope inclination towards the south and the prevailing transport direction from north to south. As the Ladinian – Carnian succession of the Slovenian Basin is dominated by shale, sandstone, and hemipelagic limestone, it is distinguished from deeper-marine successions of the same age in the Dinarides and in the Julian Nappes of the Southern Alps.

Acknowledgements

Fieldwork and laboratory work for this research were carried out in the scope of the research project “Sedimentological and geochemical research of the “Pseudozilja” and equivalent formations”. Finalization of the paper was made possible thanks to research core fundings No. P1-0011 and P1-0195 is co-funded by the Slovenian Research and Innovation Agency. We are thankful to the anonymous reviewers who carefully read the manuscript and provided constructive remarks.

References

- Babić, L. & Zupanić, J. 1978: Košmatovi »Železnikarski vapnenci i dolomiti« i »Zaliloški krovni škriljavci« upredgorju Julijskih Alpa: podaci o stratigrafiji, facijesu i paleografskom značenju. Geol. Vjesnik, 20: 21–42.
- Berra, F., Jadoul, F. & Anelli, A. 2010: Environmental control on the end of the Dolomia Principale/Hauptdolomit depositional system in the central Alps: Coupling sea-level and climate changes. Palaeogeogr., Palaeoclimatol., Palaeoecol., 290: 138–150. <https://doi.org/10.1016/j.palaeo.2009.06.037>
- Buser, S. 1974: Osnovna geološka karta SFRJ 1:100 000 list Tolmin. Geologija, 17/1: 493–496.
- Buser, S. 1986: Osnovna geološka karta SFRJ 1: 100 000. Tolmač listov Tolmin in Videm (Udine). Zvezni geološki zavod, Beograd: 103 p.
- Buser, S. 1987: Osnovna geološka karta SFRJ 1:100 000. List Tolmin in Videm (Udine). Zvezni geološki zavod, Beograd.
- Buser, S. 1989: Development of the Dinaric and the Julian carbonate platforms and of the intermediate Slovenian Basin (NW Yugoslavia). Boll. Soc. Geol. Ital., 40: 313–320.
- Buser, S. 1996: Geology of western Slovenia and its paleogeographic evolution. In: Drobne, K.,

- Goričan, Š. & Kotnik, B. (eds.): International workshop Postojna '96: The role of impact processes and biological evolution of planet Earth. Založba ZRC, Ljubljana: 111–123.
- Buser, S. & Krivic, K. 1979: Excursion M, Hudajužna in the Bača Vallex–Carnian stage. In: Drobne, K. (ed.): 16th European micropaleontological colloquium, Zagreb–Bled, Yugoslavia, 8th–16th September 1979. Croatian Geological Society & Slovenian Geological Society, Zagreb & Ljubljana: 229–232.
- Buser, S. & Ogorelec, S. 1987: Excursion II, Carnian Amphiclinia beds-Hudajužna. In: Evolution of the karstic carbonate platform, 5. June. Geological Survey, Ljubljana: 12–18.
- Buser, S., Kolar-Jurkovšek, T. & Jurkovšek, B. 2007: Triasni konodonti Slovenskega bazena. Geologija, 50/1: 19–28. <https://doi.org/10.5474/geologija.2007.002>
- Celarc, B. 2004: Problems of the “Cordevolian” Limestone and Dolomite in the Slovenian part of the Southern Alps. Geologija, 47/2: 139–149. <https://doi.org/10.5474/geologija.2004.011>
- Celarc, B. 2008: Carnian bauxite horizon on the Kopitov grič near Borovnica (Slovenia) - is there a “forgotten” stratigraphic gap in its footwall? Geologija, 51/2: 147–152. <https://doi.org/10.5474/geologija.2008.015>
- Celarc, B., Goričan, Š. & Kolar-Jurkovšek, T. 2013: Middle Triassic carbonate-platform break-up and formation of small-scale halfgrabens (Julian and Kamnik-Savinja Alps, Slovenia). Facies, 59: 583–610. <https://doi.org/10.1007/s10347-012-0326-0>
- Čar, J., Jež, J. & Milanič, B.: 2021: Structural setting at the contact of the Southern Alps and Dinarides in western Cerkljansko region (western Slovenia). Geologija, 64/2: 189–203. <https://doi.org/10.5474/geologija.2021.011>
- Čar, J., Skaberne, D., Ogorelec, B., Turnšek, D. & Placer, L. 1981: Sedimentological characteristic of Upper Triassic (Cordevolian) circular quiet water coral bioherm in Western Slovenia, Northwestern Yugoslavia. SEPM Spec. Publ., 3: 233–240.
- Demšar, M. 2016: Geological map of the Selca Valley: Explanatory book to the Geological map of the Selca Valley 1: 25.000. Geological Survey of Slovenia, Ljubljana: 72 p.
- De Zanche, V., Gianolla, P. & Roghi, G. 2000: Carnian stratigraphy in the Raibl/Cave del Predil area (Julian Alps, Italy). Eclogae Geol. Helv., 93: 331–347. <https://doi.org/10.5169/seals-168826>
- Di Capua, A., De Rosa, R., Kereszturi, G., Le Pera, E., Rosi, M. & Watt, S.F.L. 2022: Volcanically-derived deposits and sequences: a unified terminological scheme for application in modern and ancient environments. Geol. Soc. London, Spec. Publ., 520: 11–27. <https://doi.org/10.1144/SP520-2021-201>
- Dozeti, S. 2006: Ladinian beds in the Obla Gorica area, central Slovenia. RMZ – Mater. Geoenviron., 53: 367–383.
- Dozeti, S. & Buser, S. 2009: Triassic. In: Pleničar, M., Ogorelec, B. & Novak, M. (eds.): Geology of Slovenia. Geological Survey of Slovenia, Ljubljana: 161–214.
- Dunham, R.J. 1962: Classification of carbonate rocks according to depositional texture. In: Ham, W.E. (ed.): Classification of carbonate rocks. Amer. Ass. Petrol. Geol Mem., 108–121. <https://doi.org/10.1306/M1357>
- Flügel, H. & Ramovš, A. 1970: Zur Kenntnis der Amphiclinen Schichten Sloweniens. Geol. Vestnik, 23: 21–37.
- Gale, L. 2010: Microfacies analysis of the Upper Triassic (Norian) “Bača Dolomite”: early evolution of the western Slovenian Basin (eastern Southern Alps, western Slovenia). Geol. Carpathica, 61/4: 293–308. <https://doi.org/10.2478/v10096-010-0017-0>
- Gale, L. 2012: Biostratigrafija in sedimentologija norijsko-retijskih plasti zahodnega Slovenskega bazena, Južne Alpe, Slovenija. Doktorska disertacija. Univerza v Ljubljani, Naravoslovno-tehniška fakulteta, Ljubljana: 268 p.
- Gale, L., Celarc, B., Caggiati, M., Kolar-Jurkovšek, T., Jurkovšek, B. & Gianolla, P. 2015: Paleogeographic significance of Upper Triassic basinal succession of the Tamar Valley, northern Julian Alps (Slovenia). Geol. Carpathica, 66/4: 269–283. <https://doi.org/10.1515/geoca-2015-0025>
- Gale, L., Kadivec, K., Vrabec, M. & Celarc, B. 2023: Sediment infill of the Middle Triassic half-graben below Mt. Vernar in the Julian Alps, Slovenia. Geol. Croatica, 76: 1–12. <https://doi.org/10.4154/gc.2023.03>
- Gale, L., Novak, U., Kolar-Jurkovšek, T., Križnar, M. & Stare, F. 2017: Characterization of silicified fossil assemblage from upper Carnian Amphiclinia beds at Crngrob (central Slovenia). Geologija, 60/1: 61–75. <https://doi.org/10.5474/geologija.2017.005>
- Gale, L., Skaberne D., Peybernes, C., Martini, R., Čar, J. & Rožič, B. 2016: Carnian reefal blocks in the Slovenian Basin, eastern Southern Alps.

- Facies, 62: 1–15. <https://doi.org/10.1007/s10347-016-0474-8>
- Gawlick, H.-J. & Böhm, F. 2000: Sequence and isotope stratigraphy of Late Triassic distal periplatform limestones from the Northern Calcareous Alps (Kalberstein Quarry, Berchtesgaden Hallstatt Zone). *Int. J. Earth Sci. (Geol. Rund.)*, 89: 108–129. <https://doi.org/10.1007/s005310050320>
- Gerčar, D., Koceli, A., Založnik, A. & Rožič, B. 2017: Upper Carnian Clastites from the Lesno Brdo Area (Dinarides, Central Slovenia). *Geologija*, 60/2: 279–295. <https://doi.org/10.5474/geologija.2017.020>
- Gianolla, P., Caggiati, M. & Pecorari, M. 2019: Looking at the timing of Triassic magmatism in the Southern Alps. *Geo. Alp.*, 16: 65–68. <https://doi.org/10.1144/jgs2018-123>
- Gianolla P., De Zanche V. & Mietto P. 1998a: Triassic Sequence Stratigraphy in the Southern Alps. Definition of sequences and basin evolution. In: Graciansky, P.C. de, Hardenbol, J., Jacquin, T., Vail, P.R. & Ulmer-Scholle, D. (eds.): Mesozoic-Cenozoic Sequence Stratigraphy of European Basins: SEPM Spec. Publ., 60: 723–751.
- Gianolla, P., Ragazzi, E. & Roghi, G. 1998b: Upper Triassic amber from the Dolomites (Northern Italy). A paleoclimatic indicator? *Riv. Ital. Paleont. Strat.*, 104/3: 381–390. <https://doi.org/10.13130/2039-4942/5340>
- Gianolla, P., De Zanche, V. & Roghi, G. 2003: An Upper Tuvalian (Triassic) platform-basin system in the Julian Alps: the start-up of the Dolomia Principale (Southern Alps, Italy). *Facies*, 49: 125–150. <https://doi.org/10.1007/s10347-003-0029-7>
- Goričan, Š., Đaković, M., Baumgartner, P.-O., Gawlick, H.-J., Cifer, T., Djerić, N., Kocjančič, A., Kukoč D. & Mrdak, M. 2022: Mesozoic basins on the Adriatic continental margin – a cross-section through the Dinarides in Montenegro. *Folia Biol. Geol.*, 63/2: 85–150. <https://doi.org/10.3986/fbg0099>
- Grad, K. & Ferjančič, L. 1974: Osnovna geološka karta SFRJ 1:100 000. Tolmač lista Kranj L33-65. Zvezni geološki zavod, Beograd: 70 p.
- Haas, J. & Budai, T. 1999: Triassic sequence stratigraphy of the Transdanubian Range (Hungary). *Geol. Carpathica*, 50: 459–475.
- Jelaska, V. 2003: Carbonate Platforms of the External Dinarides. In: Jelaska, V., Gušić, I., Cvetko Tešović, B., Bucković, D., Benček, Đ., Fuček, L., Oštarić, N. & Korbar, N. (eds.): Initiation, Evolution and Disintegration of the Mesozoic Carbonate Platform, Central Dalmatia. Field Trip Guidebook, 22nd Meeting of Sedimentology, Opatija: 67–71.
- Jurkovšek, B. 1984: Langobardian beds with daonellas and posidonias in Slovenia. *Geologija*, 27: 41–95.
- Jurkovšek, B. 1987: Osnovna geološka karta SFRJ 1:100 000. Tolmač listov Beljak in Ponteba L33-51, L33-52. Zvezni geološki zavod, Beograd: 58 p.
- Kocjančič, A., Rožič, B., Gale, L., Vodnik, P., Kolar-Jurkovšek, T. & Celarc, B. 2022: Facies analysis of Ladinian and Carnian beds in the area of Rute Plateau (External Dinarides, central Slovenia). In: Rožič, B. & Žvab Rožič, P. (eds): 15th Emile Argand Conference on Alpine Geological Studies: 12–14 September 2022, Ljubljana, Slovenia: abstract book & fieldtrip guide. Faculty of Natural Sciences and Engineering, Department of Geology, Ljubljana: 37. <https://doi.org/10.5194/egusphere-alpshop2022-37>
- Kolar-Jurkovšek, T. 1982: Conodonts from Amphiolina beds and Baca dolomite. *Geologija*, 25: 167–188.
- Kolar-Jurkovšek, T. 1991: Microfauna of Middle and Upper Triassic in Slovenia and its biostratigraphic significance. *Geologija*, 33/1: 21–170. <https://doi.org/10.5474/geologija.1990.001>
- Kolar-Jurkovšek, T. & Jurkovšek, B. 2019: Conodonts of Slovenia. Geological Survey of Slovenia, Ljubljana: 259 p.
- Kossmat, F. 1901: Geologisches aus dem Bačathale im Küstenlande. *Verh. Geol R.-A.*, 4: 103–111.
- Kossmat, F. 1907: Geologie des wocheiner Tunnels und der südlichen Anschlusslinie. *Denkschr. der Kaiser. Akad. Wiss Math.- Naturwiss. Kl.*: 41–102.
- Kossmat, F. 1910: Erlauterung zur geologischen karte der im Reichsrat vertretenen Königreiche und Länder der Öster.- Unger. Monarchie, SW-Gruppe, Nr. 91. Bischofslack und Idria, Wien: 104 p.
- Kossmat, F. 1913: Die adriatische Umrandung in der alpinen Faltregion. *Mitt. Österr. Geol. Ges.*, 6: 61–165.
- Kralj, P. & Celarc, B. 2002: Shallow intrusive volcanic rocks on Mt. Raduha, Savinja-Kamnik Alps, Northern Slovenia. *Geologija*, 45/1: 247–253. <https://doi.org/10.5474/geologija.2002.018>
- Kukoč, D., Smirčić, D., Grgasović, T., Horvat, M., Belak, M., Japundžić, D., Kolar-Jurkovšek, T., Šegvić, B., Badurina, L., Vukovski, M. &

- Slovenec, D. 2023: Biostratigraphy and facies description of Middle Triassic rift-related volcano-sedimentary successions at the junction of the Southern Alps and the Dinarides (NW Croatia). *Int. J. Earth Sci.*, 112: 1175–1201.
- Kukoč, D., Slovenec, D., Šegvić, B., Vukovski, M., Belak, M., Grgasović, T., Horvat, M. & Smirčić, D. 2024: The early history of the Neotethys archived in the ophiolitic mélange of northwestern Croatia. *J. Geol. Soc.* <https://doi.org/10.1144/jgs2023-143>
- Lokier, S.W. & Junaibi, A. 2016: The petrographic description of carbonate facies: are we all speaking the same language? *Sedimentology*, 63: 1843–1885. <https://doi.org/10.1111/sed.12293>
- Mietto, P., Avanzini, M., Belvedere, M., Bernardi, M., Dall'Vecchia, F.M., O'orazi Porchetti, S., Gianolla, P. & Petti, F.M. 2020: Triassic tetrapod ichnofossils from Italy: the state of the art. *J. Mediterr. Earth Sci.*, 12: 83–134.
- Neri, C., Gianolla, P., Furlanis, S., Caputo, R. & Bosellini, A. 2007: *Carta Geologica d'Italia alla scala 1: 50.000, Foglio 29 Cortina d'Ampezzo, and Note illustrative*. APAT, Roma: 200 p.
- Ogorelec, B. 2011: Microfacies of Mesozoic Carbonate Rocks of Slovenia. *Geologija*, 54/2: 3–135. <https://doi.org/10.5474/geologija.2011.011>
- Oselj, K., Kolar-Jurkovšek, T., Jurkovšek, B. & Gale, L. 2023: Microfossils from Middle Triassic beds near Mišji Dol, central Slovenia. *Geologija*, 66/1: 107–124. <https://doi.org/10.5474/geologija.2023.004>
- Placer, L. 1999: Contribution to the macrotectonic subdivision of the border region between Southern Alps and External Dinarides. *Geologija*, 41/1: 223–255. <https://doi.org/10.5474/geologija.1998.013>
- Placer, L. 2008: Principles of the tectonic subdivision of Slovenia. *Geologija*, 51/2: 205–217. <https://doi.org/10.5474/geologija.2008.021>
- Placer, L. & Čar, J. 1977: The Middle Triassic Structure of the Idrija Region. *Geologija*, 20: 141–166.
- Placer, L. & Čar, J. 1998: Structure of Mt. Blegoš between the Inner and the Outer Dinarides. *Geologija*, 40/1: 305–323. <https://doi.org/10.5474/geologija.1997.016>
- Placer, L. & Kolar-Jurkovšek, T. 1990: O starosti psevdoziljskih skladov v vzhodnih Posavskih gubah. *Rudarsko metalurški zbornik*, 38: 529–534.
- Placer, L., Rajver, D., Trajanova, M., Ogorelec, B., Skaberne, D. & Mlakar, I. 2000: Borehole Ce-2/95 at Cerkno at the boundary between the Southern Alps and the External Dinarides (Slovenia). *Geologija*, 43/2: 251–266. <https://doi.org/10.5474/geologija.2000.020>
- Pristavec, M., Gale, L., Kolar-Jurkovšek, T. & Rožič, B. 2021: Sedimentološka analiza amfiklinskih plasti na Martinj vrhu pri Železnikih. In: Rožič, B. (ed.): 25th meeting of Slovenian geologists. University in Ljubljana, Faculty of Natural Sciences and Engineering, Ljubljana: 101–105.
- Rakovc, I. 1950: Pseudozilian strata in Slovenia (NW Yugoslavia). *Geogr. Vestnik*, 22: 1–24.
- Ramovš, A. 1970: Stratigrafski in tektonski problemi triasa v Sloveniji. *Geologija*, 13: 159–173.
- Ramovš, A. 1990: Razvoj ladinjske stopnje v severnih Julijskih Alpah. *Geologija*, 31: 241–266.
- Ramovš, A. 2004: Geološki razvoj Selške doline. Železne niti, 1: 17–51.
- Rožič, B., Kolar-Jurkovšek, T. & Šmuc, A. 2009: Late Triassic sedimentary evolution of Slovenian Basin (eastern Southern Alps): description and correlation of the Slatnik Formation. *Facies*, 55: 137–155. <https://doi.org/10.1007/S10347-008-0164-2>
- Rožič, B., Kocjančič, A., Gale, L., Zupančič, N., Popit, T., Vodnik, P., Kolar-Jurkovšek, T., Brajkovič, R. & Žvab Rožič, P. 2024: Architecture and sedimentary evolution of the Ladinian Kobilji curek basin (External Dinarides, central Slovenia). *Swiss J. Geosci.*, 117, 3. <https://doi.org/10.1186/s00015-023-00449-w>
- Schefer, S., Egli, D., Missoni, S., Bernoulli, D., Fügenschuh, B., Gawlick, H.-J., Jovanović, D., Krystyn, L., Lein, R., Schmid, S.M. & Sudar, M. 2010: Triassic metasediments in the internal Dinarides (Kopaonik area, southern Serbia): stratigraphy, paleogeographic and tectonic significance. *Geol. Carpathica*, 61: 89–109. <https://doi.org/10.2478/v10096-010-0003-6>
- Skaberne, D. & Čar, J. 1986: Sedimentological characteristics of “Pseudozilian” Formation in the Malenski vrh area, N from Poljane, W Slovenia. In: 5th Yugoslavian Meeting of Sedimentologists, Brioni. Croatian Geol. Soc., Zagreb: 57–60.
- Smirčić, D., Kolar-Jurkovšek, T., Aljinović, D., Barudžija, U., Jurkovšek, B. & Hrvatović, H. 2018: Stratigraphic definition and correlation of Middle Triassic volcanoclastic facies in the External Dinarides: Croatia and Bosnia and Herzegovina. *J. Earth Sci.*, 29: 864–878. <https://doi.org/10.1007/s12583-018-0789-1>

- Smirčić, D., Aljinović, D., Barudžija, U. & Kollar-Jurkovšek, T. 2020: Middle Triassic syn-tectonic sedimentation and volcanic influence in the central part of the External Dinarides, Croatia (Velebit Mts.). *Geol. Quarterly*, 64: 220–239. <https://doi.org/10.7306/gq.1528>
- Stur, D. 1858: Das Isonzo-Thal von Flitsch abwärts bis Görz, die Umgebungen von Wipptach, Adelsberg, Planina und die Wochein. *Geol. R.-A.*: 324–366.
- Šmuc, A. & Čar, J. 2002: Upper Ladinian to Lower Carnian sedimentary evolution in the Idrija-Cerkno region, western Slovenia. *Facies*, 46: 205–216. <https://doi.org/10.1007/BF02668081>
- Teller, F. 1885: Fossilführende Horizonte in der oberen Trias der Sannthaler Alpen. *Verh. Geol. R.-A.*, 355–361.
- Teller, F. 1889: Reise-Bericht. Zur Kenntniss der Tertiärablagerungen des Gebietes von Neuhau bei Cilli in Südsteiermark. *Verh. Geol. R.-A.*, 12: 234–246.
- Turnšek, D., Buser, S. & Ogorelec, B. 1982: Carnian coral-sponge reefs in the Amphiclina beds between Hudajužna and Zakriž (western Slovenia). *Razprave IV. razr. SAZU*, 24: 51–98.
- Vrabec, M. & Fodor, L. 2006: Late Cenozoic tectonics of Slovenia: structural styles at the North-eastern corner of the Adriatic microplate. In: Pinter, N., Grenerczy, G., Weber, J., Stein, S. & Medek, D. (eds.): *The Adria microplate: GPS geodesy, tectonics, and hazards*. Kluwer Academic Publishers: Dordrecht, The Netherlands: 151–168. https://doi.org/10.1007/1-4020-4235-3_10
- Walker, R.G. & Multi, E. 1973: Turbidite facies and facies associations. In: *Turbidites and deep water sedimentation*. Soc. Econ. Paleontol. Mineral. Pac. Sect., Short Course: 119–157.
- Winkler-Hermaden, A. 1936: Neuere Forschungsergebnisse über Schichtfloge und Bau der östlichen Südalpen. *Geol. Rundsch.*, 27: 156–195.
- Wright, V.P. 1992: A revised classification of limestones. *Sed. Geol.*, 76: 177–185. [https://doi.org/10.1016/0037-0738\(92\)90082-3](https://doi.org/10.1016/0037-0738(92)90082-3)



Isotopic composition of carbon ($\delta^{13}\text{C}$) and nitrogen ($\delta^{15}\text{N}$) of petrologically different Tertiary lignites and coals

Izotopska sestava ogljika ($\delta^{13}\text{C}$) in dušika ($\delta^{15}\text{N}$) petrološko različnih terciarnih lignitov in premogov

Tjaša KANDUČ^{1*} & Miloš MARKIČ²

¹Department of Environmental Sciences, Jožef Stefan Institute, Jamova cesta 39, SI–1000 Ljubljana, Slovenia;

*corresponding author: tjasa.kanduc@ijs.si

²Geological Survey of Slovenia, Dimičeva ulica 14, SI–1000 Ljubljana, Slovenia; e-mail: milos.markic@geo-zs.si

Prejeto / Received 9. 2. 2024; Sprejeto / Accepted 3. 5. 2024; Objavljeno na spletu / Published online 11. 6. 2024

Key words: lignite, coal, petrography, C and N isotopic composition, gelification, mineralization

Ključne besede: lignit, premog, petrografija, izotopska sestava C in N, gelifikacija, mineralizacija

Abstract

This study investigates the carbon ($\delta^{13}\text{C}_{\text{org}}$) and nitrogen ($\delta^{15}\text{N}$) isotopic composition of tertiary lignites and coals from six sedimentary basins: Velenje, Mura-Zala, and Zasavje in Slovenia; Sokolov in Czech Republic, Barito in Indonesia; and Istria in Croatia. The aim is to investigate the correlation between the fine detrital (fD) component and $\delta^{13}\text{C}$ and $\delta^{15}\text{N}$ in Velenje lignite samples. Additionally, we aim to evaluate the biogeochemical processes of organic substances during their deposition in all analyzed samples, calculate their $\delta^{13}\text{C}_{\text{CO}_2}$ values and compare the analyzed values of $\delta^{13}\text{C}$ and $\delta^{15}\text{N}$ to those reported in the literature. Thirty-two samples were analyzed, predominantly from the Velenje ortho-lignite (Pliocene), with additional lignites and coals from the Pannonian to Paleocene epochs for comparison. Carbon isotopic composition ($\delta^{13}\text{C}_{\text{org}}$) ranged from -27.9 to -23.6 ‰, and nitrogen isotopic composition ($\delta^{15}\text{N}$) ranged from 1.8 to 7.4 ‰. The fine-detrital lithotypes of the Velenje ortho-lignite exhibited the most negative $\delta^{13}\text{C}_{\text{org}}$ values due to anaerobic bacterial activity in an intramontane alkaline lake environment influenced by the carbonate hinterland. Moreover, gelification processes affected fine-detrital organic matter more than larger wooden pieces. Terbegovci, Hrastnik meta-lignites, and Barito sub-bituminous coal also displayed low $\delta^{13}\text{C}_{\text{org}}$ values, indicating limited gelification, while variations in the $\delta^{15}\text{N}$ values suggested differences in mineralization. The Velenje xylitic lithotypes have higher $\delta^{15}\text{N}$ values, indicating a more intense mineralization under aerobic conditions. Raša ortho-bituminous coal, deposited in a brackish environment, displayed the highest $\delta^{13}\text{C}_{\text{org}}$ values and a wide range of $\delta^{15}\text{N}$ values due to fluctuating water tables in a paralic carbonate platform environment. The lowest $\delta^{15}\text{N}$ value was observed in the Sokolov Basin lignite coal, indicating minimal mineralization and low bacterial activity. The isotopic composition of CO_2 in air ($\delta^{13}\text{C}_{\text{air}}$), which was calculated using the $\delta^{13}\text{C}$ values in lignites and coal, ranged from -8.4 to -3.4 ‰, with Velenje lignite displaying the minimum value and Raša coal showing the maximum value. The determined $\delta^{13}\text{C}$ and $\delta^{15}\text{N}$ values of the coal and lignite samples in this research fall within the typical range of world coals.

Izvleček

Ta raziskava proučuje izotopsko sestavo ogljika in dušika ($\delta^{13}\text{C}_{\text{org}}$ in $\delta^{15}\text{N}$) terciarnih lignitov in premogov iz šestih sedimentacijskih bazenov: Velenje, Mura-Zala in Zasavje v Sloveniji; Sokolov na Češkem; Barito v Indoneziji; in Istri na Hrvaškem. Cilj je iskati korelacijo med fino detritno (fD) komponento in $\delta^{13}\text{C}_{\text{org}}$, $\delta^{15}\text{N}$ v velenjskih lignitnih vzorcih ter oceniti biogeokemične procese organske snovi med odlaganjem v vseh analiziranih vzorcih, izračunati $\delta^{13}\text{C}_{\text{CO}_2}$ ter primerjati analizirane vrednosti $\delta^{13}\text{C}$ in $\delta^{15}\text{N}$ z objavljenimi literaturo. Analiziranih je bilo dvaintrideset vzorcev, večinoma iz Velenjskega orto-lignita (pliocen), za primerjava pa še ligniti in premogi od panonske do eocenske starosti. Izotopska sestava ogljika ($\delta^{13}\text{C}_{\text{org}}$) vseh vzorcev se je spremenjala od -27,9 do -23,6 ‰, in izotopska sestava dušika ($\delta^{15}\text{N}$) od 1,8 do 7,4 ‰. Fino-detritni litotipi Velenjskega orto-lignita so pokazali najbolj negativne vrednosti $\delta^{13}\text{C}_{\text{org}}$ zaradi anaerobne bakterijske aktivnosti v intramontanem alkalnem jezerskem okolju pod vplivom karbonatnega zaledja. Prosesi gelifikacije bolj vplivajo na drobno-detritno organsko snov kot na večje lesne ostanke. Meta-ligniti iz Terbegovcev in Hrastnika ter Barito sub-bituminozni premog so prav tako pokazali nizke vrednosti $\delta^{13}\text{C}_{\text{org}}$, kar kaže na omejeno gelifikacijo. Spremembe v $\delta^{15}\text{N}$ kažejo na razlike v mineralizaciji. Velenjski ksilititski litotipi so pokazali višjo $\delta^{15}\text{N}$, kar kaže na bolj intenzivno mineralizacijo v aerobnih pogojih. Raški orto-bitumenski premog, odložen v brakičnem okolju, je pokazal najvišjo $\delta^{13}\text{C}_{\text{org}}$ in širok razpon $\delta^{15}\text{N}$ vrednosti zaradi nihajočih vodnih nivojev v paraličnem karbonatnem platformnem okolju. Najnižja $\delta^{15}\text{N}$ je bila opažena v lignitnem premogu iz Sokolovskega bazena, kar kaže na minimalno mineralizacijo in nizko bakterijsko aktivnost. Izotopska sestava CO_2 v zraku ($\delta^{13}\text{C}_{\text{air}}$), ki je bila izračunana iz $\delta^{13}\text{C}$ v lignitih in premogih se je spremenjala od -8,4 do -3,4 ‰, pri čemer je velenjski lignit pokazal najnižjo vrednost, raški premog pa najvišjo. Določene vrednosti $\delta^{13}\text{C}$ in $\delta^{15}\text{N}$ vzorcev lignita in premoga v tej raziskavi padejo znotraj razpona svetovnih premogov.

Introduction

Coal, which accounts for 65 % of the world's total fossil fuel resources, is widely distributed globally and accounts for 40 % of global power generation (Shafiee & Topal, 2009; Hariana et al., 2021). Coal is a sedimentary rocks that has evolved from compressed vegetation, trapped between layers of rocks over millions of years and is combustible. Among geological materials, it is among the most intricate, composed of organic matter, elements (C, H, O, N, S), water, oil (CH), gases (mainly CH₄ and CO₂), and a variety of minerals (Rađenović, 2006). The initial phase of the coalification process (e.g. Diessel, 1992) involves the microbial degradation of plant ingredients into peat, occurring either aerobically or anaerobically. Subsequent changes in temperature with depth under overlying strata and pressure modify the physical and chemical characteristics of the sedimentary environment, during which the peat transforms into lignite and higher-ranking coals. Variations in geochemical conditions and the heterogeneity of plant tissues contribute to different coal types (Kirby et al., 2010), which comprise varying proportions of macerals (organic components) and inorganic minerals. The primary maceral groups are the huminite to vitrinite, exinite or liptinite, and inertinite groups (Stach et al., 1982; Diessel, 1992; Taylor et al., 1998; Speight, 2013; Flores & Moore, 2024).

Stable isotopes play a significant role in paleoclimate studies, as they are commonly used to track biogeochemical processes, including peatification and coalification processes (Hoefs, 1987).

It is known that photosynthesis leads to an enrichment of light isotopes, namely ¹²C and ¹⁴N, in plants (O'Leary, 1988). The typical value of $\delta^{13}\text{C}$ for C3 plants is approximately -27 ‰ (expressed relative to the Vienna PeeDee Belemnite, VPDB), while for C4 plants like *Zea mays*, $\delta^{13}\text{C}$ is around -14 ‰. The range of $\delta^{15}\text{N}$ in the biosphere varies from -10 ‰ to 10 ‰ (Peterson & Fry, 1987). The $\delta^{13}\text{C}$ values for most coals fall within the range of -29 to -20 ‰, aligning with that of modern C3 vegetation, i.e., -34 ‰ to -23 ‰ (Ding et al., 2019). However, during the early stages of organic matter diagenesis, isotopic fractionation occurs due to bacterial activity, leading to an enrichment in the heavier (¹³C and ¹⁵N) isotopes. Numerous studies have been conducted on the $\delta^{13}\text{C}$ and $\delta^{15}\text{N}$ values of the coal matrices in different sedimentary basins, and both $\delta^{13}\text{C}$ and $\delta^{15}\text{N}$ have been utilized to evaluate and understand the evolution of ecological environments. For example, $\delta^{15}\text{N}$ is employed to trace the sources of organic matter and the vege-

tation involved in peat formation and to assess the extent of bacterial activity during the peat-forming stage (Taylor et al., 1998), while $\delta^{13}\text{C}$ is used to trace air temperature, humidity, soil moisture, and precipitation rates (Bechtel et al., 2008; Xu et al., 2020; Li et al., 2022; Lin et al., 2022; Masood et al., 2022; Panda et al., 2022). Furthermore, $\delta^{13}\text{C}$ values can be used to estimate the $\delta^{13}\text{C}_{\text{air}}$ values of ancient atmospheres (Arens et al., 2000; Gröcke, 2002).

In the Velenje Basin, Pezdič et al. (1998) initiated the study of biogeochemical processes of various lithotypes (xylite, detrital lignite, fuzinite) of the ortho-lignite using $\delta^{13}\text{C}$ analysis. Subsequent research by (Kanduč et al., 2005; Kanduč et al., 2007; Kanduč et al., 2012) expanded on this work by investigating the Velenje ortho-lignite, as well as other coals such as meta-lignites from Kanižarica and Senovo, and plant tissues using both $\delta^{13}\text{C}$ and $\delta^{15}\text{N}$ tracers. These studies consistently revealed distinct $\delta^{13}\text{C}$ and $\delta^{15}\text{N}$ values among the different lignite lithotypes from the Velenje Basin, indicating variations in biochemical reactions during coalification, specifically gelification resulting in ¹²C enrichment and mineralization processes leading to ¹⁵N enrichment (Kanduč et al., 2005; Kanduč et al., 2012; Kanduč et al., 2018). Kanduč et al. (2018) also conducted a detailed investigation of authigenic mineralization associated with organic matter in lignite from the Velenje Basin, while Bangjun et al. (2019) focused on determining biomarkers in the Velenje lignite samples, which were first studied together with stable carbon isotope composition to interpret paleo-environmental conditions and early coalification processes (Bechtel et al., 2003). A similar study was performed on the Trbovlje (Zasavje) coal by Bechtel et al. (2004). The isotopic composition of sulphur ($\delta^{34}\text{S}$) and elemental composition of carbon and nitrogen in several Slovenian coals, including Velenje, Trbovlje, Senovo, and Kanižarica, were examined by Šturm et al. (2009), who observed variations between the coal seams and different coal types. These differences were attributed to SO₄²⁻ and Fe²⁺ availability and microbial activity.

The objective of the present study is to isotopically characterize ($\delta^{13}\text{C}_{\text{org}}$ and $\delta^{15}\text{N}$) samples of lignite and coals from six geological basins: Velenje, Mura-Zala, and Zasavje in Slovenia, Sokolov in Czechia, Barito in Indonesia, and Raša (Istria) in Croatia. The primary focus was to search for a correlation between the fine detrital (fD) component and their $\delta^{13}\text{C}$ and $\delta^{15}\text{N}$ values in Velenje lignite samples. Further, we determined the extent of bio-geochemical processes, such as gelification

and mineralization of organic matter. To achieve this, we compared our results with previously published isotopic data on lignites and coals and to the isotopic composition of recent plant samples to elucidate any discrepancies and highlight the degradation of organic matter during the coalification process. Additionally, we calculated $\delta^{13}\text{C}$ values in relation to atmospheric carbon dioxide ($\delta^{13}\text{C}_{\text{CO}_2}$) to determine potential differences in paleo-air among the studied coals.

Geological characteristics of sampling locations

Sampling locations from six coal-bearing sedimentary basins (Velenje, Mura-Zala, Zasavje, Sokolov, Barito, and Istria), with basic information on locality, coalification rank, and age are presented in Table 1 and Figure 1.

Knowing the geological characteristics and paleo-environment of the sampling locations in the separate basins is essential for interpreting the bio- and physicochemical coalification processes within different geological realms.

Table 1. Characteristics of studied lignites and coals.

Abbreviation of samples (and number of samples analyzed)	Lignite / Coal from a basin	Locality - seam	Coalification Rank	Age
VL (22)	Velenje (Slovenia)	Pesje – Velenje seam	Ortho-lignite	Pliocene
TL (2)	Mura-Zala (Slovenia)	Terbegovci lignite from a borehole.	Meta-lignite	Pannonian ("Pontian")
HC (1)	Zasavje (Slovenia)	Laško syncline Hrastnik seam Terežija field	Meta-lignite / sub-bituminous coal	Oligocene
JC (1)	Sokolov (Czechia)	Josef seam	Meta-lignite / sub-bituminous coal	Oligocene
BC (1)	Barito (Indonesia)	Barito seam	Sub-bituminous coal	Miocene
RC (5)	Istria (Croatia)	Raša – in-limestone seam	Ortho-bituminous coal	Paleocene

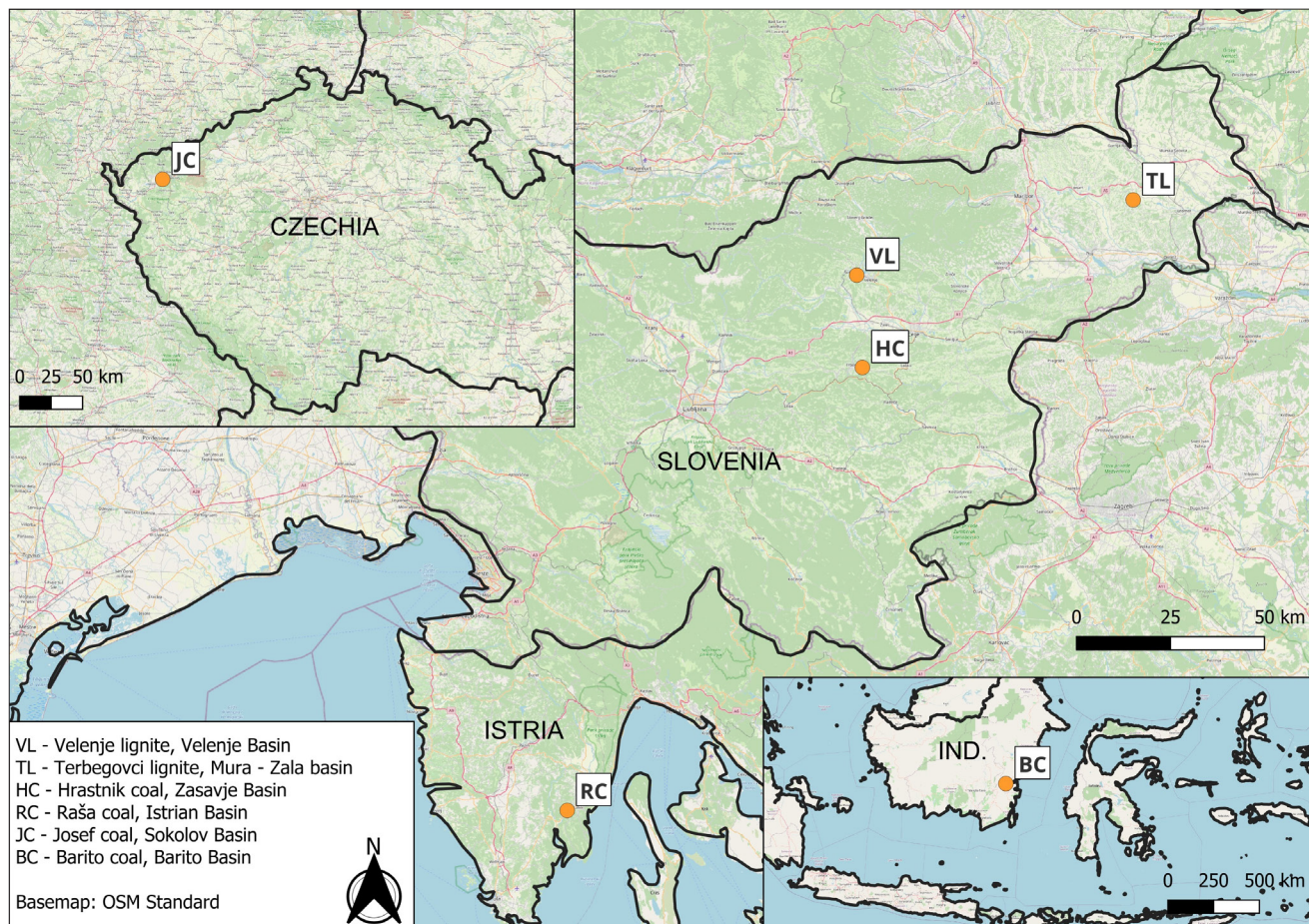


Fig. 1. Sampling locations from the six coal-bearing sedimentary basins in Slovenia, Czechia, Indonesia (Ind.) and Istria.

Velenje ortho-lignite (VL), Velenje basin, N Slovenia

The Velenje lignite-bearing basin is a typical intramontane freshwater lacustrine basin formed as a pull-apart basin (Vrabec, 1999) during the Pliocene to Quaternary times. It was created by polyphase dextral strike-slip fault tectonics be-

tween the Smrekovec and Šoštanj faults (Fig. 2). The basin contains a sequence of clastic sediments that can reach up to 1000 meters in thickness and host a single lignite seam that is exceptionally thick, measuring extremely, up to 165 meters (Brezigar, 1985).

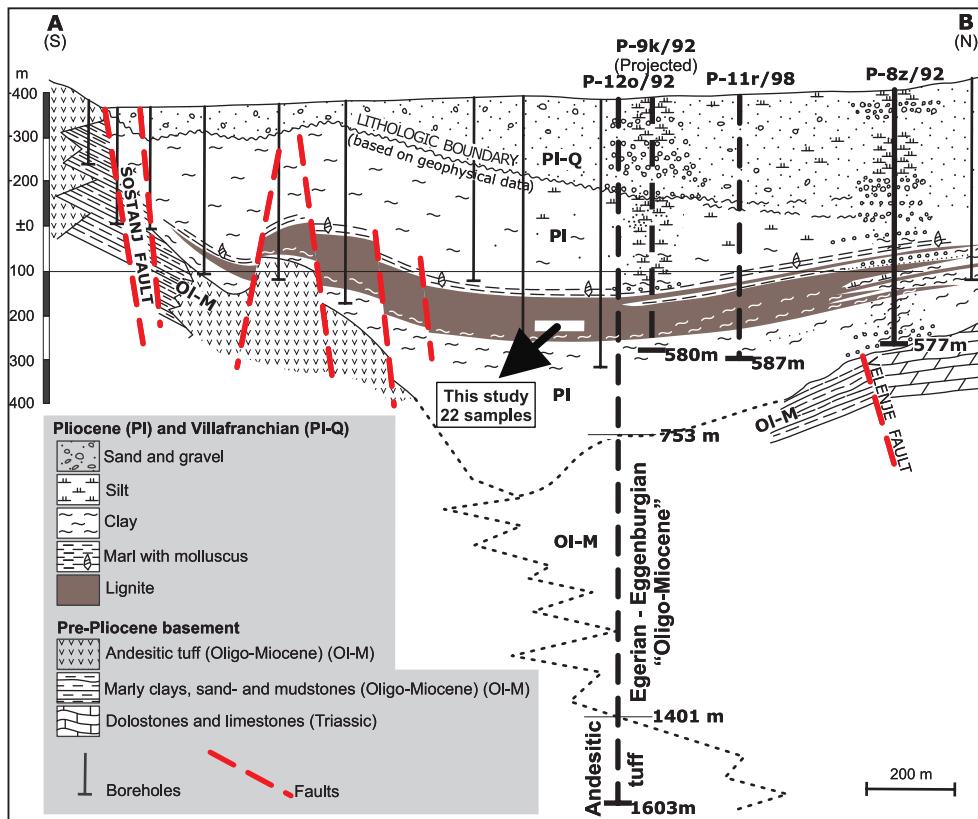
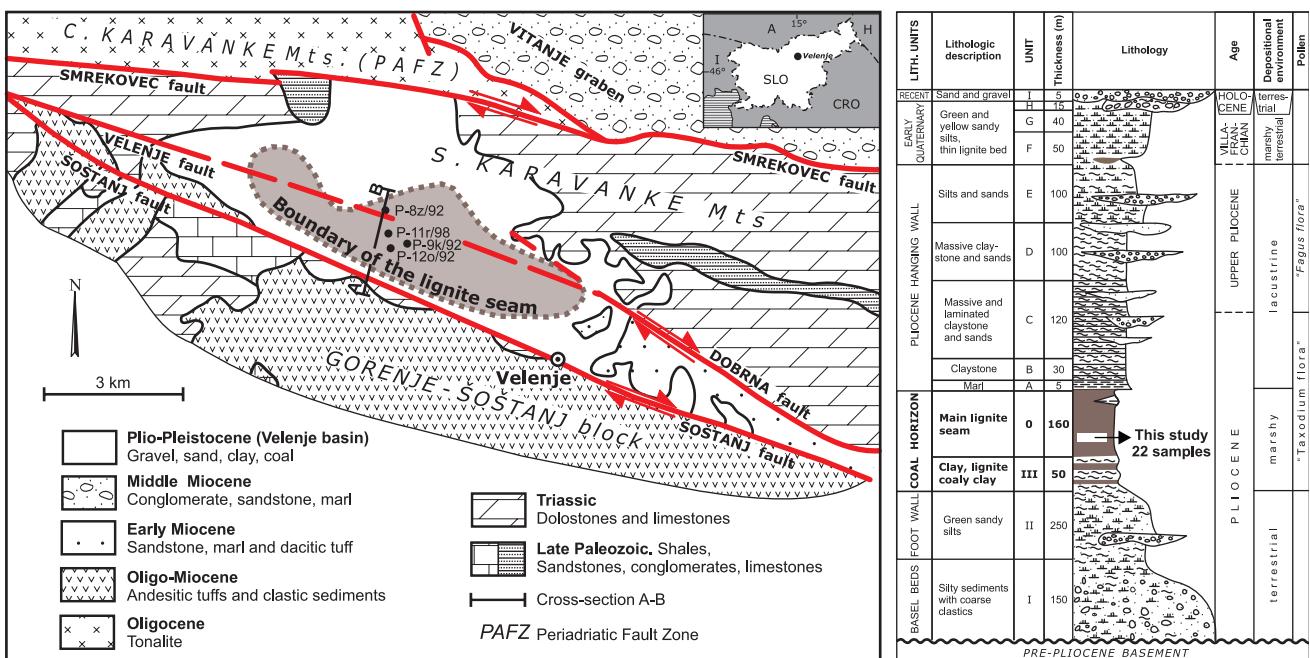


Fig. 2. The Velenje lignite basin: geological map (upper left), lithologic column (upper right), and cross-section (bottom) (Brezigar, 1985).

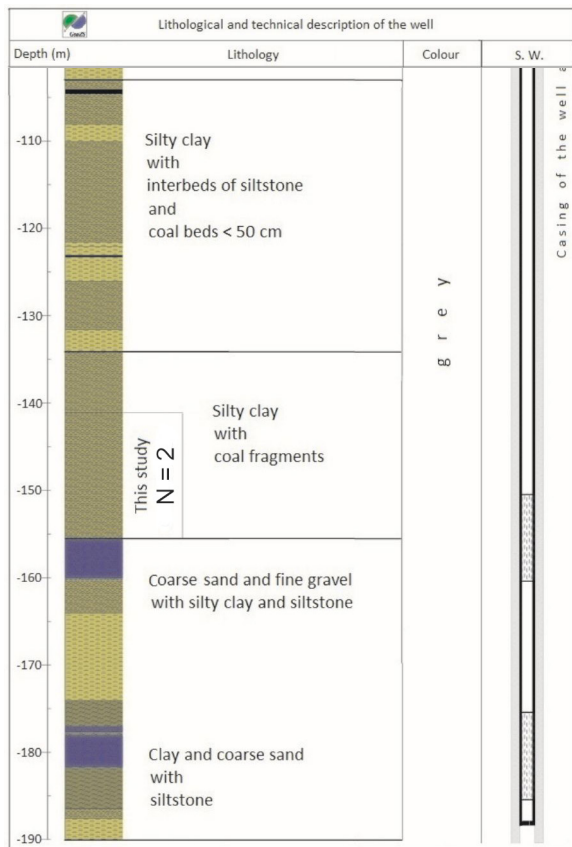


Fig. 3. Lithologic column of TER-1/03 well. The sampled coal material is from a depth interval of 141.0–155.5 m; N = number of samples; the whole column is given in Markič & Brenčič (2014).

According to the literature data, the average calorific value of the lignite, on an as-received basis (based on core data), is 10.7 MJ/kg, with a moisture content of 33.5 % and an ash content of 18.0 % (RCMWRA, 2002; Veber & Dervarič, 2004; Papež, 2019). The sulfur content, on a dry basis (db), varies from around 1.0 % to 5.5 %, with the latter being mainly detected where the lignite seam is close to the carbonate bedrock (Markič & Sachsenhofer, 2010). The Velenje lignite is classified as a typical ortho-lignite in terms of coalification rank, characterized by approximately 45 % bed moisture (ash-free basis), 62.7–66.4 % carbon content (dry, ash-free basis), 58.3–57.7 % volatile matter (dry, ash-free basis), and the gross calorific value (GCV) ranging from 12.23 to 15.25 MJ/kg (bed moist, ash-free basis) (Markič & Sachsenhofer, 2010). The reflectance (R_m %) of huminite (ulminite B) varies from 0.34 to 0.41 %, suggesting that this lignite can be classified as a meta-lignite. However, this range can also result from optical effects, such as subtle oxidation caused by pronounced aerobic bacterial and fungal activity during peatification and early coalification (Markič & Sachsenhofer, 2010).

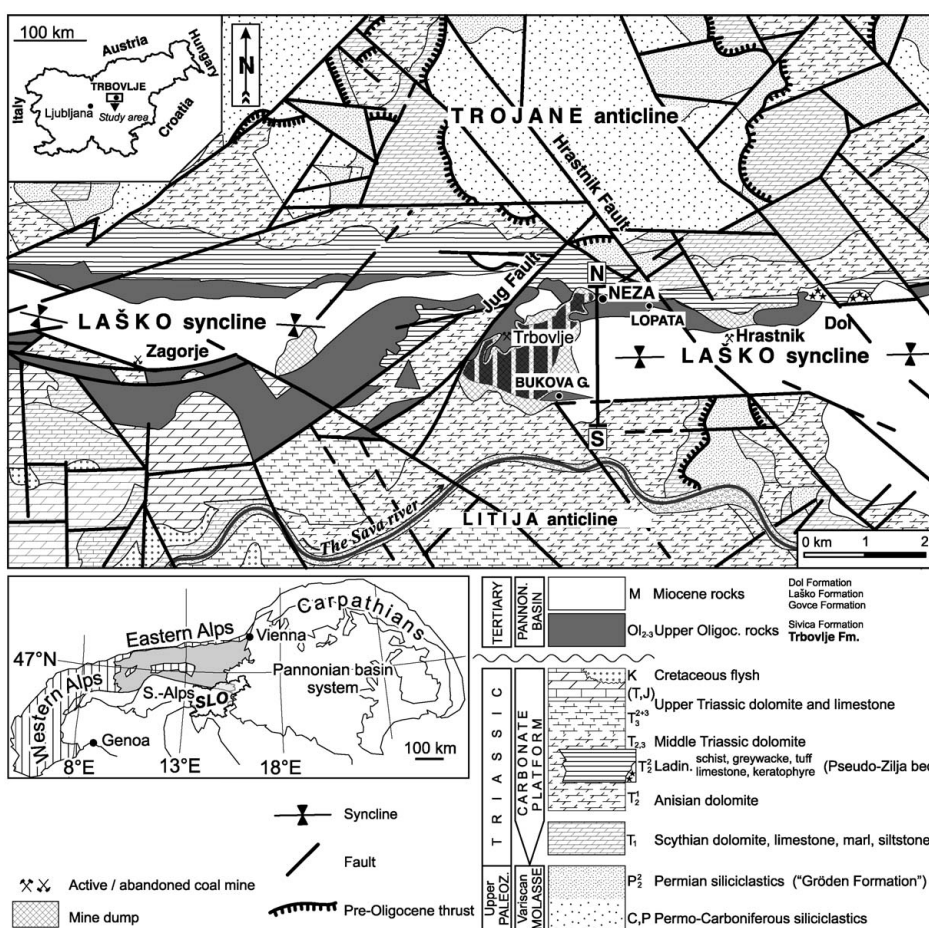


Fig. 4. Geological map of the Zasavje Basin – Laško Syncline (adapted from Buser, 1978 and Premru, 1983, taken from Bechtel et al. (2004)). Notable is the Hrastnik coal mine in the central-eastern part of the map.

Terbegovci lignite (TL), Mura–Zala Basin, NE Slovenia

Based on the gross calorific value on a dry, ash-free basis (GCV_{dab}) of 28.137 MJ/kg, the coal material was classified as a humic high-grade meta-lignite, similar in rank to the meta-lignites in the Mura Formation formed during the late Pannonian (Markič et al., 2011).

Hrastnik coal (HC), Zasavje Basin, Central Slovenia

The E-W trending Laško syncline (Fig. 4) of the Zasavje Basin is about 40 km long and up to 3 km wide, bounded by the Trojane and Litija anticlines to the north and the south, respectively (Kuščer, 1967; Buser, 1978; Premru, 1983; Placer, 1998 and references therein). The lithologies and formations

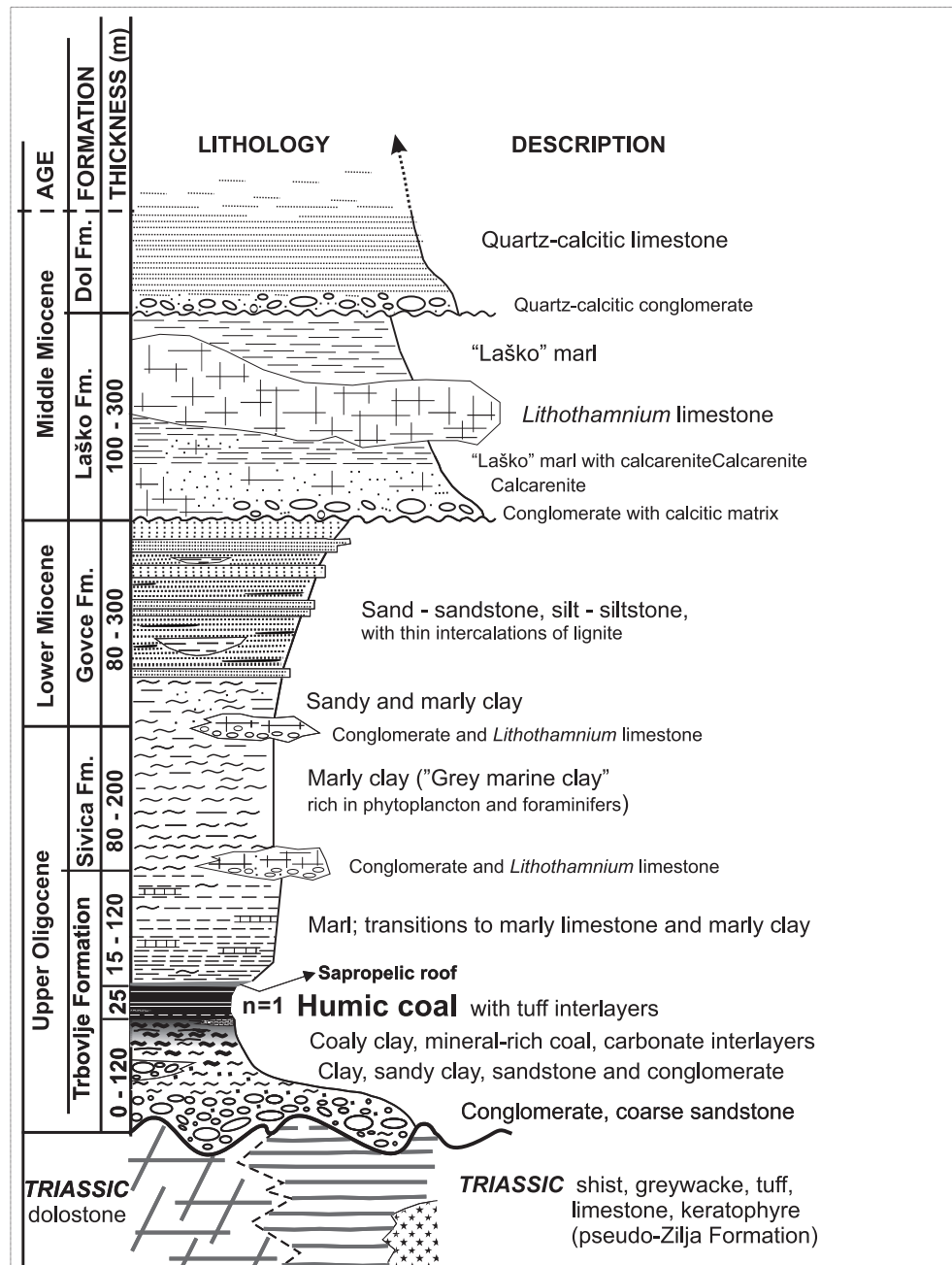


Fig. 5. Above: Schematic lithologic column of Tertiary strata in the Zasavje basin – Laško Syncline (modified after Kuščer, 1967). Below left: Zasavje humic coal with an andesitic tuff interlayer (7 cm thick). Below middle: sapropelic coal. Below right: sapropelic coal with sub-millimetre fragments of lake molluscs ("white dots"). The sample was taken from the humic coal seam.



above the coal seam are shown in the lithologic column in Figure 5.

The average coal grade and calorific value (as received basis) for the k. 34 Terezija polje (Hrastnik), from which the sample was taken, are as follows: coal moisture 19.7 %, ash yield 33.1 %, S content 4.2 %, and the net calorific value 12.8 MJ/kg (RTH d.o.o., 2013). Using the formula in (Thomas, 1992, p.30), the gross calorific value at the dry, ash-free basis (GCVdafb) is 30.2 MJ/kg, ranks the Hrastnik coal into the sub-bituminous coalification rank. This rank is generally consistent with the rank determined by vitrinite reflectance of 0.5 % R_m, as reported in Bechtel et al. (2004) for the Zasavje-Trbovlje seam.

Josef coal (JC), Sokolov Basin, W Czechia

Lignites from Czechia are thoroughly described in Pešek (2014). The Nove Sedlo Formation is composed of effusive and volcanoclastic rocks, marking the first significant stage of the extension of the Sokolov Basin associated with intense tectonic movements and volcanic activity. The lower part hosts the Josef coal seam, from which the sample was taken (Fig. 6). Its moisture content (as received basis) ranges between 28 and 43 %, the ash content (dry basis) between 2.6 and 27.3 %, and the sulphur content (dry basis) between 0.5 and 11.8 % (Rojík et al., 2014). Its gross calorific value (dry, ash-free basis) is between 29.1 and 31.5 MJ/kg, and its reflectance (R_m %) ranges from 0.3 to 0.45 %. The coal is ranked as a metalignite to sub-bituminous coal (Rojík et al., 2014; p. 134).

Barito coal (BC), Barito Basin, Indonesia

The Barito Basin is located in South Kalimantan (Fig. 1). It is one of the main geological basins in the region, containing abundant coal resourc-

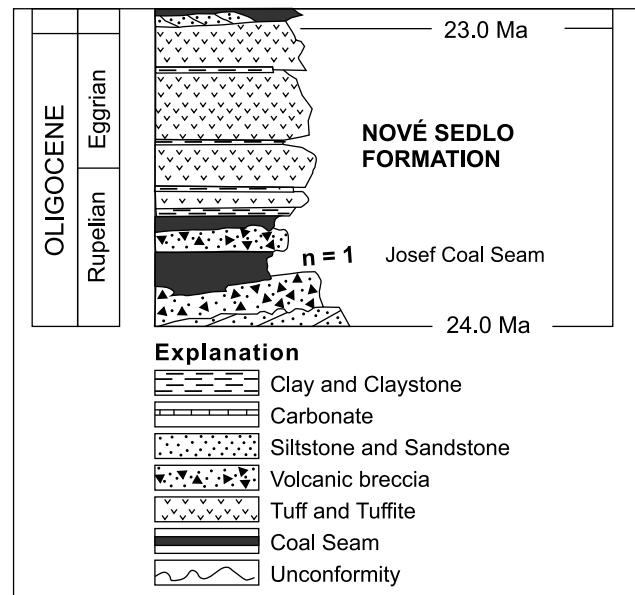


Fig. 6. Stratigraphic scheme of the Upper Oligocene of the Sokolov Basin fill, (after Rojík et al., 2014); n = number of samples taken from the Josef Coal Seam. (The Stare Sedlo Fm below the Nove Sedlo Fm is not shown).

es and reserves. Within the basin, the Warukin Formation is among those where coal is present (Fig. 7). The rocks in the Warukin Formation primarily comprise sandstones and claystones with coal deposits (Supandi & Hartono, 2020).

The coal imported from Indonesia to Slovenia is excavated in the open-cast Pasir Mine, Indonesia's third largest single mine, operated by the Kideco Jaya Agung Company. The geology of the Pasir Mine is summarized here from the work of Choi et al. (2013) and Supandi and Hartono (2020). The Barito Basin coal from the Pasir Mine is known for its low sulphur content (<0.2 %) and is considered an environmentally friendly coal-energy source due to an ash content of <5 %. The Barito coal in

PERIOD		FORMATION	THICKNESS	LITHOLOGY	DESCRIPTION
PLIOCENE	DAHOR		750 m	siltst. sandst. clayst. siltst.	Quartz sandstone with low strength and intersection with claystone and siltstone
MIOCENE	A T B	WARUKIN	250 - 750 m	coal clayst. coal siltst. sandst. clayst.	Sandstone with high strength and intersection with claystone and coal n=1

Fig. 7. Regional stratigraphic column of the Barito Basin showing the coal seams in the Warukin Formation (modified after Supandi & Hartono, 2020); n = number of samples taken.

Southern Kalimantan occurs in several widely developed beds up to 10 m thick and is sub-bituminous (Thomas, 1992; Internet 2).

Raša Coal (RC), Istrian Basin, Croatia

The Istrian coal mines in the eastern part of the Istrian Peninsula in Croatia's Northern Adriatic Sea region (Fig. 1) held the largest economically viable anthracite coal deposits in Croatia from the 18th century until 1999. One distinctive characteristic of the Raša coal is its high organic sulfur content, reaching up to 14 % (Medunić et al., 2016). During the initial phase of coalification, known as humification, organic sulphur compounds are generated as plant debris decomposes due to bacterial activity. Hamrla (1960) determined that the Raša coals were formed under anaerobic conditions. The substantial organic sulphur content in these coals is attributed to the bacterial reduction of marine sulphates, which became incorporated into the organic matrix (Medunić et al., 2016).

Raša coal is classified as an ortho-bituminous coal (Table 1) with a gross calorific value (dry, ash-free basis) of 34.3 MJ/kg and a vitrinite reflectance (R_r %) of 0.64 (Hamrla, 1959; Hamrla, 1985).

Sampling and methods

Thirty-two lignite and coal samples from six diverse sedimentary basins were collected for this study (Fig. 1). Detailed data, e.g., coordinates of origin with mine sampling locations and sampling date, are presented in the data repository (Kanduč et al., 2023). The coal samples were obtained from various locations, including underground mining areas (Velenje lignite – VL, Hrastnik coal – HC, Raša coal – RC), open-pit mines (Josef coal – JC), and boreholes (Terbegovci lignite – TL).

Twenty-two samples (Table 1) of the ortho-lignite from Velenje were collected during the macro-petrographic logging of three nearly horizontal boreholes from the Pesje and Preloge excavation fields: JPK-52 (+2°) (excavation field B-65/A, Pesje), JGM-55 (+10°) (excavation field B K. -130 Preloge, south wing), and JPK-60 (+10°) (excavation field F K.-65 Pesje). All these cores were collected in the southern central and lower part of the lignite seam (Fig. 2). The boreholes passed through intervals with different lithotype compositions, which have a more significant influence on the isotopic composition than with seam depth (Kanduč et al., 2005; Markič & Sachsenhofer, 2010). The Terbegovci meta-lignite samples (TL) were taken from a depth of 141.0–155.5 m as a composite sample of coal cuttings during

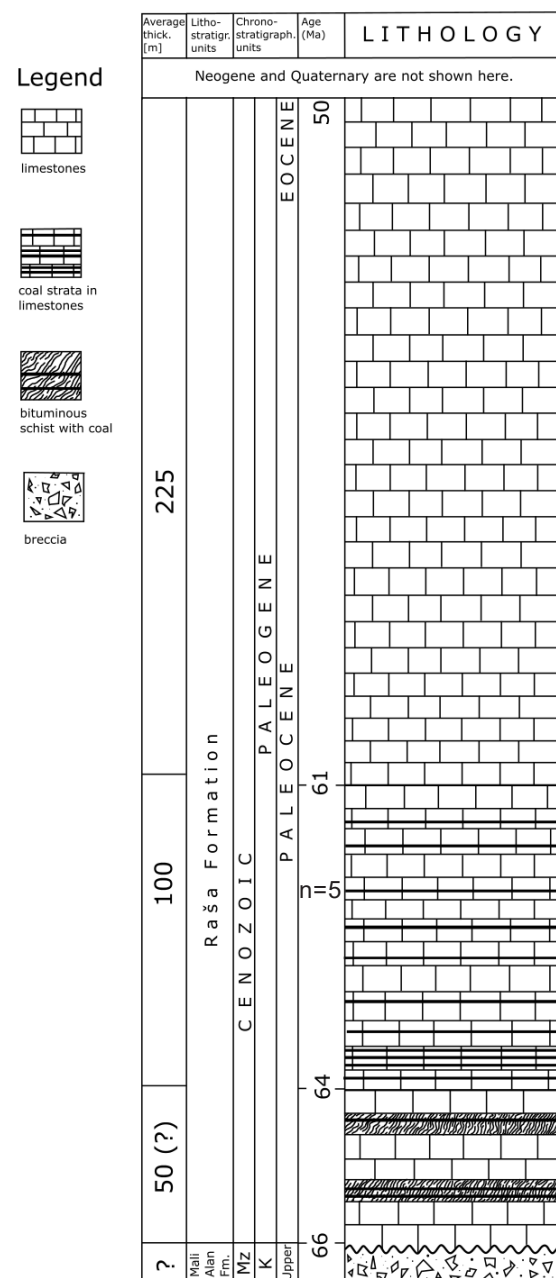


Fig. 8. Regional stratigraphic column from Medunić 2016, after Velić et al., 2015, n = number of samples taken.

the drilling of the TER-1/03 water supply well (Fig. 3), while a single bulk sample of meta-lignite/sub-bituminous coal from the Hrastnik mine was collected just before the mine ceased operation in 2012. A sample from the Josef meta-lignite/sub-bituminous coal seam was also collected (Table 1), and the Thermal-Heat Power Station Ljubljana - Termoelektrarna Toplarna Ljubljana provided a coal sample identified as a sub-bituminous coal from the Barito Basin (Pasir Mine) in Indonesia. Additionally, five samples (Table 1) of ortho-bituminous coal from Raša were collected from different seams of unique petrologic composition (Hamrla, 1959; Medunić et al., 2016).

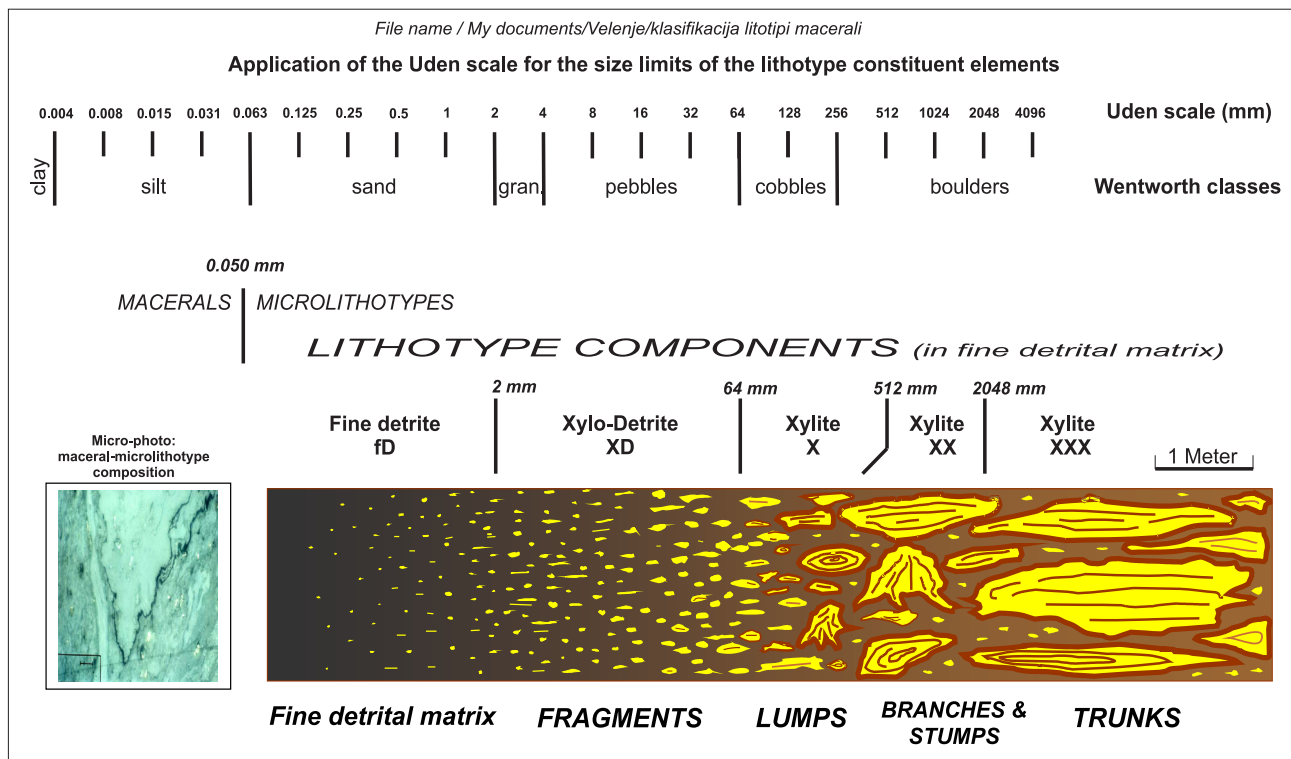


Fig. 9. Basic concept of macropetrographic classification for the Velenje ortho-lignite (Markič et al., 2001; Markič & Sachsenhofer, 2010) using a concept of lithotype components and the Uden scale for dimension limits.

Macropetrographic description of the Velenje ortho-lignite

Macropetrographic classification of the lithotype heterogeneity of the Velenje ortho-lignite has been defined and described in detail by Markič et al. (2001) and Markič & Sachsenhofer (2010). For its macropetrographic description and composition, a concept of lithotype components was introduced (Fig. 9). The classification is somewhat broader than the “official” classification by the (ICCP, 1993).

Microscopic descriptions of samples (VL3 and VL5, Table 2a) were prepared by crushing the material (<2 mm), embedding it in epoxy resin, subjecting it to vacuum, drying, and then creating polished blocks of size 2.5×2.5 cm. The investigation was conducted using Zeiss Opto Axiophot conventional optical microscopy in polarised reflected light under normal atmospheric conditions, and the results were documented photographically.

Isotopic composition of organic carbon ($\delta^{13}\text{C}_{\text{org}}$) and nitrogen ($\delta^{15}\text{N}_{\text{bulk}}$)

The stable isotopic composition of organic carbon ($\delta^{13}\text{C}_{\text{org.}}$) and nitrogen ($\delta^{15}\text{N}_{\text{bulk}}$) in different lignite and coal lithotypes was analyzed using the Europa 20–20 isotope-ratio mass spectrometer connected to an ANCA-SL preparation module. To prepare the lignite and coal samples, they were initially homogenized by grinding in an agate mortar.

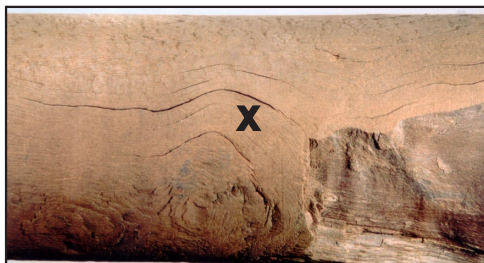
For $\delta^{13}\text{C}_{\text{org}}$ analysis, the samples were treated with 3M HCl at 60 °C overnight to eliminate carbonates. The remaining residues were washed with distilled water, dried, and homogenized. The organic fraction was filtered through a GF/F filter, and chloride ions were removed with triple washing with distilled water. The residue was then dried at 60–70 °C. Approximately 1–2 mg of the residue was used for $\delta^{13}\text{C}_{\text{org}}$ measurements. Approximately 8 mg of powdered lignite and coal were used for $\delta^{15}\text{N}$ analyses with no pretreatment. The carbon and nitrogen isotopic compositions were determined by combusting the samples in sealed tin capsules in an oxidation column using pure oxygen at 1000 °C. The generated products went through a reduction column filled with Cu at 600 °C and then separated on a chromatographic column. IAEA CH-3 ($\delta^{13}\text{C} = -24.724 \text{ ‰} \pm 0.041 \text{ ‰}$) and CH-6 ($\delta^{13}\text{C} = -10.449 \text{ ‰} \pm 0.033 \text{ ‰}$) reference materials were employed to convert the analytical results to the VPDB scale. IAEA N-1 ($\delta^{15}\text{N} = +0.4 \text{ ‰} \pm 0.2 \text{ ‰}$) and IAEA N-2 ($\delta^{15}\text{N} = +20.41 \text{ ‰} \pm 0.12 \text{ ‰}$) were used as reference materials to relate the analytical results to AIR (atmospheric nitrogen) (Coplen, 1996). The reproducibility of the samples was $\pm 0.2 \text{ ‰}$ for carbon isotopes and $\pm 0.3 \text{ ‰}$ for nitrogen isotopes. The results are expressed in the standard δ notation (in per mil, ‰) as the deviation of the sample (sp) from the standard (st) according to the following equation (Brand et al., 2014):

Basic organo-clastic lithotype components

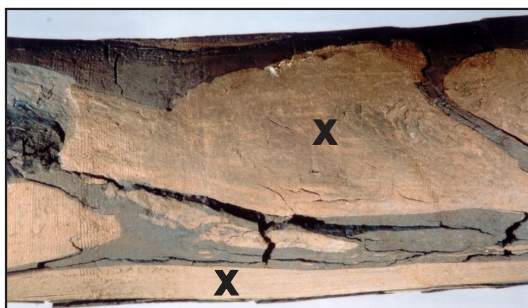
64 mm

· 1 mm

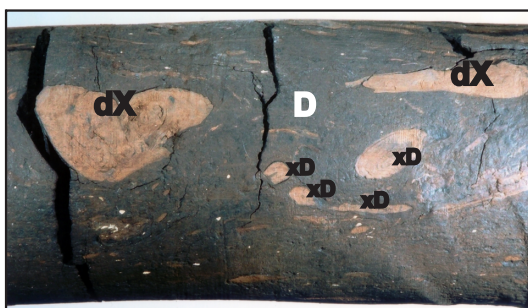
Scale ~ 1:2 (if not cited differently)



1: Xylite (X), wholly extending over dimensions of core diameter.

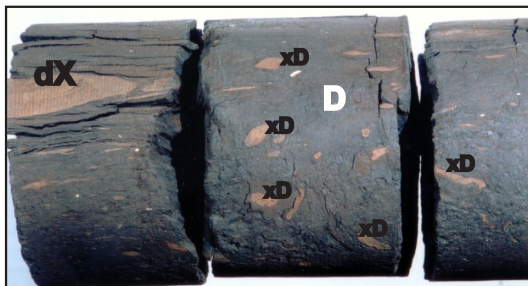


2: Xylite fragments (X) of different shapes, all longer than 64 mm.



3: The biggest two, larger than 32 mm pieces are detro-xylite (dX). Pieces between 1 and 32 mm in size are termed xylo-detrite (xD). Dark homogeneous groundmass (matrix) and the smallest (<1 mm) xylite lenses are termed fine detrite (D).

Extremely small white spots on figs. 3 and 4 are calcite.



4: Same components as in fig. 3



5: Homogeneous fine detrital lignite - as a whole fine detrite (D). On the left is typically crushed, whereas on the right typically fractured fine detrital lignite.

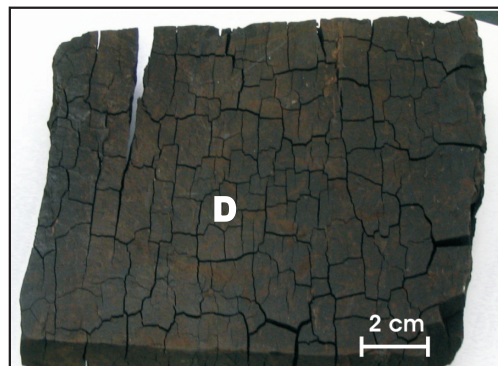


Fig. 10. Lithotype classification is employed in macro-petrographic core logging of the Velenje ortho-lignite. JGM-55 borehole (excavation field B k.-130) (this study) (see appendix) is an example of petrographic well-logging.

$$\delta^y\text{X}(\text{\textperthousand}) = (R_{\text{sp}}/R_{\text{st}} - 1) * 1000 \quad (1)$$

Where $y\text{X}$ is carbon (^{13}C) or nitrogen (^{15}N), and R the $^{13}\text{C}/^{12}\text{C}$ or $^{15}\text{N}/^{14}\text{N}$, respectively.

The $\delta^{13}\text{C}$ of air (atmospheric CO_2) was then calculated using the equations proposed by Arens et al. (2000) (equation 2) and Gröcke (2002) (equation 3).

Gröcke, 2002 suggested that the carbon isotopic composition of ancient CO_2 can be estimated using the $\delta^{13}\text{C}$ value of fossil organic matter. In this study, it is assumed that the samples with $\delta^{13}\text{C}$ values from -27 ‰ to -22 ‰ were derived from terrestrial/freshwater C3 plants ($\delta^{13}\text{C}_{\text{plant}}$) and that in Equ. 2, any carbon isotope fractionation during plant metabolism is similar to that of modern C3 plants and that the primary control on plant C iso-

topes is the carbon isotopic composition of atmospheric CO_2 ($\delta^{13}\text{C}_{\text{air}}$).

$$\delta^{13}\text{C}_{\text{air}} = (\delta^{13}\text{C}_{\text{plant}} + 18.67)/(1.10) \quad (2)$$

$$\delta^{13}\text{C}_{\text{air}} = \delta^{13}\text{C}_{\text{plant}} + 20.22 \quad (3)$$

Results

The results of the macropetrographic classification and the associated $\delta^{13}\text{C}_{\text{org}}$ and $\delta^{15}\text{N}$ values of lignites and coals and calculated $\delta^{13}\text{C}_{\text{air}}$ according to equations (2) and (3) from the six selected locations are presented in Tables 2a and 2b. The isotopic data ($\delta^{13}\text{C}_{\text{org}}$ and $\delta^{15}\text{N}$), the macropetrographic composition data obtained in this study, and previously published data have been uploaded to a public repository (Kanduč et al., 2023).

Table 2a. Results of macropetrographic composition of the Velenje lignite (this study) according to decreasing share of xylite (X) and increasing share of fine detrite (fD), with associated $\delta^{13}\text{C}_{\text{org}}$ and $\delta^{15}\text{N}$ values, $\delta^{13}\text{C}_{\text{air}}$ values calculated after Arens et al. (2000) and Gröcke (2002), and ash yields from Hann et al. (2020). Ash yields were analyzed as composites of two to five samples with similar petrographic composition.

Sample/Location	Macropetrographic composition					$\delta^{13}\text{C}_{\text{org}}$ (‰)	$\delta^{15}\text{N}$ (‰)	After Arens et al. (2000)	After Gröcke (2002)	From Hann et al. (2020)
	Interval (m)	X (%)	dX (%)	xD (%)	fD (%)			$\delta^{13}\text{C}_{\text{air}}$ (‰)	Ash yield (%)	
VL2, Velenje JPK 60	21.5-21.9	95			5	-25.3	+5.6	-6.4	-5.5	2.69
VL1, Velenje JPK 52	16.2-13.3	90			10	-26.6	+3.4	-7.2	-6.4	
VL3, Velenje JGM 55	7.0-7.2	85			15	-25.7	+7.4	-6.4	-5.5	4.93
VL4, Velenje JGM 55	9.6-9.9	85			15	-25.7	+4.0	-6.0	-5.1	
VL15, Velenje JPK 52	24.75-24.9	70			30	-25.5	+3.5	-6.2	-5.3	4.45
VL16, Velenje JPK 60	8.95-9.15	70		5	25	-25.0	+4.8	-5.8	-4.8	
VL13, Velenje JPK 60	5.5-5.85	20	10	30	40	-26.2	+4.4	-6.8	-6.0	9.91
VL12, Velenje JPK 52	22.8-22.95	40		15	45	-26.6	+3.9	-7.2	-6.4	
VL14, Velenje JPK 60	11.5-11.7	35		15	50	-25.5	+4.6	-6.2	-5.3	9.81
VL19, Velenje JPK 60	6.6-6.75	10	5	10	75	-27.2	+3.0	-7.8	-7.0	
VL20, Velenje JPK 60	15.8-16.0	10	5	10	75	-26.5	+4.5	-7.1	-6.3	9.83
VL18, Velenje JPK 60	5.85-6.15		5	15	80	-27.0	+3.6	-7.6	-6.8	
VL17, Velenje JGM 55	1.35-1.55		5	10	85	-27.3	+3.5	-7.8	-7.1	9.63
VL6, Velenje JPK 52	20.35-20.55			10	90	-27.9	+2.6	-8.4	-7.7	
VL8, Velenje JPK 60	19.65-19.8			10	90	-27.4	+4.1	-7.9	-7.2	14.73
VL9, Velenje JPK 60	20.6-21.0			5	95	-26.9	+2.7	-7.5	-6.7	
VL5, Velenje JPK 52	17.7-17.8			5	95	-27.7	+2.7	-8.2	-7.5	14.73
VL7, Velenje JPK 60	10.0-10.5			5	95	-27.2	+3.0	-7.8	-7.0	
VL10, Velenje JPK 52	21.4-21.55			5	95	-27.1	+5.3	-7.7	-6.9	23.30
VL11, Velenje JGM 55	7.2-7.4				100	-26.9	+3.5	-7.5	-6.7	
VL21, Velenje JGM 55	19.5-19.7					-27.5	+3.6	-8.0	-7.3	23.30
VL22, Velenje JPK 60	2.5-2.7			5	55min	-27.5	+3.7	-8.0	-7.3	

X – xylite, dX – detro-xylite, XD – xylo-detrite, fD – fine detrite

Table 2b. Results of macropetrographic composition analysis: TL – Terbegovci lignite (n = 2), HC – Hrastnik coal (n = 1), JC – Josef coal (n = 1), BC – Barito coal (n = 1), RC – Raša coal (n = 5) with associated $\delta^{13}\text{C}_{\text{org}}$ and $\delta^{15}\text{N}$ values, and $\delta^{13}\text{C}_{\text{air}}$ values as calculated after Arens et al. (2000) and Gröcke (2002).

Sample/Location	Coalification rank and lithotypes All are humic lignites and coals	$\delta^{13}\text{C}_{\text{org}}\text{ (‰)}$	$\delta^{15}\text{N}\text{ (‰)}$	$\delta^{13}\text{C}_{\text{air}}\text{ (‰)}\text{ After (Arens et al., 2000)}$	$\delta^{13}\text{C}_{\text{air}}\text{ (‰)}\text{ After (Gröcke, 2002)}$
TL – Terbegovci lignite, Terbegovci (TER-1/03), Mura Zala basin, NE Slovenia	Meta-lignite, high grade (high grade; <10 % ash db)	-27.0	+4.4	-7.6	-6.8
TL – Terbegovci lignite, TER-1/03, Mura Zala basin, NE Slovenia	Meta-lignite, high grade (high grade; <10 % ash db)	-27.1	+4.2	-7.7	-6.9
HC- Hrastnik coal Terezija polje - Hrastnik, Laško syncline, Central Slovenia	Meta-lignite- Durain	-27.2	+4.3	-7.8	-7.0
JC – Josef coal, Sokolov Basin, Czech Republic	Meta lignite - Durain	-25.6	+1.8	-6.3	-5.4
BC – Barito coal, Barito Basin, Indonesia	Sub-bituminous coal	-27.5	+2.7	-8.0	-7.3
RC – Raša coal, Istrian Basin, Croatia	Ortho-bituminous coal – Vitrain	-23.6	+3.2	-4.5	-3.4
RC – Raša coal, Istrian Basin, Croatia	Ortho-bituminous coal – Vitrain	-23.7	+4.6	-4.6	-3.5
RC – Raša coal, Istrian Basin, Croatia	Ortho-bituminous coal – Vitrain	-23.9	+3.8	-4.8	-3.7
RC – Raša coal, Istrian Basin, Croatia	Ortho-bituminous coal – Vitrain	-24.0	+5.5	-4.8	-3.8
RC – Raša coal, Istrian Basin, Croatia	Ortho-bituminous coal – Vitrain	-24.0	+2.9	-4.8	-3.8

The Velenje lignite comprises xylitic components of varying dimensions, shapes, packing, and orientations within a fine detrital matrix. These lithotype components can be categorized as fine detrite (fD), xylo-detrite (XD), and xylites of different sizes (X, XX, XXX) (Fig. 9). Fusite (F) often occurs as incrustations over xylite. Fusite is obtained from the so-called fusinitization pathway (Diessel, 1992), which proceeds under relatively oxygen-enriched conditions. Fusinitization may cause a loss of organic matter and relative enrichment in residual mineral matter (mineralization process). The mineral components typically consist of various forms of calcite (Markič & Sachsenhofer, 2010; Kanduč et al., 2018), consistent with the classification of this lignite as Ca-rich lignite (Markič & Sachsenhofer, 2010). Also, organic components may exhibit different degrees of gelification, classified as weak (G), moderate (GG), and strong gelification (GGG). In the Velenje lignite, huminite macerals (textinite, texto-ulminite, ulminite, attrinite, and densinite) largely predominate, with a share in a total maceral composition ranging between 85 and 95 % by volume, while liptinite

and inertinite macerals are highly subordinated (Markič & Sachsenhofer, 1997, 2010).

Xylite refers to fossilized wood pieces larger than 64 mm, i.e., larger than an average borehole-core diameter. In contrast, the detrite consists of fine plant detritus that underwent a coalification process known as biochemical gelification more readily and rapidly compared to xylites (Diessel, 1992; Stach et al., 1982; Taylor et al., 1998), resulting in structural homogeneity of the lignite. The color of detrite ranges from homogeneously dark brown (poorly gelified) to black (if strongly gelified). Detro-xylite and xylo-detrite are xylitic pieces within a fine-detrital matrix. In the case of detro-xylite, the woody pieces are larger than 32 mm, while in xylo-detrite, they are <32 mm (Figs. 9 and 10).

Other lignites and coals in this study are classified by rank (ECE-UN, 1998), for example, ortho-lignite, meta-lignite, sub-bituminous coal, bituminous coal and ortho-bituminous coal (Table 1), and in terms of well-known hard-coal lithotypes: vitrain, clarain, durain and fusain (Stach et al., 1982; Diessel, 1992; Taylor et al., 1998; Flores, 2014).

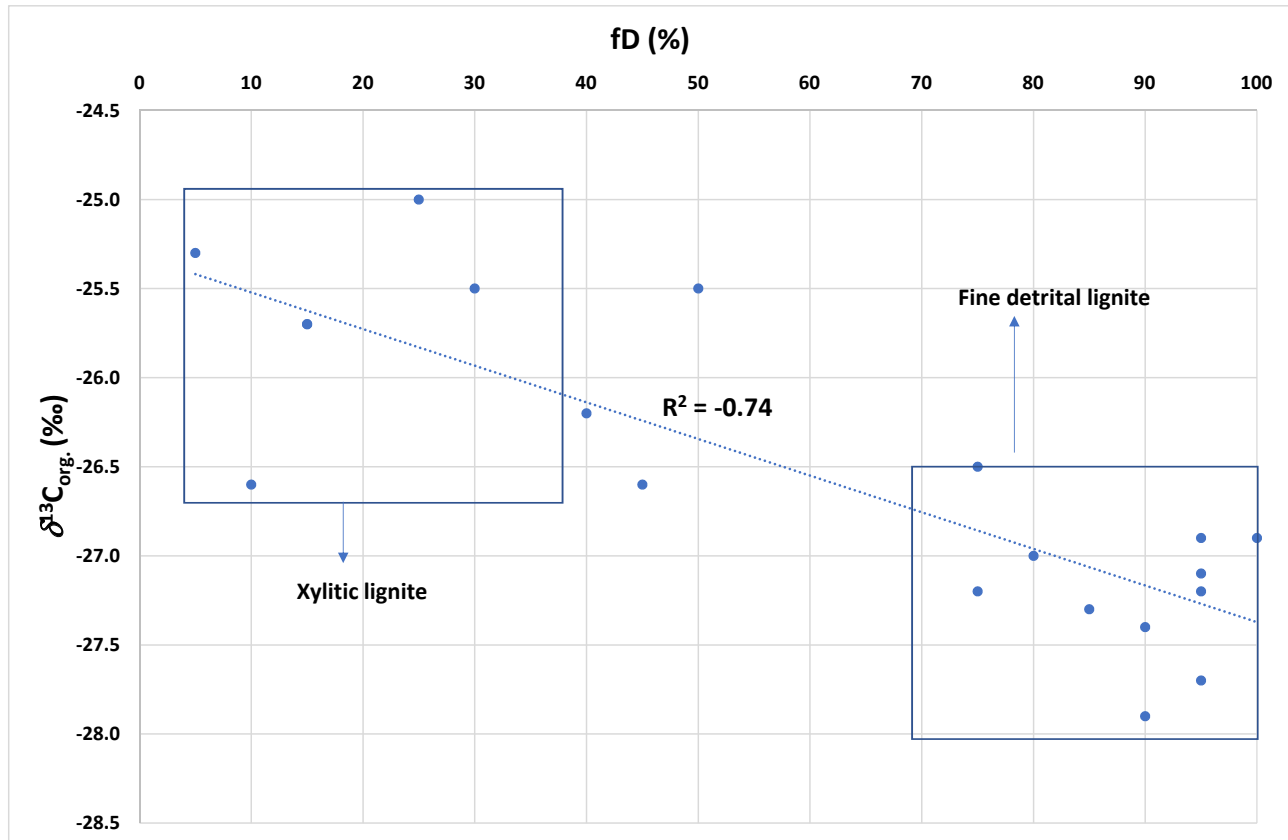


Fig. 11. $\delta^{13}\text{C}_{\text{org.}}$ values vs the share of fine detrital (fD) component of the investigated Velenje lignite samples.

Discussion

Relation between xylite, detro-xylite, xylo-detrite and fine-detrite components and associated $\delta^{13}\text{C}_{\text{org.}}$, and $\delta^{15}\text{N}$ in the Velenje lignite samples

Among the twenty-two samples of the Velenje ortho-lignite (Table 2a), the following samples with distinct lithotype compositions can be distinguished: six samples of xylite-rich lignite ($X > 70\%$), eleven samples of fine-detrital lignite ($fD > 75\%$) and three samples with a xylite-rich composition ($X + dX + xD$) $50\text{--}60\%$, $fD 40\text{--}55\%$, one sample of highly gelified xylite, and one mineral-rich fine detrital sample. In order to look for a possible relationship between fD (fine-detrital component) and $\delta^{13}\text{C}_{\text{org.}}$ in the Velenje lignite samples, we applied the Mann-Whitney U test. However, no significant difference was identified at the 0.05 significance level. The relationship between fD and $\delta^{13}\text{C}_{\text{org.}}$ (Fig. 11), using Spearman's non-parametric coefficient is -0.74. The Spearman's correlations ($p < 0.05$) for Velenje lignite samples revealed the following correlations: $X (\%)$ vs $fD (\%)$ -0.97, $X+dX (\%)$ vs $\delta^{13}\text{C} (\text{\textperthousand})$ 0.66 and $\delta^{15}\text{N} (\text{\textperthousand})$ vs $\delta^{13}\text{C} (\text{\textperthousand})$ 0.65. dX component is not significantly correlated with any parameter at a $p < 0.05$.

Samples of geloxylite (VL 21) and samples enriched with mineral matter (VL 22) are not included in Fig. 11, while two xylite samples with $\delta^{13}\text{C}_{\text{org.}}$ of -25.7 ‰ and $fD 15\%$ overlap. As observed from Figure 11, xylite-rich lignites ($X + dX + xD \geq 50\%$ vs $fD \leq 50\%$) are characterized by $\delta^{13}\text{C}_{\text{org.}}$ values from -26.6 to -25.0 ‰, while those of fine-detrital lignite ($fD \geq 75\%$) are mostly between -27.9 and -26.9 ‰, with one exception with a $\delta^{13}\text{C}_{\text{org.}}$ of -26.5 ‰.

The ash content (Table 2a) in the fine-detrital lignite is higher than in xylitic lignite. Also, the xylite samples ($X > 70\%$) have ash content from 2.69 to 4.45 % and $\delta^{13}\text{C}_{\text{org.}}$ from -26.6 to -25.0 ‰, while samples enriched with detrital component ($fD > 40\%$) have ash contents from 9.91 to 14.73 % (Table 2a) and are enriched with light ^{12}C isotope. The higher ash content for fD (Table 2a) results from water flow influx, with the lake water being subsequently alkaline, promoting gelification, which is discussed in continuation.

Biogeochemical processes reflected by $\delta^{13}\text{C}_{\text{org.}}$ and $\delta^{15}\text{N}$ in lignites and coals

Mineralization, i.e. microbial degradation of organic matter (enrichment with ^{13}C and ^{15}N isotope) and gelification processes (enrichment with

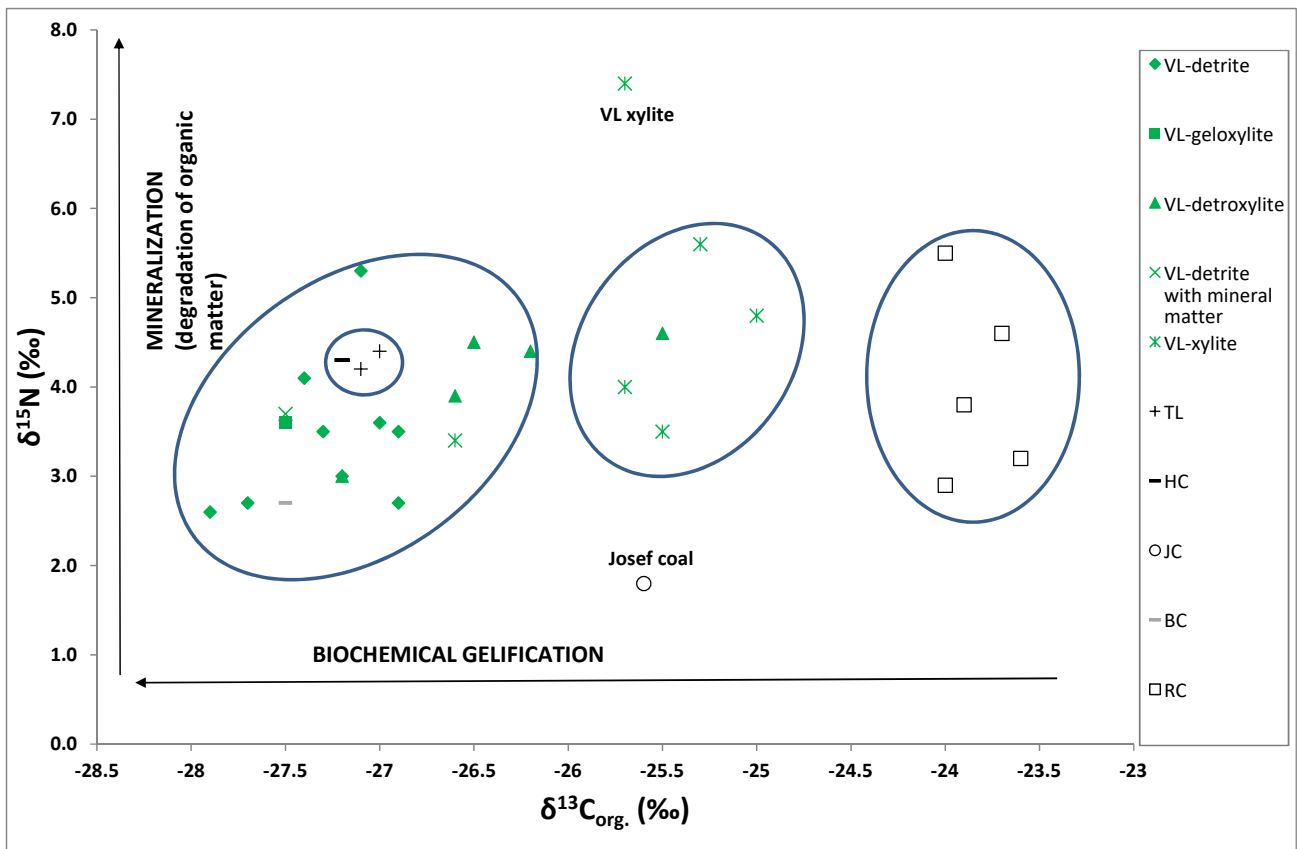


Fig. 12. $\delta^{15}\text{N}$ vs $\delta^{13}\text{C}_{\text{org}}$ for Velenje lignite – VL, Raša coal – RC, Hrastnik coal - HC, Jožef coal - JC, Barito coal - BC and Terbegovci lignite - TL. Degradation of organic matter enriches coal samples with ^{13}C and ^{15}N isotopes; different degrees of biochemical gelification (weak, moderate, strong) enriches lignite with ^{12}C and is the most expressed in Velenje lignite samples.

the light ^{12}C isotope) are best expressed in the Velenje lignite samples (Table 2a, Fig. 12). The lower $\delta^{13}\text{C}_{\text{org}}$ values ($\leq -27.9\text{ ‰}$) in the Velenje ortho-lignite indicate a high degree of gelification and are common in fine-detrital matrix. In comparison, the $\delta^{15}\text{N}$ values ($\leq 7.4\text{ ‰}$) indicate intense mineralization. The $\delta^{15}\text{N}$ value for liptinite is commonly more positive than that for vitrinite, followed by inertinite (Rimmer et al., 2006). Fine organic terrestrial detritus (giving fine detrital lignite) was accumulated in open-water environments of the inner and upper parts of the initial peatland, whereas higher bush and forest vegetation (giving xylite-rich lignite) occupied the periphery (Markič & Sachsenhofer, 2010).

Several groups indicating one or both processes (mineralization and biochemical gelification) can be distinguished (Fig. 12): lower values of $\delta^{13}\text{C}_{\text{org}}$ ($< -26.9\text{ ‰}$) are characteristic for the freshwater fine-detrital Velenje ortho-lignite formed in topogenous mire, as well as for meta-lignite from Terbegovci and Hrastnik, and sub-bituminous coal from Barito formed in a raised swamp.

The lowest $\delta^{13}\text{C}_{\text{org}}$ values (Fig. 12) are observed in the fine-detrital lignite, which is more affected by the gelification process than the xylite fragments, especially in an alkaline environment where

there is significant anaerobic bacterial activity, as in Velenje (Pliocene), Hrastnik (Zasavje Basin - Oligocene) and Terbegovci (Mura-Zala Basin – upper Pannonian). Environments with strong gelification are also characterized by low mineralization, as indicated by low $\delta^{13}\text{C}$ values. However, as the proportion of xylite components increases, $\delta^{13}\text{C}_{\text{org}}$ and $\delta^{15}\text{N}$ values increase due to weaker effects of biochemical gelification and stronger effects of mineralization (Fig. 12). This can be explained by the presence of more aerobic conditions, the subdued oxidation of organic components, and the activity of aerobic bacteria, which result in a relative loss of organic matter and an increase in mineral content. A distinctly notable pattern with a $\delta^{15}\text{N}$ value of 7.4 ‰ is observed in Velenje xylite (Fig. 12), which is attributed to the highest degree of mineralization. The lowest $\delta^{15}\text{N}$ value (1.8 ‰) was analyzed in the meta-lignite/sub-bituminous coal from the Josef seam (Oligocene) in the Sokolov Basin. The coal from the Josef seam is a predominantly “detritus-rich,” even “sapropelic-rich,” coal formed from accumulated organic matter in a low drained swamp environment (“peat bog”) with occasional input of tuffaceous material (Rojík, P. in Pešek et al., 2014, p.101). Such an environment is characterized by negligible mineralization and low

gelification, most likely due to a relatively acidic paleoenvironment.

A different isotopic composition occurs in the ortho-bituminous (black) coal from Raša (Istrian Basin - Paleocene). This coal formed in a paralic environment with a carbonate hinterland and the probable influence of brackish or marine waters. It shows a narrow range of relatively higher $\delta^{13}\text{C}_{\text{org}}$ values, from -24.0 to -23.6 ‰, and a broader range of $\delta^{15}\text{N}$ values, from 2.9 to 5.5 ‰. Higher $\delta^{13}\text{C}_{\text{org}}$ values, from -24.0 to -23.6 ‰, could be attributed to the contribution of organic matter of marine origin. A fluctuating water table (alternating transgressions and regressions) in a paralic carbonate platform environment (e.g., tidal flats, lagoons, deltas, mixing of nonmarine and marine sediments) most probably caused by significant changes in mineralization, is evidenced by a wide range of $\delta^{15}\text{N}$ values. Bacterial activity was also likely present in the brackish paralic carbonate-rich environment. However, they did not lead to intense

gelification of the organic matter; instead, bacterial degradation led to different mineralization.

The lowest $\delta^{15}\text{N}$ value (1.8 ‰) was measured in the meta-lignite/sub-bituminous coal from the Sokolov basin, indicating the lowest mineralization of organic matter among all the samples examined and a low degree of bacterial activity. The highest measured $\delta^{15}\text{N}$ value (7.4 ‰) of "pure" xylite (i.e., < 5 % ash yield, Table 2a) in the Velenje ortho-lignite indicates pronounced mineralization (Fig. 12). Microscopic inspection did not prove the effect of fuzinitization (Fig. 13a). However, cell lumina of textinites are empty implying exposure to air and thus the degradation (mineralization) of organic matter primarily filling cell lumina. The volume content of the textinite (highly prevailing), texto-ulminite and ulminite macerals (Fig. 13a) together is 75 %, corresponding to the macro-petrographic estimates (X 85 %, Table 2a).

The Velenje fine-detrital ortho-lignite (VL) composed of >90 % of the fD component (Table 2a)

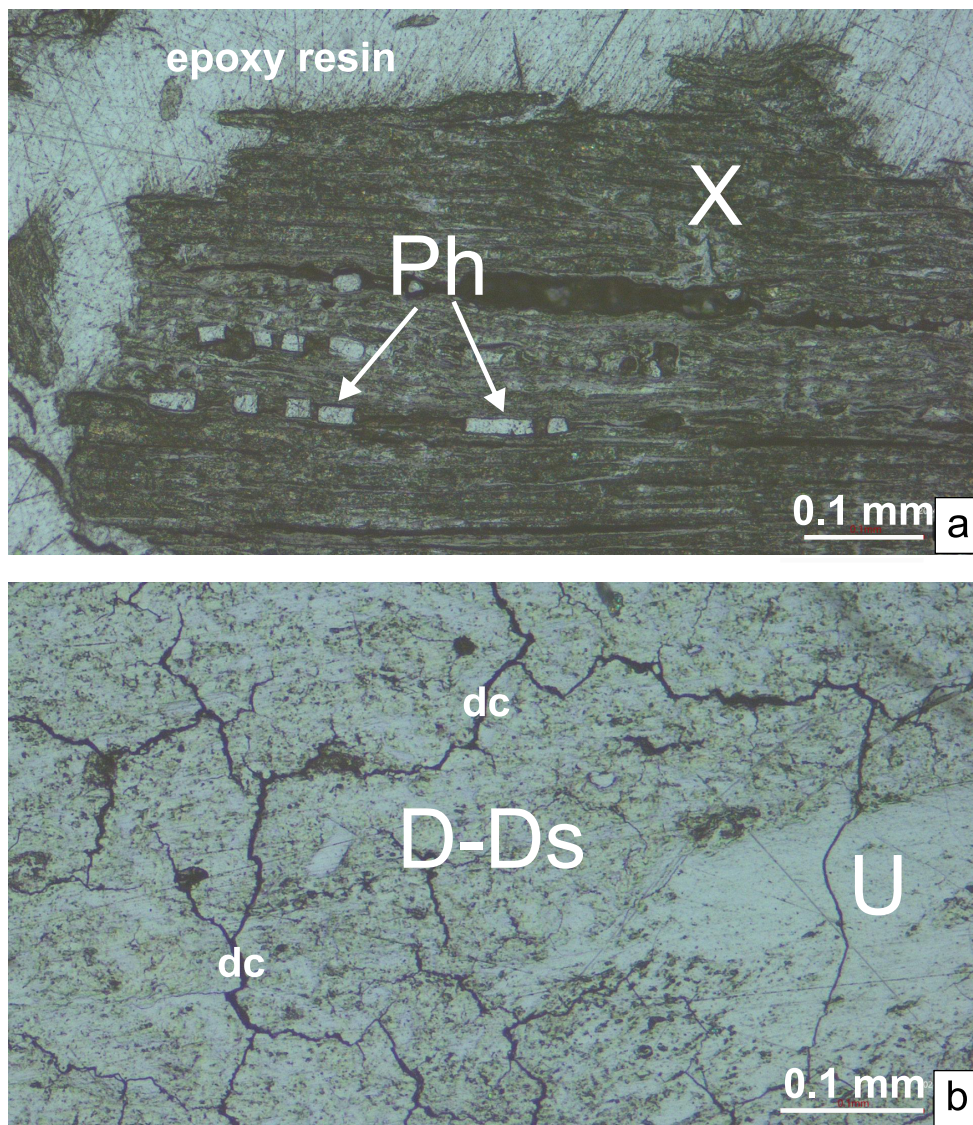


Fig. 13. Micro-petrographic appearance of two contrast lithotypes of Velenje lignite: a) sample VL-3 - Xylinite (X) with phlobaphynite (Ph) highly prevails in xylite-rich ortho-lignite; analyzed ash yield is <5 wt. % and b) sample VL-5 – Ditrinite to densinite (D-DS) highly prevails in fine detrital ortho-lignite; analysed ash yield is <10 wt. %. U is ulminite; dc are desiccation cracks.

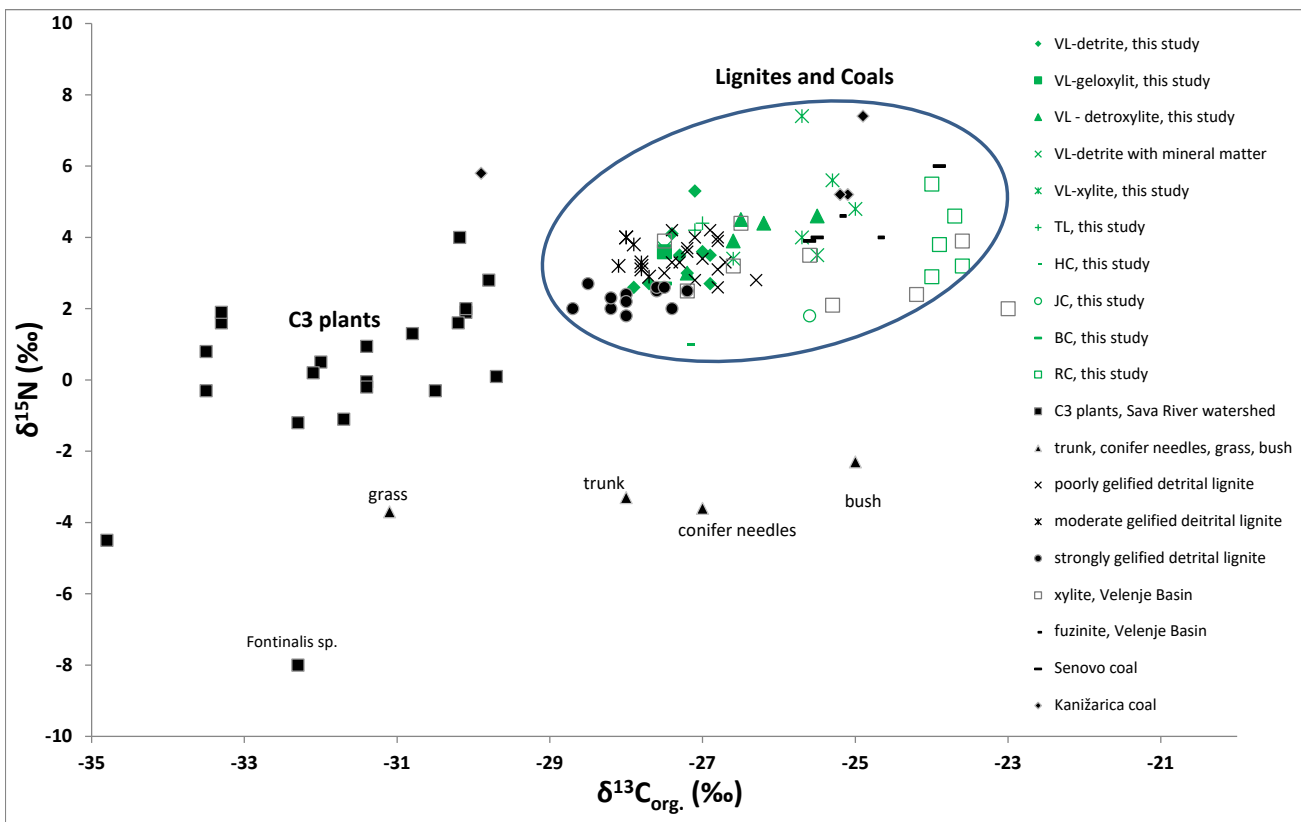


Fig. 14. $\delta^{15}\text{N}$ versus $\delta^{13}\text{C}_{\text{org}}$; plants (terrestrial and aquatic) (Kanduč et al., 2005; Kanduč et al., 2007), and lignites and coals from this and previous studies (Šlejkovec & Kanduč, 2005; Kanduč et al., 2005; Kanduč et al., 2018).

has $\delta^{13}\text{C}_{\text{org}}$ from -27.9 to -26.9 ‰ (avg.: -27.3 ‰) and $\delta^{15}\text{N}$ mostly from 2.6 to 3.5 ‰ (extremes: 4.1 ‰ and 5.3 ‰, respectively) (avg.: 3.5 ‰), both indicating considerable gelification (Table 2a and Figs. 12 and 13b). Strongly gelified samples from previous studies (excavation field -50/C, Velenje Basin) had $\delta^{13}\text{C}$ around -28.0 ‰ with the lowest $\delta^{13}\text{C}_{\text{org}}$ value of even -28.7 ‰, (Fig. 14) (strong gelification) and $\delta^{15}\text{N}$ of 2 ‰, which indicates low mineralization (Kanduč et al., 2018; Kanduč et al., 2023).

Considering $\delta^{13}\text{C}$ values, the precursor plants are C3 plants with values from -33 ‰ to -22 ‰ in all investigated coals (Figs. 12 and 14).

Recent plants collected around the Velenje Basin (Kanduč et al., 2005; Kanduč et al., 2012; Kanduč et al., 2023), such as trunks ($\delta^{13}\text{C} = -28.0$ ‰, $\delta^{15}\text{N} = -3.3$ ‰), conifer needles ($\delta^{13}\text{C} = -27.0$ ‰, $\delta^{15}\text{N} = -3.6$ ‰), grass ($\delta^{13}\text{C} = -31.1$ ‰, $\delta^{15}\text{N} = -3.7$ ‰), and bushes ($\delta^{13}\text{C} = -25.0$ ‰, $\delta^{15}\text{N} = -2.3$ ‰), exhibit more negative $\delta^{15}\text{N}$ values compared to lignites and coals (Fig. 14). Recent plants in the Sava River Basin, Slovenia, have on average $\delta^{13}\text{C}$ values of -31.6 ‰ and $\delta^{15}\text{N}$ values of 0.2 ‰ (Kanduč et al., 2007; Kanduč et al., 2023). The $\delta^{13}\text{C}$ and $\delta^{15}\text{N}$ values of parent organic matter and coalification processes depend on the source of organic

matter (bushes, grass, trunks, and conifer needles) and local meteorological conditions (Liu et al., 2020).

Calculated $\delta^{13}\text{C}$ values of atmospheric CO_2 ($\delta^{13}\text{C}_{\text{CO}_2}$)

The variation in $\delta^{13}\text{C}$ of the plants is primarily controlled by the atmospheric CO_2 isotopic composition ($\delta^{13}\text{C}_{\text{CO}_2}$) rather than the concentration of CO_2 in the atmosphere (Arens et al., 2000). Therefore, the $\delta^{13}\text{C}$ values of coal can be used to estimate the ancient $\delta^{13}\text{C}_{\text{CO}_2}$ values (Arens et al., 2000; Gröcke, 2002). The Eqs. (2) and (3) proposed by (Arens et al., 2000) and (Gröcke, 2002), respectively, have been used for estimating ancient $\delta^{13}\text{C}_{\text{CO}_2}$ using the carbon isotopic composition of organic matter ($\delta^{13}\text{C}_{\text{plant}}$). This estimation assumes that the carbon isotopic fractionation of plants with atmospheric CO_2 is a single-step process (Gröcke, 2002). Enrichment with ^{13}C in atmospheric CO_2 could be related to the burial of more terrestrial plant debris due to rising sea levels (Xu et al., 2020). Diesel (2010) also demonstrated that the late Carboniferous-early Permian was characterized by low pCO_2 and more positive $\delta^{13}\text{C}_{\text{air}}$ values, followed by an increasing atmospheric oxygen content in the mid-early Permian.

In this study from selected coals, the $\delta^{13}\text{C}_{\text{CO}_2}$ value ranges from -3.4 to -8.4 ‰ (Tables 2a, b) based on Eqs. (2) and (3) for all selected coal locations. The calculated $\delta^{13}\text{C}_{\text{CO}_2}$ of coals in our study are in the broader range of values published by Panda et al. (2022) for coals of Permian age (-5.6 to -2.3 ‰). Interestingly, Raša coals of Paleogene age have $\delta^{13}\text{C}_{\text{CO}_2}$ ranging from -4.8 to -3.4 ‰, while a broader range is observed in geologically the youngest Pliocene Velenje lignite (from -5.8 to -8.4 ‰ after (Arens et al., 2000). The global average $\delta^{13}\text{C}_{\text{CO}_2}$ value of modern atmospheric CO_2 was

reported as -8.4 ‰ in 2015 (Graven et al., 2020). Results from one year of monitoring (January 2011 to November 2011) from nine locations in the Velenje basin around thermo power plant Šoštanj indicate $\delta^{13}\text{C}_{\text{CO}_2}$ of atmospheric CO_2 in the range from -18.0 to -6.4 ‰ with an average value of -11.7 ‰ (Kanduč, 2015). This average value shows enrichment with ^{12}C compared to $\delta^{13}\text{C}_{\text{air}}$ from the Pliocene Velenje lignite formation. The pre-industrial global average was estimated for 1850 at -6.6 ‰ (Graven et al., 2020).

Table 3. The $\delta^{13}\text{C}$ values of peat (Alaska), lignites and coals from this study and of different world coals.

Country	Age	$\delta^{13}\text{C}$ (‰)	Rank	Reference
Alaska	Late galacial-E. Holocene	from -28 to -34	Peat	Panda et al., 2022 and references therein
China	Pliocene	from -28.4 to -25.4	Lignite	Panda et al., 2022 and references therein
Velenje, Slovenia	Pliocene	from -25.3 to -27.0	Lignite	Panda et al., 2022 and references therein
Austria	Miocene	from -27.4 to -23.8	Lignite	Panda et al., 2022 and references therein
Poland	Miocene	from -27.2 to -24.6	Lignite	Panda et al., 2022 and references therein
Germany	Miocene	from -27.3 to -24.6	Lignite	Panda et al., 2022 and references therein
Australia	Miocene	from -27.8 to -24.9	Lignite	Panda et al., 2022 and references therein
Australia	Oligocene	from -26.4 to -24.2		Panda et al., 2022 and references therein
Australia	Eocene	from -26.4 to -23.6		Panda et al., 2022 and references therein
India	Eocene	from -28.7 to -25.3	Lignite	Panda et al., 2022 and references therein
India	Palaeocene	from -30.7 to -25.5	Lignite	Panda et al., 2022 and references therein
Mongolia	L. Cretaceous	from -23.5 to -21.3	Lignite	Panda et al., 2022 and references therein
Australia	Jurassic	from -25.2 to -20.9	Sub-bituminous	Panda et al., 2022 and references therein
South-Africa	Permian	from -25.0 to -23.2	Bituminous	Panda et al., 2022 and references therein
North China	Permian	from -25.3 to -22.7	Sub-bituminous to bituminous	Panda et al., 2022 and references therein
Australia	Permian	from -26.6 to -21.9		Panda et al., 2022 and references therein
India	Permian	from -24.2 to -21.0	Bituminous	Panda et al., 2022 and references therein
China	Late Carboniferous	from -24.3 to -23.1	Bituminous	Panda et al., 2022 and references therein
USA	Carboniferous	from -25.1 to -23.5	Bituminous	Panda et al., 2022 and references therein
India	Permian	from -23.8 to -21.7	Sub-bituminous to bituminous	Panda et al., 2022 and references therein
Velenje, Slovenia	Pliocene	from -27.4 to -22.6	Ortho - lignite	Pezdič et al., 1998
Velenje, Slovenia	Pliocene	from -28.7 to -23.0	Ortho - lignite	Kanduč et al., 2005, Kanduč et al., 2018 Kanduč et al., 2023
Kanižarica	Miocene	from -29.9 to -24.9	Brown coal	Kanduč et al., 2018
Senovo	Oligocene	from -25.6 to -23.9	Brown coal	Kanduč et al., 2018
Velenje, Slovenia	Pliocene	from -27.9 to -25.0	Ortho - lignite	This study
Hrastnik	Oligocene	-27.2	Bituminous coal – durain	This study
TER-1/03, NE Slovenia	Upper Pannonian	from -27.0 to -27.1	Meta-lignite-durain	This study
Raša, Croatia	Paleocene	from -24.0 to -23.6	Bituminous–vitrain	This study
Sokolov, Czech Republic	Oligocene	-25.6	Brown coal	This study
Pasir mine, Indonesia	Miocene	-27.5	Humic, high-grade meta-lignite	This study

Table 4. The $\delta^{15}\text{N}$ values of lignites and coals from this study and from different world coals.

Country	$\delta^{15}\text{N}$ (%)	Rank	Reference
China	from -6 to -10	Lignite to antracite	Panda et al., 2022 and references therein
Canada	from -0.2 to 1.4	NA	Panda et al., 2022 and references therein
Russia	from 1.86 to 4.35	NA	Panda et al., 2022 and references therein
SE-Asia (Indonesia, Malaysia, Phillipines)	from 0.38 to 2.32	NA	Panda et al., 2022 and references therein
Europe	from 3.5 to 6.3	Lignite to anthracite	Panda et al., 2022 and references therein
Australia	from 0.3 to 3.7	Lignite to semi-anthracite	Panda et al., 2022 and references therein
USA	from 2.1 to 5.35	Bituminous to anthracite	Panda et al., 2022 and references therein
Germany	from 2.7 to 3.72	Anthracite	Panda et al., 2022 and references therein
India	from 1.07 to 3.44	Bituminous to anthracite	Panda et al., 2022 and references therein
India	from 0.6 to 3.4	Sub-bituminous to high volatile bituminous	Panda et al., 2022 and references therein
Velenje, Slovenia	from 1.8 to 4.6	Ortho – lignite	Kanduč et al., 2005, Kanduč et al., 2018
Kanižarica	from 5.2 to 7.4	Brown coal	Kanduč et al., 2018
Senovo	from 3.9 to 6.0	Brown coal	Kanduč et al., 2018
Velenje, Slovenia	from 2.6 to 7.4	Ortho – lignite	This study
Hrastnik, Slovenia	4.3	Bituminous coal-vitrain	This study
TER-1/03, NE Slovenia	from 4.2 to 4.4	Meta-lignite-durain	This study
Raša, Croatia	from 2.9 to 5.5	Meta-lignite-durain	This study
Sokolov, Czech Republic	1.8	Brown coal	This study
Pasir mine, Indonesia	2.7	Humic, high-grade meta-lignite	This study

Isotopic data in this study gathered with worldwide coals

The $\delta^{13}\text{C}$ and $\delta^{15}\text{N}$ values in coals analyzed in this study and previous studies and those for worldwide coals are presented in Tables 3 and 4. Data from the coalfields analyzed in our study fall within the range of isotopic values of coals worldwide, i.e., from -30.7 to -20.9 ‰. Characteristic $\delta^{13}\text{C}$ values for Paleozoic coals range from -25.7 to -20.2 ‰ (Panda et al., 2022 and references therein). Higher $\delta^{13}\text{C}$ values (up to -23.6 ‰) are also observed for Raša coals of Miocene age (Table 3).

The $\delta^{13}\text{C}_{\text{org}}$ values of Velenje lignites fall within the characteristic range for worldwide lignite, while a broader range (up to 7.4 ‰) is observed for $\delta^{15}\text{N}$ (Table 2a). The carbon isotopic composition ($\delta^{13}\text{C}_{\text{coal}}$, VPDB) of coal samples from the Taiyuan and Shanxi formations of Quinshi and North China-Boloiwan basins ranges from -25.3 ‰ to -22.7 ‰, with an average of -23.7 ‰. The average $\delta^{13}\text{C}_{\text{coal}}$ value is -23.6 ‰ in the late Carboniferous, -23.4 ‰ in the early Permian, and -20.5 ‰ in the mid-early Permian (Xu et al., 2020). Early Permian coals in the southern North China-Boloiwan Basin to the east were isotopically significantly more negative, with a $\delta^{13}\text{C}_{\text{org}}$ value of -25.2 ‰ (Table 3), likely due to regional aridity changes. Geologically younger lignites (Paleocene to Pliocene age) have more negative $\delta^{13}\text{C}$ compared to geologically older

higher rank coals (Late Carboniferous – Late Cretaceous) (Table 3).

There is also disagreement regarding the relationship between $\delta^{15}\text{N}$ and coal rank, with several authors reporting a positive correlation between $\delta^{15}\text{N}$ and coal rank (Zheng et al., 2015), while others suggest that $\delta^{15}\text{N}$ values are largely independent of maturation (Boudou et al., 2008). The $\delta^{15}\text{N}$ of the examined peats range from -1.4 to 1.6 ‰, while lignites exhibit values from -1.4 to 1.8 ‰ and coals from India show values from -2.8 to 5.0 ‰. These values indicate that each material preserves its unique organic matter source signature. Moreover, the highest $\delta^{15}\text{N}$ values found in Cenozoic lignites compared to Cenozoic sub-bituminous coal suggest regional climatic variation. Furthermore, Gondwana anthracites display elevated $\delta^{15}\text{N}$ values from 1.3 to 5.0 ‰, attributed to the tectonic influence of the Himalayan orogeny (Ganguly et al., 2023). In addition, our study observes no relationship between coal rank and $\delta^{15}\text{N}$ values; Pliocene lignites from the Velenje Basin can also be enriched with ^{15}N with $\delta^{15}\text{N}$ up to 7.4 ‰ (Table 4).

Conclusion

This study examined various ortho-lignite samples from the Velenje Basin, having homogeneous fine-detrital and heterogeneous xylite-rich lithotypes. We also analyzed higher-rank coals for

comparison, such as meta-lignites, meta-lignites/sub-bituminous coals, sub-bituminous coals and ortho-bituminous coals. The coals under study were formed in different paleoenvironments and deposited in environments influenced by seawater, as seen in the case of the Raša ortho-bituminous coal and Barito sub-bituminous coal. They were also found in freshwater lake environments, as exemplified by the Velenje ortho-lignite, Hrastnik, and Josef seam meta-lignite/sub-bituminous coals, as well as the Terbegovci meta-lignite and span different geological ages, including the Paleocene (RC), Upper Oligocene (HC, JC), Upper Miocene (JC), upper Pannonian (TL) and Pliocene (VL).

During the processes of peatification and coalification, bacterial activity differed in oxic and anoxic conditions across all the investigated sedimentary coal basins. Moreover, the coals were deposited in open waters, bush moors, and forest swamps. These variations are reflected in the $\delta^{13}\text{C}_{\text{org}}$ and $\delta^{15}\text{N}$ of coals we investigated. The wide range of $\delta^{13}\text{C}_{\text{org}}$ (from -27.9 to -23.6 ‰) and $\delta^{15}\text{N}$ (from 1.8 to 7.4 ‰) values observed in the six different coals indicates different intensities of biogeochemical processes and depositional conditions, including the source of vegetation, humification, bacterial activity, and redox conditions. Gelification, which leads to enrichment with ^{12}C and mineralization, which leads to enrichment in ^{15}N , are most evident in the Velenje ortho-lignite samples.

The detrital lignite sample exhibited the lowest $\delta^{13}\text{C}$ value of -27.9 ‰, whereas the highest value of -23.6 ‰ was measured in Raša coal. The $\delta^{15}\text{N}$ values of the coal samples also fall within the typical worldwide range, which is between -6.0 to 5.4 ‰. Only the Raša sample with a value of 5.5 ‰ and two xylite samples with $\delta^{15}\text{N}$ values of 5.5 ‰ and 7.4 ‰ from Velenje deviate from the worldwide values, indicating higher mineralization. In previous studies, the highest microbial degradation, indicating high activity, was observed in the Raša coal (Paleocene) and the Velenje xylite samples (Pliocene), with the highest $\delta^{13}\text{C}$ values of -23.6 ‰. Among all the analyzed samples, gelification was characteristic of Velenje lignite samples, with $\delta^{13}\text{C}_{\text{org}}$ ranging up to -27.9 ‰ and the lowest (-29.9 ‰) in the Kanižarica sample in previous studies. Similar $\delta^{13}\text{C}$ and $\delta^{15}\text{N}$ values were only detected in Hrastnik coal (durain maceral type) and Terbegovci lignite samples, suggesting they were deposited in freshwater environments (open water) with similar precursor plants. Both the $\delta^{13}\text{C}$ and $\delta^{15}\text{N}$ parameters indicate that C3 plants are the precursor plants in all the investigated coal locations. The precursor

plant material and microbial degradation played crucial roles during peatification and coalification, influencing both $\delta^{13}\text{C}$ and $\delta^{15}\text{N}$ values.

The calculated $\delta^{13}\text{C}_{\text{CO}_2}$ values range from -8.4 ‰ to -3.4 ‰, which is more positive in all the coal sedimentary basins compared to the $\delta^{13}\text{C}_{\text{CO}_2}$ of modern atmospheric CO_2 , reported for the year 2015 (-8.4 ‰, global average). In our study, we can conclude that biogeochemical processes in the coal basin mask the paleoclimate. However, further systematic studies based on macropetrological and microscopic analysis and using elemental ratios and biomarkers combined with $\delta^{13}\text{C}_{\text{org}}$ and $\delta^{15}\text{N}$ data are needed to understand better the biogeochemical processes involved in coalification.

Acknowledgements

We thank the Slovenian Research Agency and Innovation (ARIS) for project funding L2 – 4066: Petrology of brown coals mined and used in Slovenia, gases in them and their gas-sorption properties (2011–2014) and program fundings: P1-0143 and P1-0025. We thank Premogovnik Velenje Coalmine d.d. for providing us samples from boreholes JPK-52 (+2°), JPK-60 (+10°) and JGM-55 (+10°) for petrographic and isotopic analysis, Mrs Branka Bravec for providing us literature of Terezija polje mine (Hrastnik), Mr. Stojan Žigon for measurements of $\delta^{13}\text{C}$ and $\delta^{15}\text{N}$ and Mrs. Mateja Malovrh for providing us Indonesian coal samples from Termoelektrarna Ljubljana. We thank Mr Rok Novak for creating the QGIS map of sampling locations.

Declaration of generative AI and AI-assisted technologies in the writing process.

While preparing this work, the author(s) used Chat GPT v3.5 for minor language editing and statistical processing. After using this tool/service, the authors reviewed and edited the content as needed and takes full responsibility for the content of the publication.

References

- Arens, N.C., Jahren, A.H. & Amundson, R. 2000: Can C3 plants faithfully record the carbon isotopic composition of atmospheric carbon dioxide? *Paleobiology*, 26: 137–164. [https://doi.org/10.1666/0094-8373\(2000\)026<0137:CCPFRT>2.0.CO;2](https://doi.org/10.1666/0094-8373(2000)026<0137:CCPFRT>2.0.CO;2)
- Bangjun, L., Vrabec, M., Markič, M. & Püttman, W. 2019: Reconstruction of paleobotanical and paleo-environmental changes in the Pliocene Velenje Basin, Slovenia by molecular and stable isotope analyses of lignite. *International Journal of Coal Geology*, 206: 31–5. <https://doi.org/10.1016/j.coal.2019.03.006>

- Bechtel, A., Sachsenhofer, R.F., Markič, M., Gratzer, R., Lücke, A. & Püttmann, W. 2003: Paleo-environmental implications from biomarker and stable isotope investigations on the Pliocene Velenje lignite seam (Slovenia). *Organic Geochemistry*, 34/9: 1277–1298. [https://doi.org/10.1016/S0146-6380\(03\)00114-1](https://doi.org/10.1016/S0146-6380(03)00114-1)
- Bechtel, A., Markič, M., Sachsenhofer, R.F., Jelen, B., Gratzer, R., Lücke, A. & Püttmann, W. 2004: Paleoenvironment of the upper Oligocene Trbowlje coal seam (Slovenia). *International Journal of Coal Geology*, 57: 23–48. <https://doi.org/10.1016/j.coal.2003.08.005>
- Bechtel, A., Gratzer, R., Sachsenhofer, R.F., Gusterhuber, J., Lücke, A. & Pütman, W. 2008: Biomarker and carbon isotope variations in coal and fossil wood of Central Europe through the Cenozoic. *Palaeogeography, Palaeoclimatology, Palaeoecology*, 262/3-4: 166–175. <https://doi.org/10.1016/j.palaeo.2008.03.005>
- Boudou, J.P., Schimmelmann, A., Ader, M., Mastalerz, M., Sebilo, M. & Gengembre, L. 2008: Organic nitrogen chemistry during low-grade metamorphism. *Geochimica Cosmochimica Acta*, 72/4: 1199–1221. <https://doi.org/10.1016/j.gca.2007.12.004>
- Brand, W.A., Coplen, T.B., & Vogl J., Rosner, M & Prohaska, T. 2014: Assessment of international reference materials for isotope-ratio analysis (IUPAC Technical Report). *Pure Applied Chemistry*, 86/3: 425–467. <https://doi.org/10.1515/pac-2013-1023>
- Brezigar, A. 1985: Coal seam of the Velenje coal mine. *Geologija*, 28/29: 319–336 (in Slovene with English summary).
- Brezigar, A., Kosi, G., Vrhovšek, D. & Velkovrh, F. 1985: Paleontološke raziskave pliokvartarne skladovnice velenjske udorine = Paleontological investigations of the Plio-Quaternary beds of the Velenje depression. *Geologija*, 28/29: 93–119.
- Buser, S. 1978: Osnovna geološka karta SFRJ 1:100.000. List Celje. Zvezni Geološki zavod, Beograd.
- Choi, B.H., Ryn, C.H., Deb, D., Jung, Y.B. & Jeong, J.H. 2013: Case study of establishing a safe blasting criterion for the pit slopes of an open-pit coal mine. *International Journal of Rock Mechanics and Mining Sciences*, 57: 1–10. <https://doi.org/10.1016/j.ijrmms.2012.07.014>
- Coplen, T.B. 1996: New guidelines for reporting stable hydrogen, carbon and oxygen isotopes ratio data. *Geochimica et Cosmochimica Acta*, 60: 390–3360. [https://doi.org/10.1016/0016-7037\(96\)00263-3](https://doi.org/10.1016/0016-7037(96)00263-3)
- Diessel, C.F.K. 1992: Coal-Bearing Depositional Systems. Springer-Verlag, Berlin, Heidelberg, New York, London, Paris, Tokyo, Hong Kong: 721 p.
- Diessel, C.F.K. 2010: The stratigraphic distribution of inertinite. *International Journal of Coal Geology* 81/4: 251–268. <https://doi.org/10.1016/j.coal.2009.04.004>
- Ding, D.S., Liu, G.J. & Fu, B. 2019: Influence of carbon type on carbon isotopic composition of coal from the perspective of solid-state ^{13}C NMR. *Fuel*, 245: 174–80. <https://doi.org/10.1016/j.fuel.2019.02.072>
- ECE-UN, 1998: ECE-UN, Economic Commission for Europe, Committee on sustainable energy. International Classification of in seam coals, 1998/19 documents United Nations, Geneva: 14 p.
- Flores, R.M. 2014: Coal and Coalbed Gas. Elsevier, 697 p.
- Ganguly, M., Kumar, das S., Ekblad, A. & Behera, P.K. 2023: Variation of $\delta^{15}\text{N}$ in Indian coal, lignite and peat. *Geochemistry*, 83: 126013. <https://doi.org/10.1016/j.chemer.2023.126013>
- Graven, H., Keeling, R.F. & Rogelj, J. 2020: Changes to carbon isotopes in atmospheric CO_2 over the industrial Era and Into the Future. *Global biogeochemical cycles*, 34: e2019GB006170. <https://doi.org/10.1029/2019GB006170>
- Gröcke, D.R. 2002: The carbon isotope composition of ancient CO_2 based on higher plant organic matter. *Philosophical Transactions A, Mathematical, Physical, and Engineering Sciences*, 360/1793: 633–658. <https://doi.org/10.1098/rsta.2001.0965>
- Hamrla, M. 1959: O pogojih nastanka premogišč na krasu = On the conditions of origin of the coal beds in the karst region. *Geologija*, 5: 180–264.
- Hamrla, M. 1960: K razvoju in stratigrafiji produktivnih liburnijskih plasti Primorskega kraša. Rudarsko Metalurški zbornik, 3: 203–2016.
- Hamrla, M. 1985: Optična odsevnost nekaterih slovenskih premogov = Light reflectance of some Slovenian coals. *Geologija*, 28/29: 293–317.
- Hann, D., Žarn, J. & Markič, M. 2020: Properties of CO_2 adsorption for petrographically diverse ortho-lignites and some higher rank coals. *Acta Montanistica Slovaca*, 25/3: 324–336. <https://doi.org/10.46544/AMS.v25i3.6>
- Hariana, Prismatoko A., Putra, H.P., Nuryadi, A.P., Sugiarto, Enjang & Nielsen, C. 2021: Characteristics of low-rank and medium-rank Indonesian coal using the TG-DSC method. *International Seminar on Mineral and Coal Technology IOP Conf. Series: Earth and Envi-*

- ronmental Sciences, 882: 012031, <https://doi.org/10.1088/1755-1315/882/1/012031>
- Hoefs, J. 1987: Stable isotope geochemistry. Springer-Verlag, Heidelberg: 241 p.
- ICCP-International Committee for Coal Petrology, 1993: International Handbook of Coal Petrography, 3rd Supplement to 2nd Edition. University of Newcastle upon Tyne, England.
- Kanduč, T., Markič, M. & Pezdič, J. 2005: Stable isotope geochemistry of different lithotypes of the Velenje lignite (Slovenia). *Geologija*, 48/1: 83–95. <https://doi.org/10.5474/geologija.2005.008>
- Kanduč, T., Ogrinc, N. & Mrak, T. 2007: Characteristics of suspended matter in the River Sava watershed, Slovenia. *Isotopes in environmental and health studies*, 43/4: 369–386. <https://doi.org/10.1080/10256010701705112>
- Kanduč, T., Markič, M., Zavšek, S. & McIntosh, J. 2012: Carbon cycling in the Pliocene Velenje Coal Basin, Slovenia, inferred from stable carbon isotopes. *International Journal of Coal Geology*, 89: 70–83. <https://doi.org/10.1016/j.coal.2011.08.008>
- Kanduč, T. 2015: Isotopic composition of carbon in atmospheric air; use of a diffusion model at the water/atmosphere interface in Velenje Basin. *Geologija*, 58/1: 35–46. <https://doi.org/10.5474/geologija.2015.002>
- Kanduč, T., Vreča, P., Gregorin, Š., Vrabec, M., Vrabec, Ma. & Grassa, F. 2018: Authigenic mineralization in low-rank coals from the Velenje Basin, Slovenia. *Journal of sedimentary research*, 88/2: 201–203. <https://doi.org/10.2110/jsr.2018.7>
- Kanduč, T., Markič, M., Žigon, S. & Novak, R. 2023: Data set on petrological and isotopic composition of some selected lignites, sub-bituminous and ortho-bituminous coals. Mendeley Data, <https://doi.org/10.17632/ydc964pbdm.2>
- Kirby, B.M., Vengadajellum, C.J., Burton, S.G. & Cowan, D.A. 2010: Coal, Coal Mines and Spoil Heaps. *Handbook of Hydrocarbon and Lipid Microbiology*, 2277–2292. https://doi.org/10.1007/978-3-540-77587-4_166
- Kuščer, D. 1967: Zagorski terciar (Tertiary formations of Zagorje). *Geologija*, 10: 5–85.
- Lin, Y., Wang, S., Schobert, H. H., Guo, Q. & Li, X. 2022: Sulfur and nitrogen isotopic composition of Late Permian bark coals: source identification and associated environmental assessment. *Organic geochemistry*, 164: 104369. <https://doi.org/10.1016/j.orggeochem.2022.104369>
- Li, J., Wang, Y., Nguyen, X., Zhuang, X., Li J., Querol, X., Li B., Moreno, N., Hoang, V., Cor- doba, P. & Do, V. 2022: First insights into mineralogy, geochemistry and isotopic signatures of the Upper Triassic high-sulphur coals from the Thai Nguyen Coal Field NE Vietnam. *International Journal of Coal Geology*, 261: 104097. <https://doi.org/10.1016/j.coal.2022.104097>
- Liu, B., Vrabec, M., Markič, M. & Püttman, W. 2019: Reconstruction of paleobotanical and palaeoenvironmental changes in the Pliocene Velenje basin, Slovenia by molecular and stable isotope analysis of lignites. *International Journal of Coal Geology*, 206: 31–45. <https://doi.org/10.1016/j.coal.2019.03.006>
- Liu, J., Dai, S., Hower, J.C., Moore, T.A., Moroeng, O.M., Nechoer, V.P., Petrenko, T.I., French, D., Graham, I.T. & Song, X. 2020: Stable isotopes of organic carbon, palynology, and petrography of a thick low-rank Miocene coal within the Mile Basin, Yunnan Province, China: implications for paleoclimate and sedimentary conditions. *Organic geochemistry*, 149: 104103. <https://doi.org/10.1016/j.orggeochem.2020.104103>
- Markič, M. & Sachsenhofer, R.F. 1997: Petrographic composition and depositional environments of the Pliocene Velenje lignite seam (Slovenia). *International Journal of Coal Geology*, 33/3: 229–254. [https://doi.org/10.1016/S0166-5162\(96\)00043-2](https://doi.org/10.1016/S0166-5162(96)00043-2)
- Markič, M., Zavšek, S., Pezdič, J., Skaberne, D. & Kočevar, M. 2001: Macropetrographic characterization of the Velenje lignite (Slovenia). *Acta Universitatis Carolinae Geologica*, 45: 81–97.
- Markič, M. & Sachsenhofer, R.F. 2010: The Velenje lignite: its petrology and genesis. *Geološki zavod Slovenije*, Ljubljana: 218 p.
- Markič, M., Turk, V., Kruk, B. & Šolar, S.V. 2011: Premog v Murski formaciji (pontij) med Lendavo in Murskim središčem ter v širšem prostoru SV Slovenije = Coal in the Mura Formation (Pontian) between Lendava (Slovenia) and Mursko Središče (Croatia), and in the wide area of NE Slovenia. *Geologija*, 54/1: 97–120. <https://doi.org/10.5474/geologija.2011.008>
- Markič, M. & Brenčič, M. 2014: High arsenic (As) content in the upper Miocene coal matter from TER-1/03 borehole. *Geologija*, 57/1: 015–026. <https://doi.org/10.5474/geologija.2014.002>
- Masood, N., Zafar, T., Hudson-Edwards, K.A., Rehman, H. U. & Farooqi, A. 2022: Trace element geochemistry and stable isotopic ($\delta^{13}\text{C}$ and $\delta^{15}\text{N}$) records of the Paleocene Coals, Salt Range, Punjab, Pakistan. *International Journal of Mining Science and Technology*, 32: 551–561. <https://doi.org/10.1016/j.ijmst.2022.03.007>

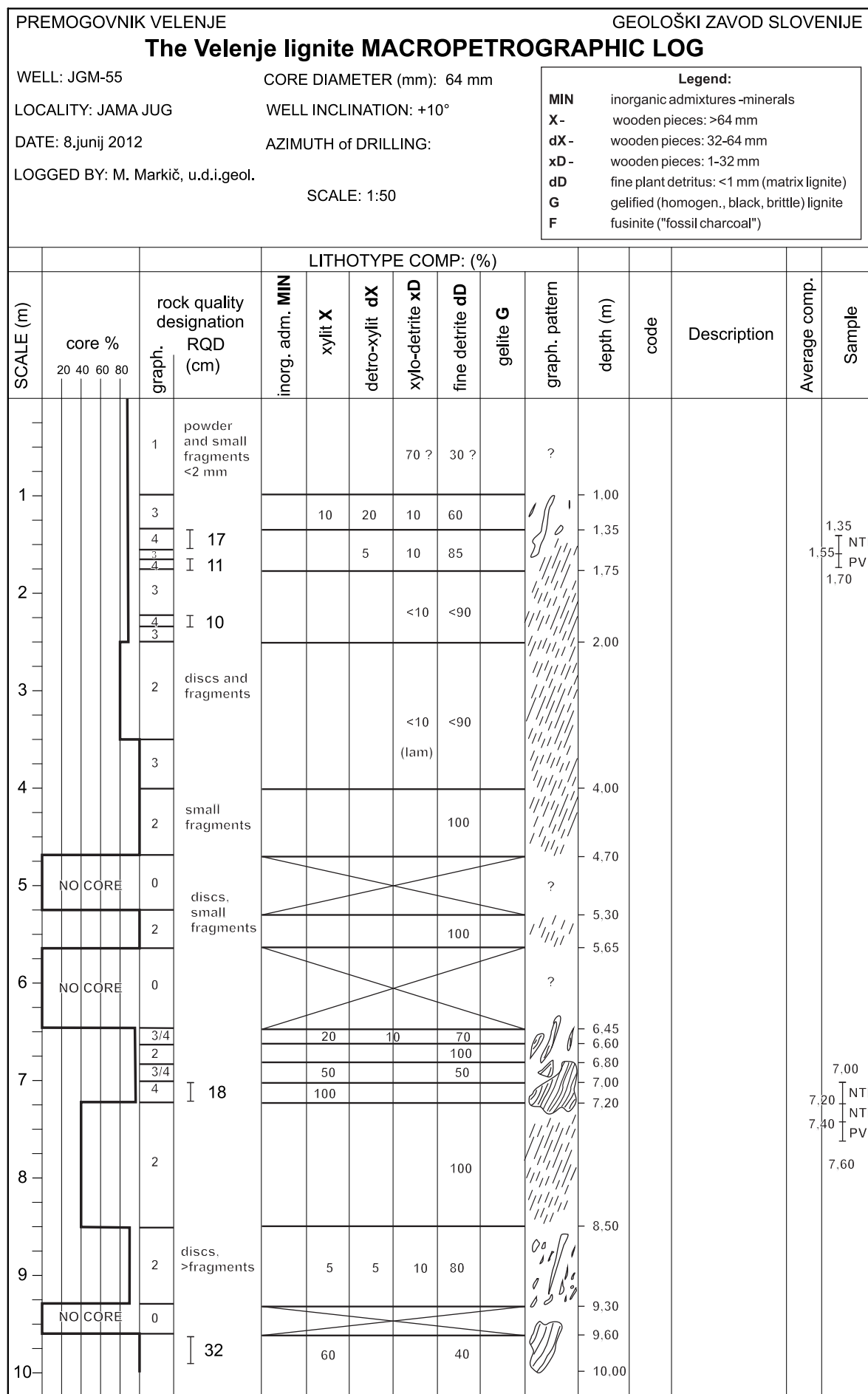
- Medunić, G., Rađenović, A., Bajramović, M., Švec, M. & Tomac, M. 2016: Once grand, now forgotten: what do we know about the superhigh – organic-sulphur Raša coal? The Mining Geology Petroleum Engineering Bulletin, 27–45. <https://doi.org/10.17794/rgn.2016.3.3>
- O'Leary, M.H. 1988: Carbon isotopes in photosynthesis. Bioscience, 38: 328–336. <https://doi.org/10.2307/1310735>
- Panda, M., Equeemuddin, Sk., Md. & Mohanty, D. 2022: Organic petrography and stable isotopic characteristics of Permian Talcher coal, India: Implications on depositional environment. International Journal of Coal Geology, 264: 104130. <https://doi.org/10.1016/j.coal.2022.104130>
- Papež, D. 2019: Elaborat o klasifikaciji in kategorizaciji izračunanih zalog in virov premoga v Premogovniku Velenje s stanjem 31.12.2018. Premogovnik Velenje (in Slovene).
- Pešek, J. et al. (23 co-authors), 2014: Tertiary basins and lignite deposits of the Czech Republic. Czech Geological Survey: 283 p.
- Peterson, B.J. & Fry, B. 1987: Stable isotopes in ecosystem studies. Annual Review of Ecology, Evolution and Systematics, 18/1: 293–320.
- Pezdič, J., Markič, M., Lojen, S., Čermelj, B., Ulrich, M. & Zavšek, S. 1998: Carbon isotope composition in the Velenje lignite mine – its role in soft brown coal genesis. Materials and geoenvironment, 45: 149–153.
- Placer, L. 1998: Structural meaning of the Sava folds. Geologija, 41/1: 191–221. <https://doi.org/10.5474/geologija.1998.012>
- Premru, U. 1983: Osnovna geološka karta SFRJ 1:100.000. List Ljubljana. List Ljubljana. Zvezni geološki zavod, Beograd.
- Rađenović, 2006: Inorganic constituents in coal. Kemija u industriji, 55: 65–71.
- RCMWRA, (Republic Commission for Mineral and Water Reserves Assessment) 2002: Annual Balance of Mineral Raw Material Reserves and Resources in Slovenia – I Energy raw materials. Ministry of Economic Affairs: Ljubljana.
- Rimmer, S.M., Rowe, D., Toulbee, D.N. & Howler, J.C. 2006: Influence of maceral content on $\delta^{13}\text{C}$ and $\delta^{15}\text{N}$ in a Middle Pennsylvanian coal. Chemical Geology, 225: 77–90.
- Rojík, P. 2004: New stratigraphic subdivision of the Tertiary in the Sokolov basin in North-western Bohemia. Journal of Czech Geological Society, 49/3–4: 173–185.
- Rojík, P., Dašková, J., Kvaček, Z., Pešek, J., Skorov Rojík, P., Dašková, J., Kváček, Z., Pesek, J., Sýkorová, I. & Teodoridis, V. 2014: The Sokolov Basin. In: Pesek, J. (ed.): Tertiary basins and lignite deposits of the Czech Republic. Czech Geol Survey, Prague: 90–142.
- RTH d.o.o. 2013: Elaborat o klasifikaciji in kategorizaciji izračunanih zalog in virov rjavega premoga na pridobivalnem prostoru Rudnika Trbovlje – Hrastnik s stanjem 31.12.2012 = Elaborate on the classification and categorization of the calculated reserves and resources of lignite in the extraction area of the Trbovlje-Hrastnik mine with the status of 31.12.2012 (in Slovene).
- Shafiee, S. & Topol, E. 2009: When will fossil fuel reserves be diminished? Energy Policy, 37: 181–189.
- Speight, J.G. 2013: Coal-Fired Power Generation Handbook. Scrivener Publishing LLC, Salem, 8–21.
- Stach, E., Mackowski, M.-Th., Teichmüller, M., Taylor, G.H., Chandra, D. & Teichmüller, R. 1982: Stach's Textbook of Coal petrology (Third Edition). Gebrüder Borntraeger, Berlin: 535 p.
- Supandi & Hartono, H.G. 2020: Geomechanic properties and provenance analysis of quartz, sandstone from the Warukin formation. International Journal of GEOMATE, 18/66: 140–149. <https://doi.org/10.21660/2020.66.50081>
- Šturm, M., Lojen, S., Markič, M. & Pezdič, J. 2009: Speciation and isotopic composition of sulphur in low rank coals from four Slovenian Coal Seams. Acta Chimica Slovenica, 56: 989–996.
- Taylor, G.H., Teichmüller, M., Davis, A., Diessel, C.F.K., Littke, R. & Robert, P. 1998: Organic Petrology. Gebrüder Borntraeger, Berlin: 704 p.
- Thomas, L. 1992: Handbook of practical coal geology. John Wiley and Sons, Chichester: 338 p.
- Veber, I. & Dervarič, E. 2004: Reserves presentation for Velenje colliery according to United Nations framework classification. First session of the ad hoc group of experts on classification of energy reserves and resources; Geneva, http://www.unece.org/ie/se/pdfs/adclass/day2/Subelj_Veber_UNFC.pdf
- Velić, J., Malvić, T., Cvetković, M. & Velić, I. 2015: Stratigraphy and petroleum geology of the Croatian part of the Adriatic basin. Journal of Petroleum Geology, 38/3: 281–300.
- Vrabec, M., 1999: Style of postsedimentary deformation in the Plio-Quaternary Velenje basin, Slovenia. N. Jb. Geol. Paläont. Mh.: 449–463.
- Xu, Z., Hamilton, S.K., Rodrigues, S., Baublys, K. A., Esterle, J. S., Liu, Q. & Golding, S.D. 2020: Palaeoenvironment and palaeoclimate during the late Carboniferous – early Permian

- in northern China from carbon and nitrogen isotopes of coals. *Palaeogeography, Palaeoclimatology, Palaeoecology*, 539: 109490. <https://doi.org/10.1016/j.palaeo.2019.109490>
- Zheng, Q., Liu, Q., Huang, B. & Zhao, W. 2015: Isotopic composition and content of organic nitrogen in the coals of Quinshui coalfield, North China. *Journal of Geochemical Exploration*, 149: 120–126. <https://doi.org/10.1016/j.gexplo.2014.12.002>

Electronic sources:

- Internet 1: <https://www.statista.com/statistics/544848/distribution-of-thermal-coal-exporting-countries-worldwide/> (accessed in 15 December 2023)
- Internet 2: https://www.gem.wiki/Pasir-coal_mine (accessed on 15 November 2023)

Appendix to Figure 10





Tectonics and gravitational phenomena, part two: The Trnovski gozd-Banjšice-Šentviška Gora degraded plain

Tektonika in gravitacijski pojavi, drugi del: Trnovsko- banjško-šentviška degradirana uravnava

Ladislav PLACER^{1*}, Tomislav POPIT² & Igor RIŽNAR³

¹Geološki zavod Slovenije, Dimičeva ul. 14, SI-1000 Ljubljana, Slovenija;

*corresponding author: ladislav.placer@telemach.net

²Univerza v Ljubljani, Naravoslovnotehniška fakulteta, Oddelek za geologijo, Aškerčeva 12, SI-1000 Ljubljana, Slovenija;
e-mail: tomi.popit@ntf.uni-lj.si

³Geološke ekspertize Igor Rižnar s. p., SI-1000 Ljubljana, Slovenija; e-mail: igor.riznar@telemach.net

Prejeto / Received 22. 3. 2024; Sprejeto / Accepted 29. 5. 2024; Objavljeno na spletu / Published online 11. 6. 2024

Key words: External Dinarides NW, geomorphology, gravitational phenomena, karst plains, degraded karst plains, Idrija fault

Ključne besede: Zunanji Dinaridi NW del, geomorfologija, gravitacijski pojavi, kraške uravnave, degradirane kraške uravnave, Idrijski prelom

Abstract

The article describes the recent conditions at the Paleogene thrust contact between the External Dinaric Thrust Belt composed of carbonate rocks and the External Dinaric Imbricate Belt composed of flysch rocks, geographically, between the Trnovski gozd (Trovski gozd plateau) and the Vipava Valley at the northwestern end of the Dinarides. Fossil and recent gravity-related phenomena that indicate the uplift of the southwestern edge of the External Dinaric Thrust Belt and the larger complex in the hinterland are found there. However, these phenomena are not related to the reactivated Paleogene thrust tectonics, but to the Neogene-recent underthrusting as a consequence of the Microadria (Adriatic Microplate) movement towards the Dinarides. Only arguments for these processes are presented in this article.

Izvleček

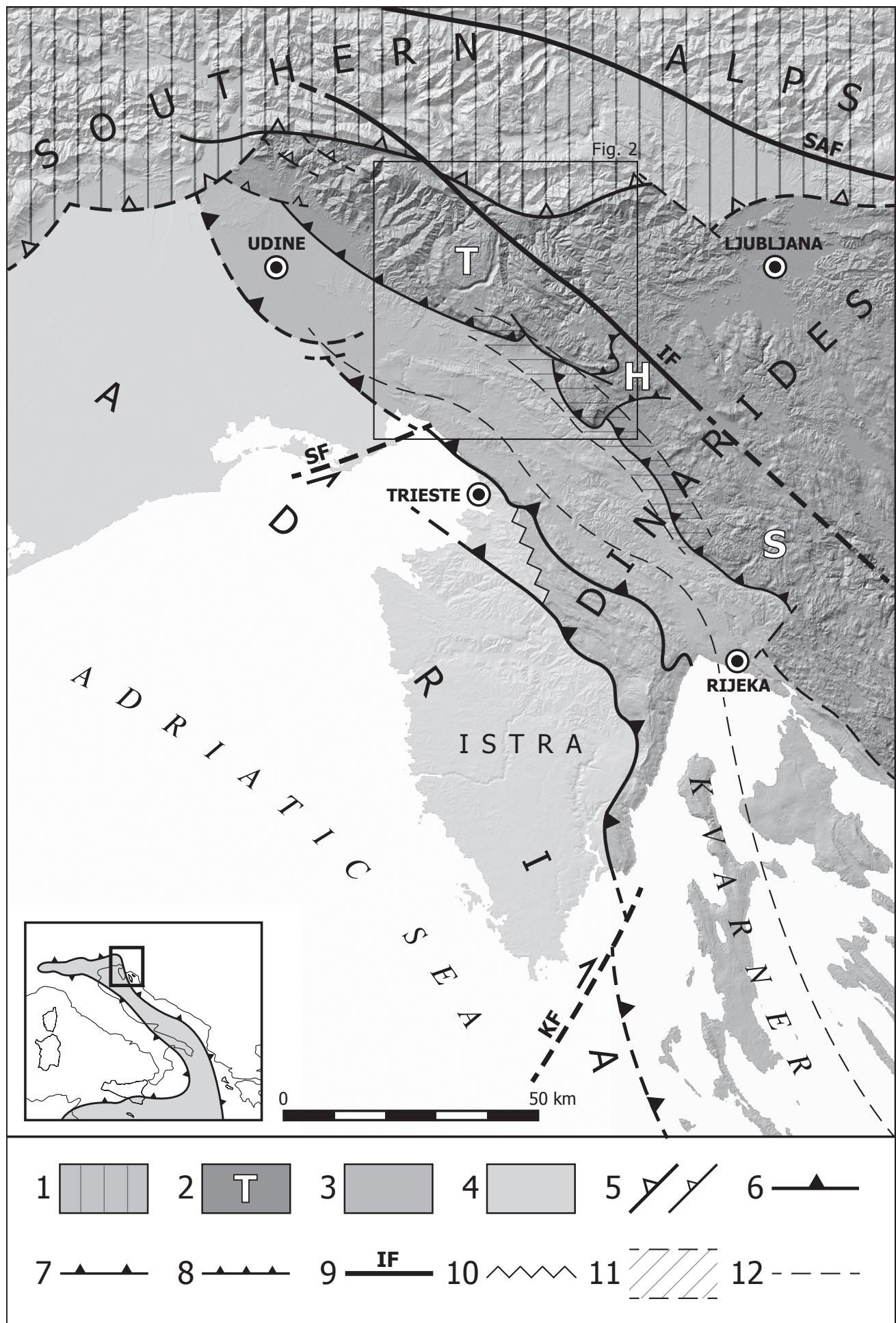
V članku so opisane recentne razmere na paleogenskem narivnem stiku med Zunanjedinarskim narivnim pasom iz karbonatnih kamnin in Zunanjedinarskim naluskanim pasom iz flišnih kamnin. Geografsko med Trnovskim gozdom (Trovsko planoto) in Vipavsko dolino na severozahodnem koncu Dinaridov. Tu najdemo fosilne in recentne gravitacijske pojave, ki kažejo na dviganje jugozahodnega obrobja Zunanjedinarskega narivnega pasu in večjega kompleksa v zaledju, vendar to ni povezano z reaktivirano paleogensko narivno tektoniko, temveč z neogensko-recentnimi procesi podrivanja, ki so posledica pomikanja Mikroadrije (Jadranska mikroplošča) proti Dinaridom. V članku so predstavljene le posledice teh procesov.

Introduction

The Microadria (Adriatic microplate) is moving towards the Dinarides, which northwestern part is described by Blašković (1991); Weber et al. (2006; 2010); Placer et al. (2010); Vrabec et al. (2018). It has not been precisely determined when the convergence process began, but in general we assume that it started in the Middle Miocene and continues today, which is why we use the term Neogene-recent activity of the Adriatic Microplate. Its characteristics have not yet been sufficiently studied, but the result of this process is the narrowing of the Dinarides, which is kinematically different from the narrowing of the Dinarides in the Paleo-

Uvod

Mikroadrija (Jadranska mikroplošča) se posluša proti Dinaridom, za njen severovzhodni del so o tem pisali Blašković (1991); Weber et al. (2006; 2010); Placer et al. (2010); Vrabec et al. (2018). Kdaj se je pričel proces približevanja ni natančneje ugotovljeno, v splošnem pa menimo, da v srednjem miocenu in traja še danes, zato uporabljamo termin neogensko-recentna dejavnost Jadranske mikroplošče. Njene značilnosti še niso dovolj raziskane, posledica tega procesa pa je oženje Dinaridov, ki se kinematsko razlikuje od oženja le-teh v paleogenu, v zaključnem obdobju nastajanja krovne zgradbe. Razlikuje se



gene, in the final period of the formation of the nappe structure. It differs mainly in that, in addition to successive deformations, new plicative and disjunctive structures also emerged.

The Istran block is located between the Sesljan and Kvarner Faults, an integral part of the Microadria which, in contrast to the other blocks of the Microadria, is noticeably pushed towards the northeast. Its visible part is Istra (Fig. 1). As a result, an extensive Istra Pushed Area was formed in the Dinaric hinterland of the block, in which longitudinal morphostructural objects are laterally bent towards the northeast (Placer et al., 2010; 2023). This situation is illustrated by the morphostructural trajectory in the figure. The two branches of the Dinaric thrust boundary in Istra are related by the Črni Kal Anomaly, which is substantiated in the article by Placer et al. (2023, p. 18–30).

This article discusses the laterally bent Paleogene thrust boundary between the External Dinaric Imbricated Belt, composed predominantly of flysch rocks, and the External Dinaric Thrust Belt, which is composed mostly of carbonate rocks. Extensive, sub-recent and recent gravity-related phenomena have developed here, which significantly affect the geomorphology of the landscape (Komac & Ribičič, 2008; Kocjančič et al., 2019; Placer et al., 2021a). The described conditions are particularly pronounced on the northeastern part of the Vipava Valley beneath the carbonate brims of the Trnovski gozd and Nanos plateaus (Popit et al., 2022), where fossil gravity bodies are stacked in several consecutive levels, and the recent ones are spread out over them; such are e.g. the recent large Slano Blato and Razdrto planar landslides (Fig. 2). The conditions therefore show that the External Dinaric Thrust Belt is being uplifted in this area

predvsem v tem, da so poleg nasledstvenih deformacij nastale tudi nove plikativne in disjunktivne strukture.

Sestavni del Mikroadrije je istrski blok med Sesljanskim in Kvarnerskim prelomom, ki je nasproti drugim blokom Mikroadrije opazno potisnjen proti severovzhodu. Njegov vidni del je Istra (sl. 1). Zaradi tega je v dinarskem zaledju bloka nastalo obsežno istrsko potisno območje v katerem so longitudinalni morfostrukturni objekti bočno usločeni proti severovzhodu (Placer et al., 2010; 2023). To stanje ponazarja morfostrukturna trajektorija na sliki. Dva kraka narivne meje Dinarirov v Istri povezuje črnokalska anomalija, ki je utemeljena v članku Placer et al. (2023, str. 17–30).

V tem članku obravnavamo bočno usločeno narivno mejo paleogenske starosti med Zunanjedinarskim naluskanim pasom, pretežno iz flišnih kamnin in Zunanjedinarskim narivnim pasom pretežno iz karbonatnih kamnin. Tu so se razvili obsežni subrecentni in recentni gravitacijski pojavi, ki pomembno vplivajo na geomorfologijo krajine (Komac & Ribičič, 2008; Kocjančič et al., 2019; Placer et al., 2021a). Opisane razmere so posebej izrazite na severovzhodnem obrobju Vipavske doline pod karbonatnimi obronki planot Trnovski gozd in Nanos (Popit et al., 2022), kjer so fosilna gravitacijska telesa naložena v več nadstropijih, recentna pa se prožijo preko njih; taka sta npr. velika recentna planarna plazova Slano blato in Razdrto (sl. 2). Razmere torej kažejo, da se enota Zunanjedinarskega narivnega pasu na tem območju dviga (Mihael Ribičič, ustna izjava 2010), kar povzroča nestabilnost pobočij, vendar dviganje ni posledica reaktivacije krovnega nariva Zunanjedinarskega narivnega pasu paleogenske

Fig. 1. Structural sketch of the northeastern margin of Microadria. Compiled from: Geological map of Slovenia 1:250 000 (ed. Buser, S. 2009); Geological map of the Friuli Venezia Giulia 1:150 000 (ed. Giovanni Battista Carulli, 2006); Placer et al. (2021; 2023).

Sl. 1. Strukturna skica severovzhodnega obroba Mikroadrije. Sestavljeno po predlogah: Geološka karta Slovenije 1:250 000 (ured. Buser, S. 2009); Carta geologica del Friuli Venezia Giulia 1:150 000 (ured. Giovanni Battista Carulli, 2006); Placer et al. (2021; 2023).

1 Southern Alps / Južne Alpe.

2 External Dinaric Thrust Belt. Front part of thrust unit: **T** – Trnovo Nappe, **H** – Hrušica Nappe, **S** – Snežnik Nappe / Zunanjedinarski narivni pas. Čelnji del krovne enote: **T** – Trnovski pokrov, **H** – Hruški pokrov, **S** – Snežniški pokrov

3 External Dinaric Imbricate Belt / Zunanjedinarski naluskani pas

4 Adria Microplate (Microadria) / Jadranska mikroplošča (Mikroadrija)

5 Thrust boundary of Southern Alps; thrust fault related to the dynamics of the Southern Alps / narivna mejna Južnih Alp; nariv povezan z dinamiko Južnih Alp

6 Thrust boundary of Dinarides / narivna mejna Dinaridov

7 Boundary of the External Dinaric Imbricate Belt / mejna Zunanjedinarskega narivnega pasu

8 Boundary of the nappe unit within the External Dinaric Thrust Belt / mejna krovne enote znotraj Zunanjedinarskega narivnega pasu

9 Subvertical fault: **SAF** – Sava Fault, **IF** – Idrija Fault, **SF** – Sistiana Fault, **KF** – Kvarner Fault / subvertikalni prelom: **SAF** – Savski prelom, **IF** – Idrijski prelom, **SF** – Sesljanski prelom, **KF** – Kvarnerski prelom

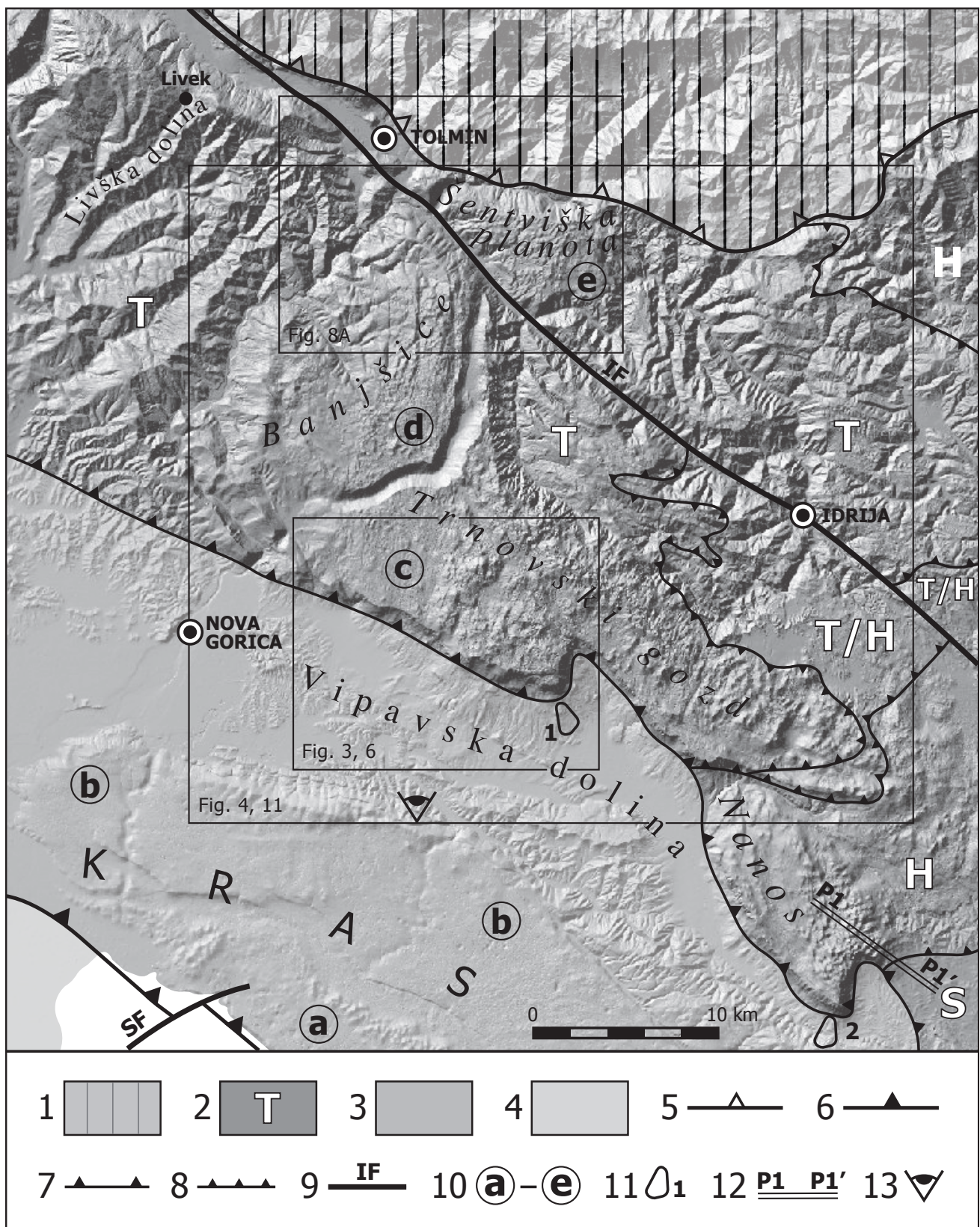
10 Črni Kal Anomaly (Placer et al., 2023, pg. 17–30) / črnokalska anomalija (Placer et al., 2023, str. 17–30)

11 Area of large gravitational phenomena / območje velikih gravitacijskih pojavov

12 Morphostructural trajectory / morfostrukturna trajektorija

(Mihael Ribičič, oral statement 2010), which introduces instability into the slopes. However, the uplift is not the result of the reactivation of the Paleogene nappe thrust of the External Dinaric Thrust Belt, but the Neogene-recent activity of the Adriatic Microplate. Paleogene overthrusts in this

starosti, temveč neogensko-recentne dejavnosti Jadranske mikroplošče. Paleogenski krovni narivi so v tem delu Dinarirov v smeri narivanja subhorizontalni in rahlo undirani (Placer et al., 2021a, str. 47; 2023, sl. 11), regionalno pa blago tonejo proti severozahodu.



part of the Dinarides are subhorizontal and slightly undulating in the direction of thrusting (Placer et al., 2021a, p. 47; 2023, fig. 11), and regionally dipping gently to the northwest.

The geomorphological step between Trnovski gozd and Nanos composed of carbonate rocks in the External Dinaric Thrust Belt and Vipava Valley composed of flysch rocks in the External Dinaric Imbricate Belt could also have been created only due to a faster denudation of flysch, however, during the mapping of the route of the highway along the Vipava Valley beneath Nanos and Trnovski gozd unequivocal signs of reverse tectonics indicating subduction (unpublished) were found. It is also important that several etages of gravity phenomena can be more easily explained by tectonic uplift than by denudation, and that a geomorphological step occurs also where both of the mentioned nappe units are composed of flysch rocks (the area of the ongoing mapping northwest of the Vipava Valley).

The events on the boundary between the Istra Autochton and the External Dinaric Imbricated Belt, where Paleogene thrust planes are antiformally folded along the Neogene-recent underthrusting reverse faults (Placer et al., 2023, Fig. 7) serve as a structural model of the recent events on the boundary between the External Dinaric Imbricated Belt and the External Dinaric Thrust Belt in the Vipava Valley. The stepped structure of the Dinarides appears to be related not only to the Paleogene nappe structure, but also to Neogene-recent underthrust reverse faults. This is also observed by Korbar et al. (2020) in the Kvarner area. Longitudinal right lateral strike-slip faults of the Dinarides are less important, only some are more important, e.g. the Idrija Fault, which it is included it in the article.

Geomorfološka stopnja med Trnovskim gozdom z Nanosom iz karbonatnih kamnin v Zunanjedinarskem narivnem pasu in Vipavsko dolino iz flišnih kamnin v Zunanjedinarskem naluskanim pasu bi lahko nastala tudi samo zaradi hitrejše denudacije fliša, vendar so bili pri kartiranju trase avtoceste po Vipavski dolini pod Nanosom in Trnovskim gozdom odkriti nedvoumni znaki reverzne tektonike, ki kažejo na podrivanje (neobjavljen). Pomembno je tudi, da je več etaž gravitacijskih pojavorov lažje razložiti s tektonskim dviganjem kot z denudacijo in da nastopa geomorfološka stopnja tudi tam, kjer sta obe omenjeni krovni enoti zgrajeni iz flišnih kamnin (območje trenutnega kartiranja severozahodno od Vipavske doline).

Kot strukturni model recentnega dogajanja na meji med Zunanjedinarskim naluskanim pasom in Zunanjedinarskim narivnim pasom v Vipavski dolini služi dogajanje na meji med avtohtonom Istre in Zunanjedinarskim naluskanim pasom, kjer so ob neogensko-recentnih podravnih reverznih prelomih paleogenske narivne ploskve antiformno usločene (Placer et al., 2023, sl. 7). Zdi se, da stopničasta zgradba Dinaričev ni povezana samo s paleogensko krovno zgradbo, temveč tudi z neogensko-recentnimi podravnimi reverznimi prelomi. To opažajo tudi Korbar et al. (2020) na območju Kvarnerja. Longitudinalni desnozmični prelomi Dinaričev imajo pri tem manjši pomen, pomembnejši so le nekateri, npr. Idrijski prelom, ki smo ga zato tudi vključili v članek.

V tem članku ni opisan strukturni mehanizem neogensko-recentnega dviganja Zunanjedinarskega narivnega pasu nad Zunanjedinarski naluskani pas v Vipavski dolini, temveč je obdelana le geomorfologija dvignjenih planot nad Vipavsko

Fig. 2. Major karst plains on the External Dinaric Thrust Belt and External Dinaric Imbricate Belt.

Sl. 2. Večje kraške uravnave na Zunanjedinarskem narivnem in Zunanjedinarskem naluskanim pasu.

1 Southern Alps / Južne Alpe

2 External Dinaric Thrust Belt: **T** – Trnovo Nappe, **H** – Hrušica Nappe, **S** – Snežnik Nappe, **T/H** – area of the interjacent nappe slices between Trnovo Nappe and Hrušica Nappe (Placer, 1981, fig. 9) / Zunanjedinarski narivni pas: **T** – Trnovski pokrov, **H** – Hrušički pokrov, **S** – Smežniški pokrov, **T/H** – območje vmesnih krovnih lusk med Trnovskim in Hrušičkim pokrovom (Placer, 1981, sl. 9)

3 External Dinaric Imbricate Belt / Zunanjedinarski naluskni pas

4 Microadria / Mikroadrija

5 Thrust boundary of the Southern Alps / narivna meja Južnih Alp

6 Thrust boundary of the Dinarides / narivna meja Dinaričev

7 Boundary of the External Dinaric Imbricate Belt / meja Zunanjedinarskega narivnega pasu

8 Boundary of the nappe unit within the External Dinaric Thrust Belt / meja krovne enote znotraj Zunanjedinarskega narivnega pasu

9 Important subvertical fault: **IF** – Idrija Fault, **SF** – Sistiana Fault / pomembnejši subvertikalni prelom: **IF** – Idrijski prelom, **SF** – Sesljanski prelom

10 Larger karst plain: **a** – Aurisina Classical Karst Region, **b** – Doberdo del Lago, Kostanjevica, and Komen Classical Karst Region, **c** – Voglarska planota (Voglarji plateau), **d** – southeastern part of Banjšice (Banjšice plateau), **e** – eastern part of Šentviška planota (Šentviška Gora plateau) / večje kraške uravnave: **a** – Nabrežinski Kras, **b** – Doberdolski, Kostanjeviški in Komenski Kras, **c** – Voglarska planota, **d** – jugovzhodni del Banjšice planote ali Banjšic, **e** – vzhodni del Šentviške planote

11 Active planar landslide: 1 – Slano blato, 2 – Razdrto / dejavni planarni plaz: 1 – Slano blato, 2 – Razdrto

12 Profile Nanos (hamlet) - Strane (village) / profil Nanos (zaselek) - Strane (vas)

13 Recording location of fig. 5A / stojišče snemanja sl. 5A

This article does not describe the structural mechanism of the Neogene-recent uplift of the External Dinaric Thrust Belt above the External Dinaric Imbricated Belt in the Vipava Valley, only the geomorphology of the raised plateaus above the Vipava Valley is covered. The elevation of the Trnovski gozd, Banjšice and Šentviška Gora plateau is reflected in the peculiarities of their geomorphology. This is not reflected only in the gravitational, but also in the intensity of the corrosive degradation of the karstic plains on the External Dinaric Thrust Belt – in this case on the Voglariji plateau in the northwestern part of the Trnovski gozd, in the southeastern part of the Banjšice plateau or Banjšice, and on the eastern part of the Šentviška Gora plateau. The phenomenon of corrosive degradation of the above-mentioned settlements is derived from the assumption that they were formed at a lower altitude than today. The increased corrosion is the result of harsher climatic conditions, which is most apparent when we compare the leveled parts of the External Dinaric Thrust Belt (c, d, e) with the leveled Karst, which lies at a lower altitude (a, b) (Fig. 2).

The Trnovski gozd and Banjšice plateaus are delimited by the Čepovan dry valley, a pradol according to Diercks et al. (2021). The latter is separated from the Šentviška Gora plateau by the Idrija Fault and was uplifted by about 200 m along the length of it.

The uplift of the Trnovski gozd and the Banjšice plateaus up to today's level is already evident in the very existence of the Čepovan dry valley, which could not have been formed at today's altitude because it does not have a hydrographic hinterland.

Stepišnik and Ferk (2023, p. 12–13, 17–18) defined the leveled area of the Trnovski gozd and Banjšice plateaus as a corrosive karst plain, which was thought to have been formed before the uplift of the Trnovski gozd plateau. Habič (1968) already thought the same about the uplift. In our article, we present a geological-structural view of the Trnovski gozd, Banjšice, and Šentviška Gora plateaus, which confirms some basic geographical findings but at the same time points to the possibility that the leveled area extended significantly further at the time of its formation than it does today.

Gravitational phenomena

Quaternary gravity-related phenomena are relatively well studied on the northeastern edge of the Vipava Valley, and research so far has shown that the structure and genesis of slope sediments

dolino. Dvig Trnovskega gozda, Banjšic in Šentviške planote se odraža v posebnostih njihove geomorfologije, ta se ne odraža samo v gravitacijskih pojavih, temveč, poleg drugega, tudi v intenzivnosti korozivne degradacije kraških uravnov na Zunanjedinarskem narivnem pasu, v tem primeru na Voglarski planoti na severozahodnem delu Trnovskega gozda, na jugovzhodnem delu Banjške planote ali Banjšic in na vzhodnem delu Šentviške planote. Pojav korozivne degradacije omenjenih uravnov izpeljujemo iz predpostavke, da so nastale na nižji nadmorski višini od današnje. Povečana stopnja korozije je posledica ostrejših klimatskih razmer, kar se najlepše opazi, ko obravnavane uravnane dele Zunanjedinarskega narivnega pasu (c, d, e) primerjamo z uravnanim Krasom, ki leži na nižji nadmorski višini (a, b) (sl. 2).

Trnovski gozd in Banjško planoto razmejuje suha dolina Čepovanski dol, po Dierks et al. (2021) pradol. Slednja je od Šentviške planote ločena z Idrijskim prelomom ter ob njem dvignjena za okoli 200 m.

Dviganje Trnovskega gozda in Banjške planote na današnji nivo se kaže že v samem obstoju Čepovanskega dola, ki ni mogel nastati na današnji nadmorski višini, ker nima hidrografskega zaledja.

Uravnano območje Trnovskega gozda in Banjšic sta Stepišnik in Ferk (2024, str. 12–13, 17–18) opredelila kot korozivni kraški ravnik, ki naj bi nastal v času pred dvigom Trnovskega gozda. Enako je o dvigu menil že Habič (1968). V našem članku podajamo geološko-strukturni pogled na kraške uravnave Trnovskega gozda, Banjšic in Šentviške planote, ki potrjuje osnovne geografske ugotovitve, hkrati pa kaže na možnost, da je imelo uravnano ozemlje ob svojem nastanku bistveno večji obseg od današnjega.

Gravitacijski pojavi

Kwartarni gravitacijski pojavi so na severovzhodnem robu Vipavske doline razmeroma dobro obdelani, dosedanje raziskave so pokazale, da je zgradba in geneza pobočnih sedimentov na tem območju izredno kompleksna. Pod celom paleogenskega narivnega roba se nahajajo obsežne akumulacije pobočnih sedimentov, ki so nastali z različnimi mehanizmi transporta in sedimentacijskimi procesi (Popit in Košir, 2003; Popit et al., 2013; Popit, 2016). Poleg regionalnih geoloških razmer, na mesta pojavljanja in vrsto pobočnih procesov neposredno vplivajo tudi krajevni strukturni, litološki, hidrološki in geokemični pogoji.

in this area is extremely complex. Extensive accumulations of slope sediments formed by various transport mechanisms and depositional processes (Popit in Košir, 2003; Popit et al., 2013; Popit, 2016) are present beneath the front of the Paleogene thrust margin. In addition to regional geological conditions, local structural, lithological, hydrological, and geochemical conditions also directly influence the places of occurrence and type of slope processes.

Quaternary slope sediments deposited below the thrust front margin appear in the highest parts of the slope in the form of scree patches and fans. These are related to the passes between the higher lying steep carbonate walls and the gentler flysch slope below them. The scree deposits cover a considerable area and are the main source of carbonate gravels, which is deposited further down the impermeable slope by various transport mechanisms and depositional processes. Numerous larger and smaller sedimentary bodies and blocks of Quaternary slope sediments cemented into slope breccia are deposited in the lower parts of the slope. The variability of Quaternary sediments in individual sedimentary bodies is extremely large, considering the geological structure of the territory. The origin of the material is represented by two main lithological differences: sediment consisting of siliciclastic flysch rocks (sandstone, siltstone, marl, and mudstone) from the flysch base and carbonate sediment from the carbonate hanging wall in the hinterland. Based on two lithological differences, the composition and structure of Quaternary sediments would be expected to be relatively simple. According to previous research, most of the profiles investigated in detail in the Rebrnice area beneath Mt. Nanos (Popit et al., 2013) and the Selo landslide (Košir & Popit, 2002; Popit & Košir, 2003; Verbovšek et al., 2017) revealed extraordinary stratigraphic variability and lateral diversity. Several distinctly layered sediments were recorded within the landslide masses, indicating several phases of sedimentation or events.

If we focus on the area between Ajdovščina and Nova Gorica (Fig. 3), the 10 km² complex Selo landslide stands out in terms of size and shape, according to Košir et al. (2015) and is described as a long runout rock avalanche. The Selo landslide measures approximately 4.5 km in length, with the distance from the crown to the toe end measuring 5.8 km. The average sediment thickness is estimated at 19 m, and the maximum measured sediment thickness in the central part is 56 m (Popit & Košir, 2003; Košir et al., 2015). The volume of the landslide, estimated with the help of

Kvartarni pobočni sedimenti, ki so odloženi pod čelom narivnega roba se v najvišjih delih pobočja pojavljajo v obliki meliščnih zaplat in pahljač. Ti so vezani na prevoje med višje ležečimi strmimi karbonatnimi stenami in položnejšim flišnim pobočjem pod njimi. Melišča obsegajo precejšnje območje in predstavljajo glavni vir karbonatnega grušča, ki se nadalje z različnimi mehanizmi transporta in sedimentacijskimi procesi odlaga nižje po neprepustnem pobočju. V nižjih delih pobočja so odložena številna manjša in velika sedimentna telesa in bloki kvartarnih pobočnih sedimentov mestoma sprijetih v pobočno brečo. Variabilnost kvartarnih sedimentov v posameznih sedimentnih telesih je glede na geološko zgradbo ozemlja izredno velika. Izvor materiala predstavljata dva glavna litološka različka: sediment sestavljen iz siliciklastičnih flišnih kamnin (peščenjak, meljevec, laporovec in muljevec) iz flišne podlage in karbonatni sediment iz karbonatne krovnine v zaledju. Na podlagi dveh litoloških različkov bi pričakovali, da bo sestava in zgradba kvartarnih sedimentov razmeroma enostavna. Po dosedanjih raziskavah pa se je v večini detajlno preiskanih profilov na območju Rebrnic pod Nanosom (Popit et al., 2013) in plazu Selo (Košir & Popit, 2002; Popit & Košir, 2003; Verbovšek et al., 2017) izkazala izjemna stratigrafska raznolikost in lateralna spremenljivost. Znotraj splazelih mas je bilo evidentiranih več izrazito plastnatih sedimentov, ki kažejo na več faz sedimentacije oziroma dogodkov.

Če se osredotočimo na območje med Ajdovščino in Novo Gorico (sl. 3), po velikosti in obliki močno izstopa 10 km² velik kompleksni plaz Selo, po Koširju et al. (2015) imenovan podorni tok velikega dosega (ang. long runout rock avalanche). Plaz Selo meri približno 4,5 km v dolžino, razdalja od odlomnega roba do največjega dosega plazu v dolini pa 5,8 km. Povprečna debelina sedimenta je ocenjena na 19 m, največja izmerjena debelina sedimenta v osrednjem delu pa 56 m (Popit & Košir, 2003; Košir et al., 2015). Volumen plazu, ki je bil ocenjen s pomočjo terenskega dela, radarskega profiliranja in GIS-a, znaša $190 \times 10^6 \text{ m}^3$ (Verbovšek et al., 2017).

Poleg manjših in večjih sedimentnih teles pahljačastih in jezičastih oblik se na pobočjih na celotnem severnem robu severovzhodnega dela Vipavske doline pogosto pojavljajo tudi planarne izravnave karbonatnih breč, nastale kot posledica velikih rotacijskih plazov, in posamezni večji ali manjši karbonatni bloki nastali z rotacijsko-translacijskimi zdrssi. Na podlagi plastnatosti breče na posameznih delih blokov lahko prepoznamo,

field work, GPR profiling, and GIS, is $190 \times 10^6 \text{ m}^3$ (Verbovšek et. al., 2017).

In addition to smaller and larger sedimentary fan- and tongue-shaped bodies, planar levelings of carbonate breccias, formed as a result of large rotational landslides, and individual larger or smaller carbonate blocks formed by rotational-translational landslides occur often on the slopes of the entire northern edge of the northeastern part of the Vipava Valley. Based on the layering of the breccia in individual parts of the blocks, we can recognize that the blocks rotated up to 60° towards the slope. Such an example occurs in the hinterland of the Šumljak landslide in Rebrnice (Popit, 2017). The leveled surface is developed mainly in the central parts of the planar surfaces, while steep margins appear on the outer parts of the levelings, which represent the main broken edges of the sedimentary bodies. These sedimentary bodies, especially in the upper part of the slope, were formed as a result of the remobilization of material from the outer parts of large rotational landslides, where the material was transported lower down the slope in the form of rock avalanches (Popit, 2017). In addition to planar levelings, individual carbonate partly-brecciated gravity blocks are exposed on the slopes in large numbers in the wider vicinity of Lokavec, but towards Šempeter they become smaller and less numerous. The exceptional amount and frequency of the occurrence of slope processes is indicated by e.g. the area around Ajdovščina, where there are many large sedimentary bodies along the edge of the Vipava Valley, e.g. the Podrta Gora and Gradiška Gmajna fossil landslides (Popit et al., 2022) and many large gravity (collapsing) carbonate blocks. Based on preliminary research by Placer et al. (2008), and later by Kocjančič et al. (2019), 10 carbonate gravity blocks. The results of the measurements showed that the lengths of the block movements along the slope ranged from 80 m to as much as 1,950 m (Kocjančič et al., 2019). The layered carbonate blocks changed their strike and dip when moving relative to the carbonate layers of the source area. Differences in the incidence of carbonate layers of the source area and carbonate blocks range from 4° to 59° . Larger gravity blocks that appear northwest of Lokavec are Zasod and Školj Sv. Pavla nad Vrtovinom (Verbovšek et al., 2019), Zasod pri plazu Selo, Kuclji nad Osekom, Vitovski hrib above the village of Vitovlje and many smaller translational gravity blocks (Fig. 6). To the northwest, the occurrence of carbonate blocks decreases considerably, and by the Lijak spring they are practically non-existent.

da so bloki rotirali tudi do 60° proti pobočju. Tak primer nastopa v zaledju plazu Šumljak na Rebrnicah (Popit, 2017). Izravnana površina je razvita predvsem v osrednjih delih planarnih površin, na zunanjih delih izravnava pa se pojavljajo strmi robovi, ki predstavljajo glavne odlomne robove sedimentnih teles. Ta sedimentna telesa, predvsem v zgornjem delu pobočja, so nastala kot posledica remobilizacije materiala z zunanjih delov velikih rotacijskih plazov, kjer se je material nato v obliki kamninskih plazov transportiral nižje po pobočju (Popit, 2017). Poleg planarnih izravnava so na pobočjih močno izpostavljeni posamezni karbonatni, deloma brečirani, gravitacijski bloki, ki se v velikem številu pojavljajo v širši okolini Lokavca, proti Šempetru pa jih je na pobočju vse manj tako po velikosti kot po njihovi številčnosti. Na izjemno količino in pogostnost pojavljanja pobočnih procesov kaže npr. območje v okolini Ajdovščine, kjer so vzdolž roba vipavske doline številna velika sedimentna telesa, npr. fosilni plaz Podrta Gora in Gradiška Gmajna (Popit et al., 2022) in številni veliki gravitacijski (podorni) karbonatni bloki. Na podlagi predhodnih raziskav Placerja in sodelavcev (2008), ter kasneje Kocjančičeve s sodelavci (2019), je bilo samo v okolini Lokavca identificiranih 10 karbonatnih gravitacijskih blokov. Rezultati meritev so pokazali, da so dolžine premikov blokov po pobočju znašale od 80 m do kar 1950 m (Kocjančič et al., 2019). Vpadi plastnih karbonatnih blokov so pri premiku, glede na karbonatne plasti izvornega območja, spremenili smer in naklon. Razlike pri vpadu karbonatnih plasti izvornega območja in karbonatnih blokov pa znašajo od 4° do 59° . Večji gravitacijski bloki, ki se pojavljajo severozahodno od Lokavca so Zasod in Školj Sv. Pavla nad Vrtovinom (Verbovšek et al., 2019), Zasod pri plazu Selo, Kuclji nad Osekom, Vitovski hrib nad Vitovljami in številni manjši translacijsko gravitacijski bloki (sl. 6). Severozahodneje se pojavnost karbonatnih blokov močno zmanjša in do izvira Lijaka jih praktično ni več.

Geomorfologija Trnovskega gozda, Banjšic in Šentviške planote

Ob pogledu na geološko karto Trnovskega gozda ter Banjške in Šentviške planote je že na prvi pogled jasno, da tvorita Trnovska in Banjška planota morfotektonski blok in da je bila nekoč Šentviška planota njegov del. Prvi dve geografsko ločuje Čepovanski dol, tretjo pa v geografskem in tektonskem pomenu od Banjšic ločuje dolina Idrije, ki si jo je izdolbla po coni Idrijskega preloma (sl. 2).

Geomorphology of the Trnovski gozd, Banjšice, and Šentviška Gora plateaus

Looking at the geological map of the Trnovski gozd and the Banjšice and Šentviška Gora plateaus, it is clear at first glance that the Trnovski gozd and Banjšice plateaus form one morphotectonic block, and that the Šentviška Gora plateau was once part

Vse tri planote so zgrajene pretežno iz karbonatnih kamnin (sl. 4), njihovo površje je razgibano, večji uravnani površini pa nastopata na Voglarski planoti na Trnovskem gozdu (c – zgornjejurski in spodnjekredni karbonati) in na jugovzhodnem delu Banjške planote (d – zgornjetriascni, jurski in spodnjekredni karbonati),

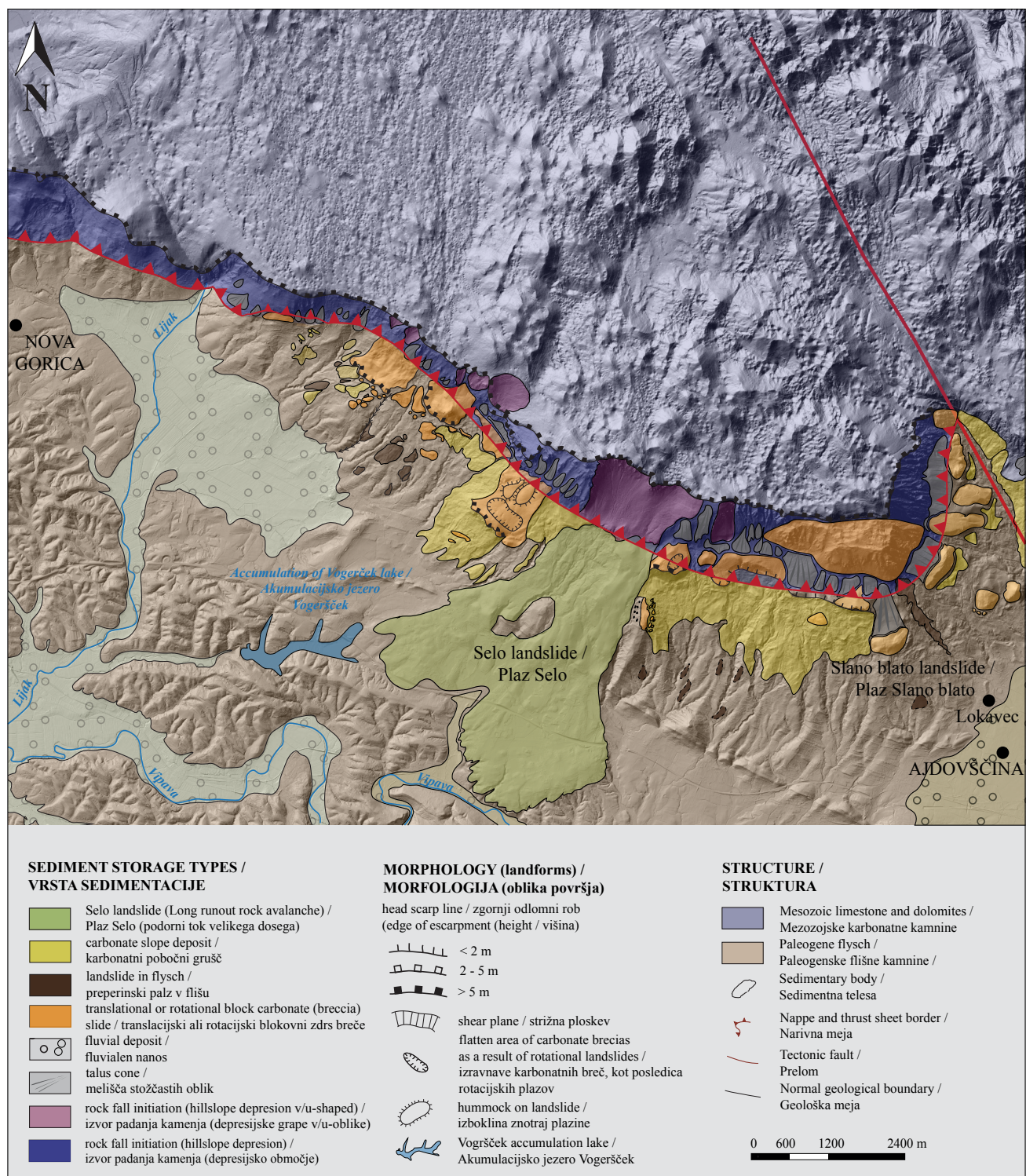


Fig. 3. Geomorphological map of the forehead of Trnovo Nappe between Lijak (spring) and Lokavec (village).

Sl. 3. Geomorfološka karta čela Trnovskega pokrova med Lijakom in Lokavcem.

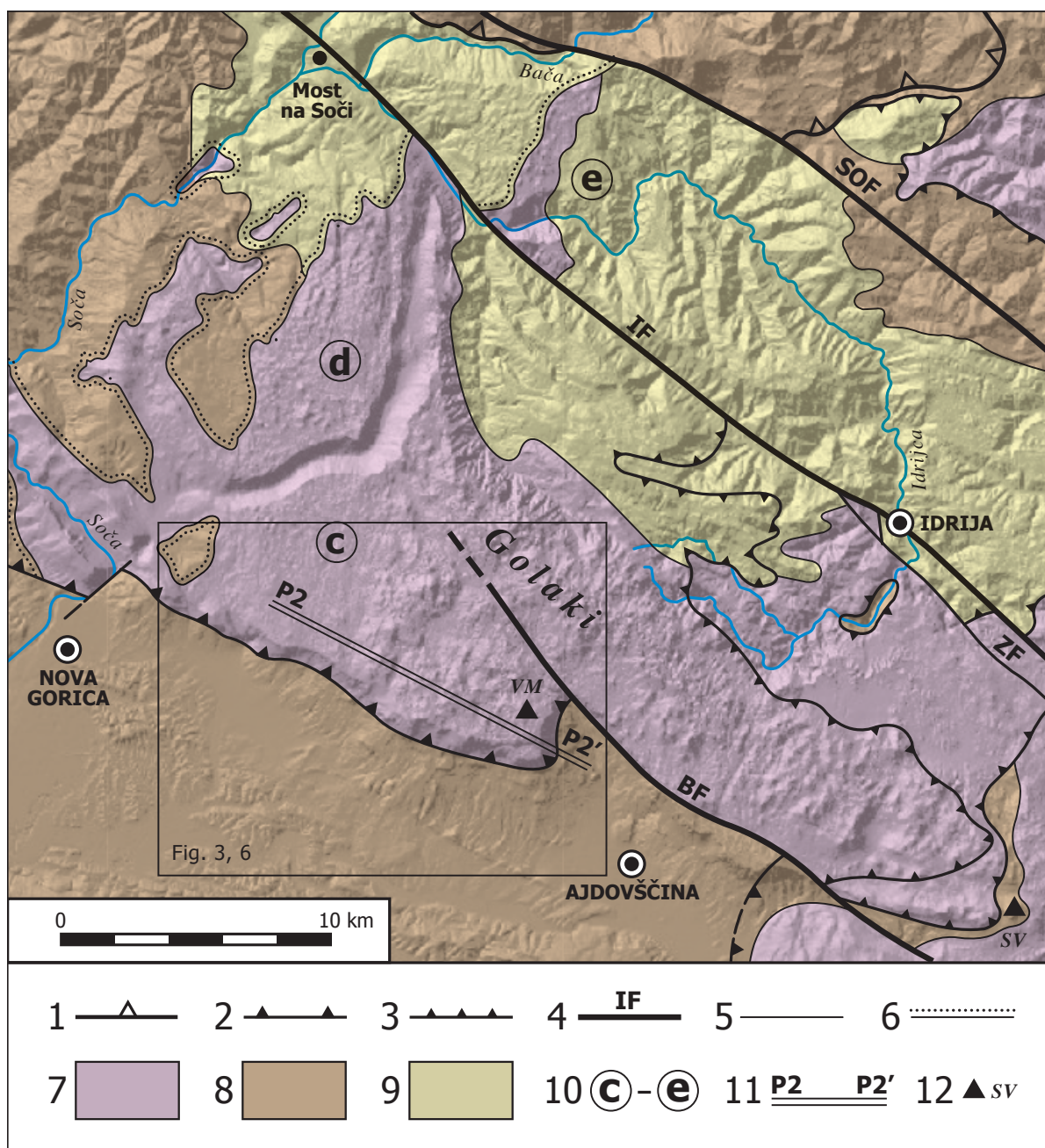


Fig. 4. Structural-lithological sketch of the Trnovski gozd, Banjšice, and Šentviška Gora plateaus. According to the Basic Geological Map of Yugoslavia 1:100 000 – OGK (sheet Gorica: Buser, 1968; sheets Tolmin in / and Videm (Üdine): Buser, 1987; sheet Kranj: Grad & Ferjančič, 1974; sheet Postojna: Buser, Grad & Pleničar, 1967), Mlakar (1969, fig. 5, fig. 8), and Placer (1973, fig. 2).

Sl. 4. Strukturno-litološka skica Trnovske, Banjške in Šentviške planote. Po podatkih Osnovne geološke karte SFRJ 1:100 000 - OGK (list Gorica: Buser, 1968; lista Tolmin in Videm: Buser, 1987; list Kranj: Grad & Ferjančič, 1974; list Postojna: Buser, Grad & Pleničar, 1967), Mlakarja (1969, sl. 5, sl. 8) in Placerja (1973, sl. 2).

1 Thrust boundary of Southern Alps / narivna meja Južnih Alp

2 Boundary of the External Dinaric Thrust Belt / meja Zunanjedinarskega narivnega pasu

3 Boundary of the nappe unit within the External Dinaric Thrust Belt / meja krovne enote znotraj Zunanjedinarskega narivnega pasu

4 Fault: **SOF** – Sovodenj Fault, **IF** – Idrija Fault, **ZF** – Zala Fault, **BF** – Belsko Fault (Placer et al., 2021, fig. 6, p. 44; Buser, 1976, p. 50, Predjama Fault) / prelom: **SOF** – Sovodenjski prelom, **IF** – Idrijski prelom, **ZF** – Zalin prelom, **BF** – Belski prelom (Placer et al., 2021, sl. 6, str. 44; Buser, 1976, str. 50, Predjamski prelom)

5 Geological boundary / konkordantna geološka meja

6 Unconformity / diskordantna geološka meja

7 Predominantly carbonates / pretežno karbonati: **T₃²⁺³, J, K₁, P_c, E₁**

8 Predominantly clastites / pretežno klastiti: **C, P₁, K₂, P_c, E**

9 Carbonates and clastites / karbonati in klastiti: **P₂, T₁₊₂, T₃¹, K₂**

10 Karst plain: **c** – Voglarska planota (Voglarski plateau), **d** – southeastern part of Banjšice (Banjšice plateau), **e** – eastern part of Šentviška planota (Šentviška Gora plateau) / kraška uravnava: **c** – Voglarska planota, **d** – jugovzhodni del Banjšice planote, **e** – vzhodni del Šentviške planote

11 Position of profile **P2 – P2'** / lega profila P2 – P2'

12 Top / vrh: **VM** – Veliki Modrasovec (1355 m), **SV** – Streliški vrh (1266 m)

of it. The first two are geographically separated by the Čepovanski dol (dry valley), and the third is separated from Banjšice in a geographical and tectonic sense by the Idrijca River Valley, which was carved out along the Idrija fault zone (Fig. 2).

All three plateaus are built mainly of carbonate rocks (Fig. 4), their surface is rugged, and larger level surfaces occur on the Voglarji plateau in the Trnovski gozd plateau (c – Upper Jurassic and Lower Cretaceous carbonates) and on the south-eastern part of the Banjšice plateau (d – Upper Triassic, Jurassic and Lower Cretaceous carbonates), and a smaller one in the eastern part of the Šentviška Gora plateau (e – Upper Triassic carbonates). Stepišnik and Ferk (2023, p. 13–14) considered the leveled part in question (which is also called the Banjšice-Trnovski gozd plain in the geographical literature) a corrosive karst plain, which rises above the primary level due to tectonic processes. Habič (1968) also thought the same.

For a complex understanding of the geomorphology, in addition to the corrosive influence, it is also necessary to take into account the structural and tectonic aspects of the genesis of the territory, which are significantly supplemented with respect to older interpretations. Therefore, we examine Trnovski gozd, and the Banjšice and Šentviška Gora plateaus from the point of view of recent research. The most important question is whether the non-peneplained areas of the plateaus under consideration were once peneplained. On the shaded digital elevation model (DMV) obtained from lidar data, three basic structural-morphological surface types can be observed on the mentioned plateaus (Fig. 4): 1. an otherwise leveled (peneplained) but corrosively affected surface, on which morphologically poorly responsive cracks in the SSW-NNE direction are noticeable, 2. sharply furrowed surface along a fracture system in the SSW-NNE direction in Trnovski gozd, which stretches from the boundary of the leveled (peneplained) Voglarji plateau to Veliki Modrasovec (1355 m) and Streliski vrh (1266 m) and 3. the softer, irregularly corroded and eroded surface on the western part of the Banjšice and Šentviška Gora plateaus, on which various structural forms such as folds, layers, and fractures can be observed. The narrow strip of peneplained territory on the southwestern side of the Trnovski gozd plateau from Predmeja to Vodice is not covered in this article, as such would require a broader structural interpretation.

We know from general data that carbonate rocks are more prone to corrosion, limestones more than

manjša pa na vzhodnem delu Šentviške planote (e – zgornjetriiasni karbonati). Del obravnavanega uravnanevga sveta, ki je v geografski literaturi poimenovan tudi Banjško-trnovski ravnik, sta Stepišnik in Ferk (2023, str. 13–14) obravnavala kot korozijsko kraško uravnavo, ki je zaradi tektonskih procesov dvignjena nad primarni nivo. Enako je menil tudi Habič (1968).

Za kompleksno razumevanje geomorfologije je poleg korozivnega vpliva potrebno upoštevati tudi strukturni in tektonski vidik geneze ozemlja, ki sta glede na starejše interpretacije bistveno dopolnjena. Zato si oglejmo Trnovski gozd ter Banjško in Šentviško planoto z vidika novejših raziskav. Kot najpomembnejše se postavlja vprašanje ali so bila neuravnana območja obravnavanih planot nekoč uravnana. Na senčenem digitalnem modelu višin (DMV) pridobljenem iz lidarskih podatkov je na omenjenih planotah opaziti tri osnovne strukturno-morfološke tipe površja (sl. 4): 1. sicer uravnano toda korozivno prizadeto površje, na katerem so opazne morfološko slabo odzivne razpoke v smeri SSW-NNE, 2. ostro razbrzdano površje po sistemu razpok v smeri SSW-NNE na Trnovskem gozdu, ki se razteza od meje uravnane Voglarske planote do Velikega Modrasovca (1355 m) in Streliskega vrha (1266 m) in 3. mehkejše nepravilno kordirano in erodirano površje na zahodnem delu Banjške in Šentviške planote, na katerem je opaziti različne strukturne oblike kot gube, plasti in prelome. Ožji pas uravnane ozemlja na jugozahodni strani Trnovske planote od Predmeje do Vodic v tem članku ni zajet, ker bi to zahtevalo širšo strukturno razlagajo.

Iz splošnih podatkov vemo, da so koroziji najbolj podvržene karbonatne kamnine, bolj apnenci kot dolomiti, manj klastične kamnine, vendar so erozijsko manj odporne, zato je na sl. 4 prikazana strukturno-litološka skica na kateri so izrisane meje treh skupin kamnin, pretežno karbonatnih, pretežno klastičnih in mešanih. Razdelitev je groba in namenjena le predstavitvi v tem članku obravnavanih vprašanj. Če se omejimo samo na Trnovski gozd, Banjšice in Šentviško planoto, je uravnano površje razvito pretežno na karbonatnih kamninah zgornjetriiasne, jurske in kredne starosti. Enako velja za močno razgibano površje. Mehkejše razgibano površje pa je razvito na območjih z mešanimi in klastičnimi kamninami zgornjekredne in paleogenske starosti.

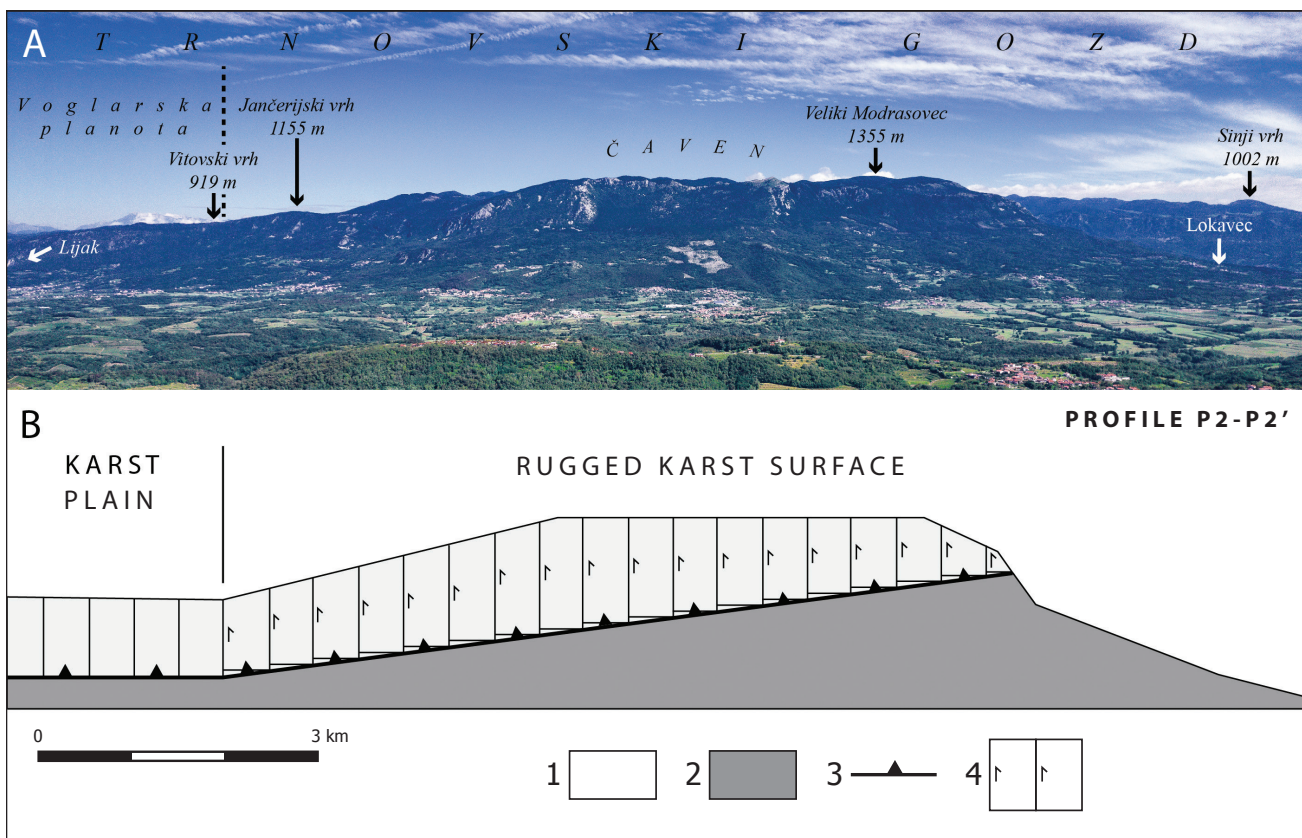


Fig. 5. Geomorphological profile P2 – P2': Voglarska planota (Voglarji plateau) – Čaven (ridge) – Veliki Modrasovec (1355 m) – Lokavec (village). Position of profile in fig. 4.

Sl. 5. Geomorfološki profil P2 – P2': Voglarska planota – Čaven – Veliki Modrasovec – Lokavec. Lega profila na sl. 4.

A – Panoramic shot of the thrust face of Trnovo Nappe. Recording location in fig. 2 / Panoramski posnetek narivnega čela Trnovskega pokrova. Stojišče snemanja na sl. 2.

B – Geomorphological profile P2 – P2' as a kinematic model of this part of the Trnovo Nappe. Profile runs perpendicular to the regional sub-vertical fractures in direction SSW-NNE / Geomorfološki profil P2 – P2' kot kinematski model tega dela Trnovskega pokrova. Profil poteka pravokotno na regionalne subverticalne razpoke v smeri SSW-NNE.

1 Carbonates / karbonati

2 Clastites (flysch) / klastiti (fliš)

3 Thrust fault surface of the Trnovo Nappes / narivna ploskev Trnovskega pokrova

4 Kinematics of regional sub-vertical fractures in direction SSW-NNE / kinematika regionalnih subvertikalnih razpok v smeri SSW-NNE

dolomites, and clastic rocks less so, but they are less resistant to erosion; so in Figure 4 a structural-lithological sketch on which the boundaries of three groups of rocks, predominantly carbonate, predominantly clastic and mixed, are drawn. The division is rough and intended only to present the issues discussed in this article. If we limit ourselves to Trnovski gozd, and the Banjšice and Šentviška Gora plateaus, the flat surface is developed mainly on carbonate rocks of Upper Triassic, Jurassic, and Cretaceous age. The same applies to highly uneven surfaces. A softer rugged surface is developed in areas with mixed and clastic rocks of Upper Cretaceous and Paleogene age.

How then do we approach the question of whether the entire area of the Trnovski gozd plateau and the Banjšice and Šentviška Gora plateaus was completely levelled before some certain time, or before the uplift of the territory? On all three

S čim torej utemeljujemo vprašanje ali je bilo celotno območje Trnovskega gozda ter Banjšice in Šentviške planote pred določenim časom, oziroma pred dvigom ozemlja, v celoti uravnano? Na vseh treh planotah, kjer nastopajo karbonatne kamnine, izstopa sistem enako usmerjenih razpok v smeri SSW-NNE, ki pa je na uravnanih delih komaj ali slabo viden, na razgibanih delih pa predstavlja glavno strukturno diskontinuiteto po kateri se je oblikovalo površje. V tem smislu je najbolj povedno ozemlje Voglarske planote in Čavna do Velikega Modrasovca (1355 m) za katerega je izdelana geomorfološka karta na sl. 3. Pri predpostavki, da je bilo celotno območje uravnano na nižjem nivoju in pozneje dvignjeno, postavljamo domnevo, da je bilo dviganje neenotno, uravnani del Trnovskega gozda (Voglarska planota) se je dvigal enakomerno, območje jugovzhodno od tod pa neenakomerno

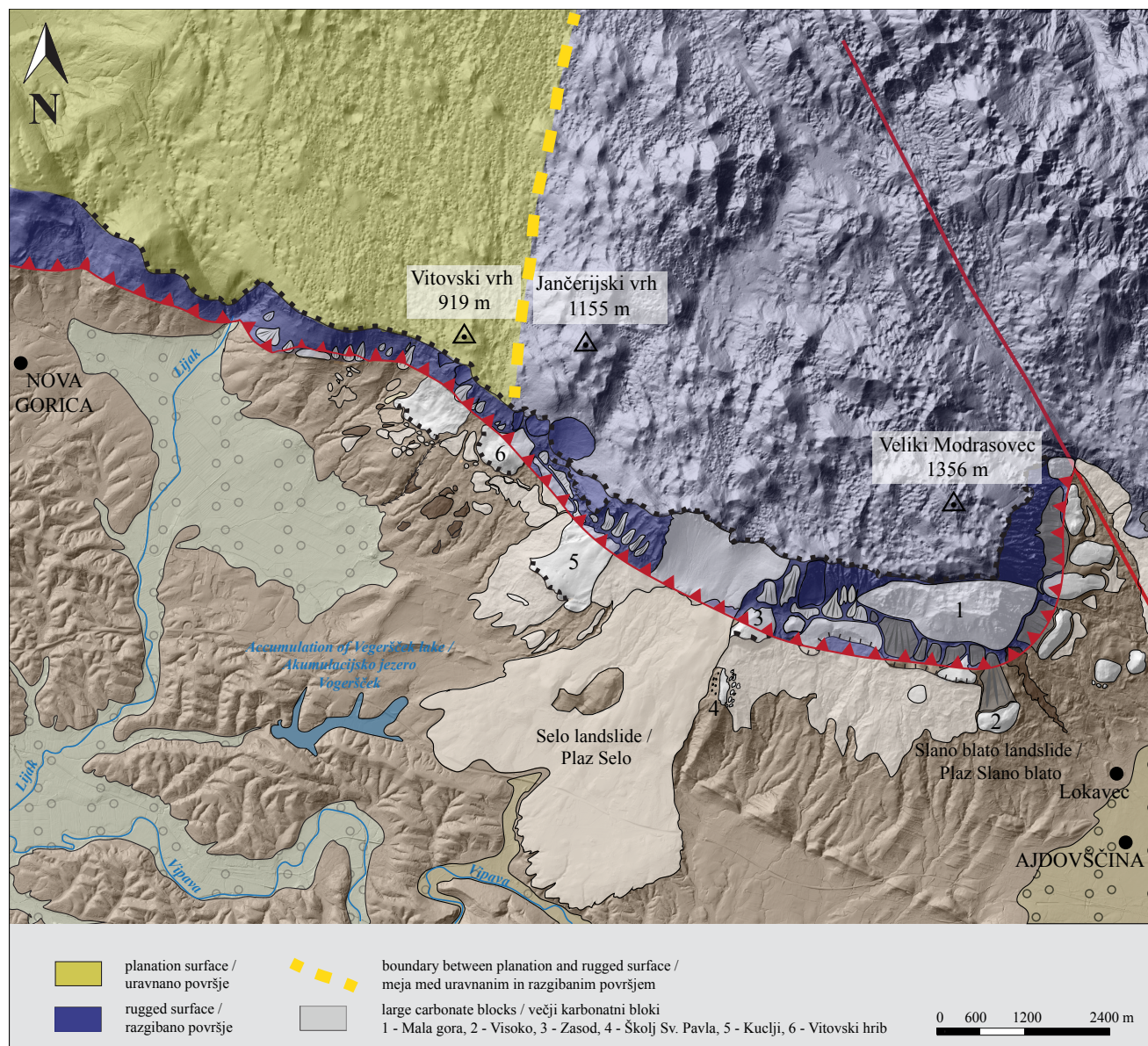


Fig. 6. Relation between geomorphology of Trnovski gozd (Trnovski gozd plateau) and gravitational phenomena.
Sl. 6. Povezava med geomorfologijo Trnovskega gozda in gravitacijskimi pojavji.

plateaus where carbonate rocks occur a system of similarly oriented fractures in the SSW-NNE direction stands out, which, however, is only barely visible on the levelled parts, and on the rugged parts represents the main structural discontinuity along which the surface was formed. In this sense, the most telling area is the territory of Voglarji plateau, Mt. Čaven and Mt. Veliki Modrasovec (1355 m), for which the geomorphological map in fig. 3. is elaborated. On the assumption that the entire area was levelled at a lower level and later uplifted, we suggest that the uplift was uneven, the levelled part of Trnovski gozd (Voglarji plateau) uplifted evenly, and the area southeast of it uplifted faster and unevenly, which resulted in successive movements along the exposed fracture system and a certain degree of crushing. This was followed by

in hitreje, zaradi česar je prišlo do nasledstvenih premikov po izpostavljenem sistemu razpok in določene stopnje drobljenja. Temu je sledila izdatnejša korozija. Učinek tega procesa je prikazan na sl. 5, panoramskemu posnetku na sl. 5A je priložena grobo shematisirana kinematska skica opisanega dogajanja v profilu med Voglarsko planoto in Velikim Modrasovcem na sl. 5B. Bloki (makrolitoni) med razpokami sistema SSW-NNE so na Voglarski planoti ostali nepremaknjeni, jugovzhodno od tod pa je med njimi prišlo do premikanja. Posledice opisanega stanja so prikazane na sl. 6, kjer so večji gravitacijski karbonatni bloki posejani le po pobočju pod robom planote z razgibanim reliefom, medtem ko jih pod robom uravnane Voglarske planote ni. Meja med obema tipoma reliefsa je zazna-

more extensive corrosion. The effect of this process is shown in Figure 5. A roughly schematic kinematic sketch of the described event in the profile between Voglarji plateau and Veliki Modrasovec in Figure 5B is attached to the panoramic snapshot in Figure 5A. The blocks (macrolithons) between the fractures of the SSW-NNE system remained unmoved on the Voglarji plateau, but movement took place between them southeast of the area. The consequences of the described condition are shown in Figure 6, where larger gravity carbonate blocks are only scattered along the slope below the edge of the plateau with rugged relief, while they are absent below the edge of the flat Voglarji plateau. The border between the two types of relief is marked by a yellow dashed line running in the SSW-NNE direction of fractures, which is why it is almost flat and, in our opinion, indirectly proves

movana z rumeno prekinjeno črto, ki poteka v smeri razpok SSW-NNE, zaradi tega je skoraj ravna in po našem mnenju posredno dokazuje, da je na tem mestu razpoklinski sistem glavni usmerjevalec geomorfološke podobe površja. Kot navidezna izjema deluje plazišče severozahodno od Vitovlja, vendar leži pod Vitovskim vrhom (919 m), za katerega menimo, da je nastal kot posledica selektivne korozije. Osameli griči so namreč pogost pojav velikih kraških uravnnav.

Profil P2 – P2' na sl. 5B je v kinematskem smislu soroden vzdolžnemu profilu P1 – P1' (sl. 7) na jugovzhodnem delu bližnjega Nanosa (sl. 2), kjer obstaja enak sistem regionalnih razpok v smeri SSW-NNE (Placer et al., 2021a, sl. 11, profil 1a). Enake razmere obstojajo tudi na ostalem delu Trnovskega gozda do Streliškega vrha (1266 m) (sl. 4).

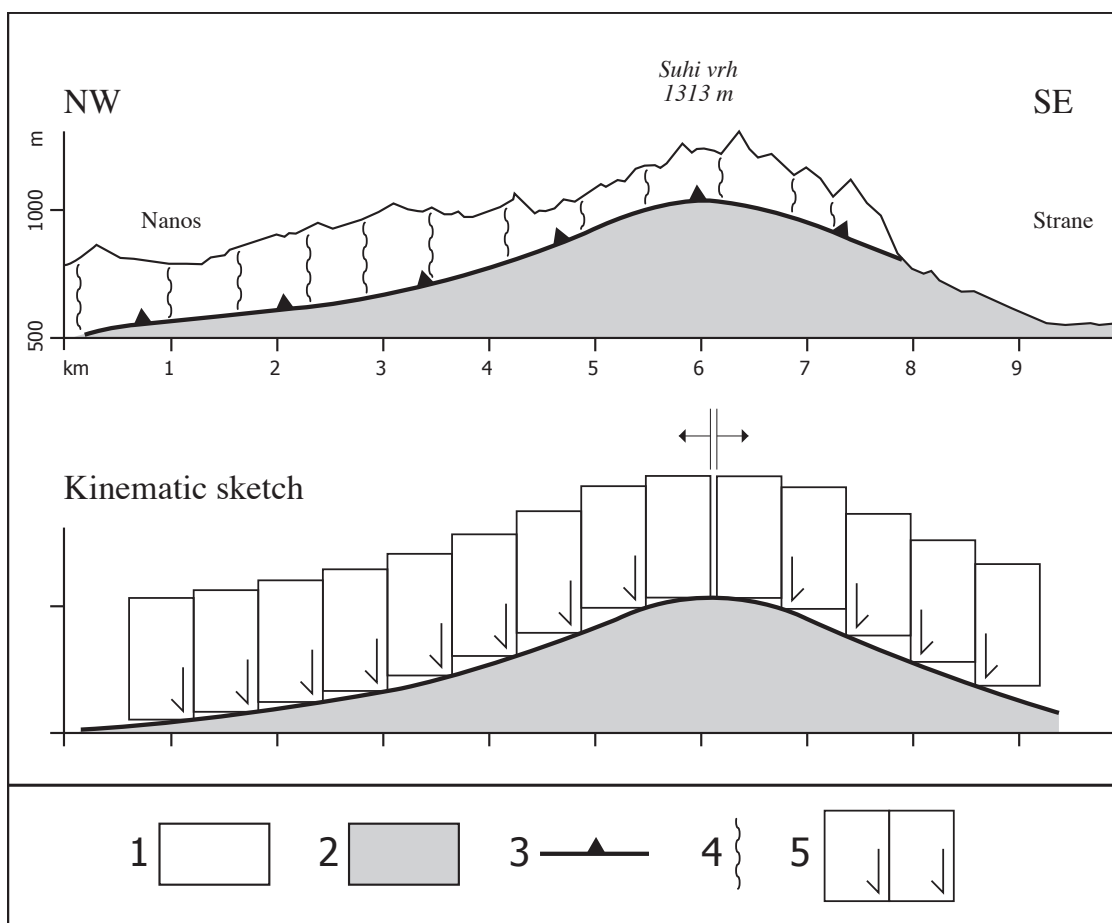


Fig. 7. Geomorphological profile P1 – P1' as a kinematic model of Hrušica Nappe unit at the southeastern end of Nanos plateau. The profile runs perpendicular to the regional sub-vertical fractures SSW-NNE. After Placer et al. (2021, fig. 11, profile 1a), Nanos (hamlet) – Strane (village). Position of profile in Fig. 2.

Sl. 7. Geomorfološki profil P1 – P1' kot kinematski model krovne grude Hrušičkega pokrova na jugovzhodnem koncu planote Nanos. Profil poteka pravokotno na regionalne subvertikalne razpoke SSW-NNE. Povzeto po Placer et al. (2021, sl. 11, profil 1a), Nanos (zaselek) – Strane (vas). Lega profila na sl. 2.

1 Carbonate / karbonati

2 Clastites (flysch) / klastiti (fliš)

3 Thrust surface of the Hrušica Nappe / narivna ploskev Hrušičkega pokrova

4 SSW-NNE system fracture / razpoka sistema SSW-NNE

5 Kinematics of regional subvertical fractures SSW-NNE / kinematika regionalnih subvertikalnih razpok SSW-NNE

that the fracture system is the main guide of the geomorphological surface image at this place. As an apparent exception, there is a landslide northwest of Vitovlje, but it lies below Mt. Vitovski vrh (919 m) which we believe was formed as a result of selective corrosion. Inselbergs are a frequent feature of large karst formations.

Profile P2 – P2' in fig. 5B is kinematically related to the longitudinal profile P1 – P1' (Fig. 7) in the southeastern part of nearby Mt. Nanos (Fig. 2), where the same system of regional fractures in the SSW-NNE direction exists (Placer et al., 2021a, Fig. 11, profile 1a). The same conditions also exist in the rest of the Trnovski gozd plateau up to Mt. Streliški vrh (1266 m) (Fig. 4).

In the area of rugged relief, the ridge of Mt. Veliki Golak and Mt. Mali Golak (Fig. 4) stands out, along with some peaks or groups of peaks raised above the surroundings. The Mt. Veliki and Mali Golak ridge was formed during a long period of selective corrosion because it lies in the area of Lower and Middle Jurassic carbonates, which in some places are relatively less soluble than those from the Upper Jurassic. Individual peaks or groups of peaks outside the ridge are the result of the general post-thrust structural and geomorphological development of the Trnovski gozd plateau, when successive and new deformations occurred. Glaciation also had a part in shaping the surface (Kodelja et al., 2013).

Čepovanski dol (Dry Valley)

The Čepovanski dol dry valley is a witness to the tectonic events in the wider area. The valley's essential characteristics consist in a river that ran along it, and that it is tectonically raised together with the Trnovski gozd and Banjšice plateaus in the northeast above the Šentviška Gora plateau and in the southwest above the Vipava Valley. Above the Šentviška Gora plateau, it is raised along the Idrija Fault, and above the Vipava Valley the uplift is the result of a temporally, dynamically, and kinematically complex post-thrust Neogene-recent process. In this article the process itself is not discussed, only its consequences are pointed out. As a result, the relief elevation above the Vipava Valley is not comparable to the elevation of the relief along the Idrija Fault.

Let's take a look at the Idrija fault. According to Mlakar (1964), the horizontal component of the offset along the fault is about 1950 m in Idrija. The horizontal component of the offset according to Placer (1982, p. 57) is about 2360 m, but this length also includes offsets along the Zala Fault and parallel faults between Zala and Idrija Faults

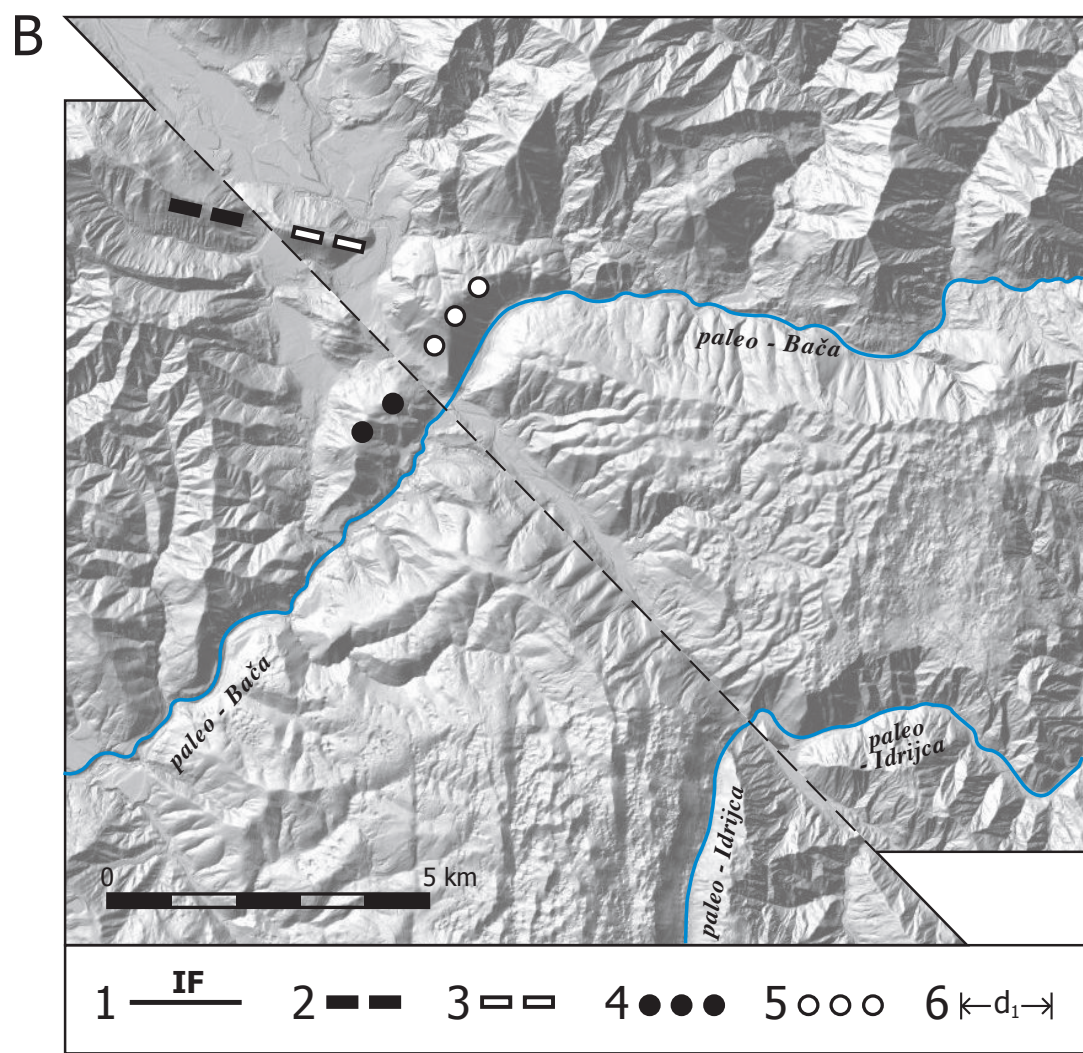
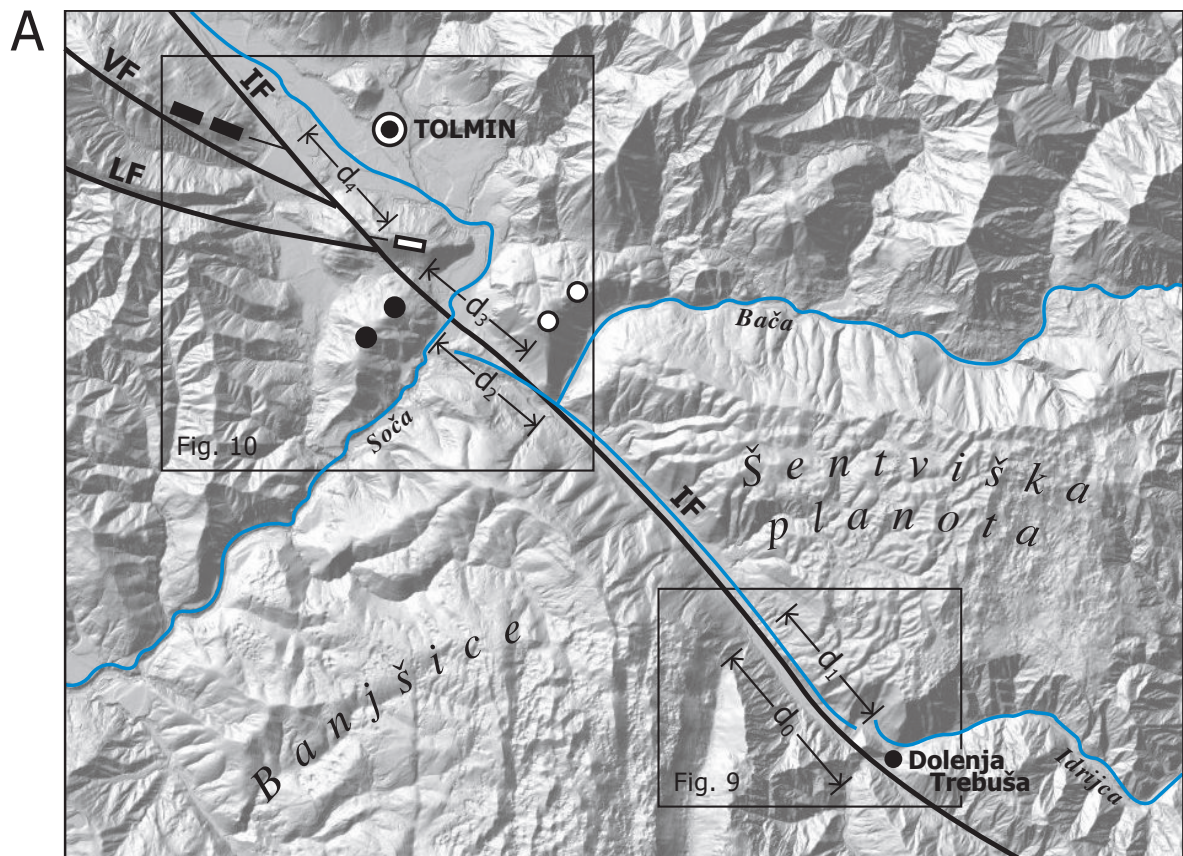
Na območju razgibanega reliefa izstopa npr. greben Golakov (sl. 4), ki leži v smeri slemenitve plasti NW-SE in nekaj vrhov ali skupin vrhov dvignjenih nad okolico. Greben Golakov je nastal skozi dolgo obdobje selektivne korozije, ker leži v območju spodnje in srednjejurskih karbonatov, ki so ponekod relativno slabše topni od zgornjejurskih. Posamezni vrhovi ali skupine vrhov izven Golakov pa so posledica splošnega postnaravnega strukturnega in geomorfološkega razvoja Trnovskega gozda, ko so nastale nasledstvene in nove deformacije. Svoj delež pri oblikovanju površja je imela tudi poledenitev (Kodelja et al., 2013).

Čepovanski dol

Čepovanski dol je pričevalec tektonskega dogajanja na širšem prostoru. Njegovi bistveni značilnosti sta, da je po njem tekla reka, in da je skupaj s Trnovsko in Banjško planoto tektonsko dvignjen; na severovzhodu nad Šentviško planoto, na jugozahodu nad Vipavsko dolino. Nad Šentviško planoto je dvignjen ob Idrijskem prelomu, nad Vipavsko dolino pa je dvig posledica časovno, dinamsko in kinematsko kompleksnega postnaravnega neogensko-recentnega procesa, ki ga v tem članku ne obravnavamo, temveč le opozarjam na njegove posledice. Dvig nad Vipavsko dolino zaradi tega ni primerljiv z dvigom ob Idrijskem prelomu.

Oglejmo si Idrijski prelom, v Idriji znaša horizontalna komponenta premika ob njem po Mlakarju (1964) okoli 1950 m, po Placerju (1982, str. 57) okoli 2360 m, vendar so v to dolžino všteti tudi premiki ob Zalinem prelomu in vzporednih prelomih med Zalinim in Idrijskim prelomom. Torej premiki ob glavni prelomni coni in ob prelomih ožjega dela idrijske izravnalne zgradbe (Placer et al., 2021b, 239). Celočni premik ob idrijski izravnalni zgradbi pa je nekaj večji, saj bi morali vrednosti 2360 m prišteti še premike širšega dela izravnalne zgradbe, kot sledi iz podatkov Geološke karte idrijsko-žirovskega hribovja med Stopnikom in Rovtami 1:25 000 (Čar, 2010). Velikost teh pa ni znana, le sklepamo lahko na okoli 100 do 200 m. Mlakarjev podatek je vezan le na premik ob glavni prelomni coni. V Idriji je severovzhodno krilo ugreznjeno, višina strukturnega skoka znaša v Idriji okoli 480 m (Placer, ibid.), vendar je ta podatek navidezen, prava višina je bistveno manjša, vendar ni bila določena.

V našem primeru opisujemo razmere med Tolminom in Dolenjo Trebušo (sl. 8A). Pri Dolenji Trebuši (sl. 9) poteka Idrijski prelom po dolini



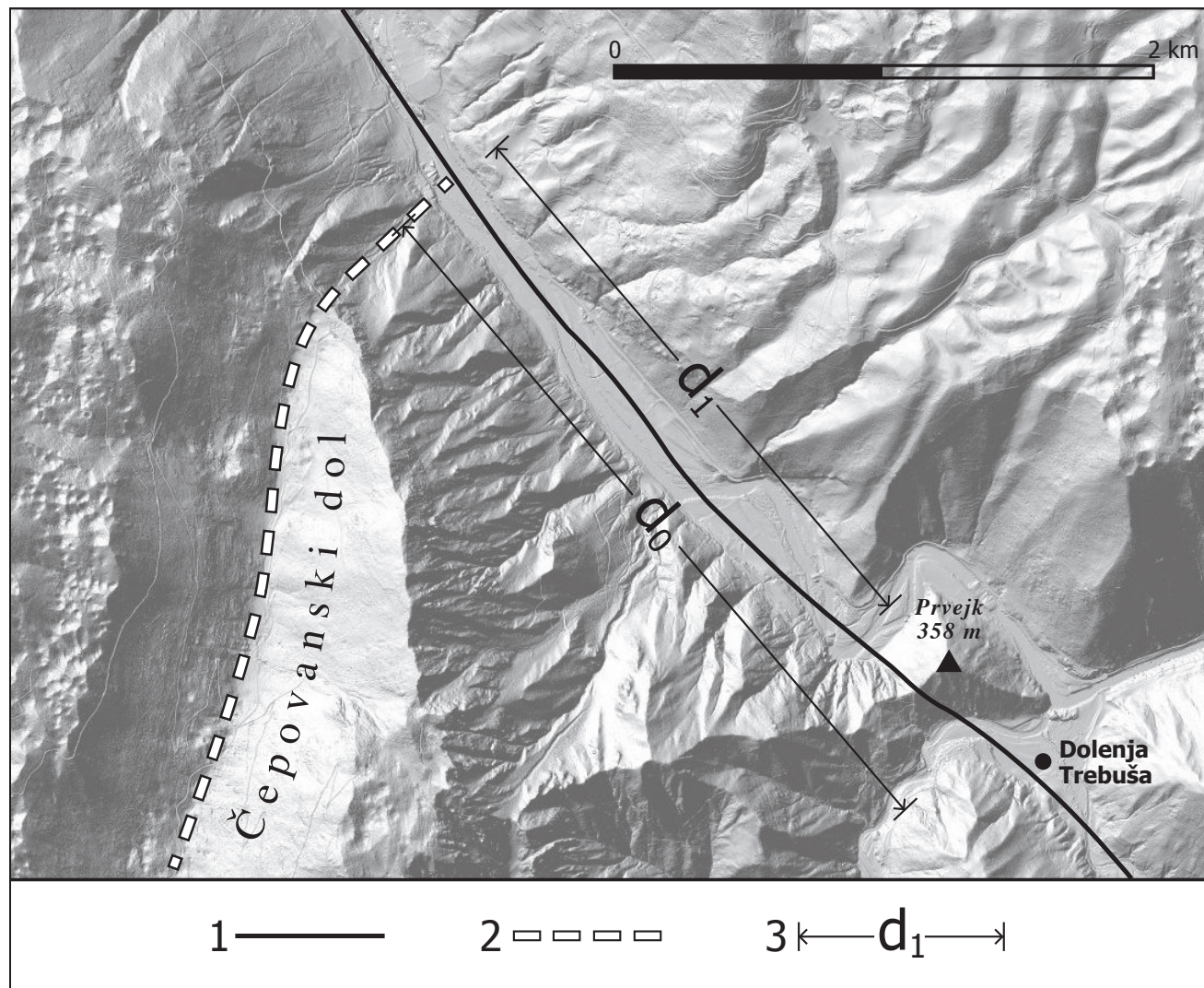


Fig. 9. Corrosive record of the Čepovanski dol (Čepovan dry valley) floor in the left slope of the Idrijca Valley indicating a connection with the Idrijca Valley under the northwestern slope of the Prvejk hill (358 m). Position of figure in fig. 8A.

Sl. 9. Korozivni odtis dna Čepovanskega dola v levem pobočju doline Idrijce, ki kaže na povezavo z dolino Idrijce pod severozahodnim pobočjem Prvejka (358 m). Lega slike na sl. 8A.

1 Idrija Fault, approximate position of the main fault zone / Idrijski prelom, približna lega glavne prelomne cone

2 Čepovanski dol (Čepovan dry valley) floor / dno Čepovanskega dola

3 Horizontal component of displacement along the Idrija Fault: **d0** – the entire movement, **d1** – segment movement / vodoravna komponenta premika ob Idrijskem prelomu: **d0** – celotni premik, **d1** – segmentni premik

Fig. 8. The influence of the Idrija Fault on the formation of the relief between Tolmin (town) and Dolenja Trebuša (village). Position of figure in fig. 2.

Sl. 8. Vpliv Idrijskega preloma na oblikovanje reliefsa med Tolminom in Dolenjo Trebušo. Lega slike na sl. 2.

A – Current situation / Sedanje stanje.

B – Situation before the formation of the Idrija Fault / Stanje pred nastankom Idrijskega preloma.

1 Fault: visible, covered or assumed: IF – Idrija Fault, VF – Volče Fault, LF – Livek Fault / prelom: viden, prekrit ali domneven: IF – Idrijski prelom, VF – Volčanski prelom, LF – Livški prelom

2 Hlevnik ridge (886 m) - Senica (576 m) / greben Hlevnik (886 m) - Senica (576 m)

3 Bučenica ridge (498 m) / greben Bučenica (498 m)

4 Selski vrh ridge (588 m) - Mrzli vrh (590 m) / greben Selski vrh (588 m) - Mrzli vrh (590 m)

5 Senica ridge (658 m) / greben Senica (658 m)

6 Horizontal component of the dextral movement of the valleys and ridges that were transversely cut by the Idrija Fault: **d0** – Idrijca Valley, Dolenja Trebuša ↔ Čepovanski dol (Čepovan dry valley), **d1** – Idrijca Valley, Mt. Prvejk ↔ Čepovanski dol, **d2** – Bača Valley ↔ Soča Valley, **d3** – Senica (658 m) ridge ↔ Selski vrh (588 m) – Mrzli vrh (590 m) ridge, **d4** – Bučenica (498 m) ridge ↔ Hlevnik (886 m) – Senica (576 m) ridge; **d1** ≈ **d2** ≈ **d3** ≈ **d4** ≈ 2200 m / vodoravna komponenta desnega premika dolin in grebenov, ki jih je prečno presekal Idrijski prelom: **d0** – dolina Idrijce, Dolenja Trebuša ↔ Čepovanski dol, **d1** – dolina Idrijce, Prvejk ↔ Čepovanski dol, **d2** – dolina Bače ↔ dolina Soče, **d3** – greben Senica (658 m) ↔ greben Selski vrh (588 m) - Mrzli vrh (590 m), **d4** – greben Bučenica (498 m) ↔ greben Hlevnik (886 m) - Senica (576 m); **d1** ≈ **d2** ≈ **d3** ≈ **d4** ≈ 2200 m

and represents the sum of offsets along the Idrija main fault zone and the offsets in the narrower zone of the Idrija adjusting structure (Placer et al., 2021b, 239). The total offset along the Idrija adjusting structure is somewhat larger, as the offsets of the wider part of the adjusting structure, should be added to the value of 2360 m as follows from the data of the Geological map of the Idrija-Žirovski vrh between Stopnik and Rovte in the 1:25,000 scale (Čar, 2010). The size of these is not known, but we can only conclude that they sum to around 100 to 200 m. Mlakar's information is only related to movement along the main fault zone. In Idrija, the northeastern block (of the Idrija Fault) is subsided, the height of the structural offset in Idrija is around 480 m (Placer, ibid.), but this information is easily available; the true height is significantly lower, but was not determined.

For our purposes, the situation between Dolenja Trebuša and Tolmin is described (Fig. 8A). At Dolenja Trebuša (Fig. 9) the Idrija Fault runs along the Hotenja Valley, across the saddle on Mt. Prvejk (358 m) and further towards Tolmin along the Idrijca Valley. The horizontal displacement along it has two measurable values, the first one is the distance between the axis of the outlet of Čepovanski dol in the left slope of the Idrijca Valley, and the axis of the Idrijca Valley northwest of Mt. Prvejk, which is denoted by d1 (around 2200 m), the second is the distance between the bottom of Čepovanski dol and the extension of the Idrijca Valley southeast of Mt. Prvejk, which is marked with d0 (around 2650 m). The distance of 2650 m is close to the total displacement in Idrija $2360 + 100$ to 200 m = 2460 to 2560 m and represents the entire displacement in the area of Dolenja Trebuša, however, we will see that the 2200 m displacement is more important for the interpretation of the relief between Dolenja Trebuša and Tolmin. The discussion about the structure of the fault zone of the Idrija Fault and the formation of the valley network around Dolenja Trebuša is beyond the scope of this article, but the important fact is that the displacement d1 (2200 m) is also reflected in the relief around Tolmin. When the axis of the Idrijca Valley on the northwestern side of Mt. Prvejk is placed opposite the bottom of the corrosive imprint of Čepovanski dol, the mouth of the Bača River is positioned opposite the middle part of the Soča Valley near the village of Most na Soči (Fig. 8B). This probably means that the Idrija Fault was originally segmented, with two segments meeting at Dolenja Trebuša, which today are combined into a single zone. This question cannot be solved without detailed mapping, which is why the area around Dolenja Trebuša in Fig. 8B is structur-

Hotenje, čez sedlo na Prvejku (358 m) in naprej proti Tolminu po dolini Idrijce. Horizontalni premik ob njem ima dve izmerljivi vrednosti, prva je razdalja med osjo izteka Čepovanskega dola v levem pobočju doline Idrijce in osjo doline Idrijce severozahodno od Prvejka, kar je označeno z d1 (okoli 2200 m), druga je razdalja med dnom Čepovanskega dola in podaljškom doline Idrijce jugovzhodno od Prvejka, kar je označeno z d0 (okoli 2650 m). Razdalja 2650 m je blizu skupnemu premiku v Idriji $2360 + 100$ do 200 m = 2460 do 2560 m in predstavlja celotni premik na območju Dolenje Trebuše, kljub temu pa bomo videli, da je za razlago reliefsa med Dolenjo Trebušo in Tolminom pomembnejši premik 2200 m. Razprava o zgradbi prelomne cone Idrijskega preloma in o nastanku dolinske mreže okoli Dolenje Trebuše presega okvir tega članka, pomembno pa je dejstvo, da se premik d₁ (2200 m) odraža tudi v reliefu okoli Tolmina, ko namreč postavimo os doline Idrijce na severozahodni strani Prvejka nasproti dna korozivnega odtisa Čepovanskega dola, se ustje Bače postavi nasproti sredine doline Soče pri Mostu na Soči (sl. 8B). To verjetno pomeni, da je bil Idrijski prelom prvotno segmentiran pri čemer sta se v Dolenji Trebuši srečala dva segmenta, ki sta danes združena v enotno cono. Tega vprašanja ni mogoče rešiti brez detajlnega kartiranja, zato je prostor okoli Dolenje Trebuše na sl. 8B strukturno neobdelan.

Ko stoji dolina Bače nasproti doline Soče (sl. 8B) se; greben Selski vrh (588 m) - Mrzli vrh (590 m) se postavi nasproti grebena Senice (658 m) nad Modrejem (sl. 8A, d3), greben Bučenice (498 m) nad Modrejcami se postavi v vzhodno-jugovzhodni podaljšek grebena Hlevnik (886 m) - Senica (576 m) nad Volčami (sl. 8A, d4). Iz slike 8B je torej mogoče povzeti, da je paleo-Idrijca tekla po Čepovanskem dolu in da je paleo-Baća tekla po sedanji dolini Soče južno od Mosta na Soči. Na podlagi gornjih ugotovitev smatramo razdaljo okoli 2200 m za referenčni premik ob Idrijskem prelому na območju Tolmina in Dolenje Trebuše. To lahko izrazimo z zapisom $d1 \approx d2 \approx d3 \approx d4 \approx 2200$ m. Do kvalitativno enake ugotovitve o vplivu Idrijskega preloma na odnos doline Idrijce do Čepovanskega dola in doline Bače do doline Soče južno od Mosta na Soči, so prišli Miklavž Feigel (ustna izjava, 1973) in Moulin et al. (2016, sl. 5).

Podatka o premiku d1 in d2 sta visoko pričevalna, medtem ko ima d3 ob d2 le vzporeden pomen. Podatek d4 je lahko realen ali slučajen, saj glede na nadaljnje izvajanje ne moremo

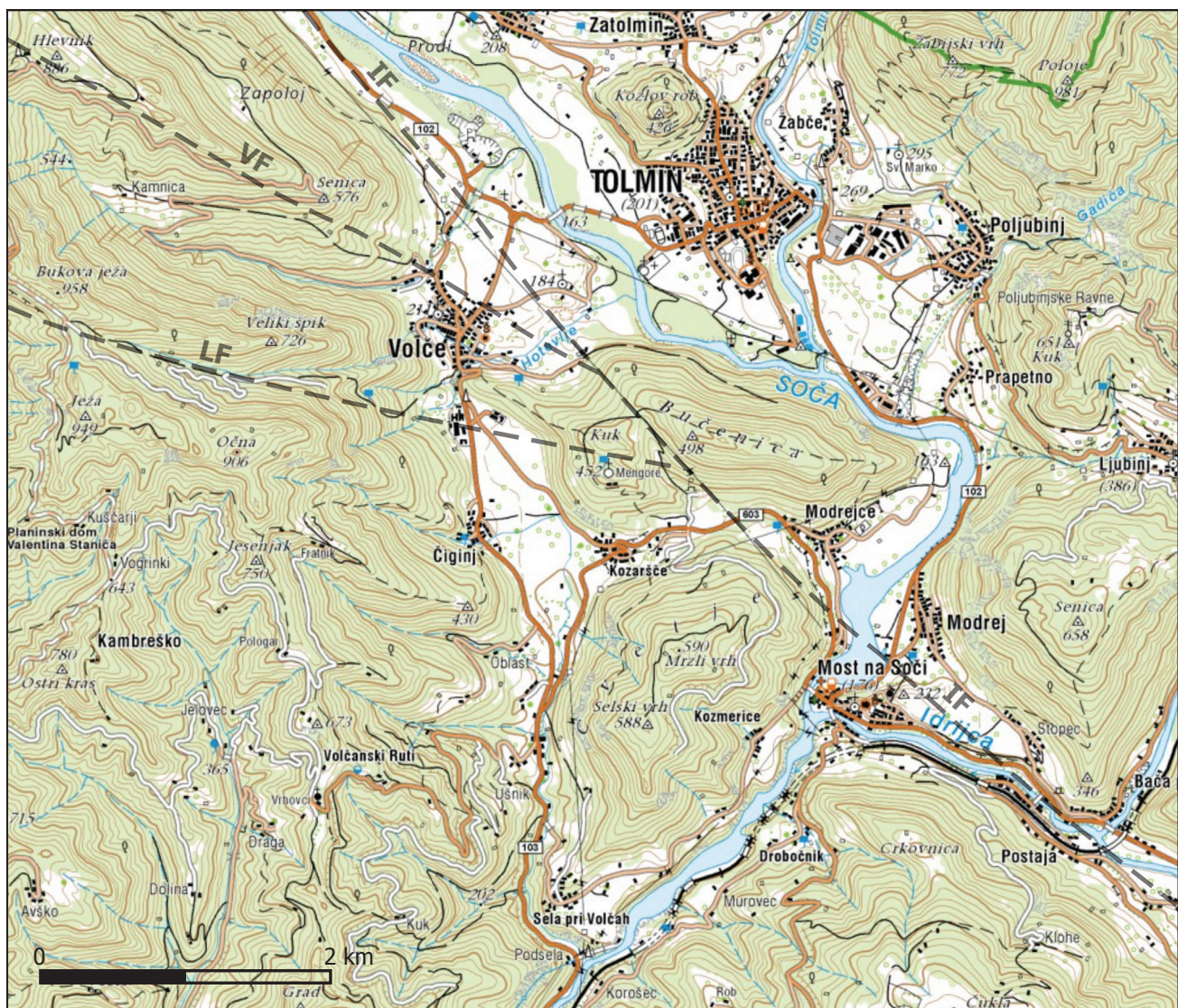


Fig. 10. Topographic map of the wider area around the Soča confluence, Tolminka, and Idrijca rivers. According to Geopedia – interactive online atlas and map of Slovenia. Explanation in Fig. 8.

Sl. 10. Topografska karta širše okolice sotočja Soče, Tolminke in Idrijce. Povzeto po Geopedia - interaktivni spletni atlas in zemljevid Slovenije. Legenda na sl. 8.

ally not resolved. The course of the Fault in the Tolmin area is described in more detail, which is why a topographical sketch is attached for easier orientation (Fig. 10). The terms “total displacement” for d0 and the “segmental displacement” for d1 in Figure 9 are only relevant for explaining the situation in the Dolenja Trebuša area.

When Bača Valley is positioned opposite the Soča Valley Mt. Selski vrh ridge (588 m) – Mt. Mrzli vrh (590 m) is located opposite the Mt. Senica ridge (658 m) above Modrej village (Fig. 8A, d3), the Mt. Bučenica ridge (498 m) above Modrej is located in the east-southeastern extension of the Mt. Hlevnik ridge (886 m) – Mt. Senica (576 m) above Volče (Fig. 8A, d4). It can therefore be concluded from Figure 8B that the paleo-Idrijca flowed along the Čepovanski dol and that the paleo-Bača flowed along the present Soča Valley south of the village of

trditi, da je greben Hlevnik - Senica - Bučenica obstajal že pred nastankom Idrijskega preloma. Trasa preloma na sl. 8 sloni na interpretaciji kot jo je podal Buser (1986; 1987) na Osnovni geološki karti, lista Tolmin in Videm; od sedla med Bučenicami in Kukom nad Kozarščem poteka proti severozahodu, oziroma proti Kobaridu, ne pa proti zahodu-severozahodu proti Volčam, kot menijo Moulin et al. (2016, sl. 5). Za tako odločitev obstoja več razlogov: 1. razvoj pliocenskega porečja Soče po Meliku (1956), 2. geološki podatki na Osnovni geološki karti 1:100.000, lista Tolmin in Videm (Buser ibid.), 3. ugrez severovzhodnega krila Idrijskega preloma in 4. kriterij desnozmičnega premika 2200 m na območju Tolmina in Dolenje Trebuše, kot je prikazan v tem članku.

Most na Soči. Based on these findings, we consider a distance of around 2,200 m as a reference offset along the Idrija fault in the area of Tolmin and Dolenja Trebuša. This can be expressed as $d_1 \approx d_2 \approx d_3 \approx d_4 \approx 2200$ m. Miklavž Feigel (oral statement, 1973) and Moulin et al. (2016, Fig. 5) came to the same qualitative conclusion about the impact of the Idrija Fault on the relationship between the Idrijca Valley, the Čepovanski dol, the Bača Valley, and the Soča Valley south of Most na Soči (2016, Fig. 5).

The data on the d_1 and d_2 offsets are highly testimonial, while d_3 has only a parallel meaning with d_2 . The d_4 data may be representative or coincidental, since according to further implementation we cannot claim that the Hlevnik - Senica - Bučenica ridge already existed before the formation of the Idrija Fault. The Idrija Fault trace in Figure 8 is based on the interpretation given by Buser (1986; 1987) on the Basic Geological Map, sheet Tolmin and Videm; from the saddle between Mt. Bučenica and Mt. Kuk above the village of Kozaršče, it runs towards the northwest, or rather towards Kobarid, but not WNW towards Volče, as Moulin et al. (2016, Fig. 5) suggested. There are several reasons for such a decision: 1. the development of the Pliocene Soča basin according to Melik (1956), 2. geological data on the basic geological map 1:100,000, the Tolmin and Videm sheets (Buser, ibid), 3. the subsidence of the northeastern block of the Idrija Fault, and 4. the criterion of a 2,200 m dextral offset in the area of Tolmin and Dolenja Trebuša, as shown in this article.

Ad 1. Melik (1956, Fig. II) in his discussion about the Middle Pliocene assumes that the paleo-Soča flowed through the valley between Kobarid and Robič, and then through the present-day Nadiža gorge towards the south. Melik (ibid) also assumed that the paleo-Idrijca river flowed through the Čepovanski dol valley, and that today's hanging Livek Valley SE of the village of Livek (Fig. 2) had a wide watershed in its hinterland, which was fed from the area northeast of Livek and today appears completely denuded. The description applies to the situation before the formation of the Idrija Fault. It is also indirectly proven by the flow of the Soča River, which flows north of Kobarid across the frontal part of the Southern Alps thrust independently of the bundle of faults that were created later and which we believe are related to the Idrija Fault. The assumption is supported by the 1:100,000 scale Basic geologic map, Tolmin and Videm sheet (Buser, 1986; 1987).

The Livek hanging valley is the main geomorphological object that indicates the flow of the paleo-Soča River towards the present-day Nadiža

Ad 1. Melik (1956, sl. II) v svoji razpravi za obdobje srednjega pliocena domneva, da je paleo-Soča tekla po dolini med Kobaridom in Robičem, nato pa po današnji soteski Nadiže proti jugu, da je paleo-Idrijca tekla po Čepovanskem dolu in da je imela danes viseča Livška dolina (sl. 2) tedaj široko zaledje. Napajala se je z območja severovzhodno od Livka, ki je danes povsem denudirano. Opis velja za stanje pred nastankom Idrijskega preloma, kar posredno dokazuje tudi tok Soče, ki severno od Kobarida teče preko čelnega dela nariva Južnih Alp neodvisno od pozneje nastalega snopa prelomov, za katere menimo, da so povezani z Idrijskim prelomom. Podlaga za to domnevo so podatki Osnovne geološke karte, lista Tolmin in Videm (Buser, 1986; 1987).

Viseča Livška dolina je glavni geomorfološki objekt, ki kaže na tok paleo-Soče proti današnji dolini Nadiže. Na območju Livka ima med Kolovratom in Matajurjem značilnosti pradoljne, katere pobočja dosežejo do 500 m višine, pri Čepovanskem dolu pa največ okoli 400 m. Na podlagi tega je moč sklepati, da je imelo denudirano porečje zgornjega dela livške paleoreke znaten obseg.

V času nastanka Melikove razprave so Idrijski prelom obravnavali kot disjunktivno deformacijo, ki naj bi imela ponekod učinek reverznega, ponekod normalnega preloma. Rakovec (1956, str. 79) ga je potegnil do Kobarida in Uče. Desnozmično komponento Idrijskega preloma je utemeljil Mlakar (1964).

Ad 2. Po podatkih Osnovne geološke karte (OGK), lista Tolmin in Videm (Buser, ibid.), je trasa Idrijskega preloma od sedla med Bučenico in Kukom nad Kozarščem (sl. 10), usmerjena proti severozahodu. Naprej poteka pod severovzhodnim pobočjem grebena Hlevnik - Senica in po Soški dolini do Kobarida ter po severovzhodnem pobočju grebena Mali vrh (1405 m) - Starijski vrh (1146 m) proti spodnjemu delu doline Uče nad Žago (Čar & Pišljar, 1993; Gosar, 2022). Pri Libušnjah se na severovzhodno stran cone Idrijskega preloma naslanja narivna meja Južnih Alp, ki se pri Kobaridu od nje odcepi. Zahodno od tod se nadaljuje pod imenom prelom Barcis - Staro selo. Premik narivne meje Južnih Alp ob Idrijskem prelому je desnozmičen, navidezna dolžina premika znaša okoli 3,5 km, vendar gre za učinek, ki je posledica ugreza severovzhodnega krila Idrijskega preloma in položnega vpada narivne meje Južnih Alp. Dejanski desnozmični premik je manjši, vendar njegove velikosti ni mogoče ugotoviti.

Valley. In the area of the village of Livek, between Mt. Kolvrat and Mt. Matajur, it has the characteristics of a deep valley, with slopes that reach a height of up to 500 m, while the maximum valley depth at Čepovanski dol is around 400 m. With this in mind, we can conclude that the denuded basin of the upper part of the Livek paleo-river had a significant extent.

At the time of Melik's treatise, the Idrija Fault was treated as a brittle deformation, which was supposed to have the effect of a reverse fault in some places, and a normal fault in others. Rakovec (1956, p. 79) drew it to Kobarid and Učja. The dextral offset component of the Idrija Fault was established by Mlakar (1964).

Ad 2. According to the Basic Geological Map 1:100,000 (OGK), sheet Tolmin and Videm (Buser, ibid.), the Idrija Fault trace from the saddle between Mt. Bučenica and Mt. Kuk above Kozaršče village (Fig. 10) is directed towards the northwest. It continues under the northeastern slope of the Mt. Hlevnik – Mt. Senica ridge and along the Soča Valley to Kobarid and along the northeastern slope of the Mt. Mali vrh (1405 m) – Mt. Starijski vrh (1146 m) ridge towards the lower part of the Učja Valley above the village of Žaga (Čar & Pišljar, 1993; Gosar, 2022). Near Libušnje, the thrust boundary of the Southern Alps leans on the northeastern side of the Idrija Fault zone, which splits off near Kobarid. To the west it continues as the Barcis - Staro selo Fault. The offset of the thrust boundary of the Southern Alps along the Idrija Fault is dextral, with an apparent offset of about 3.5 km. The actual dextral displacement is smaller due to the subsidence of the northeastern block of the Idrija Fault and the gentle dip of the Southern Alps boundary thrust. The true offset, however, cannot be ascertained.

On the saddle between Mt. Bučenica and Mt. Kuk, before Volče, the stratigraphically and geomorphologically responsive Volče Fault (Fig. 8) splits off from the Idrija Fault, which runs along the southwestern slope of the Mt. Hlevnik – Mt. Senica ridge. Due NW it continues across the saddle between Mt. Hlevnik (886 m) and the Mt. Kolvrat ridge into the Soča Valley. Between Mt. Kuk and Mt. Mengore (just south of it), another fault branches off from the Idrija Fault (Jamšek Rupnik et al., 2022), whose route, in our opinion, passes the village of Livek and continues due NW towards Robič. The fault between Robič and Livek was mapped by Buser, who marked it due southeast to the upper Idrijca River and named it the Livek Fault. However, the structural and remote detection data indicate a connection from Livek to the aforementioned saddle above Kozaršče, so we suggest that the lat-

Na sedlu med Bučenico in Kukom se pred Volčami od Idrijskega preloma odcepi stratigrafsko in geomorfološko jasno odziven Volčanski prelom (sl. 8), ki poteka po jugozahodnem pobočju grebena Hlevnik - Senica. Nato se prevesi preko sedla med Hlevnikom (886 m) in grebenom Kolovrata v Soško dolino. Med Kukom in Mengorami nad Kozarščem se od Idrijskega preloma odcepi drugi prelom (Jamšek Rupnik et al., 2022), katerega trasa po našem mnenju poteka mimo Livka in naprej proti Robiču. Prelom med Robičem in Livkom je kartiral Buser, potegnil ga je proti jugovzhodu na zgornjo Idrijco in ga poimenoval Livški prelom. Toda strukturni podatki in zaznambe daljinske detekcije, kažejo na povezavo od Livka proti omenjenemu sedlu nad Kozarščem, zato predlagamo, da se slednja varianta obravnava kot Livški prelom (sl. 8). Naše mnenje temelji na primerjavi podatkov Geološke karte Benečije Julisce krajine (Carulli, 2006) in Osnovne geološke karte Jugoslavije merila 1: 100.000, listov Tolmin in Videm (Buser, 1986; 1987). Ta je pokazala, da se zahodno od Idrijskega preloma uveljavlja drugačna dinamika neogensko-recentnih deformacij. To se odraža v njihovi smeri in kinematiki, vendar razprava o tem presega okvir tega članka.

Ad 3. Sklepamo, da je Idrijski prelom odrezal zgornje povirje livške paleoreke od njenega osrednjega in spodnjega toka. Rez je bil učinkovit zato, ker se je severovzhodno krilo preloma ugreznilo, ozziroma jugovzhodno krilo dvignilo in s tem preprečilo odtok voda zgornjega povoda livške paleoreke proti jugozahodu. Te so se potem lahko odvajale le proti severozahodu ali jugovzhodu. Pričel se je proces nastajanja doline med Kobaridom in Tolminom, ki je bil učinkovit tudi zaradi bližine narivne meje Južnih Alp. Najprej sta nastali porečji dveh potokov od katerih je eden napajal paleo-Sočo, drugi paleo-Bačo. Sčasoma je nastala dolina, v katero se je iz doslej še neraziskanih razlogov preusmerila Soča.

Dolina med Kobaridom in Tolminom bi lahko nastala tudi zaradi same narivne meje Južnih Alp brez Idrijskega preloma, vendar kažeta Volčanski prelom in desni premik narivne meje Južnih Alp med Kobaridom in Libušnjami na traso, kot so jo razumevali Rakovec (1956), Arsovski & Feigel (1973) in Buser (1986, 1987).

ter variant be considered the Livek Fault (Fig. 8). Our opinion is based on a comparison of the data of the Geological Map of the Veneto Julian Region (Carulli, 2006) and the Basic Geological Map of Yugoslavia, 1:100,000 scale, Tolmin and Videm sheet (Buser, 1986; 1987). This showed that a different dynamic of Neogene-recent deformations is taking place west of the Idrija Fault, which is reflected in their direction and kinematics, but discussion of this is beyond the scope of this article.

Ad 3. We conclude that the Idrija Fault cut off the upper headwaters of the Livek paleo-river from its central and lower course. The cut was effective because the northeastern flank of the fault subsided, or the southeastern flank rose, thereby preventing drainage of the waters of the upper catchment of the Livek paleo-river towards the southwest. These waters could then be discharged only towards the northwest or southeast. Thus, the process of formation of the valley between Kobarid and Tolmin began, which was also effective due to the proximity of the Southern Alps Thrust Boundary. First, the basins of two watersheds were formed, one of which fed the paleo-Soča, the other the paleo-Bača River. Over time, a valley was formed into which the Soča River diverted for as yet unexplained and unexplored reasons.

The valley between Kobarid and Tolmin may also have been formed by the Southern Alps Thrust Boundary without the Idrija Fault, but the Volče Fault and the right lateral shift of the Southern Alps Thrust Boundary between Kobarid and the village of Libušnje show the trace as understood by Rakovec (1956), Arsovski & Feigel (1973), and Buser (1986; 187).

Ad 4. The displacement criterion of 2200 m can be used for displacements d2, d3, and d4 in the Tolmin area (Fig. 8A), while the of valley network between Tolmin and Sela pri Volčah indicates a multiphase development. This only reinforces the assumption that before the formation of the Idrija Fault, the paleo-Soča did not flow here and that the area between Tolmin and Sela pri Volčah was formed by several streams that fed the paleo-Bača River from the northwestern side. In Figure 8B, no variant on the geomorphological development of this area is given, but we would like to draw attention to the Mt. Selski vrh – Mt. Mrzli vrh – Mt. Senica (658 m) ridge, which was probably continuous, before the formation of the Idrija Fault, so the water of all the streams flowed into the paleo-Bača River in the area of Sela pri Volčah exclusively.

The above four considerations lend a relatively high probability to the interpretation of the paleo-Soča flow from Kobarid to the west and to the

Ad 4. Kriterij zmika 2200 m je na območju Tolmina mogoče uporabiti pri premiku d2, d3 in d4 (sl. 8A), medtem ko splet dolin med Tolminom in Selami pri Volčah kaže na večfazni razvoj. To le utrjuje domnevo, da pred nastankom Idrijskega preloma paleo-Soča tu še ni tekla in da je prostor med Tolminom in Selami pri Volčah oblikovalo več potokov, ki so napajali paleo-Bačo s severozahodne strani. Na sl. 8B ni podane nobene variante o geomorfološkem razvoju tega prostora, opozorili bi pa na greben Selski vrh - Mrzli vrh -Senica (658 m), ki je bil pred nastankom Idrijskega preloma verjetno sklenjen, zato je voda vseh potokov odtekala v paleo-Bačo le na območju Sel pri Volčah.

Navedeni štirje premisleki dajejo sorazmerno visoko stopnjo verjetnosti interpretaciji toka paleo-Soče od Kobarida proti zahodu in interpretaciji trase Idrijskega preloma od sedla med Bučenico in Kukom proti severozahodu. Vendar je potrebno obe tezi kljub temu preveriti. Katera reka je urezala dolino med Robičem in Kobaridom bi se dalo ugotoviti s sondiranjem, s katerim bi določili smer imbrikacije ploščatih prodnikov; če je ta nagnjena proti zahodu je dolino izdolbla Soča, v nasprotnem primeru Nadiža. Sondiranje bi moralo odgovoriti tudi na vprašanje morebitne ojezeritve in njene starosti. Traso Idrijskega preloma je mogoče preveriti z razkopi ali geofizikalnim profiliranjem v dolini Soče, najprimernejše mesto preverbe je prostor pod severovzhodnim pobočjem grebena Hlevnik - Senica. Raziskave v Modrejcah (Jamšek Rupnik- et al., 2022) so bile izvedene korektno, niso pa mogle dati odgovora na to vprašanje.

Prispevek o genezi rečnega reliefa na območju zgornje Nadiže (Diercks et al., 2021) ne posega v to razpravo, čeprav je v njem uporabljena interpretacija Moulin et al. (2016, sl. 5), da je Nadiža urezala dolino med Robičem in Kobaridom.

Pred nastankom Idrijskega preloma sta Banjška in Šentviška planota tvorili enovito »Banjško-Šentviško planoto« (sl. 8B). Če bi hoteli bolj dosledno rekonstruirati takratno stanje, bi morali Šentviško planoto dvigniti za okoli 150 m, ali obratno, in odmisli dolino Idrijce med njima.

V tem članku ne opisujemo strukturnih razmer na jugozahodni strani Banjške in Trnovske planote nad Vipavsko dolino, ugotavljam pa, da so litolska sestava (eocenski fliš ter kredni, paleocenski in eocenski karbonati), razporeditev (fliš v talnini, karbonati v krovnini, meja med njimi subhorizontalna krovna narivna ploskev) in kinematika, primerljivi z istrsko-furlansko narivno-podrivno cono (Placer et al., 2023, sl. 1, str. 13). V profilu

interpretation of the route of the Idrija Fault from the saddle between Mt. Bučenica and Mt. Kuk to the northwest. However, it is still necessary to verify both theses. Which river cut the valley between Robič and Kobarid could be determined by probing, which would determine the direction of imbrication of flat pebbles; if it is inclined to the west, the valley was carved out by the Soča River, and if inclined otherwise by the Nadiža. Sounding should also answer the question of possible lake formation there and the age of such. The Idrija Fault trace can be verified by trenching or geophysical profiling in the Soča Valley; the most suitable place for verification is the area under the northeastern slope of the Mt. Hlevnik – Mt. Senica ridge. Research at the village of Modrejce (Jamšek Rupnik et al., 2022) was carried out correctly but did not provide a conclusive answer to the question.

The paper on the genesis of the river relief in the area of the upper Nadiža River (Diercks et al., 2021) does not play a role in this discussion, though it does use the interpretation of Moulin et al. (2016, Fig. 5) that the Nadiža cut the valley between Robič and Kobarid.

Before the formation of the Idrija Fault, the Banjšice and Šentviška Gora plateaus formed a single plateau (Fig. 8B). If we wanted to reconstruct a more consistent picture of the situation at the time, we would have to raise the Šentviška, Gora plateau by about 150 m, or vice versa, and discard the Idrijca Valley between them.

In this article we do not describe the structural conditions on the southwestern side of the Banjšice and Trnovski gozd plateaus above the Vipava Valley, but we note that the lithological composition (Eocene flysch and Cretaceous, Paleocene, and Eocene carbonates), distribution (flysch in the footwall, carbonates in the hanging wall and subhorizontal thrust plane between them) and kinematics are comparable to the Istra-Friuli Thrust-Underthrust Zone (Placer et al., 2023, Fig. 1, p. 13). In the profile of the Istra-Friuli Thrust-Underthrust Zone (*ibid.*, fig. 8), two types of deformations stand out: underthrust reverse faults and antiformally bent Paleogene thrust surfaces located next to them; both are related to the uplift of the hanging wall of the underthrust reverse faults. The equivalent of the antiformally bent nappe thrust plane on the boundary between the Vipava Valley (External Dinaric Imbricated Belt) and the Trnovski gozd plateau with Mt. Hrušica (External Dinaric Thrust Belt) is the Nanos-Čaven antiform (Placer et al., 2021a, p. 56–58; 2023, p. 38), the equivalent of the underthrust reverse faults are represented by structures whose description requires extensive substantiation, so

istrsko-furlanske narivno-podrivne cone (*ibid.*, sl. 8) izstopata dva tipa deformacij, podrivni reverzni prelomi in ob njih antiformno usločene paleogenske narivne ploskve; oboje je povezano z dvigom krovninskega krila podrivnih reverznih prelomov. Ekvivalent antiformno usločene krovne narivne ploskve na meji med Vipavsko dolino (Zunanjedinarski naluskani pas) in Trnovskim gozdom s Hrušico (Zunanjedinarski narivni pas), je nanoško-čavenska antiforma (Placer et al., 2021a, str. 56–58; 2023, str. 38), ekvivalent podrivnih reverznih prelomov pa predstavlja strukture, katerih opis zahteva obširno utemeljevanje, zato bodo predstavljene v posebnem prispevku.

Za dokaz dviga uravnana območja Trnovskega gozda in Banjške planote zadostuje že sam obstoj Čepovanskega dola, saj dol kot nekdanja rečna dolina ni mogel delovati na sedanji nadmorski višini, urezovanje v primarno uravnavo na začetku njegovega nastajanja pa se je moralo dogajati na še nižjem nivoju.

Sklep

Nad severovzhodnim obrobjem Vipavske doline, ki je zgrajena iz flišnih kamnin Zunanjedinarskega naluskanega pasu, se dvigajo karbonatne kamnine Zunanjedinarskega narivnega pasu (planote Banjšice, Trnovski gozd, Nanos), ki so bile tja narinjene v paleogenu v zaključnem obdobju narivne faze nastajanja Dinaridov. Narinjene karbonatne kamnine se danes gravitacijsko sprožajo v Vipavsko dolino, ta proces traja že subrecentno in recentno obdobje, zato sklepamo, da se omenjene planote postopoma dvigajo.

Dviganje ob severovzhodnem obrobu Vipavske doline se ne dogaja ob paleogenskih krovnih narivnih ploskvah, ki so tu subhorizontalne in blago tonejo proti severozahodu, temveč ob podrivnih reverznih prelomih smeri NW-SE, ki pa so šele v fazi proučevanja. Ti so posledica pomikanja Jadranske mikroplošče (Mikroadrija) proti Dinaridom. Desnozmični prelomi v smeri NW-SE imajo v tem primeru podrejeno vlogo.

Premikanje Mikroadrije proti Dinaridom poteka domnevno vse od srednjega miocena, zato ga obravnavamo kot neogensko-recentno dogajanje. Poleg splošnih geomorfoloških pojavov na širšem prostoru severozahodnih Dinaridov (istrsko potisno območje) to dokazujejo tudi pojavi na Banjšicah in Trnovskem gozdu: 1. Kraških uravnav na Trnovskem gozdu (Voglarska planota) in Banjšicah (jugovzhodni del) ne moremo razlagati s krajevno omejenimi procesi. 2. Korozivna degradacija teh uravnav je povezana s postritvijo klimatskih razmer zaradi dviganja Zunanjedinarskega

they are to be presented in a special, separate paper.

The very existence of the Čepovanski dol is enough to prove the elevation of the peneplained area of the Trnovski gozd and the Banjšice plateaus, since the Čepovanski dol, as a former river valley, could not function at its current altitude, and the cutting into primary regulation at the beginning of its formation had to take place at a level even lower than of today.

Conclusions

The carbonate rocks (Banjšice and Trnovski gozd plateaus, Nanos) that were overthrusted there in the Paleogene during the final period of the thrust phase of the formation of the Dinarides rise above the northeastern edge of the Vipava Valley, which is built from the flysch rocks of the External Dinaric Imbricated Belt. The eroded carbonate rocks are now gravitationally launched into the Vipava Valley, which process has been going on over the course of the sub-recent and recent periods, so we conclude that the mentioned plateaus are gradually rising.

The uplift along the northern margin of the Vipava Valley does not take place along the sub-horizontal Paleogene nappe thrust planes, dipping slightly to the northwest, but rather along the NW-SE trending underthrust reverse faults which are still in the study phase. These are a consequence of the Microadria movement towards the Dinarides where the right lateral NW-SE trending strike-slip faults play a subordinate role.

The movement of the Microadria towards the Dinarides has presumably been going on since the Middle Miocene, so we treat it as a Neogene-recent event. In addition to the general geomorphic phenomena in the wider area of the northwestern Dinarides (Istran Pushed Zone), this is also proven by phenomena in the Banjšice and Trnovski gozd plateaus: 1. The karstic peneplanation in the Trnovski gozd plateau (Voglarji plateau) and the Banjšice plateau (southeastern part) cannot be explained by locally limited processes. 2. The corrosive degradation of these peneplains (plateaus) is related to the aggravation of climatic conditions due to the uplift of the External Dinaric Thrust Belt. 3. Čepovanski dol was active (hosted a river) at a lower altitude, and at the beginning of cutting into the levelled karst surface it must have lay even lower.

We note that in addition to the existing karstic peneplanations in the Banjšice and Trnovski gozd plateaus, the rest of the Trnovski gozd area was also peneplained from the Voglarji plateau in the southeast to Mt. Veliki and Mt. Mali Modrasovec

narivnega pasu. 3. Čepovanski dol je bil prečno aktiven na nižjem nadmorskem nivoju, na začetku urezovanja v uravnano kraško površje pa je moral ležati še nižje.

Ugotavljam, da je bil poleg obstoječih kraških uravnnav na Banjšicah in Trnovskem gozdu, uravnana tudi preostali del Trnovskega gozda od Voglarske planote proti jugovzhodu do Velikega in Malega Modrasovca nad Lokavcem in Strelškega vrha nad Podkrajem pri Colu. Enako domnevamo tudi za danes neuravnani del Banjšic in Šentviške planote. Zato uvajamo termin trnovsko-banjško-šentviška degradirana uravnava.

Obseg trnovsko-banjško-šentviške degradirane uravnave je prikazan na sliki 11. Pri nižji nadmorski višini je bilo celotno območje uravnano, med dviganjem pa je strukturno in denudacijsko degradiralo. Degradacija ni bila enotna temveč podrejena litološki sestavi, strukturi in dinamiki dviganja. Danes so na tem prostoru razviti trije različni tipi reliefs, ki so nastali po načinu degradacije prvotne uravnave. Na relativno umirjenem delu iz karbonatnih kamnin, kjer struktorna degradacija ni imela vpliva, so vidne le posledice ostrejših klimatskih pogojev, ta del je označen kot korozivno degradirana kraška uravnava (I); del iz karbonatnih kamnin, ki je danes razgiban, je označen kot strukturno in korozivno degradirana kraška uravnava (II); del iz mešanih kamnin, ki je danes umirjeno razgiban je označen kot strukturno degradirana in denudirana uravnava (III), tu je delež korozivne degradacije podrejen zaradi prisotnosti klastičnih kamnin. Vplivno območje korozivno degradiranih kraških uravnav (I) je identično z vplivnimi območji c, d in e (I ≡ c, d, e) (sl. 2, 4).

Trnovsko-banjško-šentviška degradirana uravnava leži na najvišjem območju Trnovskega pokrova, ki je zgrajeno iz karbonatnih kamnin. Ta del je proti jugovzhodu ohranjen le do Strelškega vrha (1266 m), od tu naprej pa je erodiran; na mestu je torej domneva, da je bila obravnavana uravnava ob svojem nastanku večja od površine kot je predstavljena na sl. 11, zato bi sodila po definiciji Stepišnika in Ferkove (2023, 12–13) v razred korozijskih uravnav. Temu pritrjuje tudi sodobni pogled na njihovo genezo (ibid. 17–18).

V tem članku ni obdelan geološki pomen Ponikvanske tektonske krpe na Šentviški planoti. Obdelan ni tudi pomemben podatek, da je Šebreljska planota vzhodni podaljšek Šentviške planote na drugi strani doline Idrije.

Vsa našteta dejstva in domneve terjajo temeljiti premislek o ponarivni, oziroma popaleogenski genezi Dinaridov.

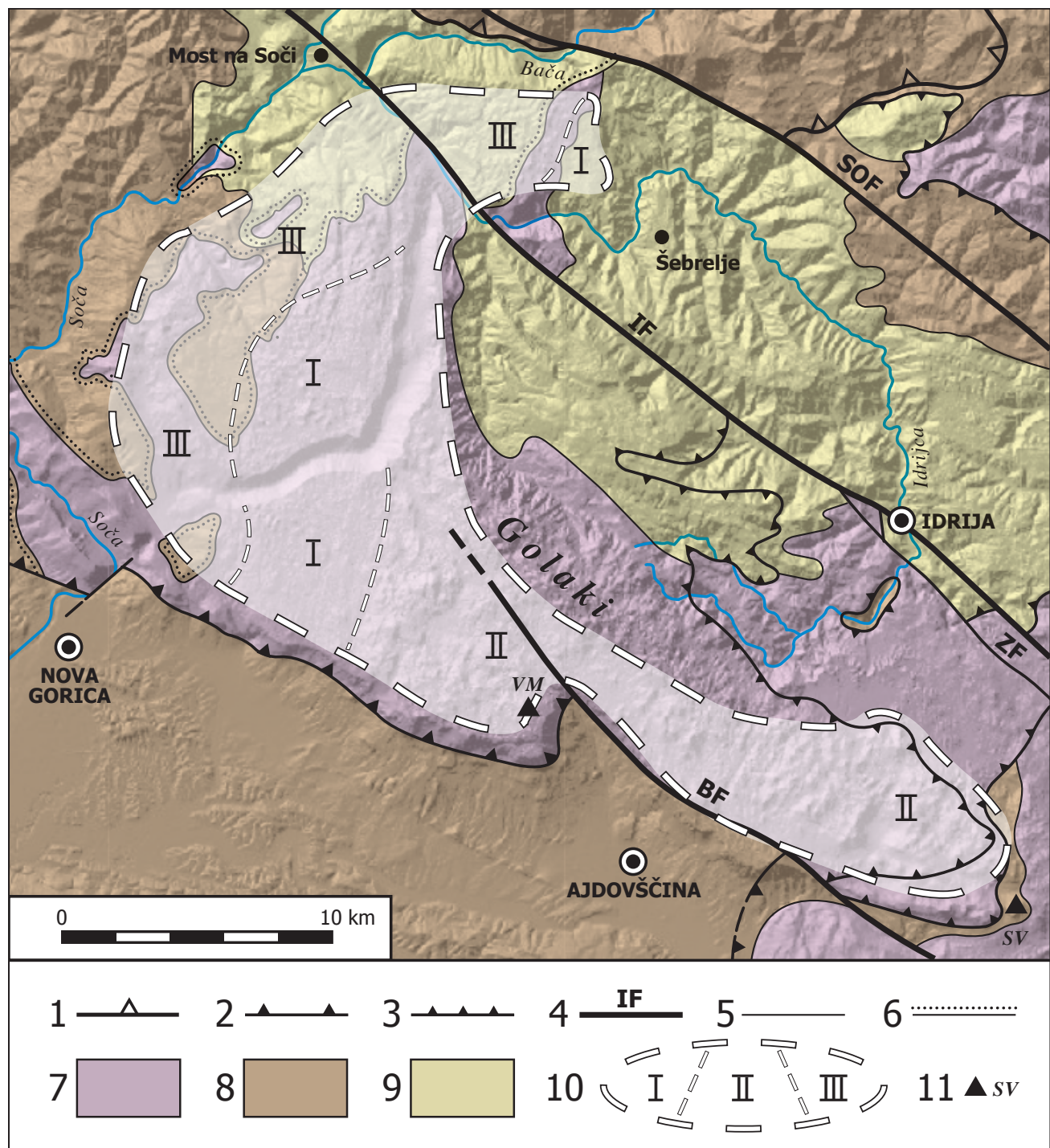


Fig. 11. Trnovski gozd-Banjšice-Šentviška planota degraded plain.

Sl. 11. Trnovsko-banjško-šentviška degradirana uravnava.

1 Thrust boundary of Southern Alps / narivna meja Južnih Alp

2 Boundary of the External Dinaric Thrust Belt / meja Zunanjedinarskega narivnega pasu

3 Boundary of the nappe unit within the External Dinaric Thrust Belt / meja krovne enote znotraj Zunanjedinarskega narivnega pasu

4 Fault: **SOF** – Sovodenj Fault, **IF** – Idrija Fault, **ZF** – Zala Fault, **BF** – Belsko Fault (Placer et al., 2021, fig. 6, p. 44; Buser, 1976, p. 50, Predjama Fault) / prelom: **SOF** – Sovodenjski prelom, **IF** – Idrijski prelom, **ZF** – Zalin prelom, **BF** – Belski prelom (Placer et al., 2021, sl. 6, str. 44; Buser, 1976, str. 50, Predjamski prelom)

5 Concordant geological border / konkordantna geološka meja

6 Discordant geological border / diskordantna geološka meja

7 Predominantly carbonates / pretežno karbonati: T_3^{2+3} , J, K₁, P_c, E₁

8 Predominantly clastites / pretežno klastiti: C, P₁, K₂, P_c, E

9 Carbonates and clastites / karbonati in klastiti: P₂, T₁₊₂, T₃¹, K₂

10 Area of the Trnovski gozd-Banjšice-Šentviška planota degraded plain / območje trnovsko-banjško-šentviške degradirane uravnave. Type of dominant degradation: I – corrosive degradation (I ≡ c, d, e: see fig. 2, fig. 4), II – structural and corrosive degradation, III – structural degradation and denudation / tip prevladajoče degradacije: I – korozivna degradacija (I ≡ c, d, e: glej sl. 2, sl. 4), II – strukturna in korozivna degradacija, III – strukturna degradacija in denudacija

11 Top / vrh: VM – Veliki Modrasovec (1355 m), SV – Streliški vrh (1266 m)

above Lokavec and Mt. Streliški vrh above Podkraj pri Colu. We assume the same for the currently non-peneplained part of Banjšice and the Šentviška Gora plateaus – which is why we here introduce the term Trnovski gozd-Banjšice-Šentviška Gora degraded peneplain.

The extent of the Trnovski gozd-Banjšice-Šentviška Gora plateaus degraded peneplanation is shown in Figure 11. At a lower altitude the entire area was levelled, but during the uplift it degraded structurally and denudationally. The degradation was not uniform but subordinated to the lithological composition, structure, and uplift dynamics. Today, three different types of relief have been developed in this area, formed according to the type of degradation of the original peneplain. On the relatively unactive part built of carbonate rocks, where structural degradation had no effect, only the consequences of harsher climatic conditions are visible; this part is designated as corrosively degraded karst plain (I); the part built of carbonate rocks, which is uneven today, is designated as a structurally and corrosively degraded karst plain (II); the part made of various (carbonate and clastic) rocks, which today is moderately rugged, is designated as structurally degraded and denuded plain (III); here the proportion of corrosive degradation is subordinate due to the presence of clastic rocks. The influence zone of corrosively degraded karst plains (I) is identical to the influence zones c, d, and e ($I \equiv c, d, e$) (Figs. 2, 4).

The Trnovski gozd-Banjšice-Šentviška Gora degraded plain lies on the highest part of the Trnovo Nappe, which is composed of carbonate rocks. This part towards the southeast is preserved only up to Mt. Streliški vrh (1266 m), while from here on it is eroded. It is appropriate, therefore, to assume that at the time of its formation the considered level was more extensive than the surface as presented in Figure 11; according then to the definition of Stepišnik and Ferk (2023, p.12–13) it would belong to the class of corrosion plains. This is also confirmed by the modern view of their genesis (*ibid.* p.17–18).

The geological significance of the Ponikve klippe on the Šentviška Gora plateau is not discussed in this article. The important fact that the Šebrelje plateau represents the eastern extension of the Šentviška Gora plateau on the other side of the Idrija Valley is also not dealt with herein.

All of the above facts and assumptions require a thorough consideration of the post-thrust or post-Paleogene genesis of the Dinarides.

References

- Arsovski, M. & Feigel, M. 1973: Neotektonika SR Slovenije. Institut za zemljotresno inženjerstvo i inženjersku seismologiju, Univerzitet Kiril i Metodij, Skopje. Arhiv Urada za seismologijo, Agencija Republike Slovenije za okolje / Archives of Office of Seismology, Agency of the Republic of Slovenia for the Environment. Report OIS 73-2: 32 p.
- Blaškovič, I. 1991: Raspored uzdužnih, reverznih i normalnih rasjeda i konstrukcija oblika i dubina ploha podvlačenja (Disposition of the longitudinal, reverse and normal faults and the construction of the forms and depths of the underthrusting surfaces). Geol. vjesnik, 4: 247–256.
- Buser, S. 1976: Tektonska zgradba južnozahodne Slovenije = Tektonischer Aufbau Südwest-Sloweniens. 8. jugoslovanski geološki kongres-Bled, 1.-5. okt. 3: 45–58.
- Buser, S. 1986: Osnovna geološka karta Jugoslavije 1:100 000 (OGK) = Basic geological map of Yugoslavia 1:100.000. Tolmač listov / Guidebooks of sheets Tolmin in Videm (Udine). Zvezni geološki zavod, Beograd.
- Buser, S. 1987: Osnovna geološka karta Jugoslavije 1:100 000 (OGK) = Basic geological map of Yugoslavia 1:100.000. Lista/sheets Tolmin in Videm (Udine). Zvezni geološki zavod, Beograd.
- Čar, J. & Pišljar, M. 1993. Presek Idrijskega preloma in potek doline Uče glede na prelomne strukture. Rudarsko-metalurški zbornik, 40/1-2: 79–91, Ljubljana
- Čar, J. 2010: Geološka zgradba idrijsko-cerkljanskega hribovja. Tolmač h Geološki karti idrijsko-cerkljanskega hribovja med Stopnikom in Rovtami v merilu 1:25.000 = Geological Structure of the Idrija-Cerkno hills. Explanatory book to the Geological map of the Idrija-Cerkno hills between Stopnik and Rovte 1:25.000. Geological Survey of Slovenia, Ljubljana: 127 p
- Diercks, M., Grützner, C., Vrabec, M. & Ustaszewski, K. 2021: A model for the formation of the Pradol (Pradolina) dry valley in W Slovenia and NE Italy. Geologija, 64/1: 21–33.
- Gosar A. 2022: Meritve tektonskih mikro-premikov v prelomni coni Idrijskega preloma v dolini Uče (Z Slovenija). 6. slovenski geološki kongres: zbornik povzetkov = book of abstracts, 37 p. <https://www.geo-zs.si/6SGK2022/>
- Habič, P. 1968: Kraški svet med Idrijeo in Vipavo: prispevek k poznavanju razvoja kraškega reliefa = The Karstic region between the Idrijea

- and Vipava rivers: a contribution to the study of development of the Karst relief. SAZU, Clasis IV, Dela-Opera 21:243 p.
- Jamšek Rupnik, P., Žebre, M., Jež, J., Zajc, M., Preusser, F. & Monegato, G. 2022: Deciphering the deformation mechanism in Quaternary deposits along the Idrija Fault in the formerly glaciated Soča Valley, southeast European Alps. *Engineering Geology*, 297. <https://doi.org/10.1016/j.enggeo.2021.106515>
- Kocjančič, M., Popit, T. & Verbovšek, T. 2019: Gravitational sliding of the carbonate megablocks in the Vipava Valley, SW Slovenia. *Acta geographica Slovenica*, 59/1: 7–22 p. <https://doi.org/10.3986/AGS.4851>
- Kodelja, B., Žebre, M. & Stepišnik, U. 2013: Poledenitev Trnovskega gozda = Glaciation of Trnovski gozd. E-knjige Založba UL. <https://doi.org/10.4312/9789612375614>
- Komac, M. & Ribičič, M. 2008: Zemljevid verjetnosti pojavljanja zemeljskih plazov v Sloveniji 1: 250.000 = Landslide susceptibility map of Slovenia 1: 250.000. Geološki zavod Slovenije, Ljubljana.
- Korbar, T., Markušić, S., Hasan, O., Fuček, L., Brunović, D., Belić, N., Palenik, D. & Kastelic, V. 2020: Active Tectonics in the Kvarner Region (External Dinarides, Croatia) – An Alternative Approach Based on Focused Geological Mapping, 3D Seismological, and Shallow Seismic Imaging Data. *Front. Earth Sci.*, 25 November. <https://10.3389/feart.2020.582797>
- Košir, A. & Popit, T. 2002: Pleistocene debris at Selu in Vipava Valley. In: Horvat, A. (ed.), et al. Knjiga povzetkov. 1. slovenski geološki kongres, Črna na Koroškem, 9.–11. oktober 2002. Geološki zavod Slovenije, Ljubljana: 43.
- Košir, A., Popit, T. & Verbovšek, T. 2015: The Selu landslide: A long runout rock avalanche? In: Rožič, B. (ed.): 22. posvetovanje slovenskih geologov = 20th Meeting of Slovenian Geologists, Ljubljana, November 2015. Univerza v Ljubljani, Naravoslovnotehniška fakulteta. Geološki zbornik, 23: 92–95.
- Melik, A. 1956: Pliocene Soča = La Soča (Isonzo) pliocene. *Geografski zbornik*, 4: 129–157. giam.zrc-sazu.si/sites/default/files/zbornik/GZ_0401_129-157.pdf
- Mlakar, I. 1964: Vloga postrudne tektonike pri iskanju novih orudnih con na območju Idrije = The Role of Postmineralization Tectonics in the Search for New Mineralized Zones in the Idria Area. Rudarsko-metalurški zbornik, 1 / Mining and Metallurgy Quarterly, 1: 19–25.
- Mlakar, I. 1969: Krovna zgradba idrijsko žirovskega ozemlja = Nappe structure of the Idrija - Žiri Region. *Geologija*, 12: 5–72.
- Moulin, A., Benedetti, L., Rizza, M., Jamšek Rupnik, P., Gosar, A., Bourlès, D., Keddadouche, K., Aumaître, G., Guillon, V. & Ritz, J. 2016: The Dinaric fault system: Large-scale structure, rates of slip, and Plio-Pleistocene evolution of the transpressive northeastern boundary of the Adria microplate. *Tectonics*, 35/10: 2258–2292. <https://doi.org/10.1002/10.2016TC004188>
- Placer, L. 1973: Rekonstrukcija krovne zgradbe idrijsko-žirovskega ozemlja = Reconstruction of the Nappe Structure of the Idrija-Žiri Region. *Geologija*, 16: 317–334.
- Placer, L. 1981: Geološka zgradba jugozahodne Slovenije = Geologic structure of southwestern Slovenia. *Geologija*, 24/1: 27–60.
- Placer, L. 1982: Tektonski razvoj idrijskega rudišča = Structural history of the Idrija mercury deposit. *Geologija*, 25/1: 7–94.
- Placer, L., Jež, J. & Atanackov, J. 2008: Strukturni pogled na plaz Slano blato = Structural aspect on the Slano blato landslide (Slovenia). *Geologija*, 51/2: 229–234. <https://doi.org/10.5475/geologija.2008.023>
- Placer, L., Vrabec, M. & Celarc, B. 2010: The bases for understanding of the NW Dinarides and Istria Peninsula tectonics. *Geologija*, 53/1: 55–86. <https://doi.org/10.5474/geologija.2010.005>
- Placer, L., Mihevc, A. & Rižnar, I. 2021a: Tectonics and gravitational phenomena (Nanos, Slovenia). *Geologija*, 64/1: 35–63, Ljubljana. <https://doi.org/10.5474/geologija.2021.003>
- Placer, L., Jamšek Rupnik, P. & Celarc, B. 2021b: The Sistiana Fault and the Sistiana Bending Zone (SW Slovenia). *Geologija*, 64/2: 221–252. <https://doi.org/10.5474/geologija.2021.013>
- Placer, L., Rižnar, I. & Novak, A. 2023: Transverse Dinaric zone of increased compression between the Kraški rob and Hrušica Regions, NE Microadria. *Geologija*, 66/1: 9–71. <https://doi.org/10.5474/geologija.2023.000>
- Popit, T. & Košir, A. 2003: Pleistocene debris flow deposits in the Vipava Valley, SW Slovenia. In: Vlahović, I. (ed.): 22nd IAS Meeting of Sedimentology, Opatija, Croatia), Institute of geology, Zagreb, pp. 161.
- Popit, T., Košir, A. & Šmuc, A. 2013: Sedimentological characteristics of Quaternary deposits of the Rebrnice slope area (SW Slovenia). Book of abstracts: 3rd Scientific Meeting Quaternary Geology in Croatia with international participation, on the occasion of the 130th

- birth anniversary of Marijan Salopek, Fellow of the Croatian Academy and in memory of Maja Paunović on her 10th death anniversary, Zagreb, March 21–23, 2013. Zagreb. Hrvatska akademija znanosti i umjetnosti, Zavod za paleontologiju i geologiju kvartara; Geološki zavod Slovenije, Ljubljana.
- Popit, T. 2016: Transport mechanisms and depositional processes of Quaternary slope deposit in Rebrnice area. Doctoral dissertation. Faculty of Civil and Geodetic Engineering and Faculty of Natural Science and Engineering, Ljubljana: 341 p.
- Popit, T. 2017: Origin of planation surfaces in the hinterland of Šumljak sedimentary bodies in Rebrnice (upper Vipava Valley, SW Slovenia) = Nastanek reliefnih izravnih v zaledju sedimentnih teles Šumljak na Rebrnicah (zgornja Vipavska dolina, SW Slovenija). Geologija, 60/2: 297–307. <https://doi.org/10.5474/geologija.2017.021>
- Popit, T., Rožič, B., Šmuc, A., Novak, A. & Verbovšek, T. 2022: Using a lidar-based height variability method for recognizing and analyzing fault displacement and related fossil mass movement in the Vipava Valley, SW Slovenia. Remote Sensing, 14/9: 1–16. <https://doi.org/10.3390/rs14092016>
- Rakovec, I. 1956: Pregled tektonske zgradbe Slovenije = A survey of the tectonic structure of Slovenia. Prvi jugoslovanski geološki kongres, Bled / 1st Geological Congress of FNR Yugoslavia, Bled. Predavanja in poročila / Transactions and reports, 73–83, Ljubljana.
- Stepišnik, U. & Ferk, M. 2024: Morphogenesis and classification of corrosion plains in Slovenia. Acta geographica Slovenica, 64/1: 7–22.
- Verbovšek, T., Teran, M., Zajc, M., Košir, A. & Popit, T. 2017: Volume determination of the Selo landslide complex (SW Slovenia): integration of field mapping, Ground Penetrating Radar and GIS approaches. Landslides: Journal of the international consortium on landslides, 14/3: 1265–1274. <https://doi.org/10.1007/s10346-017-0815-x>
- Verbovšek, T., Popit, T. & Kokalj, Ž. 2019: VAT method for visualization of mass movement features: an alternative to hillshaded DEM. Remote Sensing, 11/24: 1–14. <https://doi.org/10.3390/rs11242946>
- Vrabec, M., Pruner, P., Zupan Hajna, N., Mihevc, A. & Bosak, P. 2018: Unraveling neotectonic vertical-axis rotations in the AdriaEurasia collision zone: paleomagnetic data from Pliocene-Quaternary cave sediments (Slovenia). In: Ustaszewski, K., Grützner, Ch. & Navabpour, P. (eds.): TSK Jena 2018. 1st ed. Jena: Friedrich Schiller University Jena, Institute of Geological Sciences: 134 p.
- Weber, J., Vrabec, M., Stopar, B., Pavlovčič-Prešeren, P. & Dixon, T. 2006: The PIVO-2003 experiment: A GPS study of Istria peninsula and Adria microplate motion, and active tectonics in Slovenia. In: Pinter, N., Gyula, G., Weber, J., Stein, S. & Medak, D. (eds.): The Adria Microplate: GPS Geodesy, Tectonics and Hazards, 305–320. Nato Science Series IV, Earth and Environmental Sciences, 61. https://doi.org/10.1007/1-4020-4235-3_21
- Weber, J., Vrabec, M., Pavlovčič Prešeren, P., Dixon, T., Jiang, Y. & Stopar, B. 2010: GPS-derived motion of the Adriatic microplate from Istria Peninsula and Po Plain sites, and geodynamic implications. Tectonophysics, 483/3–4: 214–222. <https://doi.org/10.1016/j.tecto.2009.09.001>



Petrology dataset of Pliocene-Pleistocene sediments in northeastern Slovenia

Podatki o petrologiji pliocensko-pleistocenskih sedimentov severovzhodne Slovenije

Eva MENCIN GALE^{1*}, Polona KRALJ¹, Mirka TRAJANOVA¹, Luka GALE^{1,2} & Dragomir SKABERNE¹

¹ Geološki zavod Slovenije, Dimičeva ulica 14, SI–1000 Ljubljana, Slovenija

² Oddelek za geologijo, Naravoslovnotehniška fakulteta, Aškerčeva 12, 1000 Ljubljana, Slovenija

*corresponding author: eva.mencin-gale@geo-zs.si

Prejeto / Received 21. 5. 2024; Sprejeto / Accepted 6. 6. 2024; Objavljeno na spletu / Published online 11. 6. 2024

Key words: petrological analysis, clast lithological analysis, provenance of the clasts, Pliocene-Pleistocene sediments
Ključne besede: petrografska analiza, litološka analiza klastov, provenienca klastov, pliocensko-pleistocensi sedimenti

Abstract

This is a dataset of petrological analysis of Pliocene-Pleistocene fluvial sediments from 14 gravelly samples from the Slovenj Gradec, Nazarje, Celje and Drava-Ptuj Basin (northeastern Slovenia), collected for clast lithological analysis. The petrological analysis includes description of 155 thin sections of metamorphic, volcanic, volcaniclastic, clastic and carbonate rocks. This dataset provides grounds for determining the provenance of these gravel deposits, revealing possible resedimentation processes, and serves as a tool for drainage network interpretation in the Pliocene-Pleistocene.

Izvleček

V članku predstavljamo podatke o petrološki analizi rečnih pliocensko-pleistocenskih sedimentov iz 14 prodnatih vzorcev iz slovenjgraškega, nazarskega, celjskega in dravsko-ptujskega bazena (severovzhodna Slovenija), ki so bili vzorčeni za namen litološke analize klastov. Petrološka analiza obsega opise 155 zbruskov metamorfnih, vulkanskih, vulkanoklastičnih, klastičnih in karbonatnih kamnin. Ti podatki predstavljajo temelj za določitev provenience obravnavanih prodnatih sedimentov, razkrivajo morebitno resedimentacijo ter so pomembni za interpretacijo razvoja rečne mreže v pliocenu in pleistocenu.

Background

This [dataset](#) was collected to perform clast lithological analysis of Pliocene-Pleistocene fluvial sediments in the frame of research published in Mencin Gale (2021). The dataset present in this article contributes to understanding the provenance of gravelly sediments deposited in Slovenj Gradec, Nazarje, Celje and Drava-Ptuj Basins using clast lithological analysis. This method provides grounds for determining the source of gravel. Moreover, it serves as a tool for determination of possible re-sedimentation (e.g. from Miocene conglomerates) and drainage evolution.

Clast lithological analysis is traditionally performed at the macroscopic level (Bridgland et al., 2012), with efficacy and statistical validity being

its primary strengths (Bridgland, 1986; Walden, 2004; Gale and Hoare, 2011). However, it has been discovered that conducting petrographic analysis on thin sections of selected clasts significantly enhances the quality and spatial resolution of provenance analysis (Mencin Gale, 2021; Mencin Gale et al., 2019a, 2019b, 2024). This approach provides more accurate information about the composition and source formations of the studied sediments.

Detailed results and interpretations of this methodology were already published in several publications: Mencin Gale (2021), Mencin Gale et al. (2019a, 2019b, 2024). Moreover, the selected sections from where the samples were taken were in detail discussed in Mencin Gale et al., (2019a, 2019b, 2024).

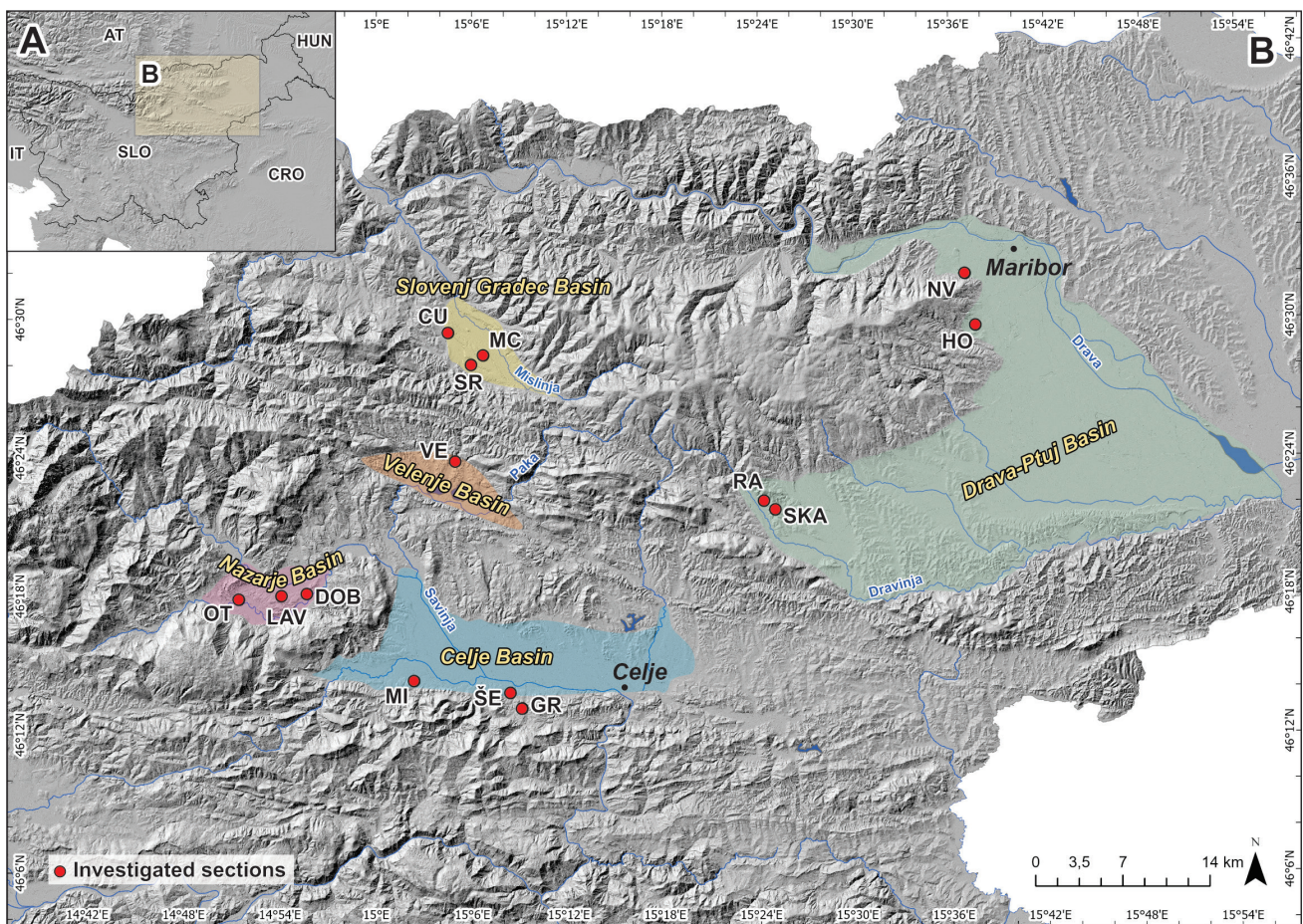


Fig. 1. Overview of the studied region. A: Map of Slovenia with marked investigated area. B: Locations of the selected basins and sections comprising the dataset presented in this paper. Basemap: shaded relief of the DEM (digital elevation model, Ministry of Environment & Spatial Planning, 2015).

Experimental design, materials, and methods

a) Gravel sampling

We selected 14 sections in Slovenj Gradec, Nazarje, Celje and Drava-Ptuj Basins for sedimentological analysis and sampling (Fig. 1). The sections were selected based on length and preservation of the clasts (avoiding weathered sections). The sections range from 1 to 14.3 m in length (Table 1). The most suitable outcrops were found on terrace risers or within areas incised by tributaries. Samples of gravel were collected from the sections, which were cleaned prior to sampling. Locations of the sections (x , y , z) were acquired with hand-held GPS device Trimble and further managed in ArcGIS Pro (ESRI).

b) Clast lithological analysis (CLA)

Clast lithological analysis was adapted from guidelines by Walden (2004), Lindsey et al. (2007), and Gale and Hoare (2011). Sampling for gravel involved bulk sampling of the exposed surface to

avoid biasing by selecting only the most obvious clasts. The Velunja section (VE; Velenje Basin) was logged and sampled with an abseiling technique and the rest of the sections were accessible from the ground. Dry-sieving was conducted in the field, with only a 1.5–6 cm fraction transported to the laboratory for further analysis. Clasts smaller than 1.5 cm are mostly too weathered to allow for reliable determination of lithology. Larger clasts also allow for better observation of the texture and bulk characteristics of the rock.

Each sample comprised 48–346 clasts, with precise counts provided in Table 1. A smaller number of counted clasts is due to the less available material for the analysis (e.g. smaller, conglomerated layers). Macroscopic examination and lithology-based grouping were followed by petrological analysis. In total 2.682 clasts were examined from which 155 were selected for detailed examination in thin sections: 14 clasts from the Slovenj Gradec Basin, 63 from the Nazarje Basin, 13 from the Celje Basin, 32 from the Drava-Ptuj Basin, and 33 from the Velenje Basin.

c) Microscopy for determination of source stratigraphic unit

We used optical polarizing microscope Opton Zeiss for microscopy in transmitted light with lenses with magnifications of 2.5 \times , 5 \times , 10 \times , 20 \times , 25 \times , 50 \times . A digital camera is attached to the microscope for production of microphotographs. Biotic components in carbonate and mixed carbonate-siliciclastic rocks, grain composition in clastic rocks, and mineral associations and mineral alterations in metamorphic, volcanic, and volcanioclastic rocks determined from thin sections crucial for the determination of source stratigraphic unit of each rock type.

Data description

All described and deposited data are analyzed data. They are represented in several figures, tables and shapefile.

Fig. 1 shows locality map of the sections. Fig. 2–5 show selected photographs of 35 thin sections in the Slovenj Gradec (5), Nazarje (10), Celje (8) and Drava-Ptuj Basin (12), respectively.

Figure 1: Locations of the sections where samples for clast lithological analysis were collected.

Figure 2: Microfacies of clasts in the Pliocene-Pleistocene sediments from the Slovenj Gradec Basin in cross-polarized light. Corresponding thin sections descriptions are presented in Table 2. Abbreviations: Qtz – quartz, Mc – microcline, Pl – plagioclase, Ep – epidote, Am – amphibole, Chl – chlorite, Bt – biotite, Ms – muscovite, Grt – garnet

Figure 3: Microfacies of clasts in the Pliocene-Pleistocene sediments from the Nazarje Basin in plain- (A, B, C, D, G, H, I, J, K, L) and cross-polarized light (E, F). Corresponding thin sections descriptions are presented in Table 3. Abbreviations: H – hyaloclasts, Lmt – laumontite, Chl – chlorite, Sme – smectite, Zeo – zeolite, Pl – plagioclase, PmL – pumice lapilli, VRF – volcanic rock fragment, Fsp – feldspar, Aug – augite, Qtz – quartz, Bt – biotite, Hbl – hornblende, M – glassy groundmass, Px – pyroxene, RF – rock fragment.

Figure 4: Microfacies of clasts in the Pliocene-Pleistocene sediments in the Celje Basin in plain- (B, C, D, E, F, G, I) and cross-polarized light (A, H). Corresponding thin sections descriptions are presented in Table 4. Abbreviations: Qtz – quartz, Ms – muscovite, CG – crystal grains, y-GS – y-shaped glass shards, VRF – volcanic lithic fragment, Fsp – feldspar, M – tuffaceous matrix, Bt – biotite, g – glassy groundmass, RF – rock fragment, Tur – tourmaline, Tur(a) – authigenic tourmaline

Figure 5: Microfacies of clasts in the Pliocene-Pleistocene sediments in the Drava-Ptuj Basin in cross- (A, B, D, G, H, I) and plain-polarized light (C, E, F, J, K, L, M, N, O). Corresponding thin sections descriptions are presented in Table 5. Abbreviations: Qtz – quartz, Qtz(m) – microcristalline quartz, Hbl – hornblende, Ep – epidote, Grt – garnet, Ms – muscovite, Ser – sericite, Chl – chlorite, Chl(a) – altered chloride, Op – opaque mineral, WGS – welded glass shards, Cl – collapsed lapilli.

Locality map of sections in Shapefile (Shapefile 1) contains following attribute: type of shapefile, section (full name), name of the section (abbreviations), section type, reference, where the results and interpretation are published, author of the mapping and year of mapping. Shapefile contains 14 data points.

Shapefile 1: Location map of sections

Table 1 contain dataset with listed sections in each basin; section names after village name; sections' lengths in meters; CLA (clast lithological analysis) sample; depth of collected clast lithological samples; number of counted clasts per sample; number of thin sections per sampling area; coordinates of the sections in EPSG Coordinate Reference System Code (code: 3794); cross-reference for petrographical data (Tables 2-5 and publications) and related research article in which results and discussions were presented. Tables 2–5 contain petrographical dataset of analyzed thin sections from the Slovenj Gradec, Nazarje, Celje and Drava-Ptuj Basins, respectively, including lithogroup, lithotype, thin section descriptions and provenance attribution. Thin sections are marked with abbreviation of the section and a consecutive number. Lithogroup marks general rock classification. Lithotype represents basic rock determination. Brief petrographic description contains information about rock structure, texture, mineralogical composition, alteration, weathering, cementation, microfossils, diagenesis and, where applicable, resemblance with a certain thin section. Provenance was determined according to petrographic descriptions and compared with published data and maps of the geological units (Mencin Gale et al., 2019a, 2019b, 2024; Mencin Gale, 2021, and references therein).

Table 1: Sections dataset

Table 2: Petrography Slovenj Gradec Basin

Table 3: Petrography Nazarje Basin

Table 4: Petrography Celje Basin

Table 5: Petrography Drava-Ptuj Basin

Data format

Figure 1–5: Raster image (.jpeg format)
 Shapefile 1: ESRI shapefile, point features (.shp format)
 Table 1–5: Microsoft Excel file (.xlsx format)

Data accessibility

The analyzed data and metadata are open access data and has been deposited in DiRROS repository. License: CC-BY 4.0. Data and metadata are accessible using the link:

Repository name: DiRROS
 Direct URL to data: <https://dirros.openscience.si/IzpisGradiva.php?id=19042&lang=slv>

Acknowledgment

This work was co-funded by the Slovenian Research and Innovation Agency (ARIS) in the frame of the Young Researchers programme under grant no. 38184, the postdoctoral project under grant no. Z1-50029 (EvoQ the past) and the research programme Regional Geology under grant no. P1-0011 carried out at the Geological Survey of Slovenia. We would like to thank dr. Petra Gostinčar and anonymous reviewer for the comments that significantly improved the earlier version of the manuscript.

References

- Bridgland, D.R. 1986: Clast Lithological Analysis. Technical Guide, 3. Quaternary Research Association, Cambridge: 207 p.
- Bridgland, D.R., Westaway, R., Romieh, M.A., Candy, I., Daoud, M., Demir, T., Galiatsatos, N., Schreve, D.C., Seyrek, A., Shaw, A.D., White, T.S. & Whittaker, J. 2012: The River Orontes in Syria and Turkey: Downstream variation of fluvial archives in different crustal blocks. *Geomorphology*, 165–166: 25–49. <https://doi.org/10.1016/j.geomorph.2012.01.011>
- Gale, S.J. & Hoare, P.G. 2011: Quaternary Sediments: Petrographic Methods for the Study of Unlithified Rocks. The Blackburn press, Caldwell, New Jersey: 325 p. <https://doi.org/10.1002/gj.2584>
- Lindsey, D.A., Langer, W.H. & Van Gosen, B.S. 2007: Using pebble lithology and roundness to interpret gravel provenance in piedmont fluvial systems of the Rocky Mountains, USA. *Sedimentary Geology*, 199: 223–232. <https://doi.org/10.1016/j.sedgeo.2007.02.006>
- Mencin Gale, E. 2021: Pliocene to Quaternary sedimentary evolution of intramountain basins at the junction of Alps, Dinarides and Pannonian Basin Faculty for Natural Sciences and Engineering. PhD thesis. Univerza v Ljubljani, Naravoslovno-tehniška fakulteta, Ljubljana: 187 p.
- Mencin Gale, E., Jamšek Rupnik, P., Trajanova, M., Bavec, M., Anselmetti, F.S. & Šmuc, A. 2019a: Morphostratigraphy and provenance of Plio-Pleistocene terraces in the south-eastern Alpine foreland: the Mislinja and Upper Savinja valleys, northern Slovenia. *Journal of Quaternary Science*, 34: 633–649. <https://doi.org/10.1002/jqs.3156>
- Mencin Gale, E., Jamšek Rupnik, P., Trajanova, M., Gale, L., Bavec, M., Anselmetti, F.S. & Šmuc, A. 2019b: Provenance and morphostratigraphy of the Pliocene-Quaternary sediments in the Celje and Drava-Ptuj Basins (eastern Slovenia). *Geologija*, 62/2: 189–218. <https://doi.org/10.5474/geologija.2019.009>
- Mencin Gale, E., Jamšek Rupnik, P., Akçar, N., Christl, M., Vockenhuber, C., Anselmetti, F. S. & Šmuc, A. 2024: The onset of Pliocene - Early Pleistocene fluvial aggradation in the South-eastern Alpine Foreland (Velenje Basin, Slovenia) and its paleoenvironmental implications. *Journal of Quaternary Science*, ISSN 0267-8179: 1–19. <https://doi.org/10.1002/jqs.3623>.
- Ministry of Environment and Spatial Planning, Slovenian Environmental Agency, 2015. Lidar data. http://gis.arso.gov.si/evode/profile.aspx?id=atlas_voda_Lidar@Arso&culture=en-US (last accessed: February, 2023)
- Walden, J. 2004: Particle lithology (or mineral and geochemical analysis). In: Evans, D.J.A. & Benn, D.I. (eds.): A practical guide to the study of glacial sediments. Hodder Education, London: 145–180.

Poročila in ostalo - Reports and More

7. svetovni geotermalni kongres WGC 2023, Peking (Kitajska)

15. – 17. september 2023

Dušan RAJVER

Geološki zavod Slovenije, Dimičeva ul. 14, SI-1000 Ljubljana, Slovenija; e-mail: dusan.rajver@geo-zs.si

Pred osmimi leti so vodilni v mednarodnem geotermalnem združenju (IGA) menili, da mora postati geotermalna energija bistveno bolj prepoznavna in vidna med svetovnimi viri energije, še posebno med obnovljivimi viri energije (OVE). Zato je Kitajska kot naslednja gostiteljica organizirala 7. svetovni geotermalni kongres že v septembru 2023, kar je le dve leti po prejšnjem na Islandiji, ki je bil sicer najavljen za leto 2020, zaradi Covid pandemije pa je bil premaknjen za eno leto naprej in izveden večinoma virtualno (Rajver, 2021). Kongres v Pekingu je trajal le tri dni, saj so organizatorji očitno dojeli, da bo prispevkov za kongres in udeležencev iz drugih držav nekaj manj kot na prejšnjih dveh kongresih. Razloga sta najmanj dva: kongres se je namreč odvijal le dve leti za prejšnjim, nekaj vpliva pa morda imajo tudi strogi in zapleteni (in posledično odvračajoči) postopki za vstop na Kitajsko. Gostitelj kongresa je bil China National Geothermal Energy Center, organizator pa China Petrochemical Corporation s štirimi so-organizatorji in tremi podpornimi korporacijami (vse tri iz naftne sfere). Glavna (diamantna) sponzorja sta bili podjetji Arctic Green Energy in Honeywell, poleg teh je bilo še deset drugih sponzorjev. Prejšnji svetovni geotermalni kongresi oziroma mednarodni geotermalni simpoziji od leta 1970 dalje so omenjeni v prejšnjih poročilih (Rajver, 2015, 2021).

Kitajska je izjemen primer, ki z leti vse bolj dokazuje, da geotermalna energija (GE) lahko znatno prispeva k daljinskemu ogrevanju in doseže ogljično neutralnost v gradbenem sektorju, četudi v vulkansko neaktivniv državi. Z ogromnim povpraševanjem po »čistem« (ne-fosilnem) ogrevanju je postopno postavila tak geotermalni razvoj s fokusom na ogrevanju in hlajenju, kar jo je pripeljalo v rabi GE za ogrevanje in hlajenje že nekaj let na prvo mesto v svetu, kakor tudi v posredovanju novih idej za mednarodni geotermalni razvoj. Kitajska je prva glede neposredne rabe toplotne iz GE, bodisi brez upoštevanja sektorja rabe plitve GE s tehnolo-

gijo geotermalnih topotnih črpalk (GTČ, angl. ground-source heat pumps, GSHP) ali pa skupaj s tem tipom postavitev (instalacije). Navajam številke iz najnovejših svetovnih pregledov o ogrevanju in hlajenju v svetu iz GE (Manzella et al., 2023) ter proizvodnji električne energije iz GE v svetu (Gutiérrez-Negrín, 2023). Prispevek kitajskih avtorjev o rabi GE na Kitajskem v letu 2022 (Guo et al., 2023) namreč še vedno ni na voljo na spletni strani IGA (Internet 1). Ob koncu 2021 je doseglj kapaciteto za ogrevanje in hlajenje iz GE na 1,33 milijard m², vključno 530 milijonov m² za geotermalno daljinsko ogrevanje in 800 milijonov m² površin, ki se ogrevajo in/ali hladijo s tehnologijo GTČ iz toplotne plitve podzemlja. V neposredni rabi za ogrevanje in hlajenje ima Kitajska nameščeno kapaciteto naprav 100.220 MW_t, iz katerih izkorišča 828.882 TJ (123.361,4 GWh, podatek za 2022), kar je 56 % svetovne izkoriščene GE za različne kategorije rabe, kar jo že 20 zaporednih let uvršča na prvo mesto. Med obsežnimi geotermalnimi aplikacijami izstopa ogrevanje in hlajenje stavb kot pomembna zgodba o uspehu z nameščeno zmogljivostjo 92.352 MW_t in letno porabo 714.236 TJ energije. Severna Kitajska, predvsem pet severnih provinc in mest Hebei, Henan, Shandong, Shaanxi in Tianjin, ki se zanašajo na bogate geotermalne vire v sedimentnih bazenih, se je postopoma razvila v glavno območje z daljinskim ogrevanjem iz hidrogeotermalnih virov. Vse to je zelo podprto s politiko čistega ogrevanja pozimi v severni regiji in z ustreznim davkom za geotermalne vire. Poleg tega se je ogrevanje iz hidrogeotermalnih virov razvilo tudi v severnih in alpskih regijah ter nekaterih provincah na jugu (Heilongjiang, Jilin, Liaoning, Notranja Mongolija, Xinjiang, Gansu, Ningxia, Qinghai, Tibet, Jiangsu, Anhui in Hubei). Sistemi GTČ so večinoma razširjeni v ravninah vzhodne Kitajske, med katerimi je najbolje razvit Bohajski rob, druga regija pa je srednji in spodnji tok ravnic reke Jangce. Druge dejavne kategorije rabe so: kmetijstvo (rastlinjaki, akvakultura) in predelava hrane,

industrijska procesna toplota, ter zdravje, rekreacija in turizem (bazenski kompleksi). - Seveda pa Kitajska nima takih geoloških danosti za proizvodnjo električne energije kot jo imajo druge države iz visokoentalpijskih geotermalnih sistemov, zato v njenih elektrarnah nameščena kapaciteta znaša le 45,1 MW_e, iz katere je proizvedla 131,2 GWh električne energije (Guo et al., 2023; v: Gutiérrez-Negrín, 2023).

Tokratni kongres je zaradi prej omenjenih razlogov težko primerjati s tistim na Islandiji leta 2020+1 ali tistim v Avstraliji 2015. Prisotno je bilo okrog 900 udeležencev, kar je precej manj kot na prejšnjih kongresih, in od tega jih je bilo manj kot polovico iz drugih držav. Potekal je le na licu mesta in ne virtualno. Za kongresni zbornik je bilo tik pred kongresom sprejeto okrog 765 prispevkov,

precej manj kot na prejšnjih kongresih, in niso bili predani udeležencem kongresa v nobeni združeni obliki zbornika (USB ali spletna povezava na vse prispevke, CD na prejšnjih kongresih), kot je bila praksa na vseh prejšnjih svetovnih kongresih. Organizatorji so namreč dopustili možnost, da so avtorji lahko svoje prispevke še po kongresu dopolnili in popravili ter jih poslali na uradno spletno stran kongresa še do 13. okt. 2023. Ni znano koliko prispevkov je bilo še naknadno poslano, sedaj (stanje 22. dec. 2023) je na spletni strani IGA naloženo še vedno le 436 prispevkov.

V tabeli 1 so vse sekcije (v angl. in slov.), s številom sprejetih prispevkov po posameznih sekcijah, kakor je bilo navedeno na spletni strani kongresa le nekaj dni pred kongresom.

Tabela 1. Seznam vseh sekcij na kongresu in število najavljenih predstavitev po sekcijah.

Session	Sekcija	Število prispevkov	
		govorno	poster
Advanced geothermal	Napredna tehnologija in pristopi (v geotermiji)	18	
Business strategies (Green Finance)	Poslovne strategije (financiranje v OVE)	7	4 (GF)
Case histories	Primeri (raziskav in/ali rabe GE)	7	
Corrosion in geothermal systems	Korozija v geotermalnih sistemih	5	
Country updates	Poročila držav o rabi GE	14	
Direct use: local solutions	Neposredna raba: lokalne rešitve	5	
Direct use: miscellaneous	Neposredna raba: razno	6	
Direct use: rural-urban use	Neposredna raba: na podeželju-v mestih	5	
Direct use: wells exploitation	Neposredna raba: vrtine v izkoriščanju	5	
District heating: sustainability	Daljinsko ogrevanje: trajnost	4	
District heating: technology	Daljinsko ogrevanje: tehnologija	4	
Drilling & completion technology	Tehnologija vrtanja & dokončanja del (druge tehnološke naprave)	28	14
Education	Izobraževanje (v geotermiji)	4	
Enhanced geothermal systems	Izboljšani geotermalni sistemi (EGS)	19	
Energy cost & efficiency	Strošek energije & učinkovitost	5	
Environmental aspects	Okoljski vidiki	4	
Exploration: exploration methods	Raziskave: raziskovalne metode	6	
Exploration (in Americas & Africa)	Raziskave (v Amerikah & Afriki)	6	
Exploration (in China & Indonesia)	Raziskave (na Kitajskem & v Indoneziji)	12	
Exploration (in Eurasia)	Raziskave (v Evropi & Aziji)	5	
Exploration (remote sensing & borehole imaging)	Raziskave (daljinsko zaznavanje & slikanje vrtin)	6	
Field management	Upravljanje z geotermalnim poljem	6	
Geochemistry low temperature fracture hotsprings	Geokemija: nizko-temperaturni razpoklinski vroči izviri	6	
Geochemistry experiment mineral	Geokemija: poskusi, minerali	4	
Geochemistry high temperature	Geokemija: visoko-temperaturno okolje	6	
Geochemistry sedimentary	Geokemija: sedimentno okolje	5	
Geology	Geologija	43	
Geophysics	Geofizika	35	

Geothermal closed loop	Geotermični sistemi na zaprti krogotok	10	
Geothermal development & utilization & Cities	Geotermalni razvoj & izkoriščanje GE & Mesta		23
Geothermal	Geotermalni (razno)		14
Heat storage	Shranjevanje topote	5	
Hydrogeology	Hidrogeologija	9	
Hydrothermal accumulation mechanism & Resource assessment	Mehanizem hidrotermalne akumulacije & Ocena virov	7	
Injection technology	Tehnologija reinjekcije	4	
Integrated energy systems & Cascaded uses	Integrirani energijski sistemi & Kaskadne rabe	7	
International collaboration	Mednarodna sodelava	6	
Life cycle analysis	Analiza življenjskega cikla (LCA)	3	
Markets	Trženje geotermije (opreme, topote)		9
Minerals, metals & hydrogen	Minerali, kovine & vodik (iz GE)	6	
Oil & gas	Toplotna iz naftnih /plinskih polj	7	9
Policy, legal & regulatory aspects	Politika, pravni in regulativni vidiki	6	2
Power generation	Proizvodnja električne energije (iz GE)	6	
Power generation (Prospective sites)	Proizvodnja električne energije (perspektivne lokacije)	5	
Production engineering, steam gathering systems	Proizvodni inženiring, sistemi zbiranja (geotermalne) pare	5	
Research & Development: drilling & completion	Raziskave & razvoj: vrstanje & dokončanje		14
Research & Development: field & production technology	Raziskave & razvoj: tehnologija geotermalnega polja & proizvodnje		26
Research & Development: geoscience	Raziskave & razvoj: geoznanost		80
Research & Development: geothermal systems	Raziskave & razvoj: geotermalni sistemi		38
Reservoir engineering	Inženiring (geotermalnih) rezervoarjev	23	
Resource assessment	Ocena (geotermalnih) virov	6	
Risk mitigation	Blaženje rizika	5	
Scaling in geothermal systems	Luščenje (odlaganje kotlovcu) v geotermalnih sistemih	14	
Societal & cultural aspects	Družbeni in kulturni vidiki	5	
Supercritical geothermal	Superkritični geotermalni viri	7	
Sustainability & climate change	Trajnost & klimatske spremembe	6	16
Technology & Innovation - Big data & data analytics	Tehnologija & inovacije - Veliki podatki & analitika podatkov	6	
Technology & Innovation - intelligent computing & AI	Tehnologija & inovacije - inteligentno računalništvo & umetna inteligenco	7	
Technology & Innovation	Tehnologija & inovacije		10
Technology & Innovation - software for geothermal applications	Tehnologija & inovacije - programska oprema za geotermalne aplikacije	6	
Top sides - case studies: heat pumps	Vrhunski dosežki - študije primerov: topotne črpalki	6	
Top sides - deep BHEs	Vrhunski dosežki - globoke geosonde	6	
Top sides - economics, exploration & financing	Vrhunski dosežki - ekonomija, raziskovanje & finančiranje	4	
Top sides - models & analysis of pilot sites	Vrhunski dosežki - modeli & analiza pilotnih lokacij	7	
Top sides	Vrhunski dosežki		19
UNFC sessions	UNFC sekcije	3	
Water use	Raba (termalne) vode	3	
SKUPAJ:	765	487	278

Opombe:

EGS=Enhanced Geothermal System; GE=geotermalna energija; UNFC=United Nations Framework Classification for resources; BHE=Borehole Heat Exchanger; GF=green finance.

Skupno je do pričetka kongresa prisvelo 765 prispevkov, in okvirno toliko naj bi bilo na kongresu tudi predstavitev (od tega 278 posterjev) v 67 sekcijah. Seveda pa se je na samem kongresu izkazalo, da precej predavateljev, predvsem iz drugih držav, sploh ni prisvelo na kongres (po okvirni oceni >10 %), tako da nekatere predstavitve niso bile izvedene.

Raznolikost v temah prispevkov je rezultat širitve svetovne dejavnosti v raziskavah in rabi geotermalne energije, kakor tudi vključenosti geotermalne energije v različnih vejah dejavnosti oziroma družbe. Iz prevladujočih sekcij po številu prispevkov se opazi, kam so usmerjeni glavni napori v raziskavah, razvoju in uveljavljanju geotermalne energije: raziskave in razvoj (štirje različni vidiki: 158, od tega geoznanost 80, geotermalni sistemi 38, tehnologija geotermalnega polja in proizvodnje 26), geologija (43), tehnologija vrtanja in dokončanja del (42), vrhunski dosežki (različni vidiki: 42), geofizika (35), tehnologija in inovacije (različni vidiki: 29), raziskave po regijah in raziskovalne metode (29), geotermalni razvoj in izkoriščanje geotermalne energije (23), inženiring (geotermalnih) rezervoarjev (23), trajnost in klimatske spremembe (22), geokemija (štirje različni vidiki: 21), neposredna raba toplotne energije (različni vidiki: 21), EGS (19), napredna tehnologija v geotermiji (18). Glede na prejšnje kongrese so nekatere dejavnosti prišle tokrat bolj v ospredje, vseeno pa so posredne in površinske metode (geofizika, geokemija in geologija) še naprej zelo pomembne v raziskavah in upravljanju geotermalnih virov. Z namenom bolj uveljaviti geotermalno energijo med OVE je viden prispevek sekcij *trajnost, trženje geotermije, politika in regulativni vidiki*. Številni prispevki o raziskavah kažejo na dejavno iskanje novih virov v raznih državah sveta. Izpostavim lahko še nekaj zanimivih prispevkov v sekciji *Vrhunski dosežki*, kot so primeri z uporabo toplotnih črpalk, primeri z globokimi geosondami ter modeli in analiza pilotnih lokacij.

Pod okriljem kongresa so se med kongresom odvijali naslednji dogodki: *Global geothermal collaboration forum*, *China-Iceland geothermal technology exchange forum*, *Geothermal youth forum*, *IGA standard release*. V kongresnem centru se je istočasno odvijala razstava opreme za raziskave in razvoj geotermalne energije (*Geothermal development technology and equipment exhibition*) z močnim deležem kitajskih podjetij (proizvodnja opreme za vrtine, cevovode, toplotne postaje, elektrarne, itd.) v geotermalnih raziskavah in

razvoju ter izkoriščanju geotermalne energije. V ponudbi kongresa je bila tudi izvedba štirih ekskurzij (2-dnevne do 6-dnevne), vse v osrednji in jugozahodni del vzhodne polovice države.

Plenarna predavanja na otvoritvi (L.C. Gutiérrez-Negrín o napredku v proizvodnji elektrike iz GE v svetu, A. Manzella o ogrevanju in hlajenju iz geotermalne energije (GE) v svetu ter X. Guo o razvoju kitajske geotermalne industrije) so pokazala vztrajno rast v geotermalnem razvoju. Za ta kongres je o *ogrevanju in hlajenju* iz GE poročalo 38 držav, za 50 držav so pridobljeni podatki iz drugih virov. Torej se je ogrevanje in hlajenje ob koncu leta 2022 odvijalo v 88 državah, enako kot tri leta prej (Manzella et al., 2023). Skupna nameščena kapaciteta za ogrevanje in hlajenje iz GE znaša 173.303,2 MW_t, kar je porast za 60 % glede na številko poročano za WGC 2020+1. Na ta znaten napredek večinoma vplivajo poročane številke o veliki širitvi rabe GE za ogrevanje in hlajenje na Kitajskem. Skupna svetovna raba GE je znašala 1.476.312,0 TJ (410 TWh), kar je porast za 44 % glede na poročano za WGC 2020+1 (Lund & Toth, 2021). Tabela 2 povzema oboje po celinah (Manzella et al., 2023). Pomembna značilnost poročanja, kot ga podajajo Manzella in sodelavci (2023), je revidirana klasifikacija kategorij rabe GE za ogrevanje in hlajenje. Kategorizacija je bila poenostavljena in zdaj obsega pet pomembnih uporab geotermalne toplotne, in sicer (I) kmetijstvo in predelava hrane, (II) industrijska procesna toplota, (III) zdravje, rekreacija in turizem, (IV) ogrevanje in hlajenje zgradb, in (V) druge uporabe. Strokovnjaki so se strinjali, da je treba kategorijo GTČ (plitva geotermija) obravnavati kot vrsto naprave in ne kot kategorijo samo po sebi. Številke zanjo so uvrščene večinoma v rabo »ogrevanje in hlajenje zgradb«. Prva novost poročila Manzelle in sodelavcev (2023) je v terminologiji in kategorizaciji, začenši s sklicevanjem na toplotno uporabo geotermalne toplotne. Geotermalna toplota se pogosto imenuje „neposredna uporaba“. Vendar to ni običajno ime zunaj geotermalne industrije. Strokovnjaki so se strinjali, da je „ogrevanje in hlajenje“ najprimernejše ime za ta sektor. Pri izbiri so odločali ozaveščenost občinstva (uporabno zunaj geotermalne industrije), inkluzivnost (plitva in globoka, nizka in visoka entalpija itd.) in celovitost (vključno z uporabo GTČ kot vrste tehnologije skupaj z drugimi vrstami). Kot predlog za opredelitev sektorja je *ogrevanje in hlajenje* „uporaba toplotne energije, ki se nahaja v podzemlju ali naravno dviga na površino tal, za katerikoli namen, razen za proizvodnjo električne energije“.

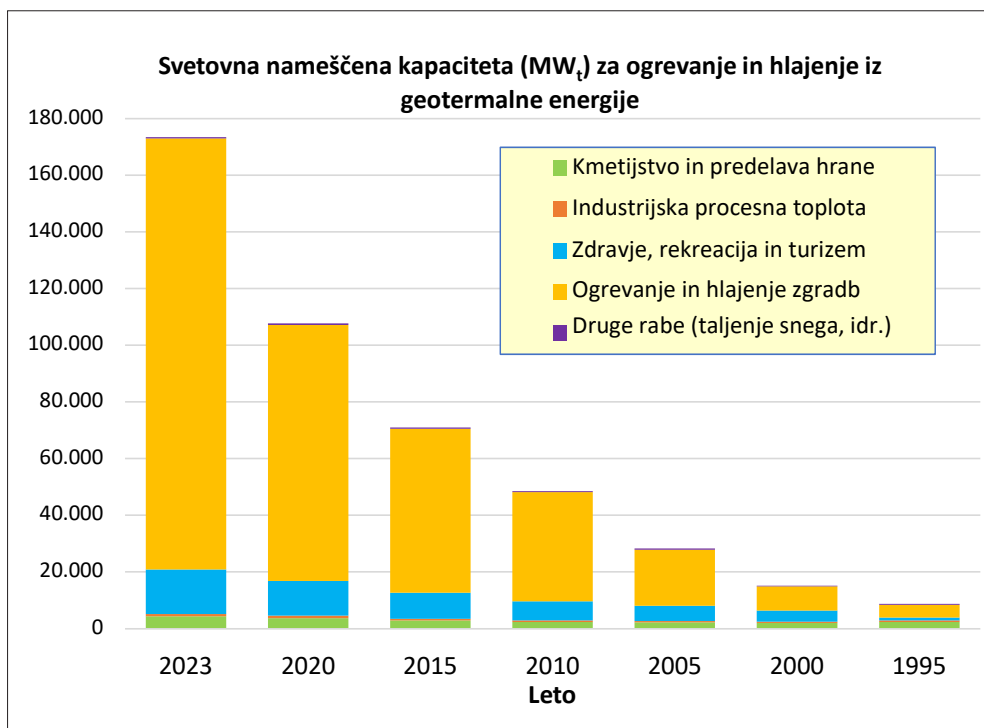
Celina (štev. držav)	MW _t	TJ/leto	GWh/leto
Afrika (11)	160,71	3.713,78	1.031,61
Amerika (17)	24.506,46	191.540,82	53.205,78
Azija (17)	105.095,70	877.957,20	243.877,00
Evropa (36)	37.051,68	291.237,47	80.899,30
Oceanija (3)	820,60	15.352,02	4.264,45
Transcelinske (4)	5.668,05	96.510,72	26.808,53
SKUPAJ (88)	173.303	1.476.312	410.087

Tabela 2. Povzetek podatkov o ogrevanju in hlajenju v svetu po celinah (za leto 2022).

Stopnje rasti instalirane moči in letne rabe GE za zadnjih 28 let so povzete na slikah 1 in 2. Kategorija z najbolj izrazitim porastom v tem obdobju je »ogrevanje in hlajenje zgradb«. Slika 1 jasno kaže znaten porast te kategorije v nameščeni kapaciteti, ki je precej podkrepljena z naraščajočim številom sistemov z enotami GTČ (izkoriščanje plitve GE), vključno za industrijske rabe. Znaten porast kategorije ogrevanja in hlajenja zgradb, viden na

sliki 2, je prvenstveno posledica močne širitve tovrstne rabe na Kitajskem.

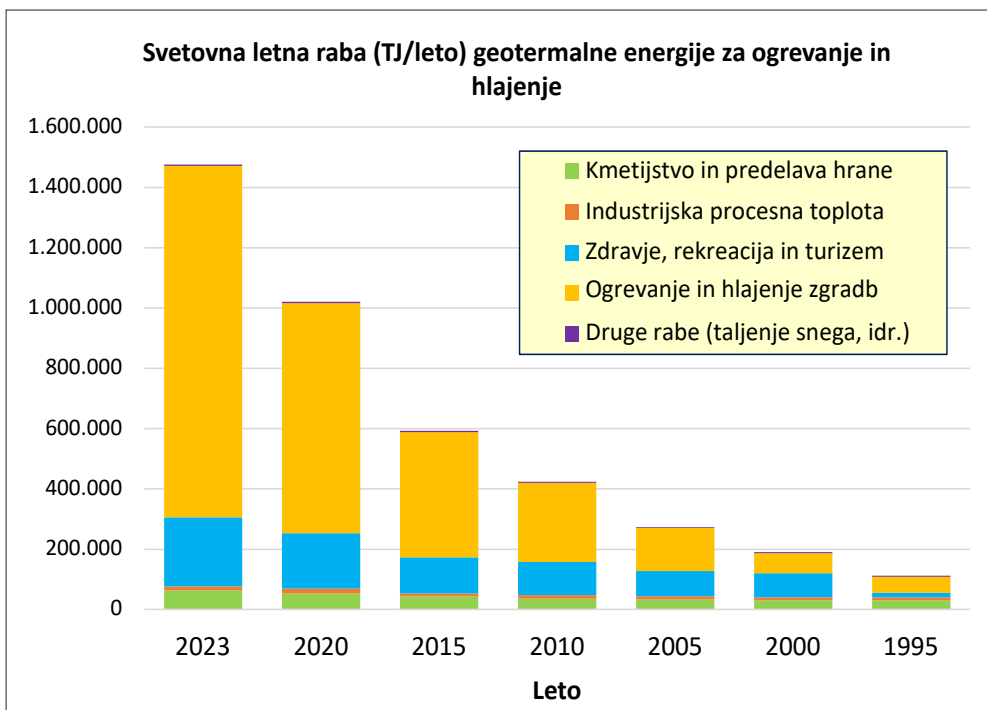
Kitajska, ZDA, Švedska, Nemčija in Turčija so države z največ nameščene kapacitete (MW_t) za ogrevanje in hlajenje iz GE (vse kategorije rabe), in v teh državah je kar 80 % svetovne kapacitete, medtem ko so države z največ izkoriščene GE na letni ravni Kitajska, ZDA, Turčija, Švedska in Islandija (Tabela 3).



Sl. 1. Nameščena kapaciteta (MW_t) za ogrevanje in hlajenje (porazdeljena po kategorijah) kot je poročano na svetovnih geotermalnih kongresih od 1995 do 2023 (Lund & Toth, 2021; Manzella et al., 2023).

Država	Kapaciteta, MW _t	Država	Energija, TJ/leto
Kitajska	100.220	Kitajska	828.882
ZDA	20.712	ZDA	152.809
Švedska	7.280	Turčija	85.000
Nemčija	5.381	Švedska	67.680
Turčija	5.113	Islandija	35.615

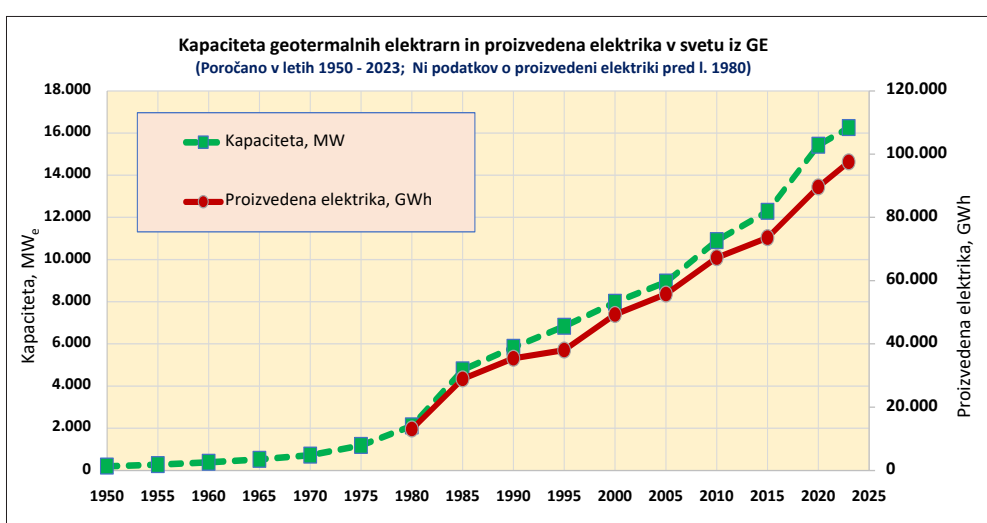
Tabela 3. Vodilne države v svetu v izkoriščanju geotermalne energije za ogrevanje in hlajenje.



Sl. 2. Letna raba geotermalne energije (TJ/leto) za ogrevanje in hlajenje (porazdeljena po kategorijah) kot je poročano na svetovnih geotermalnih konгресih od 1995 do 2023 (Lund & Tóth, 2021; Manzella et al., 2023).

Ob koncu leta 2021 so bile delajoče geotermalne elektrarne samo v 31 državah, s skupno močjo 16.260 MW_e, to je le 0,16 % vse inštalirane moči vseh elektrarn na svetu, ki je bila 10.216.390 MW_e. Geotermalne elektrarne so postavljene na 197 geotermalnih poljih s 671 posameznimi agregati (stanje v dec. 2021). Skoraj 38 % teh enot je tipa z momentnim vparevanjem (angl. flash) s skupno močjo 9.129 MW_e (52,6 % od skupne moči), sledijo binarne enote tipa ORC z 21,7 % instalirane moči. Izbrani niz držav z geotermalno proizvodnjo električne še naprej vodijo ZDA, sledijo Indonezija, Filipini in Turčija. Vse države so v letu 2021 proizvedle 96.562 GWh električne energije pri poprečnem letnem faktorju zmogljivosti 68 %, kar je predstavljalo 0,35% svetovne proizvodnje električne energije (27.834,7 TWh) in 0,90 % vse »čiste«

električne energije v svetu (10.731,3 TWh). Čista energija je definirana kot proizvedena elektrika iz nizko-ogljičnih virov, kar v osnovi vključuje vse OVE in nuklearno energijo. V vsaj sedmih državah električna energija geotermalnega izvora predstavlja več kot 10 % vse proizvedene električne energije, na čelu s Kenijo, Islandijo in Salvadorjem. Praktično vseh 197 delajočih geotermalnih polj izkorišča vire iz hidrotermalnih konvencionalnih rezervoarjev, z oceno 3700 proizvodnih vrtin z letno poprečno proizvodnjo skoraj 3 MWh na vrtino. Stvari bi lahko bile podobne v naslednjih nekaj letih, če se bo trenutni trend nadaljeval, vendar se lahko vse spremeni zaradi svetovne nujnosti ohranjanja globalnega segrevanja pod pragom 1,5 °C v naslednjih letih (Gutiérrez-Negrín, 2023).



Sl. 3. Kapaciteta geotermalnih elektrarn in njihova proizvedena elektrika v svetu med letoma 1980 in 2023. Proizvedena elektrika v letih 1980 in 1985 je le ocenjena (Gutiérrez-Negrín, 2023).

Po podatkih kot jih navaja Gutiérrez-Negrín (2023), je letna rast proizvedene geotermalne električne energije (7,4-krat) višja od rasti celotne svetovne proizvodnje električne energije v istem obdobju (5,6-krat, s 5.633 na 28.254 TWh), pa tudi od rasti nizkogljične proizvedene električne energije (4,6-krat, z 2438 na 11.143 TWh). To seveda pomeni, da je geotermalna industrija rastla nekoliko hitreje kot proizvodnja električne energije na splošno in zlasti industrija čiste energije, kar se zdi protislovno. Vendar pa tudi pojasnjuje, zakaj se je delež geotermalne energije tako v skupni kot v čisti proizvodnji električne energije v teh desetletjih povečeval z 0,23 % oziroma 0,54 %



Sl. 4. Notranjost geotermalne elektrarne z močjo 280 kW z ORC tipom turbine v Tianzhenu (SV od Datonga), Shanxi demonstration base.

na 0,34 % oziroma 0,87 %. Vsekakor gre za majhno globalno povečanje, vendar je bistveno v državah, kjer geotermalna energija prispeva pomemben del portfelja električne energije.

V izkoriščanju geotermalne energije je v Sloveniji ob koncu 2022 znašala nameščena zmogljivost naprav za neposredno rabo 318 MW_t, letna izkoriščena geotermalna energija pa 1847 TJ (ali 513 GWh) (Rajver et al., 2023a, 2023b), vključno s prispevkom geotermalnih topotnih črpalk (GTČ) v koriščenju toplote plitvega podzemlja za ogrevanje in hlajenje. Prispevek sektorja GTČ za ogrevanje in/ali hlajenje prostorov je v letu 2022 znašal 260 MW_t oziroma 1295 TJ (360 GWh). Različne kategorije rabe pa zajemajo: ogrevanje individualnih prostorov in pripravo sanitarne vode, daljinsko ogrevanje, klimatizacijo/hlajenje, ogrevanje rastlinjakov, kopanje in plavanje z balneologijo, taljenje snega ter ogrevanje in/ali hlajenje s tehnologijo GTČ.

Z Geološkega zavoda Slovenije je bil na kongresu prisoten le pisec tega poročila s prispevkom v sekciiji *Country updates* (Rajver et al., 2023a). V drugih prispevkih strokovnjaki iz Slovenije tokrat niso bili nikjer prisotni. Naslednji svetovni geotermalni kongres bo že junija 2026 v Kanadi (Calgary), še prej pa bo leta 2025 naslednji evropski geotermalni kongres v Švici (Zürich).



Sl. 5. Datong Volcanic group GeoPark, VSV od Datonga.

Viri

- Guo, X., Dang, L., Han, Z. & Guo, D. 2023: High-Quality Development of China's Geothermal Industry – China National Report of the 2023 World Geothermal Conference. Proceedings, World Geothermal Congress 2023, 15-17 Sept. 2023, Beijing, China.
- Gutiérrez-Negrín, L.C. 2023: Worldwide Geothermal Power 2020-2023 Update Report. Proceedings, World Geothermal Congress 2023, Sept. 2023, Beijing, China, 36 p.
- Lund, J.W. & Toth, A.N. 2021: Direct utilization of geothermal energy 2020 worldwide review. *Geothermics*, 90. <https://doi.org/10.1016/j.geothermics.2020.101915>
- Manzella, A., Cannone, E., Galione, M.R. & Trumpy, E. 2023: Geothermal Heating and Cooling Production, 2023 Worldwide Review. Proceedings, World Geothermal Congress 2023, 15-17 Sept. 2023, Beijing, China, 25 p.
- Rajver, D. 2015: 5. Svetovni geotermalni kongres v Melbournu (Avstralija). *Geologija*, 58/2: 263-264, Ljubljana.
- Rajver, D. 2021: 6. Svetovni geotermalni kongres WGC 2020+1, Reykjavik (Islandija). *Geologija*, 64/2: 294-298, Ljubljana.
- Rajver, D., Rman, N., Lapanje, A. & Prestor, J. 2023a: Geothermal Country Update Report for Slovenia, 2020-2022. Proceedings, World Geothermal Congress 2023, 15-17 Sept. 2023, Beijing, China, IGA, 10 p., 3 tables.
- Rajver, D., Pestotnik, S., Rman, N., Hribernik, J., Srša, A., Lapanje, A., Prestor, J. & Adrinek, S. 2023b: Pregled rabe geotermalne energije v Sloveniji v letu 2022 in način pridobivanja podatkov o trgu geotermalnih toplovnih črpalk. Mineralne surovine v letu 2022, Geološki zavod Slovenije, Ljubljana: 154-173.
- Internet 1: [Geothermal Paper Database - International Geothermal Association \(lovegeothermal.org\)](http://www.lovegeothermal.org)

Poročilo slovenskega nacionalnega odbora za geoznanosti in geoparke (IGGP) za leto 2023

Matevž NOVAK^{1,2}

¹Geološki zavod Slovenije, Dimičeva ul. 14, SI-1000 Ljubljana, Slovenija; e-mail: matevz.novak@geo-zs.si

²Slovenski nacionalni odbor za geoznanosti in geoparke

Mednarodni program za geoznanost in geoparke (*International Geoscience and Geoparks Programme* – IGGP) od leta 2015 združuje dva, prej ločena programa. To sta Mednarodni geoznanstveni program (*International Geoscience Programme* – IGCP) in program Unescovih Globalnih geoparkov (*Unesco Global Geoparks* - UGGP). Prvi je bil ustanovljen že leta 1972 v sodelovanju Unesca in Mednarodne zveze geoloških znanosti (*International Union of Geological Sciences* – IUGS). Ustanovljen je bil z imenom *International Geological Correlation Programme* (Mednarodni geološki korelacijski program) in je bil zelo usmerjen v mednarodne stratigrafske korelacije. Vanj so bili močno vpeti tudi slovenski raziskovalci. Leta 2005 je bil IGCP program prestrukturiran in preimenovan v *International Geoscience Programme*, kratica pa je ostala. Od leta 2013 ima IGCP podnaslov »Geoznanost v službi družbe« in je usmerjen v spodbujanje trajnostne rabe naravnih virov, energetskega prehoda, zmanjševanja tveganj geoloških nevarnosti ter ohranjanja geopestrosti in geološke dediščine. Program danes povezuje več kot 10.000 geoznanstvenikov iz več kot 150 držav, ki z eksperimenti in mreženjem postavljam temelje prihodnosti našega planeta. Program se izvaja skozi IGCP projekte, razdeljene v pet glavnih tematskih sklopov: Zemljini viri, Globalne spremembe in evolucija življejna, Geološko pogojene nevarnosti, Hidrogeologija in Geodinamika.

V Sloveniji je bil leta 1992 ustanovljen Slovenski nacionalni odbor IGCP, ki se je leta 2015 preimenoval v Nacionalni odbor IGGP. Deluje kot strokovno in posvetovalno telo Slovenske nacionalne komisije za Unesco (SNKU).

Na redni letni seji Nacionalnega odbora IGGP, 18. 12. 2023, so bili za člane v novem štiriletnem mandatu imenovani predstavniki inštitucij in posamezniki:

- dr. Matevž Novak, Geološki zavod Slovenije (GeoZS), predsednik NO
- doc. dr. Luka Gale, UL, Naravoslovno tehniška fakulteta, Oddelek za geologijo in GeoZS, tajnik NO
- dr. Mirka Trajanova, upokojena sodelavka GeoZS
- dr. Miloš Bavec, GeoZS

- mag. Suzana Fajmut Štrucl, Geopark Karavanke
- doc. dr. Špela Goričan, Paleontološki inštitut Ivana Rakovca, ZRC SAZU
- dr. Mateja Gosar, GeoZS
- Marjutka Hafner, Urad za UNESCO
- izr. prof. dr. Martin Knez, Inštitut za raziskovanje krasa, ZRC SAZU
- doc. dr. Tea Kolar-Jurkovšek, GeoZS
- pridr. prof. dr. Marko Komac, samostojni podjetnik
- Bojan Režun, Geopark Idrija
- Martina Stupar, Zavod RS za varstvo narave (ZRSVN)
- dr. Katica Drobne, upokojena sodelavka Paleontološkega inštituta Ivana Rakovca, ZRC SAZU, častna članica
- zaslužni prof. dr. Simon Pirc, upokojeni sodelavec UL, NTF, Oddelek za geologijo, častni član
- izr. prof. dr. Nastja Rogan Šmuc, UL, NTF, Oddelek za geologijo
- doc. dr. Petra Žvab Rožič, UL, NTF, Oddelek za geologijo
- doc. dr. Aleš Šoster, UL, NTF, Oddelek za geologijo

V letu 2023 je Nacionalni odbor IGGP koordiniral aktivnosti, ki so vključevale sodelovanje v IGCP projektih in dveh delovnih skupinah IUGS ter izvajanje programov dveh UNESCO Globalnih geoparkov, Idrija in Karavanke/Karawanken in Mednarodnega dneva geopestrosti.

Glavnino projektov je obsegal sklop IGCP s podarkom na prioritetah Unesca. Težišče dela je bilo na terenskih raziskavah, laboratorijski analitiki, mreženju in pripravi ter objavi rezultatov v domačih in tujih mednarodno priznanih znanstvenih revijah. Raziskovalci so težili k čim večji vpetosti v mednarodno sodelovanje, popularizacijo geoznanosti, prenos znanja na mlade ter širšo zainteresirano javnost in prenos dobrih praks med geoparki na mednarodnem nivoju. Povezovanje je potekalo preko spletnih in javnih medijev ter mednarodnih srečanj.

Poleg temeljnih znanj prinašajo raziskovalni projekti neposredno uporabno vrednost na področju vodnih virov, geotermalne energije, varstva okolja in naravne dediščine ter geološko pogojenih

Preglednica 1. Pregled projektov IGGP in nosilcev posameznih nalog v letu 2023.

Zap. št	Projekti	Nosilci projektov, inštitucije
1.	IUGS/IAGC: Global Geochemical Baselines	M. Gosar, GeoZS
2.	IUGS/IFG: Initiative on Forensic Geology	M. Gaberšek, GeoZS
3.	IGCP 692: Geoheritage for Geohazard Resilience	K. Ivančič, GeoZS
4.	IGCP 685: Geology for Sustainable Development	E. Mencin Gale, GeoZS
5.	IGCP 636: Geothermal resources for energy transition: direct uses and clean and renewable base-load power	N. Rman, GeoZS
6.	IGCP 684: The Water-Energy-Food and Ground-water Sustainability Nexus	M. Janža, GeoZS
7.	IGCP 710: Western Tethys meets Eastern Tethys – geodynamical, paleoceanographical and paleobiogeographical events	K. Drobne, ZRC SAZU, L. Gale, NTF, P. Miklavc, NTF
8.	IGCP 652: Reading geologic time in Paleozoic sedimentary rocks: the need for an integrated stratigraphy	M. Dolenec, NTF
9.	IGCP 683: Pre-Atlantic geological connections among northwest Africa, Iberia and eastern North America: Implications for continental configurations and economic resources	A. Šoster, NTF
10.	IGCP 737: SMART geology for better community	P. Žvab Rožič, NTF
11.	Geopark Idrija	B. Režun, Zavod za turizem Idrija
12.	Geopark Karavanke, Slovenija-Avstrija	S. Fajmut Štrucl, Podzemlje Pece
13.	Obeleževanje Mednarodnega dneva geopestrošči	M. Stupar, ZRSVN

nevarnosti. Slovenski raziskovalci so v letu 2023 sodelovali v osmih IGCP projektih. Nadaljevale so se aktivnosti v dveh delovnih skupinah IUGS in dveh UNESCO Globalnih geoparkih. Projekti in nosilci nalog so prikazani v Preglednici 1.

V delovnih skupinah IUGS/IACG in IUGS/IFG slovenski raziskovalci sodelujejo pri ugotavljanju naravnega geokemičnega ozadja in razločevanju med geološkimi materiali naravnega in antropogenega izvora.

Projekti IGCP 652, 683 in 710 so temeljne narave. Na podlagi izsledkov terenskih raziskav in laboratorijskih analiz se v teh projektih uskljuje stratigrafsko zaporednje kamnin, preko katerega se ugotavlajo razmere in dogajanja v okolju in njegove spremembe v geološki zgodovini. Nadgradnja geoloških modelov z novimi ugotovitvami je nujna za ugotavljanje geološkega razvoja posameznih območij, korelacije s sosednjimi območji, usmerjanje nadaljnjih raziskav, predvsem pa za načrtovanje rabe prostora.

Projekti IGCP 636, 684 in 685 so aplikativne narave. Obravnavajo vire geotermalne energije za prehod na pridobivanje energije iz obnovljivih virov, vodne vire za zagotavljanje pitne vode in vode za potrebe kmetijstva ter proučevanje sedimentov in sedimentacijskih procesov v obdobju kvartarja, ki so pomembni z družbeno-ekonomskega vidika, saj dajejo smernice za umeščanje infrastrukture v prostor, potresno varnost ter pridobivanje novih virov pitne vode.

Projekta IGCP 692 in 737, ter aktivnosti obeh Unescovih Globalnih geoparkov, Idrije in Karavank/Karawanken, združujejo interdisciplinarna znanja na osnovi geoznanosti. Njihov cilj je krepitev znanja o vseh vidikih geološke dediščine s širjenjem lastnih izkušenj z vzpostavljanjem in upravljanjem območij Unescove svetovne dediščine, geoparkov in drugih zavarovanih območij geološke dediščine. Oba geoparka sta uspešno opravljala vlogo informiranja, izobraževanja in ozaveščanja šolajoče se mladine in zainteresirane javnosti. S ciljem nadaljevanja aktivnosti za vzpostavitev upravljaškega načrta in trajnostnega razvoja čezmejnega geoparka Kras-Carso je bil v sodelovanju z italijanskimi partnerji prijavljen projekt INTERREG IT-SI KRAS-CARSO II – Skupno upravljanje in trajnostni razvoj območja Matičnega Krasa. Oddaja aplikacije za članstvo v Unescovi mreži Globalnih geoparkov se je žal zamknila za eno leto in je načrtovana v letu 2024.

Za obeležitev 2. Mednarodnega dneva geoprostrosti v letu 2023 je bilo s koordinacijo Zavoda RS za varstvo narave in Nacionalnega odbora IGGP izvedenih več promocijskih aktivnosti in predavanj z namenom širjenja novice o Mednarodnem dnevu geoprostrosti s poudarkom pomena tega dneva. Osrednji dogodek obeležitve je bil 6. oktobra v prostorih Glasbene šole Litija - Šmartno z okroglo mizo »Raba minaralnih surovin in njihov pomen za geoprostrost« ter obiskom Rudnika Sitarjevec.

Poročilo o aktivnostih Slovenskega geološkega društva v letu 2023

Astrid ŠVARA

Inštitut za raziskovanje krasa ZRC SAZU, Titov trg 2, SI-6230 Postojna, Slovenija;
e-mail: astrid.svara@zrc-sazu.si

V letu 2023 je bila glavna naloga vodstva društva sprememba društvenega statuta. Ker je zaradi posodobitve društvenih aktivnosti postal statut mestoma neskladen z delovanjem društva, je bila popolna prenova temeljnega akta neizogibna. Slednje smo opravili skladno z Zakonom o društvih (Uradni list RS št. 64/11-ZDru-1-UPB2), z Zakonom nevladnih organizacij (Uradni list RS št. 21/18) in s posvetovanjem z referentkama z Upravne enote Ljubljana ter Ministrstva za vzgojo in izobraževanje, kjer je Slovensko geološko društvo (SGD) registrirano. Sprememba statuta je v ožji skupini potekala aktivno in angažirano celo leto. Statut SGD je skupščina soglasno sprejela na seji 13. 3. 2024. Po potrditvi je bil poslan v pregled in overitev na UE LJ. Statut je dostopen na spletni strani društva.

Tik pred predhodno sejo skupščine se je prijetila nezgoda pri urejanju spletnne strani – stran je v minuti postala nepregledna, številni podatki so ob sesutju strani bili tudi izgubljeni. V ožjem izvršnem odboru smo sprejeli odločitev, da spletno stran iz precej zahtevne in skrbniku neprijazne domene »Joomla« s pomočjo strokovnjakije prestavimo na strežnik »Wordpress«. Slednji je enostavnejši za uporabo in upravljanje. Prenovljena spletna stran društva je bila predstavljena na skupščine in je dostopna na naslovu: www.slovenskogeoloskodrustvo.si.

Poleg nove spletnne grafične podobe društva, smo izdelali tudi dve reklamni roll-up stojali – v slovenskem in angleškem jeziku. Stojali sta primerni za uporabo na različnih dogodkih, kjer sodeluje SGD. Vsi, ki bi si žeeli stojalo izposoditi, lahko to storijo s sporočilom predsednici društva.

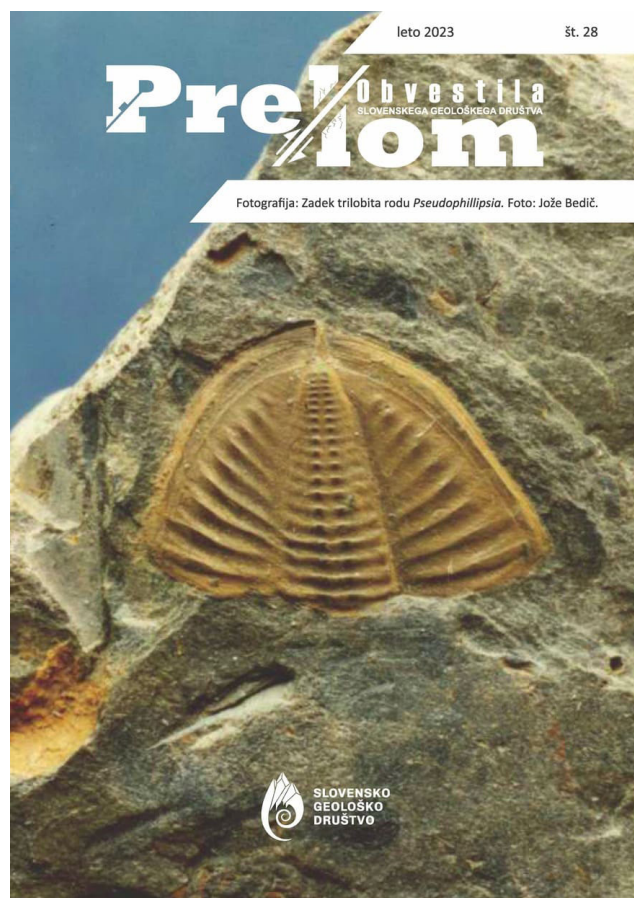
V začetku decembra 2023 je na Naravoslovno-tehniški fakulteti (NTF), na Oddelku za geologijo, v soorganizaciji z društvom potekalo 26. posvetovanje slovenskih geologov. Posvetovanja se je udeležilo 88 geologov strokovnjakov in študentov, med katerimi je velika večina izsledke svojih raziskav v obliku krajsih predavanj predstavila v 8. sekcijah in poster sekcijsi. Po uvodnih nagovorih je bilo nekaj uvodnih minut namenjenih tudi predstavitvi aktivnosti društvenega glasila Prelom. Skrbnik za glasilo je prisotne pozval k oddaji prispevkov.

Spletна stran posveta (sl. 1): <https://sites.google.com/geo.ntf.uni-lj.si/26-posvet-slovenskih-geologov>



Sl. 1. Vstopna stran na 26. posvetovanje slovenskih geologov.

Na Posvetovanju so vsi udeleženci ob registraciji prejeli brezplačen izvod **društvenega glasila Prelom**, št. 28 (sl. 2).



Sl. 2. Društveno glasilo - Prelom št. 28.

Glasilo je poželo veliko pohval, predvsem za ponovno obuditev izdajanja. Vseeno bi si želeli, da bi članke prispevalo večje število raznolikih avtorjev. Drugi izziv predstavlja tiskanje in postavitev glasila, kar je postal v tem času precejšen finančni zalogaj. S plačilom članarine aktivni člani podprejo tako delovanje društva, kot tudi obstoj glasila. Zato je društvo sprejelo odločitev, da bo od naslednje številke glasila dalje, Prelom fizično distribuiralo le aktivnim članom društva. Upamo, da bomo s tem spodbudili tudi k priključitvi tudi tiste, ki še niso včlanjeni, a si Prelom želijo prebrati. Posledično, bomo aktualno številko glasila na spletno stran naložili z zakasnitvijo. Glasilu smo na prenovljeni spletni strani namenili samostojen zavihek, kjer si lahko obiskovalci pogledajo pretekle izdaje glasila.

Po malce slabši odzivnosti v post-kovidnem času, smo v preteklem letu zelo uspešno izvedli 3 strokovna predavanja. Po tehtnem premisleku smo se odločili, da bomo uvedli predavanja v hibridni obliki, saj se jih tako lahko udeleži več ljudi in tudi tisti, ki imajo številne aktivnosti po službi ali so od fizične lokacije predavanja precej oddaljeni. Hibridna predavanja so bila dobro sprejeta. Ker nismo želeli, da bi bila predavanja omejena le na eno institucijo, smo uvedli spremembe lokacij predavanj. Dosedaj so se društvena predavanja odvila na Geološkem zavodu Slovenije (GeoZS) in NTF. Promocija predavanj je potekala preko spletnne strani SGD (Aktualne novice, Koledar, Aktualna predavanja), kjer so posamezniki imeli možnost prebrati povzetke in kratke življjenjepise predavateljev, ter preko e-poštnega seznama Georg. Deljenje novic je potekalo tudi preko institucionalnih portalov in osebnih družabnih omrežij. Tematike, ki smo jih s predavanji v letu 2023 pokrili so geotermija, geokemija in okolska geologija ter krasoslovje. Prvo predavanje je bilo izvedeno 1. 6. 2023 na GeoZS. Nina Rman, Mateja Macut in Simon Mozetič

z GeoZS so predstavili »Geološke in geotermalne zanimivosti Islandije« v okviru projekta INFO-GEOTHERMAL, ki je bil podpora študijskemu obisku Islandije. Predavanje so podprli s fotografskim gradivom in predstavitvijo naravnih in kulturnih zanimivosti Islandije. Dne 6. 11. 2023 smo na GeoZS gostovali podoktorsko raziskovalko Ines Tomašek iz Univerze Clermont Auvergne v Franciji. V predavanju z naslovom »Nevarnost za zdravje ljudi zaradi geogenih onesnaževal v mestnem zunanjem zraku: priporočila za multidisciplinarno raziskovanje« je Ines Tomašek podala pregled študij o nevarnostih vulkanskih in puščavskih emisij na zdravje ljudi ter opisala uporabo multidisciplinarnih pristopov k njihovem raziskovanju. Veliko zanimanja je 14. 12. 2023 na Oddelku za Geologijo (UL NTF) poželo predavanje Mitje Prelovška z Inštituta za raziskovanje krasa ZRC SAZU (sl. 3). S predavanjem »Kraški pojavi na trasi 2TDK«, je predstavil raziskave krasa in kraških jam na odsekih izgradnje drugega železniškega tira med Divačo in Koprom. Vabilo na predavanje smo razposlali tudi kolegom geografom in geomorfologom, kateri so se pozitivno odzvali.



Sl. 3. Predavanje M. Prelovška na OG NTF.



Slovensko
geološko društvo

GEOPESTROST PRED DOMAČIM PRAGOM

Galerija Paviljon NOB, Tržič
10.-14. maj 2023

Vabljeni na odprtje 9. maja, ob 18. uri.

Paviljon NOB
Predilniška cesta 12, 4290 Tržič
sre.–pet.: 10.00–12.00 in 16.00–18.00
sob.–ned.: 9.00–18.00

www.trzic.info



49.
MINEOS



SLOVENSKO
GEOLOŠKO
DRUŠTVO
Muzej

Sl. 4. Vabilo na razstavo »Geopestrost pred domaćim pragom«, 10. – 14. maj 2023.

Društvo je na kongresu v letu 2022, v sklopu obeležitve prvega Mednarodnega dne geopestrošči otvorilo fotografsko razstavo z naslovom »Geopestrošči pred domačim pragom«. Sklenili smo, da razstavo preselimo na številne lokacije, kjer bi dosegla še druge radovedne poglede. Skladno z dogovorom, smo jo 9. 5. 2023 na dogodku 49. MINFOS otvorili pod istim imenom (sl. 4).

Na dan, ko obeležujemo Mednarodni dan geopestrošči (6. 10. 2023), smo razstavo preselili v galerijo Mitnica pri NTF in jo poimenovali »Geopestrošči – zgodbe nežive narave« (sl. 5). Slednja je bila na voljo za ogled en mesec. Tako je postala prava potupoča »geo-fotografska« razstava.

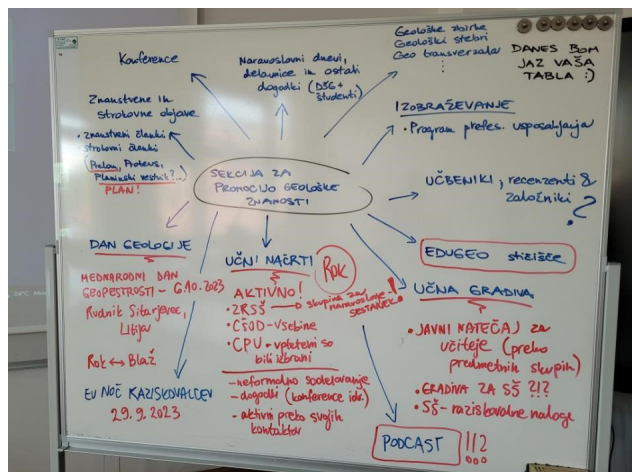


Sl. 5. Vabilo na razstavo »Geopestrošči zgodbe nežive narave« v galeriji Mitnici pred NTF, 6.10. – 6. 11. 2023.

Ena najbolj aktivnih skupin oz. sekcij Slovenskega geološkega društva ostaja **Sekcija za promocijo geološke znanosti**. Svoje aktivnosti v letu 2023 so pričeli s sestankom 8. junija, kjer so sprejeli naslednje sklepe:

SKLEP 1: Predhodni zapisnik je sprejet. Zapisan povzetek zapisnika sestanka (sl. 6).

SKLEP 2: V septembru 2023 je v planu izvedba sestanka s predmetno komisijo za Naravoslovje na ZRSŠ. Sestanek organizira Petra Žvab Rožič. Naknadno povabimo sodelujoče. Vsi člani sekcije



Sl. 6. Povzetek zapisnika sestanka, 8. 6. 2023.

bodite pozorni na informacije (formalne/neformalne), ki krožijo in jih javite Roku, ki je koordinator te aktivnosti (sestanek je bil organiziran v oktobru – glej nižje).

SKLEP 3: Nina Rman in Petra Žvab Rožič pregledata plane in tabelo iz prejšnjih let, ter naprej koordinirata vnovično vzpostavitev redne geološke rubrike v Planinskem vestniku.

SKLEP 4: Sekcija je sprejela sklep, da do nadaljnega ne izvaja javnih dogodkov. Vsi morebitni interesi, ki bi prevzeli koordinacijo in izvedbo posameznih dogodkov ali celotne aktivnosti, naj se javijo Roku po elektronski pošti (rok.brajkovic@geo-zs.si).

SKLEP 5: Predlog, da se v šolskem letu 2023/24 izvede natečaj za učitelje za naj geološko učno gradivo ni sprejet. Najprej je potrebna priprava celotnega gradiva, nato sledi izvedba.

SKLEP 6: Lea Dvorčak pripravi spisek tehnične opreme, ki jo potrebuje društvo za vzpostavitev podcasta. Rok in Lea (po želji tudi Nejc M.), pripravijo predlog uredniške politike. V septembru na sestanku SGD predstavimo zadevo in ugotovimo ali se društvo strinja z podcastom. Potencialna izvedba proti koncu leta 2023 ali v 2024.

Sekcija je sodelovala pri izvedbi dogodka 49. MINFOS - dnevi mineralov, fosilov in okolja (13. in 14. 5. 2023) ter na prireditvi Količarski dan v Dragi pri Igu (26. 8. 2023) – Geološka delavnica (sl. 7).

Sekcija je 6. 10. 2023 izvedla delavnico Dan geologije za 76 učencev Osnovnih šol Litija in Šmartno pri Litiji. Delavnica je bila izvedena v sklopu Mednarodnega dneva geopestrošči (sl. 8).

Na Zavod za šolstvo Republike Slovenije je sekcija na podlagi sestankov iz 18. 10. 2023 in 7. 11. 2023 oddala predlog popravkov in dopolnitiv obstoječih učnih načrtov, ki zajema le učne cilje, pri katerih predlagajo spremembe. Cilji, ki se ne-



Sl. 7. Geološka delavnica, Količarski dan, 26. 8. 2023.



Sl. 8. Izvajalci delavnice ob Dnevu geologije pred rudnikom Sitarjevec.

posredno ali posredno nanašajo na geološke vsebine in so bili prepoznani kot ustrezni (strokovo, taksonomsko, pravilno umeščeni), niso pa bili obravnavani. Predlagane spremembe učnih ciljev vsebujejo naslednje popravke in dopolnitve:

Učni cilji so ustrezno prerazporejeni med razrednimi stopnjami in predmeti.

Za posamezne učne cilje z geološko tematiko so predlagani strokovni popravki.

Predlog vključitve novih učnih ciljev za geološke vsebine, ki v obstoječem sistemu niso zastopane (npr. geološko pogojene nevarnosti).

Predlog razširitev ciljev z do sedaj pomanjkljivo predstavljenimi vsebinami (npr. o mineralih, tektoniki, dinamiki podzemne vode, fosilih in evoluciji) ter spremembo poučevanja o mineralnih surovinah zaradi zastarelosti ciljev v obstoječih učnih načrtih (Valand, Brajkovič in Torreggiani, 2021).

V posameznih primerih so predlagali krčenje geoloških vsebin v učnih načrtih (npr. vsebine o vulkanih, podvajanje vsebin na osnovni taksonomske stopnji).

Na konferenci Museoeurope 2023 je sekcija predstavila interpretacijo geoloških stebrov. Slednji so predstavljeni tudi na spletni strani društva (»Gradiva«). Referenca: KOČEVAR, Tanja Nuša, GABRIJELČIČ TOMC, Helena, ISKRA, Andrej, NOVAK, Matevž, ŽVAB ROŽIČ, Petra. Presentation of earth history through digital storytelling and interactive geological columns. V: KOPRIVNIK, Vesna (ur.), SALECL, Dunja (ur.). Srečanja tisočletij = The convergence of millennia: Museoeurope: the collected volume of the symposium 19.-21. 10. 2023: [Zbornik mednarodnega simpozija 19.-21. 10. 2023]. Maribor: Pokrajinski muzej = Regional Museum, 2023. Str. 155–166, ilustr. Zbirka Museoeurope, 8. https://museum-mb.si/wp-content/uploads/2023/10/MuseoEurope_2023.pdf.

Člani **sekcije za geokemijo** so v 2023 nadaljevali z delom začrtanim že v preteklih letih. Še vedno je najbolj v ospredju geokemija okolja. Raziskujejo kemične procese, vsebnosti in porazdelitve na zemeljskem površju, torej v našem okolju. V letu 2023 so bili v Sloveniji izjemni vremenski dogodki, ki so spodbudili raziskave v zvezi s premeščanjem s kovinami obremenjenih materialov. Raziskujejo tudi barja, ki so zelo zanimiva in specifična okolja.

Sekcija za geološko dediščino je svoje aktivnosti izvajala v sodelovanju z Zavodom Republike Slovenije za varstvo narave. Osrednji dogodek Mednarodnega dne geopestrosti je potekal 6. oktobra 2023 v Litiji, kjer je bila okrogla miza z naslovom »Raba mineralnih surovin in njihov pomem za geopestrost« (sl. 9). Strokovnjaki različnih področij so spregovorili o mineralnih surovinah v Sloveniji in njihovi umeščenosti v konceptu geopestrosti. Dogodek je bil tudi medijsko pokrit.



Sl. 9. Okrogla miza v Litiji, ob osrednjem dogodku Mednarodnega dne geopestrosti 2023.

Društvo je v letu 2023 organizacijsko in finančno sodelovalo z **Društvom študentov geologije (DŠG)**, ki organizira številne strokovne in zabavne vsebine za študente. Med drugim, je bil med 7. in

13. avgustom organiziran 26. Mednarodni geološki tabor EUGEN (European Geoscience Student Network), ki se ga je udeležilo več kot 90 udeležencev. Lokacija tabora je bila zaradi poplav iz Ljubnega ob Savinji prestavljena v Zavrh pri Borovnici. Člani SGD smo aktivno sodelovali tudi kot strokovni vodje ekskurzij. Odzvali smo se tudi pozivu za darovanje znanstvene in strokovne literature za študentski srečelov in študentom podaril večjo količino knjig in publikacij, ter skrbeli za redno obveščenost študentov o dogodkih, ki se odvijajo v okviru SGD. Društvo je prisluhnilo ideji o ustavitvi geološkega podcasta in pomagalo pri pripravi elaborata za potencialno izvedbo.

SGD je član **EFG – Evropskega združenja geologov**. Član društva Marko Komac ostaja predsednik EFG, 24 članov društva pa sodeluje v njegovih strokovnih svetovalnih telesih. Društvo je bilo v letu 2023 vključeno v 3 Evropske projekte Obzorje 2020 (Horizon 2020).

V sklopu že zaključenega projekta ENGIE – Vzpodbujanje deklet za izbiro poklica geoznanstvenice (Empowering Girls to become the geoscientists of tomorrow), je SGD financiral izdajo prevoda knjižice.

Projekt ROBOMINERS – Razvoj bio-navdihnjenega robotskega rudarja (Resilient Bio-Inspired Modular Robotic Miner): v letu 2023 je bilo narejenih več prevodov obvestil za javnost (PR4, PR5, PR6, PR7, prevoda Novic Brief Policy), vsi prevodi so dostopni na spletni strani SGD (<https://www.slovenskogeoloskodrustvo.si/index.php/mednarodno-sodelovanje/sodelovanje-v-mednarodnih-projektih>). Poleg tega so bile na spletno stran dodane vse povezave na video gradiva projekta, brošure, opisana je bila tudi predstavitev robota RM-1 v Mežici 25. 10. 2023 idr. Novembra 2023 so se s tem zaključile diseminacijske aktivnosti projekta – obveščanje slovenske javnosti o poteku projekta, prevodi obvestil za javnost in posredovanje vseh obvestil, za katere je bilo preko Evropske zveze geologov (EFG) zadolženo Slovensko geološko društvo.

Projekt REFLECT – Redefiniranje lastnosti geotermalnih tekočin v ekstremnih pogojih (Redefining geothermal fluid properties at extreme conditions to optimiza future geothermal energy extraction) se izvaja od maja 2020 in je bil podaljšan do junija 2023. Cilj projekta je preprečiti težave povezane s kemijo geotermalnih tekočin še preden nastanejo, tako v geosferi, vrtini in sestavnimi deli sistemov rabe toplote (izmenjevalci in elektrarne). Projekt REFLECT se je v letu 2023 zaključil. Javnost je bila obveščena o njegovih rezultatih, s katerimi je bila osvežena spletna stran:

https://geo-zs.si/?option=com_content&view=article&id=844.

Projekt **CRM-GEOTHERMAL** – Surovine iz geotermalnih fluidov (*Critical materials from geothermal fluids*) se izvaja od julija 2022 in bo potekal do maja 2027. Projekt CRM-GEOTHERMAL se ukvarja z razvojem inovativne tehnološke rešitve, ki združuje pridobivanje kritičnih surovin in energije iz geotermalnih tekočin. Ta bo pomagala Evropi izpolniti strateške cilje Zelenega dogovora EU in Agende za trajnostni razvoj, hkrati pa zmanjšala odvisnost od uvoženih CRM-jev. Kombinirano pridobivanje toplote in mineralov iz geotermalnih rezervoarjev ponuja vrsto prednosti: maksimiranje donosnosti naložbe, minimaliziranje vpliva na okolje, izogibanje dodatni rabi zemljišč, ne pušča rudarske dediščine, dosega skoraj ničeln ogljični odtis in omogoča domačo dobavo kritičnih surovin. Naša naloga bo predvsem zagotoviti podatke o potencialu geotermalnih tekočin v Sloveniji. Projekt CRM-GEOTHERMAL je nadaljeval z delom. Diseminacija rezultatov je vidna na projektni spletni strani. Njegova predstavitev je bila opravljena na letnem srečanju SZGG v Ljubljani.

Projekt **CEEGS** – Nov sistem geološkega skladanja CO₂ s pridobivanjem elektrotermalne energije (CO₂ Based Electrothermal Energy and Geological Storage System). Projekt se izvaja od novembra 2022 in bo trajal do oktobra 2025. Projekt CEEGS je 3-letni projekt, ki ga financira Horizon Europe in temelji na razvoju medsektorske tehnologije za energetski prehod. Združuje sistem za shranjevanje obnovljive energije, ki temelji na trans-kritičnem ciklu CO₂, geološkem skladanju CO₂ in pridobivanju geotermalne toplote. Glavni cilj projekta je zagotoviti znanstveni dokaz o tehnično-ekonomski izvedljivosti tehnologije in zvišati trenutno nizko raven tehnološke razvitosti (TRL) z 2 na 4 z obravnavanjem vrzeli med površinskim trans-kritičnim ciklom in podzemnim skladanjem CO₂. SGD je k projektu pristopilo maja 2023, zato se pred tem niso izvajale nobene aktivnosti. Naloga SGD v projektu je diseminacija rezultatov projekta, s čimer v letu 2023 še nismo pričeli, saj večjih rezultatov še ni bilo.

V okviru društva deluje tudi zelo aktivna strokovna skupina **Slovenski nacionalni odbor INQUA (SINQUA)**, ki povezuje raziskovalce kvartarja in skrbi za pretok informacij med slovensko in mednarodno kvartarno znanstveno sfero. Glavni cilj skupine je napredek na področju kvartarnih znanosti, pri čemer si prizadeva za interdisciplinarno zastopanost članov in večje medsebojno sodelovanje. Vpeti so v aktivnosti INQUA komisij in fokusnih skupin, sodelujejo pri organizaciji

znanstvenih srečanj in delavnic. V letu 2023 so sodelovali v aktivnostih INQUA komisij in fokusnih skupin. Predstavnik SINQUA je sodeloval na sestankih, volitvah in pri odločjanju mednarodnega Sveta INQUA. Kot člani INQUA so nadaljevali sodelovanje pri oblikovanju skupnih aktivnosti v okviru različnih komisij. Člani SINQUA smo vpeli v aktivnosti komisij CMP (Coastal and Marine Processes), PALCOM (Paleoclimates), SACCOM (Stratigraphy and Chronology) in TERPRO (Terrestrial Processes, Deposits and History). Aprila 2023 so izvedli 2. SINQUA srečanje, ki je bilo namenjeno predvsem pogovoru o organizaciji SINQUA, prihajočih kongresih in predstavitvi dela članov. Sodelovali so pri organizaciji in se udeležili kongresa »XXI Congress of the International union for Quaternary Research "Time for Change"«, ki se je odvijal julija 2023 v Rimu (sl. 10). Kongres je združil znanstvenike iz različnih strok pri preučevanju tem, kot so podnebne spremembe, nihanje morske gladine, poledenitve, rečna dinamika, potresna aktivnost in drugo. Člana SINQUA Miloš Bavec in Petra Jamšek Rupnik sta bila vpeta v »Scientific Advisory Committee«. Bili so so-sklicatelji sekcij: »Millennial paleo-landscape reconstructions of coastal areas - From field data to modelling approaches« (Ana Novak), »Quaternary Mediterranean Glaciers« (Manja Žebre) in »Discussion panel on assessing fault capability in different geodynamic and environmental settings« (Petra Jamšek Rupnik).

Več članov je prijavilo INQUA kongresni ekskurziji: »Life with geohazard at the contact of the Alps, the Dinarides and the Pannonian Basin« in »Quaternary archives in the Northeastern Adriatic karst environments«. Ekskurziji žal nista bili izvedeni zaradi nizkega števila prijav. Člani SINQUA so na INQUA kongresu predstavili več predavanj in posterjev o svojem delu in se udeležili več delovnih sestankov. Na sestankih znanstvenega svetovalnega odbora INQUA je kot član sodeloval predstavnik SINQUA Miloš Bavec. Petra Jamšek Rupnik je bila med nominiranimi za medaljo sira Nicholasa Shackletona za izjemne mlade kvartarne znanstvenike. V okviru CMP komisije so v letu 2023 v okviru projekta NEPTUNE organizirali že omenjeno sekциjo na INQUA srečanju v Rimu (sl. 10). Zaradi velikega števila prijavljenih prispevkov, so bili po kongresu povabljeni k pripravi posebne številke revije Quaternary International. V februarju bo zaključen rok za oddajo člankov in lahko pričakujemo, da bo posebna številka izšla v zadnji četrtini leta 2024. Del projektne ekipe NEPTUNE je v 2023 sodeloval pri uspešni prijavi novega CMP INQUA projekta OnSea, ki bo z aktivnostmi začel

februarja 2024 in predstavlja nadaljevanje in nadgradnjo projekta NEPTUNE. Člani SINQUA so pripravili posebno številko revije »Quaternary« z naslovom »Seas, Lakes and Rivers in the Adriatic, Alpine, Dinaric and Pannonian Regions during the Quaternary: Selected Papers from "6th RMQG"«, ki je sledila mednarodnemu znanstvenemu srečanju v organizaciji SINQUA s partnerji v letu 2021 in je bila zaključena v letu 2023.



Sl. 10. Skupina SINQUA na kongresu v Rimu.

Društvo je že peto leto zapored član **Mednarodnega združenja ProGEO**, predstavnica Slovenije je Martina Stupar. Najpomembnejša mednarodna aktivnost v letu 2023 je bil 11. simpozij ProGEO, ki je potekal v mesecu oktobru v Veliki Britaniji v »Charnwood Forest Geopark«. Mednarodno združenje ProGEO organizira simpoziji vsaki dve leti, namenjeni so predstavitvi bazičnih raziskav, varstvu in ohranjanju dediščine, geoturizmu, izobraževanju, interdisciplinarnim povezavam in drugim aspektom, ki so ključni dejavniki geološke dediščine. Sodelovali smo v soavtorstvu članka »State of the art in geoconservation and geosite inventory in ProGEO Southeast European Regional Group countries (WG1)«, katerega nosilka je Georgia Fermely iz ProGEO Grčije. Prispevek je bil rezultat sodelovanj v projektu Unesco 737 SMART GEOLOGY, ki se je že zaključil. Za namen priprave analize stanja po posameznih državah Jugovzhodne Evrope smo člani delovne skupine sodelovali z anketo o različnih vidikih na temo promocije, proučevanja in varstva geološke dediščine. Na simpoziju smo se med drugim udeležili tudi sestanka skupine za Jugovzhodno Evropo (WG1), na katerem so bili prisotni predstavniki Hrvaške, Bosne in Hercegovine, Madžarske, Grčije in Romunije. ProGEO je pridružena članica IUGS (Mednarodna zveza geoloških znanosti) in članica IUCN (Mednarodna zveza za ohranjanje narave). Smo tudi član Strokovne skupine EFG za geološko

dediščino, podelujemo tudi pri oblikovanju dokumenta »GEOHERITAGE AND GEODIVERSITY IN NATURE CONSERVATION POLICIES«, ki ga koordinira Monica Sousa v okviru EFG.

Med 20. in 24. junijem 2023 je bila v okviru **Evropske mineraloške zveze (EMU)** v Torinu organizirana šola z naslovom »Minerals in wastes«. Mednarodna šola EMU o mineralnih sestavinah odpadkov, njihovi karakterizaciji, predelavi in ravnjanju. Dogodek je bil delno financiran a žal ni bilo odziva pri študentih. V letu 2023 študentom sofinancirajo obisk na Goldschmidt konferenci v Lyonu v primeru aktivne udeležbe na konferenci.

SGD je včlanjeno v **Slovensko inženirska zbornica (SIZ)**. S tem je izpolnjen pogoj o obveznem članstvu SGD v SIZ za pridobitev naziva Evro inženir (EUR ING).

V letu 2023 (do 31. 12. 2023) je SGD štelo **rekordnih 101 aktivnih članov**, kar je bilo 10 članov več kot leto poprej. Do 13. 3. 2024 je za leto 2024 vplačalo članarino 96 članov. Na 26. Posvetovanju slovenskih geologov, je društvo podelilo

naziv **častne članice dr. Katici Drobne** (sl. 11). Čestitamo!



Sl. 11. Slika s podelitve naziva Častna članica SGD Katici Drobne.

Nove publikacije - New Publications

Decrouez, D., Finger, W., Haldimann, P., Hofstetter, J.-C., Kündig, R., Meyer, C., Mumenthaler, T., Sieber, N., Spescha, R., Testaz, G. et al. (eds.), 2018: **Stein und Wein: Entdeckungreisen durch schweizerischen Rebbaugebiete**, AS Verlag & Grafik, Zürich: 612 p.

Stone and Wine

Discovery tours through Swiss vineyards

Starting from the initial observation that enthusiasm for wine is widespread among geologists, the core of Swiss geologists came to the conclusion that they could contribute with their knowledge and personal efforts to resolve the open technical questions about the influence of rocks on the quality of wine. The Department of Earth Sciences at ETH Zurich, with the Swiss Geotechnical Commission, recently renamed the Expert Group on Earth Resources, which has been active there since 1899, is credited with launching the project. The company ‚Verein Stein und Wein‘ was set up and Reiner Kündig, Executive Director of the Swiss Geotechnical Commission, became Editor-in-Chief of the planned publication.

A ten-member editorial board coordinated the work of a 63-strong team of authors and a team of more than 40 graphic designers, illustrators, technical consultants and translators for a decade. In order to cover the necessary breadth and complexity of the subject, geologists were joined by experts in other branches of geosciences, and wine experts and winegrowers were also consulted. The result is a 612-page publication comprising a main book with 15 chapters and 10 regional volumes. Each of these presents a single geological region or landscape in more detail. The work was published simultaneously in German and French. I received the German version of this work from Dr Markus Felber, one of the co-authors, and I refer to it only in my assessment.

As early as the 12th century, Benedictine and Cistercian monks dissolved the soil in water and tasted the resulting water solution to determine the suitability of a site for planting vines. The site appropriate according to the taste of solution was then referred to as ‚climat‘ (from the ancient Greek ‚klima‘: the slope of the sun). Even in modern times, wine reviewers often write about wines with a ‚mineral‘ taste. With thousands of minerals, this is rather vague. Apparently, it is supposed to be possible to identify and smell rock materials such as gypsum, metamorphic, schist and volcanic tuff.

Kamen in vino

Odkrivatejska popotovanja skozi švicarske vinske pokrajine

Ob izhodiščni ugotovitvi, da je navdušenje nad vini med geologi splošno razširjeno, je cvet švicarskih geologov prišel do sklepa, da lahko s svojim znanjem in osebnim prizadevanjem prispeva k razrešitvi odprtih strokovnih vprašanj o vplivu kamnin na kakovost vina. Oddelku za znanosti o Zemlji ETH Zürich s tam od leta 1899 delujejoč Švicarsko geotehnično komisijo, pred kratkim preimenovano v Strokovno skupino za zemeljske vire, gre zasluga za začetek projekta. Ustanovili so družbo ‚Verein Stein und Wein‘, izvršni direktor Švicarske geotehnične komisije Reiner Kündig pa je postal glavni urednik načrtovane publikacije.

Desetglavi redakcijski odbor je celo desetletje usklajeval **delo 63-glave avtorske skupine in več kot 40**-glave skupine grafikov, ilustratorjev, strokovnih svetovalcev in prevajalcev. V njej so se zaradi potrebne širine obravnave in kompleksnosti tematike geologom pridružili še strokovnjaki drugih vej geoznanosti, kot svetovalci pa še vinogradniki ter vinarji. Rezultat je 612 strani obsegajoča publikacija, ki obsega glavno knjigo s 15 poglavji in 10 regionalnih zvezkov. Od teh vsak podrobnejše predstavlja posamezno eno-geološko regijo oziroma pokrajino. Delo je izšlo sčasno v nemški in francoski verziji. V last sem od dr. Markusa Felberja, enega od soavtorjev, dobil nemško verzijo tega dela, zato se v svoji oceni sklicujem le nanjo.

Že v 12. stoletju so benediktinski in cistercijanski menihi za ugotavljanje primernosti neke lege za sadnjo vinske trte v vodi raztopljalji njena tla in okušali nastalo vodno raztopino. Po okusu te raztopine primerni legi so nato sicer rekli ‚climat‘ (po starogrškem ‚klima‘: nagib lege sonca).

Tudi v modernem času vinski ocenjevalci vina pogosto pišejo o vinih z ‚mineralnim‘ okusom. Pri tisočih mineralov je to precej nejasno. Očitno naj bi bilo mogoče prepoznati in vonjati kamninske materiale, kot so mavc, metamorfik, skrilavec in vulkanski tuf. Celo izkušeni geologi pa enako

Even experienced geologists, however, find it as difficult as the rest of us to make the connection between such rock concepts and the sensation of tasting wine. On the other hand, the geological conditions in the vineyards undoubtedly have a significant influence on the quality of the grapes. After all, sun exposure, the water regime, the microclimate and the composition of the soil are also a reflection of geological development.

In the 20th century, the term ‚terroir‘, derived from the French word ‚terre‘ (soil), was coined to refer to vineyard sites, but it means much more than the native soil. The question remains: what all and to what extent? In 1997, the Swiss magazine Vinum published an article entitled ‚Terroir - the last secret‘, which was met with a very divergent response. „What geological factors can be traced and guessed in wine?“ is therefore a challenging question. The authors of this work cannot be faulted for tackling an irrelevant topic.

težko kot preostali ljudje vzpostavijo povezavo med takšnimi kamninskimi pojmi in občutkom okušanja vina. Po drugi strani pa geološke razmere v vinogradih nedvomno pomembno vplivajo na kakovost grozdja. Navsezadnje so tudi izpostavljenost soncu, vodni režim, mikroklima in sestava tal odraz geološkega razvoja.

Za vinske lege se je v 20. stoletju uveljavil iz francoske besede ‚terre‘ (tla) izveden izraz ‚terroir‘, ki pa pomeni veliko več kot rodna tla. Odkrito je pa ostalo vprašanje: kaj vse in v kolikšni meri? Leta 1997 je tako švicarska revija Vinum objavila članek ‚Terroir – poslednja skrivnost‘, ki je bil deležen nadvse divergentnih mnenjskih odzivov. »Kateri geološki dejavniki se lahko zasledijo in uganejo v vinu?« je torej zahtevno vprašanje. Avtorjem tega dela ni možno očitati, da so se lotili irrelevantne teme.

Povsem logično je bilo, da so se najprej spopadli s samim pojmom »terroir«. Kasneje je



It was only logical that they first tackled the very notion of ‘Terroir’. Later, the Office International du Vin gave an officially binding definition: „Terroir encompasses the specific characteristics of soil, relief, climate, landscape and biodiversity“ (OIV 2010). Unfortunately, they have forgotten about people and later revised it. It now reads: “Viticultural terroir is a site-based concept whereby a common knowledge is acquired (and defined) for a given site of the interactions between the identifiable physical and biological factors and the viticultural techniques used there that give the products of that site their uniqueness”. These are obviously very important definitions in marketing terms. Unfortunately, they have not helped to resolve the question with which the authors of ‚Stone and Wine‘ were grappling.

The chapter on ‚Terroir‘ is therefore followed by fourteen more steps in which the authors attempt to approach the question by means of an oeno-geological approach. The first eight steps correspond to the titles of the chapters that are also relevant to non-Swiss lay readers: Time, Depth, Topography, Soil, Water, Elements, Climate, Vines, and, Wine. These are followed by five more Swiss-specific chapters: Underground, Loose Underground, Solid Underground, Assemblages, and, Wine Regions/Provinces. These chapters are also of broader methodological interest to geologists.

‘Time’ tackles the relativity of the perception of time and the circulation of matter. It offers a fascinating temporal comparison of the evolution of geological and palaeontological events from the Big Bang to the present day, and of the evolution of the vine from its first known seeds 80 million years ago and from the first traces of human wine production in the Caucasus, 8,000 years ago, to the present day. It also parallels the annual growth cycle of the vine with the cycling of rock material from volcanism through erosion, sedimentation, diagenesis, subduction, metamorphism, magmatism and orogenesis. It also establishes geological (stratigraphic) time archives and time archives of vintages. Through the binoculars of time, it also peers into the temporal development of the formations and soils characteristic of the wine-growing part of Switzerland.

‘Depth’ parallels the deep structure of the earth, the lithostratigraphic column characteristic of Switzerland, the structure of the soil from the surface of the earth to the bedrock, and the development of the vine root system. The latter often extends into the bedrock. In conclusion, he notes that it is the nature of the bedrock that determines the depth range of the vine roots.

Office International du Vin (Meddržavni urad za vino) podal uradno zavezujočo definicijo: »Terroir zajema posebne značilnosti tal, reliefa, podnebja, pokrajine in biotske raznovrstnosti.« (OIV 2010). Žal pa pri tem pozabil na ljudi, zato jo je kasneje popravil. Zdaj se glasi: »Vinogradniški terroir je koncept, ki temelji na območju, pri čemer se za zadevno območje pridobi (in opredeli) skupno znanje o interakcijah med prepoznavnimi fizikalnimi in biološkimi dejavniki ter tam uporabljenimi vinogradniškimi tehnikami, ki dajejo proizvodom s tega območja njihovo edinstvenost.« Gre za marketinško očitno zelo pomembni definiciji. Žal pa nista prispevali k razrešitvi vprašanja, s katerim so se spopadali avtorji dela ‚Kamen in vino.‘

Poglavlju »Terroir« zato sledi še štirinajst korakov, v katerih se poskušajo avtorji z eno-geološkim pristopom približati odgovoru na obravnavano vprašanje. Prvih osem korakov ustreza naslovom tudi za ne-švicarske laične bralce pomembnih poglavij: Čas, Globina, Topografija, Tla, Voda, Elementi, Klima, Trta, in, Vino. Tem pa sledi še pet za Švico specifičnih poglavij: Podlaga, Nevezana podlaga, Trdna podlaga, Sklopi, in Vinske regije/pokrajine. Za geologe pa so metodološko širše zanimiva tudi ta poglavja.

»Čas« se spopade z relativnostjo zaznavanja časa in kroženja snovi. Ponuja zanimivo časovno primerjavo razvoja geoloških in paleontoloških dogajanj od velikega poka do danes in razvoja vinske trte od njenih prvih znanih semen pred 80 milijoni let in od prvih, 8.000 let starih, sledi človeške pridelave vina na Kavkazu do danes. Tudi kroženju kamninskega materiala od vulkanizma preko erozije, sedimentacije, diageneze, subdukcije, metamorfizma, magmatizma do orogeneze ponuja vzporednico letnega rastnega kroga vinske trte. Vzporeja še geološke (stratigrafske) časovne arhive in časovne arhive vinskih letnikov. Skozi časovni daljnogled pa pokuka še v časovni razvoj za vinorodni del Švice značilnih formacij in tal.

»Globina« vzporeja globinsko zgradbo Zemlje, za Švico značilni litostratigrafski stolpec, zgradbo tal od površja zemlje do kamninske podlage, ter razvoj trtnega koreninskega sistema. Slednji pogosto seže še v kamninsko podlago tal. Za sklep ugotavlja, da prav značilnost kamninske podlage določa globinski domet korenin vinske trte.

»Topografija« je specifično švicarska. Za tiste, ki smo hodili v šole še preden so na njih predavali o tektoniki plošč, pa je hkrati splošno zanimiva. Podaja na tektoniki plošč utemeljen razvoj švicarskega ozemlja, Alp, Molase in Jure. Z na tektonsko kartou Švice vrstanimi vinorodnimi legami se

‘Topography’ is specifically Swiss. Yet, for those of us who went to school before they taught plate tectonics, it is also of general interest. It traces the evolution of the Swiss territory, the Alps, Molasses and Jura, based on plate tectonics. It then asks whether vines have tectonic preferences, and consequently preferences linked to erosion and glacial and fluvial accumulation, by means of Swiss vineyard sites drawn on a tectonic map of Switzerland. All this has shaped and defined the current topography of Switzerland. Of course, it cannot avoid considering the effects of solar radiation and winds, especially the Fön.

After an introductory general explanation of soil pedogenesis, ‘Soils’ focuses on the Swiss soil types. More specifically, the soil types typical of Swiss vineyard sites. Of general interest, however, are the discussion of soil minerals and, of great interest for the soil’s ability to retain moisture and for its ability to grow plants, the chapter on ‚Clay - the ‚Protoplasm‘ of the soil‘. Agronomists and soil scientists are well aware of the role of clay minerals, but not all geologists.

‘Water’ gives first a general picture of the surface and underground water cycle, and then its features of relevance to Switzerland. It also looks at mineral waters as carriers of dissolved salts. However, it is worth highlighting the book’s objective-oriented chapter on ‚What does water do in the vineyard? The water cycle in the unsaturated and saturated zones of some characteristic geological and soil substrates is explained in a lucid manner. For a selected soil example, the depth evolution of the soil water status and the corresponding densities and thicknesses of the vine root system are given, which is rarely illustrated. The illustration allows the relationships to be understood and the situation to be extrapolated to other soil types.

‘Elements’ focuses on the chemical composition of bedrock, growing soils and wine. The starting point is an interesting comparison of the elemental composition of the Earth from the core to the surface crust, paralleled by the elemental composition of wine (major elements, trace elements and ultra- or micro-trace elements). The vines are seen to store potassium, phosphorus, sulphur, chlorine and carbon, which are rare in the Earth, in the grape berries. Silicon, iron and aluminium, which are very abundant in the Earth, are stored only in traces. The table, which gives an overview of the elemental composition and rock-forming minerals of the different types of bedrock, takes into account the types of bedrock present in Switzerland only. However, it is a good basis for an interesting illustration of the elements essential to the

nato sprašuje, ali ima vinska trta tektonske, posledično pa še z erozijo in z ledeniško ter rečno akumulacijo povezane preference. Vse to je namreč oblikovalo in opredelilo sedanjo topografijo Švice. Seveda se ob tem ne more izogniti obravnavi vplivov osončenja in vetrov, še posebej föna.

»Tla« se po uvodni splošni razlagi pedogeneze tal posvečajo predstavitvi švicarskih talnih tipov. Bolj specifično še za švicarske vinogradniške lege tipičnih talnih tipov. Splošno zanimivi pa so razprava o mineralih v tleh in za sposobnost tal za zadrževanje vlage in za njihovo rastno sposobnost zelo zanimivo poglavje »Glina – ‚Protoplazma‘ tal«. Agronomi in pedologi se te vloge glinastih mineralov dobro zavedajo, geologi pa ne čisto vsi.

»Voda« poda najprej splošno sliko površinskega in podzemnega kroženja vode, nato pa njegove za Švico pomembne značilnosti. Posveti se tudi mineralnim vodam kot nosilcem raztopljenih soli. Izpostaviti pa velja k ciljem knjige usmerjeno poglavje »Kaj dela voda v vinogradu?« V njem je na poljuden način sijajno pojasnjeno kroženje vode v nezasičeni in zasičeni coni nekaj značilnih geoloških in talnih podlag. Za izbrani talni primer je podan sicer redko prikazani globinski razvoj stanja talnih vodnih zalog in temu prilagojene gostote in debeline trtnega koreninskega sistema. Prikaz omogoča razumevanje odnosov in ekstrapolacijo razmer na druge talne tipe.

»Elementi« se posvečajo kemijski sestavi kamninske podlage, rastnih tal in vina. Izhodišče je zanimiva primerjava elementne sestave Zemlje od jedra do površinske skorje, vzporejena z elementno sestavo vina (glavni elementi, sledni elementi in ultra- oziroma mikro-sledni elementi). Vidi se, da trta v grozdne jagode skladišči v tleh redke kalij, fosfor, žveplo, klor in ogljik. V tleh zelo zastopane silicij, železo in aluminij pa skladišči le v sledeh. Tabela, ki podaja vpogled v elementno sestavo in kamninotvorne minerale posameznih tipov kamninske podlage upošteva sicer le v Švici prisotne vrste kamninske podlage. Je pa dobra osnova za zanimiv prikaz, katere za vinsko trto bistvene elemente ji ponuja posamezni talni tip in kakšne so s tem v zvezi njene elementarne potrebe. Vinska trta je sicer skromna rastlina, a brez dveh snovi ne more: vode in ogljika. Prvo zagotavlja padavine in ustrezna struktura tal, drugo pa v tleh prisotne organske substance. Z vidika kroženja snovi in fiziologije vinske trte je izjemni slikovni in tekstovni prikaz z naslovom »Elementno- in prehranjevalno- gospodinjstvo vinske trte«. V njem so z vidika izmenjave snovi prikazani vsi ključni procesi: fotosinteza nad tlemi (CO_2 , O_2 , H_2O), v tleh pa sodifikacija (Na,

vine and its elemental needs. The vine is a modest plant, but it cannot do without two substances: water and carbon, the former provided by rainfall and the appropriate soil structure, the latter by the organic substances present in the soil. From the point of view of the cycling of substances and the physiology of the vine, the pictorial and textual presentation entitled 'The elemental and nutritional household of the vine' is remarkable. It shows all the key processes from the perspective of material exchange: photosynthesis above ground (CO_2 , O_2 , H_2O), sodification in soil (Na, Cl), bacterial metabolism (NH_3 , NO_2) and the physiological role of roots and water related to mineral weathering and element uptake. Finally, it is worth noting also the interesting picture of the distribution of chemical substances from the deeper core of the grape berry and the pips to its surface skin and stalk. It shows that polyphenols (colouring agents, tannins) are only found in the skin, pips and stalk. This is why, after pressing, red wine can be coloured mainly only in contact with the grape skins.

Temperature fluctuations are then shown in more detail for the period of human evolution from the beginning of the Middle Stone Age to the Roman Optimum (labelled the 'Vine Age'), and on a modified time scale from then to the present. The medieval temperature optimum and the Little Ice Age of the last thousand years are clearly visible. Finally, for the last 160 years, the fluctuation of directly measured air temperatures is shown for Geneva. It shows the temperature maximum in 1944, the cooling between 1944 and 1973 and the subsequent rise. The latter now exceeds the temperatures measured in 1944 by a good degree Celsius. The effects of climate change on vineyard sites and vines and the resulting necessary changes in Swiss viticulture are presented. This debate is certainly of interest to a wider audience, as wine-growers in Slovenia are also facing similar problems and resorting to similar considerations.

'The Vine' gives the history of the human cultivation and spread of the 'European' grapevine and its spread to continental Europe in the Roman Empire. It cannot, of course, pass over the catastrophe caused in the second half of the 19th century by the introduction of 'American' vines from America, which brought the vine louse and, even earlier, the fungal diseases peronospora and oidium. European and Swiss viticulture recovered in the 20th century, however, thanks to the grafting of European vines onto American rootstocks. But it is no longer possible to raise and plant grafts and spray the vines without protective agents. Most of this chapter is therefore devoted to a description

Cl), bakterijski metabolizem (NH_3 , NO_2) in s pre-perevanjem mineralov in prevzemom elementov povezana fiziološka vloga korenin in vode. Navsezadnje velja omeniti tudi zanimivo sliko porazdelitve kemijskih snovi od globljega jedra grozdne jagode in pešk do njene površinske kožice in peclja. Kaže, da so polifenoli (barvila, tanini) le v jagodni kožici, peškah in peclju. Prav zato se lahko rdeče vino po stiskanjuobarva večinoma le v stiku z grozdnimi kožicami.

»Podnebje« ob spremenljivem časovnem merilu najprej prikaže nihanje temperature ozračja od začetka kambrija do danes. Nihanje temperature je nato prikazano podrobnejše za obdobje človekovega razvoja od začetka srednje kamene dobe do rimskega optima (označenega kot 'vinski čas'), ter v spremenjenem časovnem merilu od tedaj do danes. Lepo sta vidna srednjeveški temperaturni optimum in mala ledena doba v zadnjih tisoč letih. In končno je za zadnjih 160 let za Ženevo prikazano še nihanje neposredno merjenih temperatur zraka. Kaže temperaturni maksimum v letu 1944, ohladitev med leti 1944 in 1973 in kasnejši dvig. Ta zdaj že za dobro stopinjo presega v letu 1944 izmerjene temperature. Podani so iz klimatskih sprememb izhajajoči vplivi na vinogradniške lege in trto in iz njih izhajajoče potrebne spremembe v švicarskem vinogradništvu. Ta razprava je gotovo zanimiva tudi širše, saj se tudi v Sloveniji vinogradniki spopadajo s podobnimi problemi in zatekajo k podobnim razmišljanjem.

»Trta« podaja zgodovino človekovega gojenja in razširjanja »evropske« vinske trte in njen razširjenje v kontinentalno Evropo v rimskem cesarstvu. Seveda ne more mimo katastrofe, ki jo je v drugi polovici 19. stoletja povzročila z vnosom »ameriške« vinske trte iz Amerike prenešena trtna uš, še prej pa od tam izhajajoči glivični bolezni peronospora in oidij. Sledil je popoln zlom evropskega vinogradništva in vinarstva. Evropsko in švicarsko vinogradništvo sta si v 20. stoletju s pomočjo cepljenja evropske trte na ameriške podlage sicer opomogla. A brez vzgoje in sadnje cepičev ter škropljenja vinske trte z zaščitnimi sredstvi več ne gre. Večina tega poglavja se zato posveča opisu za švicarske talne in klimatske razmere potrebnih podlag, prikazu današnje sortne sestave njihovih vinogradniških regij, ter, novih sort, ki naj bi švicarskemu vinogradništvu pomagale ekonomsko preživeti v prihodnje. Za slovenske geologe in vinogradnike pa je zanimivo poglavje z naslovom »Ko vinograd plazi.« Opisan je zdrs v Opalinski glini, kjer je zdrselo 8.000 m^2 terena oziroma 70.000 m^3 materiala. Sam sem v mladih letih videl v vinogradih v Sloveniji kar nekaj plazov, ki so sicer precej

of the rootstocks needed for the Swiss soil and climate conditions, an illustration of the present-day varietal composition of their wine-growing regions, and the new varieties that should help Swiss viticulture to survive economically in the future. Of interest to Slovenian geologists and viticulturists is the chapter entitled „When the vineyard creeps“. It describes a slip in the Opalin clay, where 8 000 m² of terrain or 70 000 m³ of material slipped. I myself saw a number of landslides in vineyards in Slovenia when I was young, and although they were much smaller in size, they were no less horrific for the affected growers.

‘Wine’ pursues the goal of tasting the ‘stone’ in the wine: it therefore devotes itself first to training our tasting skills. It is common knowledge from our culture that the human palate includes the senses of sweet, sour, bitter and salty. From Japanese culture, there is a fifth taste, ‘umami’, which is sensitive to glutamic acids and their salts. Its senses have since been medically proven in humans. It is therefore necessary to accept that we have senses for five tastes, two of which are not very well activated in the perception of wine under normal conditions. ‘Wine’ therefore introduces the method of the wine sensory expert Hans Blattig, who takes into account the three senses of taste (sweet, sour, bitter) and smell when tasting wine. Blattig thus identifies primarily four building blocks in wine: 1) the soft complex (sweetness, alcohol, glycerine); 2) the acid structure; 3) the tannins or tannic structure; and, 4) the aromatic blanket. He then graphically identifies their occurrence and duration on the time course of a single wine tasting: 1) 0-2 seconds: initial tasting, 2) 0-4 seconds: two-thirds tasting, 3) 0-6 seconds: three-phase tasting, and 4) 6-12 seconds: after-tasting or finish; after 6 seconds, the wine sample to be tested must be either swallowed or spat out. The soft complex is tasted immediately, the acid structure is delayed and full within 4 seconds, and the tannins are delayed and full within 6 seconds or even later, extending with the acids into the aftertaste. The aromas are special in that they develop immediately but, due to man’s unusual physiological capacity for retro-nasal olfaction, extend far into the aftertaste. All the results of the tastings can therefore be presented in terms of taste in a sweet-sour-bitter or sweet-sour-tannin triangle.

And this is where the undeniable creativity and innovation of the authors of this work begins: they draw the SAND/silicate - CLAY/silicate - LIME/carbonate ‘rock triangle’ from the ETH scripts (ETH 1988). Taking into account the relative proportions of carbonate, quartz and clay, practical-

zaostajali po velikosti, za prizadete vinogradnike pa niso bili nič manj grozljivi.

»Vino« sledi cilju okušanja ‚kamna‘ v vinu: zato se najprej posveti šolanju naših degustacijskih sposobnosti. Splošno je iz naše kulture značno, da obsega človeški okus čutila za sladko, kislo, grenko in slano. Iz japonske kulture je znan še peti, na glutaminske kisline in njihove soli občutljiv, okus ‚umami‘. Njegova čutila so bila medtem pri človeku medicinsko dokazana. Treba je torej sprejeti dejstvo, da imamo čute za pet okusov izmed katerih pa se dva pri zaznavanju vina v normalnih razmerah ne aktivirata kaj prida. »Vino« zato predstavi metodo vinskega senzorika Hansa Blattiga, ki pri poskušanju vina upošteva tri vrste čutil za okus (sladko, kislo, grenko) in čutilo vonja. Blattig tako v vinu določa prvenstveno štiri gradnike: 1) mehki kompleks (sladkoba, alkohol, glicerin); 2) Kislinska struktura; 3) Tanini ozioroma taninska struktura; in, 4) Aromatična odeja. Nato pa na časovnem poteku posamične degustacije vina grafično opredeli njihovo pojavnost in trajanje: 1) 0-2 sekundi: začetno okušanje, 2) 0-4 sekunde: dvetretjinsko okušanje, 3) 0-6 sekund: trifazno okušanje, in 4) 6-12 sekund: pokušanje; pri čemer je treba po 6 sekundah preskušani vzorec vina bodisi pogoltniti, bodisi izpljuniti. Okušanje mehkega kompleksa se pojavi takoj, kislinske strukture z zamudo in polno v 4 sekundah, taninov pa z zamudo in polno v 6 sekundah ali še kasneje ter sega skupaj s kislinami še v pookus. Posebnost so arome, ki se razvijejo takoj, a segajo zaradi človekove nenavadne fiziološke zmožnosti retro-nazalnega voha še daleč v pookus. Vse rezultate degustacij je torej glede okusa možno predstaviti v trikotniku sladko-kislo-grenko ozioroma sladkoba-kislina-tanini.

In tu se začenja nesporna kreativnost in inovativnost avtorjev tega dela: Iz skript ETH potegnejo ‚kamninski trikotnik‘ PESEK/silikat - GLINA/silikat - APNO/karbonat (ETH 1988). Vanj je možno, ob upoštevanju relativnih deležev karbonata, kremera in glin umestiti praktično vse švicarske kamnine (peščenjaki, graniti, gnajsi, silikatni vulkaniti, laporni peščenjaki, skrilavci, apnenci, laporni apnenci, glinasti apnenci, apneni peščenjaki, laporni apneni peščenjaki, itd.). Hkrati potegnejo iz najnovejše literature ‚trikotnik okusov‘, ki ga je v letu 1995 objavil C. Sitter. V njem je izenačil pesek s kislostjo, apno s polnostjo in glico z adstringentnostjo. Sitter v svojem trikotniku okusov opredeli še 39 različnih oznak okusa, pri čemer za območje z najmanj 20 % vsake od treh kamninskih komponent določi notranji trikotnik ‚harmonično uravnoteženih okusov‘. Avtorji dela

ly all Swiss rocks (sandstones, granites, gneisses, siliceous volcanics, lacustrine sandstones, shales, limestones, lacustrine limestones, clayey limestones, calcareous sandstones, lacustrine calcareous sandstones, etc.) can be placed in it. At the same time, they draw on the most recent literature the ‚triangle of flavours‘ published by C. Sitter in 1995. In it, Sitter equated sand with acidity, lime with fullness and clay with astringency. He defines 39 different flavour codes in his triangle of flavours, identifying an inner triangle of ‚harmoniously balanced flavours‘ for an area with at least 20 % of each of the three rock components. The authors of ‚Stone and Wine‘ first rotate Sitter’s triangle of flavours by 60 °, so that in the rock triangle, sour lies between limestone and sandstone, tannic between limestone and claystone, and sweet between claystone and sandstone. They then maintain a central area of harmony and reduce the number of too many flavour notes to just three: strong towards clay, fresh towards sandstone and structured towards limestone. With this apparatus, they then set about systematically tasting the Swiss wines. The testers are all co-authors of this work and many invited winemakers and experts. In the Blattig method, the intensity of the flavours is plotted on a timeline of the development of the flavours on the ordinate axis and the results are rigorously evaluated at the end.

Through their testing method, the authors demonstrate that the rock bed has an undeniable influence on the characteristics or flavour of the wine. However, they acknowledge that this influence is sometimes quite pronounced and sometimes barely perceptible. In his review of the work, Thomas Vaterlaus, Editor-in-Chief of the Swiss wine magazine Vinum, therefore concludes: ‚Stone and Wine‘ brings us closer to the important links, clarifies them for us, which ultimately contributes to making Swiss wines even more enjoyable in the future, because we will all drink ‚with understanding‘. But the magic remains.“

“Underground”, based on the links identified in the „Wine“ chapter, present the „Oeno-geological map of Switzerland“, derived from the geotechnical map of Switzerland. It covers 8 types of solid rock, 4 types of loose rock, 2 types of assemblages (molasses and flysch) and all Swiss vineyard sites. The distribution of the underground basement rock types in each of the oeno-geological regions or areas is also shown. The chapter on ‚Underground‘ is followed by chapters on ‚Loose Underground‘, ‚Solid underground‘ and ‚Assemblages‘, which give a more detailed picture of the nature and distribution of the different types of bedrock.

„Kamen in vino“ najprej zasučujejo Sitterjev trikotnik okusov za 60°. Tako, da leži v kamninskem trikotniku kislo med apnencem in peščenjakom, taninično med apnencem in glinovcem, sladko pa med glinovcem in peščenjakom. Nato ohranijo središčno območje harmonije in zmanjšajo število preštevilnih oznak okusa na vsega tri: močno v smeri glinovca, sveže v meri peščenjaka in strukturirano v smeri apnenca. S tem aparatom se nato lotijo sistematičnega poskušanja švicarskih vin. Preizkuševalci so vsi soavtorji tega dela ter mnogi povabljeni vinarji in strokovnjaki. Pri Blattigovi metodi nanašajo ob tem na časovni diagram razvoja okusov na ordinato še njihovo intenzivnost in na koncu rigorozno vrednotijo rezultate.

S svojo preizkuševalno metodo avtorji dokažejo, da ima kamninska podlaga nedvomen vpliv na značilnosti oziroma okus vina. Priznavajo pa, da je ta vpliv včasih povsem izrazit, včasih pa komaj zaznaven. Glavni urednik švicarske vinarske revije Vinum Thomas Vaterlaus v svoji oceni dela zato ugotavlja: „Kamen in vino“ nam približa pomembne povezave, nam jih razjasni, kar na koncu prispeva k temu, da nam bodo švicarska vina v prihodnosti nudila še več užitka, saj bomo vsi pili „z razumevanjem“. Toda magija ostaja.

»Podlaga« na osnovi v poglavju »Vino« ugotovljenih povezav podaja iz geotehnične karte Švice izvedeno »Eno-geološko karto Švice«. Zajema 8 vrst trdnih kamnin, 4 vrste nevezanih kamnin, 2 vrsti sklopov kot bolj ali manj ciklično plastovitih formacij (molasa in fliš) in vse švicarske vinogradniške lege. Prikazana je tudi porazdelitev kamninskih tipov po posameznih eno-geoloških regijah oziroma območjih. Poglavlju »Podlaga sledijo še poglavja »Nevezana podlaga«, »Trdna podlaga« in »Sklopi«, ki še natančneje predstavijo značaj in razširjenost posameznih vrst kamninske podlage.

»Vinske regije« so zaključno inovativno poglavje tega dela. Avtorji na osnovi svojih v poglavjih »Vino« in »Podlaga« prikazanih dognanj opredelijo v Švici obstoj 10 eno-geoloških vinskih regij ter te regije kartografsko prikažejo v zadnjem poglavju. To je precejšnja novost. Zakonsko so v Švici namreč določene le tri vinske regije: a) Regija zahodne Švice, b) Regija nemške Švice, in, c) Regija italijanske Švice. Po politično-kulturnih kriterijih pa ločijo 6 vinskih regij. Geologi so torej zdaj njihovo število na osnovi eno-geoloških kriterijev povečali na 10.

Vinskim regijam se posveča 10 regionalnih zvezkov (zaradi jasnosti ohranjaj imena izvirnika): Jura Nord, Mittelland, Alpenseen, Alpenrhein, Tessin, Wallis, Chablais, Balcon lémanique,

‘Wine Regions’ is the final innovative chapter of this work. Based on their findings in the chapters ‘Wine’ and ‘Underground’, the authors identify 10 oeno-geological wine regions in Switzerland and map these regions in the final chapter. This is a significant innovation. Only three wine regions are legally defined in Switzerland: a) the Western Switzerland Region, b) the German Switzerland Region, and c) the Italian Switzerland Region. The 6 wine regions are separated by political-cultural criteria. Geologists have therefore now increased the number of regions to 10 on the basis of oeno-geological criteria.

The wine regions are the subject of 10 regional volumes (for the sake of clarity, I am retaining the original names): Jura Nord, Mittelland, Alpenseen, Alpenrhein, Tessin, Wallis, Chablais, Balcon lémanique, Genf, and Drei-Seen-Land. They are wonderful geological, viticultural and cultural guides through these regions. Anyone who wants to go through them as a geologist - even if they are not a wine lover - will certainly find them a valuable guide. However, wine lovers may find themselves in trouble by too much tempting information.

What to add in conclusion? What I find immensely fascinating about the main book is the approach, starting in each chapter with a popular explanation of the most general concepts of science. Then, through technically and technologically relevant explanations, it gets to the regional data and characteristics that are important for Swiss viticulture. The book is therefore a very interesting encyclopaedic source of general natural science and specific viticultural knowledge, even for non-Swiss readers. As a geologist or hydrogeologist, I am fascinated by both the clarity of the lay scientific presentations and the scientific rigour in the approach to uncovering the links between wines and the bedrock for wine tasting. As someone who was born at the Maribor Vineyard and Wine School as the son of a later university professor of viticulture and winemaking, and who has grown up and lived with vines and wine all his life, I was also touched by the clarity and precision of the presentation of the physiology of the vine and wine tasting.

I judge ‘Stone and Wine’ to be a magnificent monument to Swiss geology, viticulture and winemaking. It can be a model for all those who do not yet have something similar.

Genf, in, Drei-Seen-Land. Predstavljajo čudovite geološke, vinogradniško-vinarske in kulturološke vodnike skozi te regije. Kdor se želi skoznje podati kot geolog - celo če ni ljubitelj vina – mu bodo gotovo dragocen vodnik. Kdor je ljubitelj vina, se pa utegne znajti v težavah zaradi prevelikega števila vabljivih informacij.

Kaj dodati za zaključek? Pri glavni knjigi me neizmerno očara pristop, ki v vsakem poglavju izhaja od poljudno prikazanih najbolj splošnih naravoslovnih pojmov. Nato pa preko tehnično-tehnološko pomembnih razlag pride do za švicarsko vinogradništvo pomembnih regionalnih podatkov in značilnosti. Knjiga je zato tudi za ne-švicarske bralce nadvse zanimiv enciklopedični vir splošnih naravoslovnih in specifičnih vinogradniško/vinarskih znanj. Kot geologa oziroma hidrogeologa me fascinirata tako jasnost poljudno znanstvenih prikazov kot znanstvena rigoroznost v pristopu k odkrivanju povezav med vini in kamninskimi podlagami namenjenim vinskim degustacijam. Kot nekoga, ki je bil na mariborski vinogradniško-vinarski šoli rojen kot sin kasnejšemu univerzitetnemu profesorju vinogradništva in vinarstva, in, ki je vse življenje rasel in živel s trto in vinom, pa se me je dotaknila tudi jasnost in natančnost predstavitev fiziologije vinske trte in vinskih degustacij.

Sodim, da je delo »Kamen in vino« veličasten spomenik švicarski geologiji, vinogradništvu in vinarstvu. Lahko je vzor vsem tistim, ki česa podobnega še nimajo.

dr. Miran Veselič zasl. prof. UNG

GEOLOGIJA

št.: 67/1, 2024

www.geologija-revija.si

- 7 Žvab Rožič, P.
Hydrogeochemical and Isotopic Characterisation of the Učja Aquifer, NW Slovenia
- 25 Gale, L. & Rožič, B.
Signs of crustal extension in Lower Jurassic carbonates from central Slovenia
- 41 Gosar, M., Bavec, Š., Miler, M. & Gaberšek, M.
Vsebnosti potencialno strupenih elementov v sedimentih in vodah reke Meže in njenih pritokov,
ki odvodnjavajo odlagališča rudarskih odpadkov
- 63 Dernov, V.
Palaeoecological significance of the trace fossil *Circulichnus* Vyalov, 1971 from the Carboniferous of the
Donets Basin, Ukraine
- 71 Skaberne, D., Čar, J., Pristavec, M., Rožič, B. & Gale, L.
Middle Triassic deeper-marine volcano-sedimentary successions in western Slovenia
- 105 Kanduč, T. & Markič, M.
Isotopic composition of carbon ($\delta^{13}\text{C}$) and nitrogen ($\delta^{15}\text{N}$) of petrologically different Tertiary lignites
and coals
- 129 Placer, L., Popit, T. & Rižnar, I.
Tectonics and gravitational phenomena, part two: The Trnovski gozd-Banjšice-Šentviška Gora
degraded plain
- 157 Mencin Gale, E., Kralj, P., Trajanova, M., Gale, L. & Skaberne, D.
Petrology dataset of Pliocene-Pleistocene sediments in northeastern Slovenias

ISSN 0016-7789